NEUROCARDIOVASCULAR DISEASES: NEW ASPECTS OF THE OLD ISSUES

EDITED BY: Tijana Bojić, Antonio M. Esquinas and Tarek Francis Antonios
PUBLISHED IN: Frontiers in Neuroscience, Frontiers in Physiology and Frontiers in Neurology

frontiers Research Topics

ISSN 1664-8714
ISBN 978-2-88945-775-5
DOI 10.3389/978-2-88945-775-5

About Frontiers

Frontiers is more than just an open-access publisher of scholarly articles: it is a pioneering approach to the world of academia, radically improving the way scholarly research is managed. The grand vision of Frontiers is a world where all people have an equal opportunity to seek, share and generate knowledge. Frontiers provides immediate and permanent online open access to all its publications, but this alone is not enough to realize our grand goals.

Frontiers Journal Series

The Frontiers Journal Series is a multi-tier and interdisciplinary set of open-access, online journals, promising a paradigm shift from the current review, selection and dissemination processes in academic publishing. All Frontiers journals are driven by researchers for researchers; therefore, they constitute a service to the scholarly community. At the same time, the Frontiers Journal Series operates on a revolutionary invention, the tiered publishing system, initially addressing specific communities of scholars, and gradually climbing up to broader public understanding, thus serving the interests of the lay society, too.

Dedication to Quality

Each Frontiers article is a landmark of the highest quality, thanks to genuinely collaborative interactions between authors and review editors, who include some of the world's best academicians. Research must be certified by peers before entering a stream of knowledge that may eventually reach the public - and shape society; therefore, Frontiers only applies the most rigorous and unbiased reviews.
Frontiers revolutionizes research publishing by freely delivering the most outstanding research, evaluated with no bias from both the academic and social point of view. By applying the most advanced information technologies, Frontiers is catapulting scholarly publishing into a new generation.

What are Frontiers Research Topics?

Frontiers Research Topics are very popular trademarks of the Frontiers Journals Series: they are collections of at least ten articles, all centered on a particular subject. With their unique mix of varied contributions from Original Research to Review Articles, Frontiers Research Topics unify the most influential researchers, the latest key findings and historical advances in a hot research area! Find out more on how to host your own Frontiers Research Topic or contribute to one as an author by contacting the Frontiers Editorial Office: researchtopics@frontiersin.org

NEUROCARDIOVASCULAR DISEASES: NEW ASPECTS OF THE OLD ISSUES

Topic Editors:
Tijana Bojić, University of Belgrade, Serbia
Antonio M. Esquinas, Hospital General Universitario Morales Meseguer, Spain
Tarek Francis Antonios, St. George's, University of London, United Kingdom

Image: Jackie Niam/Shutterstock.com

Neurocardiovascular diseases and disturbances are a distinguished group of the pathological entities that demand an integrative scientific approach to be studied, treated and finally, cured. Brain-heart and vessels axes can be comprehended as a complex, bidirectional unit of utmost importance for organism survival. Harmonized functioning of this unit through the autonomic nervous system interface can be fatally compromised by stress, infection, systemic diseases, dietary habits, pharmacological and surgical interventions. The scope of this Research Topic is to emphasize the importance of the scientists' and medical practitioners' attention to molecular and

systemic modes of the brain-heart and vessels functioning and, often underestimated, neurocardiovascular pathology by a patient's bedside. In the last couple of decades, this research area flourished and contributed to the general knowledge by placing the new milestones of neurocardiovascular physiology and pathology. We hope that by this modest contribution we will provide an interesting, practical and innovative update on the novelties in the field of neurocardiovascular research.

Citation: Bojić, T., Esquinas, A. M., Antonios, T. F., eds. (2019). Neurocardiovascular Diseases: New Aspects of the Old Issues. Lausanne: Frontiers Media.
doi: 10.3389/978-2-88945-775-5

Table of Contents

SURGICAL AND PHARMACOLOGICAL INTERVENTIONS: CAVEATS FOR NEUROCARDIOVASCULAR EVENTS

CEREBRAL BLOOD FLOW IN HYPOXIA: A STEP TOWARDS AN UNDERSTANDING OF AN AUTONOMIC CONTRIBUTION?

frontiers in Neuroscience

EDITORIAL
published: 11 January 2019
doi: 10.3389/fnins.2018.01032

Editorial: Neurocardiovascular Diseases: New Aspects of the Old Issues

*Tijana Bojić**

Laboratory of Radiobiology and Molecular Genetics, Institute of Nuclear Sciences Vinča, University of Belgrade, Belgrade, Serbia

Keywords: neurocardiovascular diseases, Integrative pathology, autonomic nervous system, sympathetic, parasympathetic, development

Editorial on the Research Topic

Neurocardiovascular Diseases: New Aspects of the Old Issues

Concept of neuro-cardiovascular diseases (NCVD) is one fruitful approach that enables the comprehension of the pathological processes raising along the brain-heart & blood vessel axes from the integrative prospective. That is the reason why multidisciplinary and interdisciplinary approaches result in novel insights into pathophysiological processes bringing new directions for therapeutic development, both at the laboratory bench and at the clinical bedside. NCVD comprises the group of pathologies that have as a primary pathological substrate the changes in neurochemical, neurophysiological and neuroanatomical levels of the autonomic nervous system (ANS) and its regulated organs (e.g., heart, blood vessels).

A striking fact is that "cardiovascular disease is the leading cause of death in the world today and will remain so by the year 2020" (The WHO MONICA Project, Investigators, 1988) strongly supports the need for new insights into cardiovascular regulatory mechanisms (Bojić, 2003). A picture of the classical cardiovascular risk factors from the prospective of neural cardiovascular control, links these factors with stress. The central topic of NCV physiology is related to stress-induced disfunction (e.g., hypertension, Du et al., 2017), emotional stress coping-cigarette smoking, obesity, Strickland et al., 2007) and stress-releasing strategies (exercise, Acevedo et al., 2006; Webb et al., 2017).

Central questions of neurophysiology of stress is:

a. Identification of different brain networks activated during stress
b. Spacial and temporal patterns of their activation
c. Identification of neuronal hubs coupling cognitive-emotional neural networks with body effectors, like the hypothalamus-pituitary-adrenal (HPA) and the sympathetic-adrenomedullary axis (SAM) (Ulrich-Lai and Herman, 2009; Godoy et al., 2018).

The interaction of the heart and vessels with the central and peripheral nervous systems represents the major topic of the basic neuro-cardiovascular research, with the current aim of the field being to highlight the mechanisms of devastating effects of stress upon the cardiovascular system. In the review of Dampney the focus was on anatomical basis and functional role of the dorsolateral periaqueductal gray (dlPAG) in generating behavioral and autonomic responses to real and perceived emotional stressors. Central position and integratory function of this structure, between higher cortical regions (auditory, secondary visual, olphactory; medial prefrontal cortex -MPC, hypothalamus and lower brainstem structures), qualifies it as a crucial, emotional stress mediator neural hub. Though the review reports, parallel and comparative results obtained in

OPEN ACCESS

Edited and reviewed by:
Vaughan G. Macefield, Baker Heart and Diabetes Institute, Australia

***Correspondence:**
Tijana Bojić
tijanabojic@vinca.rs; bojictijana@gmail.com

Specialty section:
This article was submitted to Autonomic Neuroscience, a section of the journal Frontiers in Neuroscience

Received: *18 October 2018*
Accepted: *20 December 2018*
Published: *11 January 2019*

Citation:
Bojić T (2019) Editorial: Neurocardiovascular Diseases: New Aspects of the Old Issues. Front. Neurosci. 12:1032. doi: 10.3389/fnins.2018.01032

different species, the guiding theme is the enlightening of the understanding of the morpho-functional substrate affiliated with emotional stress response in humans. Crucial for understanding of the behavioral response to the perceived emotional stress are the inputs from the MPC to the dlPAG. The species-specific MPC subregion of the primate brain, the area 10 m, has the largest volume in humans with respect to other primate species. Allman and collaborates (Allman et al., 2002) describe this structure as a comparator of current and memorized behavioral states, and as a consequent decision-maker about future, potentially advantageous behavior. Its high activation and direct interface with dlPAG points to its special role in complex emotional responses, resulting from such comparisons. In conclusion, dlPAG is presented as integrator of the reactions of both the conscious and the unconscious to threatening stimuli with dependent autonomic networks (i.e., cardiorespiratory network) which support the behavioral response to stress and threatening stimuli. Future studies need to address the questions of chemical phenotyping of the dlPAG and other extensive stress mediating brain networks; the question of morpho-functional plasticity with respect to timing and duration of stress exposure; association of stress-induced morpho-functional changes of critical brain networks associated with different cardiovascular pathologies, as well as the question of genetic predisposition to developing of specific pathological entities like NCVD on the order of short or long time scales.

The impact of peripheral information on neural mediation of the cardiovascular (CVS) response can be crucial to the development of pathologies initiated by physical stressors like injury. When a physical stressor is recognized by the brainstem through pain, inflammation and other signals, both fast SAM and sluggish HPA responses are activated (Godoy et al., 2018). Up to the present it is not known what the role of pre-stimulus of the ANS regime is for development of the compartment syndrome. In this line, the study that investigated the effect of peripheral neural input to the heart rate regulating network by Watanabe and Hotta for the first time examined the specific cardiac autonomic changes induced by the bio-mechanical pressure stimulation of skeletal muscle. The authors identified sympathetic nervous system as the effector of changes in heart rate and blood pressure. In addition, it was demonstrated that the tonic level of pre-stimulus sympathetic neural activity determines the direction of induced heart rate changes and changes to blood pressure. This data could be of particular importance for understanding the compartment syndrome, the condition of muscle ischemic necrosis due to excessive intramuscular pressure and blood hypoperfusion. Future studies are necessary for revealing the site of the interaction of peripheral muscle pressure, stretching and contraction stimulus of the CVS neural networks (spinal or brainstem), and chemical phenotyping for the purpose of pharmacological intervention, and the role of tonic pre-stimulus sympathetic neural activity, for the development of the hemodynamic profiles that are susceptible to progression of the compartment syndrome.

Drug targeting of spinal and brainstem autonomic neural circuits causally involved in the genesis of different NCVD could result with long-awaited pharmacological solutions (Pierce et al., 2010; Zimmerman, 2011) for unexpected groups of pathophysiological entities, like compartment syndrome and neurogenic hypertension.

Neurogenic hypertension (NH) and vasovagal syncope (VVS) are NCV entities representing an unsolved pathophysiological puzzle. Novel data exists about the central molecular mechanisms regulating the tonic activity of preganglionic sympathetic neurons (Zimmerman, 2011), with antagonizing effects of the angiotensin II receptor and the MAS1 receptor mediated cascade offer a promising perspective for *in silico* strategies for investigation of NH. The Information Spectrum Method (ISM), a virtual spectroscopy method for studying the long-range interactions between biological macromolecules (Veljković et al., 1985), was previously successfully applied in study of HIV (Veljković et al., 2007), anthrax (Doliana et al., 2008) and the influenza virus (Perović et al., 2013). This widely accepted method (Veljković et al., 2011) was applied for the first time by Bojić et al. for the investigation of molecular targets of NH and VVS. As the result of this study, there have been proposed three novel therapeutic candidates for treatment of NH (apelin-28, apelin-31 and apelin-36) and also 12 repurposed antimuscarinic drugs potentially could be efficient in VVS treatment. Follow up with *in vitro* and *in vivo* studies will test the therapeutic capacities of drug candidates identified by ISM.

Baroreflex sensitivity (BRS) represents one of the central research topics of NCV physiology in the last few decades (Bojić, 2003; Silvani et al., 2003, 2005; Zoccoli et al., 2005; Bajić et al., 2010; Kapidžić et al., 2014; Platiša et al.) and pathophysiology (Parati et al., 2004; Glišić et al., 2016). BRS has been recognized as valuable prognostic factor for the outcome of different NCVD like myocardial infarction (La Rovere et al., 1998), heart failure (Libbus et al., 2016) and hypertension (Subha et al., 2016).The methodology of BRS estimation evolved from the classical methods of BRS estimation based on induced blood pressure changes (mechanical, pharmacological, etc.) with the related research activity achieving considerable levels since the late 1950's (Ernsting and Parry, 1957; Lamberti et al., 1968; Kirchheim, 1976), up to the BRS techniques for analysis of blood pressure and HP spontaneous fluctuations, which were introduced during the late 1980's (Fritsch et al., 1986; Bojić, 2003).

Major advantages of spontaneous fluctuations method are:

1. There is no administration of vasoactive compounds or external appliances that could influence the baroreceptor reflex by a direct action on receptor or effector sites (Coleman, 1980).
2. BRS is measured within physiological ABP ranges, allowing the computation of the gain at ABP close to the operating set point value, with minimal nonspecific effects from other efferent nerves.
3. The method does not arouse subjects or animals, thereby reducing stress induced effects.
4. In contrast with pharmacological or mechanical methods, they are suitable to assess the BRS over prolonged periods of time (Mancia and Mark, 1983; Oosting et al., 1997).

Still, time and frequency domain analysis of ANS activity in cardiovascular signals require certain conditions, with a stable baseline as one of the most important and most difficult states to obtain on long data segments. Li et al. propose a Multiple Trigonometric Regressive Spectral Analysis as a novel method for baroreflex sensibility (BRS) estimation for short (20–30's) time segments. The proposed method uses the oscillations of ABP and HP instead of their original values. The method provides reliable estimates of BRS without regard to posture change during the short data segments of 20–30 s in length. The proposed method solves several shortcomings of the sequence method by increasing the accuracy and validity of BRS estimation (Ziemssen et al., 2013), by providing a pure physiological spectrum of ABP and HP fluctuations and by reducing the influence of non-baroreflex drives. Further studies are necessary for evaluation of this promising method for studying BRS and other CVS indexes during the dynamic processes of daily life.

Atrial fibrillation (AF) presents NCVD events typically triggered by sympathovagal discharge (Goldstein, 2001), resulting in a dysfunctional atrial rhythm possessing as a consequence stroke, heart failure and risk of dementia. The electrical instability of atria, both focal and re-entrant activity, are progressive, self-feedback processes that evolve paroxysmal AF toward its persistent form. These classical experimental and clinical observations were without clear evidence-based pathophysiological explanation (Schotten et al., 2011). Ashton et al. propose the morpho-functional remodeling of ANS, both of its extrinsic (pre and post-ganglionic neurons) and intrinsic components (ganglionated plexus) that innervate the heart, as fundamentally contributing to positive feedback mechanism of AF. The ganglionated plexus, is the network of acetylcholine and other neurochemically distinct neurons, which play an important role in the modulation of cholinergic transmission and can be the site of maladaptive changes including arrhythmogenesis. These maladaptive changes could be based on both short-term and long-term plasticity mechanisms, with engagement of $5HT_3$ receptors, acetylcholine release and NO signaling in sympathetic neurons, and nicotinic expression, NO-cGMP signaling and NMDA receptor expression in vagal neurons. The neurochemical profile of synaptic plasticity of both sympathetic and vagal ganglionic transmission is promising target for future pharmacological studies aiming to intervene in AF that is morpho-functionally stabile as its persistent form. Traditional ECG and HRV linear and nonlinear indexes (Kikillus et al., 2007) could not give the answers about regulatory mechanisms of longer time scales and their differences between healthy and AF patients. Differences in nonlinear HP functional patterns between healthy and AF patients could be of major importance for the diagnosis and consequent therapy of AF forms that are of central neural origin (Andrade et al., 2014).

This was the focus of the research of Platiša et al., where novel Generalized Poincaré Plot (GPP) analysis of RR interval was proposed as a sensible method for distinction of AF from healthy subjects. GPP revealed for the first-time different system dynamics for large time scales in AF and healthy subjects. In the special case when GPP analysis was performed between 100 preceding and 100 following RR intervals, distinct regimes could be observed in healthy subjects, reflecting hypothetical different set-points of the blood pressure-heart rate baroreflex loop. In AF patients the GPP profile of RR intervals were scattered. This result suggests that AF patients have smaller adaptive capacity to internal and external perturbations. Four cluster profile of correlation maxima and their absolute values for different correlation scales were also different in healthy and AF patients. These results supported the hypothesis that regulatory regimes in healthy subjects operate in fine tuned superimposed regimes acting on different time scales-parasympathetic, sympathetic and slow regulatory mechanisms like thermoregulation, rennin-angiotensin-aldosterone-sodium system, hormones etc. The AF cluster pattern was highly distorted, shifted toward higher frequencies and with increased randomness. The new GPP methodological approach for detection and profiling cardiovascular regimes need future pharmacological evaluation and potential translatory development as a diagnostic tool for AF and other NCVD.

ANS is coupled directly to the cardiovascular system, but also through the interface of an energy regulating system. This is why an imbalance of energy regulation, as it is the case in obesity, often represents the first step, or the initial trigger of a neurally and metabolically mediated cascade of cardiovascular complications (hypertension, generalized atherosclerotic diathesis, dyslipidemia, diabetes mellitus type II). Digestion, absorption and neuroendocrine activity associated with the adoption of food has a direct effect on cardiovascular regulating centers (de Lartigue, 2014), pointing to the vagal subsystem as the potential target for neuromodulatory and pharmacological interventions in treatment of obesity, and, consequently, obesity related diseases. This important aspect of NCVD was reviewed by Guarino et al. Even though this comprehensive overview emphasizes the potential vagal route for neuromodulation and pharmacological intervention, the sympathetic route was also evaluated. This, more complex and differently structured subsystem presents itself as less understood and consequently is a significantly diminished path for obesity and related NCVD treatment. Its anatomical characteristics, i.e., approachability by external manipulations imply that the pharmacological approach should be investigated in the future, while the vagal route offers a good basis for both neuromodulatory and pharmacological strategies.. Vagal modulation, in specific transcutaneous auricular vagus nerve stimulation is a promising method for body weight reduction in obese patients, also resulting with significant improvements of cardiometabolic profile. Sympathetic modulation, with inconsistent results on body weight reduction and partial cardiometabolic effects, from a results prospective, is a less promising strategy.

Hyperadrenergic state is the classical hallmark of heart failure (HF), the clinical endpoint of the number of CVD (Marwick, 2018). Toschi-Dias et al. details elaborates the neurohumoral responses to hemodynamic stress, the common initial event of the HF hyperadrenergic state. The HF hyperadrenergic state, associated with different reductions of left ventricular ejection fraction (LVEF: preserved-p, mid-range-mr, reduced-r) is also associated with different morpho-functional remodeling of left

ventricle, specific for its ejection functioning. This interesting association, widely recognized as a valuable prognostic and diagnostic parameter (Marwick, 2018) seeks for a deeper genetic and/or environmental influence studies, due to the hypothesis that different pathophysiological patterns might sculpture different EF phenotypes in HF. Vascular remodeling in HF further complicates an ANS functional profile, pushing it toward the maintenance and/or enhancement of hyperadrenergic state. Arterial baroreceptor (ABR) dysfunction, mostly due to the decrease of large vessel elasticity following chronic hypertension, distinguishes itself as an important factor in generation of cardiac diastolic dysfunction. ABR seem to play dominant role in sustaining hyperadrenergic state both in HFrEF (low stroke volume) and HFpEF (increased vascular stiffness), by different mechanisms. This issue necessitates future investigations of the hierarchical (in sense of absolute and relative quantitative contribution to the hyperadrenergic state) and temporal order of cardiovascular reflexes engaged in HFmrEF and HFpEF. It is reasonable to hypothesize that different quantitative and temporal patterns of cardiovascular reflex response result with different HFEF phenotypes. Cardiopulmonary reflex (CPR) regulates the state of systemic blood volume by (a) sympathetic modulation (low intensity changes), (b) release of atrial Na-uretic peptide, and (c) by strengthening and enhancing ABR action at high intensity changes. In HFrEF patients, no reduction of sympathetic outflow is obtained by CPR unloading. Participation of cardiac sympathetic afferent reflex and arterial chemoreflex was thoroughly evidenced in the hyperadrenergic state of HFrEF, while their role in HFpEF and HFmrEF needs future evaluation.

A number of surgical and pharmacological interventions manifest NCV disturbances as an important caveat. For that reason, detailed and comprehensive NCV evaluation becomes a constituent part of pre-interventional evaluation of the patient and postintervention follow up. Coronary artery bypass graft (CABG) surgery can induce disbalance of sympathovagal ratio and, consequently respiratory depression, approximately 5 days after the surgery (Aronson et al., 2011; Pantoni et al., 2014; Patron et al., 2014; Ksela et al., 2015). In order to identify a prognostic marker, Costa et al. studied the prognostic significance of perioperative arterial blood pressure (ABP) variability for the occurrence of respiratory depression following CABG. The finding of Costa et al. that ABP variability parameters have prognostic value for respiratory depression has both pathophysiological and clinical significance.

Deep brain stimulation (DBS) represents an invasive, frequent and developing intervention for the treatment of a spectrum of neurological diseases, with Parkinson's disease (PD) as the most common. As reported by Chowdhury et al., hemodynamic perturbations, like hypertension, hypotension, bradycardia, tachycardia and arrhythmia are frequent side-effects of this procedure in PD patients. They can be the consequence of (a) the independent or accompanying autonomic co-morbidity of the main PD pathological process, (b) the procedures associated to the surgery (semi-sitting position, anesthetics, sedation, stress, electrode battery placement and the stimulation of brain nuclei itself). Significant predictor potential has only pre-operative ABP, with diastolic BP as the marker most associated with hemodynamic event. Hypertension, predisposing factor of cerebral hemorrhage was noted during electrode placement and nuclei stimulation. A prospective study is needed for detailed hemodynamic evaluation (a) during the DBS surgery and the estimation of (b) pre- and (c) post-operative autonomic status of the PD patients. This approach would potentially change protocols of presurgical evaluation and postsurgical treatment of PD patients subjected to DBS. After heart transplantation, the autonomic reinnervation of the transplanted heart has important consequences on its reactivity and hemodynamical adaptability (exercise capacity, coronary blood flow regulation (Grupper et al., 2018). Wdowczyk et al. present a novel tool, Transition Networks, in the case report that has potential for distinguishing HRV increase due to reinnervation. Further stratified longitudinal clinical studies are needed for evaluation of this method. However, the capacity of the method to offer an insight into dynamical inter-beat dependences of RR intervals enounce better comprehension of the transplant functional adoption into CVS neural network.

Pharmacological interventions in neuropsychiatric patients often disturb autonomic balance. Li et.al. applied their method (long-term Multiple Trigonometric Spectral Analysis, Li et al.) combined with conventional liner parameters of HRV as a tool for predicting fingolimod-induced bradycardia in patients with multiple sclerosis (MS). On the basis of their analysis they report an increased pre medication parasympathetic activity as the predisposing factor for fingolimod induced bradycardia, with pretreatment HR as the only predicting factor. Yuen et al. performed the meta-analysis on clozapine induced autonomic dysfunction in patients with schizophrenia. They conclude that the most frequent complications were myocarditis, orthostatic hypotension and tachycardia, prevalently due to sympathetic overactivity. This report emphasizes the need for introduction of post-medication NCV evaluation autonomic tests for prevention and therapeutic coping with clozapine-induced side-effects. In accordance with Li et al., an intuitive direction for future investigations would be the identification of NCV predicting parameters for clozapine induced autonomic side effects.

Cerebral blood flow (CBF) is an issue of the upmost importance for understanding the NCVD, from two aspects:

a. A growing corpus of data supports the standpoint that besides the cerebral autoregulation (Silvani et al., 2004; Zoccoli et al., 2005), sympathetic (Cassaglia et al., 2008; ter Laan et al., 2013; Frederiksen et al., 2017), parasympathetic (Purkayastha et al., 2018) and sensory innervations (Branston et al., 1995) functionally participate in the regulation of CBF.
b. Compromise of CBF, especially in the neonates, can cause serious, life threatening autonomic dysfunctions (Silvani et al., 2004; Metzler et al., 2017; Campbell et al., 2018).

Glutamate is considered to be the neurochemical initiator and executor of brain injury in hypoxic-ischemic brain disorder

(HIBD). Dang et al. report "two phase" change of basal ganglia glutamate level after HIBD, that is significantly and negatively correlated to the brain perfusion fraction. Even though this association is suggestive for negative electrochemical coupling of cerebral activity (glutamate) and brain perfusion in HIBD, further investigations are necessary for elucidating the mechanism(s) of brain activity-blood flow coupling in HIBD. Special emphasis should be on the role of sympathetic nervous system in cerebral activity-blood flow regulation in HIBD (Ainslie, 2008; Cassaglia et al., 2008; Edvinsson, 2008; Immink and Passier, 2008; Levine and Zhang, 2008; Ogoh, 2008; Paulson and Knudsen, 2008; Prakash, 2008; Visocchi, 2008; Yildiz, 2008; ter Laan et al., 2013). An important protective effect of artesunate against necrosis in cerebral infarction was reported by Shao et al., suggesting an autophagy as the most probable mechanism. Potential treatment by artesunate could have beneficiary effect for autonomic dysfunction, an important caveat of neonatal hypoxic-ischemic encephalopathy (Metzler et al., 2017; Campbell et al., 2018).

In conclusion, the presented physiological, methodological and pathophysiological aspects of NCVD point to the importance of consideration of NCVD from integrative point of view and as a constitutive part of different pathophysiological entities. Application of novel mathematical methods for molecular targeting and systemic characterizing of NCVD enounce promising lines of future research in the translational science. Neurocardiovascular side-effects of surgical and pharmacological interventions emphasize the importance of ANS evaluation before and after the intervention as the routine procedure in the clinical work. Finally, an intriguing role of autonomic networks, traditionally considered the cardiovascular neural subsystem, in the regulation of cerebral blood flow both in physiological and pathophysiological conditions is about to open a novel aspect of cerebro-cardiovascular integration.

AUTHOR CONTRIBUTIONS

The author confirms being the sole contributor of this work and has approved it for publication.

ACKNOWLEDGMENTS

This work was supported by Ministry of Education, Science and Technological Development of the Republic of Serbia, grant number III 41028.

REFERENCES

Acevedo, E. O., Webb, H. E., Weldy, M. L., Fabianke, E. C., Orndorff, G. R., and Starks, M. A. (2006). Cardiorespiratory responses of Hi Fit and Low Fit subjects to mental challenge during exercise. *Int. J. Sports Med.* 27, 1013–1022. doi: 10.1055/s-2006-923902

Ainslie, P. N. (2008). Comments on Point: Counterpoint: Sympathetic activity does/does not influence cerebral blood flow. *J. Appl. Physiol. (1985)* 105:1370. doi: 10.1152/japplphysiol.90597.2008a

Allman, J., Hakeem, A., and Watson, K. (2002). Two phylogenetic specializations in the human brain. *Neuroscientist* 8, 335–346. doi: 10.1177/107385840200800409

Andrade, J., Khairy, P., Dobrev, D., and Nattel, S. (2014). The clinical profile and pathophysiology of atrial fibrillation: relationships among clinical features, epidemiology, and mechanisms. *Circ. Res.* 114, 1453–1468. doi: 10.1161/CIRCRESAHA.114.303211

Aronson, S., Dyke, C. M., Levy, J. H., Cheung, A. T., Lumb, P. D., Avery, E. G., et al. (2011). Does perioperative systolic blood pressure variability predict mortality after cardiac surgery? An exploratory analysis of the ECLIPSE trials. *Anesth. Analg.* 113, 19–30. doi: 10.1213/ANE.0b013e3182 0f9231

Bajić, D., Lončar-Turukalo, T., Stojičić, S., Šarenac, O., Bojić, T., Murphy, D., et al. (2010). Temporal analysis of the spontaneous baroreceptor reflex during mild emotional stress in the rat. *Stress* 13, 142–154. doi: 10.3109/1025389090 3089842

Bojić, T. (2003). *Mechanisms of Neural Control and Effects of Acoustic Stimulation on Cardiovascular System During the Wake-Sleep Cycle*. Ph.D. Experimental, Alma Mater Università di Bologna.

Branston, N. M., Umemura, A., and Koshy, A. (1995). Contribution of cerebrovascular parasympathetic and sensory innervation to the short-term control of blood flow in rat cerebral cortex. *J. Cereb. Blood Flow Metab.* 15, 525–531. doi: 10.1038/jcbfm.1995.65

Campbell, H., Govindan, R. B., Kota, S., Al-Shargabi, T., Metzler, M., Andescavage, N., et al. (2018). Autonomic dysfunction in neonates with hypoxic ischemic encephalopathy undergoing therapeutic hypothermia impairs physiological responses to routine care events. *J. Pediatr.* 196, 38–44. doi: 10.1016/j.jpeds.2017.12.071

Cassaglia, P. A., Griffiths, R. I., and Walker, A. M. (2008). Sympathetic withdrawal augments cerebral blood flow during acute hypercapnia in sleeping lambs. *Sleep* 31, 1729–1734. doi: 10.1093/sleep/31.12.1729

Coleman, T. G. (1980). Arterial baroreflex control of heart rate in the conscious rat. *Am. J. Physiol.* 238, H515–520. doi: 10.1152/ajpheart.1980.238.4.H515

de Lartigue, G. (2014). Putative roles of neuropeptides in vagal afferent signaling. *Physiol. Behav.* 136, 155–169. doi: 10.1016/j.physbeh.2014.03.011

Doliana, R., Veljković, V., Prljić, J., Veljković, N., De Lorenzo, E., Mongiat, M., et al. (2008). EMILINs interact with anthrax protective antigen and inhibit toxin action *in vitro*. *Matrix Biol.* 27, 96–106. doi: 10.1016/j.matbio.2007.09.008

Du, D., Hu, L., Wu, J., Wu, Q., Cheng, W., Guo, Y., et al. (2017). Neuroinflammation contributes to autophagy flux blockage in the neurons of rostral ventrolateral medulla in stress-induced hypertension rats. *J. Neuroinflammation* 14:169. doi: 10.1186/s12974-017-0942-2

Edvinsson, L. (2008). Comments on point:counterpoint: sympathetic activity does/does not influence cerebral blood flow. sympathetic nerves influence the cerebral circulation. *J. Appl. Physiol. (1985)* 105, 1370–1371.

Ernsting, J., and Parry, D. J. (1957). Some observations on the effect of stimulating the strech receptors in the carotid artery of men. *J. Physiol. (Lond).* 137, 45–46.

Frederiksen, S. D., Haanes, K. A., Warfvinge, K., and Edvinsson, L. (2017). Perivascular neurotransmitters: regulation of cerebral blood flow and role in primary headaches. *J. Cereb. Blood Flow Metab.* 1:271678X17747188. doi: 10.1177/0271678X17747188

Fritsch, J. M., Eckberg, D. L., Graves, L. D., and Wallin, B. G. (1986). Arterial pressure ramps provoke linear increases of heart period in humans. *Am. J. Physiol.* 251(6 Pt 2), R1086–R1090. doi: 10.1152/ajpregu.1986.251.6.R1086

Glišić, S., Cavanaugh, D. P., Chittur, K. K., Senćanski, M., Perović, V., and Bojić, T. (2016). Common molecular mechanism of the hepatic lesion and the cardiac parasympathetic regulation in chronic hepatitis C infection: a critical role for the muscarinic receptor type 3. *BMC Bioinformatics* 17:139. doi: 10.1186/s12859-016-0988-7

Godoy, L. D., Rossignoli, M. T., Delfino-Pereira, P., Garcia-Cairasco, N., and de Lima Umeoka, E. H. (2018). A comprehensive overview on stress neurobiology:

basic concepts and clinical implications. *Front. Behav. Neurosci.* 12:127. doi: 10.3389/fnbeh.2018.00127

Goldstein, D. (2001). *The Autonomic Nervous System in Health and Disease. 1st Edn.* New York, NY: Marcel Dekker, Inc.

Grupper, A., Gewirtz, H., and Kushwaha, S. (2018). Reinnervation post-heart transplantation. *Eur. Heart J.* 39, 1799–1806. doi: 10.1093/eurheartj/ehw604

Immink, R. V., and Passier, R. H. (2008). Comments on point:counterpoint: sympathetic activity does/does not influence cerebral blood flow. the sympathetic "knock-out" model. *J. Appl. Physiol. (1985)* 105, 1372–1373.

Investigators, W. M. P. P. (1988). The World Health Organization MONICA Project (monitoring trends and determinants in cardiovascular disease): a major international collaboration. *J. Clin. Epidemiol.* 41, 105–114. doi: 10.1016/0895-4356(88)90084-4

Kapidžić, A., Platiša, M. M., Bojić, T., and Kalauzi, A. (2014). RR interval-respiratory signal waveform modeling in human slow paced and spontaneous breathing. *Respir. Physiol. Neurobiol.* 203, 51–59. doi: 10.1016/j.resp.2014.08.004

Kikillus, N., Hammer, G., Wieland, S., and Bolz, A. (2007). Algorithm for identifying patients with paroxysmal atrial fibrillation without appearance on the ECG. *Conf. Proc. IEEE Eng. Med. Biol. Soc.* 2007, 275–278. doi: 10.1109/IEMBS.2007.4352277

Kirchheim, H. R. (1976). Systemic arterial baroreceptor reflexes. *Physiol. Rev.* 56, 100–177. doi: 10.1152/physrev.1976.56.1.100

Ksela, J., Avbelj, V., and Kalisnik, J. M. (2015). Multifractality in heartbeat dynamics in patients undergoing beating-heart myocardial revascularization. *Comput. Biol. Med.* 60, 66–73. doi: 10.1016/j.compbiomed.2015.02.012

La Rovere, M. T., Bigger, J. T. Jr., Marcus, F. I., Mortara, A., and Schwartz, P. J. (1998). Baroreflex sensitivity and heart-rate variability in prediction of total cardiac mortality after myocardial infarction. ATRAMI (Autonomic Tone and Reflexes After Myocardial Infarction) Investigators. *Lancet* 351, 478–484. doi: 10.1016/S0140-6736(97)11144-8

Lamberti, J. J. Jr., Urquhart, J., and Siewers, R. D. (1968). Observations on the regulation of arterial blood pressure in unanesthetized dogs. *Circ. Res.* 23, 415–428. doi: 10.1161/01.RES.23.3.415

Levine, B. D., and Zhang, R. (2008). Comments on point:counterpoint: sympathetic activity does/does not influence cerebral blood flow. Autonomic control of the cerebral circulation is most important for dynamic cerebral autoregulation. *J. Appl. Physiol. (1985)* 105, 1369–1373. doi: 10.1152/japplphysiol.zdg-8199.pcpcomm.2008

Libbus, I., Nearing, B. D., Amurthur, B., KenKnight, B. H., and Verrier, R. L. (2016). Autonomic regulation therapy suppresses quantitative T-wave alternans and improves baroreflex sensitivity in patients with heart failure enrolled in the ANTHEM-HF study. *Heart Rhythm* 13, 721–728. doi: 10.1016/j.hrthm.2015.11.030

Mancia, G., and Mark, A. L. (1983). "Arterial baroreflex in humans," in *Handbook of Physiology, Section 2: The Cardiovascular System*, eds J. T. Shepherd and F. M. Abboud (Bethesda, MD: American Physiological Society), 755–793.

Marwick, T. H. (2018). Ejection fraction pros and cons: JACC state-of-the-art review. *J. Am. Coll. Cardiol.* 72, 2360–2379. doi: 10.1016/j.jacc.2018.08.2162

Metzler, M., Govindan, R., Al-Shargabi, T., Vezina, G., Andescavage, N., Wang, Y., et al. (2017). Pattern of brain injury and depressed heart rate variability in newborns with hypoxic ischemic encephalopathy. *Pediatr. Res.* 82, 438–443. doi: 10.1038/pr.2017.94

Ogoh, S. (2008). Comments on Point:Counterpoint: Sympathetic activity does/does not influence cerebral blood flow. Autonomic nervous system influences dynamic cerebral blood flow. *J. Appl. Physiol. (1985)* 105:1370.

Oosting, J., Struijker-Boudier, H. A., and Janssen, B. J. (1997). Validation of a continuous baroreceptor reflex sensitivity index calculated from spontaneous fluctuations of blood pressure and pulse interval in rats. *J. Hypertens.* 15, 391–399. doi: 10.1097/00004872-199715040-00010

Pantoni, C. B., Mendes, R. G., Di Thommazo-Luporini, L., Simoes, R. P., Amaral-Neto, O., Arena, R., et al. (2014). Recovery of linear and nonlinear heart rate dynamics after coronary artery bypass grafting surgery. *Clin. Physiol. Funct. Imaging* 34, 449–456. doi: 10.1111/cpf.12115

Parati, G., Di Rienzo, M., Castiglioni, P., Bouhaddi, M., Cerutti, C., Cividjian, A., et al. (2004). Assessing the sensitivity of spontaneous baroreflex control of the heart: deeper insight into complex physiology. *Hypertension* 43, e32–e34; author reply e32-34. doi: 10.1161/01.HYP.0000126689.12940.cd

Patron, E., Messerotti Benvenuti, S., and Palomba, D. (2014). Preoperative and perioperative predictors of reactive and persistent depression after cardiac surgery: a three-month follow-up study. *Psychosomatics* 55, 261–271. doi: 10.1016/j.psym.2013.12.011

Paulson, O. B., and Knudsen, G. M. (2008). Comments on point:counterpoint: sympathetic activity does/does not influence cerebral blood flow. Role of a rudimentary sympathetic nervous system on cerebral blood flow. *J. Appl. Physiol. (1985)* 105, 1371–1372.

Perović, V. R., Muller, C. P., Niman, H. L., Veljković, N., Dietrich, U., Tošić, D. D., et al. (2013). Novel phylogenetic algorithm to monitor human tropism in Egyptian H5N1-HPAIV reveals evolution toward efficient human-to-human transmission. *PLoS ONE* 8:e61572. doi: 10.1371/journal.pone.0061572

Pierce, M. L., Deuchars, J., and Deuchars, S. A. (2010). Spontaneous rhythmogenic capabilities of sympathetic neuronal assemblies in the rat spinal cord slice. *Neuroscience* 170, 827–838. doi: 10.1016/j.neuroscience.2010.07.007

Prakash, E. S. (2008). Comments on Point:Counterpoint: Sympathetic activity does/does not influence cerebral blood flow. When noradrenergic restraint of cerebral blood flow makes homeostatic sense. *J. Appl. Physiol.* (1985) 105:1373.

Purkayastha, S., Maffuid, K., Zhu, X., Zhang, R., and Raven, P. B. (2018). The influence of the carotid baroreflex on dynamic regulation of cerebral blood flow and cerebral tissue oxygenation in humans at rest and during exercise. *Eur. J. Appl. Physiol.* 118, 959–969. doi: 10.1007/s00421-018-3831-1

Schotten, U., Verheule, S., Kirchhof, P., and Goette, A. (2011). Pathophysiological mechanisms of atrial fibrillation: a translational appraisal. *Physiol. Rev.* 91, 265–325. doi: 10.1152/physrev.00031.2009

Silvani, A., Asti, V., Bojić, T., Ferrari, V., Franzini, C., Lenzi, P., et al. (2005). Sleep-dependent changes in the coupling between heart period and arterial pressure in newborn lambs. *Pediatr. Res.* 57, 108–114. doi: 10.1203/01.PDR.0000148065.32413.B0

Silvani, A., Bojić, T., Cianci, T., Franzini, C., Lodi, C. A., Predieri, S., et al. (2003). Effects of acoustic stimulation on cardiovascular regulation during sleep. *Sleep* 26, 201–205. doi: 10.1093/sleep/26.2.201

Silvani, A., Bojić, T., Franzini, C., Lenzi, P., Walker, A. M., Grant, D. A., et al. (2004). Sleep-related changes in the regulation of cerebral blood flow in newborn lambs. *Sleep* 27, 36–41. doi: 10.1093/sleep/27.1.36

Strickland, O. L., Giger, J. N., Nelson, M. A., and Davis, C. M. (2007). The relationships among stress, coping, social support, and weight class in premenopausal African American women at risk for coronary heart disease. *J. Cardiovasc. Nurs.* 22, 272–278. doi: 10.1097/01.JCN.0000278964.05748.d8

Subha, M., Pal, P., Pal, G. K., Habeebullah, S., Adithan, C., and Sridhar, M. G. (2016). Decreased baroreflex sensitivity is linked to sympathovagal imbalance, low-grade inflammation, and oxidative stress in pregnancy-induced hypertension. *Clin. Exp. Hypertens.* 38, 666–672. doi: 10.1080/10641963.2016.1200596

ter Laan, M., van Dijk, J. M., Elting, J. W., Staal, M. J., and Absalom, A. R. (2013). Sympathetic regulation of cerebral blood flow in humans: a review. *Br. J. Anaesth.* 111, 361–367. doi: 10.1093/bja/aet122

Ulrich-Lai, Y. M., and Herman, J. P. (2009). Neural regulation of endocrine and autonomic stress responses. *Nat. Rev. Neurosci.* 10, 397–409. doi: 10.1038/nrn2647

Veljković, N., Glišić, S., Perović, V. R., and Veljković, V. (2011). The role of long-range intermolecular interactions in discovery of new drugs. *Expert Opin. Drug Discov.* 6, 1263–1270. doi: 10.1517/17460441.2012.638280

Veljković, V., Cosić, I., Dimitrijević, B., and Lalović, D. (1985). Is it possible to analyze DNA and protein sequences by the methods of digital signal processing? *IEEE Trans. Biomed. Eng.* 32, 337–341. doi: 10.1109/TBME.1985.325549

Veljković, V., Mouscadet, J. F., Veljković, N., Glišić, S., and Debyser, Z. (2007). Simple criterion for selection of flavonoid compounds with anti-HIV activity. *Bioorg. Med. Chem. Lett.* 17, 1226–1232. doi: 10.1016/j.bmcl.2006.12.029

Visocchi, M. (2008). Comments on point:counterpoint: sympathetic activity does/does not influence cerebral blood flow. sympathetic activity does influence cerebral blood flow. *J. Appl. Physiol. (1985)* 105:1369.

Webb, H. E., Rosalky, D. A., McAllister, M. J., Acevedo, E. O., and Kamimori, G. H. (2017). Aerobic fitness impacts sympathoadrenal axis responses to concurrent challenges. *Eur. J. Appl. Physiol.* 117, 301–313. doi: 10.1007/s00421-016-3519-3

Yildiz, M. (2008). Comments on point:counterpoint: sympathetic activity does/does not influence cerebral blood flow. *J. Appl. Physiol. (1985)* 105:1371.

Ziemssen, T., Reimann, M., Gasch, J., and Rudiger, H. (2013). Trigonometric regressive spectral analysis: an innovative tool for evaluating the autonomic nervous system. *J. Neural. Transm.* 120 (Suppl. 1), S27–S33. doi: 10.1007/s00702-013-1054-5

Zimmerman, M. C. (2011). Angiotensin II and angiotensin-1-7 redox signaling in the central nervous system. *Curr. Opin. Pharmacol.* 11, 138–143. doi: 10.1016/j.coph.2011.01.001

Zoccoli, G., Bojić, T., and Franzini, C. (2005). "Regulation of cerebral circulation during sleep," in *The Physiological Nature of Sleep, 1st Edn*, eds P. L. Parmeggiani and R. Velluti (London: Imperial College Press), 351–369. doi: 10.1142/9781860947186_0016

Conflict of Interest Statement: The author declares that the research was conducted in the absence of any commercial or financial relationships that could be construed as a potential conflict of interest.

frontiers in Neuroscience

REVIEW
published: 24 May 2018
doi: 10.3389/fnins.2018.00343

Emotion and the Cardiovascular System: Postulated Role of Inputs From the Medial Prefrontal Cortex to the Dorsolateral Periaqueductal Gray

*Roger Dampney**

School of Medical Sciences (Physiology) and Bosch Institute, University of Sydney, Sydney, NSW, Australia

The midbrain periaqueductal gray (PAG) plays a major role in generating different types of behavioral responses to emotional stressors. This review focuses on the role of the dorsolateral (dl) portion of the PAG, which on the basis of anatomical and functional studies, appears to have a unique and distinctive role in generating behavioral, cardiovascular and respiratory responses to real and perceived emotional stressors. In particular, the dlPAG, but not other parts of the PAG, receives direct inputs from the primary auditory cortex and from the secondary visual cortex. In addition, there are strong direct inputs to the dlPAG, but not other parts of the PAG, from regions within the medial prefrontal cortex that in primates correspond to cortical areas 10 m, 25 and 32. I first summarise the evidence that the inputs to the dlPAG arising from visual, auditory and olfactory signals trigger defensive behavioral responses supported by appropriate cardiovascular and respiratory effects, when such signals indicate the presence of a real external threat, such as the presence of a predator. I then consider the functional roles of the direct inputs from the medial prefrontal cortex, and propose the hypothesis that these inputs are activated by perceived threats, that are generated as a consequence of complex cognitive processes. I further propose that the inputs from areas 10 m, 25 and 32 are activated under different circumstances. The input from cortical area 10 m is of special interest, because this cortical area exists only in primates and is much larger in the brain of humans than in all other primates.

Keywords: periaqueductal gray, medial prefrontal cortex, Brodmann cortical area 10, cardiovascular regulation, respiratory activity, defensive behavior, cognition

OPEN ACCESS

Edited by:
Tijana Bojić,
University of Belgrade, Serbia

Reviewed by:
Anthony E. Pickering,
University of Bristol, United Kingdom
De-Pei Li,
University of Texas MD Anderson Cancer Center, United States

***Correspondence:**
Roger Dampney
roger.dampney@sydney.edu.au

Specialty section:
This article was submitted to Autonomic Neuroscience, a section of the journal Frontiers in Neuroscience

Received: *29 December 2017*
Accepted: *02 May 2018*
Published: *24 May 2018*

Citation:
Dampney R (2018) Emotion and the Cardiovascular System: Postulated Role of Inputs From the Medial Prefrontal Cortex to the Dorsolateral Periaqueductal Gray. Front. Neurosci. 12:343. doi: 10.3389/fnins.2018.00343

INTRODUCTION

An animal's survival depends upon being able to respond appropriately to stimuli that may signal a threat, such as the presence of a predator. In the course of evolution, several different defense systems have evolved. One of the most phylogenetically old systems is subserved by neural pathways within the basal ganglia and midbrain colliculi (homologous to the optic tectum in fish, amphibian, reptiles and birds). This system, which is not dependent on inputs from the cortex and thus appears to be subconscious, produces highly coordinated and stereotyped behavioral responses to visual, auditory and somatosensory inputs, accompanied by appropriate cardiovascular and respiratory

effects (Dean et al., 1989; Dampney, 2015, 2016; Müller-Ribeiro et al., 2016). The particular type of stereotyped response that is evoked (e.g., orienting, pursuit or escape) depends upon the precise pattern of inputs that trigger the response. This type of defense response is advantageous in a situation where immediate action is required. On the other hand, such responses lack the flexibility that would be essential in a situation where the threat is sustained and changing—in that case, cognitive appraisal of the threat is required to ensure that the response is most appropriate to the particular situation.

Apart from the basal ganglia and colliculi, many other brain regions also play important roles in generating responses to threatening stimuli in mammals. These regions include the medial prefrontal cortex, amygdala, various hypothalamic nuclei, and the midbrain periaqueductal gray (PAG) (Dampney, 2015). The specific roles of these different nuclei in generating behavioral and physiological responses to threatening stimuli have been discussed in a number of recent reviews (Dampney et al., 2013; Fontes et al., 2014; Carr, 2015; Dampney, 2015; LeDoux and Pine, 2016; Myers, 2017). This review, however, shall focus on the role of the dorsolateral (dl) portion of the PAG, which, as I shall explain in the following sections, appears to be a critical component of the central pathways subserving responses to inputs arising from the medial prefrontal cortex.

ANATOMICAL AND FUNCTIONAL PROPERTIES OF THE dlPAG

The dlPAG is one of four longitudinal columns within the PAG, the others being the dorsomedial (dmPAG), lateral (lPAG), and ventrolateral (vlPAG) columns. These different components of the PAG differ greatly with respect to their functional properties, anatomical connections and chemical properties (Carrive, 1993; Bandler and Shipley, 1994; Bandler et al., 2000; Keay and Bandler, 2001; Vianna and Brandão, 2003; Dampney et al., 2013). Activation of neurons in the lPAG and dlPAG generate active defensive behavioral responses, which are characterized by increased somatomotor activity, and cardiovascular and respiratory changes that have the effect of increasing the blood flow and supply of oxygen to active skeletal muscles. Such a response can be triggered by an escapable stimulus, such as the presence of a predator or cutaneous pain (Bandler et al., 2000; Keay and Bandler, 2001). In contrast, the vlPAG is critical for the expression of passive behavioral responses, which are characterized by decreased somatomotor activity, accompanied by decreased arterial pressure and heart rate. Such responses are believed to be triggered by inescapable stimuli, such as hemorrhage or visceral pain (Bandler et al., 2000; Keay and Bandler, 2001).

The functional differences between the different subdivisions of the PAG are also reflected by their anatomical connections (**Figure 1**). In particular, the dlPAG is distinctly different from the other PAG subdivisions with respect to both its afferent inputs and efferent outputs (Dampney et al., 2013). Studies in the rat have shown that the dlPAG, but not the other PAG subdivisions, receives direct inputs from the primary auditory cortex and from the secondary visual cortex (Benzinger and Massopust, 1983; Newman et al., 1989) as well as from the superior colliculus (Rhoades et al., 1989), which in turn receives both visual and auditory inputs (May, 2006). There are also inputs to the dlPAG but not other PAG subdivisions from the nucleus praepositus hypoglossi and the periparabigeminal nucleus in the lower brainstem (Klop et al., 2005, 2006). Both of these nuclei have a role in the control of eye movements, and it has been suggested that inputs from these nuclei allow neurons in the PAG to distinguish between visual signals generated by objects that have moved into the visual field from visual signals caused only by eye movements (Klop et al., 2006).

A very dense input to the dlPAG, but not other PAG subdivisions arises from the dorsal premamillary nucleus (PMD) in the hypothalamus, especially its ventrolateral portion (Motta et al., 2009). The ventrolateral PMD receives inputs from neurons within the medial and basomedial nuclei in the amygdala, relayed via the hypothalamic ventromedial nucleus (Motta et al., 2009). The projections from these amygdaloid nuclei to the dlPAG are believed to convey signals relating to the presence of a predator (Motta et al., 2009). Consistent with this, blockade of neurons in the PMD reduces the behavioral defensive response to a predator or predator odor alone (Markham et al., 2004; Blanchard et al., 2005; Motta et al., 2009).

There are no direct inputs to the dlPAG from any part of the spinal cord, whereas all other PAG subdivisions receive direct inputs from cervical, thoracic and lumbar segments of the spinal cord (Keay and Bandler, 2001; Dampney et al., 2013). Similarly, the lPAG and vlPAG, but not the dlPAG, receive inputs from the spinal trigeminal nucleus and nucleus of the solitary tract (NTS), respectively (Keay and Bandler, 2001; Dampney et al., 2013). In summary, the dlPAG, but not other parts of the PAG, receives direct inputs that convey visual, auditory and olfactory signals, but do not receive direct inputs conveying signals from visceral or somatic receptors. In contrast, the lPAG and vlPAG both receive major inputs from visceral and somatic receptors, but not direct inputs from brain regions that receive visual, auditory or olfactory inputs.

Consistent with the fact that the dlPAG receives visual, auditory and olfactory signals, exposure to a cat generates strong c-fos expression in the dlPAG, but not in other PAG subdivisions (Canteras and Goto, 1999). Furthermore, in conscious rats the defensive behavioral responses of freezing or flight is evoked with very low intensity stimulation of the dlPAG, whereas such stimulation is ineffective in other parts of the PAG (Bittencourt et al., 2004). Finally, in anesthetized rats, stimulation of the dlPAG evokes increases in sympathetic activity and respiration (Iigaya et al., 2010). Thus, the available anatomical and functional evidence indicates that the dlPAG is a major component of the central pathways that generate behavioral defensive responses to an external perceived threat, supported by appropriate autonomic and respiratory effects.

In contrast to all other PAG regions, the dlPAG is notable for the absence of labeled neurons following injections of

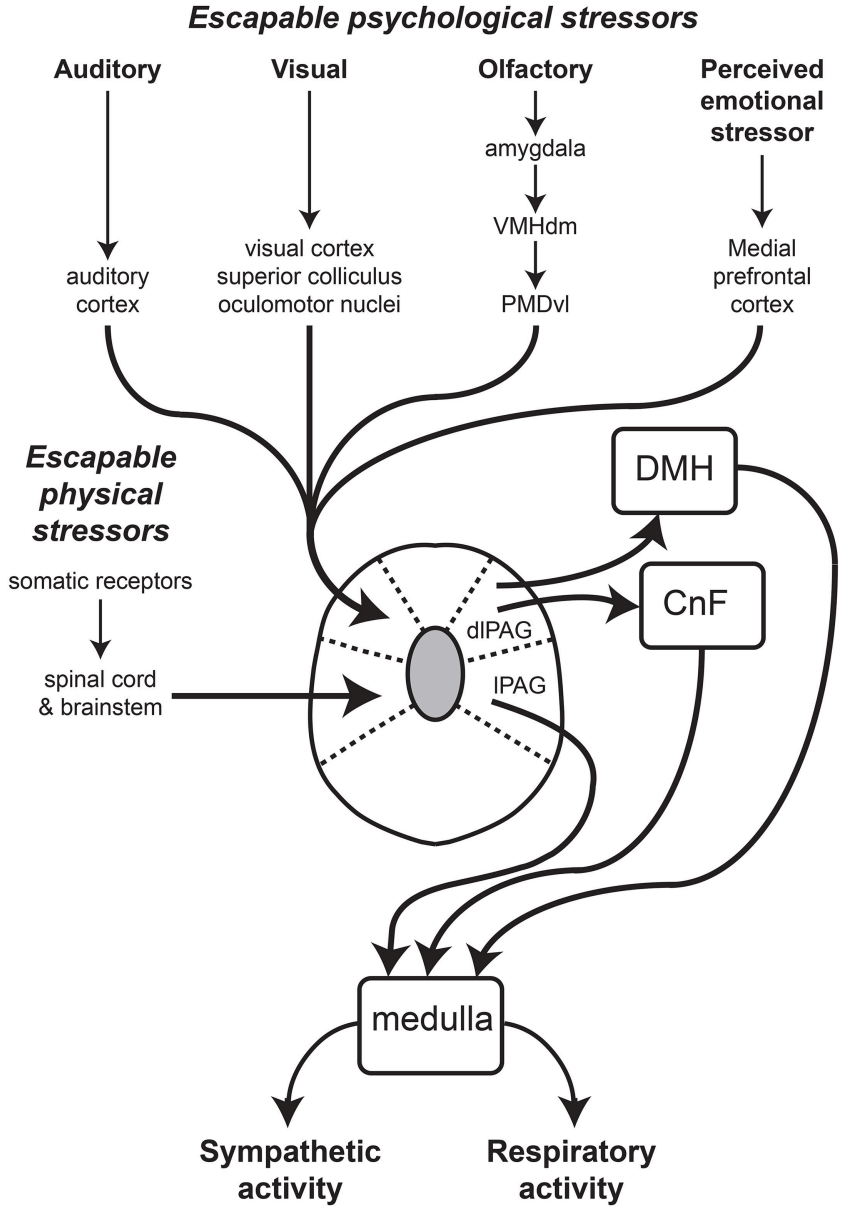

FIGURE 1 | Schematic diagram showing major inputs to the dlPAG and the proposed output pathways subserving the co-ordinated changes in sympathetic vasomotor and respiratory activity regulated by the dlPAG. The lines with arrows indicate connections, that could be either direct (monosynaptic) or indirect (polysynaptic). Other abbreviations: CnF, cuneiform nucleus; DMH, dorsomedial hypothalamus; lPAG, lateral part of the periaqueductal gray. Modified from Dampney et al. (2013).

retrogradely transported tracers into the medulla or spinal cord (Van Bockstaele et al., 1991; Cowie and Holstege, 1992; Dampney et al., 2013; **Figure 1**). Instead, neurons in the dlPAG influence autonomic and respiratory activity via direct and indirect projections to the dorsomedial hypothalamus (Horiuchi et al., 2009; Dampney et al., 2013; Dampney, 2015).

In humans, Ezra et al. (2015) used magnetic resonance imaging and probabilistic tractography to determine the functional connectivity between different PAG subregions and other brain regions. These authors found that there was functional connectivity between the dlPAG and two lower brainstem regions, the parabrachial/Kölliker-Fuse complex and the ventrolateral medulla. As Ezra et al. (2015) point out, however, the demonstrated functional connectivity may be direct or indirect. In fact, Ezra et al. (2015) also found that there was functional connectivity between the dlPAG and the midbrain cuneiform nucleus, which in rats has been shown to project to the ventrolateral medulla (Verberne, 1995). In addition, a direct projection from the dlPAG to the parabrachial/Kölliker-Fuse complex has also been demonstrated in rats (Krout et al., 1998).

Thus, the connections of the dlPAG with brainstem regions as identified in humans by Ezra et al. (2015) is entirely consistent with the anatomical connections of the dlPAG as demonstrated in rats.

FUNCTIONS OF PROJECTIONS FROM THE MEDIAL PREFRONTAL CORTEX TO THE dlPAG

There are projections from the medial prefrontal cortex to all PAG subregions (An et al., 1998; Floyd et al., 2000), but in the rat projections from the anterior cingulate and caudal prelimbic cortices terminate predominantly in the dlPAG (Floyd et al., 2000; Gabbott et al., 2005). Similarly, it has been shown in the macaque monkey that there are strong direct projections from the medial prefrontal cortex to the dlPAG, specifically from Brodmann area 10 (particularly its medial portion, area 10 m), area 25 and area 32 (An et al., 1998; Freedman et al., 2000; **Figures 2B,C**). In comparison, projections from these regions to other PAG subregions are of much smaller magnitude (**Figures 2B,C**). In the primate, Brodmann areas 25 and 32 are homologous to the infralimbic and caudal prelimbic cortices in the rat, but area 10 m has no apparent homologue in the rat or in other non-primate species (Floyd et al., 2000).

There have been few studies of the functions of the direct projections from the medial prefrontal cortex to the dlPAG. A recent study in mice, however, used optogenetics to selectively manipulate the projection from the medial prefrontal cortex to the dorsal PAG (Franklin et al., 2017). This study found that selective inhibition of this pathway produced a behavioral response that mimicked social defeat. In this study, the dorsal PAG referred to the entire dorsal half of the PAG, which includes the dmPAG, dlPAG, and lPAG, and so it is not possible on the basis of this study to determine whether the observed behavioral effects were due to activation of the pathway from the medial prefrontal cortex to the dlPAG, rather than the dmPAG or lPAG. Indeed, an earlier study by Faturi et al. (2014) found, on the basis of studies using c-fos expression and pharmacological manipulations that the dmPAG was an important node for the expression of contextual responses to social defeat.

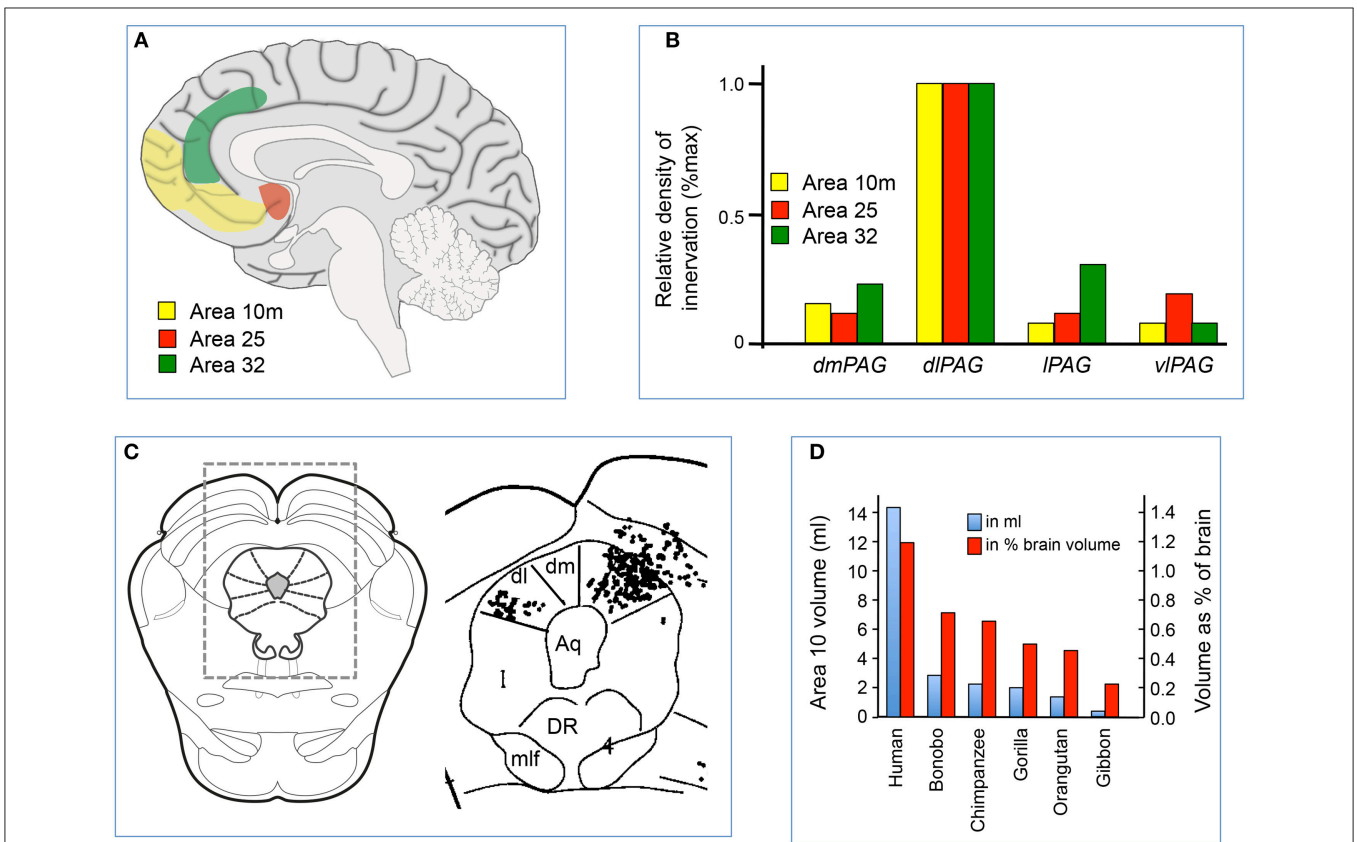

FIGURE 2 | (A) Sagittal midline section of the human brain showing the location of cortical areas 10 m, 25 and 32. **(B)** Relative density of labeled axonal terminals in the dorsomedial (dm), dorsolateral (dl), lateral (l), and ventrolateral (vl) parts of the PAG, following injection of anterograde tracer into areas 10 m, 25 and 32 in the medial prefrontal cortex of the macaque. Modified from An et al. (1998), with permission; **(C)** Example of distribution of labeled terminals in the PAG and surrounding areas following injection of anterograde tracer into areas 10 m in one experiment. The location of the area on the right is indicated by the rectangle over a standard section of the midbrain on the left. Modified from An et al. (1998). **(D)** Relative volumes of area 10 m in different primate species, expressed both as an absolute measure (in ml) or relative measure (% of brain volume). Modified from Semendeferi et al. (2001), with permission.

Area 25 (Subgenual Cingulate Cortex)

There is considerable evidence from studies in humans that area 25 (also called the subgenual cingulate cortex) has an important role in regulating emotions and the physiological response to negative emotions and threatening stimuli (Phelps et al., 2004; Milad et al., 2007). In particular, area 25 is involved in the extinction of a behavioral fear response to a conditioned stimulus, which occurs when a conditioned stimulus is presented repeatedly, without the unconditioned stimulus (Phelps et al., 2004; Milad et al., 2007). It is also interesting to note that area 25 is metabolically overactive in patients with treatment-resistant depression (Mayberg et al., 2000).

There are few studies in primates of the role of area 25 in cardiovascular regulation. In the rat, however, it has been shown that direct stimulation of the homologous region (infralimbic cortex) attenuates the cardiovascular response (increase in blood pressure and heart rate) evoked by air-jet stress (Müller-Ribeiro et al., 2012). Stimulation of the infralimbic cortex does not alter cardiovascular variables under baseline conditions (Müller-Ribeiro et al., 2012). These observations are compatible with the possibility that the direct projection from the infralimbic cortex (or area 25 in primates) inhibits neurons in the dlPAG that normally generate cardiovascular responses to threatening stimuli. Inhibition of the infralimbic cortex has no effect on these responses, however, suggesting that the neurons in the infralimbic cortex that can inhibit stress-evoked responses are not tonically active under resting conditions (Müller-Ribeiro et al., 2012).

Area 32 (Dorsal Anterior Cingulate Cortex)

In contrast to area 25, in humans activation of area 32 (also called the dorsal anterior cingulate cortex) is correlated with the magnitude of conditioned fear responses (Milad et al., 2007). Consistent with this, in rats stimulation of the homologous region (prelimbic cortex) increases conditioned fear responses (Vidal-Gonzalez et al., 2006) whereas inactivation of the prelimbic cortex reduces these responses (Corcoran and Quirk, 2007).

In a neuroimaging study in humans, Critchley et al. (2000) found that activity in area 32 correlated with increases in blood pressure during periods of psychological stress (mental arithmetic). This observation led to the prediction that lesions of area 32 would impair cardiovascular responses to psychological stress, which was tested in a group of three patients with brain lesions that included area 32 (Critchley et al., 2003). All three patients had average or above-average cognitive ability as measured in a range of tests, but all three showed reduced cardiovascular responses to psychological stress (mental arithmetic). Thus it appears that area 32 generates physiological responses associated with cognitive demands, but is not involved in the cognitive process itself.

Apart from cognition, area 32 is also believed to be a region that generates responses to pain (Etkin et al., 2011; Shackman et al., 2011; Jahn et al., 2016). There are two general theories concerning the role of area 32 in pain processing. One theory, the neural alarm hypothesis, proposes that area 32 generates immediate responses to painful stimuli, without cognitive appraisal of this stimulus (Lieberman and Eisenberger, 2015). The second theory, called the adaptive control hypothesis, proposes that area 32 acts as a hub that processes aversive stimuli regardless of modality (e.g., pain, or negative affect) and then generates an appropriate behavioral response (Shackman et al., 2011). The adaptive control hypothesis implies that cognitive processing is required to generate an appropriate response (Jahn et al., 2016). The results of recent studies using brain imaging support the neural alarm hypothesis, in that they show that pain activates a region within area 32 (Lieberman and Eisenberger, 2015; Jahn et al., 2016) that is separate from the region activated by cognitive processing. It is conceivable that neurons within area 32 that are activated by pain also project to the dlPAG, and trigger behavioral and cardiovascular responses via this pathway, but no studies have been performed to test that possibility.

Area 10

Area 10 is located in the most rostral part of the prefrontal cortex (**Figure 2A**), and is sometimes referred to as the frontopolar cortex or the rostral prefrontal cortex. In recent years area 10 has attracted much interest, for several reasons. First, as mentioned above, it is a brain structure that either does not exist in non-primate species, or is so rudimentary that it cannot be identified. Secondly, the volume of area 10 (either as an absolute measure, or as a percentage of the volume of the whole brain) is much greater in humans than in other primates (Semendeferi et al., 2001; **Figure 2D**). Thirdly, virtually all the afferent inputs to area 10 originate from higher-order association areas, suggesting this region has an important role in cognition (Barbas and Pandya, 1989; Burman et al., 2011). Finally, the maturation of area 10 occurs late in the postnatal period (Dumontheil, 2014), suggesting that it is a region where experience may affect its development, consistent with a role in higher-order cognition.

Less is known about the specific functions of area 10 than other parts of the medial prefrontal cortex. Nevertheless, some information is available. Monkeys in which area 10 was lesioned had a deficit in their ability to explore alternative goals when distracted during an ongoing behavioral task (Boschin et al., 2015; Mansouri et al., 2015). Such studies have led to the hypothesis that neurons in area 10 have an exploratory role, i.e., monitor the environment for indications that it may be advantageous to abandon the current ongoing task and pursue a different task (Mansouri et al., 2017).

Brain imaging studies in human subjects have shown that area 10 is activated when subjects perform tasks that require them to recall specific events from the past (Lepage et al., 2000). Furthermore, the medial part of area 10 (area 10 m) is specifically activated when subjects are presented with an emotionally charged dilemma that require them to make a choice between two different courses of action, each of which may affect the welfare of others (Greene et al., 2001). On the basis of these observations, Allman et al. (2002) have proposed that in humans area 10 compares the current behavioral state with past experiences, and then makes a choice with regard to future behavior. Taken together, studies in monkeys and humans suggest that area 10 continually compares the ongoing behavioral state with alternative behaviors, to determine if alternative

behaviors may be more advantageous in the light of changes in the external environment together with past experiences. The fact that area 10 m (which has a strong direct projection to the dlPAG) (**Figures 2B,C**) is specifically activated under conditions where such comparisons generate an emotional response is particularly interesting, given that emotional responses are associated with autonomic and respiratory effects.

CONCLUSIONS AND FUTURE DIRECTIONS

Cortical areas 25, 32, and 10 m in the primate medial prefrontal cortex are all involved in the regulation of behavioral responses to threatening or emotional stimuli, either real or perceived. Although there are differences in their precise functions, a common property of these regions is that all three have major direct projections to the dlPAG, but not to other PAG regions. As discussed previously, there is strong evidence that the dlPAG plays an important role in regulating behavioral responses to psychological stressors, accompanied by appropriate autonomic and respiratory changes (Dampney et al., 2013). Thus, the anatomical and functional evidence taken together suggests that the inputs to the dlPAG from areas 25, 32, and 10 m in the medial prefrontal cortex are major components of the central networks coupling emotional stimuli to behavioral and physiological responses, as previously suggested (Bandler et al., 2000; Keay and Bandler, 2001).

As discussed above, apart from inputs from the medial prefrontal cortex, the dlPAG also receives inputs related to auditory, visual and olfactory signals (**Figure 1**) that indicate a direct external threat such as the presence of a predator. In summary, the available evidence indicates that the dlPAG is a site of convergence of inputs arising from sensory receptors indicating a direct external threat, as well as inputs from the medial prefrontal cortex indicating a perceived threat based on more complex cognitive processing.

There are many unresolved issues concerning the relationship between cortical areas 25, 32, and 10 m and the dlPAG. First, while there is good evidence that areas 25 and 32 can modulate behavioral and cardiovascular responses to emotional stimuli, there is no direct evidence that these effects are mediated by direct projections from these areas to the dlPAG. In the case of neurons in area 10 m that project directly to the dlPAG, there is no information available regarding their potential role in cardiovasculat regulation. Secondly, even if the projections from areas 25, 32, and 10 m to the dlPAG do mediate behavioral and physiological responses to emotional stimuli, are these projections the only route by which such responses are generated? Finally, are the neurons within the dlPAG functionally homogeneous, or are their subsets of dlPAG neurons that receive differential inputs from areas 25, 32, and 10 m in the medial prefrontal cortex?

These questions may be answered, at least in part, by future studies using optogenetics. For example, a number of recent studies in rodents have examined the effects of selective activation or inhibition of projections from the medial prefrontal cortex to a specific target (e.g., the dorsal raphe nucleus, Warden et al., 2012), or projections to specific subregions of the PAG (e.g., to the ventral PAG from the medial preoptic area, Park et al., 2018 or the lPAG from the lateral hypothalamus, Li et al., 2018). The same methodology could be applied to selectively activate the projection to the dlPAG in rodents from the infralimbic cortex (which is analogous to cortical area 25 in primates) or from the dorsal ACC (which is analogous to cortical area 25 in primates). Such experiments would reveal the behavioral and physiological effects of activation or inhibition of these pathways in rodents. In regard to human studies, recent improvements in resolution of brain imaging technology together with new methods for determining functional connectivity in the brain have the potential for identifying the function of specific connections between the medial prefrontal cortex and subregions of the PAG, including the dlPAG (Linnman et al., 2012).

Although much remains unknown, the evidence so far suggests that the connections from the medial prefrontal cortex to the dlPAG have a critical role in generating behavioral, cardiovascular and other physiological responses associated with emotional stimuli that require cognitive appraisal.

AUTHOR CONTRIBUTION

The author confirms being the sole contributor of this work and approved it for publication.

REFERENCES

Allman, J., Hakeem, A., and Watson, K. (2002). Two phylogenetic specializations in the human brain. *Neuroscientist* 8, 335–346. doi: 10.1177/107385840200800409

An, X., Bandler, R., Öngür, D., and Price, J.L. (1998). Prefrontal cortical projections to longitudinal columns in the midbrain periaqueductal gray in macaque monkeys. *J. Comp. Neurol.* 401, 455–479. doi: 10.1002/(SICI)1096-9861(19981130)401:4<455::AID-CNE3>3.0.CO;2-6

Bandler, R., Keay, K. A., Floyd, N., and Price, J. (2000). Central circuits mediating patterned autonomic activity during active vs. passive emotional coping. *Brain Res. Bull.* 53, 95–104. doi: 10.1016/S0361-9230(00)00313-0

Bandler, R., and Shipley, M. T. (1994). Columnar organization of the midbrain periaqueductal gray: modules for emotional expression. *Trends Neurosci.* 17, 379–389. doi: 10.1016/0166-2236(94)90047-7

Barbas, H., and Pandya, D. N. (1989). Architecture and intrinsic connections of the prefrontal cortex in the rhesus monkey. *J. Comp. Neurol.* 286, 353–375. doi: 10.1002/cne.902860306

Benzinger, H., and Massopust, L. C. (1983). Brain stem projections from cortical area 18 in the albino rat. *Exp. Brain Res.* 50, 1–8. doi: 10.1007/BF00238228

Bittencourt, A. S., Carobrez, A. P., Zamprogno, L. P., Tufik, S., and Schenberg, L. C. (2004). Organization of single components of defensive behaviors within distinct columns of periaqueductal gray matter of the rat: role of *N*-methyl-D-aspartic acid glutamate receptors. *Neuroscience* 125, 71–89. doi: 10.1016/j.neuroscience.2004.01.026

Blanchard, D. C., Canteras, N. S., Markham, C. M., Pentkowski, N. S., and Blanchard, R. J. (2005). Lesions of structures showing FOS expression to cat presentation: effects on responsivity to a cat, cat odor, and nonpredator threat. *Neurosci. Biobehav. Rev.* 29, 1243–1253. doi: 10.1016/j.neubiorev.2005.04.019

Boschin, E. A., Piekema, C., and Buckley, M. J. (2015). Essential functions of primate frontopolar cortex in cognition. *Proc. Natl. Acad. Sci. U.S.A.* 112, E1020–E1027. doi: 10.1073/pnas.1419649112

Burman, K. J., Reser, D. H., Yu, H. H., and Rosa, M. G. P. (2011). Cortical input to the frontal pole of the marmoset monkey. *Cereb. Cortex* 21, 1712–1737. doi: 10.1093/cercor/bhq239

Canteras, N. S., and Goto, M. (1999). Fos-like immunoreactivity in the periaqueductal gray of rats exposed to a natural predator. *Neuroreport* 10, 413–418. doi: 10.1097/00001756-199902050-00037

Carr, J. A. (2015). I'll take the low road: the evolutionary underpinnings of visually triggered fear. *Front. Neurosci.* 9:414. doi: 10.3389/fnins.2015.00414

Carrive, P. (1993). The periaqueductal gray and defensive behavior: functional representation and neuronal organization. *Behav. Brain Res.* 58, 27–47. doi: 10.1016/0166-4328(93)90088-8

Corcoran, K. A., and Quirk, G. J. (2007). Activity in prelimbic cortex is necessary for the expression of learned, but not innate, fears. *J. Neurosci.* 27, 840-844. doi: 10.1523/JNEUROSCI.5327-06.2007

Cowie, R. J., and Holstege, G. (1992). Dorsal mesencephalic projections to pons, medulla, and spinal cord in the cat: limbic and non-limbic components. *J. Comp. Neurol.* 319, 536–559. doi: 10.1002/cne.903190406

Critchley, H. D., Corfield, D. R., Chandler, M. P., Mathias, C. J., and Dolan, R. J. (2000). Cerebral correlates of autonomic cardiovascular arousal: a functional neuroimaging investigation. *J. Physiol. (Lond).* 523, 259–270. doi: 10.1111/j.1469-7793.2000.t01-1-00259.x

Critchley, H. D., Mathias, C. J., Josephs, O., O'Doherty, J., Zanini, S., Dewar, B.-K., et al. (2003). Human cingulate cortex and autonomic cardiovascular control: converging neuroimaging and clinical evidence. *Brain* 216, 2139–2156. doi: 10.1093/brain/awg216

Dampney, R. A. L. (2015). Central mechanisms regulating coordinated cardiovascular and respiratory function during stress and arousal. *Am. J. Physiol. Regul. Integr. Comp. Physiol.* 309, R429–R443. doi: 10.1152/ajpregu.00051.2015

Dampney, R. A. (2016). Central neural control of the cardiovascular system: current perspectives. *Adv. Physiol. Educ.* 40, 283–296. doi: 10.1152/advan.00027.2016

Dampney, R. A., Furlong, T., Horiuchi, J., and Iigaya, K. (2013). Role of dorsolateral periaqueductal grey in the coordinated regulation of cardiovascular and respiratory function. *Auton. Neurosci.* 175, 17–25. doi: 10.1016/j.autneu.2012.12.008

Dean, P., Redgrave, P., and Westby, G. W. (1989). Event or emergency? two response systems in the mammalian superior colliculus. *Trends Neurosci.* 12, 137–147. doi: 10.1016/0166-2236(89)90052-0

Dumontheil, I. (2014). Development of abstract thinking during childhood and adolescence: the role of rostrolateral prefrontal cortex. *Devel. Cog. Neurosci.* 10, 57–76. doi: 10.1016/j.dcn.2014.07.009

Etkin, A., Egner, T., and Kalisch, R. (2011). Emotional processing in anterior cingulate and medial prefrontal cortex. *Trends Cogn. Sci. (Regul. Ed).* 15, 85–93. doi: 10.1016/j.tics.2010.11.004

Ezra, M., Faull, O. K., Jbabdi, S., and Pattinson, K. T. (2015). Connectivity-based segmentation of the periaqueductal gray matter in human with brainstem optimized diffusion MRI. *Hum. Brain Mapp.* 36, 3459–3471. doi: 10.1002/hbm.22855

Faturi, C. B., Rangel, M. J., Baldo, M. V., and Canteras, N. S. (2014). Functional mapping of the circuits involved in the expression of contextual fear responses in socially defeated animals. *Brain Struct. Funct.* 219, 931–946. doi: 10.1007/s00429-013-0544-4

Floyd, N. S., Price, J. L., Ferry, A. T., Keay, K. A., and Bandler, R. (2000). Orbitomedial prefrontal cortical projections to distinct longitudinal columns of the periaqueductal gray in the rat. *J. Comp. Neurol.* 422, 556–578. doi: 10.1002/1096-9861(20000710)422:4<556::AID-CNE6>3.0.CO;2-U

Fontes, M. A., Xavier, C. H., Marins, F. R., Limborco-Filho, M., Vaz, G. C., Müller-Ribeiro, F. C., et al. (2014). Emotional stress and sympathetic activity: contribution of dorsomedial hypothalamus to cardiac arrhythmias. *Brain Res.* 1554, 49–58. doi: 10.1016/j.brainres.2014.01.043

Franklin, T. B., Silva, B. A., Perova, Z., Marrone, L., Masferrer, M. E., Zhan, Y., et al. (2017). Prefrontal cortical control of a brainstem social behavior circuit. *Nat. Neurosci.* 20, 260–270. doi: 10.1038/nn.4470

Freedman, L. J., Insel, T. R., and Smith, Y. (2000). Subcortical projections of area 25 (subgenual cortex) of the macaque monkey. *J. Comp. Neurol.* 421, 172-188. doi: 10.1002/(SICI)1096-9861(20000529)421:2<172::AID-CNE4>3.0.CO;2-8

Gabbott, P. L., Warner, T. A., Jays, P. R., Salway, P., and Busby, S. J. (2005). Prefrontal cortex in the rat: projections to subcortical autonomic, motor, and limbic centers. *J. Comp. Neurol.* 492, 145–177. doi: 10.1002/cne.20738

Greene, J. D., Sommerville, R. B., Nystrom, L. E., Darley, J. M., and Cohen, J. D. (2001). An fMRI investigation of emotional engagement in moral judgement. *Science* 293, 2105–2108. doi: 10.1126/science.1062872

Horiuchi, J., McDowall, L. M., and Dampney, R. A. L. (2009). Vasomotor and respiratory responses evoked from the dorsolateral PAG are mediated by the dorsomedial hypothalamus. *J. Physiol. (Lond).* 587, 5149–5162. doi: 10.1113/jphysiol.2009.179739

Iigaya, K., Horiuchi, J., McDowall, L. M., and Dampney, R. A. L. (2010). Topographical specificity of regulation of respiratory and renal sympathetic activity by the midbrain dorsolateral periaqueductal gray. *Am. J. Physiol. Regul. Integr. Comp. Physiol.* 299, R853–R861. doi: 10.1152/ajpregu.00249.2010

Jahn, A., Nee, D. E., Alexander, W. H., and Brown, J. W. (2016). Distinct regions within medial prefrontal cortex process pain and cognition. *J. Neurosci.* 36, 12385–12392. doi: 10.1523/JNEUROSCI.2180-16.2016

Keay, K. A., and Bandler, R. (2001). Parallel circuits mediating distinct emotional coping reactions to different types of stress. *Neurosci. Biobehav. Rev.* 25, 669–678. doi: 10.1016/S0149-7634(01)00049-5

Klop, E. M., Mouton, L. J., Ehling, T., and Holstege, G. (2005). Two parts of the nucleus prepositus hypoglossi project to two different subdivisions of the dorsolateral periaqueductal gray in cat. *J. Comp. Neurol.* 492, 303–322. doi: 10.1002/cne.20728

Klop, E. M., Mouton, L. J., and Holstege, G. (2006). Periparabigeminal and adjoining mesencephalic tegmental field projections to the dorsolateral periaqueductal grey in cat - a possible role for oculomotor input in the defensive system. *Eur. J. Neurosci.* 23, 2145–2157. doi: 10.1111/j.1460-9568.2006.04740.x

Krout, K. E., Jansen, A. S., and Loewy, A. D. (1998). Periaqueductal gray matter projection to the parabrachial nucleus in rat. *J. Comp. Neurol.* 401, 437–454. doi: 10.1002/(SICI)1096-9861(19981130)401:4<437::AID-CNE2>3.0.CO;2-5

LeDoux, J. E., and Pine, D. S. (2016). Using neuroscience to help understand fear and anxiety: a two-system framework. *Am. J. Psychiatr.* 173, 1083–1093. doi: 10.1176/appi.ajp.2016.16030353

Lepage, M., Ghaffar, O., Nyberg, L., and Tulving, E. (2000). Prefrontal cortex and episodic memory retrieval mode. *Proc. Nat. Acad. Sci. U.S.A.* 97, 506–511. doi: 10.1073/pnas.97.1.506

Li, Y., Zeng, J., Zhang, J., Yue, C., Zhong, W., Liu, Z., et al. (2018). Hypothalamic circuits for predation and evasion. *Neuron* 97, 911–924. doi: 10.1016/j.neuron.2018.01.005

Lieberman, M. D., and Eisenberger, N. I. (2015). The dorsal anterior cingulate cortex is selective for pain: results from large-scale reverse inference submission. *Proc. Natl. Acad. Sci. U.S.A.* 112, 15250 −15255. doi: 10.1073/pnas.1515083112

Linnman, C., Moulton, E. A., Barmettler, G., Becerra, L., and Borsook, D. (2012). Neuroimaging of the periaqueductal gray: state of the field. *Neuroimage* 60, 505–522. doi: 10.1016/j.neuroimage.2011.11.095

Mansouri, F. A., Buckley, M. J., Mahboubi, M., and Tanaka, K. (2015). Behavioral consequences of selective damage to frontal pole and posterior cingulate cortices. *Proc. Natl Acad. Sci. U.S.A.* 112, E3940–E3949. doi: 10.1073/pnas.1422629112

Mansouri, F. A., Koechlin, E., Rosa, M. G. P., and Buckley, M. J. (2017). Managing competing goals – a key role for the frontopolar cortex. *Nat. Rev. Neurosci.* 18, 645–657. doi: 10.1038/nrn.2017.111

Markham, C. M., Blanchard, D. C., Canteras, N. S., Cuyno, C. D., and Blanchard, R. J. (2004). Modulation of predatory odor processing following lesions to the dorsal premammillary nucleus. *Neurosci. Lett.* 372, 22–26. doi: 10.1016/j.neulet.2004.09.006

May, P. J. (2006). The mammalian superior colliculus: laminar structure and connections. *Prog. Brain Res.* 151, 321–378. doi: 10.1016/S0079-6123(05)51011-2

Mayberg, H. S., Brannan, S. K., Tekell, J. L., Silva, J. A., Mahurin, R. K., McGinnis, S., et al. (2000). Regional metabolic effects of fluoxetine in major depression:

serial changes and relationship to clinical response. *Biol. Psychiatr.* 48, 830–843. doi: 10.1016/S0006-3223(00)01036-2

Milad, M. R., Quirk, G. J., Pitman, R. K., Orr, S. P., Fischl, B., and Rauch, S. L. (2007). A role for the human dorsal anterior cingulate cortex in fear expression. *Biol. Psychiatr.* 62, 1191–1194. doi: 10.1016/j.biopsych.2007.04.032

Motta, S. C., Goto, M., Gouveia, F. V., Baldo, M. V., Canteras, N. S., and Swanson, L. W. (2009). Dissecting the brain's fear system reveals the hypothalamus is critical for responding in subordinate conspecific intruders. *Proc. Natl. Acad. Sci.U.S.A.* 106, 4870–4875. doi: 10.1073/pnas.0900939106

Müller-Ribeiro, F. C. F., Goodchild, A. K., McMullan, S., Fontes, M. A. P., and Dampney, R. A. L. (2016). Coordinated autonomic and respiratory responses evoked by alerting stimuli: role of the midbrain colliculi. *Resp. Physiol. Neurobiol.* 226, 87–93. doi: 10.1016/j.resp.2015.10.012

Müller-Ribeiro, F. C. F., Zaretsky, D. V., Zaretskaia, M. V., Santos, R. A., DiMicco, J. A., and Fontes, M. A. P. (2012). Contribution of infralimbic cortex in the cardiovascular response to acute stress. *Am. J. Physiol. Regul. Integr. Comp. Physiol.* 303, R639–R650. doi: 10.1152/ajpregu.00573.2011

Myers, B. (2017). Corticolimbic regulation of cardiovascular responses to stress. *Physiol. Behav.* 172, 49–59. doi: 10.1016/j.physbeh.2016.10.015

Newman, D. B., Hileary, S. K., and Ginsberg, C. Y. (1989). Nuclear terminations of corticonuclear fiber systems in rats. *Brain Behav. Evol.* 34, 223–264. doi: 10.1159/000116508

Park, S. G., Jeong, Y. C., Kim, D. G., Lee, M. H., Shin, A., Park, G., et al. (2018). Medial preoptic circuit induces hunting-like actions to target objects and prey. *Nat. Neurosci.* 21, 364–372. doi: 10.1038/s41593-018-0072-x

Phelps, E. A., Delgado, M. R., Nearing, K. I., and LeDoux, J. E. (2004). Extinction learning in humans: role of the amygdala and vmPFC. *Neuron* 43, 897–905. doi: 10.1016/j.neuron.2004.08.042

Rhoades, R. W., Mooney, R. D., Rohrer, W. H., Nikoletseas, M. M., and Fish, S. E. (1989). Organization of the projection from the superficial to the deep layers of the hamster's superior colliculus as demonstrated by the anterograde transport of Phaseolus vulgaris leucoagglutinin. *J. Comp. Neurol.* 283, 54–70. doi: 10.1002/cne.902830106

Semendeferi, K., Armstrong, E., Schleicher, A., Zilles, K., and Van Hoesen, G. (2001). Prefrontal cortex in humans and apes: a comparative study of area 10. *Am. J. Phys. Anthrop.* 114, 224–241. doi: 10.1002/1096-8644(200103)114:3<224::AID-AJPA1022>3.0.CO;2-I

Shackman, A. J., Salomons, T. V., Slagter, H. A., Fox, A. S., Winter, J. J., and Davidson, R. J. (2011). The integration of negative affect, pain and cognitive control in the cingulate cortex. *Nat. Rev. Neurosci.*12, 154 −167. doi: 10.1038/nrn2994

Van Bockstaele, E. J., Aston-Jones, G., Pieribone, V. A., Ennis, M., and Shipley, M. T. (1991). Sub-regions of the periaqueductal gray topographically innervate the rostral ventral medulla in the rat. *J. Comp. Neurol.* 309, 305–327. doi: 10.1002/cne.903090303

Verberne, A. J. (1995). Cuneiform nucleus stimulation produces activation of medullary sympathoexcitatory neurons in rats. *Am. J. Physiol. Regul. Integr. Comp. Physiol.* 268, R752–R758. doi: 10.1152/ajpregu.1995.268.3.R752

Vianna, D. M., and Brandão, M. L. (2003). Anatomical connections of the periaqueductal gray: specific neural substrates for different kinds of fear. *Braz. J. Med. Biol. Res.* 36, 557–566. doi: 10.1590/S0100-879X2003000500002

Vidal-Gonzalez, I., Vidal-Gonzalez, B., Rauch, S. L., and Quirk, G. J. (2006). Microstimulation reveals opposing influences of prelimbic and infralimbic cortex on the expression of conditioned fear. *Learn. Mem.* 13, 728 −733. doi: 10.1101/lm.306106

Warden, M. R., Selimbeyoglu, A., Mirzabekov, J. J., Lo, M., Thompson, K. R., Kim, S. Y., et al. (2012). A prefrontal cortex-brainstem neuronal projection that controls response to behavioural challenge. *Nature* 492, 428–432. doi: 10.1038/nature11617

Conflict of Interest Statement: The author declares that the research was conducted in the absence of any commercial or financial relationships that could be construed as a potential conflict of interest.

frontiers in Neuroscience

ORIGINAL RESEARCH
published: 10 January 2017
doi: 10.3389/fnins.2016.00614

Heart Rate Changes in Response to Mechanical Pressure Stimulation of Skeletal Muscles Are Mediated by Cardiac Sympathetic Nerve Activity

Nobuhiro Watanabe and Harumi Hotta *

Department of Autonomic Neuroscience, Tokyo Metropolitan Institute of Gerontology, Tokyo, Japan

Stimulation of mechanoreceptors in skeletal muscles such as contraction and stretch elicits reflexive autonomic nervous system changes which impact cardiovascular control. There are pressure-sensitive mechanoreceptors in skeletal muscles. Mechanical pressure stimulation of skeletal muscles can induce reflex changes in heart rate (HR) and blood pressure, although the neural mechanisms underlying this effect are unclear. We examined the contribution of cardiac autonomic nerves to HR responses induced by mechanical pressure stimulation (30 s, ~10 N/cm^2) of calf muscles in isoflurane-anesthetized rats. Animals were artificially ventilated and kept warm using a heating pad and lamp, and respiration and core body temperature were maintained within physiological ranges. Mechanical stimulation was applied using a stimulation probe 6 mm in diameter with a flat surface. Cardiac sympathetic and vagus nerves were blocked to test the contribution of the autonomic nerves. For sympathetic nerve block, bilateral stellate ganglia, and cervical sympathetic nerves were surgically sectioned, and for vagus nerve block, the nerve was bilaterally severed. In addition, mass discharges of cardiac sympathetic efferent nerve were electrophysiologically recorded. Mechanical stimulation increased or decreased HR in autonomic nerve-intact rats (range: −56 to +10 bpm), and the responses were negatively correlated with pre-stimulus HR ($r = -0.65$, $p = 0.001$). Stimulation-induced HR responses were markedly attenuated by blocking the cardiac sympathetic nerve (range: −9 to +3 bpm, $p < 0.0001$) but not the vagus nerve (range: −75 to +30 bpm, $p = 0.17$). In the experiments with cardiac sympathetic efferent nerve activity recordings, mechanical stimulation increased, or decreased the frequency of sympathetic nerve activity in parallel with HR ($r = 0.77$, $p = 0.0004$). Furthermore, the changes in sympathetic nerve activity were negatively correlated with its tonic level ($r = -0.62$, $p = 0.0066$). These results suggest that cardiac sympathetic nerve activity regulates HR responses to muscle mechanical pressure stimulation and the direction of HR responses depends on the tonic level of the nerve activity, i.e., bradycardia occurs when the tonic activity is high and tachycardia occurs when the activity is low.

Keywords: skeletal muscles, mechanical pressure stimulation, somatocardiovascular reflexes, heart rate, cardiac sympathetic nerve, rats

OPEN ACCESS

Edited by:
Tijana Bojić,
University of Belgrade, Serbia

Reviewed by:
Pascal Carrive,
University of New South Wales, Australia
Philip J. Millar,
University of Guelph, Canada

***Correspondence:**
Harumi Hotta
hhotta@tmig.or.jp

Specialty section:
This article was submitted to Autonomic Neuroscience, a section of the journal Frontiers in Neuroscience

Received: *21 October 2016*
Accepted: *26 December 2016*
Published: *10 January 2017*

Citation:
Watanabe N and Hotta H (2017) Heart Rate Changes in Response to Mechanical Pressure Stimulation of Skeletal Muscles Are Mediated by Cardiac Sympathetic Nerve Activity. Front. Neurosci. 10:614. doi: 10.3389/fnins.2016.00614

INTRODUCTION

Somatosensory stimulation reflexively elicits autonomic nervous activity changes and affects cardiovascular control (somatocardiovascular reflexes) in anesthetized animals, in whom consciousness and emotions that are potentially influential are eliminated by the administration of anesthesia (Sato et al., 1997; Watanabe et al., 2015). One characteristic of somatocardiovascular reflexes is that evoked responses differ depending on the type of stimulation. For example, a strong pinch of the skin (Kimura et al., 1995; Sato et al., 1997; Suzuki et al., 2004) and noxious thermal stimulation (Kaufman et al., 1977) generally induce tachycardiac and pressor responses. In contrast, brushing and non-noxious thermal stimulation do not lead to heart rate (HR) responses or provide only a small response (Kaufman et al., 1977; Sato et al., 1997). In addition to the skin stimulation mentioned above, some skeletal muscle stimulations evoke cardiovascular responses (Sato et al., 1981, 1982; Kannan et al., 1988; Stebbins et al., 1988; Sato et al., 1997). For example, static muscle contraction and stretch induce tachycardiac and pressor responses (Coote et al., 1971; Kannan et al., 1988; Stebbins et al., 1988), whereas vibratory stimulation does not influence HR and blood pressure (Kannan et al., 1988; Sato et al., 1997). These cardiovascular responses to skin and muscle stimulation are mainly attributed to the excitation of group III and IV afferent fibers (Sato et al., 1997). HR and blood pressure responses to contraction and stretching of skeletal muscles are considered important cardiovascular regulatory mechanisms during exercise (Coote et al., 1971; Murphy et al., 2011). As the efferent of neural mechanisms, the cardiac, renal, and adrenal sympathetic nerve activities are enhanced by the static contraction of the hindlimb muscles (Matsukawa et al., 1990, 1994; Vissing et al., 1991; Koba et al., 2008).

Some mechanoreceptors in skeletal muscles are distinguished from muscle contraction- or stretch-sensitive units based on high sensitivity to pressure stimulation (Paintal, 1960; Mense and Meyer, 1985). Hence, it is possible that cardiovascular responses elicited by pressure stimulation differ from those elicited by muscle contraction. Stebbins et al. (1988) reported that static contraction of calf muscles in anesthetized cats increased HR and blood pressure (by 10 bpm and 20 mmHg, respectively), whereas the constant pressure stimulation applied externally did not change the HR and only marginally increased the blood pressure (5–10 mmHg). Uchida et al. (2003) reported that static pressure to calf muscles (∼5–8 N/cm^2) induced a depressor response in anesthetized rats. In a study by Tallarida et al. (1981), "squeeze" stimulation applied to the calf muscles caused tachycardiac and pressor responses in anesthetized rabbits, although the precise intensity of stimulation was not determined. Despite studies reporting cardiovascular responses to mechanical pressure stimulation of skeletal muscles, the neural mechanisms underlying this effect are undetermined to date.

Abbreviations: CSNA, cardiac sympathetic efferent nerve activity; CVLM, caudal ventrolateral medulla; ΔCSNA, cardiac sympathetic efferent nerve activity response, ΔHR, heart rate response; EEG, electroencephalogram; HR, heart rate; NTS, nucleus of the solitary tract; RVLM, rostral ventrolateral medulla.

Sustained muscle contraction generally induces a pressor response, whereas mechanical pressure stimulation of calf muscles can induce both pressor (Tallarida et al., 1981; Stebbins et al., 1988) and depressor (Uchida et al., 2003) responses. Even under controlled experimental conditions, it was reported that electrical stimulation of muscle afferents (Sato et al., 1981), bradykinin infusion to hindlimb muscles (Sato et al., 1982), and acupuncture-like stimulation to hindlimb muscles (Ohsawa et al., 1995) could induce tachycardiac and bradycardiac or pressor and depressor responses. The reasons for these bidirectional cardiovascular responses have not been studied. It has been documented that deeper anesthesia is more likely to induce bradycardiac and depressor responses (Gibbs et al., 1989; Sato et al., 1997). The depth of anesthesia generally affects the resting levels of HR and blood pressure.

Therefore, there were two aims of the present study. The first aim was to elucidate the contribution of cardiac autonomic nerves to HR responses induced by mechanical pressure stimulation of skeletal muscles. The second aim was to examine whether the resting (pre-stimulus) level of HR influences the direction of HR responses to skeletal muscle mechanical pressure stimulation. To maintain the constant level of anesthesia through data recordings, we used inhalation anesthesia (isoflurane) in the present study.

MATERIALS AND METHODS

Animals

Experiments in the present study were performed on Wistar male rats (4–7 months, $n = 18$) bred at the Tokyo Metropolitan Institute of Gerontology. All study protocols were approved by the animal care and use committee of the Tokyo Metropolitan Institute of Gerontology and conformed to the Guiding Principles for the Care and Use of Animals in the Field of Physiological Sciences.

Rats were anesthetized using isoflurane (Escain, Mylan Inc., Canonsburg, PA, USA). Isoflurane was vaporized by gas (O_2 30%, N_2 70%) using a vaporizer (Sigma Delta, Penlon Ltd., Abingdon, UK). The inspiratory concentration of isoflurane was set at 4% for anesthesia induction and maintained at 2.5–3.0% during surgery. Throughout data recording, isoflurane was maintained at 1.2–1.4%, which is sufficient to eliminate the corneal reflex. In all rats, catheters were implanted into the common carotid artery to continuously record arterial pressure and into the jugular vein to administer drugs and supplemental fluids. The trachea was cannulated and rats were artificially ventilated (SN-480-7; Shinano Seisakusho, Tokyo, Japan). Respiration was controlled to maintain end-tidal CO_2 at ∼3.0% (Capnostream™ 20P, Covidien, Minneapolis, MN, USA). Rectal temperature was maintained at 37.0–37.5°C using an automatically regulated heating pad and lamp (ATB-1100; Nihon Kohden, Tokyo, Japan).

HR was calculated based on recorded arterial pressure waveforms with a time constant of 5 s (Spike 2; Cambridge Electronic Design, Cambridge, England). Mean arterial pressure was obtained by smoothing arterial pressure waveforms with a time constant of 5 s (Spike 2). HR and blood pressure were continuously monitored during experiment, and mechanical

stimulation (see below) was applied after confirming that HR and blood pressure were stable for at least 1 min. The HR response (ΔHR) to stimulation was determined to be the maximum within 1 min after termination of mechanical stimulation relative to the average HR over 1 min before stimulation. The presence of a response was defined as the ΔHR value exceeding by twofold the spontaneous variability during 1 min of pre-stimulus recording (i.e., mean value ± twice the standard deviation).

Mechanical Stimulation of Muscle and Skin

Mechanical pressure stimulation was applied to the calf muscles according to previous reports (Graven-Nielsen et al., 2004; Takahashi et al., 2005; Mizumura and Taguchi, 2016). A stimulation probe 6 mm in diameter with a flat surface (contact area, ∼28 mm^2) was applied perpendicularly to the skin over the center of the inner calf with a weight of ∼290 g (≈10 N/cm^2) for 30 s. The stimulation intensity was based on previous studies showing that this pressure level increases the single unit activities of group III and IV calf muscle afferents (Berberich et al., 1988; Hoheisel et al., 2005). In a pilot study, we confirmed that mechanical pressure at 10 N/cm^2 induced clearer HR changes than stimulation at lower intensities (2–5 N/cm^2). The fur at the site of pressure stimulation was trimmed using a conventional clipper. Noxious mechanical stimulation was applied to the skin by pinching the hindpaw for 30 s using a surgical clamp (∼3 kg; Araki et al., 1984).

Autonomic Nerve Block

To identify the nerve pathway that contributes to the HR response evoked by calf muscle pressure stimulation, the influence of selective autonomic nerve block was examined. To block sympathetic nerves innervating the heart, bilateral stellate ganglia and cervical sympathetic nerves were surgically severed before the end of surgery in three rats. The second costal bone was sectioned before the stellate ganglion was crushed. To block vagus nerves, bilateral vagus nerves were surgically sectioned at the cervical level in 6 rats. In another rat, vagus efferents were pharmacologically blocked by intravenous administration of the blood–brain barrier impermeable muscarinic receptor blocker atropine methyl nitrate (2 mg/kg; Overton, 1993) purchased from Sigma-Aldrich (St. Louis, MO, USA). We confirmed that the dose of atropine was enough to prevent bradycardiac responses induced by electrical stimulation of vagus efferent nerve (Hotta et al., 2010b) at the end of the experiment. The vagotomy was performed before experiment in one rat. In the other rats, vagus nerves were blocked during experiment, and effects of mechanical stimuli were examined both before and after blocking of the vagus nerve.

Cardiac Sympathetic Efferent Nerve Activity Recording

Cardiac sympathetic efferent nerve activity was recorded in four rats by methods described in our previous study (Hotta et al., 2010a). In brief, anesthetized rats were placed in the supine position and the right second costal bone was sectioned. The right inferior cardiac sympathetic nerve was exposed, sectioned as close to the heart as possible, and isolated from surrounding connective tissue. The dissected nerve was covered with paraffin oil. The central cut end of the nerve was placed on platinum–iridium bipolar hook electrodes and mass discharges were recorded. To prevent noise contamination due to muscle contraction, rats were immobilized by intravenous administration of gallamine triethiodide (20 mg/kg). For CSNA recording, the vagus nerves were sectioned to prevent contamination of vagus nerve activity.

Nerve activity was amplified 1000× (MEG-6100, Nihon Kohden, Tokyo, Japan), filtered (bandpass filter: 150 Hz–3 kHz), and monitored visually on an oscilloscope and auditorily through loudspeakers. The amplified signals were digitized at 20 kHz (Micro 1401 mkII; Cambridge Electronic Design) and stored on a personal computer for offline analyses. Spikes of the nerve were discriminated from background noise based on the amplitude of signals, and the number of the spikes was counted every 5 s (Spike 2).

Statistical Analyses

HR and mean arterial pressure values obtained before and after the onset of stimulation were compared by paired *t*-test or Wilcoxon matched-pairs signed rank test depending on the normality of the data distribution (Prism 6; GraphPad Software Inc., La Jolla, CA, USA). Difference in variance of pre-stimulus HR and ΔHR under autonomic block conditions were examined by the *F*-test. Correlation strength was analyzed by calculating Spearman's coefficient. Statistical significance was set at $p < 0.05$. Data are expressed as mean ± standard deviation unless otherwise stated.

RESULTS

HR and Blood Pressure Responses to Mechanical Pressure Stimulation of the Calf Muscles

Resting HR of anesthetized rats ($n = 9$) prior to applying mechanical stimulation ranged from 259 to 459 bpm. Resting HR is relatively stable, but exhibited periodic step-like changes to higher or lower levels of HR (Yli-Hankala and Jäntti, 1990). In these 9 rats, 22 trials of mechanical pressure stimulation were applied to the calf. HR increased in 9 trials and decreased in 12 trials, with no change in one trial. Overall, HR significantly decreased in response to calf pressure stimulation (from 356.3 ± 59.1 to 346.8 ± 48.9 bpm, $p = 0.049$ by paired *t*-test, range −56 and +10 bpm).

Examples of increasing and decreasing responses are shown in **Figures 1A,B**, respectively. In response to pressure stimulation, HR increased slightly (e.g., maximal ΔHR = 10 bpm in **Figure 1A**) from relatively low pre-stimulus HR (e.g., 288 bpm in **Figure 1A**) or decreased more substantially (e.g., maximal ΔHR = −54 bpm in **Figure 1B**) from a relatively high pre-stimulus HR (e.g., 415 bpm in **Figure 1B**). The maximal increase or decrease was attained within a minute following the cessation of stimulation. Bradycardiac responses of >40 bpm were evoked when pre-stimulus HR was >390 bpm and smaller HR responses were produced when HR was <390 bpm. There was a significant

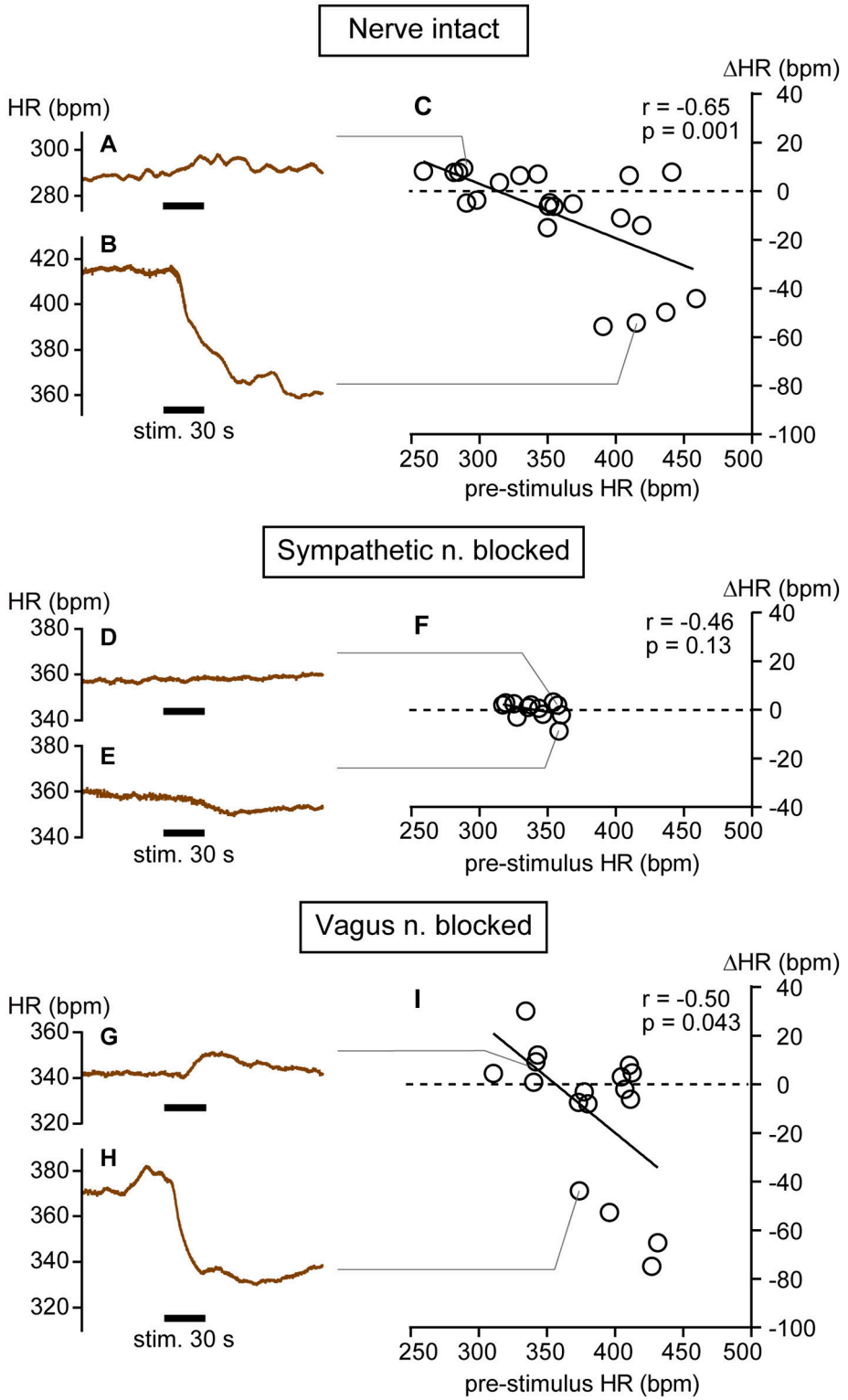

FIGURE 1 | Heart rate (HR) changes in response to calf muscle pressure stimulation in nerve intact (A–C), sympathetic nerve blocked (D–F), and vagus nerve blocked (G–I) conditions. (A,B) Bidirectional changes in heart rate (HR) in response to calf pressure stimulation in anesthetized rats with intact autonomic innervation of the heart (Nerve intact). **(C)** Correlation between pre-stimulus HR and HR responses (ΔHR). Each individual maximal ΔHR is plotted as an open circle. **(D–F)** Data obtained in rats with sympathetic nerve blocked (Sympathetic n. blocked). **(G–I)** Data obtained in rats with vagus nerve blocked (Vagus n. blocked). *r* = Spearman's correlation coefficient.

negative correlation between pre-stimulus HR and ΔHR ($r = -0.65$, $p = 0.001$; **Figure 1C**).

We also applied mechanical pressure stimulation directly to muscle (three trials in a rat) after carefully removing the overlying skin. Both increasing (from 342 to 349 bpm) and decreasing (from 349 to 328 bpm and from 339 to 305 bpm) responses were observed. The correlation between pre-stimulus HR and ΔHR was maintained. Thus, cutaneous afferents are not solely responsible for these HR responses.

On average, mean arterial pressure decreased in response to stimulation (from 113.8 ± 38.6 to 103.7 ± 30.9 mmHg, $p = 0.033$ by Wilcoxon matched-pairs signed rank test, 22 trials). Pre-stimulus mean arterial pressure level was negatively correlated with mean arterial pressure changes ($r = -0.72$, $p = 0.0002$). In majority of trials, HR and mean arterial pressure changed in the same direction (i.e., tachycardiac and pressor responses in **Figure 1A** and Supplementary Figure 1A or bradycardiac and depressor responses in **Figure 1B** and Supplementary Figure 1B). There was a significant positive correlation between HR and mean arterial pressure changes ($r = 0.83$, $p < 0.0001$, Supplementary Figure 1C).

Influence of Autonomic Nerve Block on Pre-stimulus HR and Response to Calf Pressure Stimulation

In three rats, cardiac sympathetic nerves were blocked and 12 trials of mechanical pressure stimulation were conducted. Overall, HR did not change in response to mechanical stimulation (from 340.3 ± 15.5 to 340.3 ± 14.4 bpm, $p = 0.97$ by paired *t*-test). Spontaneous fluctuations of HR during the pre-stimulus period were quite small in this condition (**Figures 1D,E**); thus, even very small changes in HR were distinguishable (e.g., from 357 to 359 bpm in **Figure 1D** and from 359 to 350 bpm in **Figure 1E**). Under sympathetic nerve block, both the range of pre-stimulus HR (317–360 bpm) and the ΔHR (−9 to +3 bpm) were significantly smaller than those in rats with intact autonomic nerves (both $p < 0.0001$ by *F*-test). There was no significant correlation between pre-stimulus HR and HR response ($r = -0.46$, $p = 0.13$; **Figure 1F**), implicating sympathetic nerve in these HR responses to mechanical pressure stimulation of calf muscle.

In seven rats, the vagus nerve was blocked and 17 trials of mechanical pressure stimulation to calf muscle were performed. In this condition, bidirectional HR responses (range: −75 to +30 bpm; **Figures 1G–I**) were observed and the range of ΔHR was not different from that in rats with intact autonomic nerves ($p = 0.17$ by *F*-test). A significant negative correlation between pre-stimulus HR and ΔHR remained ($r = -0.50$, $p = 0.043$; **Figure 1I**), although the range of pre-stimulus HR (311–431 bpm) was narrower than that in autonomic nerve intact rats ($p = 0.048$ by *F*-test). Bradycardiac responses of >40 bpm were produced when pre-stimulus HR was >370 bpm. This inverse correlation between pre-stimulus HR and ΔHR was also observed in one of the seven rats in whom the vagus efferent nerve was pharmacologically blocked by atropine administration rather than transection. Results obtained from this atropine-treated rat are grouped together with those obtained from the vagus nerve-severed rats (**Figure 1I**). When averaged, HR did not change in response to mechanical stimulation (from 380.9 ± 36.0 to 369.7 ± 31.2 bpm, $p = 0.14$ by paired *t*-test).

Response of Cardiac Efferent Nerve Activity to Calf Muscle Pressure Stimulation

The results presented above suggest that HR responses to calf pressure stimulation are mediated primarily by changes in CSNA. Hence, we electrophysiologically recorded CSNA and obtained nerve responses to calf muscle pressure stimulation. In four rats, CSNA was recorded during 17 trials of mechanical pressure stimulation. Similar to HR responses, CSNA responses (ΔCSNA) were bidirectional, increasing in 10 trials and decreasing in 6 trials with one no response trial. Sample CSNA recordings with simultaneous HR monitoring from the same rat are shown in **Figures 2A,B**. In **Figure 2A**, CSNA started to increase immediately after the onset of the calf pressure stimulation and peaked at 172.2% of pre-stimulation value. In **Figure 2B**, CSNA decreased immediately after the onset of stimulation to 41.9% below pre-stimulus value at 20 s after cessation of stimulation. In both cases, the direction of the HR change paralleled that of CSNA, and there was a strong positive correlation between ΔHR and ΔCSNA ($r = 0.77$, $p = 0.0004$; **Figure 2C**).

To identify factors influencing the direction of the CSNA response to pressure stimulation, the correlations of pre-stimulus CSNA level with ΔHR and ΔCSNA were examined. To pool pre-stimulus CSNA data from different rats, CSNA was normalized to the highest frequency value across all trials within each individual (and set to 1). The normalized pre-stimulus CSNA was significantly and negatively correlated with both ΔHR and ΔCSNA responses to calf muscle pressure stimulation ($r = -0.62$, $p = 0.0062$ and $r = -0.62$, $p = 0.0066$, respectively; **Figures 3A,B**). Thus, mechanical pressure stimulation of skeletal muscle produces decreased HR and CSNA when tonic CSNA is high and increased HR and CSNA when tonic CSNA is relatively low.

Correlation between Pre-stimulus HR and HR Response to Pinch Stimulation of the Hindpaw

We then examined whether HR responses to pinch stimulation were also influenced by the level of pre-stimulus HR. In 6 rats with intact autonomic nerves, 14 trials were performed. Overall, HR and mean arterial pressure significantly increased (from 340.3 ± 53.4 to 374.2 ± 50.5 bpm, $p = 0.0004$, and from 96.3 ± 37.9 to 125.1 ± 27.3 mmHg, $p = 0.0052$, respectively, by Wilcoxon matched-pairs signed rank test). As shown in **Figure 4A**, HR increased immediately after the onset of pinch stimulation and remained above the pre-stimulus level for more than 3 min after the cessation of stimulation in most trials. In 13 of 14 trials, HR increased in response to pinch stimulation (**Figures 4A,C**).

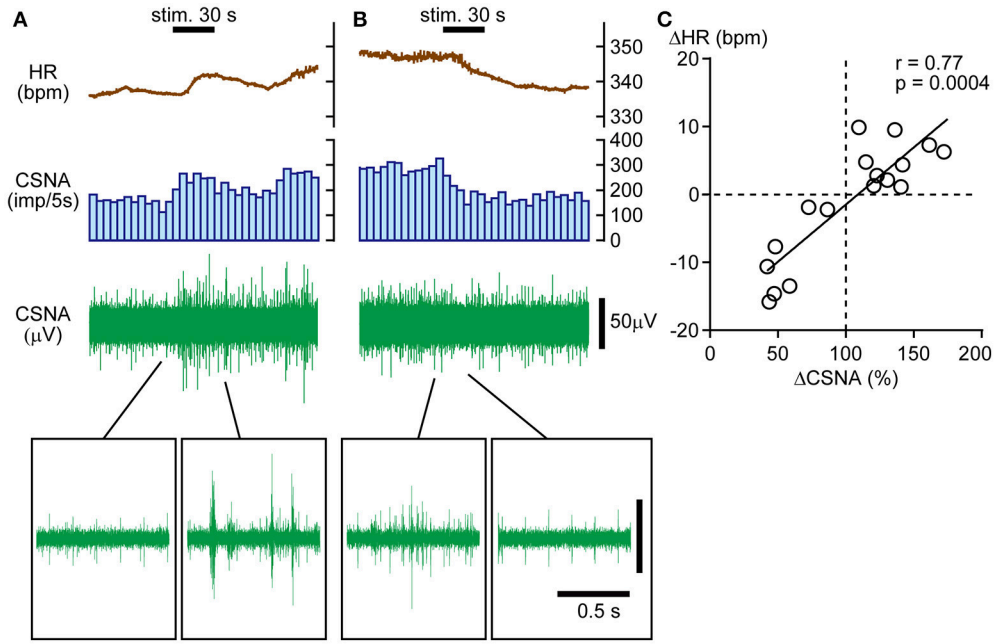

FIGURE 2 | Direct association between bidirectional heart rate (HR) and cardiac sympathetic efferent nerve activity (CSNA) changes in response to calf pressure stimulation. (A,B) Sample records showing increased **(A)** or decreased **(B)** CSNA with parallel changes in HR. The histogram illustrates the nerve discharge rate every 5 s. Raw signals are shown in the upper to lower rows. Insets in **(A,B)** show enlarged views of nerve activity. **(C)** Positive correlation between ΔCSNA and ΔHR. *r* = Spearman's correlation coefficient.

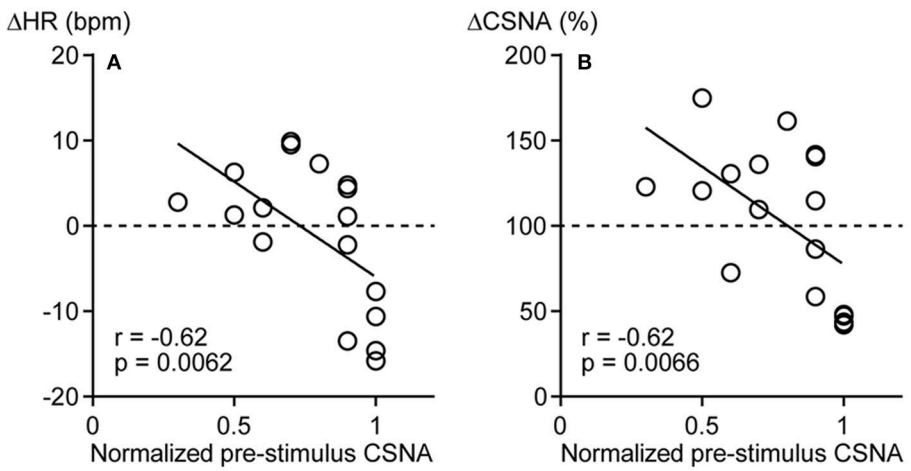

FIGURE 3 | Negative correlations between pre-stimulus cardiac sympathetic efferent nerve activity (CSNA) and changes in heart rate (ΔHR, A) and sympathetic nerve activity (ΔCSNA, B) in response to calf muscle pressure stimulation. The highest frequency value of CSNA across all trials was used to normalize the level of CSNA within each rat and expressed as 1. *r* = Spearman's correlation coefficient.

In the other trial, HR increased immediately after the onset of pinch stimulation and exhibited a larger decrease following the termination of the stimulation (**Figures 4B,C**). Like muscle stimulation, there was a significant negative correlation between pre-stimulus HR and the ΔHR responses to pinch stimulation ($r = -0.75$, $p = 0.0029$; **Figure 4C**).

DISCUSSION

The present results demonstrate that (1) calf muscle pressure stimulation induces tachycardiac or bradycardiac responses by regulating CSNA because HR responses to pressure stimulation in cardiac sympathetic nerve blocked condition were marginal and the direction of the HR change paralleled that of CSNA and

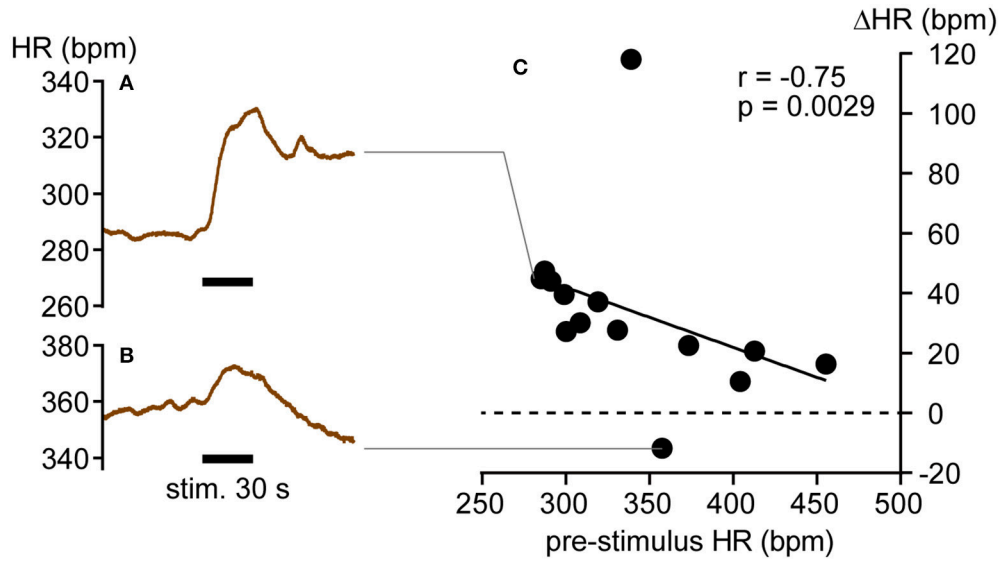

FIGURE 4 | Heart rate responses (ΔHR) to hindpaw pinch stimulation. (A,B) HR increase **(A)** and decrease **(B)** in response to pinch stimulation. **(C)** Negative correlation between individual ΔHR values (closed circles) and pre-stimulus HR. *r* = Spearman's correlation coefficient.

(2) the direction of the HR change is dependent on the tonic level of CSNA, i.e., bradycardia occurs when the tonic activity is high and tachycardia occurs when it is low.

HR Responses to Mechanical Pressure Stimulation of the Calf Muscle Were Mediated by Cardiac Sympathetic Nerves

The present observations that HR responses to calf muscle pressure stimulation were suppressed by cardiac sympathetic nerve block and strongly correlated with CSNA indicate that these responses are mediated predominantly by changes in CSNA. Furthermore, similar results were observed with direct muscle pressure after skin removal, implicating muscle mechanoreceptor afferent in this response and precluding a necessary contribution from cutaneous afferents. Moreover, since HR and blood pressure usually changed in the same direction, the HR responses likely originated from sensory inputs from the calf muscle rather than from a secondary response to blood pressure changes (i.e., baroreflexes).

In contrast to sympathetic nerve, the contribution of vagus nerve appeared negligible because there was no significant influence of vagus nerve transection on the HR response. Tallarida et al. (1981) reported that pressure stimulation of the calf muscles increased HR and this tachycardiac response was blocked by the catecholamine release inhibitor guanethidine in anesthetized vagotomized rabbits. Although, the influence of vagotomy was not reported in their study, presence of the tachycardiac response under vagotomy and blockade by inhibition of postganglionic sympathetic norepinephrine release are fundamentally consistent with our results. However, there remains a possibility that the vagus nerve may contribute to HR responses in the unanesthetized condition because cardiac vagus nerve is more susceptible to anesthetics than sympathetic nerve (Sato et al., 1997). In conscious humans, mechanical muscle stimulation by stretch is considered to increase HR through vagal withdrawal (Gladwell et al., 2005).

Tonic Level of Cardiac Sympathetic Nerve Activity Determines the Direction of the HR Response

The directions of changes in HR and blood pressure induced by muscle stimulation are reported to be affected by experimental conditions such as the depth of anesthesia (Ohsawa et al., 1995; Sato et al., 1997). However, the inhaled concentration of isoflurane was kept constant during data recording in the present study, indicating bidirectional HR responses (bradycardia or tachycardia) to the mechanical pressure stimulation were not due to shifts in anesthesia level. Rather, response direction was dependent on the pre-stimulus HR, which is a function of CSNA. Under isoflurane anesthesia, the resting HR periodically shifted ("step-like changes") during electroencephalogram (EEG) signal pattern changes, i.e., HR increases when EEG bursts occur and decreases when EEG suppression occurs (Yli-Hankala and Jäntti, 1990). Thus, the resting level of neuronal activity in the cardiovascular center may also change periodically as manifested by the resting (pre-stimulus) HR level changes observed in the present study. However, a fundamental cause of the large variability in resting HR observed in the present study has not been determined. The range of the resting HR obtained in the present study was similar to that obtained in conscious unstrained rats (Delaunois et al., 2009; Albrecht et al., 2014; Sharp et al., 2014).

Destruction of the sympathetic inputs to the heart markedly reduced pre-stimulus HR variation, although the vagus nerve block had little effect. Thus, sympathetic

inputs are the primary contributor to HR variation under these conditions. A substantial influence of sympathetic nerve block on pre-stimulus HR may be related to the inhibition of noradrenaline release from the postganglionic sympathetic terminals by the cardiac vagus nerve (Vanhoutte and Levy, 1980; Manabe et al., 1991). Thus, eliminating the tonic activity of cardiac sympathetic nerve may suppress a modulatory mechanism for resting HR driven by the vagus nerve.

We assume that the HR responses to the calf pressure stimulation are a supraspinal reflex (Sato et al., 1997). The tonic activity of sympathetic nerves innervating cardiovascular organs is thought to be generated by a core network consisting of neurons in the rostral ventrolateral medulla (RVLM), caudal ventrolateral medulla (CVLM), nucleus of the solitary tract (NTS), hypothalamus, and spinal cord (Campos and McAllen, 1997; Dampney et al., 2003; Horiuchi et al., 2004; Guyenet, 2006). Although, the central projections of pressure-sensitive muscle afferents have not been determined, muscle afferent information reportedly reaches the RVLM, CVLM, NTS, and hypothalamus (Terui et al., 1987; Kannan et al., 1988; Degtyarenko and Kaufman, 2006; McCord and Kaufman, 2010). Further, electrical stimulation to muscle afferents excited CVLM neurons and subsequently inhibited RVLM neurons (Ruggeri et al., 1995). Therefore, the direction of the HR response may be determined by the balance of excitatory and inhibitory effects on RVLM neurons. For example, at a relatively high level of RVLM neuron activity and concomitantly high CSNA, further enhancement of RVLM neuron activity by muscle afferent input may be limited due to a ceiling effect. This assumption is supported by the present result that the tachycardiac response to pinch stimulation was attenuated when pre-stimulus HR was relatively high (**Figure 4**). Hence, inhibition on RVLM neurons via CVLM neuron excitation can be dominant, leading to decreases in CSNA and HR. Conversely, when RVLM neuron activity and CSNA are low, pressure stimulation may be more likely to increase RVLM excitation, resulting in higher CSNA and HR.

It has been reported that resting HR level may also influence the bradycardiac response to acupuncture stimulation. Although, the afferent types may differ from those activated by mechanical pressure, there may be common mechanisms. Imai and Kitakoji (2003) showed that the degree of bradycardia induced by acupuncture stimulation in healthy volunteers was greater while sitting than when in the supine position, and sitting is associated with higher resting HR. On the other hand, an inhibitory effect of acupuncture-like stimulation on HR was attenuated by hypercapnia, which increases the tonic level of CSNA (Uchida et al., 2010). Therefore, HR response to somatosensory stimulation may differ, depending on the tonic CSNA level and resting HR.

Types of Somatosensory Stimulation Elicited by Calf Mechanical Pressure

In the present study, mechanical stimulation was applied to the calf over the skin. Although, this would also activate cutaneous mechanoreceptors, HR responses were inducible even when the skin over the calf was removed. Also, mechanical skin stimulation (including noxious stimulation) applied around the calf induced only a small increase in HR (Kimura et al., 1995). In addition, the pressor response to calf mechanical pressure stimulation was diminished by severing the sciatic nerve (Stebbins et al., 1988), which is the main sensory transmission pathway from calf muscles. A possibility remains that afferents responding to blood vessel distortion elicited by the pressure stimulation may contribute to the cardiovascular responses (Cui et al., 2012).

Based on single unit recordings of group III and IV muscle afferents, the stimulation intensity used in the present study (10 N/cm^2) could be considered either noxious (Berberich et al., 1988) or non-noxious (Hoheisel et al., 2005). Taguchi et al. (2005) stated that it was not possible to classify muscle afferents into low and high thresholds because the mechanical threshold of pressure stimulation is continuous. Hence, we are unable to define the stimulation used in the present study as noxious or non-noxious stimulation. Clinically, the intensity of touch-pressure stimulation for diagnosing myalgia of patients with temporomandibular joint disorders is 1 kg with a finger (Schiffman et al., 2014), estimated at 1 kg/cm^2 ($\approx$10N/cm^2). Also, the pressure pain threshold on the head in healthy adults is $\sim$4 kg/cm^2 (Antonaci et al., 1998). Taken together, the stimulation intensity used in the present study may be non-noxious in animals without injuries. However, caution is necessary when extrapolating data obtained in humans to rats because pressure stimulation to deep tissues may be influenced by the thickness of subcutaneous tissues (Takahashi et al., 2005).

Physiological Significance

We suggest that these cardiovascular responses to mechanical pressure stimulation of skeletal muscles may help control intramuscular pressure through regulation of the blood supply. In this aspect, the role of pressure sensitive mechanoreceptors may differ from those of contraction- and stretch-sensitive mechanoreceptors that increase HR and blood pressure during exercise because an adequate stimulus for each type of mechanoreceptors is different. For example, compartment syndrome is a condition that causes muscle ischemic necrosis resulting from an excessive increase in intramuscular pressure. Because 100 mmHg is approximately equivalent to 1.3 N/cm^2, force loading on muscle tissues is much greater under mechanical pressure stimulation used in the present study. Thus, such a cardiovascular response may protect muscles from potential damage by limiting blood perfusion partly due to regulating cardiac output, thereby preventing muscle edema and subsequently an abnormal intramuscular pressure. This potential function warrants further study.

In summary, the present results suggest that pressure stimulation applied to the calf excites muscle mechanoreceptors, that activate or inhibit CSNA, resulting in changes to HR. The direction of HR responses (tachycardia or bradycardia) to calf stimulation is determined by the

tonic level of CSNA, suggesting that this mechanical stimulation-induced cardiovascular reflex participates in bidirectional feedback regulation of muscle blood supply.

AUTHOR CONTRIBUTIONS

NW contributed to study design, data acquisition, data analysis, data interpretation, and manuscript writing. HH contributed to study design, data acquisition, data interpretation, and manuscript writing. All authors approved the final version of the manuscript and agreed to be accountable for all aspects of the work in ensuring that questions related to the accuracy or integrity of any part of the work are appropriately investigated and resolved.

FUNDING

The present study was supported by JSPS KAKENHI (grant number JP25871216).

ACKNOWLEDGMENTS

The authors would like to thank Professor Mark Stewart for his helpful comments.

SUPPLEMENTARY MATERIAL

The Supplementary Material for this article can be found online at: http://journal.frontiersin.org/article/10.3389/fnins.2016.00614/full#supplementary-material

REFERENCES

Albrecht, M., Henke, J., Tacke, S., Markert, M., and Guth, B. (2014). Influence of repeated anaesthesia on physiological parameters in male Wistar rats: a telemetric study about isoflurane, ketamine-xylazine and a combination of medetomidine, midazolam and fentanyl. *BMC Vet. Res.* 10:310. doi: 10.1186/s12917-014-0310-8

Antonaci, F., Sand, T., and Lucas, G. A. (1998). Pressure algometry in healthy subjects: inter-examiner variability. *Scand. J. Rehabil. Med.* 30, 3–8.

Araki, T., Ito, K., Kurosawa, M., and Sato, A. (1984). Responses of adrenal sympathetic nerve activity and catecholamine secretion to cutaneous stimulation in anesthetized rats. *Neuroscience* 12, 289–299.

Berberich, P., Hoheisel, U., and Mense, S. (1988). Effects of a carrageenan-induced myositis on the discharge properties of group III and IV muscle receptors in the cat. *J. Neurophysiol.* 59, 1395–1409.

Campos, R. R., and McAllen, R. M. (1997). Cardiac sympathetic premotor neurons. *Am. J. Physiol.* 272(2 Pt 2), R615–R620.

Coote, J. H., Hilton, S. M., and Perez-Gonzalez, J. F. (1971). The reflex nature of the pressor response to muscular exercise. *J. Physiol.* 215, 789–804.

Cui, J., McQuillan, P. M., Blaha, C., Kunselman, A. R., and Sinoway, L. I. (2012). Limb venous distension evokes sympathetic activation via stimulation of the limb afferents in humans. *Am. J. Physiol. Heart Circ. Physiol.* 303, H457–H463. doi: 10.1152/ajpheart.00236.2012

Dampney, R. A. L., Horiuchi, J., Tagawa, T., Fontes, M. A. P., Potts, P. D., and Polson, J. W. (2003). Medullary and supramedullary mechanisms regulating sympathetic vasomotor tone. *Acta Physiol. Scand.* 177, 209–218. doi: 10.1046/j.1365-201X.2003.01070.x

Degtyarenko, A. M., and Kaufman, M. P. (2006). Barosensory cells in the nucleus tractus solitarius receive convergent input from group III muscle afferents and central command. *Neuroscience* 140, 1041–1050. doi: 10.1016/j.neuroscience.2006.02.050

Delaunois, A., Dedoncker, P., Hanon, E., and Guyaux, M. (2009). Repeated assessment of cardiovascular and respiratory functions using combined telemetry and whole-body plethysmography in the rat. *J. Pharmacol. Toxicol. Methods* 60, 117–129. doi: 10.1016/j.vascn.2009.07.003

Gibbs, N. M., Larach, D. R., Skeehan, T. M., and Schuler, H. G. (1989). Halothane induces depressor responses to noxious stimuli in the rat. *Anesthesiology* 70, 503–510.

Gladwell, V. F., Fletcher, J., Patel, N., Elvidge, L. J., Lloyd, D., Chowdhary, S., et al. (2005). The influence of small fibre muscle mechanoreceptors on the cardiac vagus in humans. *J. Physiol.* 567(Pt 2), 713–721. doi: 10.1113/jphysiol.2005.089243

Graven-Nielsen, T., Mense, S., and Arendt-Nielsen, L. (2004). Painful and non-painful pressure sensations from human skeletal muscle. *Exp. Brain Res.* 159, 273–283. doi: 10.1007/s00221-004-1937-7

Guyenet, P. G. (2006). The sympathetic control of blood pressure. *Nat. Rev. Neurosci.* 7, 335–346. doi: 10.1038/nrn1902

Hoheisel, U., Unger, T., and Mense, S. (2005). Excitatory and modulatory effects of inflammatory cytokines and neurotrophins on mechanosensitive group IV muscle afferents in the rat. *Pain* 114, 168–176. doi: 10.1016/j.pain.2004.12.020

Horiuchi, J., Killinger, S., and Dampney, R. A. L. (2004). Contribution to sympathetic vasomotor tone of tonic glutamatergic inputs to neurons in the RVLM. *Am. J. Physiol. Regul. Integr. Comp. Physiol.* 287, R1335–R1343. doi: 10.1152/ajpregu.00255.2004

Hotta, H., Schmidt, R. F., Uchida, S., and Watanabe, N. (2010a). Gentle mechanical skin stimulation inhibits the somatocardiac sympathetic C-reflex elicited by excitation of unmyelinated C-afferent fibers. *Eur. J. Pain* 14, 806–813. doi: 10.1016/j.ejpain.2010.02.009

Hotta, H., Watanabe, N., Orman, R., and Stewart, M. (2010b). Efferent and afferent vagal actions on cortical blood flow and kainic acid-induced seizure activity in urethane anesthetized rats. *Auton. Neurosci.* 156, 144–148. doi: 10.1016/j.autneu.2010.04.010

Imai, K., and Kitakoji, H. (2003). Comparison of transient heart rate reduction associated with acupuncture stimulation in supine and sitting subjects. *Acupunct. Med.* 21, 133–137. doi: 10.1136/aim.21.4.133

Kannan, H., Yamashita, H., Koizumi, K., and Brooks, C. M. (1988). Neuronal activity of the cat supraoptic nucleus is influenced by muscle small-diameter afferent (groups III and IV) receptors. *Proc. Natl. Acad. Sci. U.S.A.* 85, 5744–5748.

Kaufman, A., Sato, A., Sato, Y., and Sugimoto, H. (1977). Reflex changes in heart rate after mechanical and thermal stimulation of the skin at various segmental levels in cats. *Neuroscience* 2, 103–109.

Kimura, A., Ohsawa, H., Sato, A., and Sato, Y. (1995). Somatocardiovascular reflexes in anesthetized rats with the central nervous system intact or acutely spinalized at the cervical level. *Neurosci. Res.* 22, 297–305.

Koba, S., Xing, J., Sinoway, L. I., and Li, J. (2008). Sympathetic nerve responses to muscle contraction and stretch in ischemic heart failure. *Am. J. Physiol. Heart Circ. Physiol.* 294, H311–H321. doi: 10.1152/ajpheart.00835.2007

Manabe, N., Foldes, F. F., Töröcsik, A., Nagashima, H., Goldiner, P. L., and Vizi, E. S. (1991). Presynaptic interaction between vagal and sympathetic innervation in the heart: modulation of acetylcholine and noradrenaline release. *J. Auton. Nerv. Syst.* 32, 233–242.

Matsukawa, K., Wall, P. T., Wilson, L. B., and Mitchell, J. H. (1990). Reflex responses of renal nerve activity during isometric muscle contraction in cats. *Am. J. Physiol.* 259(5 Pt 2), H1380–H1388.

Matsukawa, K., Wall, P. T., Wilson, L. B., and Mitchell, J. H. (1994). Reflex stimulation of cardiac sympathetic nerve activity during static muscle contraction in cats. *Am. J. Physiol.* 267(2 Pt 2), H821–H827.

McCord, J. L., and Kaufman, M. P. (2010). "Reflex autonomic responses evoked by group III and IV muscle afferents," in *Translational Pain Research: from Mouse to Man, 1st Edn.,* eds L. Kruger and A. R. Light (Boca Raton, FL: CRC Press), 283–299.

Mense, S., and Meyer, H. (1985). Different types of slowly conducting afferent units in cat skeletal muscle and tendon. *J. Physiol.* 363, 403–417.

Mizumura, K., and Taguchi, T. (2016). Delayed onset muscle soreness: involvement of neurotrophic factors. *J. Physiol. Sci.* 66, 43–52. doi: 10.1007/s12576-015-0397-0

Murphy, M. N., Mizuno, M., Mitchell, J. H., and Smith, S. A. (2011). Cardiovascular regulation by skeletal muscle reflexes in health and disease. *Am. J. Physiol. Heart Circ. Physiol.* 301, H1191–H1204. doi: 10.1152/ajpheart.00208.2011

Ohsawa, H., Okada, K., Nishijo, K., and Sato, Y. (1995). Neural mechanism of depressor responses of arterial pressure elicited by acupuncture-like stimulation to a hindlimb in anesthetized rats. *J. Auton. Nerv. Syst.* 51, 27–35.

Overton, J. M. (1993). Influence of autonomic blockade on cardiovascular responses to exercise in rats. *J. Appl. Physiol.* 75, 155–161.

Paintal, A. S. (1960). Functional analysis of group III afferent fibres of mammalian muscles. *J. Physiol.* 152, 250–270.

Ruggeri, P., Ermirio, R., Molinari, C., and Calaresu, F. R. (1995). Role of ventrolateral medulla in reflex cardiovascular responses to activation of skin and muscle nerves. *Am. J. Physiol.* 268(6 Pt 2), R1464–R1471.

Sato, A., Sato, Y., and Schmidt, R. F. (1981). Heart rate changes reflecting modifications of efferent cardiac sympathetic outflow by cutaneous and muscle afferent volleys. *J. Auton. Nerv. Syst.* 4, 231–247.

Sato, A., Sato, Y., and Schmidt, R. F. (1982). Changes in heart rate and blood pressure upon injection of algesic agents into skeletal muscle. *Pflügers Arch.* 393, 31–36.

Sato, A., Sato, Y., and Schmidt, R. F. (1997). The impact of somatosensory input on autonomic functions. *Rev. Physiol. Biochem. Pharmacol.* 130, 1–328.

Schiffman, E., Ohrbach, R., Truelove, E., Look, J., Anderson, G., Goulet, J. P., et al. (2014). Diagnostic criteria for temporomandibular disorders (DC/TMD) for clinical and research applications: recommendations of the international RDC/TMD consortium network and orofacial pain special interest group. *J. Oral Facial Pain Headache* 28, 6–27. doi: 10.11607/jop.1151

Sharp, J., Azar, T., and Lawson, D. (2014). Effects of a complex housing environment on heart rate and blood pressure of rats at rest and after stressful challenges. *J. Am. Assoc. Lab. Anim. Sci.* 53, 52–60.

Stebbins, C. L., Brown, B., Levin, D., and Longhurst, J. C. (1988). Reflex effect of skeletal muscle mechanoreceptor stimulation on the cardiovascular system. *J. Appl. Physiol.* 65, 1539–1547.

Suzuki, A., Uchida, S., and Hotta, H. (2004). The effects of aging on somatocardiac reflexes in anesthetized rats. *Jpn. J. Physiol.* 54, 137–141. doi: 10.2170/jjphysiol.54.137

Taguchi, T., Sato, J., and Mizumura, K. (2005). Augmented mechanical response of muscle thin-fiber sensory receptors recorded from rat muscle-nerve preparations *in vitro* after eccentric contraction. *J. Neurophysiol.* 94, 2822–2831. doi: 10.1152/jn.00470.2005

Takahashi, K., Taguchi, T., Itoh, K., Okada, K., Kawakita, K., and Mizumura, K. (2005). Influence of surface anesthesia on the pressure pain threshold measured with different-sized probes. *Somatosens. Mot. Res.* 22, 299–305. doi: 10.1080/08990220500420475

Tallarida, G., Baldoni, F., Peruzzi, G., Raimondi, G., Massaro, M., and Sangiorgi, M. (1981). Cardiovascular and respiratory reflexes from muscles during dynamic and static exercise. *J. Appl. Physiol. Respir. Environ. Exerc. Physiol.* 50, 784–791.

Terui, N., Saeki, Y., and Kumada, M. (1987). Confluence of barosensory and nonbarosensory inputs at neurons in the ventrolateral medulla in rabbits. *Can. J. Physiol. Pharmacol.* 65, 1584–1590.

Uchida, S., Hotta, H., Kagitani, F., and Aikawa, Y. (2003). Ovarian blood flow is reflexively regulated by mechanical afferent stimulation of a hindlimb in nonpregnant anesthetized rats. *Auton. Neurosci.* 106, 91–97. doi: 10.1016/s1566-0702(03)00073-0

Uchida, S., Kagitani, F., Watanabe, N., and Hotta, H. (2010). Sympatho-inhibitory response of the heart as a result of short-term acupuncture-like stimulation of the rat hindlimb is not augmented when sympathetic tone is high as a result of hypercapnia. *J. Physiol. Sci.* 60, 221–225. doi: 10.1007/s12576-009-0084-0

Vanhoutte, P. M., and Levy, M. N. (1980). Prejunctional cholinergic modulation of adrenergic neurotransmission in the cardiovascular system. *Am. J. Physiol.* 238, H275–H281.

Vissing, J., Wilson, L. B., Mitchell, J. H., and Victor, R. G. (1991). Static muscle contraction reflexly increases adrenal sympathetic nerve activity in rats. *Am. J. Physiol.* 261(5 Pt 2), R1307–R1312.

Watanabe, N., Piché, M., and Hotta, H. (2015). Types of skin afferent fibers and spinal opioid receptors that contribute to touch-induced inhibition of heart rate changes evoked by noxious cutaneous heat stimulation. *Mol. Pain* 11, 4. doi: 10.1186/s12990-015-0001-x

Yli-Hankala, A., and Jäntti, V. (1990). EEG burst-suppression pattern correlates with the instantaneous heart rate under isoflurane anaesthesia. *Acta Anaesthesiol. Scand.* 34, 665–668.

Conflict of Interest Statement: The authors declare that the research was conducted in the absence of any commercial or financial relationships that could be construed as a potential conflict of interest.

frontiers in Neuroscience

ORIGINAL RESEARCH
published: 21 January 2016
doi: 10.3389/fnins.2015.00520

In silico Therapeutics for Neurogenic Hypertension and Vasovagal Syncope

Tijana Bojić[1]*, *Vladimir R. Perović*[2] and *Sanja Glišić*[2]

[1] Laboratory of Radiobiology and Molecular Genetics-080, Institute of Nuclear Sciences Vinča, University of Belgrade, Belgrade, Serbia, [2] Center for Multidisciplinary Research-180, Institute of Nuclear Sciences Vinča, University of Belgrade, Belgrade, Serbia

Neurocardiovascular diseases (NCVD) are the leading cause of death in the developed world and will remain so till 2020. In these diseases the pathologically changed nervous control of cardiovascular system has the central role. The actual NCV syndromes are neurogenic hypertension, representing the sympathetically mediated disorder, and vasovagal syncope, which is the vagally mediated disorders. Vasovagal syncope, the disease far from its etiological treatment, could benefit from recruiting and application of antimuscarinic drugs used in other parasympathetic disorders. The informational spectrum method (ISM), a method widely applied for the characterization of protein-protein interactions in the field of immunology, endocrinology and anti HIV drug discovery, was applied for the first time in the analysis of neurogenic hypertension and vasovagal syncope therapeutic targets. *In silico* analysis revealed the potential involvement of apelin in neurogenic hypertension. Applying the EIIP/ISM bioinformatics concept in investigation of drugs for treatment of vasovagal syncope suggests that 78% of tested antimuscarinic drugs could have anti vasovagal syncope effect. The presented results confirm that ISM is a promissing method for investigation of molecular mechanisms underlying pathophysiological proceses of NCV syndromes and discovery of therapeutics targets for their treatment.

Keywords: *in silico* analysis, neurocardiovascular diseases, neurogenic hypertension, protein-protein interaction, vasovagal syncope

OPEN ACCESS

Edited by:
James J. Galligan, Michigan State University, USA

Reviewed by:
Lu Liu, University of New South Wales, Australia
Norbert Ikechukwu Nwankwo, University of Port Harcourt, Nigeria

***Correspondence:**
Tijana Bojić
tijanabojic@vinca.rs; bojictijana@gmail.com

Specialty section:
This article was submitted to Autonomic Neuroscience, a section of the journal Frontiers in Neuroscience

Received: *03 September 2015*
Accepted: *24 December 2015*
Published: *21 January 2016*

Citation:
Bojić T, Perović VR and Glišić S (2016) In silico Therapeutics for Neurogenic Hypertension and Vasovagal Syncope. Front. Neurosci. 9:520. doi: 10.3389/fnins.2015.00520

INTRODUCTION

NCVD are the syndromes where autonomic nervous system (Zoccoli et al., 2001; Bojic, 2003) dysfunction plays a dominant etiological role (Goldstain, 2001; Bojic et al., 2012a,b). NCV disorders can be classified as sympathetically mediated disorders (i.e., neurogenic hypertension, NH) vs. vagally mediated disorders (i.e., vasovagal syncope, VVS), though in many disorders both systems are dysfunctional (Goldstain, 2001).

NH is characterized by an increased level of sympathetic nervous activity (SNA) (Fisher and Paton, 2011). SNA is in reciprocal interaction with the number of important systems for the pathophysiological profile of NH, like inflammation, angiotension II system and vascular dysfunction. Recently, due to its potential causal role in the genesis of NH, an emphasis was put on the role of oxidative stress in brain stem structures.

Reactive oxygen spices (ROS) in the brain can be generated in angiotesin II dependent and angiotensin II independent manners. The most studied mechanism for investigating the potential causal treatment of NH is Ang 1-7-MAS receptor-NO mechanism (Zimmerman, 2011). This mechanism counteracts prohypertensive actions of ROS and represents a good choice for investigation of therapeutic candidate by Informational Spectrum Method (ISM).

In the case of VVS, Nucleus Tractus Solitarii (NTS) in the brain stem is stimulated either directly (central VVS) or indirectly (peripheral VVS), provoking an enhancement of vagal tone and withdrawal of SNA tone. This dual response causes a continuum of cardiovascular phenotype responses. At the "vagal end" it leads to the cardioinhibitory type of VVS (bradicardia as a dominant cause of the VVS), while on the "sympathetic end" causes the vasodepressor type of VVS (hypotension as a dominant cause of the VVS). Mixed type of VVS is on the midway between these two extremes.

The treatment of VVS involves a layered approach with a combination of lifestyle changes, physical maneuvers, medications, and implantable devices. The vast majority of patients with VVS can be adequately controlled with non-pharmacological approaches and do not require pharmacological treatment (Raj and Coffin, 2013). There is, however, the minority of patients with refractory and recurrent VVS who can benefit from effective pharmacotherapy.

Since the majority of the VVS patients suffer from mixed and cardioinhibitory type of VVS, we took under consideration the modulation of vagal tone as the *in silico* strategy for the new anti VVS drugs.

The therapy of NH and VVS is far from efficient etiological treatment. The development of new drugs for treatment of NH and VVS is time and money consuming process, which can be accelerated by *in silico* screening of the molecular libraries for candidate novel drugs and by repurposing of approved drugs.

The aim of this study was to apply EIIP/ISM approach to identify candidate neuropeptides and small-molecules for the potential therapeutics of NH and VVS. The study may lead to new insights in the field of neurocardiovascular pharmacotherapy and pathophysiology.

METHODS

The Long Range Molecular Interactions

Current concepts of intermolecular interactions in biological systems are based on the surface complementarity between interacting biomolecules and assumption that the first contact between interacting molecules is achieved accidentally by the thermal motions that cause molecular wander. If proteins are considered as spheres of 18 Å radius (typical of a small protein), and if spheres associate with every contact, without regard to orientation, the diffusion-limited association rate constant, calculated according to Smoluchowski's equation (Smoluchowski, 1916) is 7×10^9 $M^{-1}s^{-1}$. However, before chemical bond formation takes place, reacting molecular regions must be positioned close enough (at a distance of ∼2 Å) and the appropriate atoms must be held in the correct orientation for the reaction that is to follow, because the attractive forces involved in the recognition and binding of molecules include all the weak non-covalent forces. It means that the protein's binding site is only a small fraction (∼0.1%) of the surface area. Taking into account this limitation, the diffusion-limited association rate constant, predicted from a three-dimensional (3D) "random diffusion" model and calculated according Smoluchowski's equation is $\sim 10^6$ $M^{-1}s^{-1}$ for a protein-ligand and $\sim 10^3$ $M^{-1}s^{-1}$ for a protein-protein interaction. Northrup and Erickson have noted that protein-protein association generally occurs at rates that are 10^3–10^4 times faster than would be expected from simple considerations of collision frequencies and strict orientation

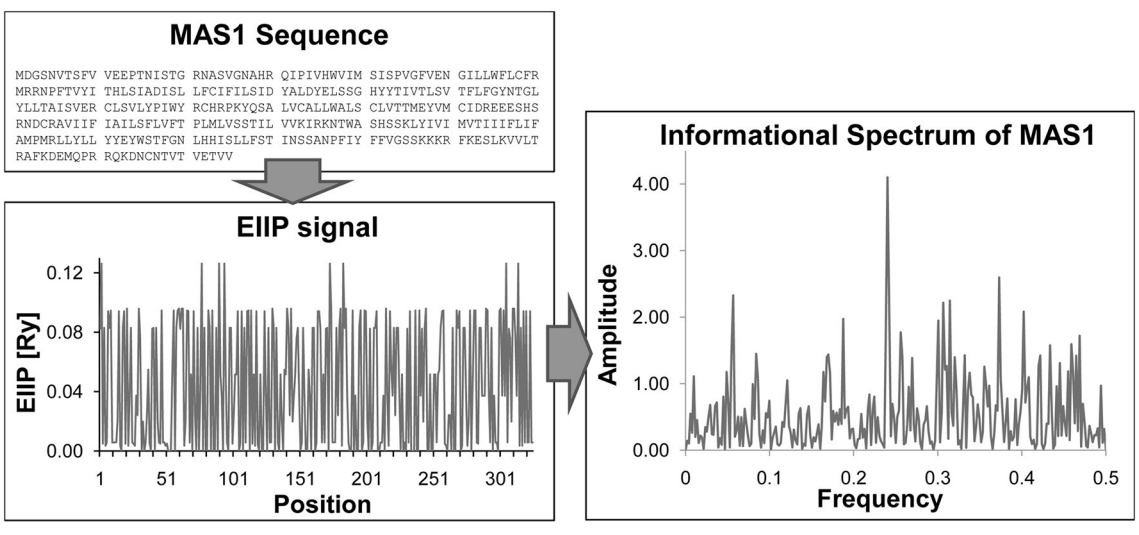

FIGURE 1 | Basic steps of ISM method. Sequence → Transformation of primary protein sequence into sequence of numbers, by assigning of EIIP to each amino acid → Numerical presentation → Discrete Fourier transformation → Informational spectrum (IS).

effects which assume that productive binding occurs only when the molecules collide within 2 Å of their final binding site (Northrup and Erickson, 1992).

Electron-Ion Interaction Potential (EIIP)

In order to overcome the discrepancy between theoretically estimated values and real values of the associated rate constant for a intermolecular interactions in biological systems, the long-range intermolecular interactions (distances between 5 and 1000 A) between interacting molecules was proposed (Veljkovic, 1980). It has been showed that the EIIP and the average quasivalence numbers (AQVN) Z* represent essential molecular descriptors which determines the long-range properties of biological molecules (Veljkovic, 1980). These two molecular descriptors are defined by the following equations:

$$Z^* = \sum^{m} n_i Z_i / N \quad (1)$$

Where:
i, Type of the chemical element;

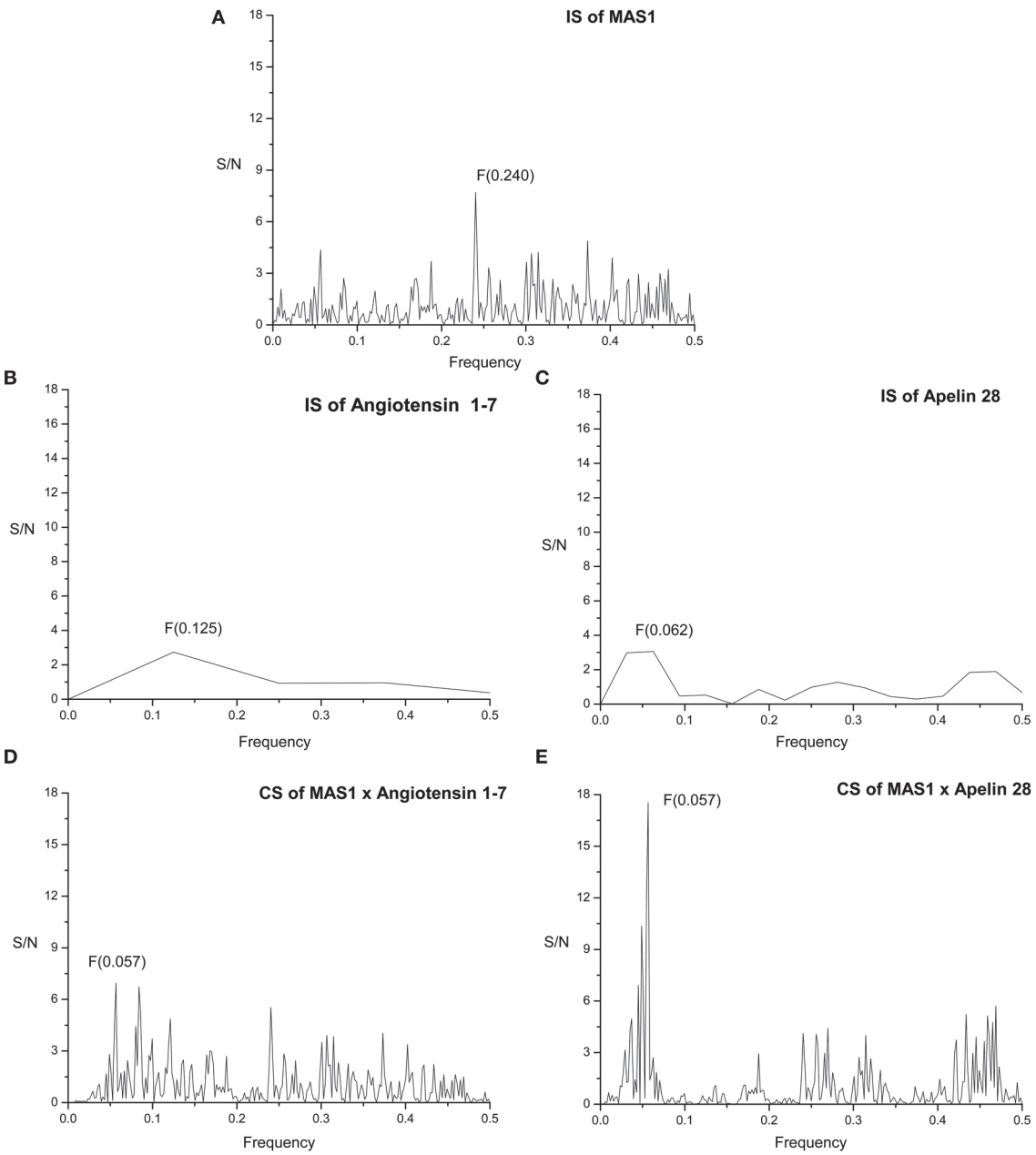

FIGURE 2 | Informational spectrum (IS) of (A) MAS1, (B) angiotensin 1-7, (C) apelin 28, and consensus informational-spectrum (CIS) of (D) MAS1 and angiotensin 1-7 and (E) MAS1 and apelin.

Z, Valence of the ith chemical element;
n, Number of the ith chemical element atoms in the compound;
m, Number of types of chemical elements in the compond;
N, total number of atoms.

$$EIIP = 0.25Z^{*}\sin(1.04\pi Z^{*})/2\pi \quad (2)$$

The EIIP values calculated according to the Equation (2) are in Rydbergs (Ry = 13.6 eV).

Informational Spectrum Method (ISM)

The ISM a virtual spectroscopy method for calculation of the long-range properties of biological macromolecules, is based on

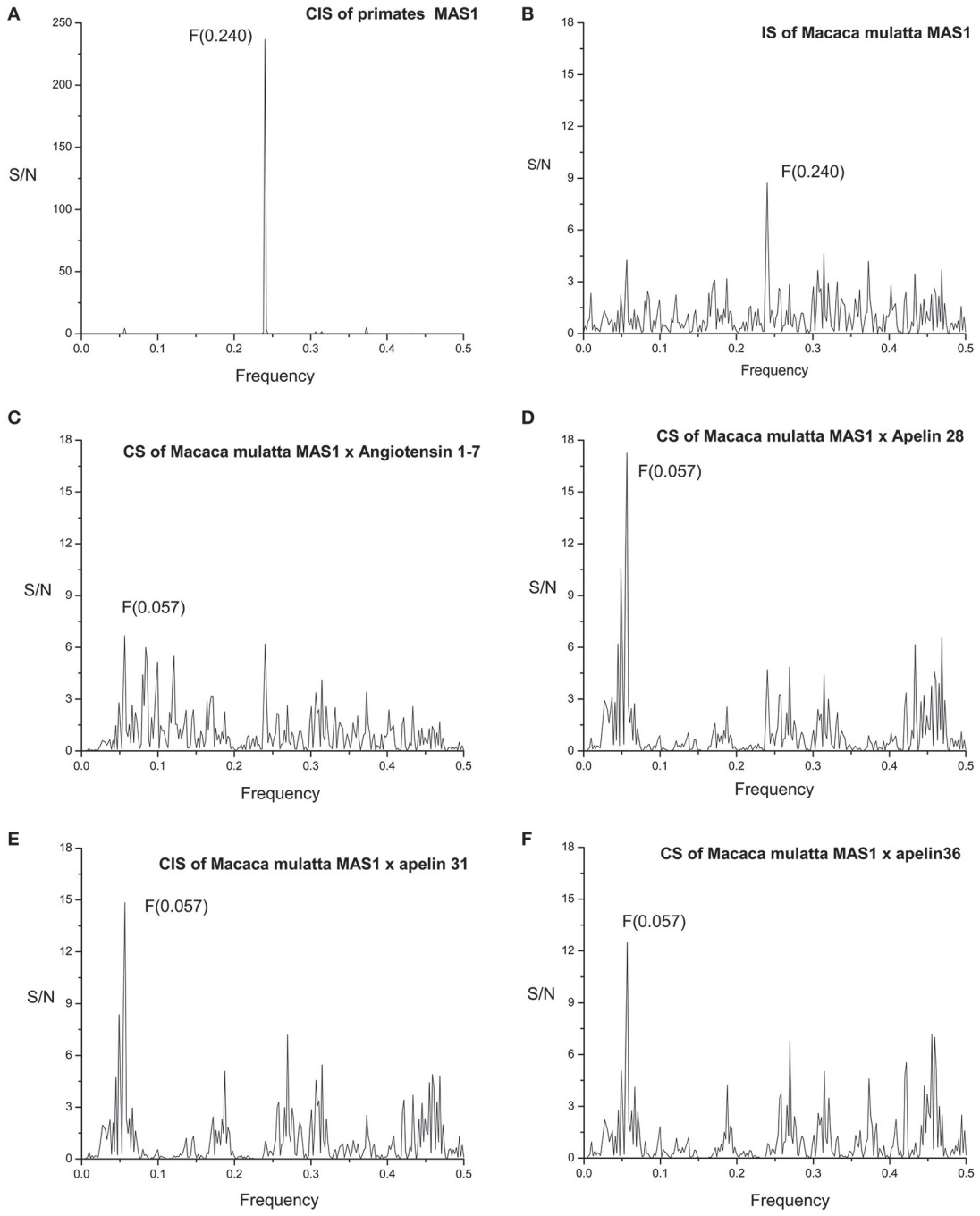

FIGURE 3 | (A) Consensus informational spectrum (CIS) of primates MAS1; **(B)** Informational spectrum (IS) of MAS1 of Macaca mulatta; **(C)** CS of Macaca mulatta MAS1 and angiotensin 1-7 and **(D)** CS of Macaca mulatta MAS1 and apelin 28, **(E)** CS of Macaca mulatta MAS1 and apelin 31 **(F)** CS of Macaca mulatta MAS1 and apelin 36.

a model that assigns to each amino acid a defined parameter describing a physico-chemical property involved in the biological activity of the protein and corresponding to electron-ion interaction potential (EIIP) (Veljkovic et al., 1985).

ISM method consists in three basic steps:

1. Transformation of alphabetic code of primary protein structure into a sequence of numbers representing EIIP of each component.
2. Conversion of numerical sequence by fast Fourier Transformation into information spectrum, which reveals dominant freqency peaks of the whole organic molecule.
3. Consensus Information Spectrum (CIS) analysis between information spectrums of two potentially similar or interactive molecules, which reveales functional locus of the interaction of two molecules.

Peak frequencies in CIS are common frequency components for the analyzed sequences. A measure of similarity for each peak is the signal-to-noise ratio (S/N), the ratio between the signal intensity at one particular IS frequency and the main value of the whole spectrum.

Schematic Presentation of ISM is given in **Figure 1**.

The strong connection between EIIP and Z* molecular descriptors of small molecules and their biological activities (carcinogenisity, antibiotic activity, antiviral activity, toxicity, etc.) has been documented (for review see Veljkovic et al., 2011 and references therein).

The method has been successful in identification of functional protein domains representing candidate therapeutic targets for anti-HIV drugs (Veljkovic et al., 2007), anthrax (Doliana et al., 2008), and human influenza viruses (Veljkovic et al., 2009a,b; Perovic et al., 2013). It is recognized and used in more than 100 research centers worldwide (Veljkovic et al., 2011).

Sequences and Molecular Formulas of Compounds

Sequences were retrieved from UniProt Database with following accession numbers: (a) sequences of primates MAS1: Homo sapiens P04201, Pan troglodytes H2QU00, Macaca mulatta F7GJU7, Pongo abelii H2PL76GN, Chlorocebus sabaeus A0A0D9RJ10, Gorilla gorilla gorilla G3R4L5, Papio anubis A0A096NZT0. (b) sequences of primates Angiotensin 1-7: Homo sapiens P01019, Pan troglodytes H2Q1B7, Macaca mulatta G7MFR4, Gorilla gorilla gorilla Q9GLP6. (C) sequences of primates Apelin: Homo sapiens Q9ULZ1, Macaca mulatta F7GX01, Gorilla gorilla gorilla G3S9L8, Chlorocebus sabaeus A0A0D9R7Q2. Sequences are shown in **Data Sheet 1**.

Molecular formulas of compounds: muscarinic modulators from US Patent 7786308, US Patent 7378447US, and Patent Application 20100311746A1.

RESULTS

The primary structure of proteins encodes the information represented by the informational spectrum (IS) frequencies that correspond to the protein biological function. Mutually interacting proteins share common information represented by peaks in their cross-spectrum (Veljkovic et al., 2008). IS of human MAS receptor (MAS1) is presented on **Figure 2A**. It contains characteristic peak at the frequency $F_{(0.240)}$.

MAS1 sequences are highly homologous among primates [see Supplementary Material: **Data Sheet 1** and Exported Multiple Sequence Alignment (Edgar, 2004) of MAS1 as artwork using Jalview (Waterhouse et al., 2009; **Image 1**)]. Informational spectrum (IS) of MAS1 of Macaca mulatta (**Figure 3B**) and consensus informational spectrum (CIS) of MAS1 of primates are shown in **Figure 3A**. It can be seen that information represented by the CIS frequency $F_{(0.240)}$, is evolutionary conserved among

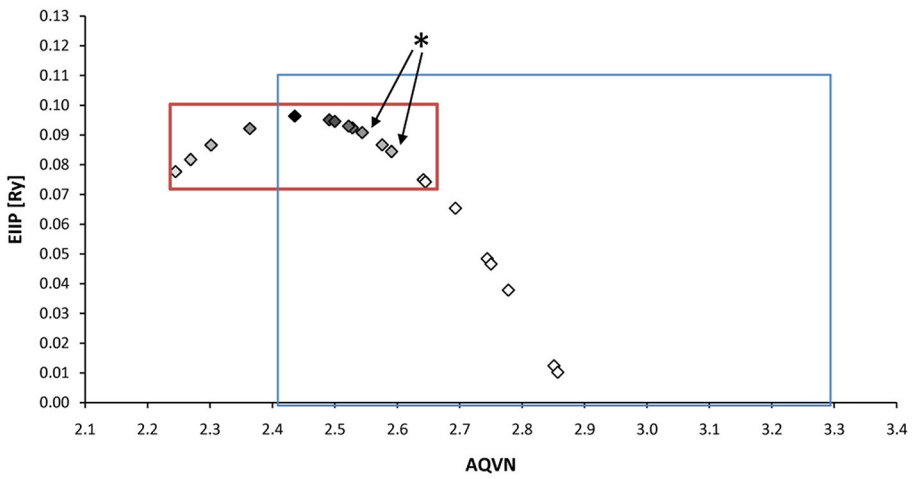

FIGURE 4 | Schematic presentation of the EIIP/AQVN criterion for selection of candidate antimuscarinic drugs with potential therapeutic effect on VVS. Active domain (red): AQVN (2.25–2.65), EIIP (0.074–0.096). Chemical space (blue) AQVN (2.40–3.30) EIIP (0.000–0.116) EIIP/AQVN domain of homologous distribution of >90% compounds from PubChem Compound Database. Statistics: inside the active domain: 21 (78%), outside the active domain: 6 (22%). Asterisk (*)-position of atropine and propentheline bromide, known anti VVS drugs, within AQVN/EIIP active domain.

proteins having the same biological function, as it was shown previously (Glisic et al., 2008).

The sequences of peptides Angiotensin 1-7 and Apelins of other primates are the same as the sequences of human peptides (**Data Sheet 1**) and consequently spectra are the same.

Figure 2B represents IS of the of human Angiotensin 1-7 (Ang 1-7). By performing cross-spectral analysis (CS) of MAS receptor and Ang 1-7 we have identified that these two molecules share common information corresponding to the IS frequency $F_{(0.057)}$ (**Figure 2D**). To confirm the reliability of our findings we have performed CS analysis of Macaca mulatta MAS1 and Ang 1-7 and identified the same frequency $F_{(0.057)}$ as dominant and evolutionary conserved (**Figure 3C**).

We further apply ISM analyses to identify new peptide interactors of human MAS1 representing potential candidate therapeutic agents. To identify peptides which share the common information represented by the frequency component $F_{(0.057)}$, 270 human peptides of the Human Neuropeptide sequence database (Kim et al., 2011) were screened by ISM and peptide apelin 28 (**Figure 2C**) was found to be among the peptides with the highest amplitudes and Signal/Noise values at the frequency $F_{(0.057)}$ in CIS with MAS1 (**Figure 2E**). Similar results were obtained for apelin-31 and apelin-36. In further analysis it was shown that the information represented by CS frequency for Macaca mulatta MAS receptor and apelins is the same (**Figures 3D–F**). According to the IS criterion these peptides are the potential candidate interactors of MAS1. Presented results indicate apelin as potential modulator of MAS1 receptor and novel candidate for treatment of NH.

With respect to the muscarinic antagonists applied in the therapy of VVS (atropine, propanteline bromide, and scopolamine), on the basis of AQVN/EIIP analysis we analyzed the distribution of other muscarinic antagonists which are not tested for their efficacy in the treatment of VVS (**Figures 4**, **5**). The analysis revealed that 78% of tested drugs are in the active AQVN/EIIP domain, implying that there is consistent number of known antimuscarinic drugs that might have a therapeutic impact on VVS.

We also analyzed muscarinic receptor modulators from three patents which are randomly selected among more than 30,000 patents from the patent database (http://www.freepatentsonline.com), in order test the suitability of the proposed EIIP/AQVN filter. Results of this analysis are presented in **Table 1**. As can

Compound	Formula	AQVN	EIIP [Ry]
Dicyclomine	$C_{19}H_{35}NO_2$	2.245	0.0777
Procyclidine	$C_{19}H_{30}ClNO$	2.269	0.0817
Trihexyphenidyl/Benzhexol	$C_{20}H_{31}NO$	2.302	0.0866
Tolterodine	$C_{22}H_{31}NO$	2.364	0.0922
Ipratropium	$C_{20}H_{30}BrNO_3$	2.436	0.0964
Oxybutynin	$C_{22}H_{31}NO_3$	2.491	0.0951
Diphenhydramine	$C_{17}H_{21}NO$	2.5	0.0946
Benzatropine	$C_{21}H_{25}NO$	2.5	0.0946
Cyclopentolate	$C_{17}H_{25}NO_3$	2.522	0.093
Hydroxyzine	$C_{21}H_{27}ClN_2O_2$	2.528	0.0924
Propantheline bromide(Yu, 1997)	$C_{23}H_{30}NO_3$	2.544	0.0908
Mebeverine	$C_{25}H_{35}NO_5$	2.576	0.0867
Atropine (Santini 1999)	$C_{17}H_{23}NO_3$	2.591	0.0844
Solifenacin	$C_{23}H_{26}N_2O_2$	2.642	0.075
Darifenacin	$C_{28}H_{30}N_2O_2$	2.645	0.0742
Tropicamide	$C_{17}H_{20}N_2O_2$	2.693	0.0654
Scopolamine (Lee 1996)	$C_{17}H_{21}NO_4$	2.744	0.0484
Aclidinium bromide	$C_{26}H_{30}BrNO_4S_2$	2.75	0.0466
Flavoxate	$C_{24}H_{25}NO_4$	2.778	0.0378
Pirenzepine	$C_{19}H_{21}N_5O_2$	2.851	0.0124
Tiotropium	$C_{19}H_{22}BrNO_4S_2$	2.857	0.0102

FIGURE 5 | The list of antimuscarinic drugs tested for their AQVN/EIIP. Shaded fields- antimuscarinic drugs within the active domain (**Figure 3**), white fields-antimuscarinic drugs out of the active domain, bordered fields- antimuscarinic drugs tested for their therapeutical effect on VVS. Probability for the anti VVS activity of muscarinicdrugs, assessed by EIIP/AQVN criterion, is represented with the gray scale (black-the highest probability, white-the lowest probability).

be seen, all patented compounds are located within the active EIIP/AQVN domain (**Figure 4**).

DISCUSSION

Brain oxidative stress/status defines the state of sympathoexcitation (increased level of ROS) or sympathoinhibition (the effect of NO), via angiotensinergic neurons (Zimmerman, 2011). Since oxidative injury contributes also to the progressive development of NH, targeting oxidative stress may represent one of promising therapeutic strategies for NH treatment.

The ISM analysis identified three forms of apelin as the potential candidates-interactors of MAS receptor on neurons in brainstem sympathetic centers and indicated apelin as potential modulator of MAS1 receptor and novel candidate for treatment of NH (**Figure 6**). There is lot of recent evidence of the role of apelin as therapeutic agent in protection of the brain against ischemic/reperfusion injury (Yang et al., 2015b), promotion of neurological function recovery after ischemic brain injury (Gu et al., 2013) and potential to cure acute and chronic neurological diseases (Cheng et al., 2012). Synthetic and biased agonists of apelin have been also developed and latter have shown in proof-of-concept studies clinical potential (Yang et al., 2015a). Apelin is adipokine secreted by peripheral tissues but also present in the hypothalamic neurons, having a major impact on the genesis and progression of diabetes (Drougard et al., 2014). This impact is obtained through ROS impact on sympathetic neuronal centers in the diencephalon which cause sympathoexcitation and consequently, the liver glycogenolysis and glusoneogenesis. Our data for the first time point on the potential role of apelin in the development of NH, again, through the action of ROS on sympathetic neuronal centers. Differently from other studies that investigate majorly apelin-APJ receptor signaling pathway (Chun et al., 2008; Yu et al., 2014) our analysis points on the novel mechanism, the apelin-MAS receptor dependent mechanism that could counterbalance sympathostimulating action of ROS. On the basis of the data in the literature (Chun et al., 2008; Yu et al., 2014) and on the basis of our results, there is high probability that apelin has sympathoinhibiting, anti ROS action also on the brainstem level. Further *in vitro* and *in vivo* studies that would elucidate the functional significance of apelin-MAS receptor interaction are needed. This finding could be of importance in designing a novel therapeutics for NH, but also for better understanding and treatment of the states like metabolic syndrome, where diabetes, hypertension, obesity, and obstructive sleep apnea occur in a cluster (Katsiki et al., 2014).

Muscarinic antagonists that were already tested for their efficacy in the treatment of VVS were:

1. atropine(*i.v.*), shown to be fully effective in the cardio-inhibitory form of tilt-induced vasovagal reflex, but with limited action in the vasodepressor form (Santini et al., 1999),

TABLE 1 | EIIP/AQVN values of patented muscarinic modulators: Muscarinic modulators (US Patent 7786308), Muscarinic agonists (US Patent 7378447), and Modulators of muscarinic receptors (US Patent Application 20100311746A1).

EIIP [RY]	AQVN	Chemical formula	Compound
Patent title: Muscarinic modulators (US Patent 7786308			
0.0845	2.590	C23H31FN2O4	ethyl 3-(4-(4-fluorophenyl)(methoxycarbonyl) amino)piperidin-1-yl)-8-azabicyclo[3.2.1]octane-8-carboxylate
0.0886	2.562	C23H33FN4O3	3-{4-[1-(4-Fluoro-phenyl)-3,3-dimethyl-ureido]-piperidin-1-yl}-8-aza-bicyclo[3.2.1]octane-8-carboxylic acid ethyl ester
0.0946	2.500	C27H38FN3O3	3-{4-[Cyclohexanecarbonyl-(4-fluoro-phenyl)-amino]-piperidin-1-yl}-8-aza-bicyclo[3.2.1]octane-8-carboxylic acid ethyl ester
0.0985	2.444	C23H35N3O2	3-[4-(ethyl-phenyl-amino)-piperidin-1-yl]-8-azabicyclo[3.2.1]octane-8-carboxylic acid ethyl ester
0.0899	2.552	C21H30FN3O3	4-[Acetyl-(4-fluoro-phenyl)-amino]-[1,4′]bipiperidinyl-1′-carboxylic acid ethyl ester
Patent title: Muscarinic agonists (US Patent 7378447)			
0.0985	2.618	C19H29N3O4	Carbamic acid tert-butyl ester (R)-(6-(1-(morpholin-4-yl)ethylideneamino)-2(R)-hydroxyindan-1-yl)amide
0.0963	2.431	C22H36BrN3O3	Biphenyl-4-carboxylic acid (R)-(6-(1-(2-methoxyethyl)methylamino)ethylideneamino)-2(R)-hydroxyindan-1-yl)amide
0.0863	2.579	C31H39N3O3	Biphenyl-1-carboxylic acid (R)-(6-(1-(2-pentoxyethyl)methylamino)ethylideneamino)-2(R)-hydroxyindan-1-yl)amide
0.0958	2.622	C31H37N3O3	Biphenyl-4-carboxylic acid (R)-(6-(1-(2-tert-butoxyethyl)methylamino)ethylideneamino)-2(R)-hydroxyindan-1-yl)amide
Patent title: Modulators of muscarinic receptors (US Patent Application 20100311746A1)			
0.0758–0.0985	2.390–2.638		1041 compounds

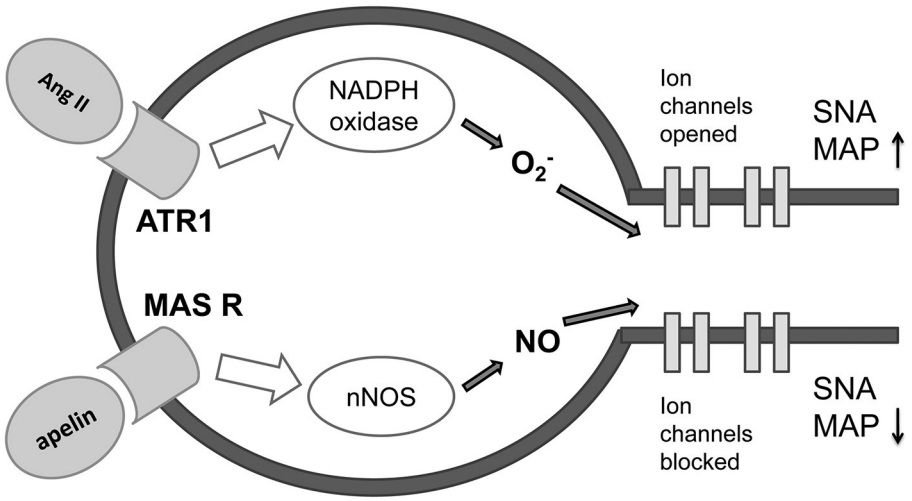

FIGURE 6 | Proposed mechanism of antagonizing effect of apeline-MAS receptor and Angiotensin II-ATR1 molecular signaling pathways on preganglionic sympathetic neurons in the brainstem (adapted from Northrup and Erickson 1992.) Ang II, angiotensin II; ATR1, angiotensin 1 receptor; MAS R, MAS receptor; O2, superoxide; NO, nitric oxide; nNOS, neural nitric oxide synthase; SNA, sympathetic nervous activity; MAP, mean arterial pressure.

2. propantheline bromide (*p.o.*), shown to be highly effective in preventing VVS. In addition, propantheline bromide's effectiveness is present in the vasodepressor VVS and supports a role of direct cholinergic control of vascular tone (Yu and Sung, 1997),
3. scopolamine (*t.d.*), which showed no effect on VVS (Lee et al., 1996).

An AQVN/EIIP approach for new candidates in pharmacotherapy of VVS reveals that on the basis of their molecular properties, the majority of antimuscarinic drugs (78% of investigated substances) might have therapeutical potential for VVS (**Figures 4**, **5**). More, the remaining 22% were out of AQVN/EIIP active domain, together with scopolamine, the drug that failed to show anti VVS therapeutical effect (**Figure 4**). Best candidates, identified by AQVN/EIIP approach, for future clinical studies are hydroxysine and cyclopentoate (**Figure 5**). The suitability of our method was further confirmed by the finding that all muscarinic modulators patented in three patents randomly selected among more than 30,000 patents from the patent database (http://www.freepatentsonline.com) have AQVN/EIIP values within AQVN/EIIP active domain (**Table 1**, **Figure 4**).

CONCLUSION

Computer-aided design techniques based on the long-range intermolecular interactions offer an insight into therapeutical and pathophysiological aspects of NH and VVS. These bioinformatics approaches also open a promising path for molecular investigation of other NCVD and could be of help in design of *in vitro* and *in vivo* animal and clinical studies of these diseases.

AUTHOR CONTRIBUTIONS

TB, VP and SG contributed equally to the conception of the work, acquisition, analysis and interpretation of data. TB, VP, and SG participated in drafting the manuscript, revisiting it critically and gave final approval of the version to be published. The authors reached the agreement to be accountable for all the aspects of the work in ensuring that questions related to the accuracy or integrity of any part of the work are appropriately investigated and resolved.

ACKNOWLEDGMENTS

This work was financed by the Ministry of Education, Science and Technological Development of the Republic of Serbia, project III 41028 and 173001.

SUPPLEMENTARY MATERIAL

The Supplementary Material for this article can be found online at: http://journal.frontiersin.org/article/10.3389/fnins.2015.00520

Data Sheet 1 | Sequences of (a) primates MAS1 (b) sequences of primates Angiotensin 1-7 (c) sequences of primates Apelin 28, Apelin 31, and Apelin 36.

Image 1 | Exported Multiple Sequence Alignment (Edgar, 2004) of MAS1 as artwork using Jalview (Waterhouse et al., 2009).

REFERENCES

Bojic, T. (2003). *Mechanisms of Cardiovascular Control and Effects of Acoustic Stimulation on Cardiovascular System during the Wake-Sleep Cycle*. Ph.D. thesis, Alma Mater Università di Bologna, Bologna.

Bojic, T., Radak, D., Putnikovic, B., Alavantic, D., and Isenovic, E. R. (2012a). Methodology of monitoring cardiovascular regulation: baroreflex and central mechanisms of cardiovascular regulation. *Vojnosanit. Pregl.* 69, 1084–1090. doi: 10.2298/VSP110707019B

Bojic, T., Sudar, E., Mikhailidis, D. P., Alavantic, D., and Isenovic, E. R. (2012b). The role of G protein coupled receptor kinases in neurocardiovascular pathophysiology. *Arch. Med. Sci.* 8, 970–977. doi: 10.5114/aoms.2012.32466

Cheng, B., Chen, J., Bai, B., and Xin, Q. (2012). Neuroprotection of apelin and its signaling pathway. *Peptides* 37, 171–173. doi: 10.1016/j.peptides.2012.07.012

Chun, H. J., Ali, Z. A., Kojima, Y., Kundu, R. K., Sheikh, A. Y., Agrawal, R., et al. (2008). Apelin signaling antagonizes Ang II effects in mouse models of atherosclerosis. *J. Clin. Invest.* 118, 3343–3354. doi: 10.1172/jci34871

Doliana, R., Veljkovic, V., Prljic, J., Veljkovic, N., De Lorenzo, E., Mongiat, M., et al. (2008). EMILINs interact with anthrax protective antigen and inhibit toxin action *in vitro*. *Matrix Biol.* 27, 96–106. doi: 10.1016/j.matbio.2007.09.008

Drougard, A., Duparc, T., Brenachot, X., Carneiro, L., Gouazé, A., Fournel, A., et al. (2014). Hypothalamic apelin/reactive oxygen species signaling controls hepatic glucose metabolism in the onset of diabetes. *Antioxid. Redox Signal.* 20, 557–573. doi: 10.1089/ars.2013.5182

Edgar, R. C. (2004). MUSCLE: multiple sequence alignment with high accuracy and high throughput. *Nucleic Acids Res.* 32, 1792–1797. doi: 10.1093/nar/gkh340

Fisher, J. P., and Paton, J. F. (2011). The sympathetic nervous system and blood pressure in humans: implications for hypertension. *J. Hum. Hypertens.* 26, 463–475. doi: 10.1038/jhh.2011.66

Glisic, S., Arrigo, P., Alavantic, D., Perovic, V., Prljic, J., and Veljkovic, N. (2008). Lipoprotein lipase: a bioinformatics criterion for assessment of mutations as a risk factor for cardiovascular disease. *Proteins* 70, 855–862. doi: 10.1002/prot.21581

Goldstain, D. (2001). *The Autonomic Nervous System in Health and Disease, 1st Edn.* New York, NY: Marcel Dekker, Inc.

Gu, Q., Zhai, L., Feng, X., Chen, J., Miao, Z., Ren, L., et al. (2013). Apelin-36, a potent peptide, protects against ischemic brain injury by activating the PI3K/Akt pathway. *Neurochem. Int.* 63, 535–540. doi: 10.1016/j.neuint.2013.09.017

Katsiki, N., Athyros, V. G., Karagiannis, A., and Mikhailidis, D. P. (2014). Metabolic syndrome and non-cardiac vascular diseases: an update from human studies. *Curr. Pharm. Des.* 20, 4944–4952. doi: 10.2174/1381612819666131206100750

Kim, Y., Bark, S., Hook, V., and Bandeira, N. (2011). NeuroPedia: neuropeptide database and spectral library. *Bioinformatics* 27, 2772–2773. doi: 10.1093/bioinformatics/btr445

Lee, T. M., Su, S. F., Chen, M. F., Liau, C. S., and Lee, Y. T. (1996). Usefulness of transdermal scopolamine for vasovagal syncope. *Am. J. Cardiol.* 78, 480–482. doi: 10.1016/S0002-9149(96)00342-6

Northrup, S. H., and Erickson, H. P. (1992). Kinetics of protein-protein association explained by Brownian dynamics computer simulation. *Proc. Natl. Acad. Sci. U.S.A.* 89, 3338–3342. doi: 10.1073/pnas.89.8.3338

Perovic, V. R., Muller, C. P., Niman, H. L., Veljkovic, N., Dietrich, U., Tosic, D. D., et al. (2013). Novel phylogenetic algorithm to monitor human tropism in Egyptian H5N1-HPAIV reveals evolution toward efficient human-to-human transmission. *PLoS ONE* 8:e61572. doi: 10.1371/journal.pone.0061572

Raj, S. R., and Coffin, S. T. (2013). Medical therapy and physical maneuvers in the treatment of the vasovagal syncope and orthostatic hypotension. *Prog. Cardiovasc. Dis.* 55, 425–433. doi: 10.1016/j.pcad.2012.11.004

Santini, M., Ammirati, F., Colivicchi, F., Gentilucci, G., and Guido, V. (1999). The effect of atropine in vasovagal syncope induced by head-up tilt testing. *Eur. Heart. J.* 20, 1745–1751. doi: 10.1053/euhj.1999.1697

Smoluchowski, M. V. (1916). Versuch einer mathematischen Theorie der Koagulationskinetik kolloider Lösungen. *Phys. Z* 17, 129–168.

Veljkovic, N., Glisic, S., Perovic, V., and Veljkovic, V. (2011). The role of long-range intermolecular interactions in discovery of new drugs. *Expert Opin. Drug. Discov.* 6, 1263–1270. doi: 10.1517/17460441.2012.638280

Veljkovic, N., Glisic, S., Prljic, J., Perovic, V., Botta, M., and Veljkovic, V. (2008). Discovery of new terapeutic targets by the informational spectrum method. *Curr. Protein Pept. Sci.* 9, 493–562. doi: 10.2174/138920308785915245

Veljkovic, V. (1980). *A Theoretical Approach to Preselection of Carcinogens and Chemical Carcinogenesis*. New York, NY: Gordon & Breach.

Veljkovic, V., Cosic, I., Dimitrijevic, B., and Lalovic, D. (1985). Is it possible to analyze DNA and protein sequences by the methods of digital signal processing? *IEEE Trans. Biomed. Eng.* 32, 337–341.

Veljkovic, V., Niman, H. L., Glisic, S., Veljkovic, N., Perovic, V., and Muller, C. P. (2009a). Identification of hemagglutinin structural domain and polymorphisms which may modulate swine H1N1 interactions with human receptor. *BMC Struct. Biol.* 9:62. doi: 10.1186/1472-6807-9-62

Veljkovic, V., Veljkovic, N., Esté, J. A., Huther, A., and Dietrich, U. (2007). Application of the EIIP/ISM bioinformatics concept in development of new drugs. *Curr. Med. Chem.* 14, 441–453. doi: 10.2174/092986707779941014

Veljkovic, V., Veljkovic, N., Muller, C. P., Müller, S., Glisic, S., Perovic, V., et al. (2009b). Characterization of conserved properties of hemagglutinin of H5N1 and human influenza viruses: possible consequences for therapy and infection control. *BMC Struct. Biol.* 9:21. doi: 10.1186/1472-6807-9-21

Waterhouse, A. M., Procter, J. B., Martin, D. M. A., Clamp, M., and Barton, G. J. (2009). Jalview Version 2-a multiple sequence alignment editor and analysis workbench. *Bioinformatics* 25, 1189–1191. doi: 10.1093/bioinformatics/btp033

Yang, P., Maguire, J. J., and Davenport, A. P. (2015a). Apelin, Elabela/Toddler, and biased agonists as novel therapeutic agents in the cardiovascular system. *Trends Pharmacol. Sci.* 36, 560–567. doi: 10.1016/j.tips.2015.06.002

Yang, Y., Lv, S. Y., Lyu, S. K., Wu, D., and Chen, Q. (2015b). The protective effect of apelin on ischemia/reperfusion injury. *Peptides* 63, 43–46. doi: 10.1016/j.peptides.2014.11.001

Yu, J. C., and Sung, R. J. (1997). Clinical efficacy of propantheline bromide in neurocardiogenic syncope: pharmacodynamic implications. *Cardiovasc. Drug. Ther.* 10, 687–692. doi: 10.1007/BF00053025

Yu, X. H., Tang, Z. B., Liu, L. J., Qian, H., Tang, S. L., Zhang, D. W., et al. (2014). Apelin and its receptor APJ in cardiovascular diseases. *Clin. Chim. Acta* 428, 1–8. doi: 10.1016/j.cca.2013.09.001

Zimmerman, M. C. (2011). Angiotensin, I. I., and angiotensin-1-7 redox signaling in the central nervous system. *Curr. Opin. Pharmacol.* 11, 138–143. doi: 10.1016/j.coph.2011.01.001

Zoccoli, G., Andreoli, E., Bojic, T., Cianci, T., Franzini, C., Predieri, S., et al. (2001). Central and baroreflex control of heart rate during the wake-sleep cycle in rat. *Sleep* 24, 753–758.

Conflict of Interest Statement: The authors declare that the research was conducted in the absence of any commercial or financial relationships that could be construed as a potential conflict of interest.

frontiers in Physiology

ORIGINAL RESEARCH
published: 22 January 2018
doi: 10.3389/fphys.2018.00010

An Innovative Technique to Assess Spontaneous Baroreflex Sensitivity with Short Data Segments: Multiple Trigonometric Regressive Spectral Analysis

Kai Li[1,2], *Heinz Rüdiger*[1], *Rocco Haase*[1] *and Tjalf Ziemssen*[1]*

[1] *Autonomic and Neuroendocrinological Lab, Department of Neurology, Center of Clinical Neuroscience, University Hospital Carl-Gustav Carus, Technical University of Dresden, Dresden, Germany,* [2] *Department of Neurology, Beijing Hospital, National Center of Gerontology, Beijing, China*

Objective: As the multiple trigonometric regressive spectral (MTRS) analysis is extraordinary in its ability to analyze short local data segments down to 12 s, we wanted to evaluate the impact of the data segment settings by applying the technique of MTRS analysis for baroreflex sensitivity (BRS) estimation using a standardized data pool.

Methods: Spectral and baroreflex analyses were performed on the EuroBaVar dataset (42 recordings, including lying and standing positions). For this analysis, the technique of MTRS was used. We used different global and local data segment lengths, and chose the global data segments from different positions. Three global data segments of 1 and 2 min and three local data segments of 12, 20, and 30 s were used in MTRS analysis for BRS.

Results: All the BRS-values calculated on the three global data segments were highly correlated, both in the supine and standing positions; the different global data segments provided similar BRS estimations. When using different local data segments, all the BRS-values were also highly correlated. However, in the supine position, using short local data segments of 12 s overestimated BRS compared with those using 20 and 30 s. In the standing position, the BRS estimations using different local data segments were comparable. There was no proportional bias for the comparisons between different BRS estimations.

Conclusion: We demonstrate that BRS estimation by the MTRS technique is stable when using different global data segments, and MTRS is extraordinary in its ability to evaluate BRS in even short local data segments (20 and 30 s). Because of the non-stationary character of most biosignals, the MTRS technique would be preferable for BRS analysis especially in conditions when only short stationary data segments are available or when dynamic changes of BRS should be monitored.

Keywords: baroreflex sensitivity, multiple trigonometric regressive spectral analysis, baroreflex function, data segment, autonomic nervous system

OPEN ACCESS

Edited by:
Tijana Bojić,
Vinča Nuclear Institute, University of Belgrade, Serbia

Reviewed by:
Michal Javorka,
Comenius University, Slovakia
Chloe E Taylor,
Western Sydney University, Australia

***Correspondence:**
Tjalf Ziemssen
tjalf.ziemssen@uniklinikum-dresden.de

Specialty section:
This article was submitted to Autonomic Neuroscience, a section of the journal Frontiers in Physiology

Received: *25 September 2017*
Accepted: *05 January 2018*
Published: *22 January 2018*

Citation:
Li K, Rüdiger H, Haase R and Ziemssen T (2018) An Innovative Technique to Assess Spontaneous Baroreflex Sensitivity with Short Data Segments: Multiple Trigonometric Regressive Spectral Analysis. Front. Physiol. 9:10. doi: 10.3389/fphys.2018.00010

INTRODUCTION

The arterial baroreflex is of fundamental importance for cardiovascular homeostasis, and its impairment may play an adverse role in several diseases (Ziemssen et al., 2013). There is an inverse relation between baroreflex sensitivity (BRS) and the risk of mortality after myocardial infarction, and interventions that improve BRS had beneficial clinical impact on cardiovascular mortality (La Rovere et al., 1988, 2002; La Rovere, 2000).

Numerous non-invasive techniques that analyze the sensitivity of spontaneous baroreflex control of heart rate and blood pressure (BP) have been developed (Bertinieri et al., 1985; Blaber et al., 1995; Ducher et al., 1995; Di Rienzo et al., 2001; Laude et al., 2004; Westerhof et al., 2004; Bernardi et al., 2010; Porta et al., 2013; Svacinova et al., 2015). They differ in their general approaches (analysis in time, frequency, or information domains; causal vs. non-causal analyses) and the applied statistical details (length of data segment analyzed, window technique, number of single BRS-values for analysis). Because of their considerable differences, studies comparing the performance of these methods are needed.

The EuroBaVar study compared 21 methods of BRS analysis (Laude et al., 2004). The multiple trigonometric regressive spectral analysis (MTRS) technique for BRS evaluation had an excellent performance in comparison with the sequence methods and the spectral analysis based on fast Fourier transform. In addition, due to the short local data segments, MTRS is able to analyze BRS in short dynamic ECG and BP recordings.

BRS-values are non-stationary and profoundly variable. We therefore shorten the window for BRS analysis. For the MTRS technique, there are two relevant types of data segments, the local and the global data segments. Each trigonometric regressive spectral analysis (TRS) spectrum is only performed within a local data segment; analyses of local data segments are repeated in successive segments shifted by one, two, or more beats within the whole global data segment (multiple TRS analysis, so called MTRS) (Rüdiger et al., 1999; Ziemssen et al., 2013). In a local data segment of 25 s, even the longest oscillation of the low frequency (LF) band can be reliably determined, but additional longer oscillations could not be accurately detected. Certainly, oscillations in the high frequency (HF) band can be well characterized in this time window. However, because of their short wavelengths, oscillations in the HF band or ultra-high frequency (UHF) band can slightly change in frequency and amplitude using a local data segment of 25 s. Therefore, there is always a compromise in the selection of the local data segment length. We have applied different lengths of local and global data segments according to the research conditions (Wright et al., 2009; Friedrich et al., 2010; Reimann et al., 2010, 2012, 2013; Gasch et al., 2011; Viehweg et al., 2016; Li et al., 2017). The most commonly used lengths of local and global data segments were 30 s and 2 min, respectively, but shorter lengths have also been applied. Until now, the effect of the lengths of local and global data segments on the BRS estimation remains unclear, and the reproducibility of selecting different global data segments in the same recording is unknown. In the present study, we aimed to investigate the influence of different local and global data segment settings on BRS assessment using the EuroBaVar dataset, which is comprised of a heterogeneous population.

SUBJECTS AND METHODS

The EuroBaVar Dataset

At first, this dataset was used as part of the EuroBaVar study to compare estimates of the BRS obtained by different research laboratories, each using its own software (Laude et al., 2004). The dataset included 46 recording files obtained from a heterogeneous population of 21 subjects. There are four duplicate recording files from two subjects (two lying recordings and two standing recordings). Thus a total of 42 recordings were analyzed in the present study. The participants (17 women, 4 men) were composed of 12 normotensive outpatients (including one diabetic patient without cardiac neuropathy, 2 treated patients with hypercholesterolemia, and one 3-month pregnant woman), one untreated hypertensive patient, two treated patients with hypertension, four healthy volunteers, and two patients with evident cardiac autonomic failure (one patient with diabetic neuropathy and the other patient recently underwent heart transplantation). All the participants underwent continuous non-invasive BP monitoring and ECG recording. These recordings were made for 10–12 min both in the supine position and in the upright position. Data were provided as the BP and ECG signals sampled at 500 Hz with a 16-bit resolution. This is a heterogeneous population characterized by a large range of BRS-values, and can thoroughly evaluate the performance of different BRS calculation methods. This challenging dataset is appropriate for measuring the consistency of BRS obtained by MTRS using different local and global data segment settings. The EuroBaVar data are from the EuroBaVar study, and publicly available for methodological studies on BRS analysis. The study was approved by the Paris-Necker committee and all the subjects had given informed consent.

The MTRS Analysis

In 1999, Rüdiger and colleagues introduced TRS, which detects true, physiological oscillations and guarantees an optimal assessment of the measured RR intervals and other parameters (Rüdiger et al., 1999). All oscillations are captured based on the following condition $\sum (RRI(t(i)) - Reg(t(i)))^2 => \text{minimum}$, with RRI(t(i)) being the original RR intervals and $Reg(t(i)) = A * \sin(\omega t(i) + \varphi(i))$ being a trigonometric function of the parameters A (amplitude), ω (frequency), and ϕ (phase shift). This trigonometric function cannot be solved as none of the three parameters in the regressive function is known. Therefore, it is necessary to set one parameter, in general the frequency ω. By the variation of this frequency ω, oscillations can be calculated with an optimal variance reduction for all target frequencies.

Computation of BRS Using MTRS

The baroreflex provides a rapid feedback loop to keep cardiovascular homeostasis. For example, an increased BP reflexively leads to a decrease of the heart rate in order

to keep the homeostasis of BP. This feedback loop works continuously during the constant fluctuations of heart rate and BP. This is the theoretical foundation of MTRS based BRS measurement.

As mentioned above, the MTRS technique uses the oscillations of SBPs and RRIs instead of their original values which are used in the sequence methods. Therefore, coherent pairs of SBP and RRI oscillations are identified, which can be correlated with one another (Gasch et al., 2011; Ziemssen et al., 2013) (**Figure 1**). The frequency distribution of individual BRS-values within two different 2-min global data segments are shown in **Figure 2**. The coherence of RRI and SBP oscillation pairs was determined by their frequencies and phase shifts. Using the TRS technique, oscillation pairs are considered coherent when the frequency difference is $\leq$0.025 Hz.

Let V_SYS (i) the variance reduction of the i-th coherent systolic BP oscillation and V_RR (i) be the variance reduction of the i-th coherent RR interval oscillation, then a variance ratio can be defined according to the following equations:

$$\text{Ratio(i)} = \text{V\_RR(i)/V\_SYS(i) for V\_RR(i)} <= \text{V\_SYS (i) or}$$
$$\text{Ratio(i)} = \text{V\_SYS(i)/V\_RR (i) for V\_RRr (i)} > \text{V\_SYS (i)}$$

This ratio can be defined for each coherent oscillation pair (i), 0 <Ratio <= 1. With all the oscillation ratios, BRS can be determined.

During the shift of the local data segments by one, two or more beats, these coherent oscillation pairs change in frequency and amplitude. Therefore, with a local data segment of 25 s, all oscillations other than the VLF band are contained at least once, and the number of individual values can be significantly increased by shifting this small data segment over a global data segment of one or more minutes.

This MTRS technique has been further developed and improved after its application in the EuroBaVar study (Ziemssen et al., 2008). In the calculations of BRS in the EuroBaVar study, all individual values have been arithmetically averaged; a weighted mean is now determined according to the following relationship:

$$\text{BRS\_opt} = \left(\sum \text{BRS(i)}^{*}\text{V\_ratio(i)}^{2}\right)/\sum \text{V\_ratio(i)}^{2}$$

With the squaring function, an even stronger weight is placed on values close to V_ratio = 1. This reduces the influence of inconsistent BP and RR interval fluctuations (such as small BP fluctuations corresponding with large RR interval fluctuations)

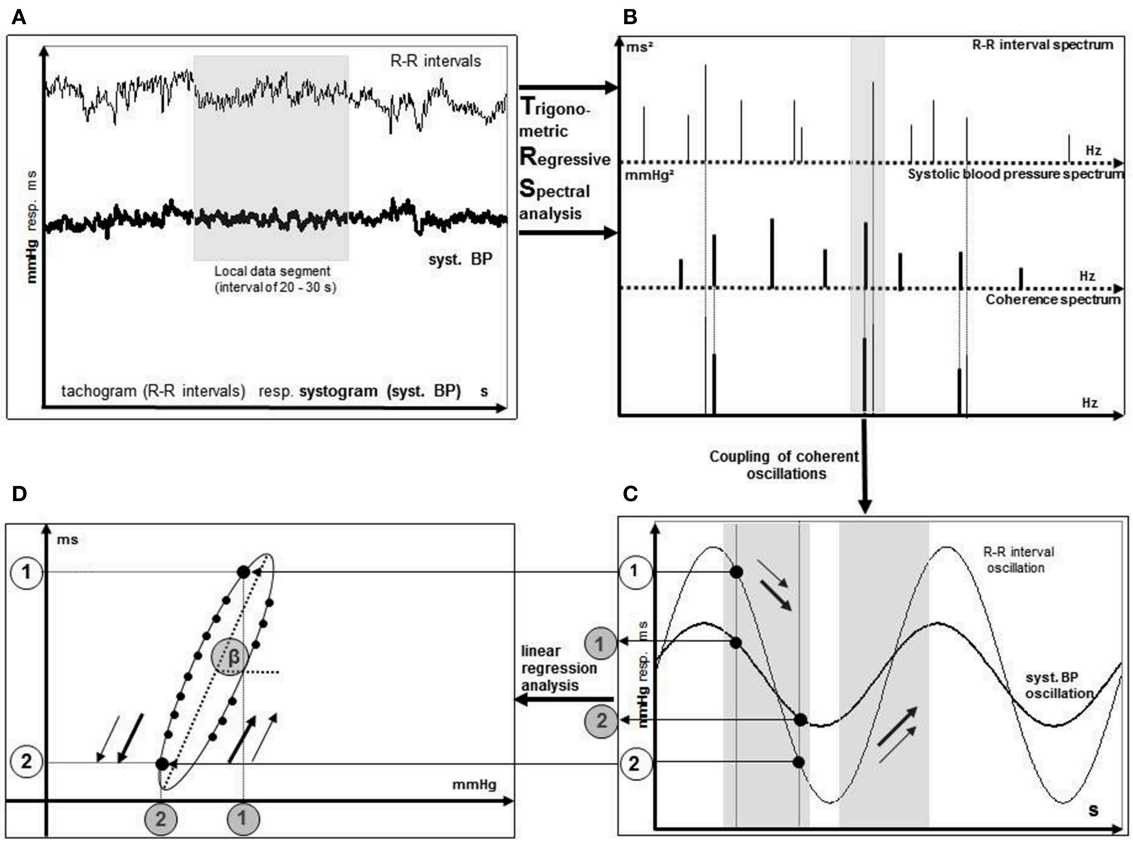

FIGURE 1 | Illustration of the BRS calculation process using TRS. Spontaneous oscillations of RR intervals and systolic blood pressure **(A)** are replaced by theoretical TRS oscillations **(B)**. Calculation of BRS as the slope of the regression line **(D)** originates from coherent oscillation pairs of RR interval and systolic blood pressure **(C)**. Points 1 and 2 are two examples of coherent oscillation pairs of RR intervals and systolic blood pressures. [Taken from Gasch et al. (2011)].

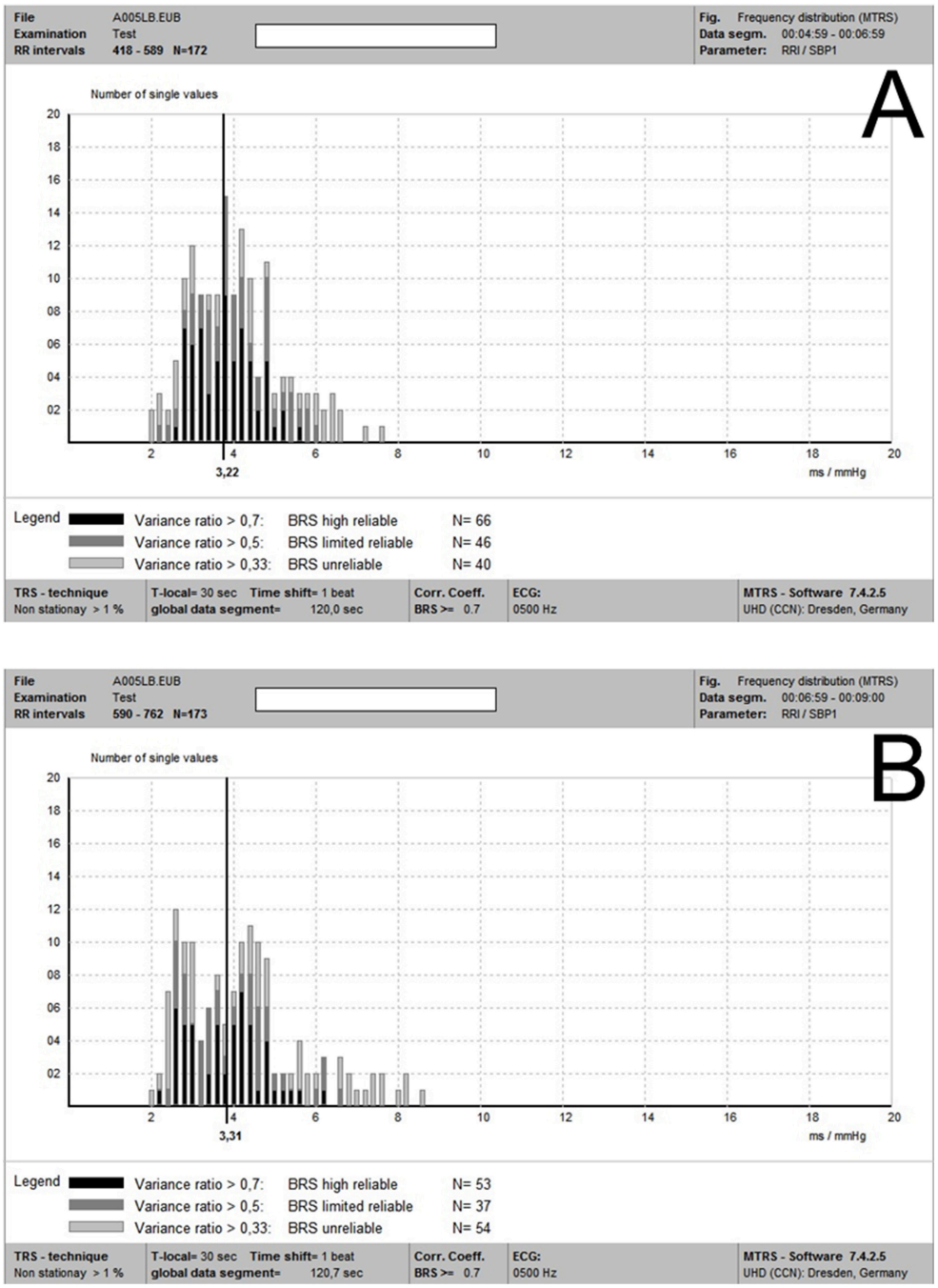

FIGURE 2 | (A,B) Individual BRS-values within two different 2-min global data segments (2a and 2b, respectively) in the same recording. It is noted that although there was some degree of variability of individual local BRS-values between these two global data segments, these two mean global BRS-values were quite close.

on the BRS calculation, because this phenomenon apparently does not reflect a baroreflex.

BRS Analyses Using Varying Local and Global Data Segments:

We used different local and global data segment settings for each recording. To assess the influence of different local data segment lengths, we calculated the BRS of a common 1-min global ECG and BP segment (1a) using local data segments of 12, 20, and 30 s, respectively. To explore the influence of the length of global data segments, we additionally computed BRS from a 2-min global data segment (2a) which extended 1 min from the aforementioned 1-min global data segment (1a) (the 1-min segment 1a was included in the 2-min segment 2a). To

test the stability of BRS analysis using MTRS, we calculated BRS from another 2-min ECG and BP data segment (2b), which had no overlap with the other two global data segments (1a and 2a). We used a common length (30 s) of local data segments when comparing BRS-values computed from different global data segments (1a, 2a, and 2b).

Statistical Analysis

All statistical analyses were performed using SPSS for Windows (Version 23.0. Armonk, NY: IBM Corp). Data are presented as mean ± standard deviation unless stated otherwise. The Kolmogorov–Smirnov test was used to evaluate data normality. Repeated measures ANOVA or Friedman's test was employed to test differences between BRS-values obtained with different settings of data segments.

To compare the BRS estimates from different local and global data segments, we performed Spearman correlation and the Bland-Altman plot. The differences between the pairs of measurements (e.g., $BRS_{2a}-BRS_{2b}$) on the vertical axis were plotted against the means of each pair [e.g., $(BRS_{2a}+BRS_{2b})/2$]. The Bland-Altman analysis requires that the differences should be normally distributed. Logarithmic (ln) transformation of the original BRS data was used if the differences of the BRS-values were not normally distributed and the logarithmic transformation solved this problem. To determine the potential proportional bias, we performed the Spearman correlation between the differences of the pairs and their means. We also calculated the 95% confidence intervals of the differences (also called limits of agreement) (Bland and Altman, 1986; Giavarina, 2015). $P \leq 0.05$ were considered statistically significant.

RESULTS

Comparisons between BRS Obtained Using Different Local and Global Data Segments

Friedman's test was used for comparisons between different data segment settings. The mean BRS-values of different global data segments (using a common local data segment length of 30 s) were 10.44 ± 8.83, 11.58 ± 11.79, and 11.07 ± 11.34 ms/mmHg for 1a, 2a, and 2b in the supine position, and 5.82 ± 3.13, 5.65 ± 3.09, and 5.39 ± 3.57 ms/mmHg in the standing position, respectively. There was no significant difference between the BRS-values obtained using different global data segments.

The mean BRS-values calculated with different local data segment lengths (using the common global data segment 1a) were 12.84 ± 11.42, 11.27 ± 9.24, and 10.44 ± 8.83 ms/mmHg for local data segment lengths of 12, 20, and 30 s in the supine position, and 6.01 ± 3.56, 5.84 ± 3.31, and 5.82 ± 3.13 ms/mmHg in the standing position, respectively. There were significant differences between 12 s and the other two local data segments in the supine position ($p = 0.013$ for 12 s vs. 20 s and $p < 0.001$ for 12 s vs. 30 s), while BRS-values obtained with local data segments of 20 and 30 s were similar. The BRS-values obtained in the standing position were similar across different local data segment settings.

Correlation Analyses between BRS-Values Obtained Using Different Data Segment Settings

There were significant correlations between all the BRS calculated using different global data segments and BRS calculated using different local data segment lengths, and all the p-values were <0.001. The correlation coefficients are shown in **Table 1**.

Bland-Altman Analyses of the BRS-Values Obtained Using Different Parameters

Comparing the BRS-values calculated using different global data segments showed no fixed bias or proportional bias, either in the supine or standing position. In addition, most of the differences between these BRS-values were relatively small regarding the corresponding mean values (**Figure 3**).

However, when calculating BRS using the common 1a global data segment in the supine position, the BRS computed using the local data segment of 12 s was higher than those using local data segments of 20 and 30 s (fixed bias). BRS estimations using local data segments of 20 and 30 s in the supine position were similar. There was no significant fixed bias comparing BRS calculated by different local data segments in the standing position. No proportional bias was found when comparing BRS using different local data segments in the supine or standing position (**Figure 4**).

DISCUSSION

This is the first study evaluating the influences of local and global data segment settings on BRS analysis by MTRS. We found very close correlations between BRS-values calculated using different global and local data segments. Both in the supine and standing positions, using different global data segments did not significantly affect the BRS estimation. However, in the supine position, local data segments that are too short, such as 12 s, lead to overestimation of BRS.

MTRS solves several shortcomings of the widely used sequence method and spectral analysis using fast Fourier transform. The sequence method requires consecutive concordant changes of BP and heart rate, thus sometimes not enough BP and heart rate pairs can be obtained for accurate BRS calculation. In the EuroBaVar study, a large proportion of the methods using the sequence approach failed to detect autonomic failure (Laude et al., 2004). The fast Fourier transform based spectral analysis requires interpolation between real RRIs which affect the accuracy of the BRS assessment, and demands a long stationary data segment of at least 5 min which restrict its usage in dynamic processes (Rüdiger et al., 1999; Ziemssen et al., 2013). MTRS has overcome these problems using a trigonometric regression and short local data segments.

On one hand, using the coherent RRI and SBP oscillations determined by TRS other than the original RRI- and SBP-values (like in the sequence methods) could substantially increase the number of single BRS-values per time. This substitution could

TABLE 1 | Spearman's correlation coefficients between different BRS-values.

	G1a						L30					
	Supine			Standing			Supine			Standing		
	L12 vs. L20	L12 vs. L30	L20 vs. L30	L12 vs. L20	L12 vs. L30	L20 vs. L30	G1a vs. G2a	G1a vs. G2b	G2a vs. G2b	G1a vs. G2a	G1a vs. G2b	G2a vs. G2b
Rho	0.98	0.95	0.97	0.95	0.89	0.93	0.97	0.88	0.92	0.93	0.91	0.87

G1a, BRS calculated using the global data segment 1a.
G2a, BRS calculated using the global data segment 2a.
G2b, BRS calculated using the global data segment 2b.
L12, BRS calculated using the local data segments of 12s.
L20, BRS calculated using the local data segments of 20s.
L30, BRS calculated using the local data segments of 30s.

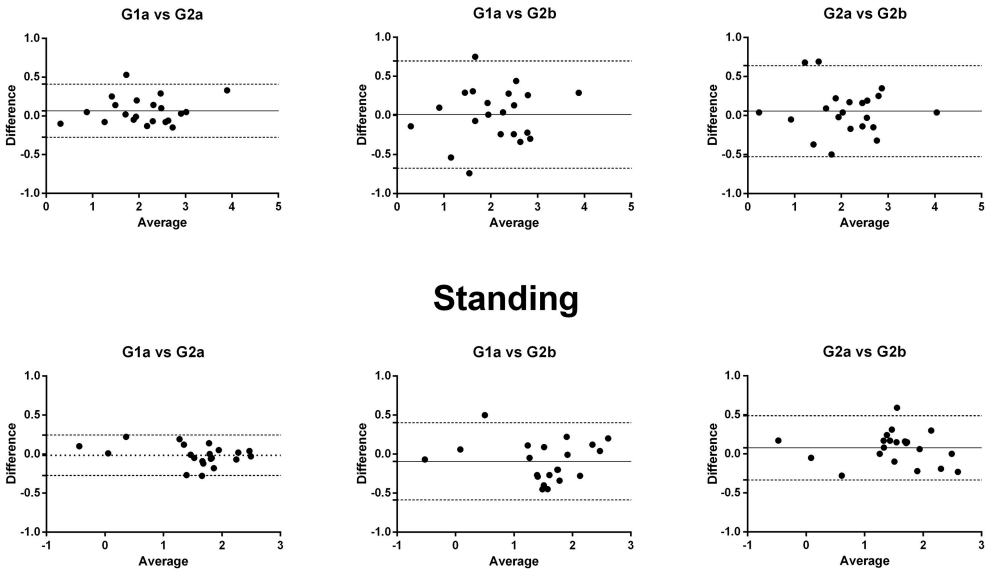

FIGURE 3 | The Bland-Altman plot of the differences and means of the logarithmic transformed BRS-values using different global data segments. There was no significant fixed or proportional bias. G1a, BRS calculated using the global data segment 1a; G2a, BRS calculated using the global data segment 2a; G2b, BRS calculated using the global data segment 2b.

improve the statistical power and validity of BRS estimation (Ziemssen et al., 2013). On the other hand, the algorithm of TRS analysis provides a pure physiological spectrum using trigonometric regression in contrast to a mathematical spectrum by using the Fast Fourier transform, thus avoiding interpolation and promote the accuracy of BRS evaluation (Ziemssen et al., 2013). **Figure 2** presents an illustration of the BRS analysis of two separate global data segments. **Figure 2A** shows the frequency distribution of individual BRS-values in a data segment of 2 min (2a) of the recording of a subject in the supine position. There are plenty of individual BRS-values detected, and the values with the greatest reliability (variance ratio $\geq$ 0.7) concentrated around the vertical line of the value 3.22 ms/mmHg. **Figure 2B** shows the individual BRS-values' distribution of another global data segment of 2min (2b) in the same recording. The averaged "optimal" BRS estimate was 3.31 ms/mmHg, which was quite close to that of the global data segment 2a. Furthermore, as mentioned in the method section, our improved MTRS analysis (after the EuroBaVar study) gives more weight on the "real" coherent SBP and RRI pairs for BRS estimation. This improvement reduces the influence of non-baroreflex mediated random fluctuations of SBP and RRI on BRS analysis. This upgrade enhances the reliability and stability of BRS analysis by MTRS, and may be part of the reason of the high consistency of BRS estimations using different global data segments.

In our study, supine BRS analysis using local data segments of 12 s produced significantly higher BRS-values compared with those using local data segments of 20 and 30 s. Because the longest LF oscillation has a wavelength of 25 s, 12 s might be too short to accurately assess the oscillations in the LF band. Increasing the local data segment length to 20 s would solve this problem and obtain similar results as those using local data segments of 30 s. Therefore, for MTRS, a local data segment length of 20–30 s is

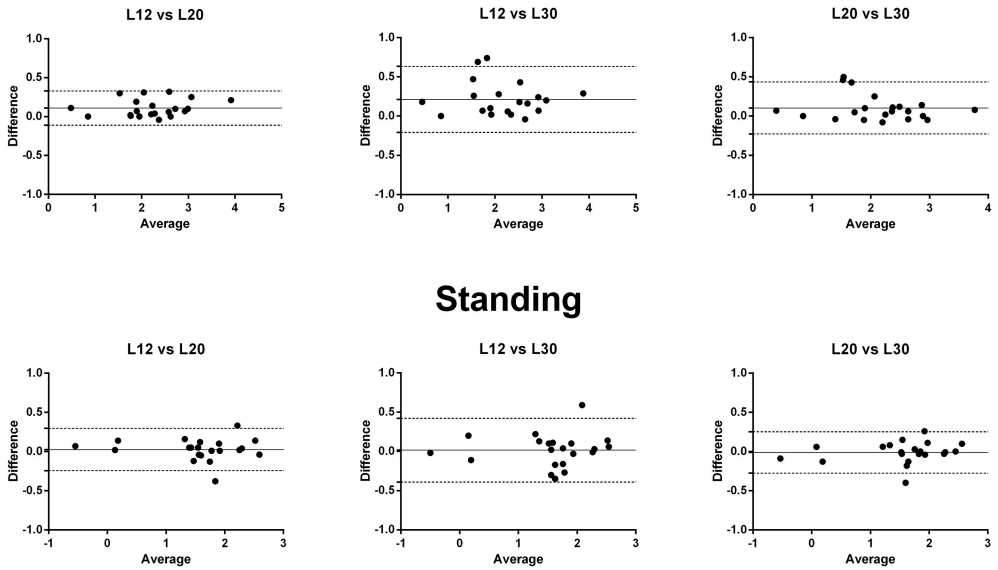

FIGURE 4 | The Bland-Altman plot of the differences and means of the logarithmic transformed BRS-values using different lengths of local data segments. BRS-values obtained using local data segments of 12 s were higher than those using local data segments of 20 and 30 s (fixed bias). There was no significant proportional bias. L12, BRS calculated using the local data segments of 12 s; L20, BRS calculated using the local data segments of 20 s; L30, BRS calculated using the local data segments of 30 s.

considered to be optimal for BRS analysis in the supine position. In a local data segment of TRS analysis, the oscillations must also remain constant similar to the fast Fourier transform. However, fast Fourier transform requires a stationary segment with the length of at least 5 min. For TRS, a stable local segment length of only 20–30 s seems to be enough. Therefore, MTRS can be utilized in BRS analysis during a dynamic process. Wright and colleagues conducted an analysis with a global data segment of 30 s and local data segments of 20 s, which is a good example of MTRS for a relatively short cardiovascular recording (Wright et al., 2009). In contrast to the BRS in the supine position, BRS-values applying different lengths of local data segments did not differ significantly in the standing position. The reason might be that BRS decreased during orthostasis (Friedrich et al., 2010; Reimann et al., 2010), and the difference also shrank to be non-significant.

A limitation of the MTRS analysis on BRS is that it could not distinguish the two directions of interactions between heart rate and SBP. Heart rate and BP can influence each other, thus form a closed loop. The change of BP would regulate heart rate through baroreflex (a feedback process), while heart rate also affects BP via the Frank–Starling mechanism and the runoff phenomenon (a feedforward non-baroreflex process) (Baselli et al., 1988; Taylor and Eckberg, 1996; Javorka et al., 2017). Recent studies have shown that causal analyses could discriminate the effect of SBP on heart rate (the feedback process, mediated by baroreflex) from the effect of heart rate to SBP (the feedforward process) (Porta et al., 2011, 2013; Svacinova et al., 2015; Javorka et al., 2017). Although MTRS based BRS analysis is a non-causal analysis, it showed good performance in the EuroBaVar study and agreed well with the modified Oxford method which was viewed as the gold standard of BRS estimation (Gasch et al., 2011). Future studies comparing causal analysis, MTRS and modified Oxford method would be helpful to clarify this issue.

In conclusion, BRS estimation by MTRS using different global data segments could acquire highly consistent results. However, too short local data segments such as 12 s would overestimate BRS in the supine position, and the optimal lengths of local data segments should be 20–30 s.

AUTHOR CONTRIBUTIONS

Conception and design of the study: TZ, HR. Acquisition, analysis and interpretation of data: KL, HR, and RH. Drafting the manuscript: KL, TZ. All the other authors critically revised the draft and approved the final version.

ACKNOWLEDGMENTS

We acknowledge support by the German Research Foundation and the Open Access Publication Funds of the SLUB/TU Dresden.

REFERENCES

Baselli, G., Cerutti, S., Civardi, S., Malliani, A., and Pagani, M. (1988). Cardiovascular variability signals: towards the identification of a closed-loop model of the neural control mechanisms. *IEEE Trans. Biomed. Eng.* 35, 1033–1046. doi: 10.1109/10.8688

Bernardi, L., De Barbieri, G., Rosengard-Barlund, M., Makinen, V. P., Porta, C., and Groop, P. H. (2010). New method to measure and improve consistency of baroreflex sensitivity values. *Clin. Auton. Res.* 20, 353–361. doi: 10.1007/s10286-010-0079-1

Bertinieri, G., di Rienzo, M., Cavallazzi, A., Ferrari, A. U., Pedotti, A., and Mancia, G. (1985). A new approach to analysis of the arterial baroreflex. *J. Hypertens. (Suppl.).* 3, S79–S81.

Blaber, A. P., Yamamoto, Y., and Hughson, R. L. (1995). Methodology of spontaneous baroreflex relationship assessed by surrogate data analysis. *Am. J. Physiol.* 268(4 Pt 2), H1682–H1687. doi: 10.1152/ajpheart.1995.268.4.H1682

Bland, J. M., and Altman, D. G. (1986). Statistical methods for assessing agreement between two methods of clinical measurement. *Lancet* 1, 307–310. doi: 10.1016/S0140-6736(86)90837-8

Di Rienzo, M., Parati, G., Castiglioni, P., Tordi, R., Mancia, G., and Pedotti, A. (2001). Baroreflex effectiveness index: an additional measure of baroreflex control of heart rate in daily life. *Am. J. Physiol. Regul. Integr. Comp. Physiol.* 280, R744–R751. doi: 10.1152/ajpregu.2001.280.3.R744

Ducher, M., Fauvel, J. P., Gustin, M. P., Cerutti, C., Najem, R., Cuisinaud, G., et al. (1995). A new non-invasive statistical method to assess the spontaneous cardiac baroreflex in humans. *Clin. Sci.* 88, 651–655. doi: 10.1042/cs0880651

Friedrich, C., Rudiger, H., Schmidt, C., Herting, B., Prieur, S., Junghanns, S., et al. (2010). Baroreflex sensitivity and power spectral analysis during autonomic testing in different extrapyramidal syndromes. *Mov. Disord.* 25, 315–324. doi: 10.1002/mds.22844

Gasch, J., Reimann, M., Reichmann, H., Rudiger, H., and Ziemssen, T. (2011). Determination of baroreflex sensitivity during the modified oxford maneuver by trigonometric regressive spectral analysis. *PLoS ONE* 6:e18061. doi: 10.1371/journal.pone.0018061

Giavarina, D. (2015). Understanding bland altman analysis. *Biochem. Med.* 25, 141–151. doi: 10.11613/BM.2015.015

Javorka, M., Czippelova, B., Turianikova, Z., Lazarova, Z., Tonhajzerova, I., and Faes, L. (2017). Causal analysis of short-term cardiovascular variability: state-dependent contribution of feedback and feedforward mechanisms. *Med. Biol. Eng. Comput.* 55, 179–190. doi: 10.1007/s11517-016-1492-y

La Rovere, M. T. (2000). Baroreflex sensitivity as a new marker for risk stratification. *Z. Kardiol.* 89(Suppl. 3), 44–50. doi: 10.1007/s003920070082

La Rovere, M. T., Bersano, C., Gnemmi, M., Specchia, G., and Schwartz, P. J. (2002). Exercise-induced increase in baroreflex sensitivity predicts improved prognosis after myocardial infarction. *Circulation* 106, 945–949. doi: 10.1161/01.CIR.0000027565.12764.E1

La Rovere, M. T., Specchia, G., Mortara, A., and Schwartz, P. J. (1988). Baroreflex sensitivity, clinical correlates, and cardiovascular mortality among patients with a first myocardial infarction. *Prospect. Study. Circ.* 78, 816–824. doi: 10.1161/01.CIR.78.4.816

Laude, D., Elghozi, J. L., Girard, A., Bellard, E., Bouhaddi, M., Castiglioni, P., et al. (2004). Comparison of various techniques used to estimate spontaneous baroreflex sensitivity (the EuroBaVar study). *Am. J. Physiol. Regul. Integr. Comp. Physiol.* 286, R226–R231. doi: 10.1152/ajpregu.00709.2002

Li, K., Konofalska, U., Akgun, K., Reimann, M., Rudiger, H., Haase, R., et al. (2017). Modulation of cardiac autonomic function by fingolimod initiation and predictors for fingolimod induced bradycardia in patients with multiple sclerosis. *Front. Neurosci.* 11:540. doi: 10.3389/fnins.2017.00540

Porta, A., Bari, V., Bassani, T., Marchi, A., Pistuddi, V., and Ranucci, M. (2013). Model-based causal closed-loop approach to the estimate of baroreflex sensitivity during propofol anesthesia in patients undergoing coronary artery bypass graft. *J. Appl. Physiol.* 115, 1032–1042. doi: 10.1152/japplphysiol.00537.2013

Porta, A., Catai, A. M., Takahashi, A. C., Magagnin, V., Bassani, T., Tobaldini, E., et al. (2011). Causal relationships between heart period and systolic arterial pressure during graded head-up tilt. *Am. J. Physiol. Regul. Integr. Comp. Physiol.* 300, R378–R386. doi: 10.1152/ajpregu.00553.2010

Reimann, M., Friedrich, C., Gasch, J., Reichmann, H., Rudiger, H., and Ziemssen, T. (2010). Trigonometric regressive spectral analysis reliably maps dynamic changes in baroreflex sensitivity and autonomic tone: the effect of gender and age. *PLoS ONE* 5:e12187. doi: 10.1371/journal.pone.0012187

Reimann, M., Hamer, M., Schlaich, M. P., Malan, N. T., Ruediger, H., Ziemssen, T., et al. (2012). Greater cardiovascular reactivity to a cold stimulus is due to higher cold pain perception in black Africans: the sympathetic activity and ambulatory blood pressure in Africans (SABPA) study. *J. Hypertens.* 30, 2416–2424. doi: 10.1097/HJH.0b013e328358faf7

Reimann, M., Julius, U., Bornstein, S. R., Fischer, S., Reichmann, H., Rudiger, H., et al. (2013). Regular lipoprotein apheresis maintains residual cardiovascular and microvascular function in patients with advanced atherosclerotic disease. *Atheroscler* (Suppl.). 14, 135–141. doi: 10.1016/j.atherosclerosissup.2012.10.009

Rüdiger, H., Klinghammer, L., and Scheuch, K. (1999). The trigonometric regressive spectral analysis–a method for mapping of beat-to-beat recorded cardiovascular parameters on to frequency domain in comparison with Fourier transformation. *Comput. Methods Programs Biomed.* 58, 1–15. doi: 10.1016/S0169-2607(98)00070-4

Svacinova, J., Javorka, M., Novakova, Z., Zavodna, E., Czippelova, B., and Honzikova, N. (2015). Development of causal interactions between systolic blood pressure and inter-beat intervals in adolescents. *Physiol. Res.* 64, 821–829.

Taylor, J. A., and Eckberg, D. L. (1996). Fundamental relations between short-term RR interval and arterial pressure oscillations in humans. *Circulation* 93, 1527–1532. doi: 10.1161/01.CIR.93.8.1527

Viehweg, J., Reimann, M., Gasch, J., Rudiger, H., and Ziemssen, T. (2016). Comparison of baroreflex sensitivity estimated from ECG R-R and inter-systolic intervals obtained by finger plethysmography and radial tonometry. *J. Neural Transm.* 123, 481–490. doi: 10.1007/s00702-016-1535-4

Westerhof, B. E., Gisolf, J., Stok, W. J., Wesseling, K. H., and Karemaker, J. M. (2004). Time-domain cross-correlation baroreflex sensitivity: performance on the EUROBAVAR data set. *J. Hypertens.* 22, 1371–1380. doi: 10.1097/01.hjh.0000125439.28861.ed

Wright, C. I., Ruediger, H., Kroner, C. I., Janssen, B. J., and Draijer, R. (2009). Acute autonomic effects of vitamins and fats in male smokers. *Eur. J. Clin. Nutr.* 63, 246–252. doi: 10.1038/sj.ejcn.1602912

Ziemssen, T., Gasch, J., and Ruediger, H. (2008). Influence of ECG sampling frequency on spectral analysis of RR intervals and baroreflex sensitivity using the EUROBAVAR data set. *J. Clin. Monit. Comput.* 22, 159–168. doi: 10.1007/s10877-008-9117-0

Ziemssen, T., Reimann, M., Gasch, J., and Rudiger, H. (2013). Trigonometric regressive spectral analysis: an innovative tool for evaluating the autonomic nervous system. *J. Neural Transm.* 120(Suppl. 1), S27–S33. doi: 10.1007/s00702-013-1054-5

Conflict of Interest Statement: The authors declare that the research was conducted in the absence of any commercial or financial relationships that could be construed as a potential conflict of interest.

frontiers in Physiology

MINI REVIEW
published: 20 March 2018
doi: 10.3389/fphys.2018.00240

Synaptic Plasticity in Cardiac Innervation and Its Potential Role in Atrial Fibrillation

Jesse L. Ashton[1], *Rebecca A. B. Burton*[2], *Gil Bub*[3], *Bruce H. Smaill*[1,4] *and Johanna M. Montgomery*[1]*

[1] Department of Physiology, University of Auckland, Auckland, New Zealand, [2] Department of Pharmacology, Oxford University, Oxford, United Kingdom, [3] Department of Physiology, McGill University, Montreal, QC, Canada, [4] Auckland Bioengineering Institute, University of Auckland, Auckland, New Zealand

Synaptic plasticity is defined as the ability of synapses to change their strength of transmission. Plasticity of synaptic connections in the brain is a major focus of neuroscience research, as it is the primary mechanism underpinning learning and memory. Beyond the brain however, plasticity in peripheral neurons is less well understood, particularly in the neurons innervating the heart. The atria receive rich innervation from the autonomic branch of the peripheral nervous system. Sympathetic neurons are clustered in stellate and cervical ganglia alongside the spinal cord and extend fibers to the heart directly innervating the myocardium. These neurons are major drivers of hyperactive sympathetic activity observed in heart disease, ventricular arrhythmias, and sudden cardiac death. Both pre- and postsynaptic changes have been observed to occur at synapses formed by sympathetic ganglion neurons, suggesting that plasticity at sympathetic neuro-cardiac synapses is a major contributor to arrhythmias. Less is known about the plasticity in parasympathetic neurons located in clusters on the heart surface. These neuronal clusters, termed ganglionated plexi, or "little brains," can independently modulate neural control of the heart and stimulation that enhances their excitability can induce arrhythmia such as atrial fibrillation. The ability of these neurons to alter parasympathetic activity suggests that plasticity may indeed occur at the synapses formed on and by ganglionated plexi neurons. Such changes may not only fine-tune autonomic innervation of the heart, but could also be a source of maladaptive plasticity during atrial fibrillation.

Keywords: atria, innervation, ganglionated plexi, synapse plasticity, atrial fibrillation, LTP

OPEN ACCESS

Edited by:
Tijana Bojić,
Vinča Nuclear Institute, University of Belgrade, Serbia

Reviewed by:
Keith L. Brain,
University of Birmingham, United Kingdom
G. Andre Ng,
University of Leicester, United Kingdom

***Correspondence:**
Johanna M. Montgomery
jm.montgomery@auckland.ac.nz

Specialty section:
This article was submitted to Autonomic Neuroscience, a section of the journal Frontiers in Physiology

Received: *20 October 2017*
Accepted: *06 March 2018*
Published: *20 March 2018*

Citation:
Ashton JL, Burton RAB, Bub G, Smaill BH and Montgomery JM (2018) Synaptic Plasticity in Cardiac Innervation and Its Potential Role in Atrial Fibrillation. Front. Physiol. 9:240. doi: 10.3389/fphys.2018.00240

INTRODUCTION

Cardiac arrhythmias are devastating disorders in which normal sinus rhythm is disrupted, resulting in the heart beating too rapidly, slowly, or erratically, thereby impairing cardiac function. The most common cardiac arrhythmia is atrial fibrillation (AF): AF affects 2.5–3.2% of people worldwide, with ∼5 million new cases reported annually (Chugh et al., 2014). In AF, atrial electrical activation is rapid and disorganized leading to irregular and often rapid ventricular rhythm. AF disrupts the reservoir and contactile functions of the atria, which impairs ventricular filling and also results in stasis of blood in the left atrium in particular (Staerk et al., 2017). The prevalence of AF increases

with aging (Benjamin et al., 1994; Chugh et al., 2014) and it has significant clinical consequences including a 5-fold increase in stroke, a 3-fold increase in heart failure and a doubling of risk for dementia (Benjamin et al., 1994; Chugh et al., 2014).

The hallmark of AF is rapid activation of the atria from one or more localized sources, which can be either focal discharges or self-sustaining circuits of re-entrant activity. Atrial myocardium distal to the arrhythmia source cannot follow the high frequency driver and consequently conduction becomes slow and irregular (Schotten et al., 2011). The progressive nature of this rhythm disturbance is acknowledged in the observation that "AF begets AF" (Wijffels et al., 1995). Repeated episodes of paroxysmal AF, which terminate spontaneously in hours, lead eventually to persistent AF. In persistent AF, atrial electrical and structural remodeling amplifies the electrophysiological instability that drives AF and the re-entrant substrates that sustain it (Iwasaki et al., 2011). It is well established that the autonomic nervous system contributes significantly to this process (Esler, 1992; Chen et al., 2014; Linz et al., 2014; Ardell and Armour, 2016). Sympathovagal discharge is a common trigger for paroxysmal AF (Tan et al., 2008; Chou and Chen, 2009). Specifically, it is thought to be proarrhythmic by enhancing delayed afterdepolarisation related ectopic activity through increasing β-adrenoceptor-dependent diastolic Ca^{2+} leak (Dobrev et al., 2011), and stabilizing re-entrant activity by reducing atrial action potential duration through increased acetylcholine-dependent K+ current (Kneller et al., 2002). Atrial sympathetic hyperinnervation and remodeling of the autonomic nervous system are both contributors to positive feedback loops that promote persistent and recurrent AF (Gould et al., 2006; Tan et al., 2008; Chou and Chen, 2009; Iwasaki et al., 2011). There is evidence of imbalance between sympathetic and parasympathetic components of the autonomic nervous system at both effector and end-organ levels (Chen and Tan, 2007; Czick et al., 2016; Kuyumcu et al., 2017). Furthermore, it is argued that progressive remodeling of the atrial neural plexus in persistent AF contributes to the maintenance of electrical instability (Chen et al., 2010, 2014; Shen et al., 2012). Despite this, we lack detailed knowledge of the structure and function of synapses formed on and by neurons within the atrial neural plexus and how these change with AF.

Extrinsic and Intrinsic Innervation of the Atria

The atria receive rich innervation from the autonomic branch of the peripheral nervous system (Hillarp, 1960; Skok, 1973; Pardini et al., 1989; Tan et al., 2006; Choi et al., 2010; Chen et al., 2014; Linz et al., 2014). Specifically, the autonomic sympathetic and parasympathetic nervous systems control normal heart rhythm and the heart's susceptibility to atrial and ventricular arrhythmias (Armour, 2008; Choi et al., 2010; Gibbons et al., 2012; Chen et al., 2014; Linz et al., 2014). Sympathetic nerves mediating control of cardiac function originate within the intermediolateral column of the spinal cord and extend to paravertebral ganglia situated from levels C1 to T5, which include the superior cervical ganglia as well as the cervico-thoracic (stellate) ganglia and thoracic ganglia (Kawashima, 2005). Cardiac nerves originating from these ganglia track to the base of the heart along the brachiocephalic trunk, common carotid and subclavian arteries as well as the superior vena cava (Kawashima, 2005). Parasympathetic cardiomotor neurons are situated in medial regions of the medulla oblongata (nucleus ambiguus and dorsal motor nucleus) and issue fibers to the atria via the bilateral vagus nerves (Spyer, 2011).

Most of the sympathetic efferent fibers directly innervate the myocardium or form synapses with neurons in cardiac ganglia located throughout the heart (Armour et al., 1997; Tan et al., 2006; Linz et al., 2014). These synapses consist of presynaptic axonal varicosities invaginated by the postsynaptic cardiomyocyte membrane which contains high densities of adrenergic receptors, adhesion and scaffold proteins (Landis, 1976; Shcherbakova et al., 2007). Hyperactive sympathetic activity is a major feature of heart disease, significantly contributing to the high arrhythmia burden and sudden cardiac death (Chen et al., 2001; Shanks et al., 2013; Ajijola et al., 2015), and recent research has revealed that this is predominantly driven by the postganglionic sympathetic neurons (Larsen et al., 2016a,b). Specifically, hypertension induces increases in membrane calcium currents, intracellular calcium, and cyclic nucleotide signaling in sympathetic stellate neurons, resulting in an increase in noradrenaline release (Shanks et al., 2013; Larsen et al., 2016a,b). Stimulation of sympathetic neurons can redistribute postsynaptic adrenergic receptors on the surface of cardiomyocytes (Shcherbakova et al., 2007). Together these data show that both pre- and post-synaptic changes can readily occur in transmission at sympathetic neuro-cardiac synapses.

Parasympathetic fibers form synapses with clusters of cardiac ganglia neurons located on the surface of the heart (**Figure 1**; Armour, 2008; Linz et al., 2014; Wake and Brack, 2016). These clusters are termed ganglionated plexi (GP), or "little brains" (Armour, 2008), and they are proposed to act as local coordinators of cardiac electrical and mechanical properties (Horackova and Armour, 1995; Choi et al., 2010; Linz et al., 2014; Ardell and Armour, 2016). In humans, approximately 14,000 GP neurons are located on the heart surface, with many clustered around the pulmonary veins (Armour et al., 1997). Increasing evidence supports the hypothesis that GP neurons can independently modulate neural control of the heart (Horackova and Armour, 1995; Arora et al., 2003; Heaton et al., 2007; Choi et al., 2010; Gibbons et al., 2012; Chen et al., 2014; Linz et al., 2014). For example, GP neurons are proposed to play a critical role in the development and propagation of arrhythmias such as AF (Choi et al., 2010; Gibbons et al., 2012; Chen et al., 2014; Linz et al., 2014), and AF can be induced by direct stimulation of GP sites (Lim et al., 2011; Gibbons et al., 2012). In addition, changes in parasympathetic tone (which increase the risk of arrhythmias, heart failure and mortality), have been proposed to occur in GP (Bibevski and Dunlap, 1999; Arora et al., 2003; Heaton et al., 2007).

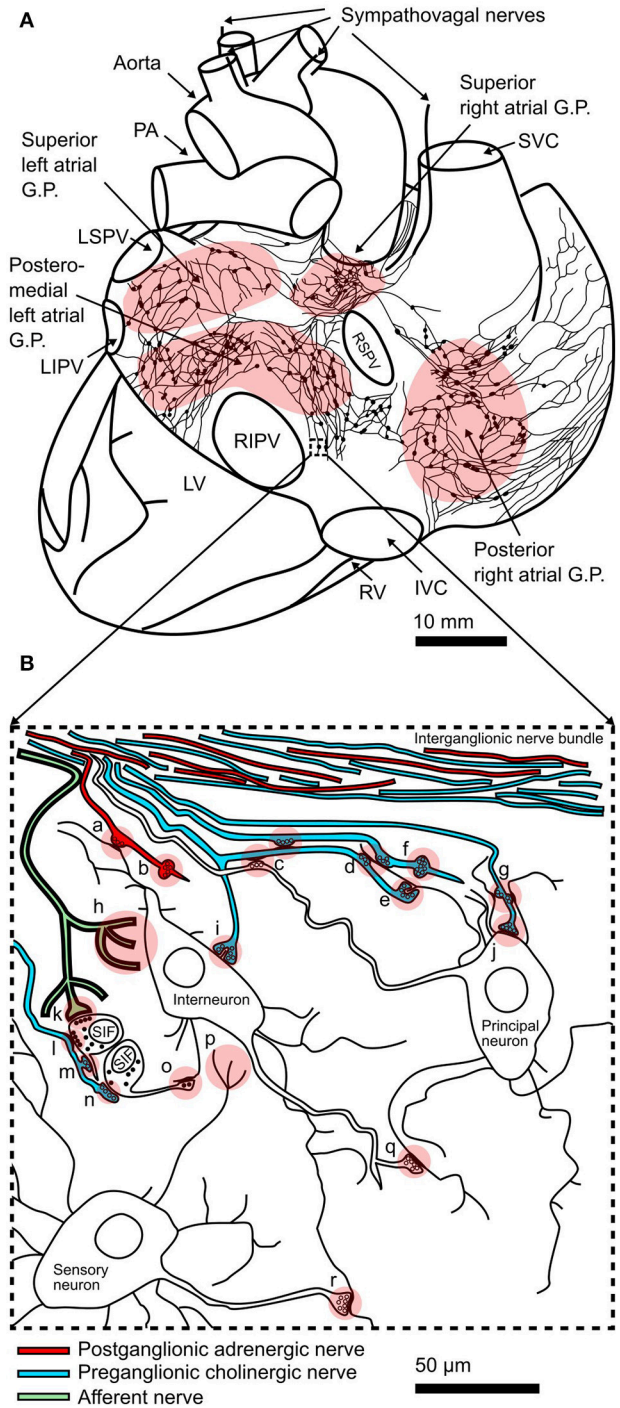

FIGURE 1 | Structure of the intracardiac plexus and synaptic connections within: **(A)** Drawing of a posterior view of the human heart and major vessels showing the locations of posterior atrial ganglionated plexi (GP) and interconnecting nerves. This schematic representation of the plexus is derived from example reconstructions of acetylcholinesterase positive nerves and ganglia on the surface of juvenile atria (Pauza et al., 2000). Sympathovagal nerves enter the heart by coursing down the aorta and superior vena cava (SVC) to innervate the superior atrial GP. The locations of the pulmonary arteries (PA), left superior pulmonary vein (LSPV), left inferior pulmonary vein (LIPV), right superior pulmonary vein (RSPV), right inferior pulmonary vein (RIPV), left ventricle (LV), right ventricle (RV), and inferior vena cava (IVC) are shown. **(B)** Schematic representation of interconnectivity in cardiac ganglia showing types of synapses seen in electron microscopy studies (Shvalev and Sosunov, 1985; Armour et al., 1997; Pauziene and Pauza, 2003): (a) axo-dendritic synapse formed by adrenergic nerve terminal; (b) adrenergic varicosity without glial sheath; (c) axo-axonal synapses; (d) two axons forming axo-dendritic synapses on a single dendrite; (e) axo-dendritic synapse on dendritic spine; (f) cholinergic varicosity without glial sheath; (g) a single axon forming axo-dendritic synapses on two dendrites; (h) afferent nerve ending; (i) axo-dendritic synapse on small spine like protrusion from soma; (j) axo-somatic synapse; (k) contact of afferent nerve terminal with SIF cell; (l) efferent (soma-axonal) synapse made by SIF cell with cholinergic nerve terminal; (m) synapse formed between cholinergic nerve terminal and process of SIF cell; (n) afferent (axo-somatic) synapse made between SIF cell and cholinergic nerve terminal; (o) synapse formed between process of SIF cell and neuronal dendrite; (p) sensory neuron afferent nerve ending; (q) axo-dendritic synapse between neurons within the GP; (r) axo-dendritic synapse between sensory neuron and other neuronal types. Modified from Shvalev and Sosunov (1985).

GANGLIONATED PLEXI

GP Structure and Neuron Function

Although initially defined as clusters of cholinergic neurons, GP neurons show significant heterogeneity in their morphology, chemical composition, and physiology (Edwards et al., 1995; Horackova et al., 1999; Richardson et al., 2003; Rimmer and Harper, 2006; Tan et al., 2006; McAllen et al., 2011; Wake and Brack, 2016). Immunocytochemical analysis has revealed multiple neurochemical subtypes of GP neurons: while choline acetyltransferase (ChAT) is expressed in all principal neurons, subpopulations express other transmitters and neuropeptides including nitric oxide, serotonin, and neuropeptide Y (Mawe et al., 1996; Horackova et al., 1999; Singh et al., 1999; Richardson et al., 2003; Adams and Cuevas, 2004; Wake and Brack, 2016). Small clusters of catecholaminergic neurons, termed SIF (small intensely fluorescent) cells, constitute 5% of GP neurons (Horackova et al., 1999; Slavíková et al., 2003) where they modulate synaptic transmission of the cholinergic neurons (McGrattan et al., 1987; Gagliardi et al., 1988; Adams and Cuevas, 2004). The presence of multiple neurochemical variants suggests differential roles for peptides and neurotransmitters in modulating GP neuron function. Distinct subtypes of neurons within GP have also been defined electrophysiologically based on action potential kinetics, ability to fire bursts of action potentials, rectification properties and synaptic input (Edwards et al., 1995; McAllen et al., 2011). This heterogeneity within GP suggests the neurons play different roles in controlling electrical signals to the heart (Ardell and Armour, 2016). Moreover, the ability of GP neurons to modulate the level of parasympathetic activity to the heart also suggests that synaptic communication from GP neurons can be altered. These synaptic changes may not only fine-tune autonomic activation of the heart, but could also likely be a source of maladaptive changes including arrhythmogenesis (Choi et al., 2010; Gibbons et al., 2012; Chen et al., 2014; Ajijola et al., 2015; Ardell et al., 2016).

Clinical Importance of GP Neurons

Clinically, AF is treated pharmacologically with rate and rhythm controllers (Lafuente-Lafuente et al., 2015; Hanley et al., 2016; which have variable efficacy and trigger ventricular arrhythmias), and by the pulmonary vein isolation procedure. In this technique, an interior ring or "firebreak" is created within each pulmonary vein to stop aberrant electrical impulses that can trigger AF from reaching the heart (Haissaguerre et al., 1998; Lancaster et al., 2016). This procedure has been most effective in reversing paroxysmal AF compared with persistent AF, however initial success rates at 12 months drop significantly beyond 2 years (Kron et al., 2010; Weerasooriya et al., 2011; Calkins et al., 2012; Zheng et al., 2013). Ablation of the GP sites has been combined with pulmonary vein isolation, and these two procedures appear to increase the numbers of patients free of AF, however results are variable, and long-term efficacy is unknown (Scherlag et al., 2006; Pokushalov et al., 2009; Kron et al., 2010; Katritsis et al., 2011; Calkins et al., 2012; Zheng et al., 2013). Moreover, GP neurons also innervate the ventricles and modulate ventricular function, raising concern of increased susceptibility to ventricular arrhythmias after ablation procedures (Pappone et al., 2004; Osman et al., 2010; Buckley et al., 2016; Jungen et al., 2017). It is critical that in order to advance GP ablation techniques and increase their reproducibility and success rates that we gain a detailed understanding of the physiological properties of the GP neurons in the aged or arrhythmic states, and how changes in their function may trigger and drive AF.

BEYOND THE BRAIN – DOES SYNAPTIC PLASTICITY OCCUR IN NEURONS INNERVATING THE HEART?

"Plasticity" is defined as the ability of neurons to alter their strength of communication at synapses (Bliss and Lomo, 1973; Dudek and Bear, 1992; Genoux and Montgomery, 2007; Nabavi et al., 2014). Synapse plasticity is a critical process in the brain, and a major area of neuroscience research as it has been shown to underlie learning and memory, as well as changes in sensory and motor functions (Genoux and Montgomery, 2007; Huang et al., 2007; Lee et al., 2014; Nabavi et al., 2014; Leighton and Lohmann, 2016). High-frequency stimulation paradigms induce increases in synaptic efficacy that last for seconds (i.e., short-term plasticity; Dobrunz et al., 1997; Jackman and Regehr, 2017), or from minutes to hours or days, referred to as long-term potentiation (LTP; Bliss and Lomo, 1973). Alternatively, low frequency stimulation paradigms induce long term depression (LTD) of synaptic efficacy (Dudek and Bear, 1992). The *induction* of LTP and LTD is dependent on activation of NMDA-type glutamate receptors (Harris et al., 1984; Morris et al., 1986; Dudek and Bear, 1992). The mechanisms underpinning the *expression* of these changes in synaptic strength vary between brain regions. Specifically, LTP/LTD paradigms can induce changes in postsynaptic receptor surface number, conductance, and distribution, the probability of presynaptic transmitter release, and/or ultrastructural changes in synaptic protein localisation (Hayashi et al., 2000; Montgomery et al., 2001; Castillo et al., 2002; Mellor et al., 2002; Ehlers et al., 2007; Volk et al., 2015; Tang et al., 2016). However, in contrast to the brain, less is known about the mechanisms of short and long-term synaptic plasticity in the neurons that innervate the heart.

Synaptic Plasticity in Cardiac Sympathetic Ganglia

Both short and long-term plasticity mechanisms have been described in the peripheral synapses within sympathetic ganglia. In the stellate and superior cervical sympathetic ganglia that innervate the heart, short-term increases in the strength of synaptic transmission occur in response to a single action potential or a short train of impulses (Bennett et al., 1976; Lin et al., 1998), and longer bursts of high frequency stimulation of the preganglionic nerve result in enhancement of postsynaptic responses and heart rate (Alonso-deFlorida et al., 1991; Bachoo and Polosa, 1991; Aileru et al., 2004). Conversely, low frequency stimulation can induce LTD (Alkadhi et al., 2008). Induction of ganglionic LTP and LTD (gLTP/gLTD) is not dependent on transmission via nicotinic, adrenergic, muscarinic or adenosine receptors, but requires activation of 5-HT_3 receptors by serotonin, potentially released from SIF cells (Alkadhi et al., 1996, 2008). Both pre- and postsynaptic expression mechanisms have been implicated in gLTP (Alkadhi et al., 2005), with increases in evoked acetylcholine (ACh) release (Briggs et al., 1985) and postsynaptic sensitivity to ACh observed (Bachoo and Polosa, 1991). More recently, both pre- and postsynaptic intracellular calcium changes have been shown to contribute equally to gLTP (Vargas et al., 2011), and the potential involvement of nitric oxide signaling (Altememi and Alkadhi, 1999) supports a trans-synaptic form of gLTP (Vargas et al., 2011) that can be enhanced by neurotrophins to regulate sympathetic tone (Arias et al., 2014).

The mechanisms underpinning gLTP likely contribute to the enhanced sympathetic drive seen in conditions associated with heart disease and AF (Alkadhi and Alzoubi, 2007). In spontaneously hypertensive rats (SHRs), synaptic transmission is augmented as shown by increased ACh release (Magee and Schofield, 1992, 1994), greater recruitment of postganglionic neurons (Magee and Schofield, 1992), and faster spike frequency adaptation in SHR ganglia (Yarowsky and Weinreich, 1985). Increased sympathetic stimulation may increase presynaptic activity to induce gLTP observed *in vivo* in sympathetic ganglia in SHRs (Alzoubi et al., 2010). Additional evidence of gLTP *in vivo* is the inhibition of baseline ganglionic transmission by 5-HT_3 receptor antagonists in sympathetic ganglia from SHRs but not age-matched controls (Alkadhi et al., 2001). Further gLTP cannot be induced, indicating occlusion of the plasticity mechanism (Alkadhi and Alzoubi, 2007). Chronic treatment with 5-HT_3 receptor antagonists also reduces blood pressure in SHRs (Alkadhi et al., 2001) but its effect on atrial arrhythmia burden in this model is unknown.

Synaptic Plasticity in the Intracardiac Plexus

Within GP, the cholinergic and catecholaminergic neurons possess large numbers of asymmetrical axodendritic synapses and

project axons to neurons within the same or different ganglion (**Figure 1**; Armour et al., 1997; Klemm et al., 1997; Horackova et al., 1999; Richardson et al., 2003; Tan et al., 2006; Armour, 2008), suggesting that significant synaptic communication occurs between networks of GP neurons. Electrophysiological recordings from synapses within the intracardiac plexus are hampered by difficulty accessing GP neurons given their proximity to the heart and great vessels, and the extensive connective tissue surrounding the ganglia. Intracellular recordings from GP neurons have been performed in the working heart-brainstem preparation (McAllen et al., 2011). These recordings revealed the presence of subthreshold synaptic potentials and silent synapses, indicating that significant capacity exists for increasing synaptic strength within GP, which could alter and/or restore vagal tone (McAllen et al., 2011). Multiple studies have measured changes in postsynaptic neuronal excitability as an indication of synaptic efficacy in the intracardiac plexus following chronic spinal cord stimulation or myocardial infarction, suggesting altered neurotransmission in the intracardiac plexus contributes to altered parasympathetic control of the heart (Bibevski and Dunlap, 1999; Ardell et al., 2014; Hardwick et al., 2014; Rajendran et al., 2016; Smith et al., 2016). After myocardial infarction, the observed overall reduction in network connectivity (Rajendran et al., 2016) suggests depression of synaptic transmission (i.e., LTD) within the intracardiac nervous system, however this may differ at afferent versus efferent synaptic inputs. With regards to AF, enhanced interaction at the level of the GP network through changes in local circuit neuron function have been proposed to be a factor contributing to AF substrate (Beaumont et al., 2013; Ardell et al., 2016). Possible factors altering ganglionic neurotransmission include changes in postsynaptic nicotinic receptor expression (Bibevski and Dunlap, 2011) and dysfunctional NO-cGMP signaling in postganglionic neurons (Heaton et al., 2007). Intriguingly, NMDA receptors are abundantly expressed in the atrium, including in the GP (Gill et al., 2007), and their activation is associated with increased arrhythmogenesis, AF inducibility, and atrial fibrosis (Shi et al., 2014, 2017). NMDA receptors are critical for the induction of synaptic plasticity in the brain, suggesting that NMDA receptors in the heart also play a role in inducing plasticity within GP, and contribute to autonomic dysfunction in arrhythmias such as AF.

Significant evidence indicates the neuropeptide pituitary adenylate cyclase-activating polypeptide (PACAP) is involved in plasticity at GP synapses. PACAP is localized to parasympathetic preganglionic fibers (Calupca et al., 2000; Richardson et al., 2003) and GP neurons express PAC_1 receptors (Braas et al., 1998). PACAP modulates nicotinic neurotransmission in the ciliary ganglion by enhancing presynaptic quantal ACh release via trans-synaptic action of NO (Pugh et al., 2010; Jayakar et al., 2014). Postsynaptically, PACAP increases the agonist affinity of GP nicotinic receptors through G-protein signaling (Liu et al., 2000). High frequency stimulation of nerve bundles within the intracardiac plexus results in a slow postsynaptic depolarisation and a sustained increase in excitability of GP neurons that is thought to be at least partially mediated by PACAP (Tompkins et al., 2007). This increase in excitability is driven by enhanced current through hyperpolarization-induced nonselective cationic (I_h; Tompkins et al., 2009) and T/R-type calcium channels (Tompkins et al., 2015). The enhanced excitability of GP neurons likely contributes to the PACAP induced AF seen in dogs (Hirose et al., 1997) and guinea pigs (Chang et al., 2005).

FUTURE DIRECTIONS

The detailed knowledge of plasticity mechanisms in the brain has resulted from precise imaging and electrophysiological analysis of synaptic properties (e.g., Hayashi et al., 2000; Montgomery et al., 2001; Ehlers et al., 2007; Fourie et al., 2014; Tang et al., 2016). To gain comparable knowledge of short and long-term plasticity mechanisms in the innervation of the heart, similar high-resolution techniques need to be applied to synapses formed on and by cardiac parasympathetic and sympathetic neurons, especially in human tissue where some aspects of GP circuitry and cell composition appear to differ (Armour et al., 1997; Pauziene and Pauza, 2003; Hoover et al., 2009). Animal models of AF are also important, as recording changes in GP neuron and synapse function during and after the onset of arrhythmia will provide evidence of whether plasticity does occur at GP synapses with changes in heart rhythm. In more intact systems, such as the working heart-brainstem and the innervated heart preparations (Brack et al., 2004; Ng et al., 2007; McAllen et al., 2011; Ashton et al., 2013), this would enable researchers to determine whether changes in synaptic strength can increase or decrease autonomic tone to the heart, and play a major role in generating the aberrant electrical impulses in the GP around the pulmonary veins that can trigger and drive AF.

AUTHOR CONTRIBUTIONS

JM and JA initiated the review topic and designed the review. All authors contributed to the writing, editing, and approval of the manuscript.

ACKNOWLEDGMENTS

The authors are grateful to the University of Auckland Faculty Research Development Fund awarded to JM and BS to support JA. We also acknowledge funding from the Heart Foundation New Zealand and the Maurice and Phyllis Paykel Trust awarded to JM to establish neuro-cardiac research. RB holds a Sir Henry Dale Royal Society and Wellcome Trust Fellowship (109371/Z/15/Z) and acknowledges support from the Nuffield Benefaction for Medicine and the Wellcome Institutional Strategic Support Fund (ISSF) Oxford and Medical Research Council; RB and JM hold a Colin Pillinger International Exchange Award (Royal Society).

REFERENCES

Adams, D. J., and Cuevas, J. (2004). "Electrophysiological properties of intrinsic cardiac neurons," in *Basic and Clinical Neurocardiology,* eds J. A. Armour and J. L. Ardell (New York, NY: Oxford University Press), 1–60.

Aileru, A. A., Logan, E., Callahan, M., Ferrario, C. M., Ganten, D., and Diz, D. I. (2004). Alterations in sympathetic ganglionic transmission in response to angiotensin II in (mRen)27 transgenic rats. *Hypertension* 43, 270–275. doi: 10.1161/01.HYP.0000112422.81661.f3

Ajijola, O. A., Howard-Quijano, K., Scovotti, J., Vaseghi, M., Lee, C., Mahajan, A., et al. (2015). Augmentation of cardiac sympathetic tone by percutaneous low-level stellate ganglion stimulation in humans: a feasibility study. *Physiol. Rep.* 3:e12328. doi: 10.14814/phy2.12328

Alkadhi, K. A., Al-Hijailan, R. S., and Alzoubi, K. H. (2008). Long-term depression in the superior cervical ganglion of the rat. *Brain Res.* 1234, 25–31. doi: 10.1016/j.brainres.2008.07.112

Alkadhi, K. A., Alzoubi, K. H., and Aleisa, A. M. (2005). Plasticity of synaptic transmission in autonomic ganglia. *Prog. Neurobiol.* 75, 83–108. doi: 10.1016/j.pneurobio.2005.02.002

Alkadhi, K. A., Otoom, S. A., Tanner, F. L., Sockwell, D., and Hogan, Y. H. (2001). Inhibition of ganglionic long-term potentiation decreases blood pressure in spontaneously hypertensive rats. *Exp. Biol. Med.* 226, 1024–1030. doi: 10.1177/153537020122601109

Alkadhi, K. A., Salgado-Commissariat, D., Hogan, Y. H., and Akpaudo, S. B. (1996). Induction and maintenance of ganglionic long-term potentiation require activation of 5-hydroxytryptamine (5-HT3) receptors. *J. Physiol.* 496, 479–489. doi: 10.1113/jphysiol.1996.sp021700

Alkadhi, K., and Alzoubi, K. (2007). Role of long-term potentiation of sympathetic ganglia (gLTP) in hypertension. *Clin. Exp. Hypertens.* 29, 267–286. doi: 10.1080/10641960701500356

Alonso-deFlorida, F., Morales, M. A., and Minzoni, A. A. (1991). Modulated long-term potentiation in the cat superior cervical ganglion *in vivo*. *Brain Res.* 544, 203–210. doi: 10.1016/0006-8993(91)90055-Z

Altememi, G. F., and Alkadhi, K. A. (1999). Nitric oxide is required for the maintenance but not initiation of ganglionic long-term potentiation. *Neuroscience* 94, 897–902. doi: 10.1016/S0306-4522(99)00362-0

Alzoubi, K. H., Aleisa, A. M., and Alkadhi, K. A. (2010). *In vivo* expression of ganglionic long-term potentiation in superior cervical ganglia from hypertensive aged rats. *Neurobiol. Aging* 31, 805–812. doi: 10.1016/j.neurobiolaging.2008.06.007

Ardell, J. L., and Armour, J. A. (2016). Neurocardiology: structure-based function. *Comp. Physiol.* 6, 1635–1653. doi: 10.1002/cphy.c150046

Ardell, J. L., Andresen, M. C., Armour, J. A., Billman, G. E., Chen, P.-S., Foreman, R. D., et al. (2016). Translational neurocardiology: preclinical models and cardioneural integrative aspects. *J. Physiol.* 594, 3877–3909. doi: 10.1113/JP271869

Ardell, J. L., Cardinal, R. R., Beaumont, E., Vermeulen, M., Smith, F. M., and Armour, A.J. (2014). Chronic spinal cord stimulation modifies intrinsic cardiac synaptic efficacy in the suppression of atrial fibrillation. *Auton. Neurosci. Basic. Clin.* 186, 38–44. doi: 10.1016/j.autneu.2014.09.017

Arias, E. R., Valle-Leija, P., Morales, M. A., and Cifuentes, F. (2014). Differential contribution of BDNF and NGF to long-term potentiation in the superior cervical ganglion of the rat. *Neuropharm* 81, 206–214. doi: 10.1016/j.neuropharm.2014.02.001

Armour, J. A. (2008). Potential clinical relevance of the little brain on the mammalian heart. *Exp. Physiol.* 93, 165–176. doi: 10.1113/expphysiol.2007.041178

Armour, J. A., Murphy, D. A., Yuan, B. X., MacDonald, S., and Hopkins, D. A. (1997). Gross and microscopic anatomy of the human intrinsic cardiac nervous system. *Anat. Rec.* 47, 289–298. doi: 10.1002/(SICI)1097-0185(199702)247:2<289::AID-AR15>3.0.CO;2-L

Arora, R. C., Cardinal, R., Smith, F. M., Ardell, J. L., Dell'Italia, L. J., and Armour, J. A. (2003). Intrinsic cardiac nervous system in tachycardia induced heart failure. *Am. J. Physiol.* 285, R1212–1223. doi: 10.1152/ajpregu.00131.2003

Ashton, J. L., Paton, J. F., Trew, M. L., LeGrice, I. J., and Smaill, B. H. (2013). A working heart-brainstem preparation of the rat for the study of reflex mediated autonomic influences on atrial arrhythmia development. *Conf. Proc. IEEE Eng. Med. Biol. Soc.* 2013, 3785–3788. doi: 10.1109/EMBC.2013.6610368

Bachoo, M., and Polosa, C. (1991). Long-term potentiation of nicotinic transmission by a heterosynaptic mechanism in the stellate ganglion of the cat. *J. Neurophysiol.* 65, 639–647. doi: 10.1152/jn.1991.65.3.639

Beaumont, E., Salavatian, S., Southerland, E. M., Vinet, A., Jacquemet, V., Armour, J. A., et al. (2013). Network interactions within the canine intrinsic cardiac nervous system: implications for reflex control of regional cardiac function. *J. Physiol.* 591, 4515–4533. doi: 10.1113/jphysiol.2013.259382

Benjamin, E. J., Levy, D., Vaziri, S. M., D'Agostino, R. B., and Belanger, A. J. (1994). Independent risk factors for atrial fibrillation in a population-based cohort the framingham heart study. *JAMA* 271, 840–844.

Bennett, M. R., Florin, T., and Pettigrew, A. G. (1976). The effect of calcium ions on the binomial statistic parameters that control acetylcholine release at preganglionic nerve terminals. *J. Physiol.* 257, 597–620. doi: 10.1113/jphysiol.1976.sp011387

Bibevski, S., and Dunlap, M. E. (1999). Ganglionic mechanisms contribute to diminished vagal control in heart failure. *Circulation* 99, 2958–2963. doi: 10.1161/01.CIR.99.22.2958

Bibevski, S., and Dunlap, M. E. (2011). Evidence for impaired vagus nerve activity in heart failure. *Heart Fail. Rev.* 16, 129–135. doi: 10.1007/s10741-010-9190-6

Bliss, T. V. P., and Lomo, T. (1973). Long-lasting potentiation of synaptic transmission in the dentate area of the anaesthetized rabbit following stimulation of the perforant path. *J. Physiol.* 232, 331–356. doi: 10.1113/jphysiol.1973.sp010273

Braas, K. M., May, V., Harakall, S. A., Hardwick, J. C., and Parsons, R. L. (1998). Pituitary adenylate cyclase-activating polypeptide expression and modulation of neuronal excitability in guinea pig cardiac ganglia. *J. Neurosci.* 18, 9766–9779.

Brack, K. E., Coote, J. H., and Ng, G. A. (2004). Interaction between direct sympathetic and vagus nerve stimulation on heart rate in the isolated rabbit heart. *Exp. Physiol.* 89, 128–39. doi: 10.1113/expphysiol.2003.002654

Briggs, C. A., Brown, T. H., and Mcafee, D. A. (1985). Neurophysiology and pharmacology of long-term potentiation in the rat sympathetic ganglion. *J. Pharmacol. Sci.* 359, 503–521. doi: 10.1113/jphysiol.1985.sp015599

Buckley, U., Rajendran, P. S., and Shivkumar, K. (2016). Ganglionated plexus ablation for atrial fibrillation: just because we can, does that mean we should? *Heart Rhythm* 14, 133–134. doi: 10.1016/j.hrthm.2016.09.001

Calkins, H., Kuck, K. H., Cappato, R., Brugada, J., Camm, A. J., Chen, S. A., et al. (2012). 2012 HRS/EHRA/ECAS expert consensus statement on catheter and surgical ablation of atrial fibrillation: recommendations for patient selection, procedural techniques, patient management and follow-up, definitions, endpoints, and research trial design. *Europace* 14, 528–606. doi: 10.1093/europace/eus027

Calupca, M. A., Vizzard, M. A., and Parsons, R. L. (2000). Origin of pituitary adenylate cyclase-activating polypeptide (PACAP)-immunoreactive fibers innervating guinea pig parasympathetic cardiac ganglia. *J. Comp. Neurol.* 423, 26–39. doi: 10.1002/1096-9861(20000717)423:1<26::AID-CNE3>3.0.CO;2-C

Castillo, P. E., Schoch, S., Schmitz, F., Südhof, T. C., and Malenka, R. C. (2002). RIM1alpha is required for presynaptic long-term potentiation. *Nature* 415, 327–330. doi: 10.1038/415327a

Chang, Y., Lawson, L. J., Hancock, J. C., and Hoover, D. B. (2005). Pituitary adenylate cyclase-activating polypeptide: localization and differential influence on isolated hearts from rats and guinea pigs. *Regul. Pept.* 129, 139–146. doi: 10.1016/j.regpep.2005.02.012

Chen, P. S., and Tan, A. Y. (2007). Autonomic nerve activity and atrial fibrillation. *Heart Rhythm.* 4, S61–S64. doi: 10.1016/j.hrthm.2006.12.006

Chen, P. S., Chen, L. S., Fishbein, M. C., Lin, S. F., and Nattel, S. (2014). Role of the autonomic nervous system in atrial fibrillation: pathophysiology and therapy. *Circ. Res.* 114, 1500–1515. doi: 10.1161/CIRCRESAHA.114.303772

Chen, P.-S., Chen, L. S., Cao, J. M., Sharifi, B., , Karagueuzian, H. S., and Fishbein, M. C. (2001). Sympathetic nerve sprouting, electrical remodeling and the mechanisms of sudden cardiac death. *Cardiovasc. Res.* 50, 409–416, doi: 10.1016/S0008-6363(00)00308-4

Chen, P.-S., Choi, E.-K., Zhou, S., Shien-Fong, L., and Chen, L. S. (2010). Cardiac neural remodelling and its role in arrhythmogenesis. *Heart Rhythm.* 7, 1512–1513. doi: 10.1016/j.hrthm.2010.05.020

Choi, E. K., Shen, M. J., Han, S., Kim, D., Hwang, S., Sayfo, S., et al. (2010). Intrinsic cardiac nerve activity and paroxysmal atrial tachyarrhythmia in ambulatory dogs. *Circulation* 121, 2615–2623. doi: 10.1161/CIRCULATIONAHA.109.919829

Chou, C. C., and Chen, P. S. (2009). New concepts in atrial fibrillation: neural mechanisms and calcium dynamics. *Cardiol. Clin.* 27, 35–43. doi: 10.1016/j.ccl.2008.09.003

Chugh, S. S., Havmoeller, R., Narayanan, K., Singh, D., Rienstra, M., Benjamin, E. J., et al. (2014). Worldwide epidemiology of atrial fibrillation: a global burden of disease 2010 study. *Circulation* 129, 837–847. doi: 10.1161/CIRCULATIONAHA.113.005119

Czick, M. E., Shapter, C. L., and Silverman, D. I. (2016). Atrial Fibrillation: the science behind its defiance. *Aging Dis.* 7, 635–656. doi: 10.14336/AD.2016.0211

Dobrev, D., Voigt, N., and Wehrens, X. H. (2011). The ryanodine receptor channel as a molecular motif in atrial fibrillation: pathophysiological and therapeutic implications. *Cardiovasc Res.* 89, 734–743. doi: 10.1093/cvr/cvq324

Dobrunz, L. E., Huang, E. P., and Stevens, C. F. (1997). Very short-term plasticity in hippocampal synapses. *Proc. Natl. Acad. Sci. U.S.A.* 94, 14843–14847. doi: 10.1073/pnas.94.26.14843

Dudek, S. M., and Bear, M. F. (1992). Homosynaptic long-term depression in area CA1 of hippocampus and effects of N-methyl-D-aspartate receptor blockade. *Proc. Natl. Acad. Sci. U.S.A.* 89, 4363–4367. doi: 10.1073/pnas.89.10.4363

Edwards, F. R., Hirst, G. D., Klemm, M. F., and Steele, P. A. (1995). Different types of ganglion cell in the cardiac plexus of guinea-pigs. *J. Physiol.* 486, 453–471. doi: 10.1113/jphysiol.1995.sp020825

Ehlers, M. D., Heine, M., Groc, L., Lee, M. C., and Choquet, D. (2007). Diffusional trapping of GluR1 AMPA receptors by input-specific synaptic activity. *Neuron* 54, 447–460. doi: 10.1016/j.neuron.2007.04.010

Esler, M. (1992). The autonomic nervous system and cardiac arrhythmias. *Clin. Auton. Res.* 2, 133–135. doi: 10.1007/BF01819669

Fourie, C., Madison, D. V., and Montgomery, J. M. (2014). Paired whole cell recordings in hippocampal organotypic slices. *J. Vis. Exp.* 91:e51958. doi: 10.3791/51958

Gagliardi, M., Randall, W. C., Bieger, D., Wurster, R. D., and hopkins, D. A. (1988). Activity of *in vivo* canine cardiac plexus neurons. *Am. J. Physiol.* 255, H789–H800. doi: 10.1152/ajpheart.1988.255.4.H789

Genoux, D., and Montgomery, J. M. (2007). Glutamate receptor plasticity at excitatory synapses in the brain. *Clin. Exp. Pharmacol. Physiol.* 34, 1058–1063. doi: 10.1111/j.1440-1681.2007.04722.x

Gibbons, D. D., Southerland, E. M., Hoover, D. B., Beaumont, E., Armour, J. A., and Ardell, J. L. (2012). Neuromodulation targets intrinsic cardiac neurons to attenuate neuronally mediated atrial arrhythmias. *J. Physiol.* 302, R357– R364. doi: 10.1152/ajpregu.00535.2011

Gill, S., Veinot, J., Kavanagh, M., and Pulido, O. (2007). Human heart glutamate receptors—implications for toxicology, food safety, and drug discovery. *Toxicol. Pathol.* 35, 411–417. doi: 10.1080/01926230701230361

Gould, P. A., Yii, M., McLean, C., Finch, S., Marshall, T., Lambert, G. W., et al. (2006). Evidence for increased atrial sympathetic innervation in persistent human atrial fibrillation. *Pacing Clin. Electrophysiol.* 29, 821–829. doi: 10.1111/j.1540-8159.2006.00447.x

Haïssaguerre, M., Jaïs, P., Shah, D. C., Takahashi, A., Hocini, M., Quiniou, G., et al. (1998). Spontaneous initiation of atrial fibrillation by ectopic beats originating in the pulmonary veins. *New Engl. J. Med.* 339, 659–666. doi: 10.1056/NEJM199809033391003

Hanley, C. M., Robinson, V. M., and Kowey, P. R. (2016). Status of antiarrhythmic drug development for atrial fibrillation: new drugs and new molecular mechanisms. *Circ. Arrhythm. Electrophysiol.* 9:e002479. doi: 10.1161/CIRCEP.115.002479

Hardwick, J. C., Ryan, S. E., Beaumont, E., Ardell, J. L., and Southerland, E. M. (2014). Dynamic remodeling of the guinea pig intrinsic cardiac plexus induced by chronic myocardial infarction. *Auton. Neurosci.* 181, 4–12. doi: 10.1016/j.autneu.2013.10.008

Harris, E. W., Ganong, A. H., and Cotman, C. W. (1984). Long-term potentiation in the hippocampus involves activation of N-methyl-D-aspartate receptors. *Brain Res.* 323, 132–137. doi: 10.1016/0006-8993(84)90275-0

Hayashi, Y., Shi, S. H., Esteban, J. A., Piccini, A., Poncer, J. C., and Malinow, R. (2000). Driving AMPA receptors into synapses by LTP and CaMKII: requirement for GluR1 and PDZ domain interaction. *Science* 287, 2262–2267. doi: 10.1126/science.287.5461.2262

Heaton, D. A., Li, D., Almond, S. C., Dawson, T. A., Wang, L., Channon, K. M., et al. (2007). Gene transfer of neuronal nitric oxide synthase into intracardiac Ganglia reverses vagal impairment in hypertensive rats. *Hypertension* 49, 380–388. doi: 10.1161/01.HYP.0000255792.97033.f7

Hillarp, N.-A. (1960). "Peripheral autonomic mechanisms," in *Handbook of Physiology*, *Section I, Neurophysiology*, ed J. Field (Washington, DC: American Physiological Society), 979–1006.

Hirose, M., Furukawa, Y., Nagashima, Y., Lakhe, M., and Chiba, S. (1997). Pituitary adenylate cyclase-activating polypeptide-27 causes a biphasic chronotropic effect and atrial fibrillation in autonomically decentralized, anesthetized dogs. *J. Pharmacol. Exp. Ther.* 283, 478–487.

Hoover, D. B., Isaacs, E. R., Jacques, F., Hoard, J. L., Pagé, P., and Armour, J. A. (2009). Localization of multiple neurotransmitters in surgically derived specimens of human atrial ganglia. *Neuroscience* 164, 1170–1179. doi: 10.1016/j.neuroscience.2009.09.001

Horackova, M., and Armour, J. A. (1995). Role of peripheral autonomic neurones in maintaining adequate cardiac function. *Cardiovasc. Res.* 30, 326–335. doi: 10.1016/0008-6363(95)00105-0

Horackova, M., Armour, J. A., and Byczko, Z. (1999). Distribution of intrinsic cardiac neurons in whole-mount guinea pig atria identified by multiple neurochemical coding a confocal microscope study. *Cell. Tissue Res.* 297, 409–421. doi: 10.1007/s004410051368

Huang, L. C., Thorne, P. R., Housley, G. D., and Montgomery, J. M. (2007). Spatiotemporal definition of neurite outgrowth, refinement and retraction in the developing mouse cochlea. *Development* 134, 2925–2933. doi: 10.1242/dev.001925

Iwasaki, Y.-K., Nishida, K., Kato, T., and Nattel, S. (2011). Atrial fibrillation pathophysiology: implications for management. *Circulation* 124, 2264–2274. doi: 10.1161/CIRCULATIONAHA.111.019893

Jackman, S. L., and Regehr, W. G. (2017). The mechanisms and functions of synaptic facilitation. *Neuron* 94, 447–464. doi: 10.1016/j.neuron.2017.02.047

Jayakar, S. S., Pugh, P. C., Dale, Z., Starr, E. R., Cole, S., and Margiotta, J. F. (2014). PACAP induces plasticity at autonomic synapses by nAChR-dependent NOS1 activation and AKAP-mediated PKA targeting. *Mol. Cell. Neurosci.* 63, 1–12. doi: 10.1016/j.mcn.2014.08.007

Jungen, C., Scherschel, K., Eickholt, C., Kuklik, P., Klatt, N., Bork, N., et al. (2017). Disruption of cardiac cholinergic neurons enhances susceptibility to ventricular arrhythmias. *Nat Commun.* 8:14155. doi: 10.1038/ncomms14155

Katritsis, D. G., Giazitzoglou, E., Zografos, T., Pokushalov, E., Po, S. S., and Camm, A. J. (2011). Rapid pulmonary vein isolation combined with autonomic ganglia modification: a randomized study. *Heart Rhythm.* 8, 672–678. doi: 10.1016/j.hrthm.2010.12.047

Kawashima, T. (2005). The autonomic nervous system of the human heart with special reference to its origin, course, and peripheral distribution. *Anat. Embriol.* 209, 425–438. doi: 10.1007/s00429-005-0462-1

Klemm, M. F., Wallace, D. J., and Hirst, G. D. S. (1997). Distribution of synaptic boutons around identified neurones lying in the cardiac plexus of the guinea-pig. *J. Auton. Nerv. Syst.* 66, 201–207. doi: 10.1016/S0165-1838(97)00084-2

Kneller, J., Zou, R., Vigmond, E. J., Wang, Z., Leon, L. J., Nattel, S., et al. (2002). Cholinergic atrial fibrillation in a computer model of a two-dimensional sheet of canine atrial cells with realistic ionic properties. *Circ. Res.* 90, E73–E87. doi: 10.1161/01.RES.0000019783.88094.BA

Kron, J., Kasirajan, V., Wood, M. A., Kowalski, M., Han, F. T., and Ellenbogen, K. A. (2010). Management of recurrent atrial arrhythmias after minimally invasive surgical pulmonary vein isolation and ganglionic plexi ablation for atrial fibrillation. *Heart Rhythm.* 7, 445–451. doi: 10.1016/j.hrthm.2009.12.008

Kuyumcu, M. S., Ozeke, O., Cay, S., Ozcan, F., Bayraktar, M. F., Kara, M., et al. (2017). The short-term impact of the catheter ablation on noninvasive autonomic nervous system parameters in patients with paroxysmal atrial fibrillation. *Pacing Clin. Electrophysiol.* 40, 1193–1199. doi: 10.1111/pace.13179

Lafuente-Lafuente, C., Valembois, L., Bergmann, J. F., and Belmin, J. (2015). Antiarrhythmics for maintaining sinus rhythm after cardioversion of atrial fibrillation. *Cochrane Database Syst. Rev.* 28:CD005049. doi: 10.1002/14651858.CD005049.pub4

Lancaster, T. S., Melby, S. J., and Damiano, R. J. Jr. (2016). Minimally invasive surgery for atrial fibrillation. *Trends Cardiovasc. Med.* 26, 268–277. doi: 10.1016/j.tcm.2015.07.004

Landis, S. C. (1976). Rat sympathetic neurons and cardiac myocytes developing in microcultures: correlation of the fine structure of endings with

neurotransmitter function in single neurons. *Proc. Nat. Acad. Sci. U.S.A.* 73, 4220–4224. doi: 10.1073/pnas.73.11.4220

Larsen, H. E., Bardsley, E. N., Lefkimmiatis, K., and Paterson, D. J. (2016a). Dysregulation of neuronal Ca^{2+} channel linked to heightened sympathetic phenotype in prohypertensive states. *J. Neurosci.* 36, 8562–8573. doi: 10.1523/JNEUROSCI.1059-16.2016

Larsen, H. E., Lefkimmiatis, K., and Paterson, D. J. (2016b). Sympathetic neurons are a powerful driver of myocyte function in cardiovascular disease. *Sci. Rep.* 6:38898. doi: 10.1038/srep38898

Lee, K. J., Rhyu, I. J., and Pak, D. T. (2014). Synapses need coordination to learn motor skills. *Rev. Neurosci.* 25, 223–230. doi: 10.1515/revneuro-2013-0068

Leighton, A. H., and Lohmann, C. (2016). The wiring of developing sensory circuits-from patterned spontaneous activity to synaptic plasticity mechanisms. *Front. Neural Circuits* 10:71. doi: 10.3389/fncir.2016.00071

Lim, P. B., Malcolme-Lawes, L. C., Stuber, T., Kojodjojo, P., Wright, I. J., Francis, D. P., et al. (2011). Stimulation of the intrinsic cardiac autonomic nervous system results in a gradient of fibrillatory cycle length shortening across the atria during atrial fibrillation in humans. *J. Cardiovasc. Electrophysiol.* 22, 1224–1231. doi: 10.1111/j.1540-8167.2011.02097.x

Lin, Y. Q., Brain, K. L., and Bennett, M. R. (1998). Calcium in sympathetic boutons of rat superior cervical ganglion during facilitation, augmentation and potentiation. *J. Autonom. Nerv. Sys.* 73, 26–37. doi: 10.1016/S0165-1838(98)00108-8

Linz, D., Ukena, C., Mahfoud, F., Neuberger, H. R., and Böhm, M. (2014). Atrial autonomic innervation: a target for interventional antiarrhythmic therapy? *J. Am. Coll. Cardiol.* 63, 215–224. doi: 10.1016/j.jacc.2013.09.020

Liu, D. M., Cuevas, J., and Adams, D. J. (2000). VIP and PACAP potentiation of nicotinic ACh-evoked currents in rat parasympathetic neurons is mediated by G-protein activation. *Eur. J. Neurosci.* 12, 2243–2251. doi: 10.1046/j.1460-9568.2000.00116.x

Magee, J. C., and Schofield, G. G. (1992). Neurotransmission through sympathetic ganglia of spontaneously hypertensive rats. *Hypertension* 20, 367–373. doi: 10.1161/01.HYP.20.3.367

Magee, J. C., and Schofield, G. G. (1994). Alterations of synaptic transmission in sympathetic ganglia of spontaneously hypertensive rats. *Am. J. Physiol. Regul. Integr. Comp. Physiol.* 267, R1397–R1407. doi: 10.1152/ajpregu.1994.267.5.R1397

Mawe, G. M., Talmage, E. K., Lee, K. P., and Parsons, R. L. (1996). Expression of choline acetyltransferase immunoreactivity in guinea pig cardiac ganglia. *Cell Tiss. Res.* 285, 281–286. doi: 10.1007/s004410050645

McAllen, R. M., Salo, L. M., Paton, J. F. R., and Pickering, A. E. (2011). Processing of central and reflex vagal drives by rat cardiac ganglion neurones: an intracellular analysis. *J. Physiol.* 589, 5801–5818. doi: 10.1113/jphysiol.2011.214320

McGrattan, P. A., Brown, J. H., and Brown, O. M. (1987). Parasympathetic effects on *in vivo* rat heart can be regulated through an alpha 1-adrenergic receptor. *Circ. Res.* 60, 465–471. doi: 10.1161/01.RES.60.4.465

Mellor, J., Nicoll, R. A., and Schmitz, D. (2002). Mediation of hippocampal mossy fiber long-term potentiation by presynaptic Ih channels. *Science* 295, 143–147. doi: 10.1126/science.1064285

Montgomery, J. M., Pavlidis, P., and Madison, D. V. (2001). Pair recordings reveal all-silent synaptic connections and the postsynaptic expression of LTP. *Neuron* 29, 691–701. doi: 10.1016/S0896-6273(01)00244-6

Morris, R. G., Anderson, E., Lynch, G. S., and Baudry, M. (1986). Selective impairment of learning and blockade of long-term potentiation by an N-methyl-D-aspartate receptor antagonist, AP5. *Nature* 319, 774–776. doi: 10.1038/319774a0

Nabavi, S., Fox, R., Proulx, C. D., Lin, J. Y., Tsien, R. Y., and Malinow, R. (2014). Engineering a memory with LTD and LTP. *Nature* 511, 348–352. doi: 10.1038/nature13294

Ng, G. A., Brack, K. E., Patel, V. H., and Coote, J. H. (2007). Autonomic modulation of electrical restitution, alternans and ventricular fibrillation initiation in the isolated heart. *Cardiovasc. Res.* 73, 750–760. doi: 10.1016/j.cardiores.2006.12.001

Osman, F., Kundu, S., Tuan, J., Jeilan, M., Stafford, P. J., and Ng, G. A. (2010). Ganglionic plexus ablation during pulmonary vein isolation–predisposing to ventricular arrhythmias? *Indian Pacing Electrophysiol. J.* 10, 104–107. www.ncbi.nlm.nih.gov/pubmed/20126597

Pappone, C., Santinelli, V., Manguso, F., Vicedomini, G., Gugliotta, F., Augello., G., et al. (2004). Pulmonary vein denervation enhances long-term benefit after circumferential ablation for paroxysmal atrial fibrillation. *Circulation* 109, 327–334. doi: 10.1161/01.CIR.0000112641.16340.C7

Pardini, B. J., Lund, D. D., and Schmid, P. G. (1989). Organization of the sympathetic postganglionic innervation of the rat heart. *J. Auton. Nerv. Syst.* 28, 193–201. doi: 10.1016/0165-1838(89)90146-X

Pauza, D. H., Skripka, V., Pauziene, N., and Stropus, R. (2000). Morphology, distribution, and variability of the epicardiac neural ganglionated subplexuses in the human heart. *Anat. Rec.* 259, 353–82. doi: 10.1002/1097-0185(20000801)259:4<353::AID-AR10>3.0.CO;2-R

Pauziene, N., and Pauza, D. H. (2003). Electron microscopic study of intrinsic cardiac ganglia in the adult human. *Ann. Anat.* 185, 135–148. doi: 10.1016/S0940-9602(03)80077-8

Pokushalov, E., Romanov, A., Shugayev, P., Artyomenko, S., Shirokova, N., Turov, A., et al. (2009). Selective ganglionated plexi ablation for paroxysmal atrial fibrillation. *Heart Rhythm.* 6, 1257–1264. doi: 10.1016/j.hrthm.2009.05.018

Pugh, P. C., Jayakar, S. S., and Margiotta, J. F. (2010). PACAP/PAC1R signaling modulates acetylcholine release at neuronal nicotinic synapses. *Mol. Cell. Neurosci.* 43, 244–257. doi: 10.1016/j.mcn.2009.11.007

Rajendran, P. S., Nakamura, K., Ajijola, O. A., Vaseghi, M., Armour, J. A., Ardell, J. L., et al. (2016). Myocardial infarction induces structural and functional remodelling of the intrinsic cardiac nervous system. *J. Physiol.* 594, 321–341. doi: 10.1113/JP271165

Richardson, R. J., Grkovic, I., and Andreson, C. R. (2003). Immunohistochemical analysis of intracardiac ganglia of the rat heart. *Cell Tissue Res.* 314, 337–350. doi: 10.1007/s00441-003-0805-2

Rimmer, K., and Harper, A. A. (2006). Developmental changes in electrophysiological properties and synaptic transmission in rat intracardiac ganglion neurons. *J. Neurophysiol.* 95, 3543–3552. doi: 10.1152/jn.01220.2005

Scherlag, B. J., Patterson, E., and Po, S. S. (2006). The neural basis of atrial fibrillation. *J. Electrocardiol.* 39, S180–S183. doi: 10.1016/j.jelectrocard.2006.05.021

Schotten, U., Verheule, S., Kirchhof, P., and Goette, A. (2011). Pathophysiological mechanisms of atrial fibrillation : a translational appraisal. *Physiol. Rev.* 91, 265–325. doi: 10.1152/physrev.00031.2009

Shanks, J., Manou-Stathopoulou, S., Lu, C. J., Li, D., Paterson, D. J., and Herring, N. (2013). Cardiac sympathetic dysfunction in the prehypertensive spontaneously hypertensive rat. *Am. J. Physiol. Heart Circ. Physiol.* 305, H980–H986. doi: 10.1152/ajpheart.00255.2013

Shcherbakova, O. G., Hurt, C. M., Xiang, Y., Dell'Acqua, M. L., Zhang, Q., Tsien, R. W., et al. (2007). Organization of b-adrenoceptor signaling compartments by sympathetic innervation of cardiac myocytes. *J. Cell Biol.* 176, 521–533. doi: 10.1083/jcb.200604167

Shen, M. J., Choi, E.-K., Tan, A. Y., Lin, S.-F., Fishbein, M. C., Chen, L. S., et al. (2012). Neural mechanisms of atrial arrhythmias. *Nat. Rev. Cardiol.* 9, 30–39. doi: 10.1038/nrcardio.2011.139

Shi, S., Liu, T., Li, Y., Qin, M., Tang, Y., Shen, J. Y.,et al. (2014). Chronic *N*-methyl-d-aspartate receptor activation induces cardiac electrical remodeling and increases susceptibility to ventricular arrhythmias. *Pacing. Clin. Electrophysiol.* 37, 1367–1377. doi: 10.1111/pace.12430

Shi, S., Liu., T., Wang, D., Zhang, Y., Liang, J., Hu, D., et al. (2017). Activation of N-methyl-d-aspartate receptors reduces heart rate variability and facilitates atrial fibrillation in rats. *EP. Europace*. 19, 1237–1243. doi: 10.1093/europace/euw086

Shvalev, V. N., and Sosunov, A. A. (1985). A light and electron microscopic study of cardiac ganglia in mammals. *Z. Mikrosk Anat. Forsch.* 99, 676–694.

Singh, S., Johnson, P. I., Javed, A., Gray, T. S., Lonchyna, V. A., and Wurster R. D. (1999). Monoamine- and histamine-synthesizing enzymes and neurotransmitters within neurons of adult human cardiac ganglia. *Circulation* 99, 411–419. doi: 10.1161/01.CIR.99.3.411

Skok, V. I. (1973). *Physiology of Autonomic Ganglia*. Tokyo: Igaku Shoin, Ltd.

Slavíková, J., Kuncová, J., Reischig, J., and Dvoráková, M. (2003). Catecholaminergic neurons in the rat intrinsic cardiac nervous system. *Neurochem. Res.* 28, 593–598. doi: 10.1023/A:1022837810357

Smith, F. M., Vermeulen, M., and Cardinal, R. (2016). Long-term spinal cord stimulation modifies canine intrinsic cardiac neuronal properties and

ganglionic transmission during high-frequency repetitive activation. *Physiol. Rep*. 4:e12855. doi: 10.14814/phy2.12855

Spyer, K. M. (2011). Vagal preganglionic neurons innervating the heart. *Compr. Physiol*. 2011, 213–239. doi: 10.1002/cphy.cp020105

Staerk, L., Sherer, J. A., Ko, D., Benjamin, E. J., and Helm, R. H. (2017). Atrial fibrillation: epidemiology, pathophysiology, and clinical outcomes. *Circ. Res.* 120, 1501–1517. doi: 10.1161/CIRCRESAHA.117.309732

Tan, A. Y., Li, H., Wachsmann-Hogiu, S., Chen, L. S., Chen, P. S., and Fishbein, M. C. (2006). Autonomic innervation and segmental muscular disconnections at the human pulmonary vein-atrial junction: implications for catheter ablation of atrial-pulmonary vein junction. *J. Am. Coll. of Cardiol.* 48, 132–143. doi: 10.1016/j.jacc.2006.02.054

Tan, A. Y., Zhou, S., Ogawa, M., Song, J., Chu, M., Li, H., et al. (2008). Neural mechanisms of paroxysmal atrial fibrillation and paroxysmal atrial tachycardia in ambulatory canines. *Circulation* 118, 916–925. doi: 10.1161/CIRCULATIONAHA.108.776203

Tang, A. H., Chen, H., Li, T. P., Metzbower, S. R., MacGillvary, H. D., and Blanpied, T. A. (2016). A trans-synaptic nanocolumn aligns neurotransmitter release to receptors. *Nature* 536, 210–214. doi: 10.1038/nature19058

Tompkins, J. D., Ardell, J. L., Hoover, D. B., and Parsons, R. L. (2007). Neurally released pituitary adenylate cyclase-activating polypeptide enhances guinea pig intrinsic cardiac neurone excitability. *J. Physiol*. 582, 87–93. doi: 10.1113/jphysiol.2007.134965

Tompkins, J. D., Lawrence, Y. T., Parsons, R. L., Dyavanapalli, J., Rimmer, K., and Harper, A. A. (2009). Enhancement of Ih , but not inhibition of IM, is a key mechanism underlying the PACAP-induced increase in excitability of guinea pig intrinsic cardiac neurons. *Am. J. Physiol. Regul. Integr. Comp. Physiol.* 297, R52–R59. doi: 10.1152/ajpregu.00039.2009

Tompkins, J. D., Merriam, L. A., Girard, B. M., May, V., and Parsons, R. L. (2015). Nickel suppresses the PACAP-induced increase in guinea pig cardiac neuron excitability. *Am. J. Physiol. Cell Physiol*. 308, C857–C866. doi: 10.1152/ajpcell.00403.2014

Vargas, R., Cifuentes, F., and Morales, M. A. (2011). Role of presynaptic and postsynaptic IP3-dependent intracellular calcium release in long-term potentiation in sympathetic ganglion of the rat. *Synapse.* 65, 441–448. doi: 10.1002/syn.20862

Volk, L., Chiu, S. L., Sharma, K., and Huganir, R. L. (2015). Glutamate synapses in human cognitive disorders. *Ann. Rev. Neurosci.* 38, 127–149. doi: 10.1146/annurev-neuro-071714-033821

Wake, E., and Brack, K. (2016). Characterization of the intrinsic cardiac nervous system. *Auton. Neurosci*. 199, 3–16. doi: 10.1016/j.autneu.2016.08.006

Weerasooriya, R., Khairy, P., Litalien, J., Macle, L., Hocini, M., Sacher, F., et al. (2011). Catheter ablation for atrial fibrillation: are results maintained at 5 years follow up? *J. Am. Coll. of Cardiol*. 57, 160–166. doi: 10.1016/j.jacc.2010.05.061

Wijffels, M. C., Kirchhof, C. J., Dorland, R., and Allessie, M. A. (1995). Atrial fibrillation begets atrial fibrillation. a study in awake chronically instrumented goats. *Circulation* 92, 1954–1968. doi: 10.1161/01.CIR.92.7.1954

Yarowsky, P., and Weinreich, D. (1985). Loss of accommodation in sympathetic neurons from spontaneously hypertensive rats. *Hypertension* 7, 268–276. doi: 10.1161/01.HYP.7.2.268

Zheng, S., Li, Y., Han, J., Zhang, H., Zeng, W., Xu, C., et al. (2013). Long-term results of a minimally invasive surgical pulmonary vein isolation and ganglionic plexi ablation for atrial fibrillation. *PLoS ONE* 8:e79755. doi: 10.1371/journal.pone.0079755

Conflict of Interest Statement: The authors declare that the research was conducted in the absence of any commercial or financial relationships that could be construed as a potential conflict of interest.

frontiers in Neuroscience

ORIGINAL RESEARCH
published: 16 February 2016
doi: 10.3389/fnins.2016.00038

Generalized Poincaré Plots-A New Method for Evaluation of Regimes in Cardiac Neural Control in Atrial Fibrillation and Healthy Subjects

Mirjana M. Platiša[1], Tijana Bojić[2], Siniša U. Pavlović[3], Nikola N. Radovanović[3] and Aleksandar Kalauzi[4]*

[1] Faculty of Medicine, Institute of Biophysics, University of Belgrade, Belgrade, Serbia, [2] Laboratory of Radiobiology and Molecular Genetics, Institute of Nuclear Sciences "Vinča," University of Belgrade, Belgrade, Serbia, [3] Faculty of Medicine, Pacemaker Center, Clinical Center of Serbia, University of Belgrade, Belgrade, Serbia, [4] Department for Life Sciences, Institute for Multidisciplinary Research, University of Belgrade, Belgrade, Serbia

Classical Poincaré plot is a standard way to measure nonlinear regulation of cardiovascular control. In our work we propose a generalized form of Poincaré plot where we track correlation between the duration of j preceding and k next *RR* intervals. The investigation was done in healthy subjects and patients with atrial fibrillation, by varying $j,k \leq 100$. In cases where $j = k$, in healthy subjects the typical pattern was observed by "paths" that were substituting scatterplots and that were initiated and ended by loops of Poincaré plot points. This was not the case for atrial fibrillation patients where Poincaré plot had a simple scattered form. More, a typical matrix of Pearson's correlation coefficients, $r(j,k)$, showed different positions of local maxima, depending on the subject's health condition. In both groups, local maxima were grouped into four clusters which probably determined specific regulatory mechanisms according to correlations between the duration of symmetric and asymmetric observed *RR* intervals. We quantified matrices' degrees of asymmetry and found that they were significantly different: distributed around zero in healthy, while being negative in atrial fibrillation. Also, Pearson's coefficients were higher in healthy than in atrial fibrillation or in signals with reshuffled intervals. Our hypothesis is that by this novel method we can observe heart rate regimes typical for baseline conditions and "defense reaction" in healthy subjects. These data indicate that neural control mechanisms of heart rate are operating in healthy subjects in contrast with atrial fibrillation, identifying it as the state of risk for stress-dependent pathologies. Regulatory regimes of heart rate can be further quantified and explored by the proposed novel method.

Keywords: Poincaré plot, autonomic nervous system, heart rate, atrial fibrillation, indexes of asymmetry, neural control regimes

OPEN ACCESS

Edited by:
Yrsa Bergmann Sverrisdóttir, University of Oxford, UK

Reviewed by:
Alberto Porta, University of Milan, Italy
Sean Parsons, McMaster University, Canada

****Correspondence:***
Mirjana M. Platiša
mirjana.platisa@gmail.com;
mirjana.platisa@mfub.bg.ac.rs

Specialty section:
This article was submitted to Autonomic Neuroscience, a section of the journal Frontiers in Neuroscience

Received: *13 November 2015*
Accepted: *01 February 2016*
Published: *16 February 2016*

Citation:
Platiša MM, Bojić T, Pavlović SU, Radovanović NN and Kalauzi A (2016) Generalized Poincaré Plots-A New Method for Evaluation of Regimes in Cardiac Neural Control in Atrial Fibrillation and Healthy Subjects. Front. Neurosci. 10:38. doi: 10.3389/fnins.2016.00038

INTRODUCTION

Standardized Poincaré plot of the first order is a graphical representation of temporal correlations within time series of inter-beat intervals in which an *RR* interval is plotted against its first predecessor. Generally it is the measure of nonlinearity in heart rate (HR) neural regulatory systems. Classically, a standardized Poincaré plot can quantitatively be evaluated by two measures

of variability, i.e., two measures of standard deviation: SD1, the measure of variability across the line of identity, measuring how big the difference in duration of two successive *RR* intervals can be; SD2, on the other hand, is the measure of variability along the identity line, measuring how dispersed successive *RR* intervals of equal or similar durations can be (Guzik et al., 2006; Porta et al., 2008). Their major contribution is in the field of recognition of different types of cardiac arrhythmias (Zhang et al., 2015), dilated cardiomyopathy (Voss et al., 2012), and in the research of physiology of aging and gender (Voss et al., 2015).

Nonlinearity is a well-known characteristic of HR regulatory systems. In physiological circumstances, different cardiovascular (Eckberg, 1980; Ottesen and Olufsen, 2011) and extra cardiovascular systems (Wu et al., 2005; Kapidžić et al., 2014) influence its dynamics. In physiological situations (Delaney and Brodie, 2000), and pathophysiological situations, like heart rate arrhythmias, nonlinearity of HR changes in a specific manner, making it possible to distinguish different types of arrhythmias. Poincaré plot is a typical example of presenting how these nonlinearities are manifested (Zhang et al., 2015).

Atrial fibrillation (AF) is a sympathovagally triggered disease with dominant vagal role in the initiation of a paroxysmal episode (Chou and Chen, 2009). It is one of the pathophysiological models where altered neural control can be observed and evaluated. Once initiated, it is characterized by multifocal atrial electrical activity that irregularly passes through atrioventricular conductive pathway and depolarizes the ventricules. Atrial fibrillation is a typical neurocardiovascular disease with specific heart rate rhythm pattern but the specificities of autonomic remodeling that takes place in this pathology are still unknown. It is known that increased sympathetic innervation is present in patients with persistent AF, testifying that autonomic remodeling is present. In order to evaluate common functional modulation of both sympathetic and parasympathetic branches of cardiac autonomic nervous system, in the sense of a "black box" system, we applied a novel generalized modality of Poincaré plot in healthy and AF subjects. This is the first time that the generalized Poincaré plot (gPp) is proposed and in order to test its potential, we applied it on healthy subjects and AF patients.

METHODS

Subjects

Ethic Committee of the Faculty of Medicine, University of Belgrade approved this study. All subjects gave written informed consent in accordance with the Declaration of Helsinki. Ambulatory patients with permanent atrial fibrillation (mean age 73; range 51–89) were included. Control subjects were gender matched, 10 men and 3 women. Control group were healthy middle aged subjects (mean age 41; range 35–45 years).

Data Acquisition

Measurements were done in the morning between 9.00 and 12.00 a.m. Subjects were supine with spontaneous breathing during 20 min of ECG measurements (without moving and verbal communications). The ECG was acquired with sampling frequency of 1 kHz by Biopac MP100 system with AcqKnowledge 3.9.1. software (BIOPAC System, Inc., Santa Barbara, CA, USA). ECG data were collected using 100C electrocardiogram amplifier module, leads and on subjects applied AgCl electrodes—Lead I. $RR(t)$ inter-beat intervals was extracted from ECG using OriginPro 8.6 (OriginLab Corporation, USA), visually checked and manually corrected if necessary.

Generalized Poincaré Plots

Further analysis was done with our original programs developed within MATLAB 6.5 (MathWorks Inc., Natick, MA 01760-2098 United States). In the following text, $RRn{-}j$ refers to summed duration of previous successive j *RR* intervals, while $RRn{+}k$ denotes the same quantity for the next successive k intervals. Both quantities were calculated by simply adding the durations of the corresponding intervals around a chosen *R* wave which was moving along the ECG signal. However, a natural limitation imposed on the number of points in these generalized Poincaré plots had to be observed: for an ECG signal with a total of N *RR* intervals, only $N - j - k$ points could be drawn. In order to differentiate results obtained with specific values of j and k, for a pair of number of intervals, *(j,k)*, we propose the term "order of the gPp." Increased complexity of gPp scatter grams, compared to classical Poincaré plots, allows one to study their different properties. In this work we concentrated mostly on their visual characterization and on the resulting Pearson's coefficients of linear correlation $r(RRn{-}j,RRn{+}k)$.

While in case of classical Poincaré plots only one value for each ECG recording is obtained, here we were dealing with matrices $r(RRn{-}j,RRn{+}k)$ which we briefly denoted as $r(j,k)$. Out of many possible characteristics of these matrices, we were interested in the asymmetry of their element values, since we noticed that this property was very sensitive to the state of patient's health. In order to quantify it, we introduce a normalized asymmetry index (*NAI*), which for a $m \times n$ type matrix is defined as

$$NAI = \frac{1}{m \times n} \frac{1}{\bar{r}} \sum_{j=1}^{m} \sum_{k=j+1}^{n} \left(r(k,j) - r(j,k) \right)$$

where $r(j,k)$ represents matrix element, while

$$\bar{r} = \frac{1}{m \times n} \sum_{j=1}^{m} \sum_{k=1}^{n} \left| r(j,k) \right| .$$

By introducing this particular type of normalization, we were able to compare asymmetry indexes calculated from matrices of different range of their element values, as well as their different sizes.

Another property of these Pearson's matrices which drew our attention was the appearance and positions of local maxima, since each local maximum of correlation could potentially signify a temporal range in which a neurocardial regulatory mechanism is operating. However, one should be very careful to verify that a physiological mechanism is lying beneath the appearance of a particular maximum, rather than any of numerous artifactual causes. It is not easy to separate these two causes, both for

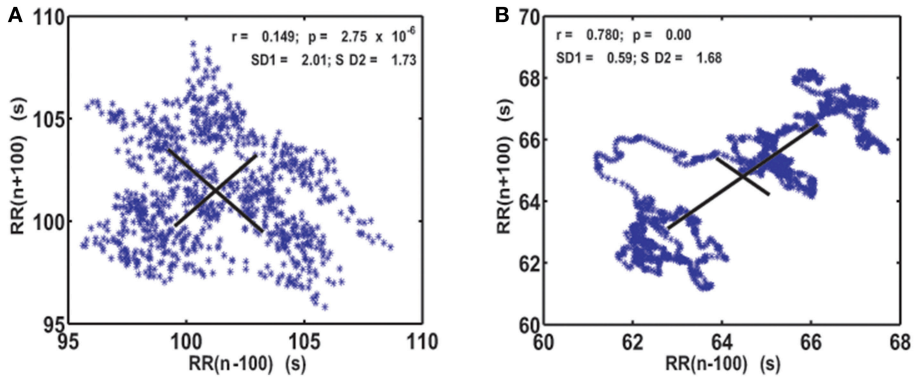

FIGURE 1 | Visualization of the system dynamics with generalized Poincaré plot for $j = k = 100$ *RR* intervals, in patient with atrial fibrillation (A) and healthy subject (B). *SD1* and *SD2*, drawn with solid lines, are measures of dispersion of 100 successive summed *RR* intervals along and away from the identity line.

asymmetry and local maxima, but one of the approaches described in the literature is the method of random reshuffling of the detected *RR* intervals, which we adopted in this work (Guzik et al., 2006; Burykin et al., 2014). More, for each individual, *r(j,k)* matrices obtained for 10 repeated reshufflings were averaged and the corresponding *NAIsh* indexes calculated. Finally, the corrected version of an asymmetry index, *NAIC*, was obtained as their difference: $NAIC = NAI - NAIsh$.

Statistics

Mann Whitney U test was used to compare indexes of asymmetry, *NAIsh* and *NAIC*, between healthy subjects and AF patients as well as their values in every group. To identify groups with different values of the Pearson's correlation coefficients maxima, a k-means clustering analysis was performed. As each local maximum was characterized by three coordinates: its position on the (j,k) plane and its value $r(j,k)$, three dimensional clustering was performed according to these variables. The number of clusters was determined by two-step clustering procedure. Pearson's coefficients, as the third coordinate of cluster centroids, were compared between AF patients and healthy subjects, also by using the Mann Whitney U test. The data are given as mean values ± standard errors. A value of $p < 0.05$ was considered significant. Statistical analyses were performed using the software package SPSS Statistics (version 17.0, SPSS Inc., USA).

RESULTS

Characterization of Generalized Poincaré Plots

As the first step of our analysis we calculated generalized Poincaré plots where $j = k$ and $(j,k) = 1, \ldots, 100$. In healthy subjects, as the order of gPp increased, classical Poincaré plots slowly changed into a more organized pattern. They were characterized by trajectories that were substituting scatterplots and which were initiated and ended by "hanks" or clustered points. This was not the case for AF patients, where Poincaré plots maintained their scattered forms (**Figure 1**).

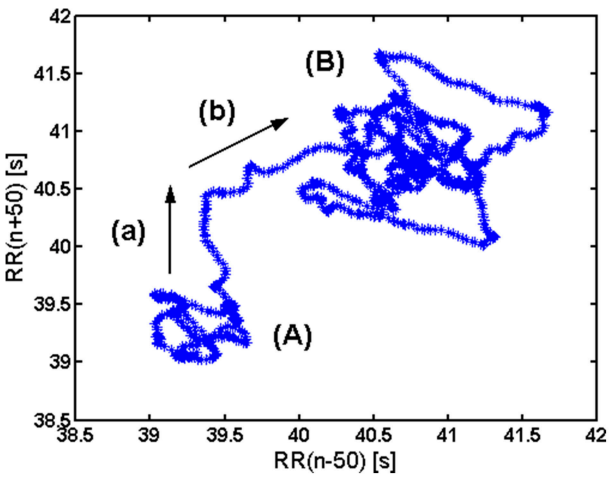

FIGURE 2 | Interpretation of elements of a generalized Poencaré plot in healthy. (A) Tachycardic "hank"; **(B)** Bradycardic "hank"; (a) longer *RR* intervals entering the analysis; (b) shorter *RR* intervals exiting the analysis.

In healthy subjects, in basal conditions, two subregimes can be observed in a gPp (**Figure 2**). One zone, denoted with **(A)**, corresponds to a tachycardic regime, while the other one **(B)** corresponds to bradycardic regime. A two-phase transition from **(A)** to **(B)** is also visible: along (a) longer *RR* intervals enter the analysis, while along (b) shorter *RR* intervals exit the analysis window.

Analysis of *r(j,k)* Matrices

The analysis was expanded to $j \neq k$, resulting in a matrix of Pearson coefficients *r(j,k)*. The reshuffled data were also analyzed and compared with measured data, generating $r_{sh}(j,k)$ matrices. Examples of two typical *r(j,k)* matrices, their reshuffled counterparts, $r_{sh}(j,k)$ and their differences $r(j,k) - r_{sh}(j,k)$, are presented on **Figures 3**, **4**.

For two groups of subjects we studied the distribution of index of asymmetry of reshuffled data *NAIsh* and corrected index

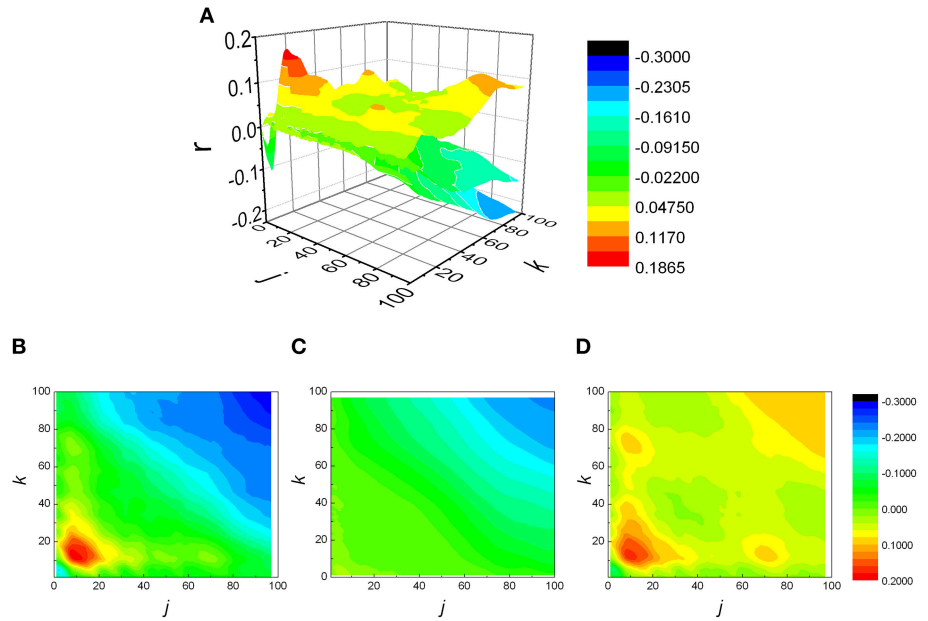

FIGURE 3 | (A) Examples of three matrices of Pearson's correlation coefficients (*r*) between *k* following and *j* preceding *RR* intervals: physiological **(B)**, reshuffled **(C),** and corrected **(D)** for generalized Poincaré plot of the 100th order in patient with atrial fibrillation.

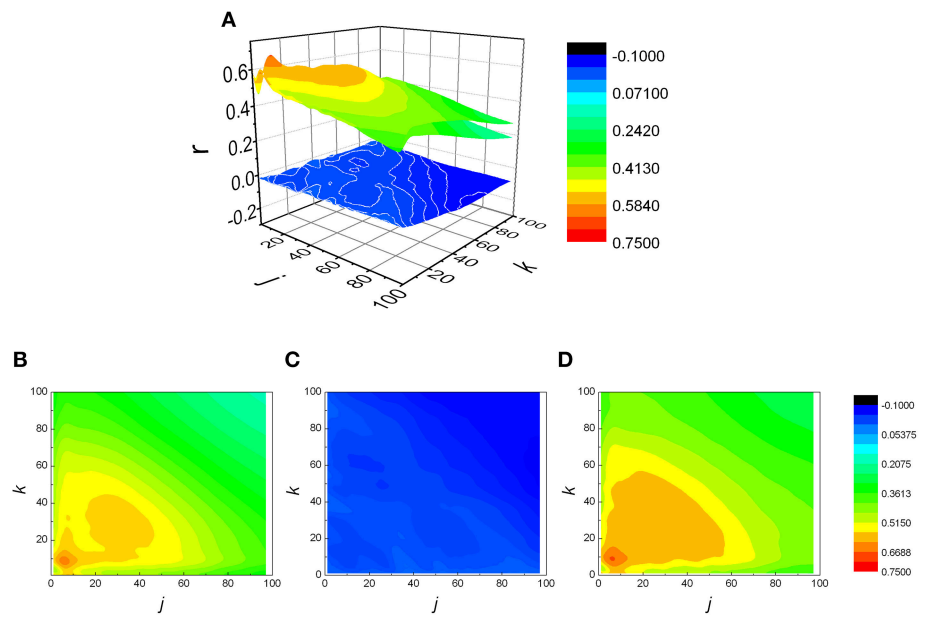

FIGURE 4 | (A) Examples of three matrices of Pearson's correlation coefficients (*r*) between *k* following and *j* preceding *RR* intervals: physiological **(B)**, reshuffled **(C)**, and corrected **(D)** for generalized Poincaré plot of the 100th order in healthy subject. Physiological and corrected matrices appear as one surface because $r_{sh}(j,k) \approx 0$.

of asymmetry *NAIC*, for $j,k \leq 100$. In AF subjects the two distributions were sharply different ($p = 0.007$, $Z = -2.691$): for reshuffled data mean values of *NAIsh* were 0.0063 ± 0.0084, while all *NAIC* values were negative and asymmetrical in shape with mean values -0.047 ± 0.014 (**Figure 5**). As expected, the *NAIsh* was not different between groups ($p = 0.801$, $Z = 0.778$), but *NAIC* was ($p < 0.001$, $Z = -4.283$) (**Figure 5**). Their mean values for healthy were 0.0025 ± 0.0063 for *NAIsh*; 0.0138 ± 0.0056 for *NAIC*.

From **Figures 3**, **4** it could be observed that local maxima of Pearson coefficients matrix were present, with different amplitudes and distributions both in AF patients and healthy

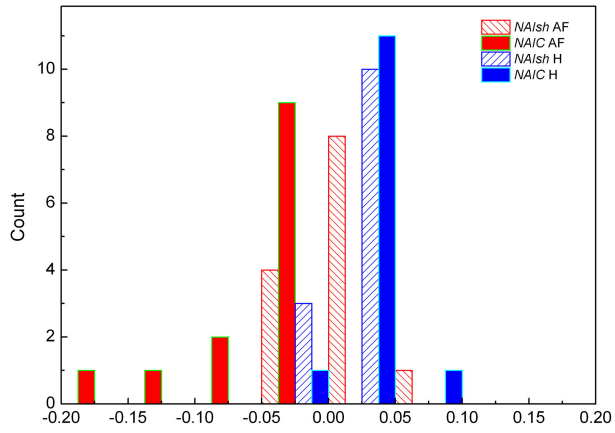

FIGURE 5 | Distributions of *NAIsh* (normalized index of asymmetry for $r_{sh}(j,k)$ matrices) and *NAIC* (corrected normalized index of asymmetry for *r(j,k)* matrices) in subjects with AF and healthy control H.

subjects. Coordinates of all detected local maxima, from 13 AF patients, as well as from their 13 averaged reshuffled data, were measured and pooled. These data are presented as points in **Figures 6A,C,E**, while the same data for healthy subjects are drawn on **Figures 6B,D,F**. Coordinates of pooled local maxima for physiological (not reshuffled) data that were subjected to four cluster k-means algorithm are presented on **Figures 7A–C**.

The first cluster is located at position corresponding to a relatively low order of the Poincaré plot for both groups ($(j,k) = 1,\ldots, 50$ in AF and $(j,k) = 1, \ldots, 30$ in healthy subjects) but the values of local maxima of Pearson's coefficients in AF were significantly different from these values obtained in healthy subjects (**Table 1**). High values in healthy subjects and low values of *r* in AF indicate that correlation between summed durations of *RR* intervals in AF diminished in this short-range of observation. In healthy subjects, maxima with the highest values of Pearson's coefficients were located at $j,k = 1$ which corresponds to values for standardized Pp (not shown in **Table 1**). There is no statistical difference in maxima of Pearson coefficients between groups in the third cluster which is characterized by low correlation between large values of *k* and small values of *j*. Contrary, in the opposite second cluster, estimated for small values of *k* and larger values of *j,* significant correlation existed only in healthy subjects. Statistically significant difference between AF and healthy subjects was also found for maxima of Pearson's coefficients in the fourth cluster determined for $j,k = 50, \ldots, 100$ (**Table 1**).

Method Validation Using Synthetic Signals

In order to validate our method, a special MATLAB program was designed to generate a series of synthetic *RR* intervals in such a way that maximal correlation should be achieved for a given pair (j,k) of *j* preceding and *k* following intervals. When choosing initial parameters of this synthesis, we tried to imitate as much as possible the physiological values that were present in our subjects. By observing a typical histogram of measured *RR* intervals (not shown), we generated in our algorithm first j+k *RR* intervals as uncorrelated, by using a normal distribution, within the range 0.75–1.2 s ("randn" command in MATLAB). Next, an iterative scheme was programmed so that, with each step, duration of the next included interval was calculated so that the value of summed next *k* intervals tends to compensate the change in duration of the previous *j* intervals. However, if this compensation resulted in a value that violated the adopted range (0.75–1.2 s), the limitation posed by this range was applied as stronger, therefore introducing a desired degree of variability within the system.

We generated two series of data, by setting maximal correlation for $j = 5$, $k = 10$ (case where $j < k$) in the first synthetic signal, and $j = 20$, $k = 15$ ($j > k$) in the second example (**Figure 8**). Each signal was subjected to the same analytical procedure as our physiological data, and the results are presented on **Figures 8A–D**. As observed, in both cases maximal correlation was detected precisely at those values of *j* and *k* which were set prior to the analysis. Regarding the sign of *NAI*, as expected, it was negative (−0. 0723) in the first case, where maximal *r* was positioned above the identity diagonal, while a positive value (0.0380) was obtained in the second synthetic signal, where it was situated below this line.

DISCUSSION

It is well-known that blood pressure–heart rate baroreflex operates under different regimes, depending on the metabolic demand and different level of "central command" input (Sagawa, 1983; Rowell, 1993; McIlveen et al., 2001; Zoccoli et al., 2001; Bojić, 2003). This "baroreflex resetting" is visible both under the exercise (dominantly metabolic demand) and "defense reaction" (dominantly central command; Bauer et al., 1988; Jansen et al., 1995). These aforementioned drives change independently both the heart rate and arterial blood pressure set point (Sagawa, 1983; Bauer et al., 1988; McIlveen et al., 2001). By our novel analysis we are able to visualize different regimes (or "set points") of heart rate control in the form of loops, which are delineating the areas of different regimes present in the conditions of basal metabolic demands. These regimes of HR regulation are connected with transitional "paths" connecting one HR regime with the other (**Figure 2**). It is plausible that in our baseline metabolic condition the HR regulatory system passes through different regimes due to different attentional and emotional states, psychological stress or even "defensive behavior" (in physiological terms—different levels and patterns of "central command"; Dampney et al., 2008; Peressutti et al., 2012). The parasympathetic control of heart rate, which is the dominant mechanism of heart rate control in basal conditions (Rowell, 1993) is shown to relate to emotional and attentional state of the subject (Porges, 1992; Suess et al., 1994; Thayer et al., 2009). The fact that "the regimes" were not registered in AF patients speaks for the presence of lower HR adaptiveness in these patients, especially in the circumstances of increased central command in different attentional and emotional states. The dominant adaptive mechanism to "defensive reaction" in AF patients is an increase of stroke volume by an increased cardiac contractility, while HR increase is less present (Goldstain, 2001). This maladaptive pattern creates the diathesis

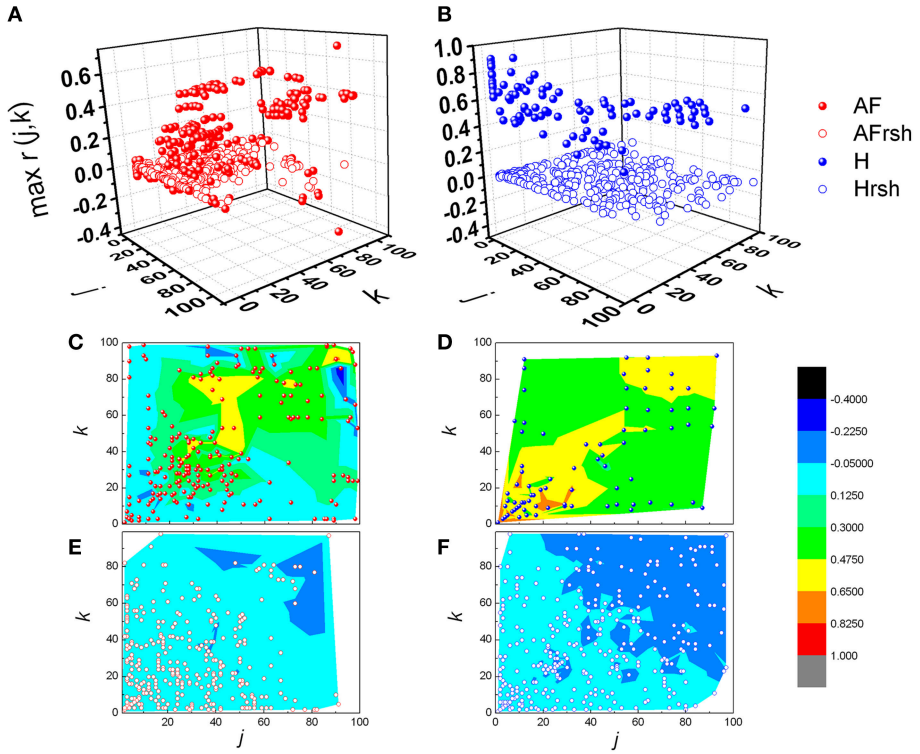

FIGURE 6 | Distribution of pooled local maxima of Pearson's correlation coefficient matrices – max *r(j,k)* in patients with atrial fibrillation (A) and healthy subjects (B) and their corresponding reshuffled data. AF, AF patients; AFrsh, AF reshuffled; H, healthy; Hrsh, H reshuffled. Contour plots are given with corresponding maxima points for patients with AF **(C)** and their reshuffled data **(E)**, and healthy subjects **(D)** and their reshuffled data **(F)**. Contour plots are surface graphs of (*j*,*k*, max *r(j,k)*) data where ranges of max *r(j,k)* values are distinguished by different colors.

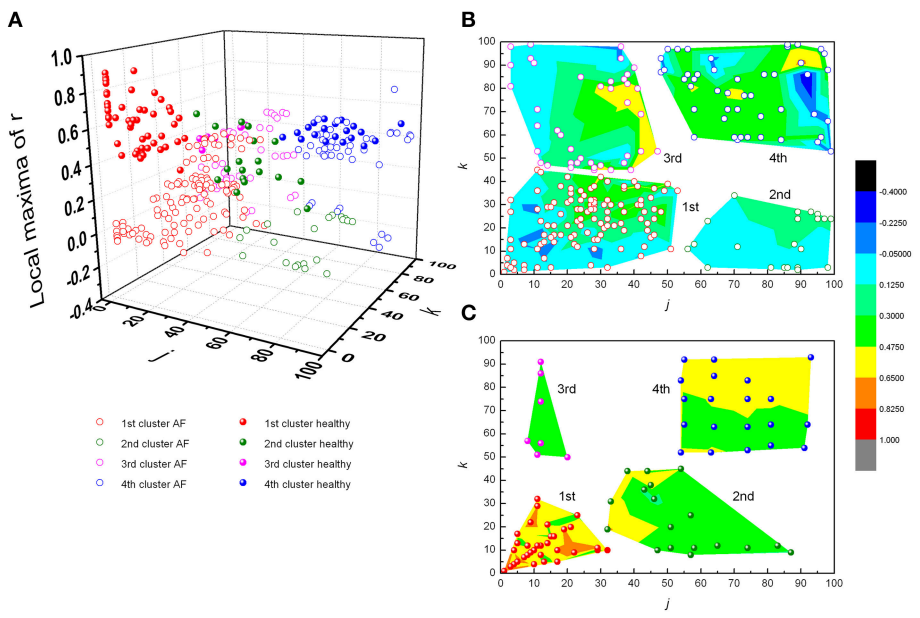

FIGURE 7 | Clusters of subjects' pooled local maxima of Pearson's correlation coefficients matrices – max *r(j,k)* in patients with atrial fibrillation and healthy subjects (A), and corresponding contour plots with local maxima points in patients with AF (B) and healthy subjects (C). Contour plots are surface graphs of (*j*,*k*, max *r(j,k)*) data where ranges of max *r(j,k)* values are distinguished by different colors.

to hypertrophic cardiomiopathy and subsequent degenerative changes of myocardium (Goldstain, 2001). The maladaptive mechanism of AF in defensive reaction is dominantly an increase of cardiac contractility (an increase of stroke volume) and less an increase of heart rate. An increase of cardiac contractility by activation of beta adrenergic receptors increases intracellular concentration of calcium by an increase of voltage gated CaV1.2 channels. An increase of intracellular calcium through different intracellular mechanisms in time results with an increase in size of cardiomyocites and consequently, the thickening of the heart muscle. This condition, known as hypertrophic cardiomyopathy is characterized by serious structural and electrical abnormalities of the heart. It is known that hypertrophic cardiomyopathy coexists with AF (Kumar et al., 2015). The fact that distinct HR regimes lack in AF patients make this group of patients especially vulnerable for the more severe development of hypertrophic cardiomyopathy with respect to subjects with normal cardiac rhythm. This is especially valid if the AF patients are exposed to repeated and continuous stressful circumstances. Future studies need to address the question whether the absence of different heart rate regimes can be considered as the data having an AF diagnostic value.

TABLE 1 | Mean values and standard errors of Pearson's correlation coefficients (*r*) between *k* and *j* intervals in clusters determined for patients with atrial fibrillation (AF) and healthy subjects.

Clusters	AF		Healthy		*Z*	*p*
	N	*r*	N	*r*		
1st	121	0.161 ± 0.016	50	0.627 ± 0.021	−9.692	0.001
2nd	21	0.084 ± 0.017	18	0.428 ± 0.027	−5.324	0.001
3rd	41	0.227 ± 0.033	7	0.388 ± 0.014	−1.738	0.082
4th	46	0.296 ± 0.034	20	0.4768 ± 0.0013	−5.302	0.001

Regarding the distribution of *NAIsh* and *NAIC* indexes presented on **Figure 5**, where AF patients exhibited negative and significantly lower *NAIC* values than in case of healthy or reshuffled data, it would be interesting to give at least a technical interpretation of the results. Let us observe the *r(j,k)* matrix and its identity diagonal ($j = k$). According to the *NAI* definition equation, *NAI* is negative if the sum of *r(j,k)* below the identity diagonal is less than the sum of *r(j,k)* above it, in the system of reference where j is on abscissa, k on the ordinate. In that case average correlation for $k > j$ should be greater than the one for $k < j$. In other words, since $k > j$ refers to shorter preceding and longer following summed *RR* intervals, negative *NAI* means that shorter preceding intervals are more correlated with longer following intervals than the other way round. An attempt to give this fact a physiological interpretation, on the other hand, is much more difficult. Probably some kind of memory mechanism is involved here, but details of this remain to be explored in our future studies. The fact is that both our groups were registered in basal conditions where, in healthy patients, 75% of heart rate control is under vagal influence. In AF patients we have strong sympathoexcitatory background even in basal conditions. We can only hypothesize that the asymmetry of *NAI* in AF can represent different dynamics of

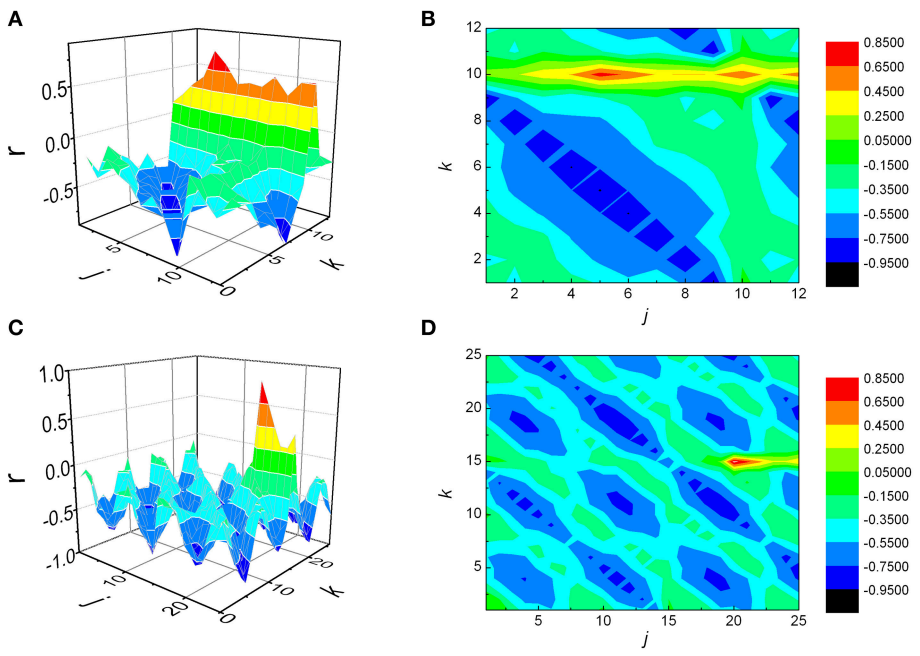

FIGURE 8 | Matrices of Pearson's correlation coefficients (*r*) between *j* preceding and *k* following *RR* intervals, obtained for two synthetic signals. The first signal was generated in such a way that maximal correlation is to be achieved when summed $j = 5$, $k = 10$ intervals are being observed (case where $j < k$, **A** and **B**), while in case of the second one the values were $j = 20$, $k = 15$ ($j > k$, **C** and **D**). As presented, in both cases the analysis was able to detect correctly positions of r_{max}.

sympathetic withdrawal (negative *NAI*, shorter preceding and longer following summed *RR* intervals) versus the effect of sympathetic stimulation on heart rate control. It is necessary to emphasize that both branches of autonomic nervous system act in synergy and that vagal contribution to this phenomenon cannot be excluded. Further pharmacological studies are needed for pathophysiological evaluation of *NAI*.

According to distance between the observed number of *RR* intervals and local maxima of their Pearson's correlation coefficients, four different clusters were recognized. In the first cluster, in healthy subjects, two such maxima were found, one for $j, k = 1$ and one for $j, k \approx 10$. Since these findings were lacking in reshuffled data, we deduced that they were the result of physiological mechanism(s). These phenomena correspond to the dynamics of two dominant neural control mechanisms - parasympathetic and sympathetic. It is known that high values of Pearson's coefficients of correlation, in case of standardized Poincaré plots ($j, k = 1$), correspond to strong correlation between each two successive *RR* intervals, independently of their duration (equally for pairs of shorter or longer *RR* intervals). Parasympathetic control acts fast, is quite powerful (efficient) and can change heart rate within one heart beat (Eckberg, 1980; Levy and Martin, 1996). Due to different dynamics of neurotransmitter release, different intracellular effector molecular mechanisms and different mechanisms of neurotransmitter removal from neuromuscular synaptic cleft, sympathetic nervous system acts slowly with respect to the parasympathetic system (with delay of ∼10 s, Rowell, 1993; Zoccoli et al., 2001; Bojić, 2003). On the basis of these data we hypothesize that the two positions of local maxima of Pearson's correlation coefficients might correspond to the zones of control of parasympathetic ($j, k = 1$) and sympathetic control ($j, k \approx 10$). In healthy subjects these two maxima are well defined, implying that both heart rate neural controls are operative, while in AF patients they are diminished. In the second cluster of Pearson's correlation coefficient maxima, defined for small values of k and larger values of j, significant correlation existed only in healthy subjects, while there was no significant difference between healthy and AF subjects in the third cluster characterized by weak correlations between small values of j and larger values of k. Again, absence of these correlations in reshuffled data and especially their asymmetry in AF patients indicates their physiological origin. According to the duration of observed *RR* intervals belonging to the third cluster, we can only conclude that here regulatory mechanisms with a slower response (in the range of a few minutes) are involved, which are again disturbed by AF. The fourth cluster of pooled subjects' local maxima of Pearson's coefficient was also influenced by AF and probably quantify very slow regulatory mechanisms with a response longer than 3 min, which include termoregulatory mechanisms, renin-angiotesin system, hormonal, metabolic, vagal influence, etc. (Task Force, 1996). In the absence of pharmacological identification of underlying functional mechanisms we can only speculate on the identity and characteristics of the AF Pearson's correlation coefficient maxima, but our approach clearly showed that the pattern of heart rate neural regulation in AF patients is highly distorted, shifted toward higher frequencies and acquired some characteristics of random pattern. However, it is important to emphasize that our results showed that high irregularity of heart rhythm in AF patients was present only in the range of short time scales (approximately shorter than 30 *RR*) when correlation between *RR* intervals didn't exist. But, in the range of larger scales (approximately larger than 30 *RR* intervals) correlations between *RR* intervals appeared. Correlations were asymmetrically distributed and in general smaller then in healthy subjects. The last feature indicates existence of specific residual determinism in AF patients' heart rhythm which probably originated from some kinds of slower regulatory mechanisms. Future pharmacological identification studies need to be done in order to clear these findings.

One more important limitation of our study is the fact that the control group and the experimental group were not age matched. The lack of age-matching could be serious bias in heart rate variability study. We could not age match the groups because it was impossible to create the control group in the range 51–89 years without some cardiovascular pathology. This finding is in accordance with World Heart Federation statement that cardiovascular disease becomes increasingly common with age (http://www.world-heart-federation.org). Inclusion of age matched control subjects with cardiovascular pathology would surely bias the results of our analysis, while, on the other side, we had an interest in heart rate pattern of AF, and there were no data in the literature that the AF pattern is age dependent. We created the control group that was in age category as close as possible to the age catergory of the experimental group. With this precaution on mind, we believe that we obtained the comparison of AF pattern with clear physiological pattern of control subjects and that obtained results can be interpreted as the result of physiological regulatory mechanisms in control group and their pathophysiological modulation due to AF in the patient group.

In our study, by a newly developed generalized Poincaré plot analysis, we gave some new insights into regulation mechanisms of heart dynamics. The proposed method revealed two phenomena: first, transient regimes of system dynamics in summed heart period time series of healthy subjects; second, asymmetry of correlations between *RR* intervals in patients with atrial fibrillation.

AUTHOR CONTRIBUTIONS

MP study protocol, calculation, statistical analysis, and writing of the manuscript. TB study design, data interpretation, and writing of the manuscript. SP clinical examination and recruitment of patients. NR ECG recordings. AK developed the method, calculation, writing of the manuscript. All authors contributed to and have approved the final version.

ACKNOWLEDGMENTS

Projects TR 31020, III 41028, and OI 173022 financed by the Ministry of Education, Science and Technological Development of the Republic of Serbia.

REFERENCES

Bauer, R. M., Vela, M. B., Simon, T., and Waldrop, T. G. (1988). A GABAergic mechanism in the posterior hypothalamus modulates baroreflex bradycardia. *Brain Res. Bull.* 20, 633–641. doi: 10.1016/0361-9230(88)90224-9

Bojić, T. (2003). *Mechanisms of Cardiovascular Control and Effects of Acoustic Stimulation on Cardiovascular System during the Wake-Sleep Cycle.* Ph.D. thesis, Department of Human and General Physiology, Alma Mater Università di Bologna, Bologna.

Burykin, A., Costa, M. D., Citi, L., and Goldberger, A. L. (2014). Dynamical density delay maps: simple, new method for visualising the behaviour of complex systems. *BMC Med. Inform. Decis. Mak.* 14:16. doi: 10.1186/1472-6947-14-6

Chou, C. C., and Chen, P. S. (2009). New concepts in atrial fibrillation: neural mechanisms and calcium dynamics. *Cardiol. Clin.* 27, 35–43. doi: 10.1016/j.ccl.2008.09.003

Dampney, R. A., Horiuchi, J., and McDowall, L. M. (2008). Hypothalamic mechanisms coordinating cardiorespiratory function during exercise and defensive behaviour. *Auton. Neurosci*, 142, 3–10. doi: 10.1016/j.autneu.2008.07.005

Delaney, J. P., and Brodie, D. A. (2000). Effects of short-term psychological stress on the time and frequency domains of heart-rate variability. *Percept. Mot. Skills.* 91, 515–524. doi: 10.2466/pms.2000.91.2.515

Eckberg, D. L. (1980). Nonlinearites of the human carotid baroreceptor-cardiac reflex. *Circ. Res.* 47, 208–216. doi: 10.1161/01.RES.47.2.208

Goldstain, D. (ed.). (2001). *The Autonomic Nervous System in Health and Disease.* New York, NY: Marcel Dekker, Inc.

Guzik, P., Piskorski, J., Krauze, T., Wykretowicz, A., and Wysocki, H. (2006). Heart rate asymetry by Poincare plots of RR intervals. *Biomed. Tech.* 51, 272–275. doi: 10.1515/BMT.2006.054

Jansen, A. S., Nguyen, X. V., Karpitskiy, V., Mettenleiter, T. C., and Loewy, A. D. (1995). Central command neurons of the sympathetic nervous system: basis of the fight-or-flight response. *Science* 270, 644–646.

Kapidžić, A., Platiša, M. M., Bojić, T., and Kalauzi, A. (2014). Nonlinear properties of cardiac rhythm and respiratory signal under paced breathing in young and middle-aged healthy subjects. *Med. Eng. Phys.* 36, 1577–1584. doi: 10.1016/j.medengphy.2014.08.007

Kumar, K. R., Mandleywala, S. N., and Link, M. S. (2015). Atrial and ventricular arrhythmias in hypertrophic cardiomyopathy. *Card. Electrophysiol. Clin.* 7, 173–186. doi: 10.1016/j.ccep.2015.03.002

Levy, M. N., and Martin, P. J. (1996). "Autonomic control of cardiac conduction and automaticity," in *Nervous Control of the Heart*, eds J. T. Shepherd and S. F. Vatner (Amsterdam: Harwood Academic Publishers), 201–223.

McIlveen, S. A., Hayes, S. G., and Kaufman, M. P. (2001). Both central command and exercise pressor reflex reset carotid sinus baroreflex. *Am. J. Physiol. Heart Circ. Physiol.* 280, H1454–H1463.

Ottesen, J. T., and Olufsen, M. S. (2011). Functionality of the baroreceptor nerves in heart rate regulation. *Comput. Methods Programs Biomed.* 101, 208–219. doi: 10.1016/j.cmpb.2010.10.012

Peressutti, C., Martín-González, J. M., and García-Manso, J. M. (2012). Does mindfulness meditation shift the cardiac autonomic nervous system to a highly orderly operational state? *Int. J. Cardiol.* 154, 210–212. doi: 10.1016/j.ijcard.2011.10.054

Porges, S. W. (1992). Vagal tone: a physiologic marker of stress vulnerability. *Pediatrics* 90(3 Pt 2), 498–504.

Porta, A., Casali, K. R., Casali, A. G., Gnecchi-Ruscone, T., Tobaldini, E., Montano, N., et al. (2008). Temporal asymmetries of short term heart period variability are linked to autonomic regulation. *Am. J. Physiol. Regul. Integr. Comp. Physiol.* 295, R550–R557. doi: 10.1152/ajpregu.00129.2008

Rowell, L. B. (1993). "What signals govern the cardiovascular responses to exercise? Role of central command," in *Human Cardiovascular Control,* ed L. B. Rowell (New York, NY: Oxford University Press, Inc.), 371–395.

Sagawa, K. (1983). "Baroreflex control of systemic arterial pressure and vascular bed," in *Handbook of Physiology. The Cardiovascular System. Peripheral Circulation and Organ Blood Flow,* Section 2, Vol. III, eds J. T. Shepherd and F. Abboud (Bethesda, MD: American Physiological Society), 453–496.

Suess, P. E., Porges, S. W., and Plude, D. J. (1994). Cardiac vagal tone and sustained attention in school-age children. *Psychophysiology* 31, 17–22. doi: 10.1111/j.1469-8986.1994.tb01020.x

Task Force of the ESC and the NASPE (1996). Standards of heart rate variability. *Eur. Heart J.* 17:354. doi: 10.1093/oxfordjournals.eurheartj.a014868

Thayer, J. F., Hansen, A. L., Saus-Rose, E., and Johnsen, B. H. (2009). Heart rate variability, prefrontal neural function, and cognitive performance: the neurovisceral integration perspective on self-regulation, adaptation, and health. *Ann. Behav. Med.* 37, 141–153. doi: 10.1007/s12160-009-9101-z

Voss, A., Fischer, C., Schroeder, R., Figulla, H. R., and Goering, M. (2012). Lagged segmented Poincaré plot analysis for risk stratification in patients with dilated cardiomyopathy. *Med. Biol. Eng. Comput.* 50, 727–736. doi: 10.1007/s11517-012-0925-5

Voss, A., Schroeder, R., Heitmann, A., Peters, A., and Perz, S. (2015). Short-term heart rate variability-influence of gender and age in healthy subjects. *PLoS ONE.* 10:e0118308. doi: 10.1371/journal.pone.0118308

Wu, G. Q., Xin, J. B., Li, L. S., Li, C., Fang, Y., and Poon, C. S. (2005). Nonlinear interaction of voluntary breathing and cardiovascular regulation. *Conf. Proc. IEEE Eng. Med. Biol. Soc.* 1, 764–767. doi: 10.1109/iembs.2005.1616527

Zhang, L., Guo, T., Xi, B., Fan, Y., Wang, K., Bi, J., et al. (2015). Automatic recognition of cardiac arrhythmias based on the geometric patterns of Poincaré plots. *Physiol. Meas.* 36, 283–301. doi: 10.1088/0967-3334/36/2/283

Zoccoli, G., Andreoli, E., Bojic, T., Cianci, T., Franzini, C., Predieri, S., et al. (2001). Central and baroreflex control of heart rate during the wake-sleep cycle in rat. *Sleep* 24, 753–758.

Conflict of Interest Statement: The authors declare that the research was conducted in the absence of any commercial or financial relationships that could be construed as a potential conflict of interest.

frontiers in Physiology

REVIEW
published: 14 September 2017
doi: 10.3389/fphys.2017.00665

The Role of the Autonomic Nervous System in the Pathophysiology of Obesity

Daniela Guarino[1,2,3], *Monica Nannipieri*[1], *Giorgio Iervasi*[2], *Stefano Taddei*[1] and *Rosa Maria Bruno*[1]*

[1] Department of Clinical and Experimental Medicine, University of Pisa, Pisa, Italy, [2] Institute of Clinical Physiology of CNR, Pisa, Italy, [3] Scuola Superiore Sant'Anna, Pisa, Italy

Obesity is reaching epidemic proportions globally and represents a major cause of comorbidities, mostly related to cardiovascular disease. The autonomic nervous system (ANS) dysfunction has a two-way relationship with obesity. Indeed, alterations of the ANS might be involved in the pathogenesis of obesity, acting on different pathways. On the other hand, the excess weight induces ANS dysfunction, which may be involved in the haemodynamic and metabolic alterations that increase the cardiovascular risk of obese individuals, i.e., hypertension, insulin resistance and dyslipidemia. This article will review current evidence about the role of the ANS in short-term and long-term regulation of energy homeostasis. Furthermore, an increased sympathetic activity has been demonstrated in obese patients, particularly in the muscle vasculature and in the kidneys, possibily contributing to increased cardiovascular risk. Selective leptin resistance, obstructive sleep apnea syndrome, hyperinsulinemia and low ghrelin levels are possible mechanisms underlying sympathetic activation in obesity. Weight loss is able to reverse metabolic and autonomic alterations associated with obesity. Given the crucial role of autonomic dysfunction in the pathophysiology of obesity and its cardiovascular complications, vagal nerve modulation and sympathetic inhibition may serve as therapeutic targets in this condition.

Keywords: autonomic nervous system, obesity, gut hormones, adipose tissue, energy expenditure, weight loss, vagal nerve stimulation, vagal nerve blockade

OPEN ACCESS

Edited by:
Tijana Bojić,
INN Vinča University of Belgrade, Serbia

Reviewed by:
Elisabeth Lambert,
Swinburne University of Technology, Australia
Geoffrey A. Head,
Baker IDI Heart and Diabetes Institute, Australia

***Correspondence:**
Rosa Maria Bruno
rosamaria.bruno@unipi.it

Specialty section:
This article was submitted to Autonomic Neuroscience, a section of the journal Frontiers in Physiology

Received: *02 February 2017*
Accepted: *22 August 2017*
Published: *14 September 2017*

Citation:
Guarino D, Nannipieri M, Iervasi G, Taddei S and Bruno RM (2017) The Role of the Autonomic Nervous System in the Pathophysiology of Obesity. Front. Physiol. 8:665. doi: 10.3389/fphys.2017.00665

INTRODUCTION

Obesity is a challenge for global public health. The worldwide prevalence of obesity has nearly doubled in the past decades (World Health Organization). Obesity may induce the onset of other conditions leading to overt cardiovascular disease, such as glucose intolerance, dyslipidemia, impaired glucose tolerance and type 2 diabetes, hypertension, and kidney failure (Martin-Rodriguez et al., 2015; Soares et al., 2015).

In this framework, there is a strong need to reach a deeper understanding of the basic mechanisms coupling energy balance with glucose homeostasis (Flier, 2001; Obici and Rossetti, 2003), in order to develop new treatments able to counteract obesity and thus decrease the risk of cardiovascular disease. The autonomic nervous system (ANS) plays a major role in the integrated regulation of food intake, involving satiety signals and energy expenditure: thus ANS dysregulation might favor body weight gain. Conversely, obesity might trigger alterations in the

sympathetic regulation of cardiovascular function, thus favoring the development of cardiovascular complications and events. This article is aimed at reviewing the role of ANS in the pathophysiology of obesity, and thus to identify possible new therapeutic targets for the treatment of obesity and its complications.

ROLE OF THE ANS IN ENERGY HOMEOSTASIS

Body weight is regulated by a complex homeostatic system, whose main components are the modulation of appetite and satiety and the modulation of energy expenditure and energy storage in the adipose tissue. This homeostatic system is aimed at maintaining a stable body weight and requires the existence of a network of signals conveying information from the periphery to the central nervous system (CNS), where these signals are integrated and contribute to long-term and short-term regulation of body weight (Cummings and Schwartz, 2003). Peripheral signals involved in energy homeostasis can be classified as short-acting signals, such as gastric distension and gut hormone release, which are acutely affected by ingested nutrients and modulating satiety, and long-acting signals, such as leptin and insulin, which regulate overall body weight and adiposity.

It is clear that any dysfunction in the pathways involved in maintaining body weight homeostasis may lead to weight gain and obesity. The ANS plays a central role in the communication between the CNS and the gastrointestinal system either in short-term or in long-term regulation of body weight (**Figure 1**). Going into detail, vagal afferents to the brain are crucial for information transfer from gut hormones and CNS and as a mediator of sense of satiety after gastric distension.

ANS and Short-Term Regulation of Body Weight

The main mediators of short-term regulation of body weight through the sensation of satiety are:

- Gastric distension (mediated by vagal afferents) (**Figure 1**);
- Gut hormones release. Indeed the gastrointestinal tract, in addition to its primary role in digestion and adsorption of nutrients, regulates food ingestion by gut hormones. Interestingly, part of their action is mediated by vagal afferents. The action of gut hormones on vagal afferent neurons is now recognized to be an early step in controlling nutrient delivery to the intestine by regulating food intake and gastric emptying. Therefore, gut hormones and vagal afferent neurons have been considered playing an important role in the pathogenesis of obesity (Dockray, 2014).

Satiety is a result of neuro-humoral stimuli generated during food intake, leading to control of meal size and termination (Woods et al., 1998): thus it is not surprising that an altered sense of satiety has been involved in the pathogenesis of obesity. The main hypothalamic areas involved in the control of both hunger and satiety are the arcuate nucleus (ARC), the paraventricular nucleus, the dorsomedial and ventromedial hypothalamus, and the lateral hypothalamic area. These areas are influenced by different peripheral signals coming from the liver and gut, the endocrine pancreas and the adipocytes, which could act directly on neurons in the CNS or through afferent neurons. Indeed, the afferent vagal pathways are probably the most important link between the gut and the brain for satiety signal modulation (Berthoud, 2008a). Vagal afferent neurons receive post-ingestive information from the gastrointestinal tract by mechanoreceptor stimulation (Ikramuddin et al., 2014) in response to gastric distension, by gut hormone release in response to nutritional composition of food consumed, and by direct action of some nutrients, such as short chain fatty acids (Baskin et al., 1999; Obici et al., 2002; Brown et al., 2006; Capasso and Izzo, 2008; Shin et al., 2009; Scherer et al., 2011; Iwasaki et al., 2013). Finally, vagal afferents receive metabolic information by chemoreceptors located in the hepatoportal system (Yi et al., 2010; **Figure 1**). Signals from peripheral receptors reach via vagal afferents the nucleus of the solitary tract/area postrema (NTS/AP) complex in the brain stem, which integrates sensory information from the gastrointestinal tract and abdominal viscera and taste information from the oral cavity

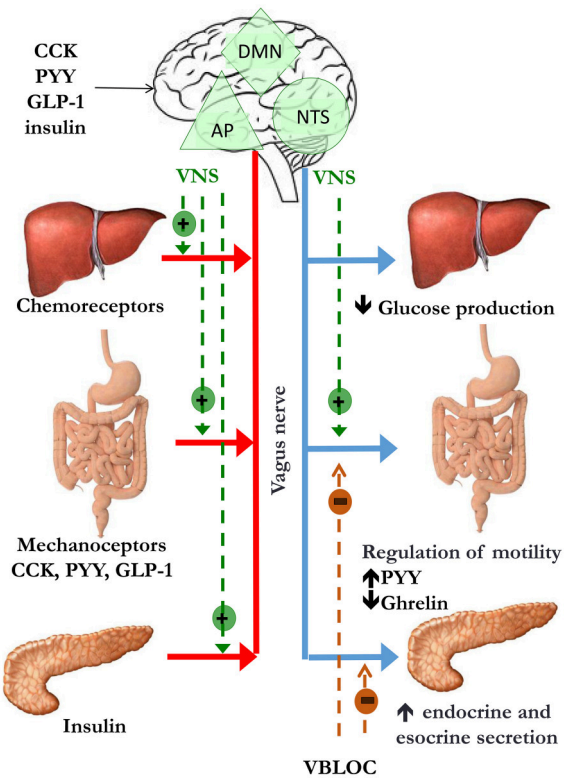

FIGURE 1 | Peripheral signals of satiety and gastric emptying reach the nucleus of the solitary tract/area postrema complex (NST/AP) via afferent vagal nerves (red line). The NTS projects to the dorsal motor nucleus (DMN). This pathway modulates intestinal motility and secretion, glucose production and pancreatic secretion via efferent vagal nerves (blue line). The suggested site of action of vagal nerve stimulation (VNS) is indicated by the dotted green lines, while mechanism of weight loss hypothesized vagal nerve blockade includes decrease in gastric emptying, increase in gut hormones release and inhibition of pancreatic esocrine secretion (dotted orange lines).

(Travers et al., 1987). NTS projects back to the gut via vago-vagal autonomic reflexes through the dorsal motor nucleus. The stimulation of this pathway leads to gut responses, including control of intestinal transit time and motility (i.e., delayed gastric emptying) (Forster et al., 1990), absorption rate and exposure of enteroendocrine cells (EECs) to nutrients, with changes in gastrointestinal hormones and pancreatic secretion, involved in satiety (Li and Owyang, 1994; Berthoud, 2008b).

ANS and Gut Hormones

Cholecystokinin (CCK)

Cholecystokinin (CCK) is an anorectic hormone secreted by different tissues, including the I-cells of the small intestine (Buffa et al., 1976), with the main effect of reducing meal size and duration (Kissileff et al., 2003). Its release pattern suggests that CCK plays a role in meal termination and early phase satiety (Burton-Freeman et al., 2002).

CCK binds A-type receptors, found either in the periphery or in the brain, and B-type receptors, found only in the brain (Fink et al., 1998). CCK may act directly on the CNS (Blessing, 1997) and/or peripherally via vagal afferent fibers (Corp et al., 1993; Burdyga et al., 2003). Some authors reported that the main mechanism trough which CCK regulates food intake is the inhibition of gastric emptying (Moran and Kinzig, 2004). Furthermore, Wank (1995) and Granger et al. (1980) CCK induces gastrointestinal vasodilation acting on CCK-A receptors placed on abdominal vagal afferents projecting to NTS. This pathway involves also caudal and rostral ventrolateral medulla neurons, thus leading to suppression of sympathetic vascular tone (Sartor and Verberne, 2002, 2006, 2008). The role of alteration of CCK secretion in obesity is uncertain: indeed, obese patients exhibit higher CCK plasmatic levels that lean individuals, either in fasting conditions or after a high-fat meal (Little et al., 2005).

Peptide YY (PYY)

Peptide YY (PYY) is released by the L-cells of the gastrointestinal tract, in response to a meal in proportion to calories, and to luminal content of fatty acids, fibers and bile acid (Adrian et al., 1985; Onaga et al., 2002). Its actions in the brainstem and in the gut are mediated by Y_1 and Y_2 receptors (Yang, 2002). PYY acts mainly via the Y_2 receptor (Dumont et al., 1995), identified on both intestinal vagal afferents and within the ARC: both pathways may thus be involved in the anorectic effects of Y_2 receptor activation (Fetissov et al., 2004; Koda et al., 2005). Central and peripheral specific binding sites of PYY have been identified in NTS/AP and in dorsal motor nucleus (Parker and Herzog, 1999), as well as in in enterocytes, myenteric and submucosal neurons (Cox, 2007a,b). PYY release in the post-prandial period seems to be induced also by the indirect stimulation of endocrine L-cells through vagal neural pathways (Fu-Cheng et al., 1997; Lin and Taylor, 2004). In animal models, PYY release was blocked by atropine, a nicotinic ganglionic blocker (Lin and Taylor, 2004), while intravenous administration of bethanechol (a muscarinic cholinergic agonist) stimulated PYY release (Dumoulin et al., 1995). PYY acts also as a counterregulatory hormone for ghrelin release via growth hormone secretagogue receptor, expressed in the nodose ganglion of vagal nerves (Neary et al., 2003) and in the ARC. PYY plasma concentrations are lower in obese in comparison to lean individuals either in the fasting period (Batterham et al., 2003) or in the post-prandial period (le Roux et al., 2006). The latter phenomenon could be responsible of impaired satiety signal in obesity, since PYY infusion reduces caloric intake both in obese and lean individuals (Batterham et al., 2003). Experimental data suggest that electrical vagal stimulation may increase PYY secretion from the isolated ileum in pigs (Sheikh et al., 1989).

Pancreatic Polypeptide (PP)

Pancreatic Polypeptide (PP) is secreted by cells located at the periphery of the pancreatic islets, in the esocrine pancreas and distal gut (Track, 1980; Ekblad and Sundler, 2002) in response to food intake. PP has inhibitory effects on gastric emptying, and delays the post-prandial rise in insulin (Schmidt et al., 2005). The vagal nerve controls both PP basal and post-prandial release. Surgical or pharmacological vagal blockade causes a marked reduction in meal-induced PP release in dogs (Niebel et al., 1987) and humans (Meguro et al., 1995).

The role of PP in obesity pathogenesis is controversial. Some authors reported a blunted post-prandial PP increase in obese individuals (Lassmann et al., 1980; Glaser et al., 1988), and no differences have been reported in circulating PP between obese subjects and lean individuals (Jorde and Burhol, 1984). However, since plasma PP concentrations are almost exclusively under vagal control, they can be used as an indicator of vagal activity in a number of experimental settings (Schwartz, 1983; Arosio et al., 2004).

Glucagon-Like Peptide-1 (GLP-1)

Glucagon-like peptide-1 (GLP-1) is an anorectic hormone, member of the incretin family. It is cleaved from preproglucagon within the intestine, where it is released by endocrine L-cells of the distal gut (Wettergren et al., 1997). GLP-1 levels rises post-prandially in response to a meal and fall in the fasting state. GLP-1 release is proportional to the calories ingested (Kreymann et al., 1987; Orskov et al., 1994) and it is particularly responsive to carbohydrates (Lavin et al., 1998) and fats (Frost et al., 2003). Some authors have suggested that circulating GLP-1 levels are reduced in obesity and normalized with weight loss (Verdich et al., 2001). GLP-1 mediates glucose-dependent insulinotropic effects in a number of species, including humans (Holst et al., 1987; Mojsov et al., 1987). Furthermore, it inhibits gastric acid secretion and gastric emptying (Imeryuz et al., 1997; Edvell and Lindstrom, 1999; Sheikh, 2013). The effects of GLP-1 on appetite regulation are mediated by the GLP-1 receptor. GLP-1 receptors are found not only in peripheral tissues (Bullock et al., 1996) but also in CNS areas (Kastin et al., 2002) involved in the regulation of satiety and induction of taste aversion, such as NTS/AP and ARC (Turton et al., 1996). In animal models GLP-1 actions on CNS seem to be mediated by afferent vagal fibers (Ronveaux et al., 2015). Indeed, vagotomy attenuates the satiating effect of GLP-1 (Nakabayashi et al., 1996; Abbott et al., 2005). Recent data showed that an intact vagal nerve is necessary for the

inhibition of food intake by intravenous GLP-1 in human patients undergoing vagotomy and pyloroplasty (Plamboeck et al., 2013). Furthermore, some evidence suggest that GLP-1 crosses the blood brain barrier to act directly on CNS receptors (Kastin et al., 2002).

Ghrelin

Ghrelin is an orexigenic hormone, primarily secreted by endocrine cells in the oxyntic mucosa of the stomach. Ghrelin stimulates eating behavior and is involved in meal initiation; ghrelin suppression after a meal is crucial to provide a feedback signaling to brain and stop food intake (Kojima et al., 1999; Cummings et al., 2001; Tschop et al., 2001). Thus it is not surprising that obese individuals, though exhibiting lower fasting ghrelin levels than lean individuals, lack the physiological ghrelin suppression in the post-prandial phase: this phenomenon could lead to increased food consumption and, finally, obesity (English et al., 2002).

Ghrelin suppression after meals, which is crucial to reduce caloric intake, is induced by several factors include changes in plasma insulin, intestinal osmolarity, and enteric neural signaling, but a key role for vagal signaling has been also hypothesized (Date et al., 2002; Lee et al., 2002). Indeed in healthy humans vagal stimulation, achieved by modified sham feeding technique (in which nutrients are chewed and tasted but not swallowed) has an inhibitory effect on ghrelin release comparable to real feeding (Arosio et al., 2004; Heath et al., 2004).

Ghrelin plays also a role in long-term body weight regulation, acting as an adiposity signal, communicating the state of energy stores to the brain. Thus fasting ghrelin levels are reduced in obese individuals, and increase after weight loss (Cummings, 2006). However, gastric bypass is associated with markedly suppressed ghrelin levels: this phenomenon possibly favor a greater weight loss after this surgical procedure (Cummings et al., 2002).

Insulin

Insulin, beyond its established role in glucose (Obici et al., 2002) and lipid metabolism (Scherer et al., 2011), is also involved in satiety pathway acting on CNS. Chronic or acute intracerebroventricular administration of insulin reduces food intake and body weight in a variety of species. Insulin receptors are expressed in the CNS neurons, especially in the ARC (Plum et al., 2005), and participate in the food intake control (Baskin et al., 1999; Brown et al., 2006). On the other hand, insulin could act on its peripheral receptors located in the nodose ganglion (Iwasaki et al., 2013). Hyperphagia and obesity could be, at least in part, caused by impaired response to insulin of nodose ganglion neurons (Iwasaki et al., 2013).

Chronic hyperinsulinemia is a feature of obesity, aimed at restoring energy balance and limiting weight gain in a compensatory fashion. However, it may act as a maladaptive mechanism, inducing sympathetic overactivity (Landsberg, 1986).

Leptin

Leptin is a hormone released by the white adipose tissue (WAT), whose main actions are to suppress appetite and to regulate glucose metabolism (Elmquist et al., 1998; Elias et al., 2000). However, leptin pathways are involved also in energy expenditure control, as reviewed below. Leptin plasma levels decrease during fasting and increase after overfeeding, whereas leptin administration decreases food intake in animals and humans (Campfield et al., 1995; Heymsfield et al., 1999). The ARC is the most important site involved in leptin-related food intake (Satoh et al., 1997; Haynes, 2000). Within the ARC, two antagonistically acting neuronal populations, the neuropeptide Y (NPY) and proopiomelanocortinergic (POMC) neurons, were identified as immediate downstream targets of leptin. Even though leptin receptors are expressed on both neuronal populations, leptin stimulation of NPY neurons decreases their firing and attenuates food intake, whereas its actions on POMC neurons are opposite (Pandit et al., 2017).

While genetic syndromes characterized by leptin deficiency present hyperfagia and obesity (Zhang et al., 1994), most obese individuals rather have hyperleptinemia (Schwartz et al., 1997), due to desensitization of its own receptor (Considine et al., 1996).

SNS is involved in regulation of secretory function of WAT, especially for leptin secretion. Indeed, acute treatment with catecholamines in *in vitro* experimental human studies reduces circulating leptin through β1 and β2 receptors (Scriba et al., 2000). Furthermore, sympathetic activation induced by cold exposure induces not only increased metabolic rate and mobilization of free fatty acids, but also a rapid decrease in leptin gene expression and plasma leptin levels (Trayhurn et al., 1995).

ANS and the Long-Term Regulation of Body Weight

The ANS seems to play a role, though not entirely clear, in energy expenditure and storage. In humans, the energy is stored mainly in the WAT under the action of insulin, from where can be mobilized mainly by activation of SNS. Furthermore, SNS might increase energy expenditure by acting either on brown adipose tissue (BAT) thermogenesis or on the cardiovascular system: this neuronal pathway is modulated by leptin (Pandit et al., 2017)

The Role of SNS in Lipolysis

It is well known that lipolysis in the WAT is regulated by SNS and insulin, the principal initiator of lipolysis and a potent inhibitor of lipolysis respectively (Goodridge and Ball, 1965; Prigge and Grande, 1971). Indeed, sympathetic nerve stimulation results in fatty acid release (Rosell, 1966), while sympathetic or ganglionic blockade inhibits lipid mobilization (Gilgen et al., 1962). On the other hand, adrenal medullary catecholamines have no effects on lipid mobilization (Takahashi and Shimazu, 1981), confirming that lipolysis is induced by increased SNS outflow directed to WAT (Rebuffe-Scrive, 1991). Kreier et al. (2002) hypothesized also a parasympathetic innervation of WAT in animal models, possibly modulating insulin-mediated glucose uptake and free fatty acid metabolism in an anabolic way, thus promoting lipid accumulation. According to this hypothesis, lipid accumulation

in obesity could be due either to a decrease in SNS activity or by an increase in parasympathetic activity (Bartness, 2002). However, other studies failed to demostrate parasympathetic innervation in WAT (Giordano et al., 2006).

The Role of SNS in Energy Expenditure

Total energy expenditure is composed of resting metabolic rate (including cardiorespiratory work and the maintenance of transmembrane ion gradients at rest), physical activity and thermogenesis (shivering and non-shivering), and the termic effect of food. SNS activation induces total energy expenditure, either increasing cardiorespiratory work or increasing thermogenesis.

It is well known that the SNS plays a pivotal role in both blood pressure and metabolic homeostatic control by regulating cardiac output, peripheral vascular resistance, and heat production, which account for a large fraction of resting metabolic rate (Goran, 2000). Indeed, pharmacological adrenergic blockade is able to reduce resting energy expenditure (Welle et al., 1991; Monroe et al., 2001; Shibao et al., 2007).

At variance to what was previously thought, BAT is not present only in children, but also in lean and obese adult humans (Virtanen et al., 2009). Its main function is to increase energy expenditure by inducing cold- or diet-stimulated heat production (van der Lans et al., 2013), and by uncoupling oxidative phosphorylation from ATP synthesis through the uncoupling protein-1 in BAT mitochondria (Cannon and Nedergaard, 2004; Saito, 2013). Functional BAT in adults is detectable after exposure to mild cold (Saito et al., 2009) and its activity is inversely related to body mass index and body fat percentage (van Marken Lichtenbelt et al., 2009). Lean subjects increase energy expenditure in response to mild cold, whereas obese subjects have a blunted cold-induced thermogenesis (Wijers et al., 2010).

BAT thermogenesis is regulated by sympathetic nerves. As previously stated, sympathetic activation results in mobilization from WAT of fatty acids, which are then used by BAT to dissipate energy as heat (**Figure 2**). As far as sympathetic control is concerned, patients with surgical unilateral sympathectomy show a detectable uptake of 18F-*f*luorodeoxyglucose (*1*8F-FDG) in BAT by positron emission tomography on the unaffected side, but not on the side of surgical sympathectomy (Lebron et al., 2010). Administration of β-adrenergic receptor blockade reduces BAT 18F-FDG uptake (Soderlund et al., 2007) in patients with known or suspected cancer as well as in a patient with paraganglioma, a condition characterized by a massively increased metabolic BAT activity, induced by excess circulating catecholamines (Cheng et al., 2012). The role of α-receptors and α-blockade is less clear. In a patient with catecholamine-secreting paraganglioma, BAT 18F-FDG uptake was suppressed after α-blockade (Sondergaard et al., 2015). The sympathomimetic drug ephedrine activates BAT in lean but not in obese subjects, though the degree of activation is substantially lower than observed after cold exposure (Carey et al., 2013). Conversely, the effect of parasympathetic nervous system on BAT appears to be indirect. Indeed, in animal models, the suppression of NE release in BAT, induced by ghrelin infusion, is abolished after vagotomy (Mano-Otagiri et al., 2009).

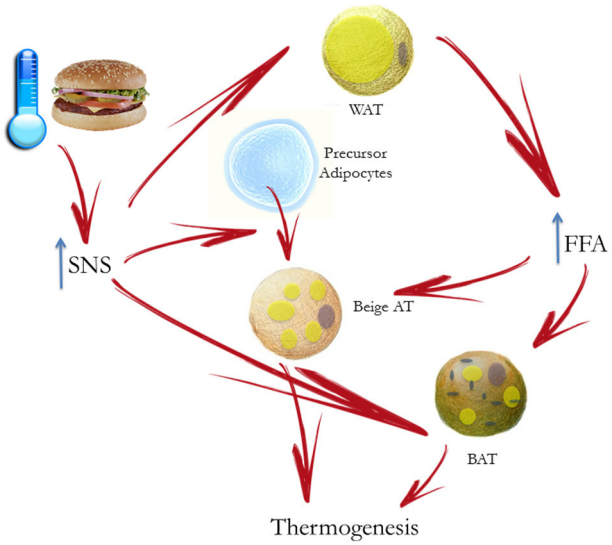

FIGURE 2 | Cold- or diet-stimulated sympathetic activation results in mobilization of free fatty acids (FFA) by white adipose tissue (WAT) and regulation of brown adipose tissue (BAT) thermogenesis. The principal substrate for BAT is constituted by fatty acids to increase energy expenditure inducing heat production. Chronic sympathetic nervous system (SNS) activation also induces the conversion of "beige" adipose tissue in WAT, which also contribute to adaptive thermogenesis.

The authors hypothesized that the vagal nerve mediates the peripheral action of ghrelin, thus inhibiting sympathetic traffic directed to BAT. The interaction between vagal and BAT activity was confirmed in patients undergoing vagal nerve stimulation (VNS) for refractory epilepsy: VNS induced a BAT-mediated increase in energy expenditure (Vijgen et al., 2013).

Furthermore, chronic sympathetic activation produces a remarkable induction of uncoupling protein1-positive brown-like adipocytes in white fat pads, called "beige" adipose tissue, which also contribute to adaptive thermogenesis and body fat reduction (Cousin et al., 1992; Inokuma et al., 2006; **Figure 2**). In humans it has been suggested that BAT is mostly composed of beige cells and is inducible in response to appropriate sympathetic stimulation. In healthy human participants, with undetectable or low BAT activity, daily 2-h cold exposure at 17°C for 6 weeks resulted in increased BAT activity. Changes in BAT activity and body fat content were negatively correlated (Yoneshiro et al., 2013).

It is important to note that leptin has a crucial role in regulation of energy expenditure through SNS. Indeed, leptin has been shown to increase energy expenditure acting both on the cardiovascular system and BAT thermogenesis via the hypothalamus (Pandit et al., 2017). The ARC represents the main site of action of leptin on SNS. In particular, CNS leptin administration does not affect sympathetic nerve activity after ARC destruction (Haynes, 2000). However, Fischer showed that leptin may increase energy expenditure by inducing a pyrexic increase in body temperature by reducing heat loss, rather than affecting BAT thermogenesis (Fischer et al., 2016).

On the other hand, in animal studies leptin administration in different CNS areas increases sympathetic outflow to the kidneys, the adipose tissue, the skeletal muscle vasculature and adrenal glands (Dunbar et al., 1997; Elmquist et al., 1997; Haynes et al., 1997), thus causing an increase in energy expenditure (Woods and Stock, 1996) and in sympathetic vasomotor activity (Marsh et al., 2003). The latter mechanism is involved in pathogenesis of obesity –induced hypertension, as explained later (see Section Sympathetic Overactivity in Obesity).

Taken together, these results suggest that BAT thermogenesis is an appealing target in obesity treatment. However, while promising evidence in experimental animals demonstrate that it is possible to impair BAT thermogenesis (i.e., by beta-adrenergic blockade), no intervention has so far been able to increase it (Tupone et al., 2014).

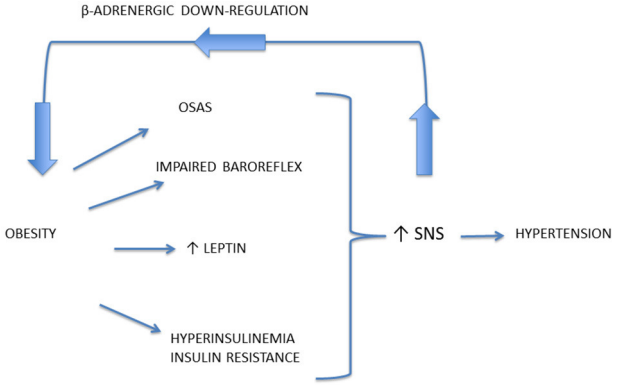

FIGURE 3 | Mechanisms responsible for the occurrence of sympathetic activation in obesity-related hypertension. Prolonged sympathetic nervous system (SNS) overactivity might induce weight gain, due to downregulation of beta-adrenoceptors, thus reducing the capacity to dissipate excessive calories.

SYMPATHETIC OVERACTIVITY IN OBESITY

An increased SNS activity has been demonstrated in obese patients, particularly in the muscle vasculature and in the kidneys, possibly contributing to increased cardiovascular risk. Though SNS activation is similar in hypertensive and normotensive obese individuals, sympathetic contribution to blood pressure via vasoconstriction is greater in the hypertensive ones, confirming a role for sympathetic activation in the pathogenesis of obesity-related hypertension. Conversely, sympathetic overactivity is not effective in favoring energy expenditure and thus weight loss. Selective leptin resistance, obstructive sleep apnea syndrome, hyperinsulinemia and low ghrelin levels are possible mechanisms underlying sympathetic activation in obesity. Weight loss is able to reverse metabolic and SNS alterations associated with obesity.

Patterns of SNS Activation in Obesity

It is well known that excess weight is associated with ANS dysfunction, and particularly with increased sympathetic traffic. Landsberg was the first researcher speculating that increased SNS activity in response to weight gain is an adaptive mechanism to increase resting energy expenditure and promote restoration of the antecedent weight (Landsberg, 1986, 2001), while other authors suggested that prolonged sympathetic overactivity might induce weight gain, due to reduced capacity to dissipate excessive calories, mediated by downregulation of β adrenoceptors (van Baak, 2001; Feldstein and Julius, 2009; **Figure 3**). On the other hand, some authors suggested that a reduced sympathetic activity is rather implied in obesity pathogenesis, inducing a lower rate of thermogenesis and a positive energy balance (Bray, 1991). However, several studies conducted with sophisticated techniques supported the Landsberg's hypothesis of SNS overactivity in obese individuals, with or without hypertension (Landsberg, 1986).

It is important to underline that obesity causes a selective and differentiated increase in sympathetic activity rather than generalized SNS activation. This crucial issue has been investigated by techniques such as microneurography, which allows recording directly spontaneous efferent activity of post-ganglionic SNS fibers controlling muscle vascular tone (Vallbo et al., 2004), and regional NE spillover, which is crucial in order to investigate organs like heart and kidney, whose efferent nerve traffic is not directly recordable in humans. Several studies highlighted that obesity is characterized by SNS overactivity directed to the muscle vasculature by means of microneurography (Grassi et al., 1995, 2004; Alvarez et al., 2004). In obese individuals, increased MSNA is obtained by recruitment of additional nervous fibers, as demonstrated by single fiber recordings, at variance to the increased firing frequency observed in essential hypertension (Lambert et al., 2007). MSNA values, although increased in both central and peripheral obesity, are greater in individuals with an abdominal or central distribution of body fat (Grassi et al., 2004), particularly with visceral obesity (Alvarez et al., 2004). Several reflex abnormalities were shown in obesity, such as impaired baroreflex sensitivity (Grassi et al., 1995), central chemoreflex hypersensitivity (Narkiewicz et al., 1999a) and blunted muscle metaboreflex (Negrao et al., 2001); conversely, MSNA responses to mental stress and cold pressure test were similar in obese and in lean subjects (Kuniyoshi et al., 2003).

Furthermore, an increased adrenergic tone in the renal district was also demonstrated, while the sympathetic outflow to the heart is not elevated or even reduced, as demonstrated by cardiac norepinephrine spillover (Esler et al., 2006). It has been hypothesized that cardiac sympathetic tone is reduced in human obesity in response to volume overload (Messerli et al., 1983), in part induced also by sodium retention mediated by high renal SNS activity (DiBona, 1992). An altered autonomic modulation of heart rate has been also demonstrated by the technique of spectral analysis of heart rate variability (Hirsch et al., 1991; Tonhajzerova et al., 2008), with conflicting findings (Matsumoto et al., 1999; Antelmi et al., 2004).

An impaired autonomic regulation in the post-prandial phase has also been suggested. As mentioned above, SNS inhibition is the physiological response to fasting, in order to limit weight loss during starvation (Young and Landsberg, 1977),

while food ingestion, particularly of carbohydrate-rich food, induces an increase in SNS activity (Young and Landsberg, 1977; Welle, 1995). This physiological response is blunted in obese individuals in comparison to lean individuals, though energy expenditure was similar and no correlation between SNS activity and the thermic effect of the food has been demonstrated (Tentolouris et al., 2003). The blunted post-prandial increase in sympathetic tone, demonstrated also in adult obese individuals (Xu et al., 2014) may thus represent a mechanism of inhibition of post-prandial thermogenesis, thus favoring weight gain, though conflicting data exist (Emdin et al., 2001). However, these results do not allow drawing firm conclusions, since only autonomic modulation of heart rate has been explored, which may not represent sympathetic traffic directed to the adipose tissue.

Finally, it is important to note that sympathetic overactivity characterizing obesity has deleterious cardiovascular consequences, including the development of hypertension, but it is not effective in increasing energy expenditure and favoring weight loss as expected (see Section Role the ANS in Energy Homeostasis). Indeed, acute ganglionic blockade (Shibao et al., 2007), did not change energy expenditure in individuals with central obesity, supporting the Landsberg's hypothesis of sympathetic activation in obesity as a compensatory but ineffective strategy induced by weight gain. However, preliminary data suggest that contribution of SNS after gastric bypass might be very small: this fact might make more difficult to maintain weight loss after surgery (Curry et al., 2013).

Mechanisms of Sympathetic Activation in Obesity and Obesity-Related Hypertension

Adrenergic activation plays an important role in pathophysiological mechanisms underlying the development, maintenance, and progression of essential hypertension (Grassi et al., 2015) and is suspected to contribute in particular to the development of hypertension in obese humans (Hall et al., 2012). Julius et al. first proposed that increased sympathetic activity in hypertension was the primary defect leading to insulin resistance and weight gain in obese adults (Julius et al., 2000). In young overweight individuals, SNS activity is directly related to the degree of cardiac, renal, and vascular dysfunction, suggesting that sympathetic neural drive may be a major player in CV risk development (Lambert et al., 2010).

Mechanisms underlying obesity-related hypertension are not fully understood. Indeed, a great importance has been given to activation of renal sympathetic nerves, causing sodium retention, increased renin secretion, and impaired renal-pressure natriuresis (Hall et al., 2012). Though renal NE spillover is similar in normotensive and hypertensive obese individuals, an exaggerated effect of SNS activation has been reported. Indeed Shibao and coauthors demonstrated that after ganglionic blockade with trimethaphan, hypertensive obese patients exhibited a greater BP fall than the normotensive ones (Shibao et al., 2007). Central mechanisms may be relevant in obesity-related hypertension and include activation of leptin and POMC pathway, and obstructive sleep apnea syndrome, with activation of chemoreceptor-mediated reflexes related to intermittent hypoxia (**Figure 3**). Furthermore, among peripheral mechanisms of sympathetic activation, hyperinsulinemia might play a role.

Leptin

As already mentioned, leptin has central sympathoexcitatory effects, demonstrated in a number of experimental studies (Haynes et al., 1999; Lim et al., 2013). Indeed, obese mice with leptin or leptin-receptor deficiency showed no increase in arterial pressure (Mark et al., 1999). The sympathoexcitatory and hypertensive effect of leptin seems to be mediated by melanocortin-4 receptor (MC4R) (Tallam et al., 2005). These findings were confirmed also in MC4R deficient humans, who show a low prevalence of hypertension, despite the presence of severe obesity (Greenfield et al., 2009).

Based on this piece of evidence, Mark et al. suggested that some forms of obesity may be characterized by a "selective leptin resistance," limited to its favorable metabolic effects (satiety and weight loss), while its sympathoexcitatory effects on the cardiovascular system are maintained (Correia et al., 2002; Mark et al., 2002; Rahmouni et al., 2005). In humans, a number of studies confirmed the association between leptin and hypertension. Human leptin deficiency was associated with early-onset morbid obesity and metabolic syndrome without SNS activation or hypertension (Ozata et al., 1999). Conversely, higher leptin levels in obese hypertensive in comparison to obese normotensive individuals have been reported (Kunz et al., 2000; Golan et al., 2002). Furthermore, in the Copenhagen City Heart Study increased plasma leptin levels predicted the risk of developing hypertension (Asferg et al., 2010). However, acute of chronic administration of leptin in humans failed to induce a sustained BP or SNS activity increase, thus the role of leptin in causing sympathetic activation in obesity still need to be fully clarified (Mark, 2013).

Obstructive Sleep Apnea Syndrome (OSAS)

OSAS is a condition characterized by repetitive episodes of upper airway narrowing or occlusion, causing chronic intermittent hypoxia and sleep fragmentation (Dempsey et al., 2010). Obesity is a major risk factor for OSAS, which in turn may induce BP increase not only during nighttime but also during daytime (Brooks et al., 1997). The role of OSAS as a determinant of sympathetic overactivity has been reported not only in obese (Somers et al., 1995; Narkiewicz et al., 1998) but also in lean subjects (Grassi et al., 2005). Interestingly, some authors suggest that obesity *per se* is not associated to increased sympathetic traffic to the muscle vasculature, but this alteration is present only when obesity is accompanied by OSAS (Narkiewicz et al., 1998). Mechanisms of hypertension development during OSAS include sympathetic activation due to chemoreflex activation, secondary to repetitive hypoxic episodes at nighttime, but also alterations in vascular function and structure caused by oxidative stress and inflammation (Bruno et al., 2013). A sustained reduction in MSNA was demonstrated in normotensive patients with OSAS after both 6 and 12 months of continuous positive airway pressure therapy (Narkiewicz et al., 1999b).

Insulin

Some authors suggest that chronic hyperinsulinemia may act as a maladaptive mechanism, inducing SNS overactivity in obesity (Landsberg, 1986, 2001). However, this hypothesis has not been supported by later studies. Indeed, insulin administration has a direct vasodilatory effect during acute euglycemic hyperinsulinemic clamp: thus the increase in MSNA and norepinephrine levels reported in healthy individuals and hypertensive patients may be a consequence of baroreflex activation (Rowe et al., 1981; Anderson et al., 1991, 1992). However, a modest increase in BP was observed in healthy individuals when supraphysiological insulin concentrations are obtained (Rowe et al., 1981). Interestingly, in elderly subjects with normal BP, acute elevations of plasma insulin during hyperinsulinemic/euglycemic clamp caused vasoconstriction, accompanied by a blunted increase in norepinephrine and heart rate, as compared to young individuals, while no changes in BP were observed in either group. The authors suggested that the insulin-induced vasoconstriction is not due to exaggerated insulin-induced sympathetic activation but rather to a reduction in the vasodilator action of insulin (Hausberg et al., 1997). Despite hyperinsulinemia, intracerebroventricular administration of insulin antagonists did not affect renal sympathetic nerve activity in experimental animals, adding to the evidence that insulin does not promote obesity hypertension by chronically stimulating the SNS (Lim et al., 2013).

Ghrelin

Beyond its established role in appetite regulation, ghrelin has beneficial effects on blood pressure (BP) and cardiovascular function (Virdis et al., 2016), possibly modulating ANS activity. In experimental animals, intracerebral infusion of ghrelin reduced BP; however, it is still not clear whether this effect was mediated by modulation of sympathetic traffic (Matsumura et al., 2002; Prior et al., 2014). Lambert et al. investigated the effects of supraphysiological doses of intravenous ghrelin in lean and obese individuals. Ghrelin did not influence SNS activity controlling resting calf vascular tone; however, ghrelin infusion blunted BP and muscle sympathetic nerve activity (MSNA) responses to acute mental stress after short-term ghrelin infusion either in lean or obese individuals (Lambert et al., 2011).

Effect of Weight Loss on the SNS

Several studies have shown that sympathetic activation reported in obese subjects is reversed by weight loss (Muscelli et al., 1998; Nault et al., 2007; Perugini et al., 2010). This topic is extensively reviewed elsewhere (Lambert et al., 2015). Straznicky reported a marked sympathoinhibition secondary to diet-induced weight loss, evaluated by MSNA and whole-body plasma norepinephrine spillover rate (Straznicky et al., 2005). However, bariatric surgery is the most effective treatment for obesity, allowing to achieve up to 70% of excess weight loss (Buchwald et al., 2004). It is also well known that bariatric surgery improves the main defects responsible for obesity-associated hyperglycaemia, namely insulin resistance and beta-cell dysfunction (Ferrannini, 1998; Nannipieri et al., 2011). Few data explored the role of bariatric surgery in reduction of SNS activity. Pontiroli et al. showed a restoration of sympathovagal balance evaluated by heart rate variability in 24 subjects with severe obesity 6 months after gastric banding (Pontiroli et al., 2013), while Lips et al. showed an improvement in heart rate variability, although explored only in the time domain, after 3 months very low-calorie diet or gastric bypass (Lips et al., 2013). However, these two studies, using spectral analysis of RR interval, did not provide a measure of sympathetic activity. In 23 severely obese, non-diabetic, individuals, MSNA was measured before and after 10% weight loss induced by laparoscopic adjustable gastric band. Noteworthy, a significant reduction in BP, MSNA, fasting insulin and creatinine clearance was found, whereas cardiac and sympathetic baroreflex sensitivity were improved (Lambert et al., 2014). Seravalle et al. evaluated the effect of weight loss secondary to sleeve gastrectomy or caloric-restricted diet on the ANS. Six months after surgery, waist circumference, leptin levels and MSNA were reduced in the surgery group, which persisted 12 months after surgery (Seravalle et al., 2014). Conversely, insulin sensitivity, evaluated by Homeostatic Model Assessment (HOMA) index, was reduced after 6 months, but returned to pre-surgery values after 12 months, suggesting that sympathetic deactivation induced by weight loss might not influence insulin sensitivity (Seravalle et al., 2014). However, this conclusion is limited by the fact that HOMA index is a rough index of insulin sensitivity; furthermore, since it is derived from fasting insulin and glucose levels, it is related to hepatic insulin sensitivity rather than peripheral insulin sensitivity, which is conceivably more influenced by changes in sympathetic tone.

SNS activity after gastric bypass surgery seem to be lower than those of obese individuals and thus might blunt energy expenditure, with negative consequences for weight maintenance (Curry et al., 2013). We do not know whether different interventions, i.e., sleeve gastrectomy might lead to the same phenomenon.

Finally, it is important to note that the surgical procedure *per se* might have a direct impact on the autonomic innervation of the gastrointestinal tract. During surgery, sleeve gastrectomy and Roux-en-Y *gastric bypass* (RYGB) may damage the gastric branches of the vagal nerve in a different manner. Infact in the sleeve gastrectomy the stomach is cut longitudinally, damaging the very distal branches of the gastric vagal nerve, while in the RYGB the stomach is cut transversely, resulting in a damage of the gastric vagal branches very close to their origin from the esophageal plexus (Ballsmider et al., 2015). Thus, it is conceivable that the effects of bariatric surgery on brain-gut axys may be influenced by the surgically-induced anatomical alterations, which may affect the integrity of vagal innervation between the hindbrain feeding centers and the gastrointestinal tract.

THE ANS AS A THERAPEUTIC TARGET IN OBESITY

Based on the physiopatological background above described, it is clear the modulation of ANS may induce weight loss and/or reduce cardiovascular risk in obese patients. VNS, achieved by implantable or transcutaneous devices, has been associated

with a significant weight loss in small, non-randomized pilot studies. Vagal nerve blockade yelded either neutral or positive effects in term of weight loss in small sham-controlled studies, but even in this case further evidence is needed. Sympathetic inhibition accompanied weight loss achieved by diet or surgery. Interventions targeting SNS are able to improve cardiometabolic profile in obese individuals.

Vagal Modulation

Since vagal afferents convey to the CNS the gastric distension signal and satiety signals evoked by gut hormones, it is not surprising that vagal stimulation has been proposed as a weight loss intervention. Several studies, carried out in obese animals, showed that VNS suppressed food intake and weight gain. Bugajski et al. suggested that VNS, achieved by implantable electronic devices, mimics activation of gastric mechanoceptors and jejunal chemoceptors, thus resulting in decreased food intake and weight loss in obese rats (Bugajski et al., 2007; **Figure 1**). The limitations of this study are the monolateral VNS and the use of constant voltage stimulation (Bugajski et al., 2007). Bilateral VNS with constant current stimulation induced stable weight loss in obese minipigs (Val-Laillet et al., 2010). Furthermore, patients treated with vagal stimulation for severe depression experienced a relevant weight loss (Pardo et al., 2007) (**Table 1**). However, this approach is limited by its high cost and invasiveness, potential need for reintervention for mechanical failure and/or battery replacement, and side effects (Ventureyra, 2000). More recently, transcutaneous auricular VNS (taVNS) has been proposed to treat disorders such as epilepsy (Miro et al., 2015) and depression, drawing inspiration from auricular acupuncture of traditional chinese medicine (Rong et al., 2016). The rationale for using taVNS is that anatomical studies showed that the ear is the only place on the surface of the human body where afferent vagal nerve distribution is present (Wang et al., 2014). Indeed, a branch of the vagal nerve provides sensory innervation of the "cymba conchae" of the external ear (Peuker and Filler, 2002). Thus, the direct stimulation of the afferent vagal nerve fibers on the ear may produce similar effects as classic VNS without the burden of surgical intervention (Henry, 2002). Indeed, cymba conchae stimulation of auricolar vagal branch activated the NTS and other vagal projections within the brainstem and forebrain in healthy adults (Frangos et al., 2015). Furthermore, in a pilot randomized clinical trial, Huang et al reported an improvement of in the 2-h glucose tolerance and systolic BP in after a 12-week treatment with taVNS in comparison with sham technique (Huang et al., 2014) (**Table 1**). Finally, taVNS is able to acutely reduce MSNA and shift cardiac autonomic function toward parasympathetic predominance in healthy volunteers (Clancy et al., 2014). These promising findings suggest that in obese and glucose-intolerant individuals, taVNS may not only restore insulin resistance and secretion, but also counteract obesity-related autonomic dysfunction (Lambert et al., 2010; Seravalle et al., 2014) and thus play a role in reducing its cardiovascular burden.

On the other hand, gastric emptying is under the control of vagal efferent fibers. Vagotomy, in experimental animals (Smith et al., 1983) as well as in humans (Kral, 1978) is able to delay gastric emptying and impair gastric accommodation to food, thus inducing weight loss. Since pancreatic secretion is under vagal control, interruption of vagal efferent fibers induces malabsorption (Camilleri et al., 2008). Furthermore, vagotomy in rats prevents the physiological ghrelin increase in fasting conditions (Williams et al., 2003). Thus, intermittent electric stimulation of vagal fibers, inducing blockade of the neural

TABLE 1 | Human studies investigating the role of VNS in weight loss and glucose control.

Study	Population	VNS duration	Clinical endpoint	Results
Pardo et al., 2007	14 patients with resistant depression	6–12 months	Change in level of depression and weight loss	Mean weight loss−7 kg; BMI change−2 kg/m^2
Huang et al., 2014	70 IGT subjects randomly assigned to the taVNS group or sham taVNS group 30 IGT controls without device	6–12 weeks	2-h plasma glucose levels (2hPG) OGTT at 6 weeks and 12 weeks.	Reduction in 2 hPG in taVNS vs sham taVNS $p = 0.004$

TABLE 2 | Human studies investigating the role of vagal nerve blockade (VBLOC) in weight loss, glucose control and caloric intake.

Study	Population	VBLOC duration	Clinical endpoint	Results
Camilleri et al., 2008	31 obese subjects	6 months	% excess weight loss (%EWL) and caloric intake	EWL 14.2% vs. baseline ($p < 0.001$) Caloric intake decreased by 30% ($p < 0.01$)
EMPOWER study Sarr et al., 2012	192 obese subjects with VBLOC 102 obese subjects with device with a lower charge delivery	12 months	% excess weight loss (%EWL)	EWL 17 ± 2% in VBLOC vs. 16 ± 2% in device with a lower charge delivery (p = ns)
Shikora et al., 2013	26 obese subjects with type 2 diabetes with VBLOC	12 months	% excess weight loss (%EWL) and glucose control	EWL 25 ± 4% ($p < 0.0001$) and mean HbA1c reduction −1 ± 0.2% ($p < 0.02$) vs. baseline
ReCharge study Ikramuddin et al., 2014	162 morbid obese subjects with VBLOC 77 morbid obese subjects with sham device	12 months	% excess weight loss (%EWL)	EWL 24,4% in VBLOC vs. 15,9% in sham device ($p = 0.002$)

transmission, has been tested as a novel weight-loss intervention (**Table 2**).

The EMPOWER study evaluated the effects of intermittent, bilateral blockade of bilateral subdiaphragmatic vagal nerves to stop both ascending and descending neural traffic, speculating its involvement in satiety, reduced food intake and weight loss in morbid obese individuals (**Figure 1**). However, despite the solid scientific background linking vagal activity and obesity, extensively described in the previous sections, the EMPOWER study yelded negative results: vagal blockade induced a similar weight loss than the control group, which had the same device with a lower charge delivery; interestingly, weight loss was related to device use time in both groups, suggesting that what was supposed to be a sham therapy was active as well (Sarr et al., 2012). This hypothesis is confirmed by the ReCharge study, in which vagal nerve blockade was obtained by using a device that delivered at least 12 h of therapy per day and was compared a sham control device that had no possibility of delivering therapy. Individuals undergoing vagal blockade therapy achieved a greater weight loss than the sham control group, although the pre-established efficacy outcomes were not achieved (Ikramuddin et al., 2014) (**Table 2**).

Sympathetic Modulation

Given the above-described role of SNS in the pathophysiology of obesity and its cardiovascular consequences, SNS inhibition is considered a potential therapeutic target in obesity. As reviewed above, it is important to underline that interventions aimed at inducing weight loss by diet or surgery are able to achieve a significant reduction in SNS tone, in particular in the muscle vasculature (Lambert et al., 2015).

Indeed, a number of mechanistic studies demonstrated that acute pharmacologic ganglionic blockade by trimetaphan is able to reduce blood pressure (Shibao et al., 2007), to improve insulin sensitivity (Gamboa et al., 2014) and to reverse endothelial function (Gamboa et al., 2016) in obesity, in particular if associated with hypertension. However, ganglionic blockers cannot be used chronically, given their unfavorable profile in terms of adverse effects.

A significant antihypertensive effect of a combined α and ß-blockade has been reported in dietary mediated obesity in dogs consuming high fat diets (Hall et al., 2001) and in obese individuals in which a greater reduction in BP in comparison to lean subjects was reported after 1 month of treatment (Wofford et al., 2001). Adrenergic blockade produced a significantly greater decrease in BP in obese than in lean patients with hypertension (Wofford et al., 2001), in line to the results reported with ganglionic blockade (Shibao et al., 2007). A study suggested also that the use of a BP-lowering central sympatholytic drug, moxonidine, might induce a small but significant weight loss, together with a reduction in blood pressure, triglycerides and fasting blood glucose (Chazova and Schlaich, 2013), though another study failed to demonstrate any impact on insulin sensitivity (Masajtis-Zagajewska et al., 2010). In contrast, β-blockers may exert negative or neutral effects on body weight and lipid and glucose profile (Lambert et al., 2015). However, some authors suggest that β-blockers may be first-choice drug in the treatment of hypertension in young adults, which is mainly linked to sympathetic overactivity due to overweight and obesity (Cruickshank, 2017).

In the past decade, great interest has been placed in device-based therapies targeting SNS for the treatment of refractory hypertension, such as renal denervation and baroceptor activating therapy (Bruno et al., 2013). Given the presence of sympathetic activation in obesity and its possible role in pathogenesis of obesity-associated hypertension, as described above, it may be expected that sympathetic inhibition might have a relevant impact in obese patients. Indeed, renal denervation seems able to restore insulin sensitivity in obese dogs (Iyer et al., 2016) but not in obese hypertensive mice (Asirvatham-Jeyaraj et al., 2016). Bilateral renal denervation greatly attenuated sodium retention and hypertension in obese dogs fed a high-fat diet (Kassab et al., 1995).

Glucose tolerance and glycemic control was significantly improved 3 and 6 months after renal denervation in 10 patients with resistant hypertension and OSAS: in this study, BP, but not BMI, was significantly reduced (Witkowski et al., 2011). This finding was confirmed in a larger cohort of resistant hypertensive patients, in whom renal denervation induced a reduction in blood fasting glucose, insulin, and HOMA-IR after 3 months (Mahfoud et al., 2011). However, the BP-lowering effect of such procedures has been recently questioned; furthermore, obese patients seem to benefit less of renal denervation in terms of BP reduction (Id et al., 2016).

CONCLUSIONS

In conclusion, obesity is accompanied by increased morbidity and mortality, mostly related to cardiovascular disease, and represents a major issue for global healthcare. Thus, the study of mechanisms underlying its pathogenesis is crucial to identify novel targets for its treatment. The ANS plays a major role in the integrated short-term regulation of weight, modulating the satiety signal and energy expenditure. The afferent vagal pathways are probably the most important link between the gut and the brain and interact in a complex way with gut hormones. SNS has the physiological function of increasing lipolysis and energy expenditure, through sympathetic innervation in white and brown adipose tissue; thus it is abnormally activated in obesity in a compensatory but ineffective fashion. Sympathetic activation may favor the development of hypertension and organ damage in obesity and lead to overt cardiovascular disease. Though preliminary clinical trials exploring autonomic modulation as a treatment for obesity yelded contrasting results, mechanistic and physiopathological studies strongly support this therapeutic strategy as an appealing and promising approach for obesity treatment.

AUTHOR CONTRIBUTIONS

DG drafted the manuscript. RMB designed and reviewed critically the article. MN, GI, and ST reviewed critically the manuscript.

REFERENCES

Abbott, C. R., Monteiro, M., Small, C. J., Sajedi, A., Smith, K. L., Parkinson, J. R., et al. (2005). The inhibitory effects of peripheral administration of peptide YY(3-36) and glucagon-like peptide-1 on food intake are attenuated by ablation of the vagal-brainstem-hypothalamic pathway. *Brain Res.* 1044, 127–131. doi: 10.1016/j.brainres.2005.03.011

Adrian, T. E., Ferri, G. L., Bacarese-Hamilton, A. J., Fuessl, H. S., Polak, J. M., and Bloom, S. R. (1985). Human distribution and release of a putative new gut hormone, peptide YY. *Gastroenterology* 89, 1070–1077. doi: 10.1016/0016-5085(85)90211-2

Alvarez, G. E., Ballard, T. P., Beske, S. D., and Davy, K. P. (2004). Subcutaneous obesity is not associated with sympathetic neural activation. *Am. J. Physiol. Heart Circ. Physiol.* 287, H414–H418. doi: 10.1152/ajpheart.01046.2003

Anderson, E. A., Balon, T. W., Hoffman, R. P., Sinkey, C. A., and Mark, A. L. (1992). Insulin increases sympathetic activity but not blood pressure in borderline hypertensive humans. *Hypertension* 19(6 Pt 2), 621–627. doi: 10.1161/01.HYP.19.6.621

Anderson, E. A., Hoffman, R. P., Balon, T. W., Sinkey, C. A., and Mark, A. L. (1991). Hyperinsulinemia produces both sympathetic neural activation and vasodilation in normal humans. *J. Clin. Invest.* 87, 2246–2252. doi: 10.1172/JCI115260

Antelmi, I., de Paula, R. S., Shinzato, A. R., Peres, C. A., Mansur, A. J., and Grupi, C. J. (2004). Influence of age, gender, body mass index, and functional capacity on heart rate variability in a cohort of subjects without heart disease. *Am. J. Cardiol.* 93, 381–385. doi: 10.1016/j.amjcard.2003.09.065

Arosio, M., Ronchi, C. L., Beck-Peccoz, P., Gebbia, C., Giavoli, C., Cappiello, V., et al. (2004). Effects of modified sham feeding on ghrelin levels in healthy human subjects. *J. Clin. Endocrinol. Metab.* 89, 5101–5104. doi: 10.1210/jc.2003-032222

Asferg, C., Mogelvang, R., Flyvbjerg, A., Frystyk, J., Jensen, J. S., Marott, J. L., et al. (2010). Leptin, not adiponectin, predicts hypertension in the Copenhagen City Heart Study. *Am. J. Hypertens.* 23, 327–333. doi: 10.1038/ajh.2009.244

Asirvatham-Jeyaraj, N., Fiege, J. K., Han, R., Foss, J., Banek, C. T., Burbach, B. J., et al. (2016). Renal denervation normalizes arterial pressure with no effect on glucose metabolism or renal inflammation in obese hypertensive mice. *Hypertension* 68, 929–936. doi: 10.1161/HYPERTENSIONAHA.116.07993

Ballsmider, L. A., Vaughn, A. C., David, M., Hajnal, A., Di Lorenzo, P. M., and Czaja, K. (2015). Sleeve gastrectomy and Roux-en-Y gastric bypass alter the gut-brain communication. *Neural Plast.* 2015:601985. doi: 10.1155/2015/601985

Bartness, T. J. (2002). Dual innervation of white adipose tissue: some evidence for parasympathetic nervous system involvement. *J. Clin. Invest.* 110, 1235–1237. doi: 10.1172/JCI0217047

Baskin, D. G., Figlewicz Lattemann, D., Seeley, R. J., Woods, S. C., Porte, D. Jr., and Schwartz, M. W. (1999). Insulin and leptin: dual adiposity signals to the brain for the regulation of food intake and body weight. *Brain Res.* 848, 114–123. doi: 10.1016/S0006-8993(99)01974-5

Batterham, R. L., Cohen, M. A., Ellis, S. M., Le Roux, C. W., Withers, D. J., Frost, G. S., et al. (2003). Inhibition of food intake in obese subjects by peptide YY3-36. *N. Engl. J. Med.* 349, 941–948. doi: 10.1056/NEJMoa030204

Berthoud, H. R. (2008a). Vagal and hormonal gut-brain communication: from satiation to satisfaction. *Neurogastroenterol. Motil.* 20(Suppl. 1), 64–72. doi: 10.1111/j.1365-2982.2008.01104.x

Berthoud, H. R. (2008b). The vagus nerve, food intake and obesity. *Regul. Pept.* 149, 15–25. doi: 10.1016/j.regpep.2007.08.024

Blessing, W. W. (1997). Inadequate frameworks for understanding bodily homeostasis. *Trends Neurosci.* 20, 235–239. doi: 10.1016/S0166-2236(96)01029-6

Bray, G. A. (1991). Obesity, a disorder of nutrient partitioning: the MONA LISA hypothesis. *J. Nutr.* 121, 1146–1162.

Brooks, D., Horner, R. L., Kozar, L. F., Render-Teixeira, C. L., and Phillipson, E. A. (1997). Obstructive sleep apnea as a cause of systemic hypertension. Evidence from a canine model. *J. Clin. Invest.* 99, 106–109. doi: 10.1172/JCI119120

Brown, L. M., Clegg, D. J., Benoit, S. C., and Woods, S. C. (2006). Intraventricular insulin and leptin reduce food intake and body weight in C57BL/6J mice. *Physiol. Behav.* 89, 687–691. doi: 10.1016/j.physbeh.2006.08.008

Bruno, R. M., Rossi, L., Fabbrini, M., Duranti, E., Di Coscio, E., Maestri, M., et al. (2013). Renal vasodilating capacity and endothelial function are impaired in patients with obstructive sleep apnea syndrome and no traditional cardiovascular risk factors. *J. Hypertens* 31, 1456–1464. discussion: 1464. doi: 10.1097/HJH.0b013e328360f773

Buchwald, H., Avidor, Y., Braunwald, E., Jensen, M. D., Pories, W., Fahrbach, K., et al. (2004). Bariatric surgery: a systematic review and meta-analysis. *JAMA* 292, 1724–1737. doi: 10.1001/jama.292.14.1724

Buffa, R., Solcia, E., and Go, V. L. (1976). Immunohistochemical identification of the cholecystokinin cell in the intestinal mucosa. *Gastroenterology* 70, 528–532.

Bugajski, A. J., Gil, K., Ziomber, A., Zurowski, D., Zaraska, W., and Thor, P. J. (2007). Effect of long-term vagal stimulation on food intake and body weight during diet induced obesity in rats. *J. Physiol. Pharmacol.* 58(Suppl.1), 5–12.

Bullock, B. P., Heller, R. S., and Habener, J. F. (1996). Tissue distribution of messenger ribonucleic acid encoding the rat glucagon-like peptide-1 receptor. *Endocrinology* 137, 2968–2978. doi: 10.1210/endo.137.7.8770921

Burdyga, G., Lal, S., Spiller, D., Jiang, W., Thompson, D., Attwood, S., et al. (2003). Localization of orexin-1 receptors to vagal afferent neurons in the rat and humans. *Gastroenterology* 124, 129–139. doi: 10.1053/gast.2003.50020

Burton-Freeman, B., Davis, P. A., and Schneeman, B. O. (2002). Plasma cholecystokinin is associated with subjective measures of satiety in women. *Am. J. Clin. Nutr.* 76, 659–667.

Camilleri, M., Toouli, J., Herrera, M. F., Kulseng, B., Kow, L., Pantoja, J. P., et al. (2008). Intra-abdominal vagal blocking (VBLOC therapy): clinical results with a new implantable medical device. *Surgery* 143, 723–731. doi: 10.1016/j.surg.2008.03.015

Campfield, L. A., Smith, F. J., Guisez, Y., Devos, R., and Burn, P. (1995). Recombinant mouse OB protein: evidence for a peripheral signal linking adiposity and central neural networks. *Science* 269, 546–549. doi: 10.1126/science.7624778

Cannon, B., and Nedergaard, J. (2004). Brown adipose tissue: function and physiological significance. *Physiol. Rev.* 84, 277–359. doi: 10.1152/physrev.00015.2003

Capasso, R., and Izzo, A. A. (2008). Gastrointestinal regulation of food intake: general aspects and focus on anandamide and oleoylethanolamide. *J. Neuroendocrinol.* 20(Suppl. 1), 39–46. doi: 10.1111/j.1365-2826.2008.01686.x

Carey, A. L., Formosa, M. F., Van Every, B., Bertovic, D., Eikelis, N., Lambert, G. W., et al. (2013). Ephedrine activates brown adipose tissue in lean but not obese humans. *Diabetologia* 56, 147–155. doi: 10.1007/s00125-012-2748-1

Chazova, I., and Schlaich, M. P. (2013). Improved hypertension control with the imidazoline agonist moxonidine in a multinational metabolic syndrome population: principal results of the MERSY study. *Int. J. Hypertens.* 2013:541689. doi: 10.1155/2013/541689

Cheng, W., Zhu, Z., Jin, X., Chen, L., Zhuang, H., and Li, F. (2012). Intense FDG activity in the brown adipose tissue in omental and mesenteric regions in a patient with malignant pheochromocytoma. *Clin. Nucl. Med.* 37, 514–515. doi: 10.1097/RLU.0b013e31824d2121

Clancy, J. A., Mary, D. A., Witte, K. K., Greenwood, J. P., Deuchars, S. A., and Deuchars, J. (2014). Non-invasive vagus nerve stimulation in healthy humans reduces sympathetic nerve activity. *Brain Stimul.* 7, 871–877. doi: 10.1016/j.brs.2014.07.031

Considine, R. V., Considine, E. L., Williams, C. J., Hyde, T. M., and Caro, J. F. (1996). The hypothalamic leptin receptor in humans: identification of incidental sequence polymorphisms and absence of the db/db mouse and fa/fa rat mutations. *Diabetes* 45, 992–994. doi: 10.2337/diab.45.7.992

Corp, E. S., McQuade, J., Moran, T. H., and Smith, G. P. (1993). Characterization of type A and type B CCK receptor binding sites in rat vagus nerve. *Brain Res.* 623, 161–166. doi: 10.1016/0006-8993(93)90024-H

Correia, M. L., Haynes, W. G., Rahmouni, K., Morgan, D. A., Sivitz, W. I., and Mark, A. L. (2002). The concept of selective leptin resistance: evidence from agouti yellow obese mice. *Diabetes* 51, 439–442. doi: 10.2337/diabetes.51.2.439

Cousin, B., Cinti, S., Morroni, M., Raimbault, S., Ricquier, D., Penicaud, L., et al. (1992). Occurrence of brown adipocytes in rat white adipose tissue: molecular and morphological characterization. *J. Cell Sci.* 103(Pt 4), 931–942.

Cox, H. M. (2007a). Neuropeptide Y receptors; antisecretory control of intestinal epithelial function. *Auton. Neurosci.* 133, 76–85. doi: 10.1016/j.autneu.2006.10.005

Cox, H. M. (2007b). Peptide YY: a neuroendocrine neighbor of note. *Peptides* 28, 345–351. doi: 10.1016/j.peptides.2006.07.023

Cruickshank, J. M. (2017). The role of beta-blockers in the treatment of hypertension. *Adv. Exp. Med. Biol.* 956, 149–166. doi: 10.1007/5584_2016_36

Cummings, D. E. (2006). Ghrelin and the short- and long-term regulation of appetite and body weight. *Physiol. Behav.* 89, 71–84. doi: 10.1016/j.physbeh.2006.05.022

Cummings, D. E., Purnell, J. Q., Frayo, R. S., Schmidova, K., Wisse, B. E., and Weigle, D. S. (2001). A preprandial rise in plasma ghrelin levels suggests a role in meal initiation in humans. *Diabetes* 50, 1714–1719. doi: 10.2337/diabetes.50.8.1714

Cummings, D. E., and Schwartz, M. W. (2003). Genetics and pathophysiology of human obesity. *Annu. Rev. Med.* 54, 453–471. doi: 10.1146/annurev.med.54.101601.152403

Cummings, D. E., Weigle, D. S., Frayo, R. S., Breen, P. A., Ma, M. K., Dellinger, E. P., et al. (2002). Plasma ghrelin levels after diet-induced weight loss or gastric bypass surgery. *N. Engl. J. Med.* 346, 1623–1630. doi: 10.1056/NEJMoa012908

Curry, T. B., Somaraju, M., Hines, C. N., Groenewald, C. B., Miles, J. M., Joyner, M. J., et al. (2013). Sympathetic support of energy expenditure and sympathetic nervous system activity after gastric bypass surgery. *Obesity* 21, 480–485. doi: 10.1002/oby.20106

Date, Y., Murakami, N., Toshinai, K., Matsukura, S., Niijima, A., Matsuo, H., et al. (2002). The role of the gastric afferent vagal nerve in ghrelin-induced feeding and growth hormone secretion in rats. *Gastroenterology* 123, 1120–1128. doi: 10.1053/gast.2002.35954

Dempsey, J. A., Veasey, S. C., Morgan, B. J., and O'Donnell, C. P. (2010). Pathophysiology of sleep apnea. *Physiol. Rev.* 90, 47–112. doi: 10.1152/physrev.00043.2008

DiBona, G. F. (1992). Sympathetic neural control of the kidney in hypertension. *Hypertension* 19, I28–I35. doi: 10.1161/01.HYP.19.1_Suppl.I28

Dockray, G. J. (2014). Gastrointestinal hormones and the dialogue between gut and brain. *J. Physiol.* 592, 2927–2941. doi: 10.1113/jphysiol.2014.270850

Dumont, Y., Fournier, A., St-Pierre, S., and Quirion, R. (1995). Characterization of neuropeptide Y binding sites in rat brain membrane preparations using [125I][Leu31,Pro34]peptide YY and [125I]peptide YY3-36 as selective Y1 and Y2 radioligands. *J. Pharmacol. Exp. Ther.* 272, 673–680.

Dumoulin, V., Dakka, T., Plaisancie, P., Chayvialle, J. A., and Cuber, J. C. (1995). Regulation of glucagon-like peptide-1-(7-36) amide, peptide YY, and neurotensin secretion by neurotransmitters and gut hormones in the isolated vascularly perfused rat ileum. *Endocrinology* 136, 5182–5188. doi: 10.1210/endo.136.11.7588257

Dunbar, J. C., Hu, Y., and Lu, H. (1997). Intracerebroventricular leptin increases lumbar and renal sympathetic nerve activity and blood pressure in normal rats. *Diabetes* 46, 2040–2043. doi: 10.2337/diab.46.12.2040

Edvell, A., and Lindstrom, P. (1999). Initiation of increased pancreatic islet growth in young normoglycemic mice (Umea +/?). *Endocrinology* 140, 778–783. doi: 10.1210/endo.140.2.6514

Ekblad, E., and Sundler, F. (2002). Distribution of pancreatic polypeptide and peptide YY. *Peptides* 23, 251–261. doi: 10.1016/S0196-9781(01)00601-5

Elias, C. F., Kelly, J. F., Lee, C. E., Ahima, R. S., Drucker, D. J., Saper, C. B., et al. (2000). Chemical characterization of leptin-activated neurons in the rat brain. *J. Comp. Neurol.* 423, 261–281. doi: 10.1002/1096-9861(20000724)423:2<261::AID-CNE6>3.0.CO;2-6

Elmquist, J. K., Ahima, R. S., Maratos-Flier, E., Flier, J. S., and Saper, C. B. (1997). Leptin activates neurons in ventrobasal hypothalamus and brainstem. *Endocrinology* 138, 839–842. doi: 10.1210/endo.138.2.5033

Elmquist, J. K., Maratos-Flier, E., Saper, C. B., and Flier, J. S. (1998). Unraveling the central nervous system pathways underlying responses to leptin. *Nat. Neurosci.* 1, 445–450. doi: 10.1038/2164

Emdin, M., Gastaldelli, A., Muscelli, E., Macerata, A., Natali, A., Camastra, S., et al. (2001). Hyperinsulinemia and autonomic nervous system dysfunction in obesity: effects of weight loss. *Circulation* 103, 513–519. doi: 10.1161/01.CIR.103.4.513

English, P. J., Ghatei, M. A., Malik, I. A., Bloom, S. R., and Wilding, J. P. (2002). Food fails to suppress ghrelin levels in obese humans. *J. Clin. Endocrinol. Metab.* 87:2984. doi: 10.1210/jcem.87.6.8738

Esler, M., Straznicky, N., Eikelis, N., Masuo, K., Lambert, G., and Lambert, E. (2006). Mechanisms of sympathetic activation in obesity-related hypertension. *Hypertension* 48, 787–796. doi: 10.1161/01.HYP.0000242642.42177.49

Feldstein, C., and Julius, S. (2009). The complex interaction between overweight, hypertension, and sympathetic overactivity. *J. Am. Soc. Hypertens.* 3, 353–365. doi: 10.1016/j.jash.2009.10.001

Ferrannini, E. (1998). Insulin resistance versus insulin deficiency in non-insulin-dependent diabetes mellitus: problems and prospects. *Endocr. Rev.* 19, 477–490. doi: 10.1210/edrv.19.4.0336

Fetissov, S. O., Kopp, J., and Hokfelt, T. (2004). Distribution of NPY receptors in the hypothalamus. *Neuropeptides* 38, 175–188. doi: 10.1016/j.npep.2004.05.009

Fink, H., Rex, A., Voits, M., and Voigt, J. P. (1998). Major biological actions of CCK–a critical evaluation of research findings. *Exp. Brain Res.* 123, 77–83. doi: 10.1007/s002210050546

Fischer, A. W., Hoefig, C. S., Abreu-Vieira, G., de Jong, J. M., Petrovic, N., Mittag, J., et al. (2016). Leptin raises defended body temperature without activating thermogenesis. *Cell Rep.* 14, 1621–1631. doi: 10.1016/j.celrep.2016.01.041

Flier, J. S. (2001). Diabetes. The missing link with obesity? *Nature* 409, 292–293. doi: 10.1038/35053251

Forster, E. R., Green, T., Elliot, M., Bremner, A., and Dockray, G. J. (1990). Gastric emptying in rats: role of afferent neurons and cholecystokinin. *Am. J. Physiol.* 258(4 Pt 1), G552–G556.

Frangos, E., Ellrich, J., and Komisaruk, B. R. (2015). Non-invasive access to the vagus nerve central projections via electrical stimulation of the external ear: fMRI evidence in humans. *Brain Stimul.* 8, 624–636. doi: 10.1016/j.brs.2014.11.018

Frost, G. S., Brynes, A. E., Dhillo, W. S., Bloom, S. R., and McBurney, M. I. (2003). The effects of fiber enrichment of pasta and fat content on gastric emptying, GLP-1, glucose, and insulin responses to a meal. *Eur. J. Clin. Nutr.* 57, 293–298. doi: 10.1038/sj.ejcn.1601520

Fu-Cheng, X., Anini, Y., Chariot, J., Castex, N., Galmiche, J. P., and Roze, C. (1997). Mechanisms of peptide YY release induced by an intraduodenal meal in rats: neural regulation by proximal gut. *Pflugers Arch.* 433, 571–579. doi: 10.1007/s004240050316

Gamboa, A., Figueroa, R., Paranjape, S. Y., Farley, G., Diedrich, A., and Biaggioni, I. (2016). Autonomic blockade reverses endothelial dysfunction in obesity-associated hypertension. *Hypertension* 68, 1004–1010. doi: 10.1161/HYPERTENSIONAHA.116.07681

Gamboa, A., Okamoto, L. E., Arnold, A. C., Figueroa, R. A., Diedrich, A., Raj, S. R., et al. (2014). Autonomic blockade improves insulin sensitivity in obese subjects. *Hypertension* 64, 867–874. doi: 10.1161/HYPERTENSIONAHA.114.03738

Gilgen, A., Maickel, R. P., Nikodijevic, O., and Brodie, B. B. (1962). Essential role of catecholamines in the mobilization of free fatty acids and glucose after exposure to cold. *Life Sci.* 1, 709–715. doi: 10.1016/0024-3205(62)90138-8

Giordano, A., Song, C. K., Bowers, R. R., Ehlen, J. C., Frontini, A., Cinti, S., et al. (2006). White adipose tissue lacks significant vagal innervation and immunohistochemical evidence of parasympathetic innervation. *Am. J. Physiol. Regul. Integr. Comp. Physiol.* 291, R1243–R1255. doi: 10.1152/ajpregu.00679.2005

Glaser, B., Zoghlin, G., Pienta, K., and Vinik, A. I. (1988). Pancreatic polypeptide response to secretin in obesity: effects of glucose intolerance. *Horm. Metab. Res.* 20, 288–292. doi: 10.1055/s-2007-1010817

Golan, E., Tal, B., Dror, Y., Korzets, Z., Vered, Y., Weiss, E., et al. (2002). Reduction in resting metabolic rate and ratio of plasma leptin to urinary nitric oxide: influence on obesity-related hypertension. *Isr. Med. Assoc. J.* 4, 426–430.

Goodridge, A. G., and Ball, E. G. (1965). Studies on the metabolism of adipose tissue. 18. *In vitro* effects of insulin, epinephrine and glucagon on lipolysis and glycolysis in pigeon adipose tissue. *Comp. Biochem. Physiol.* 16, 367–381. doi: 10.1016/0010-406X(65)90303-8

Goran, M. I. (2000). Energy metabolism and obesity. *Med. Clin. North Am.* 84, 347–362. doi: 10.1016/S0025-7125(05)70225-X

Granger, D. N., Richardson, P. D., Kvietys, P. R., and Mortillaro, N. A. (1980). Intestinal blood flow. *Gastroenterology* 78, 837–863.

Grassi, G., Dell'Oro, R., Facchini, A., Quarti Trevano, F., Bolla, G. B., and Mancia, G. (2004). Effect of central and peripheral body fat distribution on sympathetic and baroreflex function in obese normotensives. *J. Hypertens.* 22, 2363–2369. doi: 10.1097/00004872-200412000-00019

Grassi, G., Facchini, A., Trevano, F. Q., Dell'Oro, R., Arenare, F., Tana, F., et al. (2005). Obstructive sleep apnea-dependent and -independent adrenergic activation in obesity. *Hypertension* 46, 321–325. doi: 10.1161/01.HYP.0000174243.39897.6c

Grassi, G., Mark, A., and Esler, M. (2015). The sympathetic nervous system alterations in human hypertension. *Circ. Res.* 116, 976–990. doi: 10.1161/CIRCRESAHA.116.303604

Grassi, G., Seravalle, G., Cattaneo, B. M., Bolla, G. B., Lanfranchi, A., Colombo, M., et al. (1995). Sympathetic activation in obese normotensive subjects. *Hypertension* 25(4 Pt 1), 560–563. doi: 10.1161/01.HYP.25.4.560

Greenfield, J. R., Miller, J. W., Keogh, J. M., Henning, E., Satterwhite, J. H., Cameron, G. S., et al. (2009). Modulation of blood pressure by central melanocortinergic pathways. *N. Engl. J. Med.* 360, 44–52. doi: 10.1056/NEJMoa0803085

Hall, J. E., Granger, J. P., do Carmo, J. M., da Silva, A. A., Dubinion, J., George, E., et al. (2012). Hypertension: physiology and pathophysiology. *Compr. Physiol.* 2, 2393–2442. doi: 10.1002/cphy.c110058

Hall, J. E., Hildebrandt, D. A., and Kuo, J. (2001). Obesity hypertension: role of leptin and sympathetic nervous system. *Am. J. Hypertens.* 14(6 Pt 2), 103S–115S. doi: 10.1016/S0895-7061(01)02077-5

Hausberg, M., Hoffman, R. P., Somers, V. K., Sinkey, C. A., Mark, A. L., and Anderson, E. A. (1997). Contrasting autonomic and hemodynamic effects of insulin in healthy elderly versus young subjects. *Hypertension* 29, 700–705. doi: 10.1161/01.HYP.29.3.700

Haynes, W. G. (2000). Interaction between leptin and sympathetic nervous system in hypertension. *Curr. Hypertens. Rep.* 2, 311–318. doi: 10.1007/s11906-000-0015-1

Haynes, W. G., Morgan, D. A., Djalali, A., Sivitz, W. I., and Mark, A. L. (1999). Interactions between the melanocortin system and leptin in control of sympathetic nerve traffic. *Hypertension* 33(1 Pt 2), 542–547. doi: 10.1161/01.HYP.33.1.542

Haynes, W. G., Sivitz, W. I., Morgan, D. A., Walsh, S. A., and Mark, A. L. (1997). Sympathetic and cardiorenal actions of leptin. *Hypertension* 30(3 Pt 2), 619–623. doi: 10.1161/01.HYP.30.3.619

Heath, R. B., Jones, R., Frayn, K. N., and Robertson, M. D. (2004). Vagal stimulation exaggerates the inhibitory ghrelin response to oral fat in humans. *J. Endocrinol.* 180, 273–281. doi: 10.1677/joe.0.1800273

Henry, T. R. (2002). Therapeutic mechanisms of vagus nerve stimulation. *Neurology* 59(6 Suppl. 4), S3–S14. doi: 10.1212/WNL.59.6_suppl_4.S3

Heymsfield, S. B., Greenberg, A. S., Fujioka, K., Dixon, R. M., Kushner, R., Hunt, T., et al. (1999). Recombinant leptin for weight loss in obese and lean adults: a randomized, controlled, dose-escalation trial. *JAMA* 282, 1568–1575. doi: 10.1001/jama.282.16.1568

Hirsch, J., Leibel, R. L., Mackintosh, R., and Aguirre, A. (1991). Heart rate variability as a measure of autonomic function during weight change in humans. *Am. J. Physiol.* 261(6 Pt 2), R1418–R1423.

Holst, J. J., Orskov, C., Nielsen, O. V., and Schwartz, T. W. (1987). Truncated glucagon-like peptide I, an insulin-releasing hormone from the distal gut. *FEBS Lett.* 211, 169–174. doi: 10.1016/0014-5793(87)81430-8

Huang, F., Dong, J., Kong, J., Wang, H., Meng, H., Spaeth, R. B., et al. (2014). Effect of transcutaneous auricular vagus nerve stimulation on impaired glucose tolerance: a pilot randomized study. *BMC Complement. Altern. Med.* 14:203. doi: 10.1186/1472-6882-14-203

Id, D., Bertog, S. C., Ziegler, A. K., Hornung, M., Hofmann, I., Vaskelyte, L., et al. (2016). Predictors of blood pressure response: obesity is associated with a less pronounced treatment response after renal denervation. *Catheter. Cardiovasc. Interv.* 87, E30–E38. doi: 10.1002/ccd.26068

Ikramuddin, S., Blackstone, R. P., Brancatisano, A., Toouli, J., Shah, S. N., Wolfe, B. M., et al. (2014). Effect of reversible intermittent intra-abdominal vagal nerve blockade on morbid obesity: the ReCharge randomized clinical trial. *JAMA* 312, 915–922. doi: 10.1001/jama.2014.10540

Imeryuz, N., Yegen, B. C., Bozkurt, A., Coskun, T., Villanueva-Penacarrillo, M. L., and Ulusoy, N. B. (1997). Glucagon-like peptide-1 inhibits gastric emptying via vagal afferent-mediated central mechanisms. *Am. J. Physiol.* 273(4 Pt 1), G920–G927.

Inokuma, K., Okamatsu-Ogura, Y., Omachi, A., Matsushita, Y., Kimura, K., Yamashita, H., et al. (2006). Indispensable role of mitochondrial UCP1 for antiobesity effect of beta3-adrenergic stimulation. *Am. J. Physiol. Endocrinol. Metab.* 290, E1014–E1021. doi: 10.1152/ajpendo.00105.2005

Iwasaki, Y., Shimomura, K., Kohno, D., Dezaki, K., Ayush, E. A., Nakabayashi, H., et al. (2013). Insulin activates vagal afferent neurons including those innervating pancreas via insulin cascade and $Ca^{(2+)}$influx: its dysfunction in IRS2-KO mice with hyperphagic obesity. *PLoS ONE* 8:e67198. doi: 10.1371/journal.pone.0067198

Iyer, M. S., Bergman, R. N., Korman, J. E., Woolcott, O. O., Kabir, M., Victor, R. G., et al. (2016). Renal denervation reverses hepatic insulin resistance induced by high-fat diet. *Diabetes* 65, 3453–3463. doi: 10.2337/db16-0698

Jorde, R., and Burhol, P. G. (1984). Fasting and postprandial plasma pancreatic polypeptide (PP) levels in obesity. *Int. J. Obes.* 8, 393–397.

Julius, S., Valentini, M., and Palatini, P. (2000). Overweight and hypertension: a 2-way street? *Hypertension* 35, 807–813. doi: 10.1161/01.HYP.35.3.807

Kassab, S., Kato, T., Wilkins, F. C., Chen, R., Hall, J. E., and Granger, J. P. (1995). Renal denervation attenuates the sodium retention and hypertension associated with obesity. *Hypertension* 25(4 Pt 2), 893–897. doi: 10.1161/01.HYP.25.4.893

Kastin, A. J., Akerstrom, V., and Pan, W. (2002). Interactions of glucagon-like peptide-1 (GLP-1) with the blood-brain barrier. *J. Mol. Neurosci.* 18, 7–14. doi: 10.1385/JMN:18:1-2:07

Kissileff, H. R., Carretta, J. C., Geliebter, A., and Pi-Sunyer, F. X. (2003). Cholecystokinin and stomach distension combine to reduce food intake in humans. *Am. J. Physiol. Regul. Integr. Comp. Physiol.* 285, R992–R998. doi: 10.1152/ajpregu.00272.2003

Koda, S., Date, Y., Murakami, N., Shimbara, T., Hanada, T., Toshinai, K., et al. (2005). The role of the vagal nerve in peripheral PYY3-36-induced feeding reduction in rats. *Endocrinology* 146, 2369–2375. doi: 10.1210/en.2004-1266

Kojima, M., Hosoda, H., Date, Y., Nakazato, M., Matsuo, H., and Kangawa, K. (1999). Ghrelin is a growth-hormone-releasing acylated peptide from stomach. *Nature* 402, 656–660. doi: 10.1038/45230

Kral, J. G. (1978). Vagotomy for treatment of severe obesity. *Lancet* 1, 307–308. doi: 10.1016/S0140-6736(78)90074-0

Kreier, F., Fliers, E., Voshol, P. J., Van Eden, C. G., Havekes, L. M., Kalsbeek, A., et al. (2002). Selective parasympathetic innervation of subcutaneous and intra-abdominal fat–functional implications. *J. Clin. Invest.* 110, 1243–1250. doi: 10.1172/JCI0215736

Kreymann, B., Williams, G., Ghatei, M. A., and Bloom, S. R. (1987). Glucagon-like peptide-1 7-36: a physiological incretin in man. *Lancet* 2, 1300–1304. doi: 10.1016/S0140-6736(87)91194-9

Kuniyoshi, F. H., Trombetta, I. C., Batalha, L. T., Rondon, M. U., Laterza, M. C., Gowdak, M. M., et al. (2003). Abnormal neurovascular control during sympathoexcitation in obesity. *Obes. Res.* 11, 1411–1419. doi: 10.1038/oby.2003.190

Kunz, I., Schorr, U., Klaus, S., and Sharma, A. M. (2000). Resting metabolic rate and substrate use in obesity hypertension. *Hypertension* 36, 26–32. doi: 10.1161/01.HYP.36.1.26

Lambert, E. A., Rice, T., Eikelis, N., Straznicky, N. E., Lambert, G. W., Head, G. A., et al. (2014). Sympathetic activity and markers of cardiovascular risk in nondiabetic severely obese patients: the effect of the initial 10% weight loss. *Am. J. Hypertens.* 27, 1308–1315. doi: 10.1093/ajh/hpu050

Lambert, E. A., Straznicky, N. E., Dixon, J. B., and Lambert, G. W. (2015). Should the sympathetic nervous system be a target to improve cardiometabolic risk in obesity? *Am. J. Physiol. Heart Circ. Physiol.* 309, H244–H258. doi: 10.1152/ajpheart.00096.2015

Lambert, E., Lambert, G., Ika-Sari, C., Dawood, T., Lee, K., Chopra, R., et al. (2011). Ghrelin modulates sympathetic nervous system activity and stress response in lean and overweight men. *Hypertension* 58, 43–50. doi: 10.1161/HYPERTENSIONAHA.111.171025

Lambert, E., Sari, C. I., Dawood, T., Nguyen, J., McGrane, M., Eikelis, N., et al. (2010). Sympathetic nervous system activity is associated with obesity-induced subclinical organ damage in young adults. *Hypertension* 56, 351–358. doi: 10.1161/HYPERTENSIONAHA.110.155663

Lambert, E., Straznicky, N., Schlaich, M., Esler, M., Dawood, T., Hotchkin, E., et al. (2007). Differing pattern of sympathoexcitation in normal-weight and obesity-related hypertension. *Hypertension* 50, 862–868. doi: 10.1161/HYPERTENSIONAHA.107.094649

Landsberg, L. (1986). Diet, obesity and hypertension: an hypothesis involving insulin, the sympathetic nervous system, and adaptive thermogenesis. *Q. J. Med.* 61, 1081–1090.

Landsberg, L. (2001). Insulin-mediated sympathetic stimulation: role in the pathogenesis of obesity-related hypertension (or, how insulin affects blood pressure, and why). *J. Hypertens* 19(3 Pt 2), 523–528. doi: 10.1097/00004872-200103001-00001

Lassmann, V., Vague, P., Vialettes, B., and Simon, M. C. (1980). Low plasma levels of pancreatic polypeptide in obesity. *Diabetes* 29, 428–430. doi: 10.2337/diab.29.6.428

Lavin, J. H., Wittert, G. A., Andrews, J., Yeap, B., Wishart, J. M., Morris, H. A., et al. (1998). Interaction of insulin, glucagon-like peptide 1, gastric inhibitory polypeptide, and appetite in response to intraduodenal carbohydrate. *Am. J. Clin. Nutr.* 68, 591–598.

Lebron, L., Chou, A. J., and Carrasquillo, J. A. (2010). Interesting image. Unilateral F-18 FDG uptake in the neck, in patients with sympathetic denervation. *Clin. Nucl. Med.* 35, 899–901. doi: 10.1097/RLU.0b013e3181f49ff8

Lee, H. M., Wang, G., Englander, E. W., Kojima, M., and Greeley, G. H. Jr. (2002). Ghrelin, a new gastrointestinal endocrine peptide that stimulates insulin secretion: enteric distribution, ontogeny, influence of endocrine, and dietary manipulations. *Endocrinology* 143, 185–190. doi: 10.1210/endo.143.1.8602

le Roux, C. W., Batterham, R. L., Aylwin, S. J., Patterson, M., Borg, C. M., Wynne, K. J., et al. (2006). Attenuated peptide YY release in obese subjects is associated with reduced satiety. *Endocrinology* 147, 3–8. doi: 10.1210/en.2005-0972

Li, Y., and Owyang, C. (1994). Endogenous cholecystokinin stimulates pancreatic enzyme secretion via vagal afferent pathway in rats. *Gastroenterology* 107, 525–531. doi: 10.1016/0016-5085(94)90180-5

Lim, K., Burke, S. L., and Head, G. A. (2013). Obesity-related hypertension and the role of insulin and leptin in high-fat-fed rabbits. *Hypertension* 61, 628–634. doi: 10.1161/HYPERTENSIONAHA.111.00705

Lin, H. C., and Taylor, I. L. (2004). Release of peptide YY by fat in the proximal but not distal gut depends on an atropine-sensitive cholinergic pathway. *Regul. Pept.* 117, 73–76. doi: 10.1016/j.regpep.2003.10.008

Lips, M. A., de Groot, G. H., De Kam, M., Berends, F. J., Wiezer, R., Van Wagensveld, B. A., et al. (2013). Autonomic nervous system activity in diabetic and healthy obese female subjects and the effect of distinct weight loss strategies. *Eur. J. Endocrinol.* 169, 383–390. doi: 10.1530/EJE-13-0506

Little, T. J., Horowitz, M., and Feinle-Bisset, C. (2005). Role of cholecystokinin in appetite control and body weight regulation. *Obes. Rev.* 6, 297–306. doi: 10.1111/j.1467-789X.2005.00212.x

Mahfoud, F., Schlaich, M., Kindermann, I., Ukena, C., Cremers, B., Brandt, M. C., et al. (2011). Effect of renal sympathetic denervation on glucose metabolism in patients with resistant hypertension: a pilot study. *Circulation* 123, 1940–1946. doi: 10.1161/CIRCULATIONAHA.110.991869

Mano-Otagiri, A., Ohata, H., Iwasaki-Sekino, A., Nemoto, T., and Shibasaki, T. (2009). Ghrelin suppresses noradrenaline release in the brown adipose tissue of rats. *J. Endocrinol.* 201, 341–349. doi: 10.1677/JOE-08-0374

Mark, A. L. (2013). Selective leptin resistance revisited. *Am. J. Physiol. Regul. Integr. Comp. Physiol.* 305, R566–R581. doi: 10.1152/ajpregu.00180.2013

Mark, A. L., Correia, M. L., Rahmouni, K., and Haynes, W. G. (2002). Selective leptin resistance: a new concept in leptin physiology with cardiovascular implications. *J. Hypertens.* 20, 1245–1250. doi: 10.1097/00004872-200207000-00001

Mark, A. L., Shaffer, R. A., Correia, M. L., Morgan, D. A., Sigmund, C. D., and Haynes, W. G. (1999). Contrasting blood pressure effects of obesity in leptin-deficient ob/ob mice and agouti yellow obese mice. *J. Hypertens* 17(12 Pt 2), 1949–1953. doi: 10.1097/00004872-199917121-00026

Marsh, A. J., Fontes, M. A., Killinger, S., Pawlak, D. B., Polson, J. W., and Dampney, R. A. (2003). Cardiovascular responses evoked by leptin acting on neurons in the ventromedial and dorsomedial hypothalamus. *Hypertension* 42, 488–493. doi: 10.1161/01.HYP.0000090097.22678.0A

Martin-Rodriguez, E., Guillen-Grima, F., Marti, A., and Brugos-Larumbe, A. (2015). Comorbidity associated with obesity in a large population: the APNA study. *Obes. Res. Clin. Pract.* 9, 435–447. doi: 10.1016/j.orcp.2015.04.003

Masajtis-Zagajewska, A., Majer, J., and Nowicki, M. (2010). Effect of moxonidine and amlodipine on serum YKL-40, plasma lipids and insulin sensitivity in insulin-resistant hypertensive patients-a randomized, crossover trial. *Hypertens. Res.* 33, 348–353. doi: 10.1038/hr.2010.6

Matsumoto, T., Miyawaki, T., Ue, H., Kanda, T., Zenji, C., and Moritani, T. (1999). Autonomic responsiveness to acute cold exposure in obese and non-obese young women. *Int. J. Obes. Relat. Metab. Disord.* 23, 793–800. doi: 10.1038/sj.ijo.0800928

Matsumura, K., Tsuchihashi, T., Fujii, K., Abe, I., and Iida, M. (2002). Central ghrelin modulates sympathetic activity in conscious rabbits. *Hypertension* 40, 694–699. doi: 10.1161/01.HYP.0000035395.51441.10

Meguro, T., Shimosegawa, T., Kikuchi, Y., Koizumi, M., and Toyota, T. (1995). Effects of cisapride on gallbladder emptying and pancreatic polypeptide and cholecystokinin release in humans. *J. Gastroenterol.* 30, 237–243. doi: 10.1007/BF02348671

Messerli, F. H., Sundgaard-Riise, K., Reisin, E., Dreslinski, G., Dunn, F. G., and Frohlich, E. (1983). Disparate cardiovascular effects of obesity and arterial hypertension. *Am. J. Med.* 74, 808–812. doi: 10.1016/0002-9343(83)91071-9

Miro, J., Jaraba, S., Mora, J., Puig, O., Castaner, S., Rodriguez-Bel, L., et al. (2015). Vagus nerve stimulation therapy is effective and safe for startle-induced seizures. *J. Neurol. Sci.* 354, 124–126. doi: 10.1016/j.jns.2015.04.048

Mojsov, S., Weir, G. C., and Habener, J. F. (1987). Insulinotropin: glucagon-like peptide I (7-37) co-encoded in the glucagon gene is a potent stimulator of insulin release in the perfused rat pancreas. *J. Clin. Invest.* 79, 616–619. doi: 10.1172/JCI112855

Monroe, M. B., Seals, D. R., Shapiro, L. F., Bell, C., Johnson, D., and Parker Jones, P. (2001). Direct evidence for tonic sympathetic support of resting metabolic rate in healthy adult humans. *Am. J. Physiol. Endocrinol. Metab.* 280, E740–E744.

Moran, T. H., and Kinzig, K. P. (2004). Gastrointestinal satiety signals II. Cholecystokinin. *Am. J. Physiol. Gastrointest. Liver Physiol.* 286, G183–G188. doi: 10.1152/ajpgi.00434.2003

Muscelli, E., Emdin, M., Natali, A., Pratali, L., Camastra, S., Gastaldelli, A., et al. (1998). Autonomic and hemodynamic responses to insulin in lean and obese humans. *J. Clin. Endocrinol. Metab.* 83, 2084–2090. doi: 10.1210/jc.83.6.2084

Nakabayashi, H., Nishizawa, M., Nakagawa, A., Takeda, R., and Niijima, A. (1996). Vagal hepatopancreatic reflex effect evoked by intraportal appearance of tGLP-1. *Am. J. Physiol.* 271(5 Pt 1), E808–E813.

Nannipieri, M., Mari, A., Anselmino, M., Baldi, S., Barsotti, E., Guarino, D., et al. (2011). The role of beta-cell function and insulin sensitivity in the remission of type 2 diabetes after gastric bypass surgery. *J. Clin. Endocrinol. Metab.* 96, E1372–E1379. doi: 10.1210/jc.2011-0446

Narkiewicz, K., Kato, M., Pesek, C. A., and Somers, V. K. (1999a). Human obesity is characterized by a selective potentiation of central chemoreflex sensitivity. *Hypertension* 33, 1153–1158. doi: 10.1161/01.HYP.33.5.1153

Narkiewicz, K., Kato, M., Phillips, B. G., Pesek, C. A., Davison, D. E., and Somers, V. K. (1999b). Nocturnal continuous positive airway pressure decreases daytime sympathetic traffic in obstructive sleep apnea. *Circulation* 100, 2332–2335. doi: 10.1161/01.CIR.100.23.2332

Narkiewicz, K., van de Borne, P. J., Cooley, R. L., Dyken, M. E., and Somers, V. K. (1998). Sympathetic activity in obese subjects with and without obstructive sleep apnea. *Circulation* 98, 772–776. doi: 10.1161/01.CIR.98.8.772

Nault, I., Nadreau, E., Paquet, C., Brassard, P., Marceau, P., Marceau, S., et al. (2007). Impact of bariatric surgery–induced weight loss on heart rate variability. *Metab. Clin. Exp.* 56, 1425–1430. doi: 10.1016/j.metabol.2007.06.006

Neary, N. M., Small, C. J., and Bloom, S. R. (2003). Gut and mind. *Gut* 52, 918–921. doi: 10.1136/gut.52.7.918

Negrao, C. E., Trombetta, I. C., Batalha, L. T., Ribeiro, M. M., Rondon, M. U., Tinucci, T., et al. (2001). Muscle metaboreflex control is diminished in normotensive obese women. *Am. J. Physiol. Heart Circ. Physiol.* 281, H469–H475.

Niebel, W., Eysselein, V. E., and Singer, M. V. (1987). Pancreatic polypeptide response to a meal before and after cutting the extrinsic nerves of the upper gastrointestinal tract and the pancreas in the dog. *Dig. Dis. Sci.* 32, 1004–1009. doi: 10.1007/BF01297191

Obici, S., and Rossetti, L. (2003). Minireview: nutrient sensing and the regulation of insulin action and energy balance. *Endocrinology* 144, 5172–5178. doi: 10.1210/en.2003-0999

Obici, S., Zhang, B. B., Karkanias, G., and Rossetti, L. (2002). Hypothalamic insulin signaling is required for inhibition of glucose production. *Nat. Med.* 8, 1376–1382. doi: 10.1038/nm1202-798

Onaga, T., Zabielski, R., and Kato, S. (2002). Multiple regulation of peptide YY secretion in the digestive tract. *Peptides* 23, 279–290. doi: 10.1016/S0196-9781(01)00609-X

Orskov, C., Rabenhoj, L., Wettergren, A., Kofod, H., and Holst, J. J. (1994). Tissue and plasma concentrations of amidated and glycine-extended glucagon-like peptide I in humans. *Diabetes* 43, 535–539. doi: 10.2337/diab.43.4.535

Ozata, M., Ozdemir, I. C., and Licinio, J. (1999). Human leptin deficiency caused by a missense mutation: multiple endocrine defects, decreased sympathetic tone, and immune system dysfunction indicate new targets for leptin action,

greater central than peripheral resistance to the effects of leptin, and spontaneous correction of leptin-mediated defects. *J. Clin. Endocrinol. Metab.* 84, 3686–3695. doi: 10.1210/jcem.84.10.5999

Pandit, R., Beerens, S., and Adan, R. A. H. (2017). Role of leptin in energy expenditure: the hypothalamic perspective. *Am. J. Physiol. Regul. Integr. Comp. Physiol.* 312, R938–R947. doi: 10.1152/ajpregu.00045.2016

Pardo, J. V., Sheikh, S. A., Kuskowski, M. A., Surerus-Johnson, C., Hagen, M. C., Lee, J. T., et al. (2007). Weight loss during chronic, cervical vagus nerve stimulation in depressed patients with obesity: an observation. *Int. J. Obes.* 31, 1756–1759. doi: 10.1038/sj.ijo.0803666

Parker, R. M., and Herzog, H. (1999). Regional distribution of Y-receptor subtype mRNAs in rat brain. *Eur. J. Neurosci.* 11, 1431–1448. doi: 10.1046/j.1460-9568.1999.00553.x

Perugini, R. A., Li, Y., Rosenthal, L., Gallagher-Dorval, K., Kelly, J. J., and Czerniach, D. R. (2010). Reduced heart rate variability correlates with insulin resistance but not with measures of obesity in population undergoing laparoscopic Roux-en-Y gastric bypass. *Surg. Obes. Relat. Dis.* 6, 237–241. doi: 10.1016/j.soard.2009.09.012

Peuker, E. T., and Filler, T. J. (2002). The nerve supply of the human auricle. *Clin. Anat.* 15, 35–37. doi: 10.1002/ca.1089

Plamboeck, A., Veedfald, S., Deacon, C. F., Hartmann, B., Wettergren, A., Svendsen, L. B., et al. (2013). The effect of exogenous GLP-1 on food intake is lost in male truncally vagotomized subjects with pyloroplasty. *Am. J. Physiol. Gastrointest. Liver Physiol.* 304, G1117–G1127. doi: 10.1152/ajpgi.00035.2013

Plum, L., Schubert, M., and Bruning, J. C. (2005). The role of insulin receptor signaling in the brain. *Trends Endocrinol. Metab.* 16, 59–65. doi: 10.1016/j.tem.2005.01.008

Pontiroli, A. E., Merlotti, C., Veronelli, A., and Lombardi, F. (2013). Effect of weight loss on sympatho-vagal balance in subjects with grade-3 obesity: restrictive surgery versus hypocaloric diet. *Acta Diabetol.* 50, 843–850. doi: 10.1007/s00592-013-0454-1

Prigge, W. F., and Grande, F. (1971). Effects of glucagon, epinephrine and insulin on *in vitro* lipolysis of adipose tissue from mammals and birds. *Comp. Biochem. Physiol. B* 39, 69–82. doi: 10.1016/0305-0491(71)90254-9

Prior, L. J., Davern, P. J., Burke, S. L., Lim, K., Armitage, J. A., and Head, G. A. (2014). Exposure to a high-fat diet during development alters leptin and ghrelin sensitivity and elevates renal sympathetic nerve activity and arterial pressure in rabbits. *Hypertension* 63, 338–345. doi: 10.1161/HYPERTENSIONAHA.113.02498

Rahmouni, K., Morgan, D. A., Morgan, G. M., Mark, A. L., and Haynes, W. G. (2005). Role of selective leptin resistance in diet-induced obesity hypertension. *Diabetes* 54, 2012–2018. doi: 10.2337/diabetes.54.7.2012

Rebuffe-Scrive, M. (1991). Neuroregulation of adipose tissue: molecular and hormonal mechanisms. *Int. J. Obes.* 15(Suppl. 2), 83–86.

Rong, P., Liu, J., Wang, L., Liu, R., Fang, J., Zhao, J., et al. (2016). Effect of transcutaneous auricular vagus nerve stimulation on major depressive disorder: a nonrandomized controlled pilot study. *J. Affect. Disord.* 195, 172–179. doi: 10.1016/j.jad.2016.02.031

Ronveaux, C. C., Tome, D., and Raybould, H. E. (2015). Glucagon-like peptide 1 interacts with ghrelin and leptin to regulate glucose metabolism and food intake through vagal afferent neuron signaling. *J. Nutr.* 145, 672–680. doi: 10.3945/jn.114.206029

Rosell, S. (1966). Release of free fatty acids from subcutaneous adipose tissue in dogs following sympathetic nerve stimulation. *Acta Physiol. Scand.* 67, 343–351. doi: 10.1111/j.1748-1716.1966.tb03320.x

Rowe, J. W., Young, J. B., Minaker, K. L., Stevens, A. L., Pallotta, J., and Landsberg, L. (1981). Effect of insulin and glucose infusions on sympathetic nervous system activity in normal man. *Diabetes* 30, 219–225. doi: 10.2337/diab.30.3.219

Saito, M. (2013). Brown adipose tissue as a regulator of energy expenditure and body fat in humans. *Diabetes Metab. J.* 37, 22–29. doi: 10.4093/dmj.2013.37.1.22

Saito, M., Okamatsu-Ogura, Y., Matsushita, M., Watanabe, K., Yoneshiro, T., Nio-Kobayashi, J., et al. (2009). High incidence of metabolically active brown adipose tissue in healthy adult humans: effects of cold exposure and adiposity. *Diabetes* 58, 1526–1531. doi: 10.2337/db09-0530

Sarr, M. G., Billington, C. J., Brancatisano, R., Brancatisano, A., Toouli, J., Kow, L., et al. (2012). The EMPOWER study: randomized, prospective, double-blind, multicenter trial of vagal blockade to induce weight loss in morbid obesity. *Obes. Surg.* 22, 1771–1782. doi: 10.1007/s11695-012-0751-8

Sartor, D. M., and Verberne, A. J. (2002). Cholecystokinin selectively affects presympathetic vasomotor neurons and sympathetic vasomotor outflow. *Am. J. Physiol. Regul. Integr. Comp. Physiol.* 282, R1174–R1184. doi: 10.1152/ajpregu.00500.2001

Sartor, D. M., and Verberne, A. J. (2006). The sympathoinhibitory effects of systemic cholecystokinin are dependent on neurons in the caudal ventrolateral medulla in the rat. *Am. J. Physiol. Regul. Integr. Comp. Physiol.* 291, R1390–R1398. doi: 10.1152/ajpregu.00314.2006

Sartor, D. M., and Verberne, A. J. (2008). Abdominal vagal signalling: a novel role for cholecystokinin in circulatory control? *Brain Res. Rev.* 59, 140–154. doi: 10.1016/j.brainresrev.2008.07.002

Satoh, N., Ogawa, Y., Katsuura, G., Hayase, M., Tsuji, T., Imagawa, K., et al. (1997). The arcuate nucleus as a primary site of satiety effect of leptin in rats. *Neurosci. Lett.* 224, 149–152. doi: 10.1016/S0304-3940(97)00163-8

Scherer, T., O'Hare, J., Diggs-Andrews, K., Schweiger, M., Cheng, B., Lindtner, C., et al. (2011). Brain insulin controls adipose tissue lipolysis and lipogenesis. *Cell Metab.* 13, 183–194. doi: 10.1016/j.cmet.2011.01.008

Schmidt, P. T., Naslund, E., Gryback, P., Jacobsson, H., Holst, J. J., Hilsted, L., et al. (2005). A role for pancreatic polypeptide in the regulation of gastric emptying and short-term metabolic control. *J. Clin. Endocrinol. Metab.* 90, 5241–5246. doi: 10.1210/jc.2004-2089

Schwartz, M. W., Prigeon, R. L., Kahn, S. E., Nicolson, M., Moore, J., Morawiecki, A., et al. (1997). Evidence that plasma leptin and insulin levels are associated with body adiposity via different mechanisms. *Diabetes Care* 20, 1476–1481. doi: 10.2337/diacare.20.9.1476

Schwartz, T. W. (1983). Pancreatic polypeptide: a hormone under vagal control. *Gastroenterology* 85, 1411–1425.

Scriba, D., Aprath-Husmann, I., Blum, W. F., and Hauner, H. (2000). Catecholamines suppress leptin release from *in vitro* differentiated subcutaneous human adipocytes in primary culture via beta1- and beta2-adrenergic receptors. *Eur. J. Endocrinol.* 143, 439–445. doi: 10.1530/eje.0.1430439

Seravalle, G., Colombo, M., Perego, P., Giardini, V., Volpe, M., Dell'Oro, R., et al. (2014). Long-term sympathoinhibitory effects of surgically induced weight loss in severe obese patients. *Hypertension* 64, 431–437. doi: 10.1161/HYPERTENSIONAHA.113.02988

Sheikh, A. (2013). Direct cardiovascular effects of glucagon like peptide-1. *Diabetol. Metab. Syndr.* 5:47. doi: 10.1186/1758-5996-5-47

Sheikh, S. P., Holst, J. J., Orskov, C., Ekman, R., and Schwartz, T. W. (1989). Release of PYY from pig intestinal mucosa; luminal and neural regulation. *Regul. Pept.* 26, 253–266. doi: 10.1016/0167-0115(89)90193-6

Shibao, C., Gamboa, A., Diedrich, A., Ertl, A. C., Chen, K. Y., Byrne, D. W., et al. (2007). Autonomic contribution to blood pressure and metabolism in obesity. *Hypertension* 49, 27–33. doi: 10.1161/01.HYP.0000251679.87348.05

Shikora, S., Toouli, J., Herrera, M. F., Kulseng, B., Zulewski, H., Brancatisano, R., et al. (2013). Vagal blocking improves glycemic control and elevated blood pressure in obese subjects with type 2 diabetes mellitus. *J. Obes.* 2013:245683. doi: 10.1155/2013/245683

Shin, A. C., Zheng, H., and Berthoud, H. R. (2009). An expanded view of energy homeostasis: neural integration of metabolic, cognitive, and emotional drives to eat. *Physiol. Behav.* 97, 572–580. doi: 10.1016/j.physbeh.2009.02.010

Smith, D. K., Sarfeh, J., and Howard, L. (1983). Truncal vagotomy in hypothalamic obesity. *Lancet* 1, 1330–1331. doi: 10.1016/S0140-6736(83)92437-6

Soares, L. P., Fabbro, A. L., Silva, A. S., Sartorelli, D. S., Franco, L. F., Kuhn, P. C., et al. (2015). Prevalence of metabolic syndrome in the Brazilian Xavante indigenous population. *Diabetol. Metab. Syndr.* 7:105. doi: 10.1186/s13098-015-0100-x

Soderlund, V., Larsson, S. A., and Jacobsson, H. (2007). Reduction of FDG uptake in brown adipose tissue in clinical patients by a single dose of propranolol. *Eur. J. Nucl. Med. Mol. Imaging* 34, 1018–1022. doi: 10.1007/s00259-006-0318-9

Somers, V. K., Dyken, M. E., Clary, M. P., and Abboud, F. M. (1995). Sympathetic neural mechanisms in obstructive sleep apnea. *J. Clin. Invest.* 96, 1897–1904. doi: 10.1172/JCI118235

Sondergaard, E., Gormsen, L. C., Christensen, M. H., Pedersen, S. B., Christiansen, P., Nielsen, S., et al. (2015). Chronic adrenergic stimulation induces brown adipose tissue differentiation in visceral adipose tissue. *Diabet. Med.* 32, e4–e8. doi: 10.1111/dme.12595

Straznicky, N. E., Lambert, E. A., Lambert, G. W., Masuo, K., Esler, M. D., and Nestel, P. J. (2005). Effects of dietary weight loss on sympathetic activity and cardiac risk factors associated with the metabolic syndrome. *J. Clin. Endocrinol. Metab.* 90, 5998–6005. doi: 10.1210/jc.2005-0961

Takahashi, A., and Shimazu, T. (1981). Hypothalamic regulation of lipid metabolism in the rat: effect of hypothalamic stimulation on lipolysis. *J. Auton. Nerv. Syst.* 4, 195–205. doi: 10.1016/0165-1838(81)90044-8

Tallam, L. S., Stec, D. E., Willis, M. A., da Silva, A. A., and Hall, J. E. (2005). Melanocortin-4 receptor-deficient mice are not hypertensive or salt-sensitive despite obesity, hyperinsulinemia, and hyperleptinemia. *Hypertension* 46, 326–332. doi: 10.1161/01.HYP.0000175474.99326.bf

Tentolouris, N., Tsigos, C., Perea, D., Koukou, E., Kyriaki, D., Kitsou, E., et al. (2003). Differential effects of high-fat and high-carbohydrate isoenergetic meals on cardiac autonomic nervous system activity in lean and obese women. *Metab. Clin. Exp.* 52, 1426–1432. doi: 10.1016/S0026-0495(03)00322-6

Tonhajzerova, I., Javorka, M., Trunkvalterova, Z., Chroma, O., Javorkova, J., Lazarova, Z., et al. (2008). Cardio-respiratory interaction and autonomic dysfunction in obesity. *J. Physiol. Pharmacol.* 59(Suppl. 6), 709–718.

Track, N. S. (1980). The gastrointestinal endocrine system. *Can. Med. Assoc. J.* 122, 287–292.

Travers, J. B., Travers, S. P., and Norgren, R. (1987). Gustatory neural processing in the hindbrain. *Annu. Rev. Neurosci.* 10, 595–632. doi: 10.1146/annurev.ne.10.030187.003115

Trayhurn, P., Duncan, J. S., and Rayner, D. V. (1995). Acute cold-induced suppression of ob (obese) gene expression in white adipose tissue of mice: mediation by the sympathetic system. *Biochem. J.* 311(Pt 3), 729–733. doi: 10.1042/bj3110729

Tschop, M., Wawarta, R., Riepl, R. L., Friedrich, S., Bidlingmaier, M., Landgraf, R., et al. (2001). Post-prandial decrease of circulating human ghrelin levels. *J. Endocrinol. Invest.* 24(6), Rc19–Rc 21. doi: 10.1007/BF03351037

Tupone, D., Madden, C. J., and Morrison, S. F. (2014). Autonomic regulation of brown adipose tissue thermogenesis in health and disease: potential clinical applications for altering BAT thermogenesis. *Front. Neurosci.* 8:14. doi: 10.3389/fnins.2014.00014

Turton, M. D., O'Shea, D., Gunn, I., Beak, S. A., Edwards, C. M., Meeran, K., et al. (1996). A role for glucagon-like peptide-1 in the central regulation of feeding. *Nature* 379, 69–72. doi: 10.1038/379069a0

Val-Laillet, D., Biraben, A., Randuineau, G., and Malbert, C. H. (2010). Chronic vagus nerve stimulation decreased weight gain, food consumption and sweet craving in adult obese minipigs. *Appetite* 55, 245–252. doi: 10.1016/j.appet.2010.06.008

Vallbo, A. B., Hagbarth, K. E., and Wallin, B. G. (2004). Microneurography: how the technique developed and its role in the investigation of the sympathetic nervous system. *J. Appl. Physiol. (1985)* 96, 1262–1269. doi: 10.1152/japplphysiol.00470.2003

van Baak, M. A. (2001). The peripheral sympathetic nervous system in human obesity. *Obes. Rev.* 2, 3–14. doi: 10.1046/j.1467-789x.2001.00010.x

van der Lans, A. A., Hoeks, J., Brans, B., Vijgen, G. H., Visser, M. G., Vosselman, M. J., et al. (2013). Cold acclimation recruits human brown fat and increases nonshivering thermogenesis. *J. Clin. Invest.* 123, 3395–3403. doi: 10.1172/JCI68993

van Marken Lichtenbelt, W. D., Vanhommerig, J. W., Smulders, N. M., Drossaerts, J. M., Kemerink, G. J., Bouvy, N. D., et al. (2009). Cold-activated brown adipose tissue in healthy men. *N. Engl. J. Med.* 360, 1500–1508. doi: 10.1056/NEJMoa0808718

Ventureyra, E. C. (2000). Transcutaneous vagus nerve stimulation for partial onset seizure therapy. A new concept. *Childs Nerv. Syst.* 16, 101–102. doi: 10.1007/s003810050021

Verdich, C., Toubro, S., Buemann, B., Lysgard Madsen, J., Juul Holst, J., and Astrup, A. (2001). The role of postprandial releases of insulin and incretin hormones in meal-induced satiety–effect of obesity and weight reduction. *Int. J. Obes. Relat. Metab. Disord.* 25, 1206–1214. doi: 10.1038/sj.ijo.0801655

Vijgen, G. H., Bouvy, N. D., Leenen, L., Rijkers, K., Cornips, E., Majoie, M., et al. (2013). Vagus nerve stimulation increases energy expenditure: relation to brown adipose tissue activity. *PLoS ONE* 8:e77221. doi: 10.1371/journal.pone.0077221

Virdis, A., Lerman, L. O., Regoli, F., Ghiadoni, L., Lerman, A., and Taddei, S. (2016). Human ghrelin: a gastric hormone with cardiovascular properties. *Curr. Pharm. Des.* 22, 52–58. doi: 10.2174/1381612822666151119144458

Virtanen, K. A., Lidell, M. E., Orava, J., Heglind, M., Westergren, R., Niemi, T., et al. (2009). Functional brown adipose tissue in healthy adults. *N. Engl. J. Med.* 360, 1518–1525. doi: 10.1056/NEJMoa0808949

Wang, Z., Yu, L., Wang, S., Huang, B., Liao, K., Saren, G., et al. (2014). Chronic intermittent low-level transcutaneous electrical stimulation of auricular branch of vagus nerve improves left ventricular remodeling in conscious dogs with healed myocardial infarction. *Circ. Heart Fail.* 7, 1014–1021. doi: 10.1161/CIRCHEARTFAILURE.114.001564

Wank, S. A. (1995). Cholecystokinin receptors. *Am. J. Physiol.* 269(5 Pt 1), G628–646.

Welle, S. (1995). Sympathetic nervous system response to intake. *Am. J. Clin. Nutr.* 62(5 Suppl.), 1118s–1122s.

Welle, S., Schwartz, R. G., and Statt, M. (1991). Reduced metabolic rate during beta-adrenergic blockade in humans. *Metab. Clin. Exp.* 40, 619–622. doi: 10.1016/0026-0495(91)90053-Y

Wettergren, A., Maina, P., Boesby, S., and Holst, J. J. (1997). Glucagon-like peptide-1 7-36 amide and peptide YY have additive inhibitory effect on gastric acid secretion in man. *Scand. J. Gastroenterol.* 32, 552–555. doi: 10.3109/00365529709025098

Wijers, S. L., Saris, W. H., and van Marken Lichtenbelt, W. D. (2010). Cold-induced adaptive thermogenesis in lean and obese. *Obesity* 18, 1092–1099. doi: 10.1038/oby.2010.74

Williams, D. L., Grill, H. J., Cummings, D. E., and Kaplan, J. M. (2003). Vagotomy dissociates short- and long-term controls of circulating ghrelin. *Endocrinology* 144, 5184–5187. doi: 10.1210/en.2003-1059

Witkowski, A., Prejbisz, A., Florczak, E., Kadziela, J., Sliwinski, P., Bielen, P., et al. (2011). Effects of renal sympathetic denervation on blood pressure, sleep apnea course, and glycemic control in patients with resistant hypertension and sleep apnea. *Hypertension* 58, 559–565. doi: 10.1161/HYPERTENSIONAHA.111.173799

Wofford, M. R., Anderson, D. C. Jr., Brown, C. A., Jones, D. W., Miller, M. E., and Hall, J. E. (2001). Antihypertensive effect of alpha- and beta-adrenergic blockade in obese and lean hypertensive subjects. *Am. J. Hypertens* 14(7 Pt 1), 694–698. doi: 10.1016/S0895-7061(01)01293-6

Woods, A. J., and Stock, M. J. (1996). Leptin activation in hypothalamus. *Nature* 381:745. doi: 10.1038/381745a0

Woods, S. C., Seeley, R. J., Porte, D. Jr., and Schwartz, M. W. (1998). Signals that regulate food intake and energy homeostasis. *Science* 280, 1378–1383. doi: 10.1126/science.280.5368.1378

Xu, X., Chen, D. D., Yin, J., and Chen, J. D. (2014). Altered postprandial responses in gastric myoelectrical activity and cardiac autonomic functions in healthy obese subjects. *Obes. Surg.* 24, 554–560. doi: 10.1007/s11695-013-1109-6

Yang, H. (2002). Central and peripheral regulation of gastric acid secretion by peptide YY. *Peptides* 23, 349–358. doi: 10.1016/S0196-9781(01)00611-8

Yi, C. X., la Fleur, S. E., Fliers, E., and Kalsbeek, A. (2010). The role of the autonomic nervous liver innervation in the control of energy metabolism. *Biochim. Biophys. Acta* 1802, 416–431. doi: 10.1016/j.bbadis.2010.01.006

Yoneshiro, T., Aita, S., Matsushita, M., Kayahara, T., Kameya, T., Kawai, Y., et al. (2013). Recruited brown adipose tissue as an antiobesity agent in humans. *J. Clin. Invest.* 123, 3404–3408. doi: 10.1172/JCI67803

Young, J. B., and Landsberg, L. (1977). Stimulation of the sympathetic nervous system during sucrose feeding. *Nature* 269, 615–617. doi: 10.1038/269615a0

Zhang, Y., Proenca, R., Maffei, M., Barone, M., Leopold, L., and Friedman, J. M. (1994). Positional cloning of the mouse obese gene and its human homologue. *Nature* 372, 425–432. doi: 10.1038/372425a0

Conflict of Interest Statement: The authors declare that the research was conducted in the absence of any commercial or financial relationships that could be construed as a potential conflict of interest.

frontiers in Neuroscience

REVIEW
published: 30 March 2017
doi: 10.3389/fnins.2017.00162

Contribution of Autonomic Reflexes to the Hyperadrenergic State in Heart Failure

*Edgar Toschi-Dias[1,2], Maria Urbana P. B. Rondon[3], Chiara Cogliati[4], Nazareno Paolocci[5,6], Eleonora Tobaldini[2,7] and Nicola Montano[2,7]**

[1] Heart Institute (InCor) do Hospital das Clínicas da Faculdade de Medicina da Universidade de São Paulo, São Paulo, Brazil, [2] Department of Internal Medicine, Fondazione IRCCS Ca' Granda Ospedale Maggiore Policlinico, Milan, Italy, [3] School of Physical Education and Sports, University of São Paulo, São Paulo, Brazil, [4] Medicina ad Indirizzo Fisiopatologico, ASST Fatebenefratelli Sacco, Milan, Italy, [5] Division of Cardiology, Department of Medicine, Johns Hopkins Medical Institutions, Baltimore, MD, USA, [6] Dipartimento di Medicina Sperimentale, Universita' degli Studi di Perugia, Perugia, Italy, [7] Dipartimento di Dipartimento Scienze cliniche e di comunità, Università degli Studi di Milano, Milan, Italy

Heart failure (HF) is a complex syndrome representing the clinical endpoint of many cardiovascular diseases of different etiology. Given its prevalence, incidence and social impact, a better understanding of HF pathophysiology is paramount to implement more effective anti-HF therapies. Based on left ventricle (LV) performance, HF is currently classified as follows: (1) with reduced ejection fraction (HFrEF); (2) with mid-range EF (HFmrEF); and (3) with preserved EF (HFpEF). A central tenet of HFrEF pathophysiology is adrenergic hyperactivity, featuring increased sympathetic nerve discharge and a progressive loss of rhythmical sympathetic oscillations. The role of reflex mechanisms in sustaining adrenergic abnormalities during HFrEF is increasingly well appreciated and delineated. However, the same cannot be said for patients affected by HFpEF or HFmrEF, whom also present with autonomic dysfunction. Neural mechanisms of cardiovascular regulation act as "controller units," detecting and adjusting for changes in arterial blood pressure, blood volume, and arterial concentrations of oxygen, carbon dioxide and pH, as well as for humoral factors eventually released after myocardial (or other tissue) ischemia. They do so on a beat-to-beat basis. The central dynamic integration of all these afferent signals ensures homeostasis, at rest and during states of physiological or pathophysiological stress. Thus, the net result of information gathered by each controller unit is transmitted by the autonomic branch using two different codes: *intensity* and *rhythm* of sympathetic discharges. The main scope of the present article is to (i) review the key neural mechanisms involved in cardiovascular regulation; (ii) discuss how their dysfunction accounts for the hyperadrenergic state present in certain forms of HF; and (iii) summarize how sympathetic efferent traffic reveal central integration among autonomic mechanisms under physiological and pathological conditions, with a special emphasis on pathophysiological characteristics of HF.

Keywords: heart failure, autonomic nervous system, sympathetic nerve activity, cardiovascular variability

OPEN ACCESS

Edited by:
Tijana Bojić,
University of Belgrade, Serbia

Reviewed by:
Craig D. Steinback,
University of Alberta, Canada
Noah J. Marcus,
Des Moines University, USA

***Correspondence:**
Nicola Montano
nicola.montano@unimi.it

Specialty section:
This article was submitted to Autonomic Neuroscience, a section of the journal Frontiers in Neuroscience

Received: *28 October 2016*
Accepted: *13 March 2017*
Published: *30 March 2017*

Citation:
Toschi-Dias E, Rondon MUPB, Cogliati C, Paolocci N, Tobaldini E and Montano N (2017) Contribution of Autonomic Reflexes to the Hyperadrenergic State in Heart Failure. Front. Neurosci. 11:162. doi: 10.3389/fnins.2017.00162

"Most of our faculties lie dormant because they can rely upon Habit, which knows what there is to be done and has no need of their services."

Marcel Proust

INTRODUCTION

Almost all cardiovascular disease conditions eventually culminate in heart failure (HF), a complex and multifactorial syndrome that remains the main cause of morbidity and mortality worldwide (Ponikowski et al., 2016). HF stems from progressive structural and functional deterioration of the myocardium, due to chronic hemodynamic stress, whose initial trigger could be of ischemic or non-ischemic origin (Brede et al., 2002; Triposkiadis et al., 2009). Regardless of its etiology, neurohumoral activation represents a major contributor of HF pathophysiology. The neurohumoral activation arises as a compensatory response in order to adjust cardiac performance in the face of increased workload. However, persistent hemodynamic stress results in chronic release of neurohormones, particularly from sympathetic efferents and the adrenal medulla (Lymperopoulos et al., 2013), which play a major role in the progressive deterioration of cardiac function during HF (Brede et al., 2002). A hyperadrenergic state can be found in clinical conditions such as hypertension (Miyajima et al., 1991), coronary artery disease and myocardial infarction (Graham et al., 2002). As mentioned above, presence of a chronic hyperadrenergic state paves the way for HF (Notarius et al., 2007), yet also serves as a major index in the prognosis of HF (Barretto et al., 2009) and as a central therapeutic target.

Depending on the status of left ventricular (LV) performance, HF is currently classified in three clinically distinct syndromes (Ponikowski et al., 2016). Patients exhibiting signs and/or symptoms of HF that display LV ejection fraction (LVEF) <40% are categorized as HF patients with reduced ejection fraction (HFrEF) (Ponikowski et al., 2016). HF patients with preserved systolic function (LVEF >50%), but with diastolic dysfunction (LV end-diastolic volume index <97 ml/m^2) are now defined as HF patients with preserved ejection fraction (HFpEF) (Ponikowski et al., 2016; van Heerebeek and Paulus, 2016). Finally, based on more recent international guidelines on HF, a third group of HF subjects has now been identified. Those patients who display symptoms of HF with moderately reduced systolic function (LVEF between 40 and 50%) are now classified as HF with mid-range EF (HFmrEF) (Ponikowski et al., 2016).

Clinically, dyspnea and exercise intolerance are fundamental symptoms of HF. They arise at the onset of disease, and progress according to the severity of cardiac dysfunction (Ponikowski et al., 2016). Complex neuro-hormonal alterations are at the foundation of these symptoms, and act in concert with increased pulmonary venous pressure, decreased peripheral blood flow, endothelial dysfunction and skeletal muscle abnormalities (Floras and Ponikowski, 2015). It is well established that perturbed reflex mechanisms sustain sympathetic hyperactivity during HFrEF. However, substantial efforts are needed to identify changes in neural-cardiovascular regulatory pathways in HFpEF patients. Indeed, these patients also have prominent autonomic dysfunction (Verloop et al., 2015). However, little is known about the role of neural mechanisms that govern the amplitude or frequency of bursts of autonomic activity, or the pattern of active fiber discharge. Likewise, the central pathways that affect sympathetic burst generation in HFmrEF and HFpEF patients are not fully understood.

In this article, we will review and discuss old and new acquisitions on (i) the principal neural/reflex mechanisms accounting for cardiovascular homeostasis, (ii) how perturbations in these "controller units" account for the hyperadrenergic state characterizing HF; and (iii) how these mechanisms interact under physiological conditions as well as in subjects affected by HF of different categories.

HYPERADRENERGIC STATE IN HEART FAILURE

Under physiological conditions, several regulatory mechanisms work in concert in order to modulate the activity of the autonomic nervous system. By regulating heart rate, blood pressure and peripheral blood flow, the autonomic nervous system dynamically adjusts the functions of the cardiovascular system to ensure adequate levels of cardiac output will meet the perfusion and metabolic requirements of peripheral organ systems (Salman, 2016).

The past few decades have seen a growing research interest in the studying of neural mechanisms of cardiovascular regulation. This investigative attention was, and still is, justified by the recognition that these autonomic reflex controls are critical in the detection and correction of spontaneous changes in arterial blood pressure, thoracic blood volumes and pressures, humoral factors produced during myocardial ischemia and changes in arterial concentration of oxygen, carbon dioxide and pH. These reflexes are indeed essential to maintain whole-body homeostasis at rest (Salman, 2016), or during ordinary physiological events, such as, (i) changes in posture (i.e., clinostatic vs. orthostatic; Montano et al., 1994), (ii) alterations in the sleep-wake cycle (Narkiewicz et al., 1998; Tobaldini et al., 2017), (iii) in response to exercise (Negrão et al., 2001), or (iv) during emotional stress (Durocher et al., 2011).

However, during disease states affecting the cardiovascular system, the disturbance in regulatory mechanisms may cause autonomic dysfunction, in one or more of these neural/reflex mechanisms, ultimately resulting in an overall sympathetic hyperactivation and/or vagal impairment. When chronically sustained, the resulting autonomic imbalance triggers a complex "vicious cycle" that contributes to the onset of cardiovascular disease (Floras and Ponikowski, 2015).

As mentioned above, a hallmark of HF is the hyperadrenergic state, characterized by an exacerbated sympathetic nerve discharge and a progressive loss of rhythmical sympathetic oscillation (van de Borne et al., 1997; Barretto et al., 2009) (**Figure 1**). In particular, patients with HFrEF, display eccentric LV remodeling and systolic dysfunction, yet cardiac output and tissue perfusion pressures are maintained. The latter two are maintained, at least initially, by the sustained activation

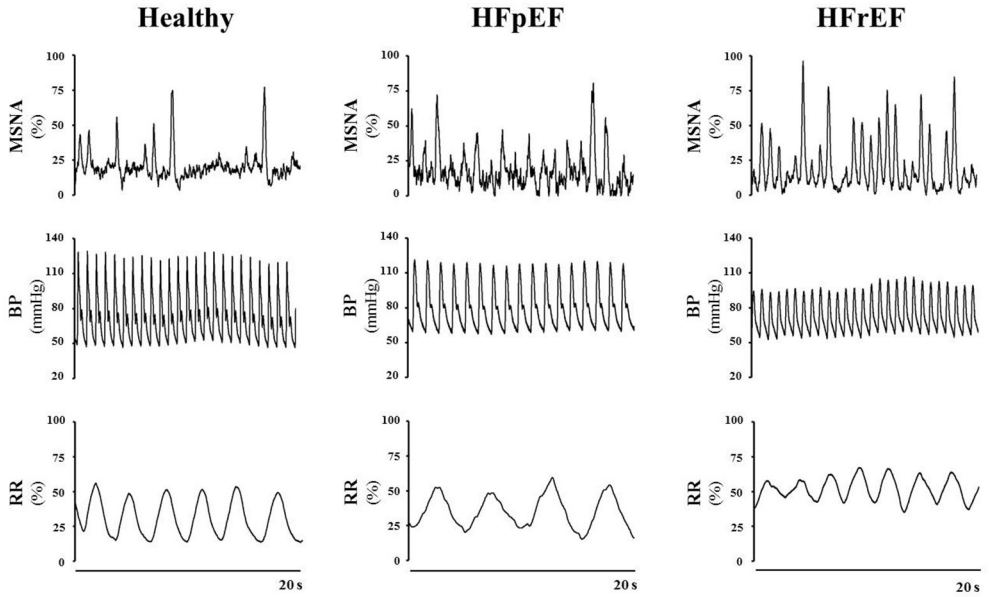

FIGURE 1 | Representative tracings of muscle sympathetic nerve activity (MSNA), blood pressure (BP) and respiration rate (RR) in a healthy subject, a patient with heart failure with preserved ejection fraction (HFpEF) and a patient with heart failure with reduced ejection fraction (HFrEF), at rest. Note the difference in the discharge patterns of the sympathetic outflow between healthy control subjects vs. HFpEF vs. HFrEF patients. Representative tracings of MSNA, BP and RR are unpublished material.

of the sympathetic nervous system (SNS) and the renin-angiotensin aldosterone system (Roig et al., 2000; Notarius et al., 2007). Conversely, HFpEF patients exhibit LV concentric hypertrophy, interstitial fibrosis and capillary rarefaction, with the main functional defect contributing to diastolic dysfunction is impaired cardiomyocyte relaxation (Paulus and Tschope, 2013). Sympathetic overdrive has been documented in these patients as well. Verloop and colleagues recently concluded that the current availability of knowledge does not permit a distinguishment on whether enhanced sympathetic activity results in HFpEF, or HFpEF results in enhanced sympathetic activity (Verloop et al., 2015). Moreover, whether patients with HFmrEF present with a hyperadrenergic state, and the eventual magnitude of this alteration, remains to be documented clinically.

Arterial Baroreflex Control

Arterial baroreflex (ABR) control is an integrated negative-feedback system whose main role is to stabilize arterial blood pressure in response to changes of circulatory homeostasis, in the short-term (Salman, 2016). Stretch-sensitive receptors located in specialized regions of the aortic arch and carotid sinus are innervated by branches of the IX and X cranial nerves. They discharge in response to an increase in arterial pressure. The central projections of baroreceptor afferents terminate primarily in the intermediate portion of the nucleus tractus solitarii (NTS) that form asymmetric (excitatory) synaptic contacts through glutamatergic receptors with caudal ventrolateral medulla (CVLM) (**Figure 2A**). In turn, CVLM efferent terminals form symmetric (inhibitory) synaptic contacts through GABAergic receptors with reticulospinal and adrenergic neurons of the rostral ventrolateral medulla (RVLM), thus inhibiting sympathetic outflow (Pilowsky and Goodchild, 2002) (**Figure 2A**). In parallel, other second-order NTS neurons form asymmetric synaptic contacts with the dorsal motor nucleus of the vagus nerve, maintaining an excitatory influence upon preganglionic parasympathetic neurons (Pilowsky and Goodchild, 2002) (**Figure 2A**).

Thus, an elevation in arterial blood pressure triggers an increase in the baroreceptor firing rate to medullary nuclei of central integration, leading to an increased discharge of vagal efferent fibers and a decreased sympathetic outflow. The physiological response of these combined effects results in bradycardia and a decrease in cardiac contractility, peripheral vascular resistance, and venous return, all acting to counter the rise in arterial blood pressure (Kirchheim, 1976; Tank et al., 2005). Conversely, a decrease in arterial blood pressure results in a reduced baroreceptor firing rate. Culminating in sympathetic excitation and parasympathetic withdrawal, thus leading to tachycardia, increased cardiac inotropy, vascular resistance, and venous return (Kirchheim, 1976; Tank et al., 2005).

During each beat, the ABR control is the main modulator of the activity of the autonomic nervous system during short-term variation of arterial pressure (Pagani and Malliani, 2000; Tank et al., 2005). Classical studies in humans and animals have clearly proved that the hyperadrenergic state of HFrEF is accompanied by blunting of ABR (Ferguson et al., 1992; Grassi et al., 2001) (**Table 1**).

As we learned before, in HFrEF patients that display eccentric remodeling and systolic dysfunction, cardiac output and tissue perfusion pressure are maintained via sustained neurohormonal

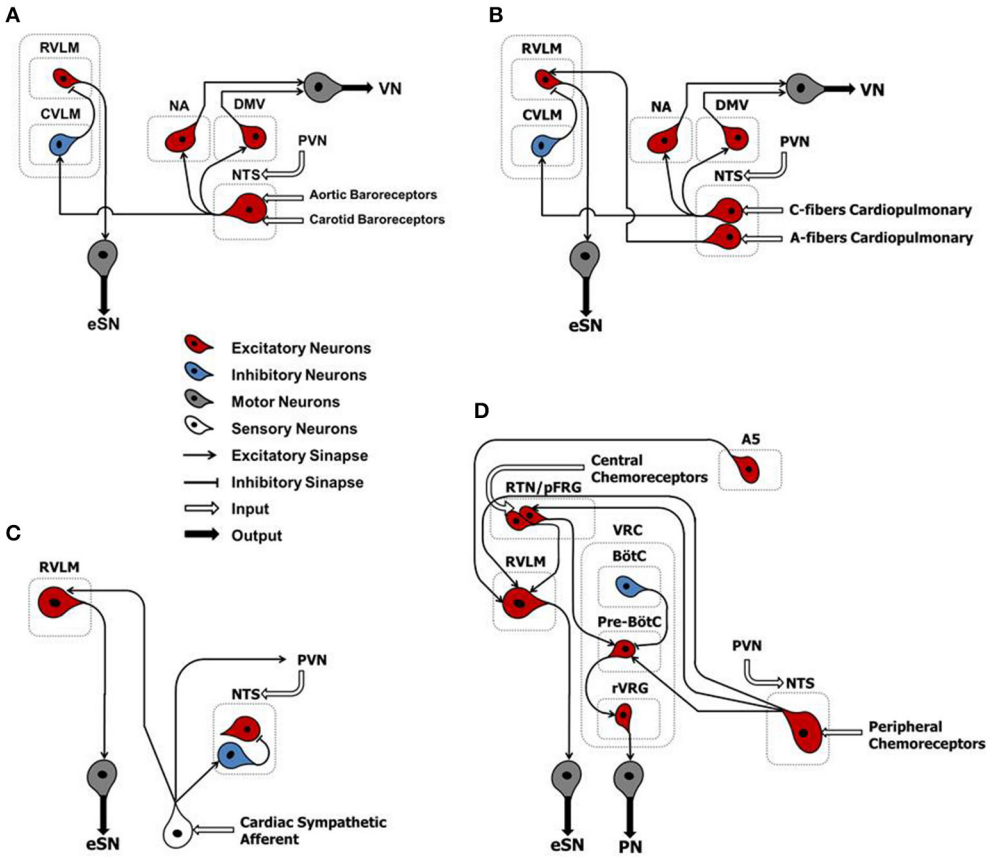

FIGURE 2 | Classical schematic diagram of arterial baroreflex control (A), cardiopulmonary reflex **(B)**, cardiac sympathetic afferent reflex **(C)**, and arterial chemoreflex **(D)**. NTS, nucleus tractus solitarii; NA, nucleus ambiguus; DMV, dorsal motor nucleus of the vagus; CVLM, caudal ventrolateral medulla; RVLM, rostral ventrolateral medulla; PVN, paraventricular nucleus of the hypothalamus; A5, noradrenergic neurons of the ventrolateral pons; RTN/pFRG, retrotrapezoid nucleus/parafacial respiratory group; VRC, ventral respiratory column; BötC, Bötzinger complex; pre-BötC, pre-Bötzinger complex; Rvrg, rostral ventral respiratory group; eSN, efferent sympathetic nerve; PN, phrenic nerve; VN, vagus nerve.

TABLE 1 | Autonomic reflex control of sympathetic nerve activity in patients with heart failure.

	HFrEF	HFpEF
Arterial Baroreflex	Blunted	–
Cardiopulmonary Reflex	Paradoxical	–
Cardiac Sympathetic Afferents Reflex	Exacerbated[a]	–
Arterial Chemoreflex	Exacerbated	Exacerbated[a]

HFrEF, heart failure with reduced ejection fraction; HFmrEF, heart failure with mid-range ejection fraction; HFpEF, heart failure with preserved ejection fraction.
[a]*Only in animal model.*

activation (Zucker et al., 2004). In the heart, chronic sympathetic activation promotes myocardial hypertrophy and vascular remodeling (Zucker et al., 2004; Floras and Ponikowski, 2015). Moreover, vascular remodeling could play an important role in the maintenance of sympathetic drive in HF, by affecting the afferent branch of ABR. In rats with ischemia-induced HF, the gain of afferent aortic depressor nerve is reduced (Rondon et al., 2006). Thus, arterial stiffness could impair the mechanical transduction of baroreceptors, therefore affecting afferent traffic.

No studies, to our knowledge, have directly examined the impact of ABR control on sympathetic nerve activity in patients with HFpEF and HFmrEF (**Table 1**). However, data from an experimental study suggest that baroreflex dysfunction of heart rate is associated with cardiac diastolic dysfunction in rats, independent of other present risk factors (Mostarda et al., 2011). Moreover, patients with HFpEF are generally older, more often female, and have a high prevalence of comorbidities, such as chronic hypertension, obesity, metabolic syndrome and type 2 diabetes mellitus (Paulus and Tschope, 2013; van Heerebeek and Paulus, 2016). All these conditions have been associated, in part, with baroreflex dysfunction (Matsukawa et al., 1991, 1994; Trombetta et al., 2010; Holwerda et al., 2016). In particular, an association exists between hypertension and vascular injury (Dao et al., 2005), affecting the elastic properties of the large vessels (Humphrey et al., 2016; Smulyan et al., 2016). This, in turn, could impact the efficiency of ABR control in patients with HFpEF. Therefore, myocardial remodeling and arterial stiffness can affect ABR arc function through different pathophysiological mechanisms, leading to sympathetic hyperactivation both in HFrEF and HFpEF patients.

Cardiopulmonary Reflex

The cardiopulmonary reflex arc is liable for detecting filling pressure in low-pressure cardiac chambers. In doing so, it contributes to the control of volemic conditions through the interaction between negative- and positive-feedback mechanisms (Salman, 2016). Several receptor subtypes, located in the heart and lungs, contribute to this reflex arc. They are mechano-sensitive and closely linked to neuronal pathways via overlapping brainstem networks. Whereas, most of these receptors are innervated by unmyelinated afferents of the vagus nerve (Type C) and are activated at higher intensities, a smaller portion is made of myelinated fibers of the vagus nerve (Type A) and are activated at lower intensities (Salman, 2016). Cardiopulmonary vagal afferents are mainly involved in neurohumoral regulation of systemic blood volume. When stimulated, they convey information to medullary nuclei of central integration (i.e., NTS) that form a trisynaptic intramedullary pathway similar to that described for the ABR (Salman, 2016) (**Figure 2B**).

Firstly, fluctuations of lower intensities activate sensory afferent fibers (Type A) located in the walls of the atria and in the atrial-caval junction, determining tachycardia through sympathetic activation. Atrial stretch results in the release of atrial natriuretic peptide by atrial myocytes, which act to increase renal blood flow and Na^+ diuresis, reducing volume and keeping cardiac output relatively constant during the increase of venous return (Salman, 2016). In stark contrast, fluctuations of higher intensities activate Type C sensory afferent fibers located in cardiac chambers, strengthening and enhancing the action of ABR by means of similar negative-feedback mechanisms. However, during hypovolemia, the neurohormonal response acts to reduce heart rate (bradycardia) and urinary volume in order to correct the initial drop in venous return (Salman, 2016).

In 1990, Seals and colleagues observed that during controlled tidal breathing (30% of inspiratory capacity at 12 breath/min), approximately 65% of the sympathetic bursts occur during the expiratory phase, suggesting an influence of breathing on sympathetic outflow (Seals et al., 1990). In turn, increasing the depth of breathing (e.g., 70% of inspiratory capacity at 12 breath/min) has great influence on the within-breath modulation of muscle sympathetic nerve activity (MSNA), producing near complete sympathoinhibition from onset-mid inspiration to early-mid expiration (Seals et al., 1990).

The effects of cardiopulmonary reflex activation and deactivation on sympathetic outflow has been evaluated in humans via MSNA recording during lower body negative/positive pressures. Previously demonstrated, deactivation of cardiopulmonary reflex during application of non-hypotensive lower body negative pressure (LBNP) showed an increase in the sympathetic efferent traffic in healthy subjects (Millar et al., 2015). Conversely, activation of cardiopulmonary reflex during application of non-hypertensive lower body positive pressure (LBPP) was associated with a decrease in sympathetic activity in healthy subjects (Millar et al., 2015).

Alterations of the autonomic neural reflex responses due to changes in cardiopulmonary loading conditions have been well documented in HFrEF patients (Azevedo et al., 2000; Floras and Ponikowski, 2015). Recently, Millar and colleagues reported that despite a preserved response of MSNA during deactivation of the cardiopulmonary reflex arc, non-hypertensive LBPP does not change the burst frequency of sympathetic outflow in patients with HFrEF (Millar et al., 2015). This paradoxical sympathetic activation in response to increasing filling pressure suggests that cardiopulmonary reflex contributes to the complex generation of autonomic dysregulation of HFrEF. Similar evidence in HFpEF and HFmrEF patients is lacking (**Table 1**).

Cardiac Sympathetic Afferent Reflex

The cardiac sympathetic afferent reflex (CSAR) is a positive feedback mechanism involved in the central transmission of nociceptive information from the heart (Chen et al., 2015). The receptors of this reflex arc are the cardiac sympathetic afferent endings that innervate the superficial epicardial layers of the ventricles. Although the exact neural pathways of CSAR are not yet well understood, there is a growing consensus of opinion that the central projections of sympathetic afferents located in the dorsal root ganglia of the C8–T9 spinal segments (especially T2–T6) form excitatory synapses in the hypothalamic paraventricular nucleus (PVN), NTS and RVLM. These stations in turn centrally process the peripheral information and, when stimulated, induce an increase in sympathetic outflow (Chen et al., 2015) (**Figure 2C**). Thus, mechanical distension of the ventricles and/or endogenous humoral factors produced in myocardium during myocardial ischemia, such as bradykinin, adenosine and reactive oxygen species (ROS), can stimulate cardiac sympathetic afferents, thereby increasing the sympathetic outflow directed to the heart, arteries and kidneys (Chen et al., 2015). All these mechanisms take part in the excessive sympathetic outflow that characterizes HF (Malliani and Montano, 2002; Zhu et al., 2004; Wang et al., 2014) (**Table 1**). Furthermore, once overtly dilated, the heart tends to utilize more oxygen, owing to increased cardiac wall tension. This need renders the heart more prone to "relative ischemia," a functional feature often observed in HF patients. In turn, this condition is accompanied by the release of endogenous substances such as bradykinin and adenosine that stimulate the ventricular sympathetic afferents endings, resulting in increased sympathetic outflow due to positive feedback mechanism. Furthermore, chronic myocardial stretch due to volume overload can cause an upregulation of the kallikrein-kinin system, followed by an increase in bradykinin content in the interstitial fluid that ultimately mediates mast cell infiltration and extracellular matrix loss (Wei et al., 2012).

In a clinical context, it is well known that patients with acute decompensated HF are very sensitive to volume overload because they have volume intolerance, regardless of the magnitude of residual LVEF. Moreover, during acute decompensated HF and pulmonary congestion, both arterial pressure and heart rate are frequently more elevated (De Luca et al., 2007). It is still unclear how the positive feedback mechanism mediated by CSAR would eventually prevail over the negative one mediated by the vagal afferents. However, there is an attractive corollary hypothesis to consider (Malliani and Montano, 2002). For example, afferent vagal fibers from the atria normally display a burst of impulses per cardiac cycle. In the case of Type A

receptors, this event occurs in coincidence with atrial systole (Paintal, 1971). In central structures, rhythmic afferent bursts can prompt a sequence of excitatory and inhibitory postsynaptic potentials (Spyer, 1982). During volume loading, Type A atrial vagal receptors also discharge during diastole (Recordati et al., 1976), and this more continuous firing may blunt the capability of generating inhibitory postsynaptic potentials in the central circuitry. Similar changes in firing patterns may characterize the majority of vagal cardiopulmonary receptors, thus explaining their reduced efficacy in exerting an efficient reflex restraint on the sympathetic outflow (Malliani and Montano, 2002). Conversely, under normal conditions, sympathetic afferent fibers do not display bursts of impulses. Rather, at most, they exhibit a more sparse and spontaneous activity with one action potential per cardiac cycle (Malliani, 1982). Thus, independent of its rhythmic relationship with the cardiac cycle, an increased afferent sympathetic barrage would retain its capability of exciting the sympathetic outflow (Malliani and Montano, 2002).

Arterial Chemoreflex

In response to environmental challenges, the maintenance of homeostasis depends also on the integration between neural mechanisms that adjust arterial levels of oxygen (O_2), carbon dioxide (CO_2) and potential of hydrogen (pH). To this end, the arterial chemoreflex control comprises *central chemoreceptors* in the brainstem that respond to hypercapnia and respiratory acidosis; and *peripheral chemoreceptors* in the carotid bodies (located near the internal carotid arteries) that respond primarily to hypoxia (Guyenet, 2000; Barnett et al., 2017).

During hypercapnia and respiratory acidosis, chemosensitive neurons located in retrotrapezoid nucleus/parafacial respiratory group (RTN/pFRG) are stimulated, sending excitatory inputs to the pre-sympathetic neurons of the RVLM that form excitatory synaptic contacts with noradrenergic neurons (A5 group) in the ventrolateral pons (Barnett et al., 2017) (**Figure 2D**). In parallel, second-order neurons of RTN/pFRG send excitatory inputs to the pre-Bötzinger complex–a cluster of neurons responsible for generating the breathing rhythm located in the ventral respiratory column (VRC). Here, they form excitatory synaptic contacts with the rostral ventral respiratory group (rVRG) and project to motor neurons that give rise to the phrenic nerve (Barnett et al., 2017) (**Figure 2D**).

During hypoxia, the central projections of peripheral chemoreceptor afferents (cranial nerve IX) terminate primarily in the commissural portion of the NTS that, by means of second-order neurons, then form excitatory synapses with RVLM, RTN/pFRG and the pre-Bötzinger complex (Guyenet, 2000; Barnett et al., 2017) (**Figure 2D**).

Therefore, the stimulation of chemoreflex by hypoxia and/or hypercapnia induces a simultaneous increase of sympathetic outflow and ventilation, thus optimizing tissue perfusion and blood gas uptake/delivery (Guyenet, 2000; Barnett et al., 2017) (**Figure 2D**).

In HFrEF, reduction in organ perfusion due to reduced cardiac output, promotes changes in oxygen delivery, thereby impairing peripheral chemoreflex function in HFrEF patients. In turn, chemoreflex dysfunction contributes to sympathetic hyperactivity, hyperventilation and the associated breathing instability typically found in HFrEF subjects (Schultz et al., 2015). Accordingly, Di Vanna and collaborators demonstrated that the activity of muscle sympathetic nerves in response to central and peripheral chemoreceptor stimulation is exacerbated in patients with HFrEF (Di Vanna et al., 2007) (**Table 1**).

In addition, it has been postulated that oxidative stress (i.e., increased ROS emission mainly from enhanced NADPH oxidase activity) is also central in activating chemoreceptors of the carotid bodies (Morgan et al., 2016). Oxidative stress is known to activate the carotid body in HF (Schultz et al., 2015). We now know that both circulating and local tissue levels of the pro-oxidant angiotensin II peptide are elevated in HF (Li et al., 2006). Angiotensin II activates NADPH oxidase to enhance superoxide production, which in turn enhances the excitability of the carotid body glomus cells and central autonomic neurons via the AT1 receptor (Li et al., 2007). The angiotensin II-superoxide pathway augments the sensitivity of the carotid body chemoreceptors, at least in part, by inhibiting oxygen-sensitive potassium channels in the carotid body glomus cells (Schultz et al., 2015).

Regardless of the low cardiac output, diverse comorbidities such as hypertension (Touyz, 2004), diabetes (Henriksen et al., 2011), and obstructive sleep apnea (Lavie, 2015) are associated with increased oxidative stress that may lead to carotid body chemoreceptor dysfunction. These comorbidities are frequent in patients with HFpEF or HFmrEF, thus suggesting the presence of chemoreflex dysfunction in these patients. In fact, Toledo and colleagues recently reported that the central chemoreflex is enhanced in HFpEF (Toledo et al., 2017). These authors observed that the activation of the central chemoreflex pathway by hypercapnia exacerbates sympatho-vagal imbalance in HFpEF rats, and that sympathetic blockade with propranolol attenuates the response of cardiac sympathetic modulation. In addition, these authors showed that neuronal activation in the RVLM was increased in HFpEF rats compared with sham rats (Toledo et al., 2017). However, further studies are needed to better understand the mechanistic intricacies of these new findings.

Further to this, to the best of our knowledge, there are no studies testing sympathetic nerve activity in response to chemoreceptor stimulation in patients with HFpEF or HFmrEF.

Central Integration of Autonomic Reflexes

Autonomic reflexes are considered as distinct controllers units. However, multiple sites of interaction among these reflex arcs have been documented (Du and Chen, 2006; Chen et al., 2015). They are outlined in **Figure 3**. NTS is the first synaptic station of the afferents in the central nervous system. It plays a pivotal role in the modulation of the autonomic efferent activity directed to the cardiovascular system (Machado et al., 1997). In order to produce a proper autonomic response, information from several relay stations must be processed at the NTS level, where all the projections of many and complex neural networks are then organized in different hierarchical levels (Smith et al., 2009; Chen et al., 2015). For instance, activation of CSAR depresses ABR and enhances the arterial chemoreflex via central integration (Du and Chen, 2006; Chen et al., 2015) (**Figure 3A**). The afferent pathways of these

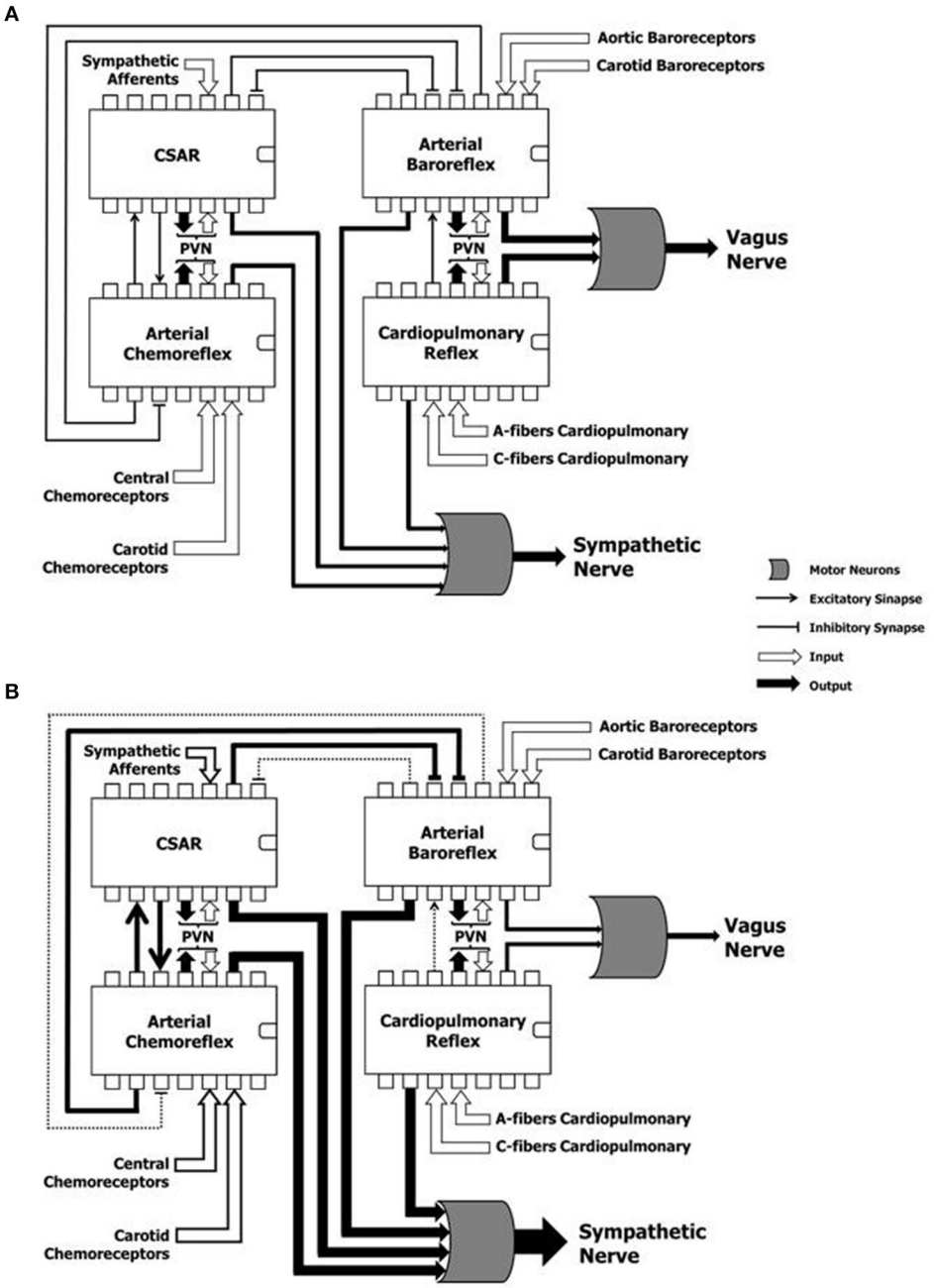

FIGURE 3 | Hypothetical representation of the reflex mechanisms considered as "controller units," and their complex and dynamic interaction in a physiological condition (A) and during heart failure **(B)**. CSAR, cardiac sympathetic afferents reflex; PVN, paraventricular nucleus of the hypothalamus; SN, sympathetic nerve; VN, vagus nerve. Note that the sustained hyperadrenergic state in patients with HF occurs due to the predominance of inputs of excitatory mechanisms on inhibitory mechanisms.

reflex mechanisms project to the NTS, and numerous lines of investigation attests that baroreflex dysfunction of the MSNA is the consequence of and not the cause of the reflex sympathetic excitation seen in HF patients (Du and Chen, 2006; Despas et al., 2012) (**Figure 3B**). In this regard, an experimental study showed that electrical stimulation of the central end of the left cardiac sympathetic nerve blunts ABR sensitivity by 42% (**Figure 3A**), and this effect is abolished after intracerebroventricular injection of losartan (Gao et al., 2004). This evidence suggests that stimulation of cardiac sympathetic afferents reduces ABR sensitivity via central AT1 receptors (Gao et al., 2004).

AngII is expressed in the NTS, and one of the signaling mechanisms by which AT1 receptors influence the NTS neurons

involves the production of ROS by NADPH oxidase. NADPH oxidase activation in turn enhances voltage-gated L-type Ca^{2+} currents in the medial NTS neurons, thereby contributing to the deleterious effects exerted by AngII in the cardiovascular system (Wang et al., 2004, 2006). As such, we cannot rule out a priori that AngII, via the AT1 receptor, plays a pivotal role in both inhibitory and excitatory reflexes in the central nervous system during HF. Accordingly, the augmented cardiac sympathetic afferent input can contribute to the exacerbated chemoreflex function in HF in a AT1 receptor-dependent manner in the NTS (Wang et al., 2008). Indeed, AT1 receptors in the NTS are upregulated, and blockade of these receptors normalized the exaggerated response of the chemoreflex/CSAR in HF (Wang et al., 2008).

In another study, Gan and colleagues observed that the CSAR is enhanced not only in HF rats, but also in rats with HF harboring bilateral vagotomy and ABR denervation (Gan et al., 2011). However, vagotomy and baroreceptor denervation augmented basal and AngII-stimulated CSAR response in the PVN (Gan et al., 2011). This study revealed that the activity of arterial baroreceptor and vagal afferents inhibit the CSAR (**Figure 3B**), while enhancing the CSAR discharge in response to AngII in the PVN of HF rats (Gan et al., 2011).

When the interaction between the chemoreflex and ABR is concerned (**Figure 3A**), we know that isocapnic hyperventilation (i.e., ventilation > 35 l/min at 15 breath/min) stimulates the chemoreflex and blunts ABR gain (van de Borne et al., 2000). On the other hand, the cardiovascular effect of chemoreflex stimulation also encompasses a rise in arterial blood pressure, which in turn, stimulates the arterial baroreceptors, while blunting the chemoreflex response (Somers et al., 1991) (**Figure 3A**).

Interestingly, Despas and colleagues have shown that elevated chemosensitivity attenuated ABR control of sympathetic nerve activity, and that deactivation of carotid chemoreceptors increased the ABR gain in patients with HFrEF (Despas et al., 2012) (**Figure 3B**). Together, this evidence suggests that the chemoreflex-related rise in sympathetic activity is not only mediated by an oxygen sensing mechanism, but also indirectly (i.e., through the involvement of ABR in patients with HFrEF; Despas et al., 2012). In stark contrast, the central integration among autonomic reflexes in patients with HFpEF and HFmrEF remains to be decodified.

QUESTIONS TO PONDER FOR FUTURE STUDIES

The relevance of the role and the modalities by which altered autonomic reflexes contribute to sympathetic hyperactivation in HFrEF are becoming increasingly clear. In contrast, little knowledge is currently available regarding this aspect in subjects with HFpEF or HFmrEF. Therefore, the new HF classification is likely to bring to the table additional, important questions concerning the role of autonomic control/reflexes in HF onset and progression. Notwithstanding, there are still major, general questions that pertain to the role of autonomic reflexes in HF pathophysiology, irrespective of its etiology or clinical classification. First and foremost, it is still unknown what is the cutoff and saturation point of the autonomic nervous system in the effector organ. As mentioned earlier, the information emanating from the central integration of many reflex mechanisms is transmitted by the autonomic fibers using *intensity* and *rhythm* of firing as codes. Importantly, certain clinical conditions can lead to the collapse of the autonomic nervous system and to the loss of rhythmicity of cardiovascular variability (Montano et al., 2009). Due to random distribution of spikes during time, the sympathetic afferent can be expressed in terms of phasic and tonic activities, thus reflecting the dynamic integration of the reflex mechanisms controlling cardiovascular functions. The tonic and phasic activities of cardiovascular variabilities are coupled and synchronized in healthy individuals. However, HFrEF patients with NYHA functional classes III and/or IV can have a paradoxical pattern of sympathetic outflow, with a marked increase in tonus in the absence of low frequency oscillations, not only in heart rate variability, but also in sympathetic nerve variability (van de Borne et al., 1997). Thus, the interpretation of oscillatory patterns of sympathetic activity, together with the analysis of heart rate and arterial pressure variability's, could shed new light on the saturation of the autonomic nervous system; not only in HFrEF patients, but also in those suffering from HFpEF or HFmrEF patients. Another aspect that warrants further investigation is the interpretation of both codes. More specifically, an additional approach should be envisioned to obtain a distinctive profile of autonomic nervous control on the effector organ (autonomic modulation), or put differently, on the ability of autonomic nervous system to induce variations (i.e., heart rate and/or arterial pressure). The clinical significance of this ability is not yet completely understood, but it appears to have clinically relevant implications. In contrast to HFrEF, no clinical trials have documented an effective treatment for patients with HFmrEF and/or HFpEF. Therefore, due to the new classifications of HF, revisiting the autonomic reflexes and hyperadrenergic state in these new categories of HF patients could certainly offer new angles into the exploration of autonomic nervous system and therapeutic perspectives for these patients.

AUTHOR CONTRIBUTIONS

All authors contributed to the preparation, revision and approval of the final manuscript.

ACKNOWLEDGMENTS

The authors are very grateful to Dr. Stephen P. Chelko for careful editing of the manuscript. ETD is supported by Fundação de Amparo à Pesquisa do Estado de São Paulo (FAPESP # 2013/07651-7 and # 2015/17642-0). MR is supported by Conselho Nacional de Desenvolvimento Científico e Tecnológico (CNPq # 309821/2014-2). NM is supported by an Italian Space Agency Grant.

REFERENCES

Azevedo, E. R., Newton, G. E., Floras, J. S., and Parker, J. D. (2000). Reducing cardiac filling pressure lowers norepinephrine spillover in patients with chronic heart failure. *Circulation* 101, 2053–2059. doi: 10.1161/01.CIR.101.17.2053

Barnett, W. H., Abdala, A. P., Paton, J. F., Rybak, I. A., Zoccal, D. B., and Molkov, Y. I. (2017). Chemoreception and neuroplasticity in respiratory circuits. *Exp. Neurol.* 287, 153–164. doi: 10.1016/j.expneurol.2016.05.036

Barretto, A. C., Santos, A. C., Munhoz, R., Rondon, M. U., Franco, F. G., Trombetta, I. C., et al. (2009). Increased muscle sympathetic nerve activity predicts mortality in heart failure patients. *Int. J. Cardiol.* 135, 302–307. doi: 10.1016/j.ijcard.2008.03.056

Brede, M., Wiesmann, F., Jahns, R., Hadamek, K., Arnolt, C., Neubauer, S., et al. (2002). Feedback inhibition of catecholamine release by two different α_2-adrenoceptor subtypes prevents progression of heart failure. *Circulation* 106, 2491–2496. doi: 10.1161/01.CIR.0000036600.39600.66

Chen, W. W., Xiong, X. Q., Chen, Q., Li, Y. H., Kang, Y. M., and Zhu, G. Q. (2015). Cardiac sympathetic afferent reflex and its implications for sympathetic activation in chronic heart failure and hypertension. *Acta Physiol. (Oxf).* 213, 778–794. doi: 10.1111/apha.12447

Dao, H. H., Essalihi, R., Bouvet, C., and Moreau, P. (2005). Evolution and modulation of age-related medial elastocalcinosis: impact on large artery stiffness and isolated systolic hypertension. *Cardiovasc. Res.* 66, 307–317. doi: 10.1016/j.cardiores.2005.01.012

De Luca, L., Fonarow, G. C., Adams, K. F. Jr., Mebazaa, A., Tavazzi, L., Swedberg, K., et al. (2007). Acute heart failure syndromes: clinical scenarios and pathophysiologic targets for therapy. *Heart Fail. Rev.* 12, 97–104. doi: 10.1007/s10741-007-9011-8

Despas, F., Lambert, E., Vaccaro, A., Labrunee, M., Franchitto, N., Lebrin, M., Galinier, M., Senard, J. M., et al. (2012). Peripheral chemoreflex activation contributes to sympathetic baroreflex impairment in chronic heart failure. *J. Hypertens.* 30, 753–760. doi: 10.1097/HJH.0b013e328350136c

Di Vanna, A., Braga, A. M., Laterza, M. C., Ueno, L. M., Rondon, M. U., Barretto, A. C., et al. (2007). Blunted muscle vasodilatation during chemoreceptor stimulation in patients with heart failure. *Am. J. Physiol. Heart Circ. Physiol.* 293, H846–H852. doi: 10.1152/ajpheart.00156.2007

Du, Y. H., and Chen, A. F. (2006). A "love triangle" elicited by electrochemistry: complex interactions among cardiac sympathetic afferent, chemo-, and baroreflexes. *J. Appl. Physiol.* 102, 9–10. doi: 10.1152/japplphysiol.01032.2006

Durocher, J. J., Klein, J. C., and Carter, J. R. (2011). Attenuation of sympathetic baroreflex sensitivity during the onset of acute mental stress in humans. *Am. J. Physiol. Heart Circ. Physiol.* 300, H1788–H1793. doi: 10.1152/ajpheart.00942.2010

Ferguson, D. W., Berg, W. J., Roach, P. J., Oren, R. M., and Mark, A. L. (1992). Effects of heart failure on baroreflex control of sympathetic neural activity. *Am. J. Cardiol.* 69, 523–531. doi: 10.1016/0002-9149(92)90998-E

Floras, J. S., and Ponikowski, P. (2015). The sympathetic/parasympathetic imbalance in heart failure with reduced ejection fraction. *Eur. Heart J.* 36, 1974–1982b. doi: 10.1093/eurheartj/ehv087

Gan, X. B., Duan, Y. C., Xiong, X. Q., Li, P., Cui, B. P., Gao, X. Y., et al. (2011). Inhibition of cardiac sympathetic afferent reflex and sympathetic activity by baroreceptor and vagal afferent inputs in chronic heart failure. *PLoS ONE* 6:e25784. doi: 10.1371/journal.pone.0025784

Gao, L., Zhu, Z., Zucker, I. H., and Wang, W. (2004). Cardiac sympathetic afferent stimulation impairs baroreflex control of renal sympathetic nerve activity in rats. *Am. J. Physiol. Heart Circ. Physiol.* 286, H1706–H1711. doi: 10.1152/ajpheart.01097.2003

Graham, L. N., Smith, P. A., Stoker, J. B., Mackintosh, A. F., and Mary, D. A. (2002). Time course of sympathetic neural hyperactivity after uncomplicated acute myocardial infarction. *Circulation* 106, 793–797. doi: 10.1161/01.CIR.0000025610.14665.21

Grassi, G., Seravalle, G., Bertinieri, G., Turri, C., Stella, M. L., Scopelliti, F., et al. (2001). Sympathetic and reflex abnormalities in heart failure secondary to ischaemic or idiopathic dilated cardiomyopathy. *Clin. Sci.* 101, 141–146. doi: 10.1042/cs1010141

Guyenet, P. G. (2000). Neural structures that mediate sympathoexcitation during hypoxia. *Respir. Physiol.* 121, 147–162. doi: 10.1016/S0034-5687(00)00125-0

Henriksen, E. J., Diamond-Stanic, M. K., and Marchionne, E. M. (2011). Oxidative stress and the etiology of insulin resistance and type 2 diabetes. *Free Radic. Biol. Med.* 51, 993–999. doi: 10.1016/j.freeradbiomed.2010.12.005

Holwerda, S. W., Vianna, L. C., Restaino, R. M., Chaudhary, K., Young, C. N., and Fadel, P. J. (2016). Arterial baroreflex control of sympathetic nerve activity and heart rate in patients with type 2 diabetes. *Am. J. Physiol. Heart Circ. Physiol.* 311, H1170–H1179. doi: 10.1152/ajpheart.00384.2016

Humphrey, J. D., Harrison, D. G., Figueroa, C. A., Lacolley, P., and Laurent, S. (2016). Central artery stiffness in hypertension and aging: a problem with cause and consequence. *Circ. Res.* 118, 379–381. doi: 10.1161/CIRCRESAHA.115.307722

Kirchheim, H. R. (1976). Systemic arterial baroreceptor reflexes. *Physiol. Rev.* 56, 100–177.

Lavie, L. (2015). Oxidative stress in obstructive sleep apnea and intermittent hypoxia-revisited-the bad ugly and good: implications to the heart and brain. *Sleep Med. Rev.* 20, 27–45. doi: 10.1016/j.smrv.2014.07.003

Li, Y. L., Gao, L., Zucker, I. H., and Schultz, H. D. (2007). NADPH oxidase-derived superoxide anion mediates angiotensin II-enhanced carotid body chemoreceptor sensitivity in heart failure rabbits. *Cardiovasc. Res.* 75, 546–554. doi: 10.1016/j.cardiores.2007.04.006

Li, Y. L., Xia, X. H., Zheng, H., Gao, L., Li, Y. F., Liu, D., et al. (2006). Angiotensin II enhances carotid body chemoreflex control of sympathetic outflow in chronic heart failure rabbits. *Cardiovasc. Res.* 71, 129–138. doi: 10.1016/j.cardiores.2006.03.017

Lymperopoulos, A., Rengo, G., and Koch, W. J. (2013). Adrenergic nervous system in heart failure: pathophysiology and therapy. *Circ. Res.* 113, 739–753. doi: 10.1161/CIRCRESAHA.113.300308

Machado, B. H., Mauad, H., Chianca Junior, D. A., Haibara, A. S., and Colombari, E. (1997). Autonomic processing of the cardiovascular reflexes in the nucleus tractus solitarii. *Braz. J. Med. Biol. Res.* 30, 533–543. doi: 10.1590/S0100-879X1997000400015

Malliani, A. (1982). Cardiovascular sympathetic afferent fibers. *Rev. Physiol. Biochem. Pharmacol.* 94, 11–74. doi: 10.1007/bfb0031332

Malliani, A., and Montano, N. (2002). Emerging excitatory role of cardiovascular sympathetic afferents in pathophysiological conditions. *Hypertension* 39, 63–68. doi: 10.1161/hy0102.099200

Matsukawa, T., Gotoh, E., Hasegawa, O., Shionoiri, H., Tochikubo, O., and Ishii, M. (1991). Reduced baroreflex changes in muscle sympathetic nerve activity during blood pressure elevation in essential hypertension. *J. Hypertens.* 9, 537–542. doi: 10.1097/00004872-199106000-00009

Matsukawa, T., Sugiyama, Y., Iwase, S., and Mano, T. (1994). Effects of aging on the arterial baroreflex control of muscle sympathetic nerve activity in healthy subjects. *Environ. Med.* 38, 81–84.

Millar, P. J., Murai, H., and Floras, J. S. (2015). Paradoxical muscle sympathetic reflex activation in human heart failure. *Circulation* 131, 459–468. doi: 10.1161/CIRCULATIONAHA.114.010765

Miyajima, E., Yamada, Y., Yoshida, Y., Matsukawa, T., Shionoiri, H., Tochikubo, O., et al. (1991). Muscle sympathetic nerve activity in renovascular hypertension and primary aldosteronism. *Hypertension* 17, 1057–1062. doi: 10.1161/01.HYP.17.6.1057

Montano, N., Furlan, R., Guzzetti, S., McAllen, R. M., and Julien, C. (2009). Analysis of sympathetic neural discharge in rats and humans. *Philos. Trans. A Math. Phys. Eng. Sci.* 367, 1265–1282. doi: 10.1098/rsta.2008.0285

Montano, N., Ruscone, T. G., Porta, A., Lombardi, F., Pagani, M., and Malliani, A. (1994). Power spectrum analysis of heart rate variability to assess the changes in sympathovagal balance during graded orthostatic tilt. *Circulation* 90, 1826–1831. doi: 10.1161/01.CIR.90.4.1826

Morgan, B. J., Bates, M. L., Rio, R. D., Wang, Z., and Dopp, J. M. (2016). Oxidative stress augments chemoreflex sensitivity in rats exposed to chronic intermittent hypoxia. *Respir. Physiol. Neurobiol.* 234, 47–59. doi: 10.1016/j.resp.2016.09.001

Mostarda, C., Moraes-Silva, I. C., Moreira, E. D., Medeiros, A., Piratello, A. C., Consolim-Colombo, F. M., et al. (2011). Baroreflex sensitivity impairment is associated with cardiac diastolic dysfunction in rats. *J. Card. Fail.* 17, 519–525. doi: 10.1016/j.cardfail.2011.02.007

Narkiewicz, K., Montano, N., Cogliati, C., van de Borne, P. J., Dyken, M. E., and Somers, V. K. (1998). Altered cardiovascular variability in obstructive sleep apnea. *Circulation* 98, 1071–1077. doi: 10.1161/01.CIR.98.11.1071

Negrão, C. E., Rondon, M. U., Tinucci, T., Alves, M. J., Roveda, F., Braga, A. M., et al. (2001). Abnormal neurovascular control during exercise is linked to heart failure severity. *Am. J. Physiol. Heart Circ. Physiol.* 280, H1286–H1292.

Notarius, C. F., Spaak, J., Morris, B. L., and Floras, J. S. (2007). Comparison of muscle sympathetic activity in ischemic and nonischemic heart failure. *J. Card. Fail.* 13, 470–475. doi: 10.1016/j.cardfail.2007.03.014

Pagani, M., and Malliani, A. (2000). Interpreting oscillations of muscle sympathetic nerve activity and heart rate variability. *J. Hypertens.* 18, 1709–1719. doi: 10.1097/00004872-200018120-00002

Paintal, A. S. (1971). Action of drugs on sensory nerve endings. *Annu. Rev. Pharmacol.* 11, 231–240. doi: 10.1146/annurev.pa.11.040171.001311

Paulus, W. J., and Tschope, C. (2013). A novel paradigm for heart failure with preserved ejection fraction: comorbidities drive myocardial dysfunction and remodeling through coronary microvascular endothelial inflammation. *J. Am. Coll. Cardiol.* 62, 263–271. doi: 10.1016/j.jacc.2013.02.092

Pilowsky, P. M., and Goodchild, A. K. (2002). Baroreceptor reflex pathways and neurotransmitters: 10 years on. *J. Hypertens.* 20, 1675–1688. doi: 10.1097/00004872-200209000-00002

Ponikowski, P., Voors, A. A., Anker, S. D., Bueno, H., Cleland, J. G., Coats, A. J., et al. (2016). 2016 ESC Guidelines for the diagnosis and treatment of acute and chronic heart failure: the Task Force for the diagnosis and treatment of acute and chronic heart failure of the European Society of Cardiology (ESC). Developed with the special contribution of the Heart Failure Association (HFA) of the ESC. *Eur. J. Heart Fail.* 18, 891–975. doi: 10.1002/ejhf.592

Recordati, G., Lombardi, F., Bishop, V. S., and Malliani, A. (1976). Mechanical stimuli exciting type A atrial vagal receptors in the cat. *Circ. Res.* 38, 397–403. doi: 10.1161/01.RES.38.5.397

Roig, E., Perez-Villa, F., Morales, M., Jiménez, W., Orús, J., Heras, M., et al. (2000). Clinical implications of increased plasma angiotensin II despite ACE inhibitor therapy in patients with congestive heart failure. *Eur. Heart J.* 21, 53–57. doi: 10.1053/euhj.1999.1740

Rondon, E., Brasileiro-Santos, M. S., Moreira, E. D., Rondon, M. U., Mattos, K. C., Coelho, M. A., et al. (2006). Exercise training improves aortic depressor nerve sensitivity in rats with ischemia-induced heart failure. *Am. J. Physiol. Heart Circ. Physiol.* 291, H2801–H2806. doi: 10.1152/ajpheart.01352.2005

Salman, I. M. (2016). Major autonomic neuroregulatory pathways underlying short- and long-term control of cardiovascular function. *Curr. Hypertens. Rep.* 18, 18. doi: 10.1007/s11906-016-0625-x

Schultz, H. D., Marcus, N. J., and Del Rio, R. (2015). Mechanisms of carotid body chemoreflex dysfunction during heart failure. *Exp. Physiol.* 100, 124–129. doi: 10.1113/expphysiol.2014.079517

Seals, D. R., Suwarno, N. O., and Dempsey, J. A. (1990). Influence of lung volume on sympathetic nerve discharge in normal humans. *Circ. Res.* 67, 130–141. doi: 10.1161/01.RES.67.1.130

Smith, J. C., Abdala, A. P., Rybak, I. A., and Paton, J. F. (2009). Structural and functional architecture of respiratory networks in the mammalian brainstem. *Philos. Trans. R. Soc. Lond. B Biol. Sci.* 364, 2577–2587. doi: 10.1098/rstb.2009.0081

Smulyan, H., Mookherjee, S., and Safar, M. E. (2016). The two faces of hypertension: role of aortic stiffness. *J. Am. Soc. Hypertens.* 10, 175–183. doi: 10.1016/j.jash.2015.11.012

Somers, V. K., Mark, A. L., and Abboud, F. M. (1991). Interaction of baroreceptor and chemoreceptor reflex control of sympathetic nerve activity in normal humans. *J. Clin. Invest.* 87, 1953–1957. doi: 10.1172/JCI115221

Spyer, K. M. (1982). Central nervous integration of cardiovascular control. *J. Exp. Biol.* 100, 109–128.

Tank, J., Diedrich, A., Szczech, E., Luft, F. C., and Jordan,. J. (2005). Baroreflex regulation of heart rate and sympathetic vasomotor tone in women and men. *Hypertension* 45, 1159–1164. doi: 10.1161/01.HYP.0000165695.98915.9a

Tobaldini, E., Costantino, G., Solbiati, M., Cogliati, C., Kara, T., Nobili, L., et al. (2017). Sleep, sleep deprivation, autonomic nervous system and cardiovascular diseases. *Neurosci. Biobehav. Rev.* 74, 321–329. doi: 10.1016/j.neubiorev.2016.07.004

Toledo, C., Andrade, D. C., Lucero, C., Arce-Alvarez, A., Díaz, H. S., Aliaga, V., et al. (2017). Cardiac diastolic and autonomic dysfunction are aggravated by central chemoreflex activation in HFpEF rats. *J. Physiol.* 8. doi: 10.1113/JP273558. [Epub ahead of print].

Touyz, R. M. (2004). Reactive oxygen species, vascular oxidative stress, and redox signaling in hypertension: what is the clinical significance? *Hypertension* 44, 248–252. doi: 10.1161/01.HYP.0000138070.47616.9d

Triposkiadis, F., Karayannis, G., Giamouzis, G., Skoularigis, J., Louridas, G., and Butler, J. (2009). The sympathetic nervous system in heart failure physiology, pathophysiology, and clinical implications. *J. Am. Coll. Cardiol.* 54, 1747–1762. doi: 10.1016/j.jacc.2009.05.015

Trombetta, I. C., Somers, V. K., Maki-Nunes, C., Drager, L. F., Toschi-Dias, E., Alves, M. J., et al. (2010). Consequences of comorbid sleep apnea in the metabolic syndrome: implications for cardiovascular risk. *Sleep* 33, 1193–1199. doi: 10.1093/sleep/33.9.1193

van de Borne, P., Mezzetti, S., Montano, N., Narkiewicz, K., Degaute, J. P., and Somers, V. K. (2000). Hyperventilation alters arterial baroreflex control of heart rate and muscle sympathetic nerve activity. *Am. J. Physiol. Heart Circ. Physiol.* 279, H536–H541.

van de Borne, P., Montano, N., Pagani, M., Oren, R., and Somers, V. K. (1997). Absence of low-frequency variability of sympathetic nerve activity in severe heart failure. *Circulation* 95, 1449–1454. doi: 10.1161/01.CIR.95.6.1449

van Heerebeek, L., and Paulus, W. J. (2016). Understanding heart failure with preserved ejection fraction: where are we today? *Neth. Heart J.* 24, 227–236. doi: 10.1007/s12471-016-0810-1

Verloop, W. L., Beeftink, M. M., Santema, B. T., Bots, M. L., Blankestijn, P. J., Cramer, M. J., et al. (2015). A systematic review concerning the relation between the sympathetic nervous system and heart failure with preserved left ventricular ejection fraction. *PLoS ONE* 10:e0117332. doi: 10.1371/journal.pone.0117332

Wang, G., Anrather, J., Glass, M. J., Tarsitano, M. J., Zhou, P., Frys, K. A., et al. (2006). Nox2, Ca^{2+}, and protein kinase C play a role in angiotensin II-induced free radical production in nucleus tractus solitarius. *Hypertension* 48, 482–489. doi: 10.1161/01.HYP.0000236647.55200.07

Wang, G., Anrather, J., Huang, J., Speth, R. C., Pickel, V. M., and Iadecola, C. (2004). NADPH oxidase contributes to angiotensin II signaling in the nucleus tractus solitarius. *J. Neurosci.* 24, 5516–5524. doi: 10.1523/JNEUROSCI.1176-04.2004

Wang, H. J., Wang, W., Cornish, K. G., Rozanski, G. J., and Zucker, I. H. (2014). Cardiac sympathetic afferent denervation attenuates cardiac remodeling and improves cardiovascular dysfunction in rats with heart failure. *Hypertension* 64, 745–755. doi: 10.1161/HYPERTENSIONAHA.114.03699

Wang, W.-Z., Gao, L., Wang, H.-J., Zucker, I. H., and Wang, W. (2008). Interaction between cardiac sympathetic afferent reflex and chemoreflex is mediated by the NTS AT1 receptors in heart failure. *Am. J. Physiol. Heart Circ. Physiol.* 295, H1216–H1226. doi: 10.1152/ajpheart.00557.2008

Wei, C. C., Chen, Y., Powell, L. C., Zheng, J., Shi, K., Bradley, W. E., et al. (2012). Cardiac kallikrein-kinin system is upregulated in chronic volume overload and mediates an inflammatory induced collagen loss. *PLoS ONE* 7:e40110. doi: 10.1371/journal.pone.0040110

Zhu, G. Q., Gao, L., Patel, K. P., Zucker, I. H., and Wang, W. (2004). ANG II in the paraventricular nucleus potentiates the cardiac sympathetic afferent reflex in rats with heart failure. *J. Appl. Physiol.* 97, 1746–1754. doi: 10.1152/japplphysiol.00573.2004

Zucker, I. H., Schultz, H. D., Li, Y. F., Wang, Y., Wang, W., and Patel, K. P. (2004). The origin of sympathetic outflow in heart failure: the roles of angiotensin II and nitric oxide. *Prog. Biophys. Mol. Biol.* 84, 217–232. doi: 10.1016/j.pbiomolbio.2003.11.010

Conflict of Interest Statement: The authors declare that the research was conducted in the absence of any commercial or financial relationships that could be construed as a potential conflict of interest.

frontiers in Neuroscience

CLINICAL TRIAL
published: 11 January 2016
doi: 10.3389/fnins.2015.00506

ICU Blood Pressure Variability May Predict Nadir of Respiratory Depression After Coronary Artery Bypass Surgery

*Anne S. M. Costa[1,2], Paulo H. M. Costa[3], Carlos E. B. de Lima[3,4], Luiz E. M. Pádua[4], Luciana A. Campos[1] and Ovidiu C. Baltatu[1]**

[1] Center of Innovation, Technology and Education, Camilo Castelo Branco University, Sao Jose dos Campos, Brazil, [2] Health Sciences Center, State University of Piaui, Teresina, Brazil, [3] Hospital Sao Marcos, Teresina, Brazil, [4] Health Sciences Center, Federal University of Piaui, Teresina, Brazil

Objectives: Surgical stress induces alterations on sympathovagal balance that can be determined through assessment of blood pressure variability. Coronary artery bypass graft surgery (CABG) is associated with postoperative respiratory depression. In this study we aimed at investigating ICU blood pressure variability and other perioperative parameters that could predict the nadir of postoperative respiratory function impairment.

Methods: This prospective observational study evaluated 44 coronary artery disease patients subjected to coronary artery bypass surgery (CABG) with cardiopulmonary bypass (CPB). At the ICU, mean arterial pressure (MAP) was monitored every 30 min for 3 days. MAP variability was evaluated through: standard deviation (SD), coefficient of variation (CV), variation independent of mean (VIM), and average successive variability (ASV). Respiratory function was assessed through maximal inspiratory (MIP) and expiratory (MEP) pressures and peak expiratory flow (PEF) determined 1 day before surgery and on the postoperative days 3rd to 7th. Intraoperative parameters (volume of cardioplegia, CPB duration, aortic cross-clamp time, number of grafts) were also monitored.

Results: Since, we aimed at studying patients without confounding effects of postoperative complications on respiratory function, we had enrolled a cohort of low risk EuroSCORE (European System for Cardiac Operative Risk Evaluation) with <2. Respiratory parameters MIP, MEP, and PEF were significantly depressed for 4–5 days postoperatively. Of all MAP variability parameters, the ASV had a significant good positive Spearman correlation (rho coefficients ranging from 0.45 to 0.65, $p < 0.01$) with the 3-day nadir of PEF after cardiac surgery. Also, CV and VIM of MAP were significantly associated with nadir days of MEP and PEF. None of the intraoperative parameters had any correlation with the postoperative respiratory depression.

Conclusions: Variability parameters ASV, CV, and VIM of the MAP monitored at ICU may have predictive value for the depression of respiratory function after cardiac surgery as determined by peak expiratory flow and maximal expiratory pressure.

ClinicalTrials.gov Identifier: NCT02074371.

Keywords: CABG, blood pressure variability, ICU, autonomic nervous system, respiratory function, perioperative parameters

OPEN ACCESS

Edited by:
Tijana Bojić,
University of Belgrade, Serbia

Reviewed by:
Kurt Kimpinski,
University of Western Ontario, Canada
Andrei Brateanu,
Cleveland Clinic Foundation, USA

****Correspondence:***
Ovidiu C. Baltatu
ocbaltatu@gmail.com

Specialty section:
This article was submitted to Autonomic Neuroscience, a section of the journal Frontiers in Neuroscience

Received: *30 October 2015*
Accepted: *21 December 2015*
Published: *11 January 2016*

Citation:
Costa ASM, Costa PHM, de Lima CEB, Pádua LEM, Campos LA and Baltatu OC (2016) ICU Blood Pressure Variability May Predict Nadir of Respiratory Depression After Coronary Artery Bypass Surgery. Front. Neurosci. 9:506. doi: 10.3389/fnins.2015.00506

INTRODUCTION

Blood pressure variability reflects different physiological phenomena and represents a subject of actual investigation as potential prognostic value and risk stratification (Boggia et al., 2014). Novel indices of blood pressure variability, as assessed by 24-h ambulatory monitoring have been proposed to provide a more accurate and elaborate estimation of cardiovascular risk (Campos et al., 2013). Blood pressure variability is controlled by neurohumoral factors and it has frequently been used as marker of autonomic tone and sympathovagal balance (Charkoudian and Wallin, 2014).

Surgical stress induces alterations of blood pressure variability as result of neurohumoral and autonomic reactions to stress (Souza Neto et al., 2004). Perioperative blood pressure variability has been associated with 30-day mortality after cardiac surgery (Aronson et al., 2011), possible mechanisms including autonomic imbalance (Pantoni et al., 2014), sympathetic overdrive, and parasympathetic withdrawal (Patron et al., 2014; Ksela et al., 2015).

Autonomic system controls both cardiovascular and respiratory systems through a single neural system conceiving a reciprocal interaction between the respiratory and autonomic control. This reciprocal interaction between the autonomic cardiovascular and respiratory control systems postulates the principle of cardiorespiratory coupling (Dick et al., 2014). Alterations in the cardiorespiratory coupling appear after surgery (Murray et al., 2009; Politano et al., 2013). In fact, among the most serious postoperative adverse events commonly occurring in cardiac surgery is respiratory depression, which can potentially lead to subsequent pulmonary complications and death (Pompei and Della Rocca, 2013). Such pulmonary complications include alveolar atelectasis, acute lung injury/pulmonary edema, acute cardiogenic pulmonary edema (CPE), pulmonary embolism or infection (Neves et al., 2013).

In this study, we hypothesized that the blood pressure variability at the post surgery intensive care unit (ICU) that may reflect the perioperative neurohumoral challenges and autonomic alterations of cardiorespiratory coupling could further predict the respiratory depression occurring after the postoperative ICU period. Postoperative respiratory depression was investigated after coronary artery bypass graft (CABG) since it has been described as a decrease in respiratory pressures (maximum inspiratory pressure—MIP and maximum expiratory pressure—MEP) and peak expiratory flow (PEF) in comparison to preoperative values (Westerdahl et al., 2005; Stein et al., 2009; Hirschhorn et al., 2012). The primary endpoint of this study was to investigate whether the blood pressure variability in the intensive care unit (ICU) is correlated with the nadir of postoperative respiratory function impairment after CABG with cardiopulmonary bypass (CPB).

Abbreviations: CABG, coronary artery bypass surgery; CPB, with cardiopulmonary bypass; ICU, intensive care unit; MIP, maximal inspiratory pressure; MEP, maximal expiratory pressure; PEF, peak expiratory flow; MAP, mean arterial pressure; SD, standard deviation; CV, coefficient of variation; VIM, variation independent of mean; ASV, average successive variability.

METHODS

A prospective observational study was conducted on 44 patients with coronary artery disease submitted to elective CABG with CPB at Hospital Sao Marcos, Teresina, Brazil. Data were collected preoperatively, intraoperatively and up to the 7th postoperative day.

The study was approved by the Research Ethics Committee of the Faculty of Medical Sciences, State University of Piauí, and by the Ethics Committee of Hospital São Marcos, in accordance with Resolution 466/12 of the National Health Council (Ministry of Health) for research on human beings (Permit No. 128/11). Written informed consent was obtained from all patients before enrollment.

The CABG surgery and perioperative medication and monitoring management were standardized according with the 2011 ACCF/AHA Guideline for Coronary Artery Bypass Graft Surgery (Hillis et al., 2011).

The patient inclusion criteria were: patients of both sexes older than 18 years of age submitted to CABG with CPB with coronary disease confirmed by coronary angiography, with no chronic or acute pulmonary disease, with bypass graft of the left internal thoracic artery and/or saphena, who remained in spontaneous ventilation on the first postoperative day, discharged from ICU in the 3rd day followed by 7 days stay at the postoperative unit, and with an EuroSCORE (European System for Cardiac Operative Risk Evaluation) of <2. EuroSCORE is a well-established method of calculating predicted operative mortality for patients undergoing cardiac surgery. It includes patient-related factors (age, sex, chronic pulmonary disease, extracardiac arteriopathy, neurological dysfunction disease, previous cardiac surgery, serum creatinine over 200 μmol/l, active endocarditis, and critical preoperative state), cardiac factors (unstable angina on intravenous nitrates, reduced left ventricular ejection fraction, recent myocardial infarction and pulmonary hypertension), and operation-related factors (emergency, major cardiac procedure other than isolated coronary surgery, thoracic aorta surgery and surgery for postinfarct septal rupture; Nashef et al., 1999). EuroSCORE has been utilized in quality control in cardiac surgery and offers risk stratification for the prediction of hospital mortality and the assessment of quality of care (De Maria et al., 2005).

Exclusion criteria were: intraoperative change of the surgical technique, surgical complications, or complications occurring in the ICU, emergency reoperation, renal failure, failure to agree to continue in the study, presence of other types of heart disease, and of pulmonary diseases.

The respiratory function of all patients was assessed by measuring MIP (cmH_2O), MEP (cmH_2O), and PEF (l/min) determined 1 day before the surgical procedure and during the period from the third to the seventh postoperative day. To evaluate maximal respiratory muscle force, the MIP and the MEP were measured with a digital pressure manometer WIKA-MV300 (WIKA Brasil Indústria Comércio, Iperó, Brazil), and PEF (l/min) determined with Assess peak flow meter (Philips Respironics). During the postoperative period in the ICU, the blood pressure of the patients was monitored at intervals of

30 min for 3 days and the mean arterial pressure (MAP) was thus obtained. MAP variability was determined on the basis of the standard deviation (SD), coefficient of variation (CV), variation independent of mean (VIM), average successive variability (ASV; Dolan and O'Brien, 2010).

The following time frame of outcome measures was followed:

1. preoperative: demographic, clinical EuroSCORE and respiratory measures (day-1)
2. intraoperative: volume of cardioplegia, CPB duration, aortic cross-clamp time, number of grafts
3. postoperative ICU (from surgery to 3rd day): blood pressure monitoring
4. postoperative (from 3rd to the 7th postoperative day): respiratory measures (day 3 to 7).

STATISTICAL ANALYSIS

Data were tested for normality using the D'Agostino & Pearson omnibus normality test. Data normally distributed are represented by mean (SE), and data that are not normally distributed are represented by median (interquartile range). Differences between different day-groups of respiratory parameters were examined using nonparametric test followed by Dunn's multiple comparisons against the group of the day before surgery ($p < 0.05$ was regarded as being statistically significant). Spearman's correlation coefficient r was used to quantify a relationship between two or more variables; a two-tailed p-value < 0.05 was considered statistically significant. Data were analyzed using statistical software (Prism 6 for Mac OS X).

RESULTS

Demographic, Euroscore, and Intraoperative Parameters

The study sample was composed of 44 patients with mean age of 62 ± 8.2 years. Demographic, clinical and surgical parameters were normally distributed within the study group (**Table 1**). None of the intraoperative parameters (cardioplegia volume, extracorporeal circulation time, aortic clamping time, number of grafts) was related to postoperative respiratory depression (data not shown).

Respiratory Parameters MIP, MEP and PEF are Significantly Depressed Postoperatively

Respiratory parameters MIP, MEP, and PEF were assessed preoperatively (day-1) and from the third to the seventh postoperative day (post-ICU) (**Figure 1**). A marked reduction in lung function was present the first week after surgery, which was consistent with previous findings (Savci et al., 2011). Comparisons of respiratory parameters in the postoperative days after the ICU to those in the preoperative day revealed a significant depression on days 3–4 for MIPs (which reflects the strength of the diaphragm and other inspiratory muscles), days 3–4 for MEPs (which reflects the strength of the abdominal muscles and intercostal muscles) and days 3–5 for PEF (which is considered as a measure of pulmonary physiology and is being used as a surrogate for the more sensitive measurement of forced expiratory volume in 1 s; Slieker and van der Ent, 2003; **Figure 1**). As determined by MIP, MEP and PEF, the nadir of respiratory depression during the first week after cardiac surgery is the critical period when most of the respiratory complications occur (Albu et al., 2010).

TABLE 1 | Demographical, clinical, and intraoperative data for patients undergoing GABG.

VARIABLES	
Age (years)	62 ± 8.2
Sex (Male/Female, %)	75%/25%
BMI (kg/m^2)	26 [24–29]
Euroscore (%)	0.68 [0.54–0.77]
COMORBIDITIES	
Hypertension (%)	30.23
Diabetes (%)	6.98
Dyslipidaemia (%)	2.33
Hypertension + Diabetes (%)	16.28
Hypertension + Dyslipidaemia (%)	18.60
Hypertension + Diabetes + Dyslipidaemia (%)	2.33
Smoking (%)	6.82
INTRAOPERATIVE VARIABLES	
Volume of cardioplegia (ml)	1374 ± 440
CPB duration (min)	95 ± 29
Aortic cross-clamp time (min)	67 ± 27
Number of grafts (%)	
1	9.09
2	15.91
3	52.27
4	20.45
more than 4	2.27

Data are presented as Mean ± SD, median [interquartile range].

ICU Blood Pressure Variability Parameters Associations with Respiratory Parameters

Of all the parameters of MAP variability, ASV showed a stronger positive and significant Spearman correlation (coefficients of 0.45–0.65, $p < 0.01$) with the aggravation of depression expressed by PEF up to the fifth day after heart surgery (**Table 2**).

VIM MAP correlated with only the first day (of 2) of postoperative MEP nadir and the first 2 days (of 3) of postoperative PEF nadir (**Table 2**).

CV MAP was associated with the 2 days of postoperative MEP nadir but also with the 3rd day of MEP depression (**Table 2**). Also, CV MAP correlated with the first 2 days but not the 3rd day of postoperative PEF nadir.

SD of MAP at the ICU was not correlated with any respiratory parameter at any time (**Table 2**).

DISCUSSION

The main findings of this study are that the MAP variability monitored at ICU may have predictive value for the depression of

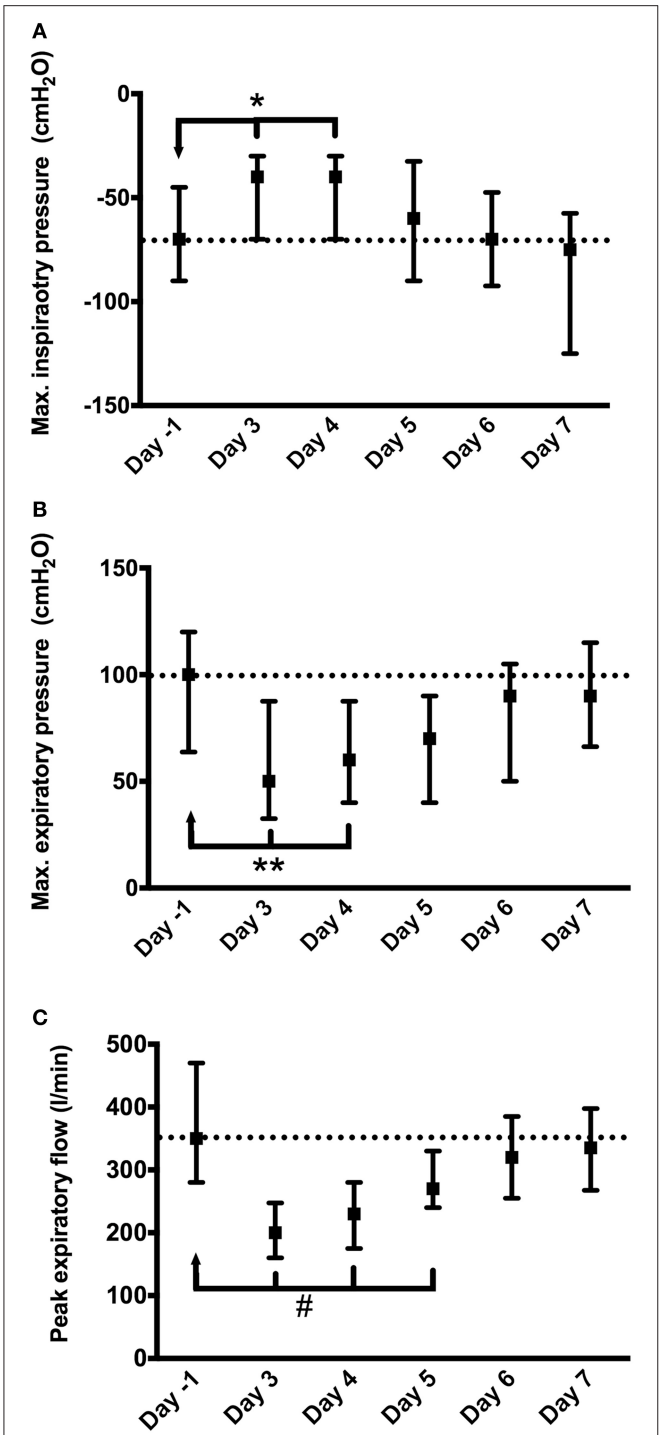

FIGURE 1 | Depression of respiratory function after CABG surgery: (A) maximal inspiratory pressure (MIP); (B) maximal expiratory pressure (MEP); (C) peak expiratory flow (PEF). Day-1, day before surgery; Day 3–7, days after surgery ICU (days 1–3 were at ICU). Statistical significance is in comparison to the day before surgery: *$p < 0.05$; **$p < 0.01$; #$p < 0.001$.

TABLE 2 | Spearman's rank correlations (ρ) between the ICU MAP variability parameters (ASV, average successive variability; VIM, variation independent of mean; CV, coefficient of variation; SD, standard deviation) and respiratory parameters (PEF, peak expiratory flow; MEP, maximal expiratory pressure; MIP, maximal inspiratory pressure).

	Day -1	Day 3	Day 4	Day 5	Day 6	Day 7
	PEF	**PEF**	**PEF**	**PEF**	**PEF**	**PEF**
ASV	0.32	0.49*	0.56*	0.67*	0.53	0.30
VIM	−0.01	0.64*	0.46*	0.32	0.08	−0.50
CV	0.10	0.44*	0.48*	0.35	0.34	0.50
SD	0.15	0.36	0.42	0.32	0.33	0.50
	MEP	**MEP**	**MEP**	**MEP**	**MEP**	**MEP**
ASV	0.05	0.34	0.25	0.37	0.15	0.06
VIM	−0.18	0.49*	0.38	0.27	0.26	0.11
CV	−0.06	0.49*	0.55*	0.52*	0.39	−0.21
SD	0.00	0.39	0.49	0.46	0.30	0.32
	MIP	**MIP**	**MIP**	**MIP**	**MIP**	**MIP**
ASV	0.27	0.19	0.21	0.44	0.16	0.07
VIM	0.10	0.19	0.11	0.13	0.01	0.00
CV	0.16	0.15	0.27	0.20	−0.10	−0.60
SD	0.21	0.12	0.34	0.20	−0.14	−0.60

*Gray shadowed cells correspond to the day when nadir of respiratory parameter depression occurs; *, significant Spearman's rank correlation $p < 0.05$.*

respiratory function after ICU as determined by peak expiratory flow and maximal expiratory pressure. The ASV of ICU MAP correlated with the nadir of peak expiratory flow in all 3 days of depression in the week following ICU after cardiac surgery. The ICU blood pressure variability measures reflecting a sum-up of the perioperative measures producing neurohumoral challenges may predict respiratory outcomes after cardiac surgery.

The pathophysiological determinants of the cardiac surgery-induced cardiovascular and respiratory dysfunction are subject of actual research and comprise a complex combination of intraoperative factors such as general anesthesia (Hachenberg et al., 1993), surgical injury caused by sternotomy (Berrizbeitia et al., 1989), damage of phrenic nerve (Mok et al., 1991), mechanical ventilation (Roosens et al., 2002), cardiopulmonary bypass (Babik et al., 2003), and postoperative airway narrowing (Babik et al., 2003; Albu et al., 2010). Cardiac surgery-induced respiratory function can be afflicted not only directly through mechanisms described above but also through systemic reactions including sympathetic stress response, pain (Ledowski et al., 2012), and inflammation (Paparella et al., 2002).

Cardiovascular and respiratory systems have vital functions in the general adaptation to stress, and both are coordinated by the autonomic nervous system. Surgery-associated stress induces a dysautonomia that afflicts cardiovascular and respiratory functions (Garcia et al., 2013). Cardiovascular and respiratory activities are intricately coupled through highly overlapping brainstem autonomic control centers. This cardiorespiratory coupling involves multiple mechanisms mediating the bidirectional influences between the cardiovascular and respiratory activity (Dick et al., 2014). The intraoperative blood pressure variability is a strong predictor of 30-day postoperative mortality after CABG surgery (Aronson et al.,

2010). On the other hand, inspiratory muscle fatigue may increase sympathetic vasomotor outflow (Katayama et al., 2012). These interrelations may contribute to the pathophysiology of cardiorespiratory coupling, and indicate a possible bidirectional connection between alterations of respiratory function and blood pressure variability. Indeed, our study suggests that MAP variability assessment during ICU, which may reflect the autonomic and neurohumoral reaction to perioperative stress, is a good predictor of the nadir of respiratory depression that occurs in the first postoperative week of CABG surgery. These complex mechanisms involved in the surgery-associated stress induced by composite intraoperative factors affecting autonomic nervous system and cardiorespiratory coupling may explain the predictive nature between cardiovascular and respiratory functions observed in our study.

Predictive biomarkers should be considered to recognize and manage postoperative complications (Gonzalez et al., 2014). Perioperative assessment of surgery is important in order to minimize the surgical risks and to prevent postoperative complications (Task Force et al., 2013). Our findings may indicate ICU MAP variability as a measure in order to initiate inspiratory muscle training programs (Westerdahl et al., 2005; Savci et al., 2011) or physiotherapy programs (Stein et al., 2009; Hirschhorn et al., 2012) for faster recovery and improved pulmonary function after CABG.

In summary, our study evidenced a predictive value of ICU MAP variability on postoperative respiratory depression. Further studies may uncover if there may be additional benefit in also reducing MAP variability to prevent postoperative cardiovascular events (Dolan and O'Brien, 2010).

Some limitations must be considered.

Since we aimed at studying patients without confounding effects of postoperative complications on respiratory function, we had enrolled a cohort without intraoperative complications and of low risk EuroSCORE (European System for Cardiac Operative Risk Evaluation) with <2. Therefore, there were no prolonged stay of intensive care and no postoperative complications were observed in the investigated period. Nevertheless, the timeframe of the investigation did not allow further monitoring in order to observe influences on clinical outcomes. Thus, we don't know if the respiratory depression further translated or not in clinical events.

Another limitation is the small sample size of the study. Also, since exclusion criteria were very strict, the results cannot be generalized to a broader range of patients such as the ones with perioperative complications. This strict selection process was intended to control several biases that may otherwise have limited the validity of the analysis. Our results are likely to be transferable to cardiac surgery patients without perioperative complications and further studies with broader inclusion criteria and longer timeframe of investigations are necessary.

AUTHOR CONTRIBUTIONS

AC carried out the postoperative patient care including the respiratory function evaluations and perioperative data collection, and participated in the design of the study. PC carried out the cardiac surgery and patient selection. CD carried out the cardiac surgery and patient selection. LP participated in the statistical analysis. LC participated in the design of the study and coordination, statistical analysis, and contributed to the interpretation of the results and the drafting of the manuscript. OB conceived the study, and participated in its design and coordination and drafted the manuscript.

FUNDING

This work was supported by the São Paulo Research Foundation (grant numbers FAPESP 2013/14724-0, FAPESP 13/06698-0). OB is supported by the National Council for Scientific and Technological Development (CNPq, 301706/2013-1).

REFERENCES

Albu, G., Babik, B., Késmárky, K., Balázs, M., Hantos, Z., and Peták, F. (2010). Changes in airway and respiratory tissue mechanics after cardiac surgery. *Ann. Thorac. Surg.* 89, 1218–1226. doi: 10.1016/j.athoracsur.2009.12.062

Aronson, S., Dyke, C. M., Levy, J. H., Cheung, A. T., Lumb, P. D., Newman, M. F., et al. (2011). Does perioperative systolic blood pressure variability predict mortality after cardiac surgery? An exploratory analysis of the ECLIPSE trials. *Anesth. Analg.* 113, 19–30. doi: 10.1213/ANE.0b013e31820f9231

Aronson, S., Stafford-Smith, M., Phillips-Bute, B., Shaw, A., Gaca, J., Newman, M., et al. (2010). Intraoperative systolic blood pressure variability predicts 30-day mortality in aortocoronary bypass surgery patients. *Anesthesiology* 113, 305–312. doi: 10.1097/ALN.0b013e3181e07ee9

Babik, B., Asztalos, T., Peták, F., Deák, Z. I., and Hantos, Z. (2003). Changes in respiratory mechanics during cardiac surgery. *Anesth. Analg.* 96, 1280–1287. doi: 10.1213/01.ANE.0000055363.23715.40

Berrizbeitia, L. D., Tessler, S., Jacobowitz, I. J., Kaplan, P., Budzilowicz, L., and Cunningham, J. N. (1989). Effect of sternotomy and coronary bypass surgery on postoperative pulmonary mechanics. Comparison of internal mammary and saphenous vein bypass grafts. *Chest* 96, 873–876.

Boggia, J., Asayama, K., Li, Y., Hansen, T. W., Mena, L., and Schutte, R. (2014). Cardiovascular risk stratification and blood pressure variability on ambulatory and home blood pressure measurement. *Curr. Hypertens. Rep.* 16, 470. doi: 10.1007/s11906-014-0470-8

Campos, L. A., Pereira, V. L. Jr., Muralikrishna, A., Albarwani, S., Brás, S., and Gouveia, S. (2013). Mathematical biomarkers for the autonomic regulation of cardiovascular system. *Front. Physiol.* 4:279. doi: 10.3389/fphys.2013.00279

Charkoudian, N., and Wallin, B. G. (2014). Sympathetic neural activity to the cardiovascular system: integrator of systemic physiology and interindividual characteristics. *Compr. Physiol.* 4, 825–850. doi: 10.1002/cphy.c130038

De Maria, R., Mazzoni, M., Parolini, M., Gregori, D., Bortone, F., Arena, V., et al. (2005). Predictive value of EuroSCORE on long term outcome in cardiac surgery patients: a single institution study. *Heart* 91, 779–784. doi: 10.1136/hrt.2004.037135

Dick, T. E., Hsieh, Y. H., Dhingra, R. R., Baekey, D. M., Galán, R. F., Morris, K. F., et al. (2014). Cardiorespiratory coupling: common rhythms in cardiac, sympathetic, and respiratory activities. *Prog. Brain Res.* 209, 191–205. doi: 10.1016/B978-0-444-63274-6.00010-2

Dolan, E., and O'Brien, E. (2010). Blood pressure variability: clarity for clinical practice. *Hypertension* 56, 179–181. doi: 10.1161/HYPERTENSIONAHA.110.154708

Garcia, A. J. III, Koschnitzky, J. E., Dashevskiy, T., and Ramirez, J. M. (2013). Cardiorespiratory coupling in health and disease. *Auton. Neurosci.* 175, 26–37. doi: 10.1016/j.autneu.2013.02.006

Gonzalez, A. A., Dimick, J. B., Birkmeyer, J. D., and Ghaferi, A. A. (2014). Understanding the volume-outcome effect in cardiovascular surgery: the role of failure to rescue. *JAMA Surg.* 149, 119–123. doi: 10.1001/jamasurg.2013.3649

Hachenberg, T., Tenling, A., Rothen, H. U., Nyström, S. O., Tyden, H., and Hedenstierna, G. (1993). Thoracic intravascular and extravascular fluid volumes in cardiac surgical patients. *Anesthesiology* 79, 976–984. doi: 10.1097/00000542-199311000-00016

Hillis, L. D., Smith, P. K., Anderson, J. L., Bittl, J. A., Bridges, C. R., Byrne, J. G., et al. (2011). 2011 ACCF/AHA guideline for coronary artery bypass graft surgery. A report of the American College of Cardiology Foundation/American Heart Association Task Force on Practice Guidelines. Developed in collaboration with the American Association for Thoracic Surgery, Society of Cardiovascular Anesthesiologists, and Society of Thoracic Surgeons. *J. Am. Coll. Cardiol.* 58, e123–e210. doi: 10.1016/j.jacc.2011.08.009

Hirschhorn, A. D., Richards, D. A., Mungovan, S. F., Morris, N. R., and Adams, L. (2012). Does the mode of exercise influence recovery of functional capacity in the early postoperative period after coronary artery bypass graft surgery? A randomized controlled trial. *Interact. Cardiovasc. Thorac. Surg.* 15, 995–1003. doi: 10.1093/icvts/ivs403

Katayama, K., Iwamoto, E., Ishida, K., Koike, T., and Saito, M. (2012). Inspiratory muscle fatigue increases sympathetic vasomotor outflow and blood pressure during submaximal exercise. *Am. J. Physiol. Regul. Integr. Comp. Physiol.* 302, R1167–R1175. doi: 10.1152/ajpregu.00006.2012

Ksela, J., Avbelj, V., and Kalisnik, J. M. (2015). Multifractality in heartbeat dynamics in patients undergoing beating-heart myocardial revascularization. *Comput. Biol. Med.* 60, 66–73. doi: 10.1016/j.compbiomed.2015.02.012

Ledowski, T., Reimer, M., Chavez, V., Kapoor, V., and Wenk, M. (2012). Effects of acute postoperative pain on catecholamine plasma levels, hemodynamic parameters, and cardiac autonomic control. *Pain* 153, 759–764. doi: 10.1016/j.pain.2011.11.002

Mok, Q., Ross-Russell, R., Mulvey, D., Green, M., and Shinebourne, E. A. (1991). Phrenic nerve injury in infants and children undergoing cardiac surgery. *Br. Heart J.* 65, 287–292. doi: 10.1136/hrt.65.5.287

Murray, A., Drummond, G. B., Dodds, S., and Marshall, L. (2009). Low-frequency changes in finger volume in patients after surgery, related to respiration and venous pressure. *Eur. J. Anaesthesiol.* 26, 9–16. doi: 10.1097/EJA.0b013e328318c6bd

Nashef, S. A., Roques, F., Michel, P., Gauducheau, E., Lemeshow, S., and Salamon, R. (1999). European system for cardiac operative risk evaluation (EuroSCORE). *Eur. J. Cardiothorac. Surg.* 16, 9–13. doi: 10.1016/S1010-7940(99)00134-7

Neves, F. H., Carmona, M. J., Auler, J. O. Jr., Rodrigues, R. R., Rouby, J. J., and Malbouisson, L. M. (2013). Cardiac compression of lung lower lobes after coronary artery bypass graft with cardiopulmonary bypass. *PLoS ONE* 8:e78643. doi: 10.1371/journal.pone.0078643

Pantoni, C. B., Mendes, R. G., Di Thommazo-Luporini, L., Simões, R. P., Amaral-Neto, O., Arena, R., et al. (2014). Recovery of linear and nonlinear heart rate dynamics after coronary artery bypass grafting surgery. *Clin. Physiol. Funct. Imaging* 34, 449–456. doi: 10.1111/cpf.12115

Paparella, D., Yau, T. M., and Young, E. (2002). Cardiopulmonary bypass induced inflammation: pathophysiology and treatment. An update. *Eur. J. Cardiothorac. Surg.* 21, 232–244. doi: 10.1016/s1010-7940(01)01099-5

Patron, E., Messerotti Benvenuti, S., Favretto, G., Gasparotto, R., and Palomba, D. (2014). Depression and reduced heart rate variability after cardiac surgery: the mediating role of emotion regulation. *Auton. Neurosci.* 180, 53–58. doi: 10.1016/j.autneu.2013.11.004

Politano, A. D., Riccio, L. M., Lake, D. E., Rusin, C. G., Guin, L. E., Josef, C. S., et al. (2013). Predicting the need for urgent intubation in a surgical/trauma intensive care unit. *Surgery* 154, 1110–1116. doi: 10.1016/j.surg.2013.05.025

Pompei, L., and Della Rocca, G. (2013). The postoperative airway: unique challenges? *Curr. Opin. Crit. Care* 19, 359–363. doi: 10.1097/MCC.0b013e3283632ede

Roosens, C., Heerman, J., De Somer, F., Caes, F., van Belleghem, Y., and Poelaert, J. I. (2002). Effects of off-pump coronary surgery on the mechanics of the respiratory system, lung, and chest wall: comparison with extracorporeal circulation. *Crit. Care Med.* 30, 2430–2437. doi: 10.1097/00003246-200211000-00005

Savci, S., Degirmenci, B., Saglam, M., Arikan, H., Inal-Ince, D., Turan, H., et al. (2011). Short-term effects of inspiratory muscle training in coronary artery bypass graft surgery: a randomized controlled trial. *Scand. Cardiovasc. J.* 45, 286–293. doi: 10.3109/14017431.2011.595820

Slieker, M. G., and van der Ent, C. K. (2003). The diagnostic and screening capacities of peak expiratory flow measurements in the assessment of airway obstruction and bronchodilator response in children with asthma. *Monaldi Arch. Chest Dis.* 59, 155–159.

Souza Neto, E. P., Loufouat, J., Saroul, C., Paultre, C., Chiari, P., Lehot, J. J., et al. (2004). Blood pressure and heart rate variability changes during cardiac surgery with cardiopulmonary bypass. *Fundam. Clin. Pharmacol.* 18, 387–396. doi: 10.1111/j.1472-8206.2004.00244.x

Stein, R., Maia, C. P., Silveira, A. D., Chiappa, G. R., Myers, J., and Ribeiro, J. P. (2009). Inspiratory muscle strength as a determinant of functional capacity early after coronary artery bypass graft surgery. *Arch. Phys. Med. Rehabil.* 90, 1685–1691. doi: 10.1016/j.apmr.2009.05.010

Task Force, M., Montalescot, G., Sechtem, U., Achenbach, S., Andreotti, F., Arden, C., et al. (2013). 2013 ESC guidelines on the management of stable coronary artery disease: the Task Force on the management of stable coronary artery disease of the European Society of Cardiology. *Eur. Heart J.* 34, 2949–3003. doi: 10.1093/eurheartj/eht296

Westerdahl, E., Lindmark, B., Eriksson, T., Friberg, O., Hedenstierna, G., and Tenling, A. (2005). Deep-breathing exercises reduce atelectasis and improve pulmonary function after coronary artery bypass surgery. *Chest* 128, 3482–3488. doi: 10.1378/chest.128.5.3482

Conflict of Interest Statement: The authors declare that the research was conducted in the absence of any commercial or financial relationships that could be construed as a potential conflict of interest.

frontiers in Neuroscience

ORIGINAL RESEARCH
published: 28 August 2017
doi: 10.3389/fnins.2017.00477

Hemodynamic Perturbations in Deep Brain Stimulation Surgery: First Detailed Description

*Tumul Chowdhury *, Marshall Wilkinson and Ronald B. Cappellani*

University of Manitoba, Winnipeg, MB, Canada

Background: Hemodynamic perturbations can be anticipated in deep brain stimulation (DBS) surgery and may be attributed to multiple factors. Acute changes in hemodynamics may produce rare but severe complications such as intracranial bleeding, transient ischemic stroke and myocardium infarction. Therefore, this retrospective study attempts to determine the incidence of hemodynamic perturbances (rate) and related risk factors in patients undergoing DBS surgery.

Materials and Methods: After institutional approval, all patients undergoing DBS surgery for the past 10 years were recruited for this study. Demographic characteristics, procedural characteristics and intraoperative hemodynamic changes were noted. Event rate was calculated and the effect of all the variables on hemodynamic perturbations was analyzed by regression model.

Results: Total hemodynamic adverse events during DBS surgery was 10.8 (0–42) and treated in 57% of cases.

Conclusion: Among all the perioperative variables, the baseline blood pressure including systolic, diastolic, and mean arterial pressure was found to have highly significant effect on these intraoperative hemodynamic perturbations.

Keywords: deep brain stimulation, Parkinson disease, cardio-vascular changes, sub-thalamic nucleus

OPEN ACCESS

Edited by:
Tijana Bojić,
University of Belgrade, Serbia

Reviewed by:
Alberto Porta,
Università degli Studi di Milano, Italy
Helio Cesar Salgado,
University of São Paulo, Brazil

****Correspondence:***
Tumul Chowdhury
tumulthunder@gmail.com

Specialty section:
This article was submitted to Autonomic Neuroscience, a section of the journal Frontiers in Neuroscience

Received: *19 June 2017*
Accepted: *10 August 2017*
Published: *28 August 2017*

Citation:
Chowdhury T, Wilkinson M and Cappellani RB (2017) Hemodynamic Perturbations in Deep Brain Stimulation Surgery: First Detailed Description. Front. Neurosci. 11:477. doi: 10.3389/fnins.2017.00477

INTRODUCTION

Deep brain stimulation (DBS) has become an established surgical therapy for patients with Parkinson's disease (PD) who are refractory to standard medical management, as well as being used for other chronic neurological conditions (Shindo et al., 2013). This procedure requires precise stimulation of different thalamic and sub thalamic nuclei, intraoperative neurological monitoring and patient's cooperation to perform certain neurological examinations (Camerlingo et al., 1990).

Hemodynamic perturbations can be anticipated in this type of surgery due to a number of reasons including age related factors, anxiety, semi sitting position, surgical procedure (electrode insertion), presenting disease (autonomic dysfunctions), presence of other co morbidities and effect of concurrent medications (Haapaniemi et al., 2001; Mata et al., 2012; Vigneri et al., 2012). The effects of stimulation of different thalamic and sub thalamic nuclei on cardiovascular changes are still a matter of investigation (Jain et al., 2012; Zrinzo et al., 2012). A recent study highlighted that cardiovascular changes (carotid stenosis or ECG changes) usually precedes motor symptoms or these may be independent predictors of PD (Chakrabarti et al., 2014). Added to these, the use of

anesthetic agents for conscious sedation can also affect the hemodynamic changes adversely (Green et al., 2010). Acute changes in hemodynamics may produce some unwanted complications such as intracranial bleeding, transient ischemic stroke, myocardium infarction etc. (Hyam et al., 2012). However, the literature revealing hemodynamic disturbances in this type of surgery is still largely unknown.

Therefore, this retrospective study attempts to determine the incidence of total hemodynamic perturbances (rate) and related risk factors in patients undergoing DBS surgery.

MATERIALS AND METHODS

After the local institutional ethics committee [HS15730] approval, all patients undergoing DBS surgery from April 1, 2000 to July 31, 2012 were recruited for this study. For retrieving the data, the Canadian Classification of Health Interventions (CCI) codes (1.AN.53.SZ.JA or 1.AN.53.SE.JA) and the International Classification of Diseases (ICD) code (ICD-9-CM code 02.93) were used. Demographic characteristics including patient's characteristics, disease and risks factors characteristics, procedural characteristics and intraoperative hemodynamic changes were noted. Event rate (total hemodynamic perturbations in relation to total anesthesia time) was calculated and the effect of all the variables on hemodynamic perturbations was analyzed by regression model.

Hemodynamic perturbations- These are defined (number of episodes) as below. Hypotension- less than 90 mm Hg systolic BP:

Hypertension-more than 140 systolic and 90 mm Hg of diastolic BP
Bradycardia-Heart rate less than 50 bpm
Tachycardia-Heart rate more than 90 bpm
Any ECG changes other than normal sinus rhythm

These events were noted during two-phases: first during electrode (nuclei) stimulation, and second-during the battery placement. During the electrode stimulation, hemodynamic events were again noted in two phases, specifically, the right and left sided electrode (nuclei) stimulation related. The total hemodynamic events were calculated as events during electrode stimulation plus events during battery placement. To match the accuracy of data, neurophysiologist was asked to provide the time at which he started to stimulate the electrode (nuclei) and hemodynamic events during 20 min from the start of simulation time (as reported by the neurophysiologist) was taken for the calculation purpose. Events were noted every 5 min.

Anesthesia Protocol

Standard monitors including EKG, pulse oximetry and invasive blood pressure monitoring (IBP) were applied and for the initial phase (placement of burr hole) of DBS surgery, all patients received monitored anesthesia care (midazolam 1–2 mg or/and propofol 25–50 mcg/kg/min and/or remifentanil 0.02–0.05 mcg/kg/min and/or fentanyl 25–50 mcg bolus). The infusions were stopped approximately 30 min before the actual testing and re-started once the testing was completed.

For the battery placement procedure, all patients were given general anesthesia with tracheal intubation. As per the anesthesiologist discretion, the standard induction technique involved combination of remifentanil/fentanyl/sufentanil plus propofol plus rocuronium. The anesthesia was maintained with volatile anesthetics (desflurane or sevoflurane) and opioids as needed. At the end of procedure, the muscle relaxant was reversed with the reversal (neostigmine and glycopyrrolate) and the trachea was extubated after ascertaining four twitches on train of four monitor as well as full recovery of consciousness. All the patients were transferred to post-anesthesia care unit for further observation.

Surgery Protocol

The DBS procedure was performed either in one stage (both the electrode placement and the battery placement on the same day) or two stage (the battery placement on other day). The same surgeon performed all the procedures from 2003 till 2012. On the morning of the operation, a rigid head frame (Leksell) was placed on the patient by the surgeon utilizing local anesthesia (0.25% bupivacaine 5–10 ml) and magnetic resonance imaging was performed in order to delineate the x, y, and z coordinates of defined structures. After this, the patient was transferred to the operating room where he/she was positioned in semi-sitting position. The stimulation involved certain thalamic/subthalamic nuclei [ventralis intermedius nucleus (VIM), the sub-thalamic nucleus (STN), and the globus pallidus (GPI)]. The whole procedure consisted of three parts: first, localization; second, insertion of electrodes and stimulation, and third, internalization of leads and battery placement. The first two procedures were done under monitored anesthesia care and third procedure (battery placement) was performed under general anesthesia.

Neurophysiology Protocol

After scalp opening and burr hole placement, microelectrode recordings were carried out using the FHC electronic Microdrive and micro/macro electrode (Frederic Hare Corp., USA) and the Lead point recording/stimulation system (Medtronic Corp.). Target acquisition was obtained from AC-PC coordinates derived from preoperative MRI sequences in conjunction with the Leksell frame system and a custom targeting software. Microelectrode impedances were acceptable between 0.5 and 2 MΩ. A survey of electrical activity was conducted from 10 mm above to 5 mm below the putative target. The depths of the top of the target nucleus (usually STN) and the bottom were noted and the appropriate changes in aggregate cellular activity observed for transitions into and out of the target nucleus. Monopolar test stimulation was conducted for each electrode trajectory above and below the putative target. The stimulus parameters were pulse duration of 0.06 ms, frequency of 130 Hz and stimulus amplitude ranging from 0.1 to 5 mA. During test stimulation, relief of parkinsonian symptoms was noted as well as any side effects due to activation of neighboring structures, the most common of which was the internal capsule or sensory apparatus. Stimulus thresholds for evoking side effects were noted and compared to the clinical benefit. Generally, a side effect produced

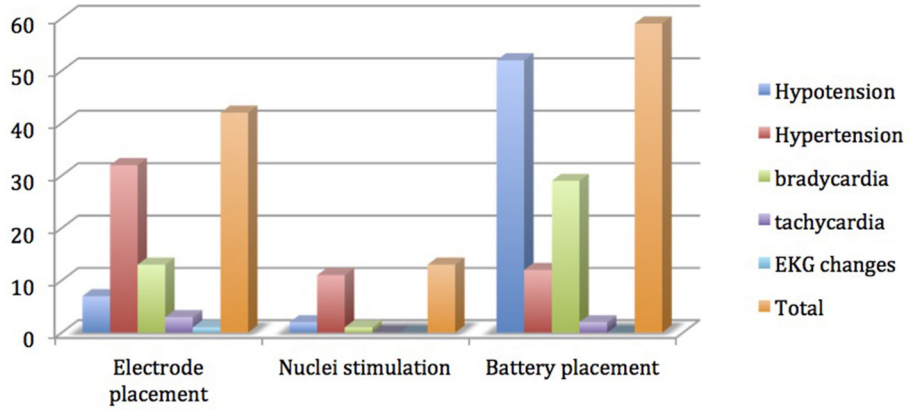

FIGURE 1 | Distribution of hemodynamic events among various steps of deep brain stimulation surgery.

by stimuli of ≤ 3 mA indicated unacceptable electrode proximity and an alternate trajectory was conducted.

Statistical Analysis

Rate ratios and their confidence intervals were estimated via negative binomial regression models. SAS version 9.3 (SAS Institute, Cary NC) was used for all analyses. Since each subject was under anesthesia for varying lengths of time, we did not compare the raw number of events during surgery between groups. Instead, we calculated event rates with minutes of anesthesia as the denominator, and used this as the outcome. The raw numbers were used to describe various hemodynamic events only in **Figure 1**. The continuous variables are reported as mean, min-max, and standard deviation. The *p*-value less than 0.05 is considered as statistically significant for this study purpose.

RESULTS

Data from 79 procedures were included for the final analysis. Among various characteristics noted, male patients (64.6%), Parkinson disease (50.6%), history of smoking (25.3%), hypertension (33%), bilateral electrode placement (73.4%) and same day battery placement (58.2%) were found to be more common variables in their respective groups (**Table 1**). Total hemodynamic adverse events during DBS surgery was 10.8 (0–42) and treated in 57% of cases. Baseline blood pressure including systolic, diastolic and mean arterial pressure was found to have highly significant effect [14, 31, and 19% greater chance of adverse hemodynamic event per 10 mm Hg increase in value respectively] on intraoperative hemodynamic perturbations (**Table 2**). DBP had the greatest impact among all the hemodynamic parameters. Other variables including type of disease, duration of symptoms, number of medications used, type of nuclei stimulated, laterality of DBS implants and battery placement on the same day had no significant effect on hemodynamic perturbations during DBS surgery (**Table 3**). The distribution of hemodynamic events among various steps of DBS surgery is shown in **Figure 1**. It is evident that most of the hemodynamic events were noted during battery placement. The hypotension was the most common hemodynamic perturbation observed during battery placement while hypertensive episodes were common events during both electrode placement and nuclei stimulation. Two patients had intracranial hemorrhage and one patient developed ST elevation during the electrode placement. No mortality was noted during the procedure.

TABLE 1 | Demographic characteristics of patients.

Characteristics	Frequency/Mean ($n = 79$)	Percentage/Range
Age (years)	57.0	21–80
GENDER		
Male: Female	51: 28	64.6: 35.4
BMI	28.0	19.5–57.5
ASA GRADE		
1	10	12.6
2	36	45.6
3	33	41.8
COMORBIDITIES		
Hypertension	33	41.8
Diabetes	14	17.7
Coronary disease	7	8.9
Asthma	3	3.8
RISK FACTORS		
Smoking	20	25.3
Alcohol	13	16.5
OSA	7	8.9
MAJOR DIAGNOSES		
Parkinson	40	50.6
Essential Tremor	25	31.7
Dystonia	10	12.6
Multiple sclerosis	4	5.1
Duration of symptoms (years)	13.0	3–47
Number of Medications	3.4	0–8

OSA, Obstructive sleep apnea.

TABLE 2 | Disease and procedure related characteristics.

Characteristics	Frequency ($n = 79$)	Percentage
TYPE OF NUCLEI STIMULATED		
STN	40	50.6
VIM	30	38.0
GPi	9	11.4
DBS IMPLANTS SITE		
Unilateral	21	26.6
Bilateral	58	73.4
BATTERY PLACEMENT DAY		
Same	46	58.2
Other	33	41.8
Complications	32	40.5
BASELINE HEMODYNAMICS (mm Hg)		
Systolic BP	140.0	104–200
Diastolic BP	75.4	54–110
Mean BP	95	65–140
Total no of events	10.8	0–42
Drugs for hemodynamic	45	57.0
Total duration surgery (min)	384.8	200–590
Total duration anesthesia (min)	451.1	260–630
Total duration battery (min)	116.3	70–194

STN, Sub thalamic nucleus; VIM, Ventral intermediate, GPi, Internal globus pallidus; BP, Blood pressure.

TABLE 3 | Regression model; event rate predicated by various demographic variables.

Factor	Rate ratio	95% confidence interval	*p*-value
Age per 10 y	1.16	0.96-1.40	0.13
Sex			
F/M	0.90	0.54–1.51	0.69
BMI per 5 Kg	0.91	0.74–1.11	0.38
Duration of symptoms (Per 10 y)	0.95	0.73–1.23	0.70
ASA GRADE			
Gr1/Gr2	1.28	0.60–2.70	0.52
Gr1/Gr3	0.78	0.36–1.65	0.51
Gr2/Gr3	0.61	0.36–1.01	0.05
COMORBIDITIES (ABSENCE/PRESENCE)			
Hypertension	0.63	0.39–1.02	0.06
Diabetes	1.05	0.56–1.98	0.88
RISK FACTORS			
Smoking	1.32	0.76–2.31	0.34
Alcohol	0.95	0.50–1.83	0.89
MAJOR DIAGNOSES (ABSENCE/PRESENCE)			
Parkinson	0.71	0.44–1.16	0.18
Essential tremor	1.06	0.63–1.79	0.82
Dystonia	1.66	0.74–3.72	0.24
Multiple sclerosis	1.59	0.51–4.92	0.44

DISCUSSION

Cardiovascular changes in DBS surgery are complex and multifactorial in origin. Three common factors can be delineated as the plausible causes. First, the neurological diseases including PD, multiple sclerosis (MS), and essential tremors may present with autonomic dysfunctions and these changes can be detected by various parameters including variability in heart rate (R-R variability), postural changes in blood pressure, Valsalva maneuver, cold pressor test, head-up tilt test, and other continuous robust monitoring methods; however, being a retrospective study, we just presented the hemodynamic parameters (Acevedo et al., 2000; Micieli et al., 2003; Jain and Goldstein, 2012). Secondly, the semi-sitting position combined with anesthetics may produce negative hemodynamic changes (Cicolini et al., 2011). And thirdly, the use of sedation as well as general anesthesia itself can also cause these perturbations. In addition, there are other contributing factors including procedure, side effects of anti-Parkinson medications, anxiety, pain, fatigue, and pre-existing comorbidities (diabetes, hypertension etc.) (Nicholson et al., 2002). We tried to note the effect of various pre/intraoperative variables on hemodynamic perturbations; however, our study did not show any association with these.

The main finding of our present study is that out of 79 DBS procedures, approximately 82% showed hemodynamic events, and there were approximately 11 hemodynamic events per DBS procedure. Importantly, more than half of these events were treated, therefore suggesting clinically significant cardiovascular alterations. On the regression analysis model, only the pre-operative blood pressure and its all components (SBP, DBP, and MAP) have shown significant association with these hemodynamic perturbations (**Table 4**). Among all the components, the DBP shows the greatest association for causing adverse hemodynamic events. A study by Tsukamoto et al. has shown that patients with PD can present wide fluctuations in blood pressure readings (more than 100 mm HG difference) in a day, and contrary to common observation of orthostatic hypotension in such disease, these patients may also experience very high SBP (200 mmHg or more) (Tsukamoto et al., 2013). Therefore, it is imperative to stabilize the blood pressure swings in such patients.

One of the most serious complications of DBS surgery is intracranial bleed and its incidence can vary from 0.5 to 5% (Jain et al., 2012). Though it is a rare event it can be associated with permanent neurological deficit or even death (Jain et al., 2012; Wang et al., 2017). In our study, two patient developed neurological deficits due to intracranial hemorrhage. In a large case series and systemic review, age and hypertension are linked with increased incidence of intracranial bleed during functional neurosurgery (Sansur et al., 2007; Jain et al., 2012). In our study, approximately 75% of the patients having battery placement, 53% during electrode placement and 13% during nuclei stimulation showed hemodynamic perturbations. Strikingly, procedures involving electrode placement and nuclei stimulation were commonly associated with hypertensive episodes. One patient who had an intracranial bleed in our study showed hypertensive episodes during both the electrode placement and the stimulation phases. The mechanism of hypertension is not clearly understood yet; however, in a small case series (Green et al., 2010), the precise stimulation of periaqueductal gray matter incited cardiovascular changes including BP and HR changes (Hyam et al., 2012).

TABLE 4 | Regression model: event rate predicted by laterality of procedure and day of the procedure.

Factor	Rate ratio	95% confidence interval	*p*-value
TYPE OF NUCLEI			
GPi/STN	0.57	0.25–1.31	0.19
GPi/VIM	0.70	0.30–1.63	0.40
STN/VIM	1.21	0.72–2.03	0.46
BASELINE HEMODYNAMICS (PER 10 mmHg)			
Systolic BP	1.14	1.03–1.28	**0.01**
Diastolic BP	1.31	1.08–1.60	**0.01**
Mean BP	1.19	1.02–1.37	**0.02**
Baseline HR	1.23	0.94–1.60	0.11
LATERALITY OF DBS IMPLANTS			
Unilateral/Bilateral	0.99	0.57–1.72	0.98
BATTERY PLACEMENT DAY			
Same/Other	0.84	0.51–1.37	0.49

STN, Sub thalamic nucleus; VIM, Ventral intermediate; GPi, Internal globus pallidus; BP, Blood pressure.

Similarly, the STN stimulation may also cause hemodynamic perturbations that include a rise in HR (25 bpm) and BP (20 mm Hg). Our study also supports these findings. However, the laterality of these stimulations does not effect these changes (Sauleau et al., 2005) as also noted in our study. On the other hand, the battery placement was linked with more hypotensive and bradycardia episodes. These negative hemodynamic changes could be due to the combined effect of general anesthesia and autonomic dysfunctions related to neurodegenerative diseases. In our study, the day of battery placement did not reveal any association with such adverse events.

Limitation

This is a retrospective study and the clinical correlation of the findings would be more justifiable if a prospective study could be done with a continuous hemodynamic monitoring during various surgical steps. Further to this, tests to detect autonomic changes can be applied to detect the actual nature and cause of these hemodynamic events.

CONCLUSION

This study is the first detailed description of hemodynamic perturbations associated with DBS surgery in relation to influencing preoperative and intraoperative factors. Among all the factors, the baseline blood pressure does significantly affect the hemodynamic perturbations during the procedure and the DBP component has the highest impact on these events. Management of preoperative as well as intraoperative blood pressure is crucial to prevent major catastrophes during DBS procedure.

DISCLOSURE

This study abstract was submitted to 41st Annual Meeting of the Society for Neuroscience in Anesthesiology and Critical Care, San Francisco, CA and subsequently published in Journal of Neurosurgical Anesthesiology. 25(4): 440-501, October 2013. This abstract was also presented at Canadian anesthesia society meeting 2015, Ottawa.

ETHICS STATEMENT

This is a retrospective study and Ethics approval was given by Ethics committee, the University of Manitoba and Health Sciences Center [HS15730], Winnipeg, Canada.

AUTHOR CONTRIBUTIONS

TC is the primary author who has assisted substantially in developing the hypothesis, collecting and interpretation of the data, writing and editing the manuscript. MW has assisted in writing and providing the neurophysiological monitoring data. RC has assisted in developing the concept, writing and editing the manuscript.

FUNDING

This study is funded by the anesthesia oversight committee grant, department of anesthesiology and perioperative medicine, university of Manitoba, Winnipeg, Canada.

ACKNOWLEDGMENTS

We thank Dr. Jerry Krcek for giving his valuable insight for this study as well as our statistician Brenden Dufault for his valuable assistance in data analysis.

REFERENCES

Acevedo, A. R., Nava, C., Arriada, N., Violante, A., and Corona., T. (2000). Cardiovascular dysfunction in multiple sclerosis. *Acta Neurol. Scand.* 101, 85–88. doi: 10.1034/j.1600-0404.2000.101002085.x

Camerlingo, M., Ferraro, B., Gazzaniga, G. C., Casto, L., Cesana, B. M., and Mamoli, A. (1990). Cardiovascular reflexes in Parkinson's disease: long-term effects of levodopa treatment on de novo patients. *Acta Neurol. Scand.* 81, 346–348. doi: 10.1111/j.1600-0404.1990.tb01568.x

Chakrabarti, R., Ghazanwy, M., and Tewari, A. (2014). Anesthetic challenges for deep brain stimulation: a systematic approach. *North Am. J. Med. Sci.* 6, 359–369. doi: 10.4103/1947-2714.139281

Cicolini, G., Pizzi, C., Palma, E., Bucci, M., Schioppa, F., Mezzetti, A., et al. (2011). Differences in blood pressure by body position (supine, Fowler's, and sitting) in hypertensive subjects. *Am. J. Hypertens.* 24, 1073–1079. doi: 10.1038/ajh.2011.106

Green, A. L, Hyam, J. A, Williams, C., Wang, S., Shlugman, D., Stein, J. F, et al. (2010). Intra-operative deep brain stimulation of the periaqueductal grey matter modulates blood pressure and heart rate variability in humans. *Neuromodulation* 13, 174–181. doi: 10.1111/j.1525-1403.2010.00274.x

Haapaniemi, T. H., Pursiainen, V, Korpelainen, J. T., Huikuri, H. V., Sotaniemi, K. A., and Myllylä, V. V. (2001). Ambulatory ECG and analysis of heart rate variability in Parkinson's disease. *J. Neurol. Neurosurg. Psychiatry* 70, 305–310. doi: 10.1136/jnnp.70.3.305

Hyam, J. A., Kringelbach, M. L., Silburn, P. A, Aziz, T. Z, and Green, A. L. T. (2012). The autonomic effects of deep brain stimulation–a therapeutic opportunity. *Nat. Rev. Neurol.* 8, 391–400. doi: 10.1038/nrneurol.2012.100

Jain, S., and Goldstein, D. S. (2012). Cardiovascular dysautonomia in Parkinson disease: from pathophysiology to pathogenesis. *Neurobiol. Dis.* 46, 572–580. doi: 10.1016/j.nbd.2011.10.025

Jain, S., Ton, T. G., Perera, S., Zheng, Y., Stein, P. K., Thacker, E., et al. (2012). Cardiovascular physiology in premotor Parkinson's disease: a neuroepidemiologic study. *Mov. Disord.* 27, 988–995 doi: 10.1002/mds.24979

Mata, M., Toquero, J., and Lopez Lozano, J. J. (2012). Cardiovascular effects of deep brain stimulation of the subthalamic nucleus (DBS-STN) in Parkinson's disease (PD) [abstract]. *Mov. Disord.* 27(Suppl. 1), 1349.

Micieli, G., Tosi, P., Marcheselli, S., and Cavallini, A. (2003). Autonomic dysfunction in Parkinson's disease. *Neurol. Sci.* 24(Suppl. 1), S32–S34. doi: 10.1007/s100720300035

Nicholson, G., Pereira, A. C., and Hall, G. M. (2002). Parkinson's disease and anaesthesia. *Br. J. Anaesth.* 89, 904–916. doi: 10.1093/bja/aef268

Sansur, C. A., Frysinger, R. C., Pouratian, N., Fu, K. M., Bittl, M., Oskouian, R. J., et al. (2007). ncidence of symptomatic hemorrhage after stereotactic electrode placement. *J. Neurosurg.* 107, 998–1003. doi: 10.3171/JNS-07/11/0998

Sauleau, P., Raoul, S., Lallement, F., Rivier, I., Drapier, S., Lajat, Y., et al. (2005). Motor and non motor effects during intraoperative subthalamic nucleus stimulation for Parkinson's disease. *J. Neurol.* 252, 457–464. doi: 10.1007/s00415-005-0675-5

Shindo, K., Watanabe, H., Tanaka, H., Ohashi, K., Nagasaka, T., Tsunoda, S., et al. (2013). Age and duration related changes in muscle sympathetic nerve activity in Parkinson's disease. *J. Neurol. Neurosurg. Psychiatr.* 74, 1407–1411. doi: 10.1136/jnnp.74.10.1407

Tsukamoto, T., Kitano, Y., and Kuno, S. (2013). Blood pressure fluctuation and hypertension in patients with Parkinson's disease. *Brain Behav.* 3, 710–714. doi: 10.1002/brb3.179

Vigneri, S., Guaraldi, P., Calandra-Buonaura, G., Terlizzi, R., Cecere, A., Barletta, G., et al. (2012). Switching on the deep brain stimulation: effects on cardiovascular regulation and respiration. *Auton Neurosci.* 166, 81–84. doi: 10.1016/j.autneu.2011.09.002

Wang, X, Wang, J., Zhao, H., Li, N., Ge, S., Chen, L., et al. (2017). Clinical analysis and treatment of symptomatic intracranial hemorrhage after deep brain stimulation surgery. *Br. J. Neurosurg.* 31, 217–222. doi: 10.1080/02688697.2016.1244252

Zrinzo, L., Foltynie, T., Limousin, P., and Hariz, M. I. (2012). Reducing hemorrhagic complications in functional neurosurgery: a large case series and systematic literature review. *J. Neurosurg.* 116, 84–94. doi: 10.3171/2011.8.JNS101407

Conflict of Interest Statement: The authors declare that the research was conducted in the absence of any commercial or financial relationships that could be construed as a potential conflict of interest.

frontiers in Physiology

CASE REPORT
published: 07 March 2016
doi: 10.3389/fphys.2016.00079

Visualization of Heart Rate Variability of Long-Term Heart Transplant Patient by Transition Networks: A Case Report

Joanna Wdowczyk[1], Danuta Makowiec[2]*, Karolina Dorniak[3] and Marcin Gruchała[1]*

[1] 1st Chair and Clinic of Cardiology, Medical University of Gdańsk, Gdańsk, Poland, [2] Institute of Theoretical Physics and Astrophysics, University of Gdańsk, Gdańsk, Poland, [3] Department of Noninvasive Cardiac Diagnostics, 2nd Chair of Cardiology, Medical University of Gdańsk, Gdańsk, Poland

We present a heart transplant patient at his 17th year of uncomplicated follow-up. Within a frame of routine check out several tests were performed. With such a long and uneventful follow-up some degree of graft reinnervation could be anticipated. However, the patient's electrocardiogram and exercise parameters seemed largely inconclusive in this regard. The exercise heart rate dynamics were suggestive of only mild, if any parasympathetic reinnervation of the graft with persisting sympathetic activation. On the other hand, traditional heart rate variability (HRV) indices were inadequately high, due to erratic rhythm resulting from interference of the persisting recipient sinus node or non-conducted atrial parasystole. New tools, originated from network representation of time series, by visualization short-term dynamical patterns, provided a method to discern HRV increase due to reinnervation from other reasons.

Keywords: heart transplantation, heart rate variability, cardiac autonomic modulation, reinnervation, arrhythmias, hearth rhythm dynamics

OPEN ACCESS

Edited by:
Tijana Bojić,
University of Belgrade, Serbia

Reviewed by:
Gavin W. Lambert,
Baker IDI Heart and Diabetes Institute, Australia
Kurt Kimpinski,
University of Western Ontario, Canada

****Correspondence:***
Joanna Wdowczyk
wdowczyk@gumed.edu.pl;
Danuta Makowiec
fizdm@ug.edu.pl

Specialty section:
This article was submitted to Autonomic Neuroscience, a section of the journal Frontiers in Physiology

Received: *15 November 2015*
Accepted: *17 February 2016*
Published: *07 March 2016*

Citation:
Wdowczyk J, Makowiec D, Dorniak K and Gruchała M (2016) Visualization of Heart Rate Variability of Long-Term Heart Transplant Patient by Transition Networks: A Case Report. Front. Physiol. 7:79. doi: 10.3389/fphys.2016.00079

1. INTRODUCTION

In patients with end-stage heart disease, heart transplantation (HTx) is associated with significant improvement in survival and in quality of life. However, after HTx multiple adverse events may occur, including acute rejections, graft failure, infections, allograft vasculopathy and arrhythmias including atrial fibrillation, all of which adversely affect long term survival. Complete denervation of the transplant significantly affects reactivity of transplanted heart and hemodynamics of circulation (Willmann et al., 1963).

Cardiac reinnervation, both sinus and myocardial, was extensively studied with a variety of methods, including heart rate variability (HRV), PET with C-11 hydroxyephedrine, MIBI-SPECT and others, and proved non-uniform and occurring at variable time (Kaye et al., 1993; Uberfuhr et al., 2000; Vanderlaan et al., 2012; Imamura et al., 2014). Higher HRV indices were associated with graft reinnervation by many authors (Uberfuhr et al., 2000; Cornelissen et al., 2012; Vanderlaan et al., 2012). On the other hand, low HRV values were associated with hypertension and increased incidence of graft vasculopathy, even in pediatric patients (Giordano et al., 2013). Moreover, HRV values in HTx patients can be confounded by certain transplant-specific factors, such as type of the surgery and time passed after the surgery (Uberfuhr et al., 2000). Nevertheless, HRV analysis is commonly assumed as providing insight in both sympathetic and parasympathetic allograft sinus reinnervation, which was demonstrated to improve outcome (Vanderlaan et al., 2012).

We present a HTx patient at his 17th year of uncomplicated follow-up. Within a frame of routine check out several tests were performed. With such a long and uneventful follow-up some degree of graft reinnervation could be anticipated. However, the patient's ECG Holter and exercise parameters seemed largely inconclusive in this regard. The exercise heart rate (HR) dynamics were suggestive of only mild, if any parasympathetic reinnervation of the graft with persisting sympathetic activation via plasma catecholamines. On the other hand, traditional HRV indices were inadequately high, due to erratic rhythm resulting from interference of the persisting recipient sinus node or non-conducted atrial parasystole.

To elucidate post-HTx HRV values (e.g., to discern between HRV increase due to post-HTx rhythm alterations such as non-conducted atrial parasystole, recipient sinus activity or true reinnervation effect), new tools are clearly needed. Here we represent the short-term dynamics of nocturnal RR-intervals by the novel complex network tools (a transition network and its adjacency matrix, Donner et al., 2010; Makowiec et al., 2014, 2015) and explore the visualization of this representation in assessment of HRV.

2. BACKGROUND

2.1. Case Presentation

A 68-year-old male patient 17 years after heart transplant was referred to our outpatient clinic for a regular follow-up. The patient was transplanted by biatrial method due to end-stage heart failure following a viral infection in July 1997. The Donor was a 37-year-old male without known risk factors. Postoperative course was uneventful under immunosuppression therapy with cyclosporin with no rejection episodes. The patient's post-HTx history included well controlled hypertension, mild chronic kidney disease, and prostatic hypertrophy.

Physical examination revealed good overall clinical condition, with normal blood pressure of 140/90 and a regular heart rate of 85/min. Standard laboratory findings were within reference ranges except for creatinine level of 1.5 mg/dL and GFR of 45 mL/min. Standard ECG demonstrated a regular sinus rhythm of 85 bpm, QRS duration within normal range and no ST segment deviation or T-wave abnormalities. Echocardiography revealed normal left ventricular function with EF of 60% and mild left ventricular hypertrophy of the graft that was noted during follow-up. Coronary angiography (2 years prior) showed normal coronary arteries without features of graft vasculopathy. Last myocardial biopsy performed in 2013 showed no signs of cellular rejection (ACR Grade 0 R). Standard graded cycle ergometry exercise test limited by exhaustion was performed (target HR was not used). Resting heart rate (82 beats/min) and BP values (140/84 mmHg), slowly increased up to 100 beats/min and 185/90 mmHg, respectively over 7 min. Maximal workload achieved was 75 W. During recovery phase a delayed HR recovery was noted, with HR gradually returning to its baseline value over 9 min.

2.2. HRV analysis

24-h Holter monitoring was performed. The recording was first analyzed using Del Mar Impresario Software. Time domain and frequency domain analysis of HRV was carried out, preceded by visual inspection of the automatic ECG recording. All supraventricular and ventricular extrasystoles were excluded. The nocturnal 6-h part was determined following the evident day-night switch in the length of RR-intervals. Highly irregular sinus rhythm pattern erratic rhythm - together with values of basic indices of HRV can be seen in **Figure 1** (by Kubios HRV Pro V 2.0, Tarvainen et al., 2014). Close ECG examination revealed non-conducted atrial parasystole and P wave originated from the recipient sinus rhythm resulting in inappropriately high values of time and frequency measures. Non-linear analysis methods were also used. Long-term fractal scaling exponent measured by the detrended fluctuation analysis method in long-term RR-interval fluctuations and the shape of Poincare plot of each RR-interval vs the next, demonstrated increased randomness of heart rate patterns.

For additional analysis, a transition network—a novel network tool of time series representation (Donner et al., 2010; Makowiec et al., 2014, 2015), was applied to changes in subsequent RR-intervals, called RR-increments. The transition network is constructed from ordered RR-increments (called vertices) which are connected by an edge if two RR-increments are adjacent in time. Repetitive edges are represented by a weight of an edge. In consequence, each vertex has the weight (a total of weights of adjacent edges) which means probability of a given RR-increment. In **Figure 2**, the probabilities of RR-increments are shown. Additionally, there are given probabilities obtained for a healthy typical coeval, a typical HTX patient early after surgery, and the same patient but 7 years earlier. The noticeable over-presence of large accelerations (larger than 100 ms) and large deceleration (larger than 100ms) in the signal of the considered patient explains huge values of standard HRV indices.

An adjacency matrix is a mathematical representation of weights of edges in a transition network. It shows probability that a pair of RR-increments appears consecutively in a time series. In **Figure 3**, the adjacency matrices are shown as density plots of the same signals as in **Figure 2**. These plots present the probabilities of physiologically justified accelerations and decelerations (RR-increments smaller than 100 ms). The resulting density plot organization in the patient at 17th year post-HTx is markedly different from the respective plots in a recently transplanted HTx patient (1 year post-HTx) or in a healthy sexagenarian volunteer. It is also clearly different from previous examinations of our patient (conducted at the 10th year post-HTx).

3. DISCUSSION

Following HTx, the loss of autonomic input to the allograft, (with greater impact of reduced parasympathetic activity), results in persistently elevated resting heart rate and decreased chronotropic reserve (Willmann et al., 1963). This is illustrated by the highly condensed adjacency matrix in a patient 1 year post-transplant (see, **Figure 3**). Decreased HRV indices at various time

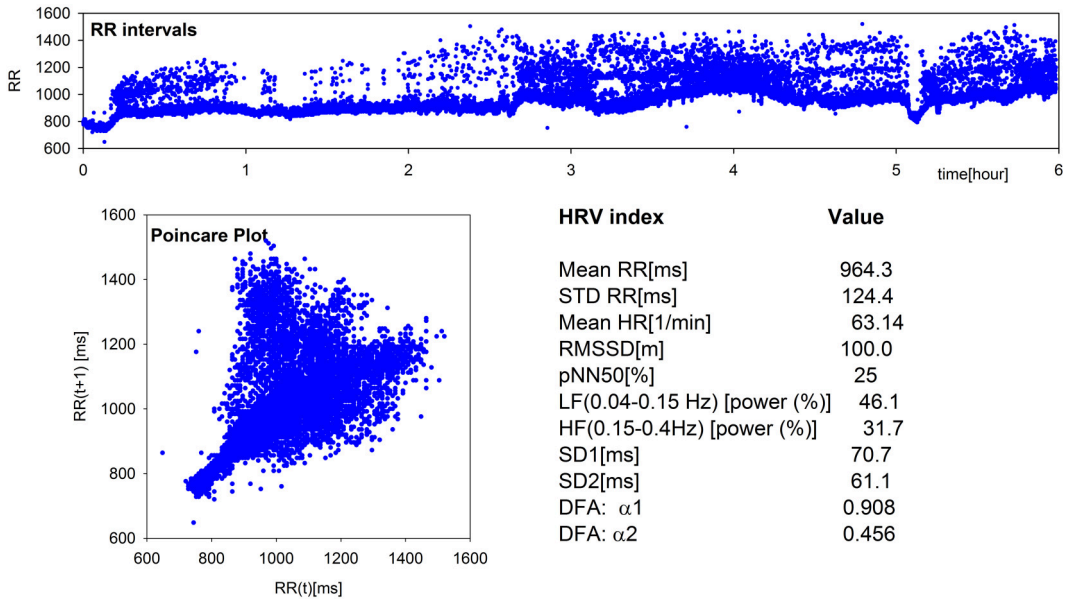

FIGURE 1 | Elements of standard and non-linear HRV analysis: plot of RR-intervals time series, Poincare Plot, and values of the main HRV indices obtained from the 6-h nocturnal RR-signal of the patient under study. Estimates were performed by Kubios HRV Pro V2.0 (Tarvainen et al., 2014).

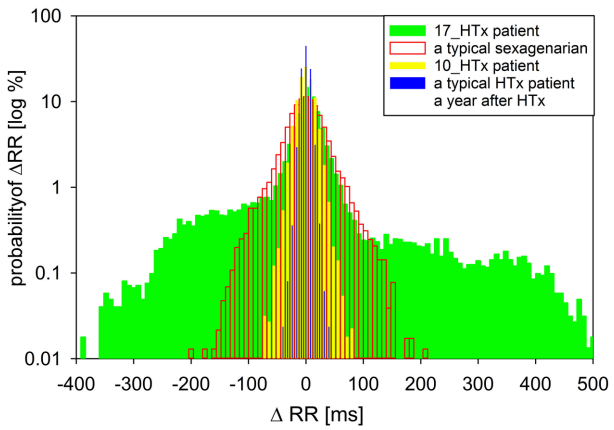

FIGURE 2 | A comparison of the distribution of increments $\Delta RR(t) = RR(t) - RR(t-1)$ for the nocturnal 6-h signal obtained from the patient under study when he was 17 years after HTx to distributions of RR-increments obtained from nocturnal recordings of a typical sexagenarian, the patient under study when he was 10 years after HTx and a typical HTx patient when a person was a year after HTx.

points of the post-transplant period suggest that the transplanted heart may have not be reinnervated. However, a degree of vagal reinnervation as assessed by HF power spectral analysis was demonstrated as early as in the first 6 months post-HTx (Imamura et al., 2014). Sympathetic reinnervation (as assessed by increased LF/HF and total power) has also been documented over the first 18 months post-HTx, though it is not simply a function of time. Reinnervation was shown to be more likely at younger age, after short uncomplicated surgery, and with low rejection rates (Bengel et al., 2002). Moreover, HRV indices can potentially be misleading due to interfering recipient sinus activity or non-conducted arrhythmias in some patients. Nevertheless, HRV analysis was used extensively to assess autonomic reinnervation in HTx recipients as it still is the most accessible clinical surrogate of reinnervation (Bengel et al., 2001; Imamura et al., 2014).

In our patient, HR response to workload during the first minutes of exercise was restored to some extent, not only due to some degree of reinnervation but also it continues to respond to plasma catecholamines (Kaye et al., 1993). Also, his baseline HR was close to 80 bpm, which is similar to resting HR reported by Imamura in patients with presumed post-HTx reinnervation (Imamura et al., 2014) as opposed to those lacking innervation in whom resting HR was at the level of 90 bpm (Wilson et al., 2000). HR recovery, however, was suggestive of poor parasympathetic reinnervation in our patient (Imamura et al., 2015).

When the biatrial method of heart transplantation is used, several specific heart rhythm alterations may occur. Activation of the recipient atrial tissue may be evident on ECG. In combination with graft P waves the native P waves may mimic atrial flutter (Elsik et al., 2012). Reestablishment of conduction across atrial anastomosis may produce recipient-to-donor conduction of sinus beats, atrial parasystole or tachycardia because of fibrillatory activity in the recipient atrium. Sinus activity of the recipient atrium may also escape into the donor atrium intermittently. Thus, in addition to reinnervation, an increasingly conduction of the suture line between the recipient atrium and the donor atrium could produce atrio-atrial on/off mechanism, predisposing to erratic rhythm and falsely increased HRV. The scars in the atria act as conduction barriers and can also predispose to atrial flutter (Elsik et al., 2012). In this case part of the heart rate variability (HRV) arises from a biatrial surgical technique and interference of the persisting recipient sinus node,

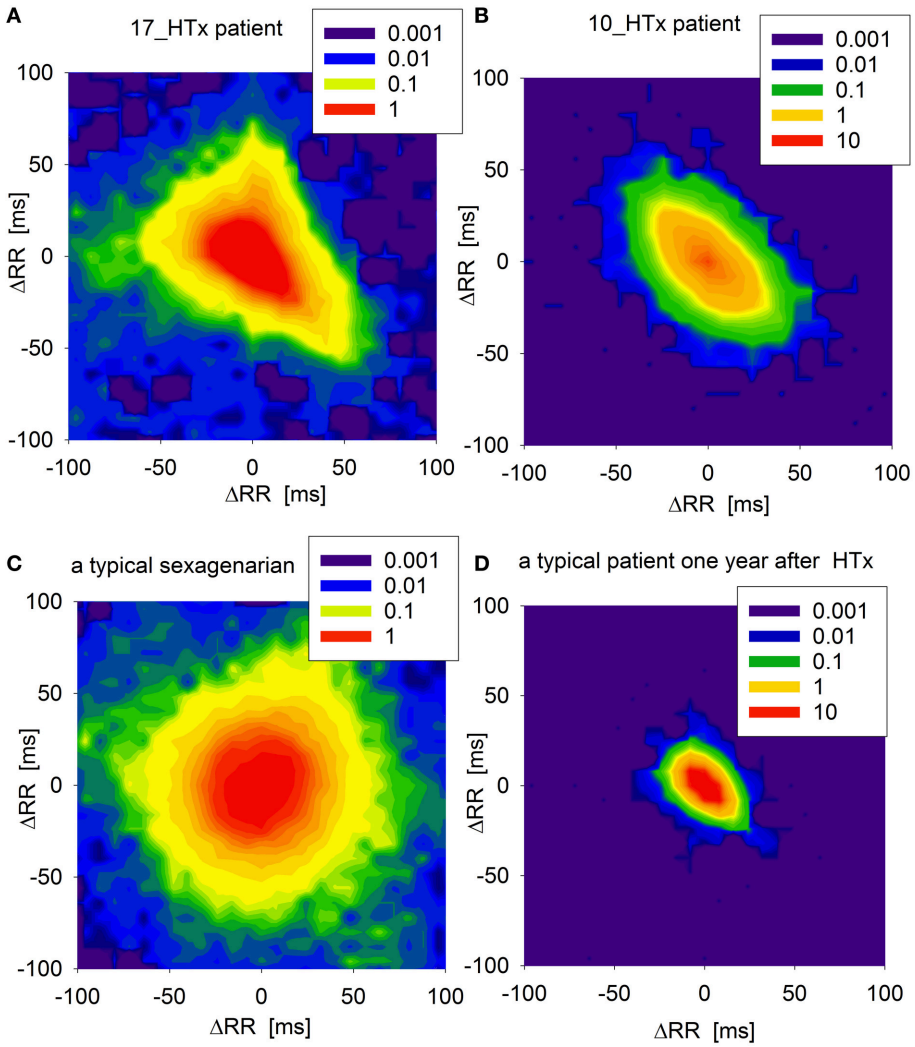

FIGURE 3 | Adjacency matrices of transition networks obtained from increments ΔRR as probability density plots (in log[%]) of the core parts of networks, (i.e., when accelerations and decelerations ΔRR are smaller than 100 ms) for: (A) the patient under study when he was 17 years after HTx , (B) the patient under study when he was 10 years after HTX, (C) a typical sexagenarian, and (D) a typical HTx patient a year after HTx.

see **Figure 2**. This situation makes it questionable whether any type of analysis of the HRV allows conclusions about the degree of reinnervation.

Sleep, in general, can be assumed as a period of human activity which is free of external stimulation. Therefore, the nocturnal part of a 24-h Holter recording provides a good possibility of observing the state of the autonomic baseline (Stein and Pu, 2012; Chouchou and Desseilles, 2014; Makowiec et al., 2015). A recent review (Stein and Pu, 2012) advocates using nocturnal records for HRV analysis. However, as sleep is organized in cycles, switches between non-REM (with high vagal activity) and REM (increased sympathetic stimulation) sleep may contribute to the observed erratic patterns.

As shown in **Figure 3**, signals from a healthy volunteer result in transition networks with many dynamics patterns playing an equivalent role. Signals from a typical HTx patient in the early post-transplant period provide networks in which accelerations are more probable to be followed by decelerations and vice verse. Moreover, the transitions are concentrated around the smallest RR-increments possible.The similar structure, but extended to RR-increments of larger size, can be read from the plot of the patient 10 years after HTx. Such a picture can be seen as the increase of direct autonomic regulation resulting from the emergence of reinnervation. However, the signal from our patient recorded 17 years post-HTx shows strange asymmetry between accelerations and decelerations suggesting that the basic dynamical pattern is distinct from both a healthy sexagenarian and a healthy post-HTx patient.

4. CONCLUDING REMARKS

We have presented a case of a patient, many years after heart transplant, with good functional status, and discussed if dynamics of RR-intervals and RR-increments as assessed

by tools based on complex network analysis applied to 24-h ECG recording, could provide more insight into physiological background of the standard HRV measures. Especially we expected to find means for assessing the reinnervation process. However, we have found a strong presence of erratic rhythms which dominated the classic HRV information and gave the false description about the activity of autonomic system. Nevertheless, this finding is important for the patient as it could switch further to supraventricular arrhythmia.

The method used—graphs of adjacency matrices of transition networks, can be compared to the technique of Poincare plots, now applied to signals of RR-increments. By its very nature it offers insight into dynamical interbeat dependencies: are they stochastic like (rhythm of sexagenarians) or fixed (a year after HTx) or structured irregular (with erratic rhythms). Obviously, our analysis can be extrapolated to larger group of subjects, especially, in a follow-up study because development of arrhythmias increases with time passed after the HTx (Thajudeen et al., 2012). We work on a full paper regarding validity of the method in which we compare groups of patients at different stages after HTx.

Further research based on augmented pool of data is needed, to assess clinical applicability of the new tools and their potential to provide additional insight in graft electrophysiology beyond standard surrogate measures of reinnervation, such as classical HRV analysis and HR response to workload. High vigilance and advanced diagnostic tools to assess allograft status are mandatory to allow for appropriate intervention in allograft-related syndromes that may emerge with improved survival of patients after transplantation.

INFORMED CONSENT STATEMENT

The study complied with the Declaration of Helsinki and was approved by the Bioethics Commission for Research of the Medical University of Gdańsk. The written informed consent was obtained from the study subject.

AUTHOR CONTRIBUTIONS

JW, DM, and MG: substantial contributions to the conception and design of the work; JW: the acquisition of the data; KD: interpretation of data, revising it critically for important intellectual conent; MG: final approval of the version to be published; JW, DM: analysis, and interpretation of data, drafting the work, revising it critically for important intellectual content and approval of the final version to be submitted; the final revision of the resubmission. All authors agreed to be accountable for all aspects of the work in ensuring that questions related to the accuracy or integrity of any part of the work are appropriately investigated and resolved.

ACKNOWLEDGMENTS

The authors acknowledge the financial support of the National Science Centre, Poland, UMO: 2012/06/M/ST2/00480.

REFERENCES

Bengel, F. M., Ueberfuhr, P., Hesse, T., Schiepel, N., Ziegler, S. I., Scholz, S., et al. (2002). Clinical determinants of ventricular sympathetic reinnervation after orthotopic heart transplantation. *Circulation* 106, 831–835. doi: 10.1161/01.CIR.0000025631.68522.9D

Bengel, F. M., Ueberfuhr, P., Schiepel, N., Nekolla, S. G., Reichart, B., and Schwaiger, M. (2001). Effect of sympathetic reinnervation on cardiac performance after heart transplantation. *N. Engl. J. Med.* 345, 731–738. doi: 10.1056/NEJMoa010519

Chouchou, F., and Desseilles, M. (2014). Heart rate variability: a tool to explore the sleeping brain? *Front. Neurosci.* 8:402. doi: 10.3389/fnins.2014.00402

Cornelissen, V. A., Vanhaecke, J., Aubert, A. E., and Fagard, R. H. (2012). Heart rate variability after heart transplantation: a 10-year longitudinal follow-up study. *J. Cardiol.* 59, 220–224. doi: 10.1016/j.jjcc.2011.12.002

Donner, R. V., Zou, Y., Donges, J. F., Marwan, N., and Kurths, J. (2010). Recurrence networks - a novel paradigm for nonlinear time series analysis. *N. J. Phys.* 12, 033025. doi: 10.1088/1367-2630/12/3/033025

Elsik, M., Teh, A., Ling, L.-H., Virdee, M., Parameshwar, J., Fynn, S. P., et al. (2012). Supraventricular arrhythmias late after orthotopic cardiac transplantation: electrocardiographic and electrophysiological characterization and radiofrequency ablation. *Europace* 14, 1498–1505. doi: 10.1093/europace/eus092

Giordano, U., Michielon, G., Calò Carducci, F., Ravàà, L., Alfieri, S., Parisi, F., et al. (2013). Heart rate variability arterial hypertension in young heart-transplanted recipients: association progression of cardiac allograft vasculopathy? *Pediatr. Transplant.* 17, 441–444. doi: 10.1111/petr.12105

Imamura, T., Kinugawa, K., Fujino, T., Inaba, T., Maki, H., Hatano, M., et al. (2014). Recipients with shorter cardiopulmonary bypass time achieve improvement of parasympathetic reinnervation within 6 months after heart transplantation. *Int. Heart J.* 55, 440–444. doi: 10.1536/ihj.14-111

Imamura, T., Kinugawa, K., Okada, I., Kato, N., Fujino, T., Inaba, T., et al. (2015). Parasympathetic reinnervation accompanied by improved post-exercise heart rate recovery and quality of life in heart transplant recipients. *Int. Heart J.* 56, 180–185. doi: 10.1536/ihj.14-292

Kaye, D. M., Esler, M., Kingwell, B., McPherson, G., Esmore, D., and Jennings, G. (1993). Functional and neurochemical evidence for partial cardiac sympathetic reinnervation after cardiac transplantation in humans. *Circulation* 88, 1110–1118. doi: 10.1161/01.CIR.88.3.1110

Makowiec, D., Wejer, D., Kaczkowska, A., Zarczynska-Buchowiecka, M., and Struzik, Z. R. (2015). Chronographic imprint of age-induced alterations in heart rate dynamical organization. *Front. Physiol.* 6:201. doi: 10.3389/fphys.2015.00201.

Makowiec, D., Struzik, Z. R., Graff, B., Żarczyńska-Buchowiecka, M., and Wdowczyk, J. (2014). Transition network entropy in characterization of complexity of heart rhythm after heart transplantation. *Acta Phys. Pol. B* 45, 1771–1781. doi: 10.5506/APhysPolB.45.1771

Stein, P. K., and Pu, Y. (2012). Heart rate variability, sleep and sleep disorders. *Sleep Med. Rev.* 16, 47–66. doi: 10.1016/j.smrv.2011.02.005

Tarvainen, M. P., Niskanen, J.-P., Lipponen, J. A., Ranta-Aho, P. O., and Karjalainen, P. A. (2014). Kubios hrv - heart rate variability analysis software. *Comput. Methods Prog. Biomed.* 113, 210–220. doi: 10.1016/j.cmpb.2013.07.024

Thajudeen, A., Stecker, E. C., Shehata, M., Patel, A., Wang, X., McAnulty, J. H., et al. (2012). Arrhytmias after heart transplantation: mechanisms and management. *J. Am. Heart Assoc.* 1:e6001461. doi: 10.1161/JAHA.112.001461

Uberfuhr, P., Frey, A. W., and Reichart, B. (2000). Vagal reinnervation in the long term after orthotopic heart transplantation. *J. Heart Lung. Transplant.* 19, 946–950. doi: 10.1016/S1053-2498(00)00181-9

Vanderlaan, R. D., Conway, J., Manlhiot, C., McCrindle, B. W., and Dipchand, A. I. (2012). Enhanced exercise performance and survival associated with evidence of autonomic reinnervation in pediatric heart transplant recipients. *Am. J. Transplant.* 12, 2157–2163. doi: 10.1111/j.1600-6143.2012.04046.x

Willmann, V., Cooper, T., Cian, L., and Rollins, C. (1963). Neural responses following autotransplantation of the canine heart. *Circulation* 27, 713–716. doi: 10.1161/01.CIR.27.4.713

Wilson, R. F., Johnson, T. H., Haidet, G. C., Kubo, S. H., and Mianuelli, M. (2000). Sympathetic reinnervation of the sinus node and exercise hemodynamics after cardiac transplantation. *Circulation* 101, 2727–2733. doi: 10.1161/01.CIR.101.23.2727

Conflict of Interest Statement: The authors declare that the research was conducted in the absence of any commercial or financial relationships that could be construed as a potential conflict of interest.

frontiers in Neuroscience

ORIGINAL RESEARCH
published: 12 October 2017
doi: 10.3389/fnins.2017.00540

Modulation of Cardiac Autonomic Function by Fingolimod Initiation and Predictors for Fingolimod Induced Bradycardia in Patients with Multiple Sclerosis

Kai Li[1,2], *Urszula Konofalska*[3], *Katja Akgün*[3], *Manja Reimann*[1], *Heinz Rüdiger*[1], *Rocco Haase*[1] *and Tjalf Ziemssen*[1,3*]

[1] *Autonomic and Neuroendocrinological Lab, Center of Clinical Neuroscience, University Hospital Carl Gustav Carus, Dresden University of Technology, Dresden, Germany,* [2] *Department of Neurology, Beijing Hospital, National Center of Gerontology, Beijing, China,* [3] *MS Center, Center of Clinical Neuroscience, University Hospital Carl Gustav Carus, Dresden University of Technology, Dresden, Germany*

Objective: It is well-known that initiation of fingolimod induces a transient decrease of heart rate. However, the underlying cardiac autonomic regulation is poorly understood. We aimed to investigate the changes of autonomic activity caused by the first dose of fingolimod using a long-term multiple trigonometric spectral analysis for the first time. In addition, we sought to use the continuous Holter ECG recording to find predictors for fingolimod induced bradycardia.

Methods: Seventy-eight patients with relapsing-remitting multiple sclerosis (RRMS) were included. As a part of the START study (NCT01585298), continuous electrocardiogram was recorded before fingolimod initiation, and until no <6 h post medication. Time domain and frequency domain heart rate variability (HRV) parameters were computed hourly to assess cardiac autonomic regulation. A long-term multiple trigonometric regressive spectral (MTRS) analysis was applied on successive 1-h-length electrocardiogram recordings. Decision tree analysis was used to find predictors for bradycardia following fingolimod initiation.

Results: Most of the HRV parameters representing parasympathetic activities began to increase since the second hour after fingolimod administration. These changes of autonomic regulations were in accordance with the decline of heart rate. Baseline heart rate was highly correlated with nadir heart rate, and was the only significant predicting factor for fingolimod induced bradycardia among various demographic, clinical and cardiovascular variables in the decision tree analysis.

Conclusions: The first dose application of fingolimod enhances the cardiac parasympathetic activity during the first 6 h post medication, which might be the underlying autonomic mechanism of reduced heart rate. Baseline heart rate is a powerful predictor for bradycardia caused by fingolimod.

Keywords: fingolimod, multiple sclerosis, cardiac autonomic function, multiple trigonometric regressive spectral analysis, bradycardia, heart rate variability (HRV)

OPEN ACCESS

Edited by:
Tijana Bojić,
University of Belgrade, Serbia

Reviewed by:
Michal Javorka,
Comenius University, Slovakia
Max-Josef Hilz,
University of Erlangen-Nuremberg, Germany

***Correspondence:**
Tjalf Ziemssen
tjalf.ziemssen@uniklinikum-dresden.de

Specialty section:
This article was submitted to Autonomic Neuroscience, a section of the journal Frontiers in Neuroscience

Received: *28 March 2017*
Accepted: *15 September 2017*
Published: *12 October 2017*

Citation:
Li K, Konofalska U, Akgün K, Reimann M, Rüdiger H, Haase R and Ziemssen T (2017) Modulation of Cardiac Autonomic Function by Fingolimod Initiation and Predictors for Fingolimod Induced Bradycardia in Patients with Multiple Sclerosis. Front. Neurosci. 11:540. doi: 10.3389/fnins.2017.00540

INTRODUCTION

Fingolimod is highly effective for the treatment of relapsing-remitting multiple sclerosis (RRMS; Cohen et al., 2010; Calabresi et al., 2014). Its therapeutic effect is mediated by the modulation of sphingosine-1-phosphate (S1P) receptors in the lymphocytes and neural cells. Besides, S1P receptors also exist in cardiac myocytes (Brinkmann et al., 2010; Camm et al., 2014). Therefore, the first dose of fingolimod can lead to a transient decrease of heart rate (HR), which has been a major concern in the first years after its approval (Camm et al., 2014). A lot of clinical data have proven the cardiac safety of fingolimod in the real world until now (Limmroth et al., 2017; Ziemssen et al., 2017). That is why a specific first dose monitoring procedure should be included in the risk-management plan of fingolimod (Thomas et al., 2017).

HR is regulated by the autonomic nervous system. Spectral analysis of heart rate variability (HRV) is a valuable tool for the quantitative evaluation of the fluctuations of HR, and can reflect the parasympathetic activities of cardiac autonomic function (Task Force of the European Society of Cardiology and the North American Society of Pacing and Electrophysiology, 1996). Unlike the well-known HR change caused by fingolimod, the alteration of cardiovascular autonomic function following fingolimod initiation has been less described. Recently, Simula et al. (2017) and Hilz et al. (2017) reported the sequence of cardiovascular autonomic parameter changes following fingolimod initiation. These two studies showed that HRV parameters representing parasympathetic modulation increased after fingolimod initiation, but there are some inconsistencies between them and both studies enrolled a relatively small sample of patients with RRMS. It should be noted that they applied different approaches, Simula et al. employed an hourly spectral analysis with fast Fourier transform on continuous ECG recordings of several hours and Hilz et al. utilized a spectral analysis with trigonometric regressive spectral (TRS) analysis on short ECG and beat-to-beat blood pressure recording segments of 2 min.

Most commonly, a power spectral analysis of HRV is performed through the fast Fourier transform, which requires equal distance between adjacent heart beats (RR interval, RRI). However, RRIs are non-equidistant and therefore interpolation is needed. The interpolation for the fast Fourier transform can affect the accuracy of spectral analysis (Rudiger et al., 1999; Ziemssen et al., 2008, 2013). Unlike the fast Fourier transform, TRS analysis does not need interpolation on non-equidistant RRIs. Alternatively, it analyzes the original RRI and blood pressure data and obtains the spectral components more accurately by using a trigonometric regression (Rudiger et al., 1999; Ziemssen et al., 2013). Its excellent performance has been verified by the EuroBaVar study (Laude et al., 2004). TRS analysis has not been employed in the analyses of the hourly HRV changes following the first dose of fingolimod using continuous Holter ECG recordings so far. Furthermore, TRS analysis is traditionally applied on the manually chosen 1–2 min electrocardiogram (ECG) segments (Reimann et al., 2010, 2012). In the present study, we are the first to use a long-term spectral analysis technique via TRS to calculate hourly HRV parameters using Holter ECG recordings. To achieve this aim, we developed a strategy of analyzing all the successive 1-min-length ECG segments of the entire ECG time window, and then we can generate the hourly averaged HRV parameters. This approach would make full use of the recorded continuous ECG information and yield more stable results.

In clinical practice, a predictor for fingolimod induced bradycardia would help physicians select appropriate patients and decide proper monitoring strategies. Several studies explored the relationship between autonomic function testing before fingolimod administration and the fingolimod-induced HR response. Simula et al. (2016) demonstrated that the percentage of successive normal RR intervals differing by >50 ms (pNN50) calculated by the 24-h ECG recording at baseline was associated with HR decline caused by fingolimod. Rossi and colleagues revealed the correlation between Valsalva ratio, HR variation in metronomic deep breathing and bradycardia resulted from fingolimod (Rossi et al., 2015). Hilz et al. (2015) demonstrated that a comprehensive autonomic battery could detect autonomic dysfunction in patients with delayed HR recovery after fingolimod intake. Although these studies used a small sample size, they suggested that HRV might be promising in predicting fingolimod induced HR decline. But their approaches require a professional autonomic testing laboratory or a 24-h ECG recording before medication. A continuous ECG monitoring after the first dose of fingolimod is recommended by the European Medicine Agency (EMA) and commonly used in clinical practice. We assumed that the HRV parameters obtained from continuous ECG might facilitate the identification of patients with high risk for bradycardia after fingolimod initiation, and might provide a convenient predictor for daily clinical use (Thomas et al., 2017).

This study sought to demonstrate the change of HRV parameters within 6 h after fingolimod intake, and tried to find convenient predictors for bradycardia induced by fingolimod in a relatively large patient sample.

METHODS

Participants

Eighty-one patients with RRMS were consecutively included in this study as a Dresden sub-study of the multicenter START study (NCT01585298; Limmroth et al., 2017). The diagnosis of RRMS was based on the McDonald criteria (Polman et al., 2011). Fingolimod was prescribed at a daily dose of 0.5 mg according to the label set by the EMA. The patients were either with highly disease activity despite an adequate treatment with at least one disease modifying therapy, or with rapidly evolving severe RRMS. Only patients older than 18 years were enrolled. Exclusion criteria included: using antiarrhythmic medication or other drugs which may reduce HR; with a history of second degree Mobitz Type II or higher-degree AV block, sick-sinus syndrome, sinoatrial heart block, significant QT prolongation, symptomatic bradycardia or recurrent syncope; with known ischemic heart disease, cerebrovascular disease, myocardial infarction, hypokalemia, congestive heart failure,

cardiac arrest, uncontrolled hypertension, or severe sleep apnea. Demographical and clinical information including the Expanded Disability Status Scale (EDSS) scores of the patients was collected.

The study was in accordance with relevant guidelines and regulations, and approved by the Institutional Review Board of University Hospital Carl Gustav Carus. This study was carried out according to the Declaration of Helsinki. All the subjects gave written informed consent prior to participation.

Study Procedures

Fingolimod was administered before 10:00 in the morning. The patients' brachial blood pressure (using the mercury sphygmomanometer) and HR were measured before medication and every hour for at least 6 h after medication. Continuous 12-lead ECG recording was performed using CardioMed CM3000-12 (Getemed, Teltow, Germany) since 1 h before medication, and until no <6 h post medication. In general, the patients were in a sedentary state in the waiting room of our hospital during the ECG monitoring, although their physical activity was not restricted and they breathed freely. All the ECG recordings were checked by a cardiology expert for any abnormalities.

Heart Rate Variability Analysis

Mean HR was computed from mean RRI of each hour, and bradycardia was defined as a HR < 60 bpm (Camm et al., 2014). Time domain parameters including the standard deviation of normal RR intervals (SDNN), the root mean square of successive differences of RR-intervals (RMSSD), and pNN50 were calculated hourly according to well-accepted standards (Task Force of the European Society of Cardiology and the North American Society of Pacing and Electrophysiology, 1996). The frequency domain parameters were computed by the long-term multiple trigonometric regressive spectral (MTRS) analysis.

In general, TRS analysis is working with a single time window (local data segments) in the range of 20–60 s. The regression function in TRS has a general form: Reg (t) = A∗sin(ωt+ψ); A is the amplitude, ωt is the angular frequency, and ψ is the phase shift of the trigonometric regression function Reg (t). To determine the function Reg (t), we need to make the deviations of Reg (t) from the original values minimal: F = Σ (RRI (t) –Reg (t))2 = Min and /or dF = 0. By pursuing a minimal deviation of Reg (t), we can determine the variables A, ω, and ψ with the help of partial differential quotients through the following equations: dF/dA = 0; df/dω = 0; df/d ψ = 0. Then optimal oscillations can be found by variation of the frequency for a maximal adaption to the original RR intervals (Rudiger et al., 1999; Ziemssen et al., 2013).

By shifting these local data segments with one, two or more beats, it is possible to measure the time variability over a global ECG data segment of 1–3 min (consisting of *multiple* local data segments). In this case TRS analysis is called MTRS analysis. This procedure guarantees a statistically representative spectral analysis for the global data segment (Rudiger et al., 1999; Ziemssen et al., 2013). Traditionally, we manually chose a stable segment of 1–2 min as the global data segment, within which local data segments of 30 s were analyzed and shifted beat by beat to determine the frequency domain parameters of the selected global data segment (Reimann et al., 2010, 2012). In the present study, we also used a local time window of 30 s, and this was shifted beat by beat within a global data segment of 1 min. After that, spectral results obtained from these global 1-min segments (60 global segments in an hour) were averaged over the entire hour. Artifacts and extrasystoles were manually identified and corrected. Low frequency power of HRV (LF), and high frequency power of HRV (HF) were calculated through the long-term MTRS analysis. LF power is the spectral component between 0.04 and 0.15 Hz, and HF power is the spectral component between 0.15 and 0.4 Hz. LF and HF were expressed as absolute values, as well as relative values which were the proportions (in percent) of LF and HF powers in the total power. HF represents mainly the parasympathetic cardiovagal tone, while there are controversies in the interpretation of LF. The Task Force of the European Society of Cardiology and the North American Society of Pacing and Electrophysiology (1996) considered LF as a parameter that included both sympathetic and vagal influences, while some researchers disagree with this opinion (Reyes del Paso et al., 2013).

Statistical Analysis

All statistical analyses were performed using SPSS for Windows (Version 23.0. Armonk, NY: IBM Corp). Data are presented as mean ± standard error of the mean (SEM) unless stated otherwise. Normality of variables was assessed by the Kolmogorov–Smirnov test. Logarithmic (ln) transformation was used in right-skewed variables if applicable. Changes of the measurements across different time points were tested by the repeated measures ANOVA. Greenhouse-Geisser correctional adjustment was applied if the assumption of sphericity was violated. To explore potential modifying factors, sex was included as a between-subjects factor, while age and EDSS were added as covariates. For variables with a non-normal distribution, Friedman test was performed to assess the changes between different time points. *Post-hoc* analyses were adjusted by the Bonferroni method.

Based on the data distribution, Pearson (normal) or Spearman's (non-normal) correlation was used to explore the associations between demographic and clinical variables, cardiovascular parameters and the nadir HR. Decision tree analysis is a powerful statistical tool for prediction, and can effectively subdivide continuous variables into subgroups (Song and Ying, 2015). The exhaustive Chi-squared automatic interaction detection method (CHAID) was utilized. Nadir HR after fingolimod intake and the categorical variable whether the patient had bradycardia were used as the dependent variables. The independent variables were demographic and clinical information, and cardiovascular parameters prior to fingolimod intake. A 10-fold cross-validation was adopted. The maximum tree depth was set as three levels, the minimum parent and child node sizes were 10 and five, respectively. The significance level for splitting was 0.05. Bonferroni correction was applied during the decision tree analysis. For all the above analyses, results were considered statistically significant when $p < 0.05$.

RESULTS

Study Population

Three of the recruited patients lacked part of the required time window of continuous ECG monitoring and were excluded for further analyses. Finally, 78 patients with RRMS were included for the analyses. Their demographic and clinical characteristics are shown in **Table 1**. The mean (SEM) age of the male and female patients were 38.7 (2.2) and 39.9 (1.6) years, and there was no significant difference between their ages ($t = -0.442$, $p = 0.66$). One patient underwent an extended monitoring of 2 h due to delayed HR recovery. There was no rebound arrhythmia in the included participants. All the patients' concomitant diseases were in a stable state. Patients with depression were mainly treated by selective serotonin reuptake inhibitors or serotonin norepinephrine reuptake inhibitors. Three patients with hypertension underwent angiotensin-converting enzyme inhibitor monotherapy, one hypertensive patient took Ramipril and hydrochlorothiazide, and the other hypertensive patient took telmisartan and amlodipine. The patients diagnosed with hypothyroidism were treated with L-thyroxin. There was no patient with diabetes mellitus.

Changes of Cardiovascular Parameters after Fingolimod Administration

The changes of HR, systolic and diastolic blood pressure, SDNN, pNN50, RMSSD, absolute and relative values of LF and HF powers, and LF/HF ratio were presented in **Figures 1**, **2**. The mean HR was lowest at the fourth hour after medication, and the nadir HR was 65.4 ± 0.8 bpm. Bradycardia (HR < 60 bpm) appeared in 19 patents. The decrease of HR from baseline to nadir was 11.5 ± 0.7 bpm. Except for SDNN, blood pressure, absolute values of LF and HF powers, all the other variables showed a consistent trend: the value deviated from baseline since the second hour after fingolimod intake, arrived at their peaks or nadirs at the fourth, fifth, or sixth hour after medication. Although the time points of their peaks/nadirs were not exactly the same, the pairwise comparisons between the fourth, fifth and sixth hours obtained non-significant results in all these parameters. SDNN decreased at the first hour post medication, and then began to increase since the second hour after fingolimod initiation. *Post-hoc* pairwise comparison did not reveal a significant decrease of systolic blood pressure after medication, while diastolic blood pressure during the third and fifth hour was significantly lower than baseline. Absolute LF power increased after fingolimod initiation, with a significant difference from baseline at the third and fourth hour. Absolute HF power also increased after fingolimod administration, with a significant difference from baseline at the third, fourth, and fifth hour. Sex, age, and EDSS had no significant interaction with the effect of fingolimod in these parameters. Sex had a significant main effect in frequency domain parameters, female patients had a lower relative value of LF power and LF/HF ratio than male patients (all $p < 0.001$), and a higher relative value of HF than male patients ($p = 0.002$; **Figure 3**).

TABLE 1 | Demographic and clinical features of the participants.

Number of patients	78
Sex (female/male)	47/31
Age (years)	39.4 ± 1.3
Disease duration since RRMS diagnosis (years)	6.9 ± 0.6
EDSS	3.1 ± 0.2
Height (cm)	172.1 ± 1.1
Weight (kg)	73.5 ± 1.7
Concomitant diseases (number of patients)*	
Depression	8
Hypertension	5
Hypothyroidism	5

*Values are presented as mean ± SEM. *The concomitant diseases which occurred in at least two patients are displayed. EDSS, Expanded Disability Status Scale; RRMS: relapsing-remitting multiple sclerosis.*

Correlation Analysis

The results of the correlation analyses between nadir HR during the 6 h after fingolimod administration and various demographic, clinical, and cardiovascular parameters are shown in **Table 2**. Age, weight, baseline HR, and time domain parameters were significantly correlated with nadir HR. In particular, baseline HR had the strongest association with the nadir HR, while other variables had only weak associations.

Decision Tree Analysis

In the decision tree analysis, the demographic, clinical, and cardiovascular variables in **Table 2** were used as independent variables. Because the aim was to find predicting factors for fingolimod induced bradycardia, two patients with a baseline HR lower than 60 bpm were excluded. The models using nadir HR after fingolimod intake and whether the patient had bradycardia caused by fingolimod obtained similar results. Baseline HR was the only significant predicting factor (**Figure 4**). According to baseline HR, the patients were divided into three groups: 85.7% of the patients with a baseline HR < 65.3 bpm had bradycardia during post medication monitoring, 43.8% of the patients with a baseline HR between 65.3 and 71.3 bpm had bradycardia, and only 7.5% of the patients with a baseline HR higher than 71.3 had bradycardia within 6 h after fingolimod initiation.

DISCUSSION

This is the first study which implemented long-term MTRS analysis in successive 1-h-length ECG segments analysis. Our results disclosed the consistent changes of HR and HRV parameters after fingolimod initiation, and indicated that baseline HR was the strongest predictor for nadir HR among various cardiovascular parameters.

Because the changes of cardiac parameters after fingolimod intake is a dynamic process over several hours, manually choosing or recording a several-minute-length ECG segment from each hour for analysis might be affected by subjectivity of the selection and inconsistency of the exact position of chosen segments between patients, thus could increase systematic bias. This is also the case for delineating slower alterations such as

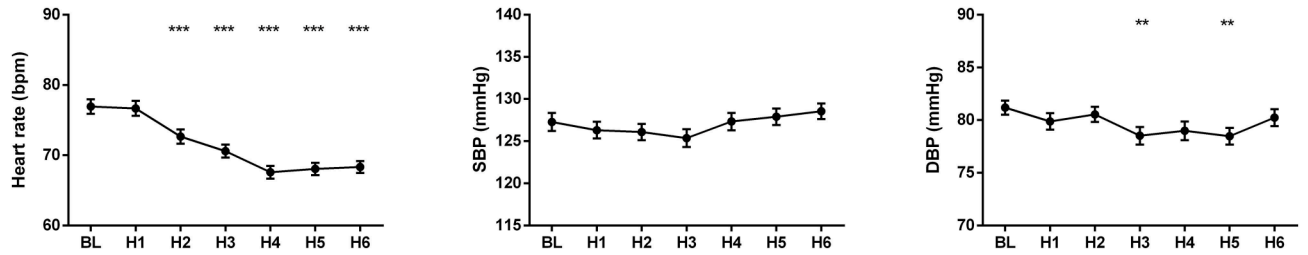

FIGURE 1 | Changes of heart rate and blood pressure after fingolimod administration. BL, baseline; DBP, diastolic blood pressure; H1, H2, H3, H4, H5, H6, the first, second, third, fourth, fifth, and sixth hour after fingolimod intake; SBP, systolic blood pressure. Values are presented as mean ± SEM. $^{**}p < 0.01$ compared with baseline, $^{***}p < 0.001$ compared with baseline.

circadian changes of cardiac autonomic regulation (Parati et al., 1990; Bilan et al., 2005). Automatically calculating the hourly HR and HRV parameters can solve these problems. Previous long-term spectral analyses of HRV were mainly performed with the fast Fourier transform. The most commonly used time windows for long-term spectral analyses of HRV were 1 and 24 h. There has been two main approaches: viewing the target time window as a whole data segment or averaging the spectral results of all the shorter segments (e.g., 2 min) within the whole time window. Generally, these two approaches yield similar results for LF and HF power components and the averaging process is more popular (Rottman et al., 1990; Task Force of the European Society of Cardiology and the North American Society of Pacing and Electrophysiology, 1996; Kleiger et al., 2005). In addition, long-term spectral analysis especially for 24 h can be used to evaluate cardiac autonomic regulations during normal daily activities, and is valuable for prognosis prediction (Task Force of the European Society of Cardiology and the North American Society of Pacing and Electrophysiology, 1996; Kleiger et al., 2005). To some extent, the comparison between 24-h long-term and short-term spectral analysis is similar as the comparison between 24-h ambulatory and clinic blood pressure measurements (Chobanian et al., 2003). However, there are some shortcomings of the long-term spectral analysis. Cardiac autonomic regulations underlying LF and HF power components cannot be deemed as stationary in long-term spectral analysis. Additionally, the averaging process integrate the dynamic alterations of autonomic tone within the specified time window, which prevents assessing autonomic function fluctuations in this time widow. Nevertheless, long-term spectral analysis have been widely applied and considered useful in evaluating cardiac autonomic function changes in various conditions and risk stratifications in cardiovascular diseases (Pagani et al., 1988; Parati et al., 1990; Tsuji et al., 1994, 1996; Task Force of the European Society of Cardiology and the North American Society of Pacing and Electrophysiology, 1996; Rossinen et al., 1997; Bilan et al., 2005; Kleiger et al., 2005), In this study, we utilized the long-term MTRS analysis using a strategy that averaged the results of 60 one-minute global segments within an hour, and applied this long-term MTRS in estimating HRV change for the first time.

The present study showed that parameters reflecting parasympathetc function such as RMSSD, pNN50, and HF power increased after fingolimod intake, while HR, LF power and LF/HF ratio decreased after medication. This phenominan can be explained by the vagomimetic effect of fingolimod. During the first several hours after fingolimod administration, this medication activates the S1P G protein-gated potassium channels in the myocytes, which is a vagomimetic effect and similar to the action of acetylcholine on muscarinic receptors (Camm et al., 2014; Vanoli et al., 2014). This can explain our findings that parameters representing parasympathetic activities initially increased after fingolimod intake, and heart rate decreased accordingly. Then several hours later, the down-regulation of S1P receptors in the myocytes mediates the restoration of the cardiovascular autonomic function (Camm et al., 2014; Vanoli et al., 2014). This S1P receptor down-regulation accounts for the decline of parasympathetic HRV parameters since the fifth or the sixth hour after fingolimod intake in our study.

In the present study, heart rate and most of the HRV parameters showed a consistent deviation from baseline since the second hour after fingolimod application. This is incompatible with the study by Simula et al. (2017). In their study, the time points when RR interval and HRV parameters deviated from baseline varied. The significant change occurred at the first, second or third hour after fingolimod administration (Simula et al., 2017). In that study, only 27 patients were recruited, and *post-hoc* multiple pairwise comparisons were not corrected. Since we enrolled a much larger sample size, and used the Bonfferoni correction during pairwise comparisons to avoid false positivities, our results of this concordant change of the above cardiac parameters are more trustworthy.

Hilz et al. (2017) showed the changes of cardivascular autonomic parameters after fingolimod initiation also using TRS. In that study, they analyzed eight 2-min ECG and blood pressure data segments from baseline to 6 h after medication. In their study, RRI, SDNN, RMSSD began to deviate from baseline since the first hour after fingolimod adminiatration, and achieved their peak 5, 2, and 4 h after medication respectively. The absolute values of LF and HF both increased 1 h after fingolimod intake. Then the absolute value of HF continued to increase until its peak 4 h after medication, while the absolute value of LF underwent a transient significant increase 1 h after fingolimod intiation and then went back to the baseline value. In addition, the normalized

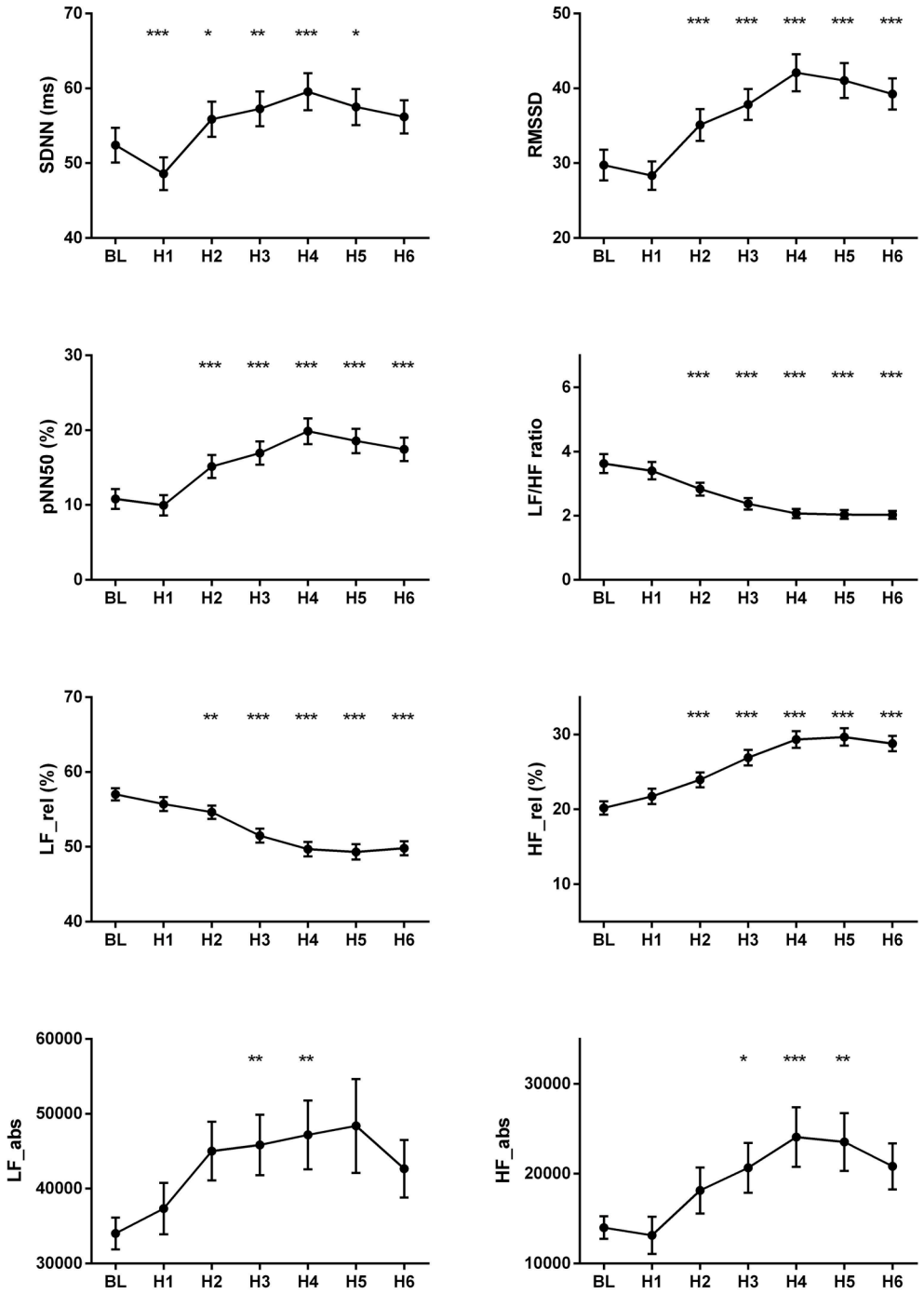

FIGURE 2 | Changes of the cardiovascular parameters after fingolimod administration. BL, baseline; H1, H2, H3, H4, H5, H6, the first, second, third, fourth, fifth, and sixth hour after fingolimod intake; HF_abs, absolute value of high frequency power; HF_rel, relative value of high frequency power; LF_abs, absolute value of low frequency power; LF_rel, relative value of low frequency power; pNN50, percentage of successive normal RR intervals differing by >50 ms; RMSSD, the root mean square of successive differences of RR-intervals; SDNN, the standard deviation of normal RR intervals. Values are presented as mean ± SEM. *$p < 0.05$ compared with baseline, **$p < 0.01$ compared with baseline, ***$p < 0.001$ compared with baseline.

values of LF and HF began to deviate from baseline since 3 h after medication, and achieved their peak/nadir 4 h after medication. The length of data analyzed affects time domain and frequency domain HRV parameters, especially SDNN is vulnerable to the influence of data length (Task Force of the European Society of Cardiology and the North American Society of Pacing and

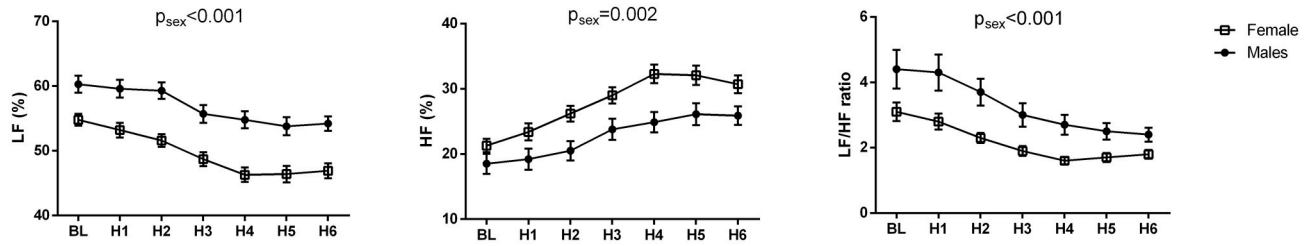

FIGURE 3 | Change of frequency domain parameters in male and female patients after fingolimod administration. BL, baseline; H1, H2, H3, H4, H5, H6, the first, second, third, fourth, fifth, and sixth hour after fingolimod intake; HF, relative value of high frequency power; LF, relative value of low frequency power. Values are presented as mean ± SEM. p_{sex}, the significance of sex as a main effect.

TABLE 2 | Correlation analysis between demographic, clinical, and cardiovascular parameters and nadir heart rate.

	Correlation coefficient with nadir heart rate	*p*-value
Age	**−0.249**	**0.028**
Weight	**−0.238**	**0.036**
BMI	−0.151	0.188
EDSS*	−0.063	0.581
Disease duration since RRMS diagnosis*	0.014	0.903
Baseline heart rate	**0.709**	**<0.001**
Baseline SBP	−0.084	0.465
Baseline DBP	0.148	0.197
Baseline SDNN	**−0.354**	**0.001**
Baseline RMSSD	**−0.333**	**0.003**
Baseline pNN50	**−0.288**	**0.010**
Baseline LF	0.179	0.118
Baseline HF	−0.168	0.141
Baseline LF/HF ratio	0.157	0.170

**For EDSS and disease duration since RRMS diagnosis, Spearman correlation was employed. For other variables, Pearson correlation was adopted. BMI, body mass index; DBP, diastolic blood pressure; EDSS, Expanded Disability Status Scale; HF, relative value of high frequency power; LF, relative value of low frequency power; pNN50, percentage of successive normal RR intervals differing by >50 ms; RMSSD, the root mean square of successive differences of RR-intervals; RRMS, relapsing-remitting multiple sclerosis; SBP, systolic blood pressure; SDNN, the standard deviation of normal RR intervals. Significant correlations are shown in bold font.*

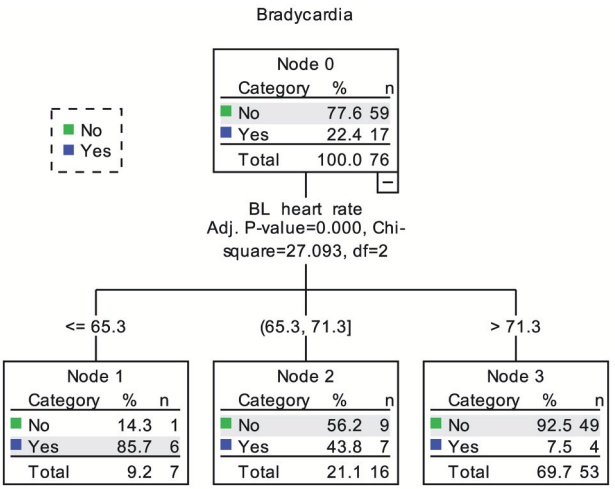

FIGURE 4 | Decision tree of predictors for bradycardia caused by fingolimod. BL, baseline. In node 1, 2 patients already had bradycardia before fingolimod intake were not included.

Electrophysiology, 1996). Although, the exact time points of changes of these paramters were not the same as our study, considering the methodological differences, the trends of changes were similar in RRI (HR in our study), RMSSD, LF/HF ratio of RRI, and LF and HF powers in our study and the study by Hilz et al. The absolute value of HF reflects parasympathetic activity and the absolute value of LF contains both parasympathetic and sympathetic regulations, this might partially explains the increase of absolute LF power after fingolimod intake in both studies (due to the increase of its parasympathetic component).

It is noteworthy that the decrease of SDNN in the first hour after fingolimod intake was not consistent with other parameters in the present study. In the study by Simula et al. (2017), SDNN was similar to baseline in the first hour after medication, while other time domain HRV parameters consistently increased since the first hour after fingolimod intake. In the study by Hilz et al., SDNN increased 1 h after medication together with RRI and RMSSD, but the time points of their peaks were different. One of the reason of this inconsistency is that SDNN represents all the cyclic components responsible for variability of analyzed RRI (Task Force of the European Society of Cardiology and the North American Society of Pacing and Electrophysiology, 1996), its underlying mechanism is different from the other cardiovascular autonomic parameters in our study and the study by Simula et al. Another reason of this inconsistency change of SDNN during the first hour post medication might be the emotional excitement of receiving a new oral treatment for their disease. It is reported that emotional change could affect HRV parameters (Pagani et al., 1989; Appelhans and Luecken, 2006; Hilz et al., 2017). Whether and how emotional response to the initiation of fingolimod affect cardiovascular autonomic function in patients with multiple sclerosis warrant further investigation.

The diastolic blood pressure decreased significantly in the third and fifth hour after fingolimod administration in our

study. Previous studies including very large patient samples demonstrated that fingolimod could slightly decrease blood pressure in the first several hours (Camm et al., 2014). However, studies enrolling small patient samples reported inconsistent results (Hilz et al., 2017; Simula et al., 2017). It is common that a small sample size is not sensitive to detecting minor differences.

A previous study showed that pNN50 might predict the HR decrease caused by fingolimod (Simula et al., 2016). However, in our study, baseline HR was the strongest predictor for bradycardia caused by fingolimod. Time domain HRV parameters also had significant correlations with nadir HR, but their associations were much weaker than baseline HR. The results of decision tree analysis also underlined the importance of baseline HR, which was the only dominant predicting factor among various demographic, clinical and cardiovascular variables. Patients with a baseline HR higher than 71.3 bpm had the lowest risk for bradycardia. This result is reasonable, as the mean maximum decrease of HR due to fingolimod was 11.5 bpm in the present study. The mean maximum HR decrease in preceding studies was between 8 and 12 bpm (Cohen et al., 2010; Calabresi et al., 2014; Camm et al., 2014). It is also intuitive that patients with a lower baseline HR are at high risk for fingolimod induced bradycardia. Although our sample is not very large, and decision tree analysis might not be highly stable in this case (Song and Ying, 2015). Considering the significance of baseline HR in both the correlation and decision tree analyses, baseline HR is the most powerful predictor for nadir HR after fingolimod initiation in our study. In future studies trying to find predictors for finglimod induced bradycardia, we suggest that comparison between potential predictors with baseline HR should be performed. In clinical practice, we need to pay more attention to patients with a lower baseline HR bpm because of their higher risk for bradycardia.

In the present study, we found that female patients with RRMS had a higher relative value of HF, and a lower relative value of LF and LF/HF ratio than male patients. Thus, the female patients had higher parasympathetic activity compared with the male patients. As far as we know, our study is the first to report this sex difference in RRMS. It has been reported that healthy females had a higher HF, as well as lower LF and LF/HF ratio compared with healthy males. This gender difference in autonomic balance may be attributed to several factors: estrogen, oxytocin, and neuro controls (Koenig and Thayer, 2016). However, whether the mechanism underlying gender difference in RRMS is the same as that in the healthy subjects needs further investigation.

Our study has several limitations. Firstly, respiration was not controlled in the study, and the patients' activity was not strictly restricted. Although the patients were generally in a sedentary state and breathed peacefully, physical activity and breathing rate/tidal volume can potentially affect both time and frequency domain HRV parameters, and this could be a confounding factor in the analysis of the effects of fingolimod and gender on the HRV parameters (Yamamoto et al., 1991; Brown et al., 1993; Osterhues et al., 1997; Gąsior et al., 2016). Secondly, as we have mentioned in the Method section, there are controversies in the interpretation of LF and LF/HF ratio of heart rates. Whether they can reflect cardiac sympathetic activity is still unsure. We include the results of LF and LF/HF ratio for potential comparison with similar studies. Thirdly, continuous beat-to-beat blood pressure monitoring was not performed together with ECG monitoring. As LF oscillations of systolic blood pressure reflects sympathetically mediated peripheral vasomotor tone, this limitation restrains us from evaluating the vascular sympathetic modulation.

In conclusion, the present study showed that long-term MTRS was a useful tool for the determination of the dynamic change of HRV. Our findings demonstrated the consistent changes of cardiovascular parasympathetic activity and HR after fingolimod administration. Furthermore, among various demographic, clinical, and cardiovascular parameters, baseline HR was the strongest predictor for nadir HR after fingolimod initiation.

AUTHOR CONTRIBUTIONS

Conception and design of the study: TZ, UK, KA. Recruiting the patients and collecting demographic and clinical information: TZ, UK, KA. Acquisition, analysis and interpretation of data: KL, RH, HR, MR. Drafting the manuscript: KL, TZ, all the other authors critically revised the draft and approved the final version.

FUNDING

The Holter ECG was performed as part of the START study which was sponsored by Novartis Pharma GmbH.

REFERENCES

Appelhans, B. M., and Luecken, L. J. (2006). Heart rate variability as an index of regulated emotional responding. *Rev. Gen. Psychol.* 10, 229–240. doi: 10.1037/1089-2680.10.3.229

Bilan, A., Witczak, A., Palusiński, R., Myśliński, W., and Hanzlik, J. (2005). Circadian rhythm of spectral indices of heart rate variability in healthy subjects. *J. Electrocardiol.* 38, 239–243. doi: 10.1016/j.jelectrocard.2005.01.012

Brinkmann, V., Billich, A., Baumruker, T., Heining, P., Schmouder, R., Francis, G., et al. (2010). Fingolimod (FTY720): discovery and development of an oral drug to treat multiple sclerosis. *Nat. Rev. Drug Discov.* 9, 883–897. doi: 10.1038/nrd3248

Brown, T. E., Beightol, L. A., Koh, J., and Eckberg, D. L. (1993). Important influence of respiration on human R-R interval power spectra is largely ignored. *J. Appl. Physiol.* 75, 2310–2317.

Calabresi, P. A., Radue, E. W., Goodin, D., Jeffery, D., Rammohan, K. W., Reder, A. T., et al. (2014). Safety and efficacy of fingolimod in patients with relapsing-remitting multiple sclerosis (FREEDOMS II): a double-blind, randomised, placebo-controlled, phase 3 trial. *Lancet Neurol.* 13, 545–556. doi: 10.1016/S1474-4422(14)70049-3

Camm, J., Hla, T., Bakshi, R., and Brinkmann, V. (2014). Cardiac and vascular effects of fingolimod: mechanistic basis and clinical implications. *Am. Heart J.* 168, 632–644. doi: 10.1016/j.ahj.2014.06.028

Chobanian, A. V., Bakris, G. L., Black, H. R., Cushman, W. C., Green, L. A., Izzo, J. L. Jr., et al. (2003). The Seventh Report of the Joint National Committee on

Prevention, Detection, Evaluation, and Treatment of High Blood Pressure: the JNC 7 report. *JAMA* 289, 2560–2572. doi: 10.1001/jama.289.19.2560

Cohen, J. A., Barkhof, F., Comi, G., Hartung, H. P., Khatri, B. O., Montalban, X., et al. (2010). Oral fingolimod or intramuscular interferon for relapsing multiple sclerosis. *N. Engl. J. Med.* 362, 402–415. doi: 10.1056/NEJMoa0907839

Gąsior, J. S., Sacha, J., Jeleń, P. J., Zieliński, J., and Przybylski, J. (2016). Heart rate and respiratory rate influence on heart rate variability repeatability: effects of the correction for the prevailing heart rate. *Front Physiol.* 7:356. doi: 10.3389/fphys.2016.00356

Hilz, M. J., Intravooth, T., Moeller, S., Wang, R., Lee, D.-H., Koehn, J., et al. (2015). Central autonomic dysfunction delays recovery of fingolimod induced heart rate slowing. *PLoS ONE* 10:e0132139. doi: 10.1371/journal.pone.0132139

Hilz, M. J., Wang, R., de Rojas Leal, C., Liu, M., Canavese, F., and Roy, S. (2017). Fingolimod initiation in multiple sclerosis patients is associated with potential beneficial cardiovascular autonomic effects. *Ther. Adv. Neurol. Disord.* 10, 191–209.doi: 10.1177/1756285616682936

Kleiger, R. E., Stein, P. K., and Bigger, J. T. Jr. (2005). Heart rate variability: measurement and clinical utility. *Ann. Noninvasive Electrocardiol.* 10, 88–101. doi: 10.1111/j.1542-474X.2005.10101.x

Koenig, J., and Thayer, J. F. (2016). Sex differences in healthy human heart rate variability: a meta-analysis. *Neurosci. Biobehav. Rev.* 64, 288–310. doi: 10.1016/j.neubiorev.2016.03.007

Laude, D., Elghozi, J. L., Girard, A., Bellard, E., Bouhaddi, M., Castiglioni, P., et al. (2004). Comparison of various techniques used to estimate spontaneous baroreflex sensitivity (the EuroBaVar study). *Am. J. Physiol. Regul. Integr. Comp. Physiol.* 286, R226–R231. doi: 10.1152/ajpregu.00709.2002

Limmroth, V., Ziemssen, T., Lang, M., Richter, S., Wagner, B., Haas, J., et al. (2017). Electrocardiographic assessments and cardiac events after fingolimod first dose - a comprehensive monitoring study. *BMC Neurol.* 17:11. doi: 10.1186/s12883-016-0789-7

Osterhues, H. H., Hanzel, S. R., Kochs, M., and Hombach, V. (1997). Influence of physical activity on 24-hour measurements of heart rate variability in patients with coronary artery disease. *Am. J. Cardiol.* 80, 1434–1437. doi: 10.1016/S0002-9149(97)00705-4

Pagani, M., Furlan, R., Pizzinelli, P., Crivellaro, W., Cerutti, S., and Malliani, A. (1989). Spectral analysis of R-R and arterial pressure variabilities to assess sympatho-vagal interaction during mental stress in humans. *J. Hypertens.* 7(Suppl.), S14–S15. doi: 10.1097/00004872-198900076-00004

Pagani, M., Somers, V., Furlan, R., Dell'Orto, S., Conway, J., Baselli, G., et al. (1988). Changes in autonomic regulation induced by physical training in mild hypertension. *Hypertension* 12, 600–610. doi: 10.1161/01.HYP.12.6.600

Parati, G., Castiglioni, P., Di Rienzo, M., Omboni, S., Pedotti, A., and Mancia, G. (1990). Sequential spectral analysis of 24-hour blood pressure and pulse interval in humans. *Hypertension* 16, 414–421. doi: 10.1161/01.HYP.16.4.414

Polman, C. H., Reingold, S. C., Banwell, B., Clanet, M., Cohen, J. A., Filippi, M., et al. (2011). Diagnostic criteria for multiple sclerosis: 2010 revisions to the McDonald criteria. *Ann. Neurol.* 69, 292–302. doi: 10.1002/ana.22366

Reimann, M., Hamer, M., Schlaich, M. P., Malan, N. T., Ruediger, H., Ziemssen, T., et al. (2012). Greater cardiovascular reactivity to a cold stimulus is due to higher cold pain perception in black Africans: the Sympathetic Activity and Ambulatory Blood Pressure in Africans (SABPA) study. *J. Hypertens.* 30, 2416–2424. doi: 10.1097/HJH.0b013e328358faf7

Reimann, M., Julius, U., Haink, K., Lippold, B., Tselmin, S., Bornstein, S. R., et al. (2010). LDL apheresis improves deranged cardiovagal modulation in hypercholesterolemic patients. *Atherosclerosis* 213, 212–217. doi: 10.1016/j.atherosclerosis.2010.07.019

Reyes del Paso, G. A., Langewitz, W., Mulder, L. J., van Roon, A., and Duschek, S. (2013). The utility of low frequency heart rate variability as an index of sympathetic cardiac tone: a review with emphasis on a reanalysis of previous studies. *Psychophysiology* 50, 477–487. doi: 10.1111/psyp.12027

Rossi, S., Rocchi, C., Studer, V., Motta, C., Lauretti, B., Germani, G., et al. (2015). The autonomic balance predicts cardiac responses after the first dose of fingolimod. *Mult. Scler.* 21, 206–216. doi: 10.1177/1352458514538885

Rossinen, J., Viitasalo, M., Partanen, J., Koskinen, P., Kupari, M., and Nieminen, M. S. (1997). Effects of acute alcohol ingestion on heart rate variability in patients with documented coronary artery disease and stable angina pectoris. *Am. J. Cardiol.* 79, 487–491. doi: 10.1016/S0002-9149(96)00790-4

Rottman, J. N., Steinman, R. C., Albrecht, P., Bigger, J. T. Jr., Rolnitzky, L. M., and Fleiss, J. L. (1990). Efficient estimation of the heart period power spectrum suitable for physiologic or pharmacologic studies. *Am. J. Cardiol.* 66, 1522–1524. doi: 10.1016/0002-9149(90)90551-B

Rudiger, H., Klinghammer, L., and Scheuch, K. (1999). The trigonometric regressive spectral analysis–a method for mapping of beat-to-beat recorded cardiovascular parameters on to frequency domain in comparison with Fourier transformation. *Comput. Methods Programs Biomed.* 58, 1–15. doi: 10.1016/S0169-2607(98)00070-4

Simula, S., Laitinen, T. P., Laitinen, T. M., Hartikainen, P., and Hartikainen, J. E. (2016). Heart rate variability predicts the magnitude of heart rate decrease after fingolimod initiation. *Mult. Scler. Relat. Disord.* 10, 86–89. doi: 10.1016/j.msard.2016.09.012

Simula, S., Laitinen, T. P., Laitinen, T. M., Hartikainen, P., and Hartikainen, J. E. (2017). Sequence of cardiovascular autonomic alterations after fingolimod initiation. *Ann. Noninvasive Electrocardiol.* 22:e12443. doi: 10.1111/anec.12443

Song, Y. Y., and Ying, L. (2015). Decision tree methods: applications for classification and prediction. *Shanghai Arch. Psychiatry.* 27, 130–135. doi: 10.11919/j.issn.1002-0829.215044

Task Force of the European Society of Cardiology and the North American Society of Pacing and Electrophysiology. (1996). Heart rate variability: standards of measurement, physiological interpretation and clinical use. *Circulation* 93, 1043–1065. doi: 10.1161/01.CIR.93.5.1043

Thomas, K., Proschmann, U., and Ziemssen, T. (2017). Fingolimod hydrochloride for the treatment of relapsing remitting multiple sclerosis. *Expert Opin. Pharmacother.* doi: 10.1080/14656566.2017.1373093. [Epub ahead of print].

Tsuji, H., Larson, M. G., Venditti, F. J. Jr, Manders, E. S., Evans, J. C., Feldman, C. L., et al. (1996). Impact of reduced heart rate variability on risk for cardiac events. The Framingham Heart Study. *Circulation* 94, 2850–2855. doi: 10.1161/01.CIR.94.11.2850

Tsuji, H., Venditti, F. J. Jr., Manders, E. S., Evans, J. C., Larson, M. G., Feldman, C. L., et al. (1994). Reduced heart rate variability and mortality risk in an elderly cohort. The Framingham Heart Study. *Circulation* 90, 878–883. doi: 10.1161/01.CIR.90.2.878

Vanoli, E., Pentimalli, F., and Botto, G. (2014). Vagomimetic effects of fingolimod: physiology and clinical implications. *CNS Neurosci. Ther.* 20, 496–502. doi: 10.1111/cns.12283

Yamamoto, Y., Hughson, R. L., and Peterson, J. C. (1991). Autonomic control of heart rate during exercise studied by heart rate variability spectral analysis. *J. Appl. Physiol.* 71, 1136–1142.

Ziemssen, T., Gasch, J., and Ruediger, H. (2008). Influence of ECG sampling frequency on spectral analysis of RR intervals and baroreflex sensitivity using the EUROBAVAR data set. *J. Clin. Monit. Comput.* 22, 159–168. doi: 10.1007/s10877-008-9117-0

Ziemssen, T., Medin, J., Couto, C. A., and Mitchell, C. R. (2017). Multiple sclerosis in the real world: a systematic review of fingolimod as a case study. *Autoimmun. Rev.* 16, 355–376. doi: 10.1016/j.autrev.2017.02.007

Ziemssen, T., Reimann, M., Gasch, J., and Rudiger, H. (2013). Trigonometric regressive spectral analysis: an innovative tool for evaluating the autonomic nervous system. *J. Neural Transm.* 120(Suppl. 1), S27–S33. doi: 10.1007/s00702-013-1054-5

Conflict of Interest Statement: KA received personal compensation from Novartis, Biogen Idec, and Roche for the consulting service. TZ received personal compensation from Biogen Idec, Bayer, Novartis, Sanofi, Teva, and Synthon for the consulting services. TZ received additional financial support for the research activities from Bayer, Biogen Idec, Novartis, Teva, and Sanofi Aventis. UK received travel support by Teva.

The other authors declare that the research was conducted in the absence of any commercial or financial relationships that could be construed as a potential conflict of interest.

frontiers in Neuroscience

SYSTEMATIC REVIEW
published: 04 April 2018
doi: 10.3389/fnins.2018.00203

Clozapine-Induced Cardiovascular Side Effects and Autonomic Dysfunction: A Systematic Review

*Jessica W. Y. Yuen[1], David D. Kim[2], Ric M. Procyshyn[3], Randall F. White[3], William G. Honer[3] and Alasdair M. Barr[2]**

[1] Faculty of Medicine and Centre for Brain Health, University of British Columbia, Vancouver, BC, Canada, [2] Department of Anesthesiology, Pharmacology and Therapeutics, University of British Columbia, Vancouver, BC, Canada, [3] Department of Psychiatry, Faculty of Medicine Faculty of Medicine, University of British Columbia, Vancouver, BC, Canada

Background: Clozapine is the antipsychotic of choice for treatment-resistant schizophrenia and has minimal risk for extrapyramidal symptoms. Therapeutic benefits, however, are accompanied by a myriad of cardiometabolic side-effects. The specific reasons for clozapine's high propensity to cause adverse cardiometabolic events remain unknown, but it is believed that autonomic dysfunction may play a role in many of these.

Objective: This systematic review summarizes the literature on autonomic dysfunction and related cardiovascular side effects associated with clozapine treatment.

Method: A search of the EMBASE, MEDLINE, and EBM Cochrane databases was conducted using the search terms antipsychotic agents, antipsychotic drug*, antipsychotic*, schizophrenia, schizophren*, psychos*, psychotic*, mental ill*, mental disorder*, neuroleptic*, cardiovascular*, cardiovascular diseases, clozapine*, clozaril*, autonomic*, sympathetic*, catecholamine*, norepinephrine, noradrenaline, epinephrine, adrenaline.

Results: The search yielded 37 studies that were reviewed, of which only 16 studies have used interventions to manage cardiovascular side effects. Side effects reported in the studies include myocarditis, orthostatic hypotension and tachycardia. These were attributed to sympathetic hyperactivity, decreased vagal contribution, blockade of cholinergic and adrenergic receptors, reduced heart rate variability and elevated catecholamines with clozapine use. Autonomic neuropathy was identified by monitoring blood pressure and heart rate changes in response to stimuli and by spectral analysis of heart rate variability. Metoprolol, lorazepam, atenolol, propranolol, amlodipine, vasopressin and norepinephrine infusion were used to treat tachycardia and fluctuations in blood pressure, yet results were limited to case reports.

Conclusion: The results indicate there is a lack of clinical studies investigating autonomic dysfunction and a limited use of interventions to manage cardiovascular side effects associated with clozapine. As there is often no alternative treatment for refractory schizophrenia, the current review highlights the need for better designed studies, use of autonomic tests for prevention of cardiovascular disease and development of novel interventions for clozapine-induced side effects.

Keywords: clozapine, schizophrenia, autonomic, cardiovascular, catecholamine, heart rate, blood pressure

OPEN ACCESS

Edited by:
Tijana Bojić,
Vinča Nuclear Institute, University of Belgrade, Serbia

Reviewed by:
Sushil Kumar Mahata,
University of California, San Diego, United States
David Wright,
University of Guelph, Canada

***Correspondence:**
Alasdair M. Barr
al.barr@ubc.ca

Specialty section:
This article was submitted to Autonomic Neuroscience, a section of the journal Frontiers in Neuroscience

Received: *10 October 2016*
Accepted: *14 March 2018*
Published: *04 April 2018*

Citation:
Yuen JWY, Kim DD, Procyshyn RM, White RF, Honer WG and Barr AM (2018) Clozapine-Induced Cardiovascular Side Effects and Autonomic Dysfunction: A Systematic Review. Front. Neurosci. 12:203. doi: 10.3389/fnins.2018.00203

INTRODUCTION

Clozapine (CLZ) is the antipsychotic drug of choice for treatment-resistant schizophrenia, displaying superior efficacy in an estimated 30% of patients who are persistently unresponsive to other antipsychotic drugs (Kane et al., 1988; Meltzer, 1997; Honer et al., 2015). CLZ has been shown to effectively reduce suicidality in patients with treatment-resistant schizophrenia (Meltzer and Okayli, 1995; Reinstein et al., 2002) and is the sole agent approved by the U.S. Food and Drug administration to manage suicidal behavior in persons with schizophrenia or schizoaffective disorder (Citrome et al., 2016). Compared to most first generation antipsychotics (FGAs) and many second generation antipsychotics (SGAs), CLZ has minimal risk for extrapyramidal symptoms (EPS) (Lindström, 1988; Casey, 1989) and does not induce hyperprolactinemia (Kane et al., 1981; Melkersson, 2005). In a study comparing treatment duration between FGAs and SGAs as an indicator of overall effectiveness, CLZ was an important factor in lengthening the time to medication discontinuation of SGAs as a group (Ascher-Svanum et al., 2006). Furthermore, fewer relapses and rehospitalization rates are reduced with CLZ use (Essock et al., 1996; Conley et al., 1999; Essali et al., 2009). The abovementioned superiority has been attributed to CLZ's diverse receptor binding profile (Bymaster et al., 1996; Nasrallah, 2008), although the exact mechanism remains unknown. CLZ has a high-affinity for adrenergic receptors α_1, α_2 (Kalkman et al., 1998), dopamine receptors D_1 (Kalkman et al., 1998), D_2 (Masri et al., 2008), and D_4 (Van Tol et al., 1991), serotonin receptors 5-HT_6 (Monsma et al., 1993) and 5-HT_7 (Shen et al., 1993), muscarinic receptors (Richelson and Souder, 2000) and histaminergic receptors H_1 and H_3 (Bymaster et al., 1997). CLZ may also show superior efficacy in treating psychostimulant drug-induced psychosis (Seddigh et al., 2014), which is associated with neuropsychiatric and structural brain changes similar to those of schizophrenia (Tang et al., 2015; Willi et al., 2016a,b).

Any therapeutic benefit from CLZ treatment, however, must take into consideration the high incidence of non-EPS side-effects associated with the drug (Andreazza et al., 2015; Thornton et al., 2015; Tse et al., 2015; Lee et al., 2016). An estimated 10–20% of eligible patients are prescribed with CLZ in the U.S., a number indicative that CLZ is vastly underutilized due to concern for its side effects (Meltzer, 2012; Kar et al., 2016). One of the most concerning side effects of CLZ is agranulocytosis, which occurs in approximately 1% of patients receiving CLZ (Alvir et al., 1993) and only rarely with other antipsychotics (Vila-Rodriguez et al., 2013). Critically, there is a large body of evidence of CLZ's high propensity to induce cardiometabolic side effects, such as orthostatic hypotension (Mackin, 2008), tachycardia (Safferman et al., 1991; Young et al., 1998), myocarditis (Kilian et al., 1999; Merrill et al., 2005), dyslipidemia (Olfson et al., 2006; Procyshyn et al., 2007, 2009), weight gain and obesity (Henderson et al., 2000; Whitney et al., 2015). Increased cardiovascular risk is of concern, especially when coronary heart disease (CHD) is the leading cause of premature death in schizophrenia (Hennekens et al., 2005). Indeed, a 10 year naturalistic study of CLZ-treated patients estimated the 10 year mortality from cardiovascular disease (CVD) to be at 9% (Henderson et al., 2005). While the increased liability for cardiovascular risk in patients with schizophrenia has been linked to lifestyle habits such as smoking, physical inactivity/sedentary behavior and unhealthy diet (McEvoy et al., 2005; Bobes et al., 2010; Lang et al., 2013; Fredrikson et al., 2014), antipsychotic use, in particular CLZ, has increased the risk of sudden cardiac deaths (Modai et al., 2000; Ray et al., 2009). The exact cause is unknown, however, myocarditis (La Grenade et al., 2001; Fineschi et al., 2004) and pulmonary embolism (Walker et al., 1997) resulting from CLZ treatment have been implicated.

The abovementioned cardiovascular side effects stem largely from autonomic dysregulation, namely antagonism of adrenergic and cholinergic receptors that influence autonomic function (Leung et al., 2012). Briefly, cardiovascular function is regulated by the autonomic nervous system (ANS), which is further divided into the sympathetic nervous system (SNS) and the parasympathetic nervous system (PNS). The SNS is comprised of neurons that relay impulses to and from the central nervous system (CNS). The SNS efferent neurons consist of 2 groups of neurons, the preganglionic and postganglionic sympathetic neurons. Preganglionic sympathetic neurons originate from the CNS and synapse with postganglionic sympathetic neurons at peripheral sympathetic ganglia either located in the sympathetic chain adjacent to the spinal cord or near target organs (Jänig, 2006; Triposkiadis et al., 2009). The postganglionic sympathetic neurons release the neurotransmitter norepinephrine (NE) upon stimulation, which in turn stimulates adrenergic receptors to influence physiological functions such as increasing heart rate (HR) and blood pressure (BP) (Jänig, 2006; Triposkiadis et al., 2009). The PNS acts in opposition to the SNS to achieve cardiac homeostasis, although there are exceptions to this conventional view. As reviewed by Paton et al., parasympathetic and sympathetic nerves innervating the heart can act in synergy during reflex responses including the startle, diving and somatic nociceptor reflexes (2005). The combined contribution from both the PNS and SNS to the heart can result in arrhythmia and possibly contribute to cardiac pathophysiology, a subject that warrants further electrophysiological experiments (Paton et al., 2005).

Schizophrenia has been associated with autonomic dysregulation, possibly due to imbalance of sympathetic and vagal control (Bär et al., 2007, 2010; Chang et al., 2009). Antipsychotic medication can also influence autonomic function (Buckley and Sanders, 2000), with CLZ consistently viewed as one of the SGAs with the highest risk for CVD and Type 2 diabetes (Henderson et al., 2005; De Hert et al., 2011). Risk for CVD was investigated in a study conducted by Henderson et al. (2005), where medical records of 96 patients with schizophrenia were screened over 10 years for metabolic and cardiovascular anomalies as a result of CLZ treatment. Results indicate time-dependent significant increases in body mass index (BMI) and average weight gain of 30 lbs, as well as an increase in the number of cardiovascular risk factors that were assessed yearly, including hypertension, smoking and cholesterol or triglyceride levels. Multiple cardiovascular-related adverse events were also

reported in this study ($n = 11$), with 7 deaths, 3 myocardial infarctions and 1 cerebrovascular accident (Henderson et al., 2005). An especially grave adverse effect of CLZ is myocarditis. Haas et al. (2007) identified 116 case reports for myocarditis-related fatality in CLZ-treated patients. Of these cases, 17 failed to recover and 12 patients died from suspected myocarditis (Haas et al., 2007). The authors noted myocarditis occurs within 4 weeks of administering CLZ at 100–450 mg/day, with a prevalence of 0.7–1.2% in CLZ-treated patients.

Given the evidence of cardiovascular complications resulting from CLZ treatment, it is imperative to understand how CLZ influences cardiovascular function and identify methods to balance the costs and benefits of prescribing CLZ. This systematic review is a comprehensive search of the literature for cardiovascular incidents resulting from CLZ use, with a specific emphasis on the ANS. We aim to compile reports of CLZ-induced cardiovascular side effects from past research, identify methods for early detection and describe clinical interventions to minimize CVD risk in CLZ-treated patients.

METHODS

The EMBASE, MEDLINE and EBM Cochrane databases were searched using the following key words: antipsychotic agents, antipsychotic drug, antipsychotic, schizophrenia, psychotic, mental illness, mental disorder, neuroleptic, cardiovascular, cardiovascular diseases, clozapine, clozaril, autonomic, sympathetic, catecholamine, norepinephrine, noradrenaline, epinephrine and adrenaline. The date range was set to 1959 (first introduction of CLZ) to March 2, 2016. Case reports, animal studies and clinical studies published in English were included. Additional records were identified from reference lists and independent searches. Human studies were excluded if subjects were under 18 years of age. The primary author conducted all screening and extraction of relevant articles from the search. Due to the mixed nature and amount of articles identified, the authors conducted a systematic review instead of a meta-analysis for better representation of the available literature.

RESULTS

The literature search identified 208 studies as outlined in **Figure 1** ($n = 180$ from Embase, $n = 13$ from MEDLINE and $n = 15$ from EBM Cochrane). Additional records were identified from other sources (gray literature and reference lists) ($n = 33$) and 11 duplicates were found. Twenty-one studies were excluded due to publication in a language other than English and 147 studies were excluded for irrelevance based on screening of abstracts and titles. The remaining 66 full-text articles were assessed and 29 full-text articles were excluded with reasons (i.e. CLZ was not administered, the study did not involve patients with schizophrenia, autonomic function was not discussed, human subjects were under 18 years of age and/or the article is a review). The final 37 articles comprised of case reports and studies evaluating the effects of CLZ on autonomic function. See Table 1 in Supplementary Material for full summary of results.

Autonomic Function Tests

Various tests have been developed to assess autonomic function and screen for autonomic neuropathies (see Table 2 in Supplementary Material for summary). These tests evaluate HR and/or BP response to stimuli, thus reflecting sympathetic and parasympathetic regulation of cardiovascular function. The following sections summarize commonly used tests for non-invasive assessment of autonomic function.

Heart Rate Variability

Spectral analysis of heart rate variability (HRV) is a noninvasive, beat-to-beat analysis of fluctuations in HR (Wheeler and Watkins, 1973). HRV assesses both sympathetic and parasympathetic function via time and frequency domain measurements (1996). Time domain measures are based on interbeat HR or HR between successive cycles (Stein et al., 1994). One simple measure based on interbeat HR is the standard deviation of all NN intervals (SDNN), where NN refers to normal-to-normal intervals or intervals between successive QRS complexes (1996). SDNN is commonly calculated over a 24 h period and reflects the total HRV for the duration of the recording (1996). Each measure of interbeat variability reflects individual contributions from the parasympathetic, sympathetic and renin-angiotensin systems to sinus rhythm control (outlined in Table 2 in Supplementary Material, Akselrod et al., 1981). The second class of time domain measurements is based on interval differences between successive cycles and a typical example is the square root of the mean squared differences of successive NN intervals (RMSSD). This measure is an estimate of the short-term components of HRV and generally reflects vagal activity (Stein et al., 1994). Frequency domain measures describe how variance is distributed as a function of frequency, generally divided into short-term and long-term spectral components (1996). Short-term spectral recordings consist of high frequency (HF), low frequency (LF), and very low frequency (VLF) components, where HF is generally linked to parasympathetic regulation whereas LF is mediated by both the SNS and PNS (Stein et al., 1994). Long term recordings measure the variance of all NN intervals in a 24 h period (1996). Reduced HRV has been linked to increased risk of mortality from cardiac disease and predicts risk for future cardiac events, thus generating an increasing interest in the clinical value of HRV (Tsuji et al., 1996; La Rovere et al., 1998; Nolan et al., 1998; Dekker et al., 2000).

Cohen et al. (2001b) compared HRV in patients with schizophrenia treated with CLZ ($n = 21$) to those treated with haloperidol (HAL, $n = 18$) or olanzapine (OLA, $n = 17$) and found CLZ induced tachycardia while significantly lowering the total variability of HR. They also found an increased LF/HF ratio in CLZ-treated patients, indicative of increased sympathetic activity associated with CLZ (Cohen et al., 2001a). Spectral analysis can also be applied toward respiratory sinus arrhythmia (RSA), derived from the HF band of HRV, and is a measure of parasympathetic activity (Mathewson et al., 2012). The relationship between RSA and cognitive function was assessed in CLZ-treated patients. Results show CLZ worsened performance in the Wisconsin Card Sorting Test (WCST) and

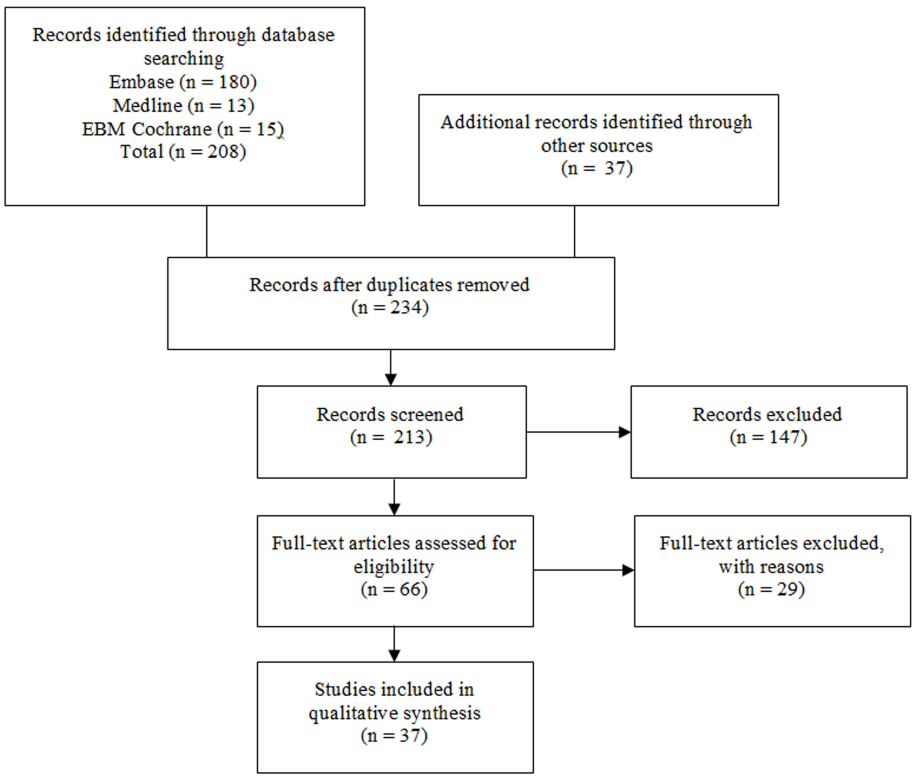

FIGURE 1 | Flow diagram for identification of studies. Original studies discussing clozapine, cardiovascular disease and autonomic function are reviewed. Keywords used: antipsychotic agents, antipsychotic drug*, antipsychotic*, schizophrenia, schizophren*, psychos*, psychotic*, mental ill*, mental disorder*, neuroleptic*, cardiovascular*, cardiovascular diseases, clozapine*, clozaril*, autonomic*, sympathetic*, catecholamine*, norepinephrine, noradrenaline, epinephrine, and adrenaline.

significantly decreased parasympathetic control, compared to healthy controls and patients treated with other antipsychotics. However, the inverse relationship between parasympathetic control and number of perseverative errors committed in patients with schizophrenia did not change with CLZ use (Mathewson et al., 2012).

CLZ's anti-cholinergic effects were investigated in a study comparing HRV in patients with schizophrenia receiving antipsychotics with high affinity for muscarinic receptors (HMA) to those with low affinity (LMA), with CLZ belonging to the HMA group (Huang et al., 2013). Of the 55 subjects recruited, 28 received HMA and displayed perturbed sympathetic and parasympathetic regulation. Correlation and multiple linear regression analyses revealed muscarinic receptor affinity was negatively associated with HRV profiles, namely HF, LF, and TP (Huang et al., 2013). Due to suppression of both the LF and HF components, the LF/HF ratio in the HMA group was not significantly different from that of the LMA group. Interestingly, the authors show the suppression of HRV in the HMA group was still present after controlling for metabolic factors, suggesting the metabolic syndrome does not significantly influence cardiovascular function. The study repeated with a larger sample size, in particular with CLZ-treated patients, will help clarify the role of antipsychotics with high metabolic liability in cardiovascular function. CLZ, as a HMA, may also contribute to increased motivation for smoking (Barr et al., 2008), which adds to cardiovascular burden.

Tümüklü et al. (2008) studied CLZ-induced arrhythmia in patients with schizophrenia over a course of 10 weeks. Parameters measured included HRV, QT dispersion (myocardial repolarization) and late potentials (delayed ventricular conduction). Both QT dispersion and late potentials displayed an increasing trend following CLZ treatment, yet the changes were statistically insignificant. HRV, however, was suppressed in CLZ-treated patients, with LF/HF significantly influenced by age and gender (i.e., patients <35 years old, female patients). Decreased sympathetic activity was attributed to CLZ's potent antagonism of muscarinic and α-adrenergic receptors (Tümüklü et al., 2008).

Reduced HRV from CLZ treatment was also noted in a prospective clinical study comparing the effects of amisulpride, OLA, CLZ, and sertindole on HRV (Agelink et al., 2001). CLZ was the only neuroleptic to significantly reduce parasympathetic activity, with half of the CLZ-treated patients showing signs of suppressed HRV (Agelink et al., 2001). Interestingly OLA, a SGA with comparable anticholinergic properties with CLZ *in vitro*, did not demonstrate the same extent of drug-induced tachycardia and parasympathetic inhibition as CLZ (Agelink et al., 2001). This was suggested to be the result of CLZ's extreme cholinergic receptor inhibition coupled with antagonism

of the α-adrenoceptors. This was supported by another case report of a treatment-resistant patient with schizophrenia who developed tachycardia and reduced HRV after commencing CLZ treatment, with increased LF and decreased HF thereby indicative of increased sympathetic control (Cohen et al., 2001b). The cardiovascular signs subsided after switching to OLA.

Pulse rate variability (PRV) was further investigated in a study comparing CLZ ($n = 10$) and OLA ($n = 18$). The authors had previously found that PRV yielded results comparable to HRV, with parameters calculated from finger pulses instead of electrocardiograms for the PRV (Mueck-Weymann et al., 2002). CLZ-treated patients displayed significantly increased HR and diminished HRV parameters compared to healthy controls. OLA-treated patients displayed the same trend, albeit to a much lesser extent (Mueck-Weymann et al., 2002). The authors attribute the observed autonomic changes to the presence of CLZ in plasma at high levels and CLZ's strong antagonism of cholinergic and adrenergic receptors.

As mentioned above, multiple studies have noted reduced HRV with CLZ use, an observation believed to be due to antagonism of muscarinic receptors in the vagus nerve. Rechlin et al. (1998) sought to expand upon this research by further including measurements of plasma CLZ drug levels in their study. Plasma CLZ levels were found to be inversely correlated with HRV parameters, with the largest decrease in HRV occurring during periods of deep breathing and rest (Rechlin et al., 1998). The authors speculate that HRV parameters are increased in the standing position due to higher sympathetic activity (Rechlin et al., 1998). The authors have previously shown non-medicated patients with schizophrenia have elevated HR and normal HRV compared to healthy controls, whilst CLZ-treated patients had tachycardia and diminished HRV (Rechlin et al., 1994). Based on these results, Rechlin et al. raise the possibility of using HRV to predict plasma CLZ concentration when blood sampling is unavailable, yet sensitivity of this method can be an issue since multiple factors such as age and concomitant medication can affect HRV (1998). Alternatively, measurement of plasma CLZ concentration can be used to determine the threshold of HRV decrement to elicit a therapeutic response, but will require further studies which may prove difficult (i.e., controlled studies with differing doses; Rechlin et al., 1998).

Although the use of HRV in reporting autonomic dysfunction in psychotic patients has become increasingly popular, most of the studies performed have focused on linear components of HRV rather than non-linear measures (Kim et al., 2004). Non-linear measures of HRV take into consideration that HR is part of a dynamic biological system, and although unpredictable in the long run (i.e., in a non-linear manner), the trajectory of the system can be theoretically determined using complex mathematical equations dependent on initial conditions of the system (Mansier et al., 1996). Kim et al. (2004) incorporated non-linear HRV parameters into their assessments of CLZ-induced autonomic dysfunction in patients with schizophrenia, demonstrating non-linear parameters were diminished with CLZ treatment, thereby indicating decreased autonomic control over cardiac function. Of note, the lack of correlation between sample entropy (SampEn) and CLZ dosage suggests psychosis directly influences autonomic function (Kim et al., 2004). SampEn is a complexity and regularity measure of time series data that removes bias by not including self-matches in calculations of probability and is largely independent of data length (Richman and Moorman, 2000). SampEn is inversely correlated with regularity, where higher values reflect randomness in the time series of HR recordings and thus arrhythmia (Kim et al., 2004). The authors propose to include non-linear HRV parameters to associate symptom severity with cardiac function.

Another study connecting psychosis symptom severity with cardiac function was conducted by Bär et al. (2005) in paranoid patients with schizophrenia, with HRV assessments taken before and after neuroleptic treatment. It was shown non-medicated patients displayed tachycardia and decreased HRV with no change after initiating antipsychotic treatment, suggesting schizophrenia directly affects autonomic activity (Bär et al., 2005). However, the study included a range of antipsychotics at inconsistent dosing regimens and will need to be replicated in a larger sample population.

The sole HRV preclinical study identified in our literature search was conducted by Wang et al. (2012), on male Wistar-Kyoto rats. This study also took into consideration the influence of antipsychotics on sleeping patterns and consequently autonomic activity during sleep-wake cycles. Results show rats treated with CLZ displayed accelerated HR and decreased RR, TP, HF, and LF%. When sleep-wake cycles were accounted for, the CLZ group demonstrated longer periods of wakefulness, to which the magnitude of the RR decrease was found to be less than that during sleep, implying CLZ-induced tachycardia was more severe during sleep (Wang et al., 2012). Of note, only animals treated with CLZ displayed significantly different RR, TP, and LF% values compared to controls regardless of consciousness. HAL and risperidone did not significantly influence HRV in the same manner as CLZ, which the authors attributed to CLZ's strong anticholinergic and antiadrenergic properties (Wang et al., 2012).

Postural Hypotension and Respiratory Sinus Arrhythmia

Several non-invasive cardiovascular tests have been developed to identify abnormalities in the ANS. These include recording HR response to the Valsalva maneuver, postural change and deep breathing, and BP response to sustained handgrip and postural change. Although these conventional tests are not as informative as spectral analysis of HRV, they are still used due to ease of implementation and they offer early detection of autonomic dysfunction when continuous ECG monitoring is unfeasible (Ewing and Clarke, 1986).

HR changes in response to posture and deep breathing reflect both sympathetic and parasympathetic reflex activity. HR is expected to increase rapidly when the subject moves from a supine to a standing position, then decreases as reflex bradycardia ensues. The characteristic increase in HR will be compromised in diseased states, such as diabetes (Ewing and Clarke, 1986). In a similar test, BP is first recorded while the subject is in a supine position and repeated when the subject is standing.

The difference in systolic BP (SBP) in the supine position and SBP when standing reflects postural fall in SBP, which normally should be <10 mmHg since sympathetic vasoconstriction rapidly restores SBP (Ewing and Clarke, 1982).

Testing HR response during deep breathing involves asking the subject to breathe deeply at a constant rate and calculating the differences between the maximal and minimal HRs during each cycle. Autonomic neuropathy will abolish the HRV that usually varies in sync with breathing cycles (Ewing and Clarke, 1982).

The Valsalva maneuver requires the seated subject to maintain a mercury manometer at 40 mmHg for 15 s by blowing into a mouthpiece. The results are expressed as ratios, where the longest RR interval in the 20 heart beats immediately after the maneuver is divided by the shortest RR interval during the maneuver. The maneuver is intended to induce stress where a drop in BP is accompanied by HR elevation. In healthy individuals, there is a reflexive overshooting of BP above baseline values and decreasing of HR after stress. Compromised parasympathetic regulation prevents BP from overshooting and HR remains unchanged following stress (Ewing and Clarke, 1982).

BP response during sustained handgrip evaluates sympathetic function, where sustained isometric muscular contraction increases cardiac output and results in a sharp increase in BP (Ewing and Clarke, 1982). The subject's maximum grip on a dynamometer is recorded and 30% of the recorded power is maintained over 5 min. Results are expressed in terms of diastolic BP (DBP) differences, where the difference between resting DBP is subtracted from the highest DBP during sustained handgrip. DBP should rise rapidly when commencing the handgrip from increased cardiac output, where individuals with autonomic neuropathy will show minimal increases in DBP (Ewing and Clarke, 1982).

Nielsen et al. (1988) studied the influence of postural change and breathing on HR in medicated and non-medicated patients with schizophrenia compared to healthy controls. Antipsychotics taken by the medicated group included flupentixol, CLZ and sulpiride. HR was continuously recorded over 15 min in the supine position and followed by a period of 5 min in the standing position. The difference in HR between the supine and standing positions were used to assess sympathetic activity, where an elevation of HR over 30 bpm was considered abnormal (Nielsen et al., 1988). In the resting supine position, medicated patients with schizophrenia had significantly higher HR than the non-medicated and control groups (Nielsen et al., 1988). However, postural changes resulted in significant HR responses in both medicated and non-medicated patients in comparison to healthy controls.

Testing for changes in HR during stages of respiration consisted of a 5 min resting period with normal breathing, followed by complete exhalation then deep and rapid inspiration. Subjects were asked to hold their breath for 20 s after inhaling and the difference between the maximal and minimal HR immediately after inspiration was used to denote HR response. Abnormal HR response was defined as a difference of <10 bpm compared to the norm of >15 bpm (Nielsen et al., 1988). HR response to deep inspiration was significantly higher in non-medicated patients with schizophrenia compared to both the medicated group and controls. However, all 3 groups had normal HR response ranging from 23 to 31 bpm, with only the medicated group showing any abnormality (3 out of 28 subjects).

In a later study, Agelink et al. (1998) modified the postural testing procedure to 10 min in the supine position preceding immediate standing, with the ratio of the 15th and 30th heartbeat reflecting sympathetic activity (30:15 ratio). The 15th heartbeat is indicative of the maximal increase of HR following the change in posture, whereas the 30th heartbeat represents peak reflex bradycardia (Agelink et al., 1998). Unlike Nielsen et al's. study (1988) where data of several different medications were pooled, Agelink et al. (1998) focused on comparing the individual drug effects of HAL and CLZ on cardiovascular autonomic parameters. A total of 46 inpatients with schizophrenia were recruited, where $n = 20$ received CLZ and $n = 26$ received HAL. The control group consisted of 30 healthy subjects. Resting HR and BP were significantly higher in the CLZ-treated group compared to HAL and controls. In addition, CLZ treatment significantly reduced 30:15 ratios, HR during deep breathing and BP during sustained handgrip, suggestive of autonomic dysfunction.

Electrodermal Activity

Electrodermal activity (EDA) or skin conductance is another widely used measure for sympathetic activity. Arousal of the SNS is directly correlated to sweat gland activity, as measured by electrical conductivity in the skin. There is evidence of both extremes of the EDA spectrum in patients with schizophrenia, known as non-responders (hypoactivity) and responders (hyperactivity), respectively (Ohman, 1981; Dawson and Nuechterlein, 1984; Nilsson et al., 2015). EDA is also indicative of social cognition regulation, as non-responders comprise a subgroup of patients with schizophrenia who display less empathy and are comparable to healthy controls, in contrast to responders who demonstrate significantly higher EDA and self-reported distress (Dawson and Schell, 2002; Schell et al., 2005; Ikezawa et al., 2012). In a study combining EDA and HRV, Zahn and Pickar (1993) demonstrate CLZ induced tachycardia, suppressed HRV and decreased skin conductance responses in comparison to placebo. Of interest, fluphenazine despite possessing anticholinergic properties, did not significantly affect HR to the same extent as CLZ. The authors suggest the discrepancy is due to CLZ being a more potent cholinergic and α_2-adrenoceptor antagonist than fluphenazine (Zahn and Pickar, 1993).

Catecholamines

Due to accessibility issues and invasiveness of measuring direct neuronal activity in humans, sampling of the major catecholamines norepinephrine (NE), epinephrine (E), and dopamine in plasma or urine has become increasingly popular for assessing sympathetic activity in health and disease (Esler et al., 1990; Forslund et al., 2002). Elevated plasma NE levels have been linked to a number of cardiovascular anomalies including heart failure (Thomas and Marks, 1978; Cohn et al., 1984; Hasking et al., 1986), hypertension (Rumantir et al., 2000; Masuo et al., 2003; Schlaich et al., 2004), left ventricular hypertrophy (Zoccali

et al., 2002; Schlaich et al., 2003) and postural tachycardia (Shannon et al., 2000; Goldstein et al., 2002; Mayer et al., 2006). Importantly, CLZ is known to substantially increase plasma NE spillover compared to conventional antipsychotics (Pickar et al., 1992; Green et al., 1993; Brown et al., 1997; Spivak et al., 1998).

There is evidence of elevated catecholamines associated with the use of CLZ. Li et al. (1997) reported a rise in BP from a low of 110/70 mmHg to a maximum of 146/106 mmHg in a patient during the course of 10 weeks of CLZ treatment. The hypertension was accompanied by rise in urinary E and NE, to which all 3 anomalies subsided after interventions were introduced and CLZ was discontinued (Li et al., 1997). Paroxysmal hypertension was diagnosed, as with multiple other case reports of CLZ-associated hypertension and raised urinary catecholamines (Krentz et al., 2001; Akinsola and Ong, 2011; Sara et al., 2013). In addition to hypertension, Akinsola and Ong (2011) reported tachycardia of 140 bpm in a patient and Krentz et al. (2001) reported 3 cases of accelerated HR ranging from 104 to 130 bpm. The authors postulated CLZ-induced paroxysmal hypertension arose from the increase in NE spillover due to reduced reuptake into sympathetic nerve endings, α-adrenoceptor antagonism and/or increased vesicular fusion (Li et al., 1997; Krentz et al., 2001; Akinsola and Ong, 2011; Sara et al., 2013).

A single-blinded study of in-patients with schizophrenia showed that CLZ-induced tachycardia and orthostatic hypotension were accompanied with a rise in cerebrospinal fluid homovanillic acid (HVA), a product of dopamine metabolism, in the first 5 days of treatment (Gerlach et al., 1974). Subsequently, Breier et al. (1994) investigated the role of catecholamines and their metabolites in a randomized, double-blinded study. Psychiatric outpatients were given either CLZ or HAL, for a period of 10 weeks. Blood samples, BP and HR were taken prior to the initiation of and during the 5th week of treatment. Apart from NE, catecholamine metabolites including 3,4-dihyroxy-$_L$-phenylalanine (dopa), dihydroxyphenylacetic acid (DOPAC), 3,4-dihydroxyphenylglycol (DHPG) were analyzed to reflect adrenergic action. A significant surge in plasma NE was evident in the CLZ group, which was statistically correlated with an increase in dopa (Breier et al., 1994). Despite a notable increase in HR, it was not correlated with the change in plasma NE (Breier et al., 1994). Of interest, the change in NE was correlated with positive outcome as indicated by lower scores in the Brief Psychiatric Rating Scale (BPRS) and Simpson-Angus Scale, suggestive of noradrenergic contribution to clinical efficacy (Breier et al., 1994). Due to unchanged DHPG levels, an increase in the intraneuronal metabolism of NE does not explain the observed surge in plasma NE. The authors speculate NE transporter (NET) inhibition played a role in increased circulating NE (Breier et al., 1994).

As elevated catecholamines have been linked to myocarditis, Wang et al. (2008) used a mouse model to investigate the effect of CLZ on heart structure and the release of NE, E, and the inflammatory marker TNF-α. CLZ was administered daily to young mice at varying doses, over a period of 7 or 14 days. Histological analysis revealed inflammation of the myocardium peaked on day 7, whereas NE and E were persistently elevated (Wang et al., 2008). Of note, TNF-α was only measured on day 14 and was found to be significantly elevated after CLZ treatment in a dose dependent manner (Wang et al., 2008).

Interventions

Of the 37 studies in our systematic review, 16 studies have reported using interventions and/or discontinuing CLZ to treat cardiovascular side effects. Commonly occurring side effects and their respective interventions will be discussed below.

Tachycardia

Tachycardia is defined by a HR above 100 bpm, accompanied by a mean HR of more than 90 bpm within a 24 h period (Sheldon et al., 2015). Accelerated HR is a commonly reported side-effect of CLZ and can precede fatal cardiac myopathies (Jones et al., 2014). Baciewicz et al. (2002) reported a patient who adversely responded to CLZ, with HR elevated to 150 bpm after 3 weeks of treatment. The patient received 5 mg of metoprolol, a β-adrenoceptor blocker, to alleviate the tachycardia (Baciewicz et al., 2002). Hypotension resulted from the metoprolol intervention, but symptoms subsided upon CLZ discontinuation.

Pereira et al. (2010) noted a case of neuroleptic malignant syndrome (NMS) in a 56 year old male patient with schizophrenia, characterized by profuse sweating, hand tremors, tachycardia and rigid limbs resulting from antipsychotic medication. The patient was previously on chronic chlorpromazine (150 mg/day, 10 years), CLZ (200 mg/day, 3 years) and atenolol (50 mg/day, 15 years). The patient's condition worsened as he developed convulsions on the 14th day of hospitalization, to which he was treated with phenytoin, divalproex sodium and bromocriptine. Discontinuation of CLZ resolved the NMS. The authors attribute the NMS to CLZ, since NMS should be apparent within the first month of chlorpromazine treatment while it can still emerge beyond 3 years of CLZ treatment (Pereira et al., 2010). Further evidence is provided by another 2 case reports of patients diagnosed with NMS (Yacoub and Francis, 2006). Both patients were given CLZ at 100–175 mg/day before NMS was diagnosed within 2 weeks of initiating CLZ treatment. Symptoms included unstable BP and HR as well as diaphoresis for one of the patients, which were resolved by withdrawing CLZ and introducing lorazepam.

Sinus tachycardia developed in a patient who attempted suicide by CLZ overdose, accompanied by sedation, hypothermia and hypersalivation (Thomas and Pollak, 2003). The patient ingested 3,500 mg of CLZ, resulting in hospitalization and treatment with naloxone and thiamine for the overdose. Serum drug levels deviated from the known CLZ half-life of 12 h, remaining at therapeutic levels of >300 ng/ml for 6 days instead of declining to negligible levels within 2 days (Thomas and Pollak, 2003). High HR also persisted (110–136 bpm) for 6 days, coinciding with the duration of the elevated serum CLZ levels. The plot of serum concentration versus time was of a biphasic pattern and consistent with a sustained release model, believed to be the result of CLZ accumulation and/or decreased bowel movements in the patient (Thomas and Pollak,

2003). Leo et al. (1996) also report a patient with sinus tachycardia after commencing CLZ at 750 mg/day. The dose was eventually lowered to 700 mg/day for 5 months, until persistent tachycardia and left ventricular (LV) abnormalities arose, to which CLZ was discontinued and digoxin (0.25 mg/day) was prescribed. Digoxin inhibits sodium-potassium ATPase to increase myocardial contractile force, sensitizes baroreceptors and promotes vagal control (Gheorghiade et al., 2004). The patient's cardiac anomalies were attributed to an existing cardiomyopathy exacerbated by CLZ (Leo et al., 1996).

Koren et al. (1997) reported a patient whose conditions deteriorated rapidly despite tolerating CLZ treatment for 11 weeks. The patient developed ventricular tachycardia and was treated unsuccessfully with lidocaine, eventually passing away within 36 h of hospitalization. The authors postulate the fatality was due to agranulocytosis and cardiomyopathy caused by lactic acidosis or myocarditis (Koren et al., 1997). The direct action of CLZ on membrane proteins may play a role in lactic acidosis, specifically CLZ's suppression of calcium-dependent potassium permeability leading to decreased insulin secretion (Koren et al., 1997).

A sixth report is of a young patient with schizophrenia who developed persistent tachycardia as a result of initiating CLZ for 1 week (Ennis and Parker, 1997). HR notably increased from 80 bpm to a maximum of 130 bpm, accompanied by hypertension upon commencement of CLZ.

Hypertension

Hypertension refers to a SBP above 120 mm Hg and a DBP above 80 mmHg, where individuals with chronically elevated BP above 140/90 mmHg are at a higher risk of developing premature CVD (Giles et al., 2005). In addition to persistent tachycardia that was noted in the previously mentioned case report, Ennis and Parker (1997) also noted hypertension in their patient. The authors ruled out common causes of hypertension, since blood tests, urinary catecholamines and physical examinations showed no obvious abnormalities (Ennis and Parker, 1997). Atenolol, a β_1-adrenoceptor antagonist, successfully stabilized the BP and HR, suggesting circulating catecholamines play a role in causing the hypertension (Ennis and Parker, 1997).

Li et al. (1997) reported a case of CLZ-induced pseudophaeochromocytoma, with the patient's BP rising up to 146/106 mmHg from 110/70 mmHg. The patient initially received CLZ at a dose of 25 mg/day, which was gradually titrated to 300 mg/day over the course of 10 weeks. Propranolol (PRO) and amlodipine were administered to reverse the hypertension. PRO and amlodipine lowers BP via β_1-adrenoceptor and calcium channel antagonism, respectively (Li et al., 1997). The patient's hypertension resolved after medication, although this may also be due to withdrawal of CLZ.

Similarly, Prasad and Kennedy (2003) noted hypertension in their patient 5 days after commencing CLZ at 50 mg/day. However, treatment with amlodipine at 5 mg/day was ineffective and the hypertension persisted until CLZ was withdrawn at 13 weeks. The authors postulate CLZ's hypertensive effects likely resulted from pseudophaeochromocytoma and the effects were transient (Prasad and Kennedy, 2003).

Hypotension

CLZ impeded vasopressor responses in a patient with schizophrenia suffering hemodynamic complications stemming from a subarachnoid hemorrhage (Leung et al., 2015). The patient developed hypotension (mid-90s mmHg) and tachycardia (>120 bpm), despite infusion of phenylephrine, NE, E, and dobutamine. Hypotension is commonly defined as a SBP lower than 90 mmHg, however, 110 mmHg has more recently been suggested (Eastridge et al., 2007). Mean arterial pressure (MAP) was restored following vasopressin administration and temporarily discontinuing CLZ, which removed the influence of CLZ's adrenoceptor antagonism as with the previous vasopressors (Leung et al., 2015).

Another example of CLZ interfering with treatment of hemodynamic disturbances is of a patient with schizophrenia who developed intraoperative hypotension following intubation under anesthesia (John et al., 2010). The patient's MAP decreased from 85 mmHg to 40 mmHg and was unresponsive to E administration. Further decrements in MAP led to the administration of vasopressin, which restored MAP to >65 mmHg. It was suggested CLZ blocked α_1-adrenergic receptors and caused vasodilation via reflex β_2-adrenoceptor activation, thereby worsening the already declining MAP (John et al., 2010). Vasopressin successfully induced vasoconstriction since its actions were mediated through the non-adrenergic receptor, V_1 receptor, thus bypassing the α_1-adrenergic inhibition. This mechanism perhaps explains the failure of E to raise SBP in the case presented by Koren et al. (1997).

Donnelly and MacLeod (1999) have also presented a clinical case report of a patient on chronic CLZ medication that developed hypotension after a cardiopulmonary bypass procedure. Methoxamine, metaraminol, dopamine and E infusions all failed to maintain the SBP above 60 mmHg, which was eventually restored to >80 mmHg by infusion of NE (Donnelly and MacLeod, 1999). The hypotension was attributed to CLZ-induced vasodilation.

Since melatonin has known benefits in reducing SGA-induced metabolic side effects in animal studies and regulates BP, Romo-Nava et al. (2014) sought to replicate the results in a randomized, double-blinded clinical trial. Patients with schizophrenia ($n = 24$) or bipolar disorder ($n = 20$) were given placebo ($n = 24$) or melatonin ($n = 20$, 5 mg/day) for 8 weeks and anthropometric variables were measured prior to and after the trial. All subjects were previously on SGA medication (CLZ, OLA, risperidone or quetiapine) for ≤3 months before recruitment. Although melatonin lowered DBP in all patients, the decrease was not statistically different from that of the placebo group in patients with schizophrenia. Metabolic measures also did not improve with melatonin use in patients with schizophrenia, while patients with bipolar disorder showed favorable outcome. The lack of therapeutic benefits for the schizophrenia patients is perhaps due to pooling data from 4 SGAs with varying risk for adverse cardiometabolic side effects instead of assessing the neuroleptics individually (Romo-Nava et al., 2014).

DISCUSSION

This review is a compilation of literature concerning cardiovascular anomalies associated with autonomic dysfunction in CLZ-treated patients with schizophrenia. We have highlighted case reports, clinical trials and animal studies to demonstrate the importance of monitoring cardiovascular parameters when administering CLZ. Patients with schizophrenia inherently have a higher risk for CVD than the general population, due to unhealthy lifestyle habits and use of SGAs (Kelly et al., 2010). Indeed, our results show CLZ is associated with fatal myocarditis, orthostatic hypotension, paradoxical hypertension and tachycardia. The results identified several characteristic features of CLZ's effects on the ANS: increased sympathetic activity, decreased vagal contribution, strong anticholinergic and antiadrenergic properties, increased E and NE and decreased HRV (Thomas and Marks, 1978; Nielsen et al., 1988; Zahn and Pickar, 1993; Ennis and Parker, 1997; Li et al., 1997; Agelink et al., 2001; Cohen et al., 2001a,b; Tümüklü et al., 2008; Wang et al., 2008, 2012; John et al., 2010; Mathewson et al., 2012; Huang et al., 2013; Sara et al., 2013; Leung et al., 2015). The studies, however, are short in duration with the longest clinical trial lasting 6 months (Huang et al., 2013). Side effects such as cardiomyopathy can occur after 12 months, hence future studies need to factor in the time of onset of relevant symptoms (Iqbal et al., 2003). CLZ is also frequently combined with other antipsychotic drugs (Honer et al., 2007, 2009; Procyshyn et al., 2010), even though the evidence indicates that polypharmacy has no therapeutic benefit and may increase metabolic side-effects (Boyda et al., 2010, 2013). It will therefore be important to determine if CLZ's cardiovascular effects are exacerbated by antipsychotic polypharmacy.

Less than half (16 out of 37) of the included studies have used interventions that have successfully attenuated CLZ-induced cardiovascular complications. These interventions include metoprolol, lorazepam, atenolol, PRO, amlodipine, vasopressin and NE infusion (Ennis and Parker, 1997; Li et al., 1997; Donnelly and MacLeod, 1999; Baciewicz et al., 2002; Yacoub and Francis, 2006; John et al., 2010; Leung et al., 2015). The drugs were administered in response to tachycardia, hypotension or paradoxical hypertension in individual case reports. Replication of the beneficial results in randomized, placebo-controlled trials with larger sample sizes is therefore warranted.

In contrast to the numerous reports of cardiovascular anomalies from CLZ use, there is a lack of in-depth investigations on the underlying causes of these adverse events. Breier et al.'s (1994) study of plasma NE metabolites is a rare trial that had explored mechanistic relationships between CLZ's superior efficacy and adrenergic function. A hallmark of CLZ-treated patients is the dramatic elevation of plasma NE levels, caused by inhibition of NE reuptake into postganglionic terminals, increased NE vesicular fusion, downregulation of β-adrenoceptors and/or inhibition of NET. It is widely believed increased sympathetic nerve traffic reflects increased NE spillover and plasma NE levels, but this is not always the case since vesicular leakage is also a major determinant of plasma NE levels as extensively reviewed elsewhere (Giles et al., 2005; Sheldon et al., 2015). Often underappreciated, vesicular leakage of NE into the cytoplasm ensures sustainable release beyond the maximal rate of synthesis by tyrosine hydroxylase activation to keep pace with NE release (Sheldon et al., 2015). Through measuring multiple plasma catecholamine metabolites that served as indicators of NE synthesis, release and reuptake, Breier et al. (1994) showed the surge in plasma NE levels was likely the result of combined inhibition of α-adrenoceptors and NET. A follow-up study from the same group further pinpointed the mechanism to be one of increased NE spillover, explained by increased vesicular fusion at the axonal membrane (Elman et al., 1999). Although these observations are pure speculation without further pharmacological studies, the inclusion of specific intraneuronal indicators of NE turnover and metabolism (i.e., DHPC, dopa, DOPAC) suggest increased NE spillover from vesicular fusion is possible. The studies, however, only document the acute effects of CLZ treatment on adrenergic function. Chronic studies are needed to determine the long-term role of NE spillover in autonomic neuropathy.

Autonomic tests such as changes in BP and HR in response to standing or deep breathing are also indicative of irregularities in the ANS. While test results are commonly used to reflect damage to the SNS and/or the PNS, they are unlikely to be solely parasympathetic or sympathetic in nature and instead represent a complex intertwine of the 2 branches of the ANS (Ewing and Clarke, 1982). Results from the "battery" of autonomic tests should be interpreted with caution as significant differences may not necessarily indicate severe autonomic neuropathy. Agelink et al. (1998) report significant differences in CLZ-treated groups, yet when the actual values are considered, the anomalies are categorized as "borderline" instead of "pathological." The reported 30:15 ratio, deep breathing HR response and handgrip BP response in CLZ-treated patients in this study all fall under the borderline category (Ewing and Clarke, 1982; Agelink et al., 1998). Nevertheless, autonomic tests remain as important indicators of autonomic dysfunction and are pivotal in early prevention of CLZ-induced CVD.

It is important to note our results yielded only 1 publication concerning myocarditis and cardiomyopathy. Given the grave consequences of myocarditis and cardiomyopathy, further elaboration of our results and pathogenesis of these cardiac disorders are warranted. Firstly, the focus of our review is on autonomic dysfunction associated with CLZ while it is believed CLZ-induced myocarditis arises from type 1 hypersensitivity mediated by immunoglobulin E (IgE) (Kilian et al., 1999) or of viral origin (Merrill et al., 2006). IgE-mediated hypersensitivity is the most convincing and widely accepted hypothesis to date, as the time to emergence of eosinophilic infiltrates corresponds accordingly to the time course of a type I allergic reaction and duration of CLZ treatment (Kilian et al., 1999; Ronaldson et al., 2015). Ensuing cardiomyopathy is believed to be the result of the direct cardiotoxic effects of CLZ or a type III hypersensitivity reaction (Merrill et al., 2005; Ronaldson et al., 2010). While there has been suggestion of catecholamine involvement in myocarditis and subsequent cardiomyopathy (Merrill et al., 2006; Wang et al., 2008), no definitive clinical evidence has been

presented thus far. Secondly, underreporting and misdiagnosis of the disorders frequently occur due to the variability of the symptoms associated with myocarditis (Ronaldson et al., 2015). CLZ-induced myocarditis can be overlooked as initial symptoms such as fever and tachycardia closely resemble normal CLZ dose titration and are typically resolved by discontinuation of CLZ before myocarditis can be diagnosed (Merrill et al., 2006; Ronaldson et al., 2015). Fatalities associated with myocarditis can also be missed since diagnosis would require an autopsy and histological assessment of the myocardial region concerned (Ronaldson et al., 2015). Under these circumstances the suspicion for myocarditis is low and would not generally warrant further monitoring and investigation. The correct diagnosis of myocarditis necessitates relevant cardiac monitoring at the time of onset of myocardial damage and awareness from psychiatrists. The abovementioned factors may have contributed to the lack of publications involving myocarditis and cardiomyopathy in our results.

Lastly, we summarize and propose additional measures to the current cardiac monitoring procedures to minimize risk for cardiac complications when commencing CLZ. The first 4 weeks of starting CLZ treatment should incorporate weekly monitoring of inflammatory (C-reactive protein; CRP) and myocardial damage (troponin I or T) markers in routine blood work for signs of myocarditis. As the onset of myocarditis is typically within 14 – 22 days of the start of CLZ treatment, it is critical to closely monitor patients for fever, troponin I or T and CRP levels for the first 28 days of treatment (Ronaldson et al., 2010, 2011). In a systematic review of CLZ-induced myocarditis, Ronaldson et al. noted the onset of fever and other symptoms non-specific for myocarditis after 10–19 days of commencing CLZ (2011). These symptoms should not be ignored especially when accompanied by CRP levels over 50 mg/L, which signify the onset of myocarditis (Ronaldson et al., 2011). Vital signs including BP, body temperature, HR and respiratory rate should be recorded every second day. Elevations in HR above 20–30 bpm can occur with the onset of initial symptoms and precede rising troponin I/T levels. In the event of CRP levels rising above 100 mg/L or troponin levels greater than 2 ULN, CLZ should be immediately discontinued, as these 2 measures represent the best sensitivity for symptomatic cases (Ronaldson et al., 2011; Freudenreich, 2015). Baseline echocardiography and weekly ECGs are ideal, but the former is unnecessary for identifying pre-existing cardiac complications and the latter lacks sensitivity in detecting myocarditis (Stein et al., 1994; Ronaldson et al., 2011). Since there is concern for exhausting available health care resources, it has been suggested that an ECG is required only when myocarditis is suspected (Freudenreich, 2015). However, we recommend the inclusion of a weekly ECG to detect abnormal changes in HRV and performing weekly autonomic tests during the critical first 4 weeks of CLZ treatment. These measures can be incorporated with the mandatory blood sampling each week to reduce any burden on health care resources. Early detection of cardiac abnormalities is not only crucial for preventing fatalities, but will also reduce the eventual costs of health care in the long run. Every effort should be made in maximizing the therapeutic benefits of CLZ, which remains heavily underutilized in managing treatment-resistant schizophrenia (Kar et al., 2016).

CONCLUSION

Reduced HRV, elevated catecholamines, tachycardia and hypotension are known effects of CLZ treatment. Yet there is a lack of controlled trials to confirm that these autonomic abnormalities are caused specifically by CLZ. Future studies should incorporate both mechanistic relationships as well as interventions to minimize CLZ's adverse effects on cardiovascular function, such as different dosing strategies (Procyshyn et al., 2014). Moreover, CLZ's strong antagonistic properties on multiple receptors should be considered before prescribing CLZ to patients with cardiovascular complications, as evidenced by failure to restore cardiac homeostasis in several patients using conventional adrenergic agonists. Clinicians should consider the use of HRV and conventional autonomic tests to preliminary screen for patients with a higher risk for cardiovascular adverse events before commencing CLZ treatment and to continuously monitor cardiovascular function once CLZ is prescribed.

AUTHOR CONTRIBUTIONS

JY performed the systematic search and wrote the manuscript, in collaboration with AB. All other authors assisted with the review and contributed to the final draft of the manuscript.

ACKNOWLEDGMENTS

This work was supported by a grant from NSERC to AB, and support from the BC Provincial Health Services Authority.

SUPPLEMENTARY MATERIAL

The Supplementary Material for this article can be found online at: https://www.frontiersin.org/articles/10.3389/fnins.2018.00203/full#supplementary-material

REFERENCES

(1996). Heart rate variability: standards of measurement, physiological interpretation and clinical use. Task Force of the European Society of Cardiology and the North American Society of Pacing and Electrophysiology. *Circulation* 93, 1043–1065. doi: 10.1161/01.CIR.93.5.1043

Agelink, M. W., Majewski, T., Wurthmann, C., Lukas, K., Ullrich, H., Linka, T., et al. (2001). Effects of newer atypical antipsychotics on autonomic neurocardiac function: a comparison between amisulpride, olanzapine, sertindole, and clozapine. *J. Clin. Psychopharmacol.* 21, 8–13. doi: 10.1097/00004714-200102000-00003

Agelink, M. W., Malessa, R., Kamcili, E., Zeit, T., Lemmer, W., Bertling, R., et al. (1998). Cardiovascular autonomic reactivity in schizophrenics

under neuroleptic treatment: a potential predictor of short-term outcome? *Neuropsychobiology* 38, 19–24. doi: 10.1159/000026512

Akinsola, O., and Ong, K. (2011). Pseudophaeochromocytoma associated with clozapine therapy: a case report. *Afr. J. Psychiatry (Johannesbg).* 14, 406–408. doi: 10.4314/ajpsy.v14i5.9

Akselrod, S., Gordon, D., Ubel, F. A., Shannon, D. C., Berger, A. C., and Cohen, R. J. (1981). Power spectrum analysis of heart rate fluctuation: a quantitative probe of beat-to-beat cardiovascular control. *Science* 213, 220–222. doi: 10.1126/science.6166045

Alvir, J. M., Lieberman, J. A., Safferman, A. Z., Schwimmer, J. L., and Schaaf, J. A. (1993). Clozapine-induced agranulocytosis. Incidence and risk factors in the United States. *N. Engl. J. Med.* 329, 162–167. doi: 10.1056/NEJM199307153290303

Andreazza, A. C., Barakauskas, V. E., Fazeli, S., Feresten, A., Shao, L., Wei, V., et al. (2015). Effects of haloperidol and clozapine administration on oxidative stress in rat brain, liver and serum. *Neurosci. Lett.* 591, 36–40. doi: 10.1016/j.neulet.2015.02.028

Ascher-Svanum, H., Zhu, B., Faries, D., Landbloom, R., Swartz, M., and Swanson, J. (2006). Time to discontinuation of atypical versus typical antipsychotics in the naturalistic treatment of schizophrenia. *BMC Psychiatry* 6:8. doi: 10.1186/1471-244X-6-8

Baciewicz, A. M., Chandra, R., and Whelan, P. (2002). Clozapine-associated neuroleptic malignant syndrome. *Ann. Inter. Med.* 137(5Pt 1):74. doi: 10.7326/0003-4819-137-5_Part_1-200209030-00034

Bär, K. J., Berger, S., Metzner, M., Boettger, M. K., Schulz, S., Ramachandraiah, C. T., et al. (2010). Autonomic dysfunction in unaffected first-degree relatives of patients suffering from schizophrenia. *Schizophr. Bull.* 36, 1050–1058. doi: 10.1093/schbul/sbp024

Bär, K. J., Boettger, M. K., Berger, S., Baier, V., Sauer, H., Yeragani, V. K., et al. (2007). Decreased baroreflex sensitivity in acute schizophrenia. *J. Appl. Physiol. (1985)* 102, 1051–1056. doi: 10.1152/japplphysiol.00811.2006

Bär, K. J., Letzsch, A., Jochum, T., Wagner, G., Greiner, W., and Sauer, H. (2005). Loss of efferent vagal activity in acute schizophrenia. *J. Psychiatr. Res.* 39, 519–527. doi: 10.1016/j.jpsychires.2004.12.007

Barr, A. M., Procyshyn, R. M., Hui, P., Johnson, J. L., and Honer, W. G. (2008). Self-reported motivation to smoke in schizophrenia is related to antipsychotic drug treatment. *Schizophr. Res.* 100, 252–260. doi: 10.1016/j.schres.2007.11.027

Bobes, J., Arango, C., Garcia-Garcia, M., and Rejas, J. (2010). Healthy lifestyle habits and 10-year cardiovascular risk in schizophrenia spectrum disorders: an analysis of the impact of smoking tobacco in the CLAMORS schizophrenia cohort. *Schizophr. Res.* 119, 101–109. doi: 10.1016/j.schres.2010.02.1030

Boyda, H. N., Procyshyn, R. M., Tse, L., Xu, J., Jin, C. H., Wong, D., et al. (2013). Antipsychotic polypharmacy increases metabolic dysregulation in female rats. *Exp. Clin. Psychopharmacol.* 21, 164–171. doi: 10.1037/a0031228

Boyda, H. N., Tse, L., Procyshyn, R. M., Wong, D., Wu, T. K., Pang, C. C., et al. (2010). A parametric study of the acute effects of antipsychotic drugs on glucose sensitivity in an animal model. *Prog. Neuropsychopharmacol. Biol. Psychiatry* 34, 945–954. doi: 10.1016/j.pnpbp.2010.04.024

Breier, A., Buchanan, R. W., Waltrip, R. W. II., Listwak, S., Holmes, C., and Goldstein, D. S. (1994). The effect of clozapine on plasma norepinephrine: relationship to clinical efficacy. *Neuropsychopharmacology* 10, 1–7. doi: 10.1038/npp.1994.1

Brown, A. S., Gewirtz, G., Harkavy-Friedman, J., Cooper, T., Brebion, G., Amador, X. F., et al. (1997). Effects of clozapine on plasma catecholamines and relation to treatment response in schizophrenia: a within-subject comparison with haloperidol. *Neuropsychopharmacology* 17, 317–325. doi: 10.1016/S0893-133X(97)00073-0

Buckley, N. A., and Sanders, P. (2000). Cardiovascular adverse effects of antipsychotic drugs. *Drug Saf.* 23, 215–228. doi: 10.2165/00002018-200023030-00004

Bymaster, F. P., Calligaro, D. O., Falcone, J. F., Marsh, R. D., Moore, N. A., Tye, N. C., et al. (1996). Radioreceptor binding profile of the atypical antipsychotic olanzapine. *Neuropsychopharmacology* 14, 87–96. doi: 10.1016/0893-133X(94)00129-N

Bymaster, F. P., Rasmussen, K., Calligaro, D. O., Nelson, D. L., DeLapp, N. W., Wong, D. T., et al. (1997). *In vitro* and *in vivo* biochemistry of olanzapine: a novel, atypical antipsychotic drug. *J. Clin. Psychiatry* 58 (Suppl. 10), 28–36.

Casey, D. E. (1989). Clozapine: neuroleptic-induced EPS and tardive dyskinesia. *Psychopharmacology (Berl).* 99 (Suppl.), S47–S53. doi: 10.1007/BF00442559

Chang, J. S., Yoo, C. S., Yi, S. H., Hong, K. H., Oh, H. S., Hwang, J. Y., et al. (2009). Differential pattern of heart rate variability in patients with schizophrenia. *Prog. Neuropsychopharmacol. Biol. Psychiatry* 33, 991–995. doi: 10.1016/j.pnpbp.2009.05.004

Citrome, L., McEvoy, J. P., and Saklad, S. R. (2016). A guide to the management of clozapine-related tolerability and safety concerns. *Clin. Schizophr. Relat. Psychoses*. 10, 163–177. doi: 10.3371/1935-1232.10.3.163

Cohen, H., Loewenthal, U., Matar, M. A., and Kotler, M. (2001b). Reversal of pathologic cardiac parameters after transition from clozapine to olanzapine treatment: a case report. *Clin. Neuropharmacol.* 24, 106–108. doi: 10.1097/00002826-200103000-00008

Cohen, H., Loewenthal, U., Matar, M., and Kotler, M. (2001a). Association of autonomic dysfunction and clozapine. Heart rate variability and risk for sudden death in patients with schizophrenia on long-term psychotropic medication. *Br. J. Psychiatry* 179, 167–171. doi: 10.1192/bjp.179.2.167

Cohn, J. N., Levine, T. B., Olivari, M. T., Garberg, V., Lura, D., Francis, G. S., et al. (1984). Plasma norepinephrine as a guide to prognosis in patients with chronic congestive heart failure. *N. Engl. J. Med.* 311, 819–823. doi: 10.1056/NEJM198409273111303

Conley, R. R., Love, R. C., Kelly, D. L., and Bartko, J. J. (1999). Rehospitalization rates of patients recently discharged on a regimen of risperidone or clozapine. *Am. J. Psychiatry* 156, 863–868. doi: 10.1176/ajp.156.6.863

Dawson, M. E., and Nuechterlein, K. H. (1984). Psychophysiological dysfunctions in the developmental course of schizophrenic disorders. *Schizophr. Bull.* 10, 204–232. doi: 10.1093/schbul/10.2.204

Dawson, M. E., and Schell, A. M. (2002). What does electrodermal activity tell us about prognosis in the schizophrenia spectrum? *Schizophr. Res.* 54, 87–93. doi: 10.1016/S0920-9964(01)00355-3

De Hert, M., Detraux, J., van Winkel, R., Yu, W., and Correll, C. U. (2011). Metabolic and cardiovascular adverse effects associated with antipsychotic drugs. *Nat. Rev. Endocrinol.* 8, 114–126. doi: 10.1038/nrendo.2011.156

Dekker, J. M., Crow, R. S., Folsom, A. R., Hannan, P. J., Liao, D., Swenne, C. A., et al. (2000). Low heart rate variability in a 2-minute rhythm strip predicts risk of coronary heart disease and mortality from several causes: the ARIC Study. Atherosclerosis Risk In Communities. *Circulation* 102, 1239–1244. doi: 10.1161/01.CIR.102.11.1239

Donnelly, J. G., and MacLeod, A. D. (1999). Hypotension associated with clozapine after cardiopulmonary bypass. *J. Cardiothorac. Vasc. Anesth.* 13, 597–599. doi: 10.1016/S1053-0770(99)90016-2

Eastridge, B. J., Salinas, J., McManus, J. G., Blackburn, L., Bugler, E. M., Cooke, W. H., et al. (2007). Hypotension begins at 110 mm Hg: redefining "hypotension" with data. *J. Trauma 63*, 291–297; discussion 297–299. doi: 10.1097/TA.0b013e31809ed924

Elman, I., Goldstein, D. S., Eisenhofer, G., Folio, J., Malhotra, A. K., Adler, C. M., et al. (1999). Mechanism of peripheral noradrenergic stimulation by clozapine. *Neuropsychopharmacology* 20, 29–34. doi: 10.1016/S0893-133X(98)00047-5

Ennis, L. M., and Parker, R. M. (1997). Paradoxical hypertension associated with clozapine. *Med. J. Aust.* 166:278.

Esler, M., Jennings, G., Lambert, G., Meredith, I., Horne, M., and Eisenhofer, G. (1990). Overflow of catecholamine neurotransmitters to the circulation: source, fate, and functions. *Physiol. Rev.* 70, 963–985. doi: 10.1152/physrev.1990.70.4.963

Essali, A., Al-Haj Haasan, N., Li, C., and Rathbone, J. (2009). Clozapine versus typical neuroleptic medication for schizophrenia. *Cochr. Datab. Syst. Rev.* CD000059. doi: 10.1002/14651858.CD000059.pub2

Essock, S. M., Hargreaves, W. A., Covell, N. H., and Goethe, J. (1996). Clozapine's effectiveness for patients in state hospitals: results from a randomized trial. *Psychopharmacol. Bull.* 32, 683–697.

Ewing, D. J., and Clarke, B. F. (1982). Diagnosis and management of diabetic autonomic neuropathy. *Br. Med. J.* 285, 916–918. doi: 10.1136/bmj.285.6346.916

Ewing, D. J., and Clarke, B. F. (1986). Autonomic neuropathy: its diagnosis and prognosis. *Clin. Endocrinol. Metab.* 15, 855–888. doi: 10.1016/S0300-595X(86)80078-0

Fineschi, V., Neri, M., Riezzo, I., and Turillazzi, E. (2004). Sudden cardiac death due to hypersensitivity myocarditis during clozapine treatment. *Int. J. Legal Med.* 118, 307–309. doi: 10.1007/s00414-004-0464-1

Forslund, L., Björkander, I., Ericson, M., Held, C., Kahan, T., Rehnqvist, N., et al. (2002). Prognostic implications of autonomic function assessed by analyses of catecholamines and heart rate variability in stable angina pectoris. *Heart* 87, 415–422. doi: 10.1136/heart.87.5.415

Fredrikson, D. H., Boyda, H. N., Tse, L., Whitney, Z., Pattison, M. A., Ott, F. J., et al. (2014). Improving metabolic and cardiovascular health at an early psychosis intervention program in vancouver, Canada. *Front. Psychiatry* 5:105. doi: 10.3389/fpsyt.2014.00105

Freudenreich, O. (2015). Clozapine-induced myocarditis: prescribe safely but do prescribe. *Acta Psychiatr. Scand.* 132, 240–241. doi: 10.1111/acps.12425

Gerlach, J., Koppelhus, P., Helweg, E., and Monrad, A. (1974). Clozapine and haloperidol in a single-blind cross-over trial: therapeutic and biochemical aspects in the treatment of schizophrenia. *Acta Psychiatr. Scand.* 50, 410–424. doi: 10.1111/j.1600-0447.1974.tb09706.x

Gheorghiade, M., Adams, K. F. Jr., and Colucci, W. S. (2004). Digoxin in the management of cardiovascular disorders. *Circulation* 109, 2959–2964. doi: 10.1161/01.CIR.0000132482.95686.87

Giles, T. D., Berk, B. C., Black, H. R., Cohn, J. N., Kostis, J. B., Izzo, J. L. Jr., et al. (2005). Expanding the definition and classification of hypertension. *J. Clin. Hypertens. (Greenwich).* 7, 505–512. doi: 10.1111/j.1524-6175.2005.04769.x

Goldstein, D. S., Holmes, C., Frank, S. M., Dendi, R., Cannon, R. O. III., Sharabi, Y., et al. (2002). Cardiac sympathetic dysautonomia in chronic orthostatic intolerance syndromes. *Circulation* 106, 2358–2365. doi: 10.1161/01.CIR.0000036015.54619.B6

Green, A. I., Alam, M. Y., Sobieraj, J. T., Pappalardo, K. M., Waternaux, C., Salzman, C., et al. (1993). Clozapine response and plasma catecholamines and their metabolites. *Psychiatry Res.* 46, 139–149. doi: 10.1016/0165-1781(93)90016-A

Haas, S. J., Hill, R., Krum, H., Liew, D., Tonkin, A., Demos, L., et al. (2007). Clozapine-associated myocarditis: a review of 116 cases of suspected myocarditis associated with the use of clozapine in Australia during 1993-2003. *Drug Saf.* 30, 47–57. doi: 10.2165/00002018-200730010-00005

Hasking, G. J., Esler, M. D., Jennings, G. L., Burton, D., Johns, J. A., and Korner, P. I. (1986). Norepinephrine spillover to plasma in patients with congestive heart failure: evidence of increased overall and cardiorenal sympathetic nervous activity. *Circulation* 73, 615–621. doi: 10.1161/01.CIR.73.4.615

Henderson, D. C., Cagliero, E., Gray, C., Nasrallah, R. A., Hayden, D. L., Schoenfeld, D. A., et al. (2000). Clozapine, diabetes mellitus, weight gain, and lipid abnormalities: a five-year naturalistic study. *Am. J. Psychiatry* 157, 975–981. doi: 10.1176/appi.ajp.157.6.975

Henderson, D. C., Nguyen, D. D., Copeland, P. M., Hayden, D. L., Borba, C. P., Louie, P. M., et al. (2005). Clozapine, diabetes mellitus, hyperlipidemia, and cardiovascular risks and mortality: results of a 10-year naturalistic study. *J. Clin. Psychiatry* 66, 1116–1121. doi: 10.4088/JCP.v66n0905

Hennekens, C. H., Hennekens, A. R., Hollar, D., and Casey, D. E. (2005). Schizophrenia and increased risks of cardiovascular disease. *Am. Heart J.* 150, 1115–1121. doi: 10.1016/j.ahj.2005.02.007

Honer, W. G., Jones, A. A., Thornton, A. E., Barr, A. M., Procyshyn, R. M., and Vila-Rodriguez, F. (2015). Response trajectories to clozapine in a secondary analysis of pivotal trials support using treatment response to subtype schizophrenia. *Can. J. Psychiatry* 60(3Suppl. 2), S19–S25.

Honer, W. G., Procyshyn, R. M., Chen, E. Y., MacEwan, G. W., and Barr, A. M. (2009). A translational research approach to poor treatment response in patients with schizophrenia: clozapine-antipsychotic polypharmacy. *J. Psychiatry Neurosci.* 34, 433–442.

Honer, W. G., Thornton, A. E., Sherwood, M., MacEwan, G. W., Ehmann, T. S., Williams, R., et al. (2007). Conceptual and methodological issues in the design of clinical trials of antipsychotics for the treatment of schizophrenia. *CNS Drugs* 21, 699–714. doi: 10.2165/00023210-200721090-00001

Huang, W. L., Chang, L. R., Kuo, T. B., Lin, Y. H., Chen, Y. Z., and Yang, C. C. (2013). Impact of antipsychotics and anticholinergics on autonomic modulation in patients with schizophrenia. *J. Clin. Psychopharmacol.* 33, 170–177. doi: 10.1097/JCP.0b013e3182839052

Ikezawa, S., Corbera, S., Liu, J., and Wexler, B. E. (2012). Empathy in electrodermal responsive and nonresponsive patients with schizophrenia. *Schizophr. Res.* 142, 71–76. doi: 10.1016/j.schres.2012.09.011

Iqbal, M. M., Rahman, A., Husain, Z., Mahmud, S. Z., Ryan, W. G., and Feldman, J. M. (2003). Clozapine: a clinical review of adverse effects and management. *Ann. Clin. Psychiatry* 15, 33–48. doi: 10.3109/10401230309085668

Jänig, W. (2006). *The Integrative Action of the Autonomic Nervous System: Neurobiology of Homeostasis.* New York, NY: Cambridge University Press.

John, A., Yeh, C., Boyd, J., and Greilich, P. E. (2010). Treatment of refractory hypotension with low-dose vasopressin in a patient receiving clozapine. *J. Cardiothorac. Vasc. Anesth.* 24, 467–468. doi: 10.1053/j.jvca.2009.09.005

Jones, W. R., Narayana, U., Howarth, S., Shinners, J., and Nazar, Q. (2014). Cardiovascular monitoring in patients prescribed clozapine. *Psychiatr. Bull.* 38:140. doi: 10.1192/pb.38.3.140a

Kalkman, H. O., Neumann, V., Hoyer, D., and Tricklebank, M. D. (1998). The role of alpha2-adrenoceptor antagonism in the anti-cataleptic properties of the atypical neuroleptic agent, clozapine, in the rat. *Br. J. Pharmacol.* 124, 1550–1556. doi: 10.1038/sj.bjp.0701975

Kane, J. M., Cooper, T. B., Sachar, E. J., Halpern, F. S., and Bailine, S. (1981). Clozapine: plasma levels and prolactin response. *Psychopharmacology (Berl).* 73, 184–187. doi: 10.1007/BF00429215

Kane, J., Honigfeld, G., Singer, J., and Meltzer, H. (1988). Clozapine for the treatment-resistant schizophrenic. A double-blind comparison with chlorpromazine. *Arch. Gen. Psychiatry* 45, 789–796. doi: 10.1001/archpsyc.1988.01800330013001

Kar, N., Barreto, S., and Chandavarkar, R. (2016). Clozapine monitoring in clinical practice: beyond the mandatory requirement. *Clin. Psychopharmacol. Neurosci.* 14, 323–329. doi: 10.9758/cpn.2016.14.4.323

Kelly, D. L., McMahon, R. P., Liu, F., Love, R. C., Wehring, H. J., Shim, J. C., et al. (2010). Cardiovascular disease mortality in patients with chronic schizophrenia treated with clozapine: a retrospective cohort study. *J. Clin. Psychiatry* 71, 304–311. doi: 10.4088/JCP.08m04718yel

Kilian, J. G., Kerr, K., Lawrence, C., and Celermajer, D. S. (1999). Myocarditis and cardiomyopathy associated with clozapine. *Lancet* 354, 1841–1845. doi: 10.1016/S0140-6736(99)10385-4

Kim, J. H., Yi, S. H., Yoo, C. S., Yang, S. A., Yoon, S. C., Lee, K. Y., et al. (2004). Heart rate dynamics and their relationship to psychotic symptom severity in clozapine-treated schizophrenic subjects. *Prog. Neuropsychopharmacol. Biol. Psychiatry* 28, 371–378. doi: 10.1016/j.pnpbp.2003.11.007

Koren, W., Kreis, Y., Duchowiczny, K., Prince, T., Sancovici, S., Sidi, Y., et al. (1997). Lactic acidosis and fatal myocardial failure due to clozapine. *Ann. Pharmacother.* 31, 168–170. doi: 10.1177/106002809703100206

Krentz, A. J., Mikhail, S., Cantrell, P., and Hill, G. M. (2001). Drug points: pseudophaeochromocytoma syndrome associated with clozapine. *BMJ* 322:1213. doi: 10.1136/bmj.322.7296.1213

La Grenade, L., Graham, D., and Trontell, A. (2001). Myocarditis and cardiomyopathy associated with clozapine use in the United States. *N. Engl. J. Med.* 345, 224–225. doi: 10.1056/NEJM200107193450317

La Rovere, M. T., Bigger, J. T. Jr., Marcus, F. I., Mortara, A., and Schwartz, P. J. (1998). Baroreflex sensitivity and heart-rate variability in prediction of total cardiac mortality after myocardial infarction. ATRAMI (Autonomic Tone and Reflexes After Myocardial Infarction) Investigators. *Lancet* 351, 478–484. doi: 10.1016/S0140-6736(97)11144-8

Lang, D. J., Barr, A. M., and Procyshyn, R. M. (2013). Management of medication-related cardiometabolic risk in patients with severe mental illness. *Curr. Cardiovasc. Risk Rep.* 7, 283–287. doi: 10.1007/s12170-013-0321-1

Lee, L. H., White, R. F., Barr, A. M., Honer, W. G., and Procyshyn, R. M. (2016). Elevated clozapine plasma concentration secondary to a urinary

tract infection: proposed mechanisms. *J. Psychiatry Neurosci.* 41, E67–E68. doi: 10.1503/jpn.150156

Leo, R. J., Kreeger, J. L., and Kim, K. Y. (1996). Cardiomyopathy associated with clozapine. *Ann. Pharmacother.* 30, 603–605. doi: 10.1177/1060028096030 00606

Leung, J. G., Nelson, S., and Hocker, S. (2015). Failure of induced hypertension for symptomatic vasospasm in the setting of clozapine therapy. *Neurocrit. Care* 23, 409–413. doi: 10.1007/s12028-015-0129-6

Leung, J. Y., Barr, A. M., Procyshyn, R. M., Honer, W. G., and Pang, C. C. (2012). Cardiovascular side-effects of antipsychotic drugs: the role of the autonomic nervous system. *Pharmacol. Ther.* 135, 113–122. doi: 10.1016/j.pharmthera.2012.04.003

Li, J. K., Yeung, V. T., Leung, C. M., Chow, C. C., Ko, G. T., So, W. Y., et al. (1997). Clozapine: a mimicry of phaeochromocytoma. *Aust. N.Z.J. Psychiatry* 31, 889–891. doi: 10.3109/00048679709065519

Lindström, L. H. (1988). The effect of long-term treatment with clozapine in schizophrenia: a retrospective study in 96 patients treated with clozapine for up to 13 years. *Acta Psychiatr. Scand.* 77, 524–529. doi: 10.1111/j.1600-0447.1988.tb05164.x

Mackin, P. (2008). Cardiac side effects of psychiatric drugs. *Hum. Psychopharmacol.* 23(Suppl. 1), 3–14. doi: 10.1002/hup.915

Mansier, P., Clairambault, J., Charlotte, N., Médigue, C., Vermeiren, C., LePape, G., et al. (1996). Linear and non-linear analyses of heart rate variability: a minireview. *Cardiovasc. Res.* 31, 371–379. doi: 10.1016/S0008-6363(96)00 009-0

Masri, B., Salahpour, A., Didriksen, M., Ghisi, V., Beaulieu, J. M., Gainetdinov, R. R., et al. (2008). Antagonism of dopamine D2 receptor/beta-arrestin 2 interaction is a common property of clinically effective antipsychotics. *Proc. Natl. Acad. Sci. U.S.A.* 105, 13656–13661. doi: 10.1073/pnas.08035 22105

Masuo, K., Kawaguchi, H., Mikami, H., Ogihara, T., and Tuck, M. L. (2003). Serum uric acid and plasma norepinephrine concentrations predict subsequent weight gain and blood pressure elevation. *Hypertension* 42, 474–480. doi: 10.1161/01.HYP.0000091371.53502.D3

Mathewson, K. J., Jetha, M. K., Goldberg, J. O., and Schmidt, L. A. (2012). Autonomic regulation predicts performance on Wisconsin Card Sorting Test (WCST) in adults with schizophrenia. *Biol. Psychol.* 91, 389–399. doi: 10.1016/j.biopsycho.2012.09.002

Mayer, A. F., Schroeder, C., Heusser, K., Tank, J., Diedrich, A., Schmieder, R. E., et al. (2006). Influences of norepinephrine transporter function on the distribution of sympathetic activity in humans. *Hypertension* 48, 120–126. doi: 10.1161/01.HYP.0000225424.13138.5d

McEvoy, J. P., Meyer, J. M., Goff, D. C., Nasrallah, H. A., Davis, S. M., Sullivan, L., et al. (2005). Prevalence of the metabolic syndrome in patients with schizophrenia: baseline results from the Clinical Antipsychotic Trials of Intervention Effectiveness (CATIE) schizophrenia trial and comparison with national estimates from NHANES III. *Schizophr. Res.* 80, 19–32. doi: 10.1016/j.schres.2005.0 7.014

Melkersson, K. (2005). Differences in prolactin elevation and related symptoms of atypical antipsychotics in schizophrenic patients. *J. Clin. Psychiatry* 66, 761–767. doi: 10.4088/JCP.v66n0614

Meltzer, H. Y. (1997). Treatment-resistant schizophrenia–the role of clozapine. *Curr. Med. Res. Opin.* 14, 1–20. doi: 10.1185/03007999709113338

Meltzer, H. Y. (2012). Clozapine: balancing safety with superior antipsychotic efficacy. *Clin. Schizophr. Relat. Psychoses* 6, 134–144. doi: 10.3371/CSRP.6.3.5

Meltzer, H. Y., and Okayli, G. (1995). Reduction of suicidality during clozapine treatment of neuroleptic-resistant schizophrenia: impact on risk-benefit assessment. *Am. J. Psychiatry* 152, 183–190. doi: 10.1176/ajp.152. 2.183

Merrill, D. B., Ahmari, S. E., Bradford, J. M., and Lieberman, J. A. (2006). Myocarditis during clozapine treatment. *Am. J. Psychiatry* 163, 204–208. doi: 10.1176/appi.ajp.163.2.204

Merrill, D. B., Dec, G. W., and Goff, D. C. (2005). Adverse cardiac effects associated with clozapine. *J. Clin. Psychopharmacol.* 25, 32–41. doi: 10.1097/01.jcp.0000150217.51433.9f

Modai, I., Hirschmann, S., Rava, A., Kurs, R., Barak, P., Lichtenberg, P., et al. (2000). Sudden death in patients receiving clozapine treatment: a preliminary investigation. *J. Clin. Psychopharmacol.* 20, 325–327. doi: 10.1097/00004714-200006000-00006

Monsma, F. J. Jr., Shen, Y., Ward, R. P., Hamblin, M. W., and Sibley, D. R. (1993). Cloning and expression of a novel serotonin receptor with high affinity for tricyclic psychotropic drugs. *Mol. Pharmacol.* 43, 320–327.

Mueck-Weymann, M., Rechlin, T., Ehrengut, F., Rauh, R., Acker, J., Dittmann, R. W., et al. (2002). Effects of olanzapine and clozapine upon pulse rate variability. *Depress. Anxiety* 16, 93–99. doi: 10.1002/da. 10037

Nasrallah, H. A. (2008). Atypical antipsychotic-induced metabolic side effects: insights from receptor-binding profiles. *Mol. Psychiatry* 13, 27–35. doi: 10.1038/sj.mp.4002066

Nielsen, B. M., Mehlsen, J., and Behnke, K. (1988). Altered balance in the autonomic nervous system in schizophrenic patients. *Clin. Physiol.* 8, 193–199. doi: 10.1111/j.1475-097X.1988.tb00208.x

Nilsson, B. M., Holm, G., Hultman, C. M., and Ekselius, L. (2015). Cognition and autonomic function in schizophrenia: inferior cognitive test performance in electrodermal and niacin skin flush non-responders. *Euro. Psychiatry* 30, 8–13. doi: 10.1016/j.eurpsy.2014.06.004

Nolan, J., Batin, P. D., Andrews, R., Lindsay, S. J., Brooksby, P., Mullen, M., et al. (1998). Prospective study of heart rate variability and mortality in chronic heart failure: results of the United Kingdom heart failure evaluation and assessment of risk trial (UK-heart). *Circulation* 98, 1510–1516. doi: 10.1161/01.CIR.98.15.1510

Ohman, A. (1981). Electrodermal activity and vulnerability to schizophrenia: a review. *Biol. Psychol.* 12, 87–145. doi: 10.1016/0301-0511(81)90008-9

Olfson, M., Marcus, S. C., Corey-Lisle, P., Tuomari, A. V., Hines, P., and L'Italien, G. J. (2006). Hyperlipidemia following treatment with antipsychotic medications. *Am. J. Psychiatry* 163, 1821–1825. doi: 10.1176/ajp.2006.163.10.1821

Paton, J. F., Boscan, P., Pickering, A. E., and Nalivaiko, E. (2005). The yin and yang of cardiac autonomic control: vago-sympathetic interactions revisited. *Brain Res. Brain Res. Rev.* 49, 555–565. doi: 10.1016/j.brainresrev.2005.0 2.005

Pereira, Y. D., Srivastava, A., Cuncoliencar, B. S., and Naik, N. (2010). Resolution of symptoms in neuroleptic malignant syndrome. *Ind. J. Psychiatry* 52, 264–266. doi: 10.4103/0019-5545.70988

Pickar, D., Owen, R. R., Litman, R. E., Konicki, E., Gutierrez, R., and Rapaport, M. H. (1992). Clinical and biologic response to clozapine in patients with schizophrenia. Crossover comparison with fluphenazine. *Arch. Gen. Psychiatry* 49, 345–353. doi: 10.1001/archpsyc.1992.018200500 09001

Prasad, S. E., and Kennedy, H. G. (2003). Pseudophaeochromocytoma associated with clozapine treatment. *Ir. J. Psychol. Med.* 20, 132–134. doi: 10.1017/S0790966700007941

Procyshyn, R. M., Honer, W. G., and Barr, A. M. (2009). Do serum lipids predict response to clozapine treatment? *J. Psychiatry Neurosci.* 34:168.

Procyshyn, R. M., Honer, W. G., Wu, T. K., Ko, R. W., McIsaac, S. A., Young, A. H., et al. (2010). Persistent antipsychotic polypharmacy and excessive dosing in the community psychiatric treatment setting: a review of medication profiles in 435 Canadian outpatients. *J. Clin. Psychiatry* 71, 566–573. doi: 10.4088/JCP.08m04912gre

Procyshyn, R. M., Vila-Rodriguez, F., Honer, W. G., and Barr, A. M. (2014). Clozapine administered once versus twice daily: does it make a difference? *Med. Hypoth.* 82, 225–228. doi: 10.1016/j.mehy.2013.11.043

Procyshyn, R. M., Wasan, K. M., Thornton, A. E., Barr, A. M., Chen, E. Y., Pomarol-Clotet, E., et al. (2007). Changes in serum lipids, independent of weight, are associated with changes in symptoms during long-term clozapine treatment. *J. Psychiatry Neurosci.* 32, 331–338.

Ray, W. A., Chung, C. P., Murray, K. T., Hall, K., and Stein, C. M. (2009). Atypical antipsychotic drugs and the risk of sudden cardiac death. *N. Engl. J. Med.* 360, 225–235. doi: 10.1056/NEJMoa0806994

Rechlin, T., Beck, G., Weis, M., and Kaschka, W. P. (1998). Correlation between plasma clozapine concentration and heart rate variability in schizophrenic patients. *Psychopharmacology (Berl).* 135, 338–441. doi: 10.1007/s002130050520

Rechlin, T., Claus, D., and Weis, M. (1994). Heart rate variability in schizophrenic patients and changes of autonomic heart rate parameters during treatment

with clozapine. *Biol. Psychiatry* 35, 888–892. doi: 10.1016/0006-3223(94)90026-4

Reinstein, M. J., Chasonov, M. A., Colombo, K. D., Jones, L. E., and Sonnenberg, J. G. (2002). Reduction of suicidality in patients with schizophrenia receiving clozapine. *Clin. Drug Investig.* 22, 341–346. doi: 10.2165/00044011-200222050-00008

Richelson, E., and Souder, T. (2000). Binding of antipsychotic drugs to human brain receptors focus on newer generation compounds. *Life Sci.* 68, 29–39. doi: 10.1016/S0024-3205(00)00911-5

Richman, J. S., and Moorman, J. R. (2000). Physiological time-series analysis using approximate entropy and sample entropy. *Am. J. Physiol. Heart Circ. Physiol.* 278, H2039–H2049. doi: 10.1152/ajpheart.2000.278.6.H2039

Romo-Nava, F., Alvarez-Icaza González, D., Fresán-Orellana, A., Saracco Alvarez, R., Becerra-Palars, C., Moreno, J., et al. (2014). Melatonin attenuates antipsychotic metabolic effects: an eight-week randomized, double-blind, parallel-group, placebo-controlled clinical trial. *Bipolar Disord.* 16, 410–421. doi: 10.1111/bdi.12196

Ronaldson, K. J., Fitzgerald, P. B., and McNeil, J. J. (2015). Clozapine-induced myocarditis, a widely overlooked adverse reaction. *Acta Psychiatr. Scand.* 132, 231–240. doi: 10.1111/acps.12416

Ronaldson, K. J., Fitzgerald, P. B., Taylor, A. J., Topliss, D. J., and McNeil, J. J. (2011). A new monitoring protocol for clozapine-induced myocarditis based on an analysis of 75 cases and 94 controls. *Aust. N.Z.J. Psychiatry* 45, 458–465. doi: 10.3109/00048674.2011.572852

Ronaldson, K. J., Taylor, A. J., Fitzgerald, P. B., Topliss, D. J., Elsik, M., and McNeil, J. J. (2010). Diagnostic characteristics of clozapine-induced myocarditis identified by an analysis of 38 cases and 47 controls. *J. Clin. Psychiatry* 71, 976–981. doi: 10.4088/JCP.09m05024yel

Rumantir, M. S., Kaye, D. M., Jennings, G. L., Vaz, M., Hastings, J. A., and Esler, M. D. (2000). Phenotypic evidence of faulty neuronal norepinephrine reuptake in essential hypertension. *Hypertension* 36, 824–829. doi: 10.1161/01.HYP.36.5.824

Safferman, A., Lieberman, J. A., Kane, J. M., Szymanski, S., and Kinon, B. (1991). Update on the clinical efficacy and side effects of clozapine. *Schizophr. Bull.* 17, 247–261. doi: 10.1093/schbul/17.2.247

Sara, J., Jenkins, M., Chohan, T., Jolly, K., Shepherd, L., Gandhi, N. Y., et al. (2013). Clozapine use presenting with pseudopheochromocytoma in a schizophrenic patient: a case report. *Case Rep. Endocrinol.* 2013:194927. doi: 10.1155/2013/194927

Schell, A. M., Dawson, M. E., Rissling, A., Ventura, J., Subotnik, K. L., Gitlin, M. J., et al. (2005). Electrodermal predictors of functional outcome and negative symptoms in schizophrenia. *Psychophysiology* 42, 483–492. doi: 10.1111/j.1469-8986.2005.00300.x

Schlaich, M. P., Kaye, D. M., Lambert, E., Sommerville, M., Socratous, F., and Esler, M. D. (2003). Relation between cardiac sympathetic activity and hypertensive left ventricular hypertrophy. *Circulation* 108, 560–565. doi: 10.1161/01.CIR.0000081775.72651.B6

Schlaich, M. P., Lambert, E., Kaye, D. M., Krozowski, Z., Campbell, D. J., Lambert, G., et al. (2004). Sympathetic augmentation in hypertension: role of nerve firing, norepinephrine reuptake, and Angiotensin neuromodulation. *Hypertension* 43, 169–175. doi: 10.1161/01.HYP.0000103160.35395.9E

Seddigh, R., Keshavarz-Akhlaghi, A. A., and Shariati, B. (2014). Treating methamphetamine-induced resistant psychosis with clozapine. *Case Rep. Psychiatry* 2014:845145. doi: 10.1155/2014/845145

Shannon, J. R., Flattem, N. L., Jordan, J., Jacob, G., Black, B. K., Biaggioni, I., et al. (2000). Orthostatic intolerance and tachycardia associated with norepinephrine-transporter deficiency. *N. Engl. J. Med.* 342, 541–549. doi: 10.1056/NEJM200002243420803

Sheldon, R. S., Grubb, B. P. II., Olshansky, B., Shen, W. K., Calkins, H., Brignole, M., et al. (2015). 2015 heart rhythm society expert consensus statement on the diagnosis and treatment of postural tachycardia syndrome, inappropriate sinus tachycardia, and vasovagal syncope. *Heart Rhythm* 12, e41–e63. doi: 10.1016/j.hrthm.2015.03.029

Shen, Y., Monsma, F. J. Jr., Metcalf, M. A., Jose, P. A., Hamblin, M. W., and Sibley, D. R. (1993). Molecular cloning and expression of a 5-hydroxytryptamine7 serotonin receptor subtype. *J. Biol. Chem.* 268, 18200–18204.

Spivak, B., Roitman, S., Vered, Y., Mester, R., Graff, E., Talmon, Y., et al. (1998). Diminished suicidal and aggressive behavior, high plasma norepinephrine levels, and serum triglyceride levels in chronic neuroleptic-resistant schizophrenic patients maintained on clozapine. *Clin. Neuropharmacol.* 21, 245–250.

Stein, P. K., Bosner, M. S., Kleiger, R. E., and Conger, B. M. (1994). Heart rate variability: a measure of cardiac autonomic tone. *Am. Heart J.* 127, 1376–1381. doi: 10.1016/0002-8703(94)90059-0

Tang, V. M., Lang, D. J., Giesbrecht, C. J., Panenka, W. J., Willi, T., Procyshyn, R. M., et al. (2015). White matter deficits assessed by diffusion tensor imaging and cognitive dysfunction in psychostimulant users with comorbid human immunodeficiency virus infection. *BMC Res. Notes* 8:515. doi: 10.1186/s13104-015-1501-5

Thomas, J. A., and Marks, B. H. (1978). Plasma norepinephrine in congestive heart failure. *Am. J. Cardiol.* 41, 233–243. doi: 10.1016/0002-9149(78)90162-5

Thomas, L., and Pollak, P. T. (2003). Delayed recovery associated with persistent serum concentrations after clozapine overdose. *J. Emerg. Med.* 25, 61–66. doi: 10.1016/S0736-4679(03)00130-6

Thornton, A. E., Procyshyn, R. M., Barr, A. M., MacEwan, G. W., and Honer, W. G. (2015). Cognition and plasma ratio of clozapine to N-desmethylclozapine in patients with clozapine-resistant schizophrenia. *Am. J. Psychiatry* 172:1259. doi: 10.1176/appi.ajp.2015.15070899

Triposkiadis, F., Karayannis, G., Giamouzis, G., Skoularigis, J., Louridas, G., and Butler, J. (2009). The sympathetic nervous system in heart failure physiology, pathophysiology, and clinical implications. *J. Am. Coll. Cardiol.* 54, 1747–1762. doi: 10.1016/j.jacc.2009.05.015

Tse, L., Barr, A. M., Scarapicchia, V., and Vila-Rodriguez, F. (2015). Neuroleptic malignant syndrome: a review from a clinically oriented perspective. *Curr. Neuropharmacol.* 13, 395–406. doi: 10.2174/1570159X13999150424113345

Tsuji, H., Larson, M. G., Venditti, F. J. Jr., Manders, E. S., Evans, J. C., Feldman, C. L., et al. (1996). Impact of reduced heart rate variability on risk for cardiac events. The Framingham Heart Study. *Circulation* 94, 2850–2855. doi: 10.1161/01.CIR.94.11.2850

Tümüklü, M. N., Alptekin, K., Kirimli, Ö., Aslan, Ö., Akdede, B. B., Badak, Ö., et al. (2008). Arrhythmic markers and clozapine in patients with schizophrenia: effect of 10 weeks clozapine treatment on heart rate variability, late potentials and QT dispersion. *Klinik Psikofarmakoloji Bülteni* 18, 167–173.

Van Tol, H. H., Bunzow, J. R., Guan, H. C., Sunahara, R. K., Seeman, P., Niznik, H. B., et al. (1991). Cloning of the gene for a human dopamine D4 receptor with high affinity for the antipsychotic clozapine. *Nature* 350, 610–614. doi: 10.1038/350610a0

Vila-Rodriguez, F., Tsang, P., and Barr, A. M. (2013). Chronic benign neutropenia/agranulocytosis associated with non-clozapine antipsychotics. *Am. J. Psychiatry* 170, 1213–1214. doi: 10.1176/appi.ajp.2013.13020215

Walker, A. M., Lanza, L. L., Arellano, F., and Rothman, K. J. (1997). Mortality in current and former users of clozapine. *Epidemiology* 8, 671–677. doi: 10.1097/00001648-199711000-00014

Wang, J. F., Min, J. Y., Hampton, T. G., Amende, I., Yan, X., Malek, S., et al. (2008). Clozapine-induced myocarditis: role of catecholamines in a murine model. *Eur. J. Pharmacol.* 592, 123–127. doi: 10.1016/j.ejphar.2008.06.088

Wang, Y. C., Chen, C. Y., Kuo, T. B., Lai, C. J., and Yang, C. C. (2012). Influence of antipsychotic agents on heart rate variability in male WKY rats: implications for cardiovascular safety. *Neuropsychobiology* 65, 216–226. doi: 10.1159/000337459

Wheeler, T., and Watkins, P. J. (1973). Cardiac denervation in diabetes. *Br. Med. J.* 4, 584–586. doi: 10.1136/bmj.4.5892.584

Whitney, Z., Procyshyn, R. M., Fredrikson, D. H., and Barr, A. M. (2015). Treatment of clozapine-associated weight gain: a systematic review. *Eur. J. Clin. Pharmacol.* 71, 389–401. doi: 10.1007/s00228-015-1807-1

Willi, T. S., Barr, A. M., Gicas, K., Lang, D. J., Vila-Rodriguez, F., Su, W., et al. (2016a). Characterization of white matter integrity deficits in

cocaine-dependent individuals with substance-induced psychosis compared with non-psychotic cocaine users. *Addict. Biol.* 22, 873–881.

Willi, T. S., Lang, D. J., Honer, W. G., Smith, G. N., Thornton, A. E., Panenka, W. J., et al. (2016b). Subcortical grey matter alterations in cocaine dependent individuals with substance-induced psychosis compared to non-psychotic cocaine users. *Schizophr. Res.* 176, 158–163. doi: 10.1016/j.schres.2016.08.001

Yacoub, A., and Francis, A. (2006). Neuroleptic malignant syndrome induced by atypical neuroleptics and responsive to lorazepam. *Neuropsychiatr. Dis. Treat.* 2, 235–240. doi: 10.2147/nedt.2006.2.2.235

Young, C. R., Bowers, M. B. Jr., and Mazure, C. M. (1998). Management of the adverse effects of clozapine. *Schizophr. Bull.* 24, 381–390. doi: 10.1093/oxfordjournals.schbul.a033333

Zahn, T. P., and Pickar, D. (1993). Autonomic effects of clozapine in schizophrenia: comparison with placebo and fluphenazine. *Biol. Psychiatry* 34, 3–12. doi: 10.1016/0006-3223(93)90250-H

Zoccali, C., Mallamaci, F., Tripepi, G., Parlongo, S., Cutrupi, S., Benedetto, F. A., et al. (2002). Norepinephrine and concentric hypertrophy in patients with end-stage renal disease. *Hypertension* 40, 41–46. doi: 10.1161/01.HYP.0000022063.50739.60

Conflict of Interest Statement: AB has received grants from Bristol-Myers Squibb. WH has received consulting fees or sat on paid advisory boards for *in silico*, Lundbeck, Otsuka, Roche, and Eli Lilly, and received honoraria from Rush University, University of Calgary, University of Hong Kong, Massachusetts General Hospital, British Columbia Health Authorities, the British Association for Psychopharmacology and the Canadian Psychiatric Association. RP has been a member of the following advisory boards in the past 3 years: Janssen, Lundbeck, and Otsuka.

The other authors declare that the research was conducted in the absence of any commercial or financial relationships that could be construed as a potential conflict of interest.

frontiers in Physiology

ORIGINAL RESEARCH
published: 25 April 2017
doi: 10.3389/fphys.2017.00237

Early Changes in Glutamate Metabolism and Perfusion in Basal Ganglia following Hypoxia-Ischemia in Neonatal Piglets: A Multi-Sequence 3.0T MR Study

Yu-xue Dang[1], *Kai-ning Shi*[2] *and Xiao-ming Wang*[1]*

[1] Department of Radiology, Shengjing Hospital of China Medical University, Shenyang, China, [2] Department of Imaging Systems Clinical Science, Philips Healthcare, Beijing, China

The excitotoxicity of glutamate metabolism as well as hemodynamic disorders of the brain are both risk factors for neonatal hypoxic–ischemic brain damage (HIBD). In the present study, changes in glutamate metabolism in the basal ganglia were detected by proton magnetic resonance spectroscopy (^{1}H-MRS) at 0–6, 8–12, 24–30, and 48–60 h after the induction of hypoxia-ischemia (HI) in newborn piglets. Meanwhile, correlation analysis was performed by combining the microcirculatory perfusion informations acquired by intravoxel incoherent motion (IVIM) scan to explore their possible interaction mechanism. The results suggested that Glu level in the basal ganglia underwent a "two-phase" change after HI; perfusion fraction *f*, an IVIM-derived perfusion parameter, was clearly decreased in the early stage after HI, then demonstrated a transient and slight recovery process, and thereafter continued to decrease. The changes in *f* and Glu level were in a significant negative correlation ($r = -0.643$, $P = 0.001$). Our study results revealed that Glu level is closely associated with the microcirculatory perfusion changes in the acute stage of HIBD.

Keywords: hypoxic–ischemic brain damage, ^{1}H-MRS, IVIM, glutamate, perfusion

OPEN ACCESS

Edited by:
Tijana Bojić,
Institut za Nuklearne Nauke Vinča,
University of Belgrade, Serbia

Reviewed by:
Ji-Hong Chen,
Wuhan University, China
Huiyin Tu,
Zhengzhou University, China

***Correspondence:**
Xiao-ming Wang
wangxm024@163.com

Specialty section:
This article was submitted to Autonomic Neuroscience, a section of the journal Frontiers in Physiology

Received: *30 January 2017*
Accepted: *05 April 2017*
Published: *25 April 2017*

Citation:
Dang Y-x, Shi K-n and Wang X-m (2017) Early Changes in Glutamate Metabolism and Perfusion in Basal Ganglia following Hypoxia-Ischemia in Neonatal Piglets: A Multi-Sequence 3.0T MR Study. Front. Physiol. 8:237. doi: 10.3389/fphys.2017.00237

INTRODUCTION

Basal ganglia injury (BGI) is a common type of hypoxic–ischemic brain damage (HIBD) and also the main cause of permanent dysneuria and cerebral palsy in perinatal full-term neonates. The basal ganglia are very sensitive to hypoxia–ischemia (HI) damage and susceptible to selective neuronal injury (Martin et al., 1997; Rocha-Ferreira and Hristova, 2016). Glutamate (Glu), as the most important excitatory neurotransmitter in animals, plays a crucial role in maintaining the function of glutamatergic neurons in the basal ganglia (Alexander and Crutcher, 1990). The excitotoxicity caused by the massive accumulation of Glu after HI is the central link for HIBD and is also the initiator and executer of brain injury (Hagberg et al., 1987; Choi and Rothman, 1990; Coyle and Puttfarcken, 1993; Rego et al., 1996).

Normally the release and reuptake of Glu are in a dynamic balance. The efficient Glu uptake system enables low, extracellular concentrations of Glu in order to avoid excitotoxicity, and only a small amount of Glu is involved in signal transduction as an excitatory neurotransmitter (D'souza and Slater, 1995; Cooper and Jeitner, 2016; Danbolt et al., 2016). However, HI leads to an increase in Glu release and/or damages the Glu uptake system, thus causing a sharp elevation of extracellular

Glu; its level and the excessive activation of relevant receptors contributes to nervous excitotoxicity and results in generalized pathological brain lesions. Of these excessively activated receptors, the N-methyl-D-aspartic acid receptor plays an important role in neuronal injury after mediating HI as outlined in our preliminary study (Wang X. Y. et al., 2012).

Perinatal HIBD has a complex pathophysiological mechanism. In addition to the excitotoxicity of Glu, hemodynamic disorders of the brain are also a risk factor for HIBD (Pryds et al., 1990; Howlett et al., 2013; Massaro et al., 2015). Hemodynamic disorders of the brain can contribute to secondary energy dysmetabolism after HI, and thus have a role in pathological mechanisms involved in brain damage secondary to HI. The pathogenesis of brain damage can be revealed by evaluating cerebral perfusion. For example, a pivotal question arises concerning cerebral metabolism in a HI environment in response to changes in cerebral perfusion: do mutual effects and interactions exist between such variables? In order to understand HIBD mechanisms, it is essential to explore the relationship between changes in Glu metabolism and changes in microcirculatory perfusion after HI.

Proton magnetic resonance spectroscopy (^{1}H-MRS), as a non-invasive technique, provides information on changes of metabolites in brain tissues. At present, two major functional magnetic resonance imaging (MRI) techniques are available to measure cerebral perfusion: perfusion-weighted imaging (PWI) and arterial spin labeling (ASL). Considering the specificity of the newborns, invasive PWI cannot be used as it requires the use of exogenous contrast media. With regard to ASL, this can only evaluate a single parameter—cerebral blood flow (CBF)—which does not allow the all-round comprehension of a hemodynamic reserve. This leads us to the question of whether an MRI technique exists that can not only meet the special requirements of non-invasive examinations in newborns, but also support the comprehensive evaluation of cerebral perfusion? Intravoxel incoherent motion (IVIM), a non-invasive MR perfusion imaging technique, can quantify the microcirculation of blood in the capillary network (perfusion) and the diffusion composition of true water molecules in tissues *in vivo* using a bi-exponential model (Le Bihan et al., 1986, 1988). Measurements using IVIM are based on the premise that the microcirculation of blood, or perfusion, is a kind of non-uniform, irregular random motion (i.e., incoherent motion) (Le Bihan et al., 1988). A linear correlation exists between IVIM-derived perfusion parameters (pseudo-diffusion coefficient D^* and perfusion fraction f) and conventional perfusion parameters (Le Bihan and Turner, 1992; Federau et al., 2014a,b). In theory, therefore, IVIM-derived perfusion parameters can be used to evaluate the microcirculatory perfusion of the brain after HI and thus provide more comprehensive information. Currently, the successful application of IVIM in the central nervous system focuses on studies to recognize the ischemic semi-dark band (Federau et al., 2014b; Hu et al., 2015), identify the benignity and malignancy of tumors(Bisdas et al., 2014; Hu et al., 2014; Suh et al., 2014) and evaluate the efficacy of radiochemotherapy (Hauser et al., 2014; Cui et al., 2015; Xiao et al., 2015). In this context, IVIM, perhaps, will become a new MR perfusion technique useful in the study of perfusion of the microcirculation in newborns.

Studies are urgently required on the critical changes that occur at the Glu level during the development of HIBD and its relationship with microcirculatory perfusion. In this study, we measured Glu-related metabolites and microcirculatory perfusion separately by ^{1}H-MRS and IVIM in a HI animal model. We investigated the dynamic changes in Glu and microcirculatory perfusion after HI and preliminarily explored their possible interaction mechanism.

MATERIALS AND METHODS

Preparation of Experimental Animals and Establishment of HIBD Model

All animal experiments were reported in accordance with Animal Research: Reporting of *In vivo* Experiments guidelines. This study was approved by the Institutional Animal Care and Use Committee of Shengjing Hospital of China Medical University. Twenty-five newborn male or female Yorkshire piglets (P3–5 d; weight: 1.5–2 kg) were randomly selected from the Laboratory Animal Center of Shengjing Hospital of China Medical University. All animal models were established according to the Regulations for the Animal Care and Use published by the Shengjing Hospital of China Medical University.

The newborn piglets were anesthetized by an intramuscular injection of 0.6 mL/kg Su-Mian-Xin (xylazine hydrochloride) in the buttocks. During anesthesia, the animals' vital signs were closely observed. When the piglets were found to become comatose, as evidenced by muscle relaxation, decreased limb muscular tension and a delayed corneal reflex, the animals were placed in a supine position on a bench prior to each operation. A laryngoscopic tracheal cannulation (φ 2.5 mm) was performed, and each animal was then connected to a TKR-200C small animal ventilator (Jiangxi Teli Anesthesia and Respiratory Equipment Co., Ltd, Jiangxi, China) for mechanical ventilation with 100% oxygen. Ventilator parameters were as follows: respiration ratio inspiration/expiration (I/E) = 1:1.5; and respiration frequency = 30 bpm. Heart rate and peripheral oxygen saturation were monitored using a TuffSat handheld pulse oximeter (GE, Boston, MA, USA). The incision area and adjacent skin were then disinfected and a median incision was made in the neck. Bilateral common carotid arteries and adjacent internal jugular veins and vagus nerves were dissected, and a 5.0 mm silk suture was indwelled. After the condition of animals stabilized for 30 min, the bilateral common carotid arteries were clipped with small artery clamps to interrupt their blood flow, and 6% oxygen–containing mixed gas was delivered mechanically for 40 min. Thereafter, the HI induction procedure was completed, the small artery clamps removed, and the blood flow of the bilateral common carotid arteries was recovered. Oxygen (100%) was mechanically delivered again, and the incision was sutured. After the operation, the animals were transferred to an incubator (37°C) to ensure a body temperature in the normal range during postoperative recovery. This well-established model was used to

induce bilateral HI injury, as documented in our previous studies (Wang H. et al., 2012; Zhang et al., 2012).

Grouping of Experimental Animals

All newborn piglets were randomly divided into the control group (sham-operation group, $n = 5$) and the HI model group ($n = 20$), and the HI model group was then further divided into 4 subgroups according to different time points after HI: 0–6, 8–12, 24–30, and 48–60 h ($n = 5$ per group). The animals in the pseudo-operation group underwent preoperative preparation similar to those in the model group but without a HI induction procedure.

MR Scans and Data Post-Processing

At different time points after HI, a conventional MR scan was performed on all animals using a 3.0T MRI system (Achieva 3.0T TX; Philips Healthcare Systems, Best, The Netherlands) with an eight-channel phased array head coil. Images (including axial and sagittal T_1-weighted images [T_1WI] and axial T_2-weighted images [T_2WI] of the head) were acquired by fast gradient echo. The relevant scan parameters used were: T_1WI Repetition time (TR) 200 ms; Echo time (TE) 2.3 ms; matrix 224 × 162; slice thickness 5 mm; T_2WI TR 5000 ms; TE 80 ms; matrix 224 × 162; and slice thickness 5 mm.

Measurements by single-voxel ^{1}H-MRS were completed with a point-resolved spectroscopy (PRESS) sequence using one 90° and two 180° radio frequency pulses (13.2224 ms; bandwidth = 1,231 Hz). The following parameters were used: TR = 2,000 ms; TE = 37 ms; bandwidth = 2,000 Hz; number of signal acquisitions = 64; and a volume of interest (VOI; 10 × 10 × 10 mm) was positioned in the left basal ganglia. A plain scan was performed on newborn piglets to acquire coronal scan images of the basal ganglia as a region of interest (ROI). After the completion of a ^{1}H-MRS scan, the raw data were then entered into LCModel (Linear Combination Model) software (version 6.3-1B) (Provencher, 2001) for quantification, with an unsuppressed water signal used as an internal reference, as well as automatic processing and analysis. The LCModel software supported automatic baseline corrections and the smoothing of spectrum raw data, as well as the absolute concentration measurement of several metabolites, including alanine (Ala), aspartic acid (Asp), creatine (Cr), phosphocreatine (PCr), γ-aminobutyric acid (GABA), glucose (Glc), glutamate (Glu), glutamine (Gln), glycerylphosphorylcholine (GPC), phosphatidylcholine (PCh), glutathione (GSH), inositol (Ins), lactic acid (Lac), N-acetylaspartate (NAA), N-acetylaspartate glutamate (NAAG), scyllo-inositol (Src) and taurine (Tau). Glu is the most abundant excitatory neurotransmitter in the brain and is essential for normal brain function; its complex signals were generated at 2.04–2.35 ppm (ppm: 10^{-6}) and 3.75 ppm. The peak of Gln overlapped with that of Glu at approximately 2.35 ppm. LCModel software can automatically distinguish the overlapping signals of different metabolites with a similar chemical shift in the same frequency area (Wisnowski et al., 2013). The spectral fitting was performed with a range from 0.2 to 4.0 ppm (see **Figure 1**). In this study, we quantified the concentrations of Glu, Gln and Glx (Glu + Gln complex). Cramér–Rao lower bounds (CRLBs), which were provided by LCModel software, were used in assessing the precision of the quantification of metabolites. Spectrum data were included in the statistical analysis, which met the following criteria: (1) signal–to–noise ratio (SNR) ≥ 5; and (2) CRLBs for the concentrations of metabolites obtained were < 50%, and generally < 25%.

An IVIM scan was performed with a single-shot spin echo planar imaging (EPI) sequence; TR/TE 4,000 ms/90 ms; matrix 228 × 231; slice thickness 5 mm; and 16 b-values (0, 10, 20, 40, 80, 110, 140, 170, 200, 300, 400, 500, 600, 700, 800, and 900 s/mm^2). IVIM analysis was performed using in-house MATLAB software (R2010a, The MathWorks, Inc., Natick, MA, USA) and a bi-exponential model. The relation between the signal attenuation and b is expressed by the following formula (Le Bihan et al., 1988, 1989):

$$S_b/S_0 = (1-f)\cdot\exp(-b\cdot D) + f\cdot\exp(-b\cdot D^*) \quad (1)$$

Where S_b and S_0 stand for signal intensity at $b \neq 0$ and $b = 0$, respectively. The relevant parameters finally obtained by least squares (Pfeuffer et al., 1999) are as follows: diffusion coefficient D (given in units of $\times 10^{-3}$ mm^2/s) denotes the true molecular diffusion; the pseudo-diffusion coefficient D^* (given in units of $\times 10^{-3}$ mm^2/s) represents the diffusion linked to microcapillary perfusion; and the perfusion fraction f (given as a percentage) indicates the proportion of microcirculatory perfusion-related diffusion in the total diffusion. As there is a variation in the speed of motion of different molecules, D^* is markedly greater than D. At $b < 200$ s/mm^2, the perfusion effect is dominant and the signal attenuation detected reflects information from perfusion; at $b > 200$ s/mm^2, the microcirculatory perfusion effect can be neglected, and the signal attenuation detected nearly reflects the true diffusion of water molecules in voxels.

Firstly, IVIM raw data were imported into post-processing software, and then post-processed using a bi-exponential model to give pseudo-color images of D, D^*, and f. Secondly, the ROI was manually marked on the left basal ganglia in images at $b = 0$ s/mm^2 (see **Figure 2**) by combining T_2WI scan images (avoiding the adjacent cerebrospinal fluid [CSF], blood vessels and noise areas), and then D, D^*, and f values were calculated. If the calculated results were < 0, f, D, and D^* were set to 0 to comply with actual physiology. If f was > 0.3 and D^* was > 0.05 as calculated, f and D^* were also set to 0 because such calculated results may be caused by the effects of SNR or CSF flow, and were therefore not physiological values (Federau et al., 2012). Finally, the relevant parameters of ROI in model and control groups were measured repeatedly three times and results then averaged. Differences in various parameters between model and control groups were analyzed.

Statistical Analysis

SPSS 20.0 statistical software was used for analyses. All data were expressed as mean ± standard deviation (SD). Multiple comparisons of data with a homogeneity of variance were performed by one-way analysis of variance (ANOVA), and those of data with a heterogeneity of variance by a Kruskal–Wallis H test. Correlations between the Glu level and IVIM-derived perfusion parameters (D^* and f) were analyzed by Spearman

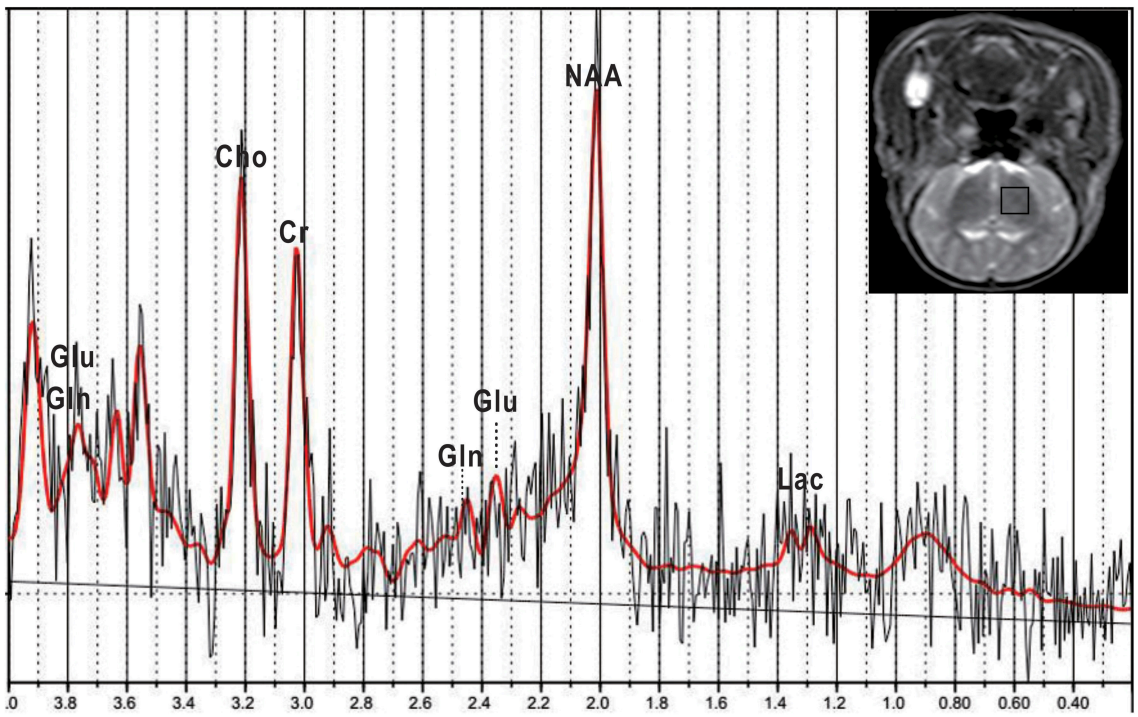

FIGURE 1 | Representative T_2-weighted image and corresponding ^{1}H-MRS of a normal piglet. A MRS voxel was placed in the left basal ganglia (black square). LCModel fitting results (red), fit from 0.2 to 4.0 ppm, are presented. Glu, glutamate; Gln, glutamine; NAA, N-acetylaspartate; Lac, lactate; Cho, choline; Cr, creatine.

rank correlation analysis. The correlation level indicated by the correlation coefficient was defined as follows: $r > 0.8$, very high correlation; $0.6 < r \leq 0.8$, significant correlation; $0.4 < r \leq 0.6$, ordinary correlation; $0.2 \leq r \leq 0.4$, low correlation; and $0 \leq r < 0.2$, weak or no correlation (Fujima et al., 2014). $P < 0.05$ suggested that a difference was statistically significant.

RESULTS

In this study, ^{1}H-MRS and IVIM scans were performed on the newborn piglets in the control group and HI model group at different time points of 0–6, 8–12, 24–30, and 48–60 h after HI. The results are described below.

^{1}H-MRS

The representative ^{1}H-MRS in the basal ganglia at different time points after HI are shown in **Figure 3**. **Figure 4** shows the mean levels of Glu, Gln, and Glx in the control group and model group. After HI, there was a sharp increase in Glu level in the basal ganglia at 0–6 h, followed by a transient decrease at 8–12 h, to a level that was still higher than that in the control group; thereafter, it increased again, demonstrating a "two-phase" change. Compared with the control group, the Glu level was increased at different time points after HI, and differences were statistically significant (0–6 h group, $P < 0.001$; 8–12 h group, $P = 0.016$; 24–30 h group, $P < 0.001$; 48–60 h group, $P < 0.001$). There was a statistically significant difference between the HI 0–6 and 8–12 h groups ($P = 0.007$) and between HI 8–12 and 24–30, or 48–60 h groups ($P < 0.001$, $P = 0.021$, respectively), but no statistically significant difference was observed between other groups.

Figure 4B demonstrated that Gln level tended to increase slightly and then decrease after HI, but there were no statistically significant differences between the different groups.

Figure 4C showed that there was a similar change in Glx level as in Glu level, where the difference between the control group and the HI 24–30 h group was statistically significant ($P = 0.009$).

IVIM Data Processing

Figure 5 shows the changes in D, D^*, and f in the control group and model group as detected by IVIM. After HI, D in the basal ganglia was markedly decreased at 0–6 h (compared with the control group, $P < 0.001$) and then gradually recovered over time, but it was still slightly lower than that in the control group (no statistically significant differences between different HI time point subgroups and the control group, $P > 0.05$).

Figure 5B showed the changes in D^* in the different groups. After HI, D^* was decreased at 0–6 and 8–12 h, then increased at 24–30 h and thereafter decreased again at 48–60 h. However, there were no statistical differences in D^* between the different groups.

As shown in **Figure 5C**, f was clearly decreased at 0–6 h after HI and then began to recover at 8–12 h, but it was still

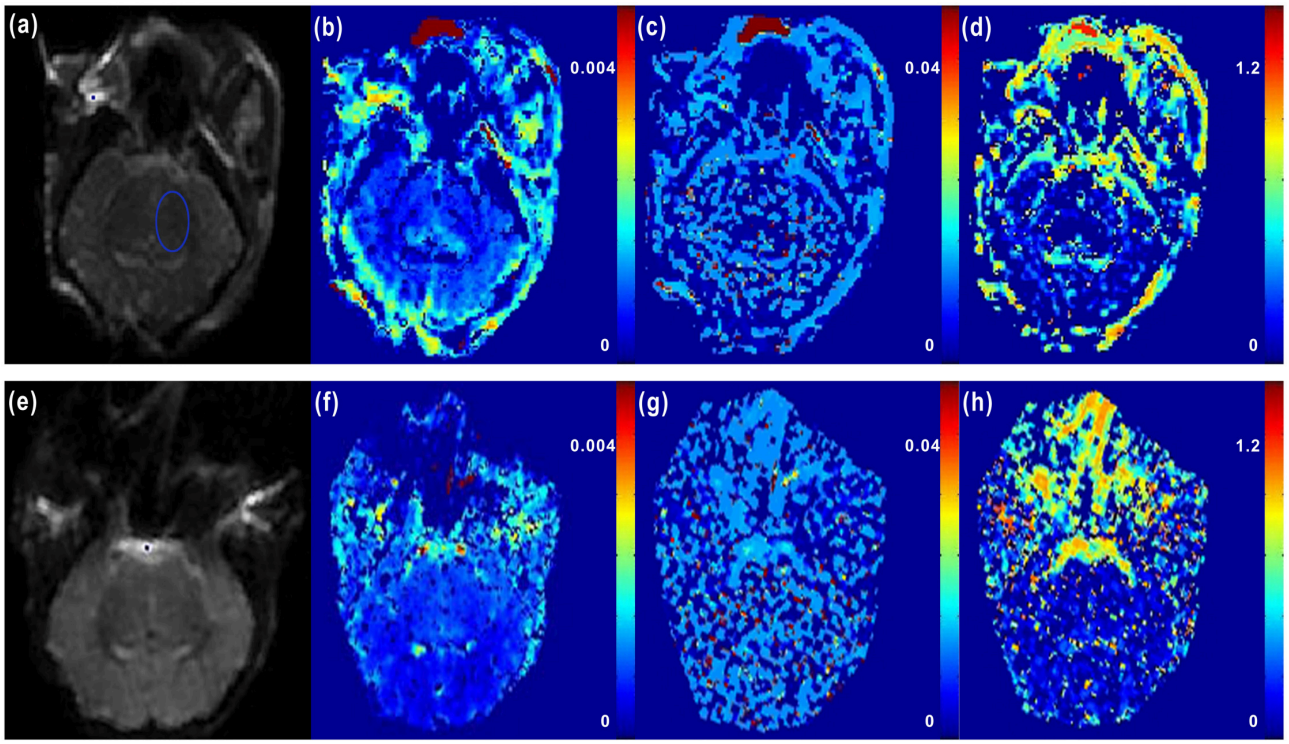

FIGURE 2 | Representative IVIM images of newborn piglets before and after HI. (a–d) showed the axial diffusion-weighted imaging (DWI) image ($b = 0$ s/mm^2) of a normal newborn piglet **(a)** (where the blue ellipse highlights the region of interest (ROI) marked in the left basal ganglia region), and the corresponding D, D^*, and f images obtained by IVIM post-processing software (**b–d**; $D = 0.642 \times 10^{-3}$ mm^2/s, $D^* = 13.207 \times 10^{-3}$ mm^2/s, $f = 12.753\%$). **(e–h)** showed the axial DWI image ($b = 0$ s/mm^2) of a newborn piglet at 6 h after HI **(e)**, and the corresponding D, D^*, and f images (**f–h**; $D = 0.269 \times 10^{-3}$ mm^2/s, $D^* = 5.412 \times 10^{-3}$ mm^2/s, $f = 7.197\%$). From the axial DWI images, we could see that at 6 h after HI, the signals of cerebral parenchyma were evidently enhanced, the cerebral cortex was obviously swollen and edematous, and the cortical sulci and gyrus became shallower; in the D and f images, weakened signals of cerebral parenchyma were observed after HI correspondingly, but the difference in the image of D^* was not significant.

lower than that in the control group; at 24–30 and 48–60 h, f continued to decrease again. The difference in f was statistically significant between the control group and the HI model group at different time points ($P < 0.001$, for both). There was a statistically significant difference between 0–6 and 8–12 h groups and between 8–12 and 24–30, or 48–60 h groups ($P < 0.001$, for both). The specific data for D, D^*, and f are shown in **Table 1**.

Analysis of Correlations between Metabolites of Glu Metabolism and IVIM-Derived Perfusion Parameters, *D** and *f*

After HI, the Glu concentration in the basal ganglia showed a significant negative correlation with f ($r = -0.643$, $P = 0.001$; **Figure 6A**); similarly, there was an ordinary negative correlation between the Glx concentration and f ($r = -0.478$, $P = 0.016$; **Figure 6C**). However, no significant correlation was observed between the Gln concentration and f (**Figure 6B**). In addition, D^* did not correlate with the concentration of Glu, Gln, or Glx (**Figures 6D–F**).

DISCUSSION

In the present study, we established a HI newborn piglet model and then investigated the level of Glu metabolism and the microcirculatory perfusion changes in the brain by multi-sequence MRI. The results showed that the change in Glu level was closely related to the microcirculatory perfusion level in the acute stage of HIBD. Since the occurrence of HIBD is a result of the interactions and influences of multiple factors that contribute to an abnormal pathological environment in the brain. On one hand, the development of dysmetabolism in cerebral energy causes a massive extracellular accumulation of Glu. The resultant excitotoxicity is one of the key factors inducing neuronal injury and death. On the other hand, hemodynamic disorders of the brain can also lead to damaged brain cells. In the brain, the neurons are located nearby small blood vessels, so the neurotransmitters released by synapses can also regulate the functions of these vessels (Huang et al., 1994) and nerve activities are tightly coupled with the degree of vascular perfusion (Busija et al., 2007; Jackman and Iadecola, 2015). In this study, we performed a preliminary exploration of relevant pathological mechanisms by multi-sequence MRI.

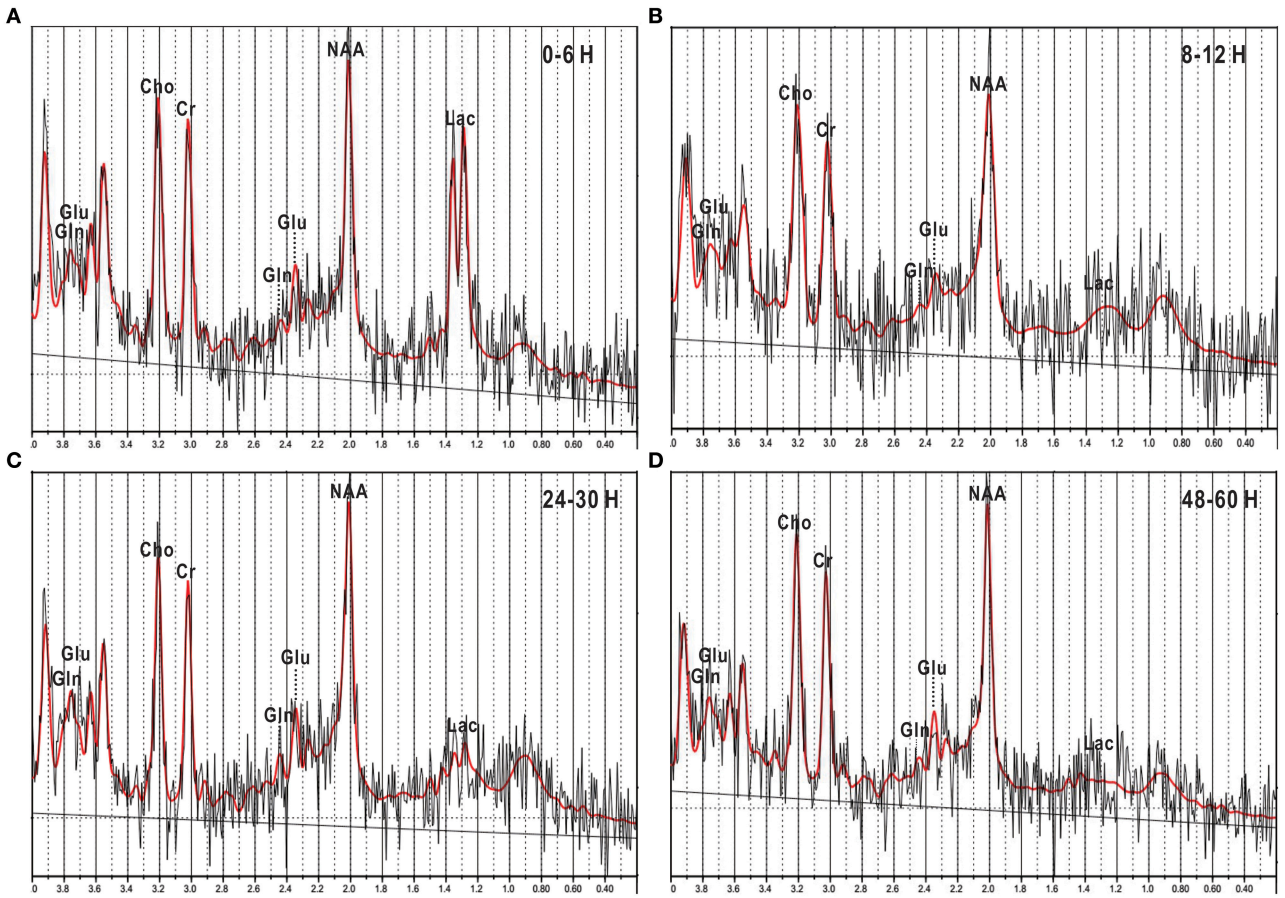

FIGURE 3 | ^{1}H-MRS images of newborn piglets at different times points after HI injury. (A–C) and **(D)** represented four different time points after HI operation: 0–6, 8–12, 24–30, and 48–60 h. In the spectra, the Glu peak was elevated at 0–6 h **(A)**, then slightly depressed at 8–12 h **(B)**, and thereafter elevated again at 24–30 h **(C)**, and 48–60 h **(D)**. However, the Gln peak did not show significant changes in the above image. Glu, glutamate; Gln, glutamine; NAA, N-acetylaspartate; Lac, lactate; Cho, choline; Cr, creatine.

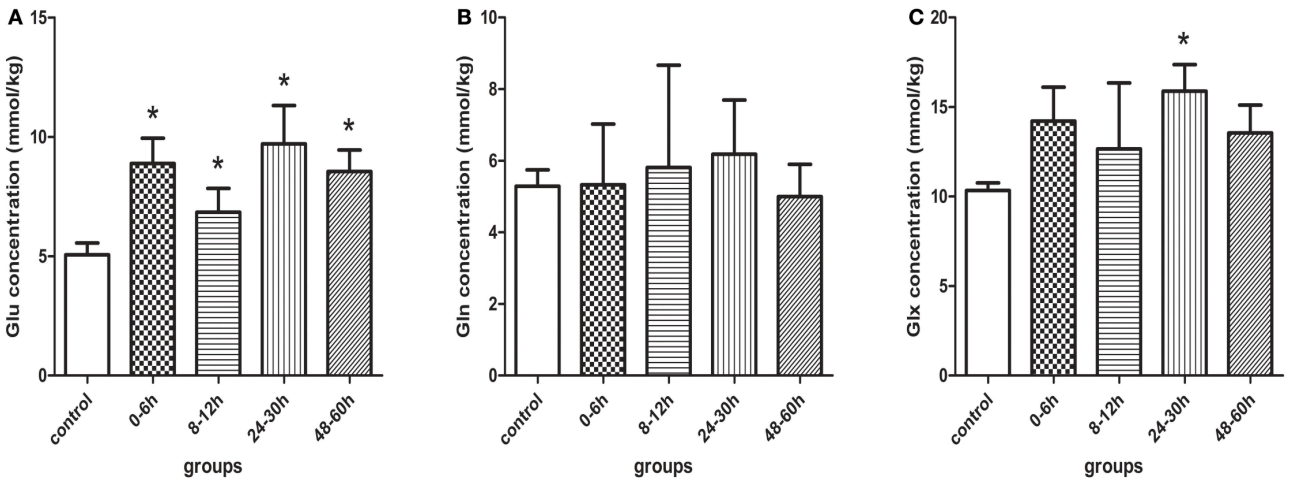

FIGURE 4 | Quantification results measured by ^{1}H-MRS in control and model piglets at different time-points after HI insult , **(A)** Glu, **(B)** Gln, and **(C)** Glx. Errors bars indicate standard deviation values. *Compared with the control group, $P < 0.05$. Glu, glutamate; Gln, glutamine; Glx, glutamate + glutamine.

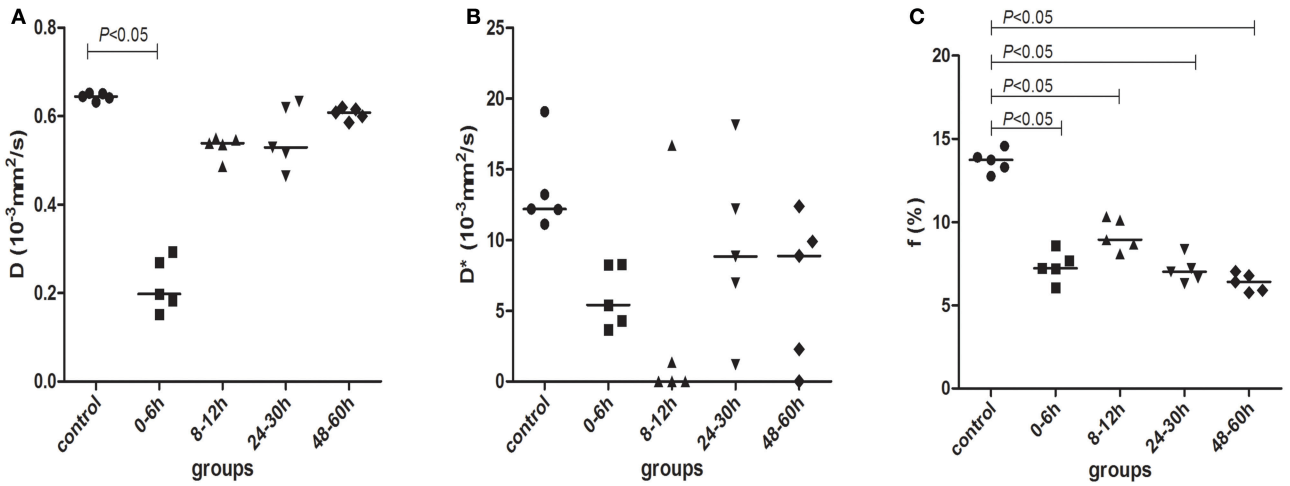

FIGURE 5 | *D* **(A)**, *D** **(B)**, and *f* **(C)** parameters measured by IVIM scanning in control (black circles) and model piglets at different time-points, 0–6 h (black squares); 8–12 h (black regular triangles); 24–30 h (black inverted triangles); and 48–60 h (black diamonds). The horizontal lines in the scatter plots represent medians.

TABLE 1 | *D*, *D, and *f* parameters measured in newborn piglets from all groups.**

Parameter	Model group				
	Control group ($n = 5$)	0–6 h ($n = 5$)	8–12 h ($n = 5$)	24–30 h ($n = 5$)	48–60 h ($n = 5$)
D ($\times 10^{-3}$mm^2/s)	0.644 ± 0.008	0.219 ± 0.060*	0.532 ± 0.026$^{\#}$	0.552 ± 0.071	0.606 ± 0.014
*D** ($\times 10^{-3}$mm^2/s)	13.546 ± 3.175	5.979 ± 2.174	3.609 ± 7.336	9.459 ± 6.276	6.683 ± 5.284
f (%)	13.650 ± 0.676$^{\#}$	7.350 ± 0.914*	9.231 ± 0.957*$^{\#}$	7.103 ± 0.778*	6.375 ± 0.551*

Data are shown as mean ± standard deviation.
Compared with the control group,$P < 0.05$*
Compared with HI 48–60 h group, $^{\#}P < 0.05$
D, diffusion coefficient; D, pseudo-diffusion coefficient; f, perfusion fraction.*

Our study results showed that Glu level underwent a "two-phase" change after HI. The sharp rise in Glu level in the 0–6 h group can be explained by the following mechanism. Energy dysmetabolism in nerve cells occured in the early stage, and the neurons were then depolarized, which caused a substantial release of excitable Glu into the extracellular spaces (Phillis et al., 1994; D'souza and Slater, 1995; Guo et al., 2011; Rocha-Ferreira and Hristova, 2016). Meanwhile, increased NADH/NAD$^+$ ratio may directly promote the de novo synthesis of Glu (Ottersen et al., 1996), and the Glu level in astrocytes was then increased accordingly. In the 8–12 h group, the Glu concentration reached a transiently low peak due to the work of Glu transporters (GluTs), responsible for taking up extracellular Glu into astrocytes. On this basis, excessive Glu is transformed into Gln and then returns back to neurons, completing the "Glu (in neuron)–Gln (in astrocyte)" cycle (Bacci et al., 2002). Excessive Glu then suppresses the excessive excitation of basal ganglia, in a possible self-protective mechanism within human astrocytes (Sofroniew and Vinters, 2010; Ouyang et al., 2014). In the 24–30 h group, the Glu concentration increased again due to two causes: cell rupture caused by reperfusion injury led to an increase in Glu release; and the Glu reuptake mechanism was damaged in the late stages of the disease's course and thus resulted in the massive extracellular accumulation of Glu (Matsumoto et al., 1996). Meanwhile, the severe shortage of ATP inhibited the activity of glutamine synthetase (which is responsible for transforming Glu into non-excitatory Gln in the Glu-Gln cycle) (Dao et al., 1991), thus causing the accumulation of residual Glu in astrocytes (Torp et al., 1993).

Moreover, we did not find statistically significant differences in Gln concentration between the different groups in the present study, and this was perhaps associated with the PRESS sequence ($TE = 37$ ms) used for the ^{1}H-MRS scan. A PRESS sequence ($TE = 37$ ms) is not the best choice to study Gln. Henry et al. (2011) believed that two-dimensional (2D) J-resolved MRS could completely disperse the peak overlapping on the 2D plane, which is caused by the approximate coupling constants in a one-dimensional plane, and had good stability and no susceptibility to linewidth fluctuation. Therefore, 2D J-resolved MRS is the optimal spectrum study method available for Gln quantification. In the future, we may be able to further investigate and explore Gln by 2D J-resolved MRS.

However, changes in local microcirculatory perfusion in the brain and their association with Glu level have not yet been fully clarified. In this study, we quantitatively evaluated changes in microcirculatory perfusion after HIBD using IVIM. As is well

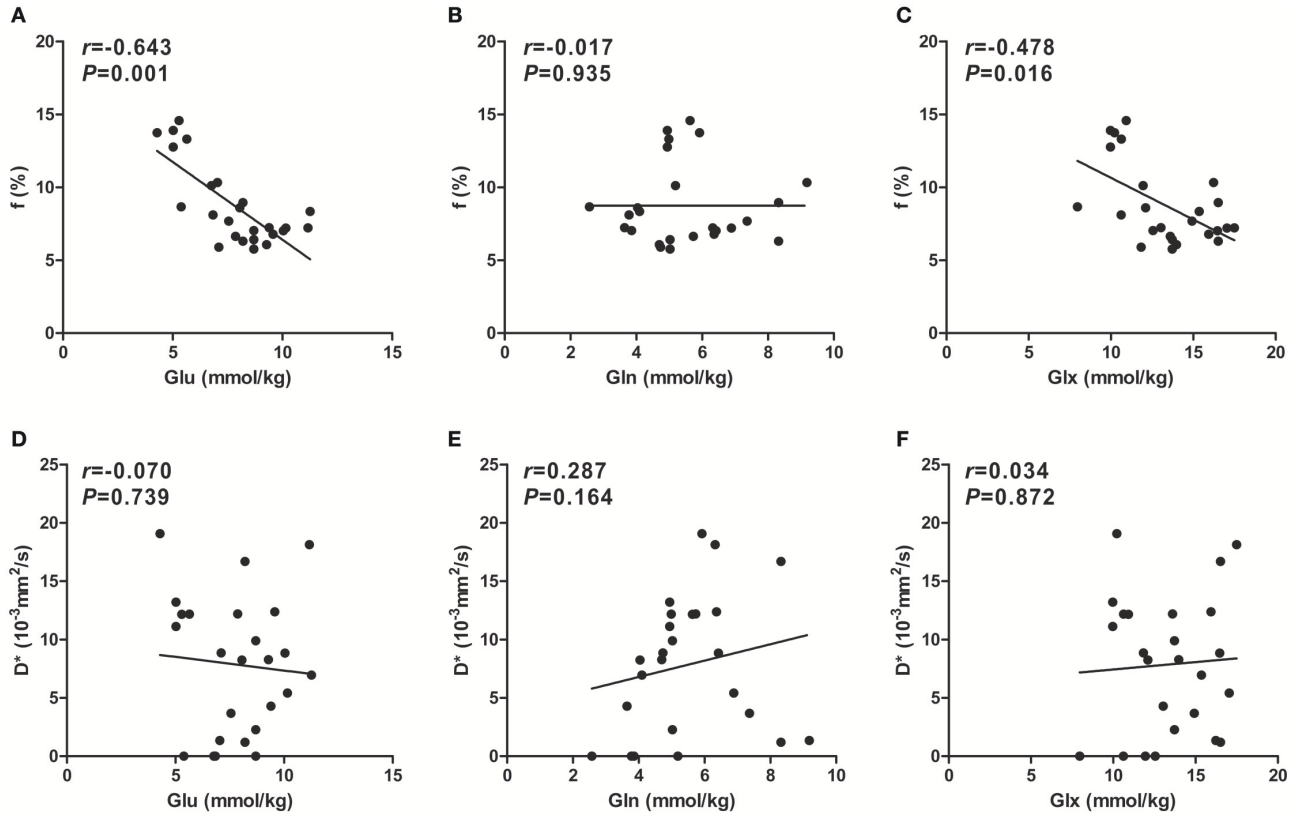

FIGURE 6 | Scatter plots of IVIM-derived *f* (%) and *D (×10^{-3}mm^2/s) parameters over concentrations (mmol/kg) of Glu, Gln, and Glx.** A significant negative correlation between *f* values and the Glu concentration was observed **(A)**, whereas an ordinary negative correlation between *f* values and the Glx concentration was observed **(C)**. However, there was no correlation between *f* values and the Gln concentration **(B)**. Unlike for *f* values, no correlation between *D** values and Glu **(D)**, Gln **(E)**, or Glx **(F)** concentrations was observed. Spearman's rank correlation coefficient *r* was calculated. Glu, glutamate; Gln, glutamine; Glx, glutamate + glutamine.

known, water molecules flow with blood (except for Brownian motion) within the capillary network of the microcirculation, and thus capillary blood flow can be regarded as another form of water diffusion. At the voxel level, the water flowing in randomly oriented capillaries can be regarded as an irregular random motion (Le Bihan et al., 1988) known as "pseudo-diffusion" due to the pseudo random organ distribution of the capillary network, and is related to the structure and blood flow rate of the capillary network. In the present study, perfusion was defined as the incoherent motion of water molecules in capillaries at the voxel level (Hu et al., 2015). The analysis of multiple *b*-value diffusion-weighted imaging (DWI) with an IVIM model is applicable to the quantification of two motion components, including water molecule diffusion and microcirculatory perfusion. Three parameters (*D*, *D**, and *f*) are then finally calculated using a Levenberg–Marquardt non-linear least square fitting routine, of which *D** and *f* both provide information on microcirculatory perfusion. The perfusion fraction *f* represents the volume percentage of perfusion-related diffusion effect in total diffusion effect, and it is positively correlated with the cerebral blood volume of the brain (Federau et al., 2014a,b); the pseudo-diffusion coefficient *D**, i.e., the capillary perfusion-related diffusion coefficient, is determined depending on the blood flow rate and geometry of capillaries. Therefore, the changes in *f* and *D** can be regarded as the changes in microcirculatory perfusion.

This study showed that after HI, *f* decreased at 0–6 h and then transiently recovered at 8–12 h but was still lower than that in the control group, and thereafter, it continued to decrease (see **Table 1** and **Figure 5C**). Several investigators (Pulsinelli et al., 1982; Qiao et al., 2004; Ohshima et al., 2012) have measured changes in local perfusion in the HI brain of animal models using 4-iodo-[14C]-antipyrine, ASL and laser speckle flowmetry (LSF), respectively. They found a transient recovery in cerebral perfusion volume, followed by a decrease in perfusion, which is consistent with our study results. A transient increase in cerebral perfusion volume in the early stages of HIBD may be attributed to the activation of a cerebral vascular self-regulatory mechanism (Grant et al., 2005) (a self-protective mechanism of the body) after the recovery of blood reperfusion in the bilateral common carotid arteries. Blood perfusion decreased in the late stages, after HI. Such delayed hypoperfusion in the clinic is controversial, but most evidence suggests that it is closely related to secondary brain damage after HI (Jensen et al., 2006).

In the present study, the Glu concentration in the basal ganglia of newborn piglets significantly correlated with f in a negative manner ($r = -0.643$, $P = 0.001$). At 8–12 h after HI, f increased transiently (**Table 1** and **Figure 5C**), corresponding to a transient low peak of Glu release (see **Figure 4A**), which indicates that the excessively accumulated Glu was cleared due to the recovery of perfusion in the early stages after HI. (Yamaguchi, 1977) The majority of current studies (Busija et al., 2007; Longo and Goyal, 2013) have shown that Glu and its synthetic analogs can dilate small arteries and veins in the brain and thus increase f. The Glu concentration increased while f decreased again, perhaps because delayed hypoperfusion can mediate the release of this excitatory neurotransmitter (Matsumoto et al., 1996). In turn, the abovementioned vasodilatory effect of Glu may be weakened with the progression of disease, and Glu may even constrict small arteries in the cerebral pia mater. As the Glu concentration increased, cerebral vasospasms may have become aggravated and may have even induced the breakage of postcapillary venules, thus causing severe microcirculatory disturbances (Huang et al., 1994), decreasing f further. Based on this finding, we postulate that the disturbances in microcirculatory perfusion and Glu release may result from, and contribute to, each other, and both may induce neuronal injury following HI.

However, our study results showed no statistically significant difference in D^*. A possible reason may be the big limitation of D^*, which results from uncertainty and very poor reproducibility (Wu et al., 2015; Nougaret et al., 2016; Yang et al., 2016). We found that D^* displayed a large degree of dispersion during post-processing computations, maybe because of a high variation in D^* within brain tissues due to the blood–brain barrier; f usually shows a small value in brain tissues. That is to say, D^* is more likely to have an error when the proportion of perfusion is lower (King et al., 1992; Bisdas et al., 2013). In addition, the movements of animals and the partial volume effect of CSF during scanning can influence the measuring accuracy of D^*. Some investigators have proposed that the accurate measurement of D^* was also affected by the cardiac cycle, with the measurement value of D^* significantly higher in the systole than in the diastole (Federau et al., 2013; Xu et al., 2016). Relative to D^*, f was less affected by these physiological factors, had lower noise and was more uniform.

In addition, this study also demonstrated that the diffusion coefficient D, a parameter reflecting the true diffusion motion of water molecules, was markedly decreased at 0–6 h after HI and then gradually recovered over time, but was still slightly lower than that in the control group (see **Figure 5A**). This was perhaps due to increased glycolysis in the tissues in the early stage of HI, with more and more lactate accumulated, resulting in intracellular acidosis and cytotoxic edema. This subsequently led to the reduction of extracellular spaces (Tuor et al., 2014), which limited the diffusion of water molecules and decreased D. Subsequently, cellular swelling caused by cytotoxic edema compressed the capillaries and then resulted in the further hypoxia of brain tissues. Such hypoxia acted on vascular endothelial cells to increase vascular permeability, resulting in vascular edema. As a result, water molecules were retained extracellularly, the extracellular space became enlarged (Wang H. et al., 2012), the diffusion of water molecules was enhanced, and D increased. Conventional DWI reflects the microstructural changes in brain tissues with changes of the apparent diffusion coefficient (ADC). However, diffusions in biotic tissues actually measured by ADC include both the true diffusion of water molecules and capillary perfusion effects, which can be distinguished by IVIM (Le Bihan et al., 1986, 1988). Therefore, multiple b-value DWI, based on an IVIM bi-exponential model, can provide a value of D without the effects of perfusion factors, and thus can more accurately measure the diffusion of water molecules. In short, the early pathological changes in brain tissues after HI are indicated by changes in D.

Of course, our study had several limitations. Firstly, a small sample size was used, which may have caused a bias in results. However, we hope our results lay the basis for further, larger studies. Secondly, the coil diameter used in this study was relatively bigger than the head of the newborn piglets, and the SNR of images was not high enough. Therefore, work must focus on seeking a better SNR for future studies. Finally, the IVIM sequence was scanned with 16 b-values (including 9 b-values within a range of 0–200 s/mm^2) in the present study, which took a long time, though more accurate and detailed perfusion information was provided; the motion displacement during scanning may have affected the accuracy of results. However, in order to overcome this limitation, data with severe motion was excluded.

CONCLUSION

In this study, we evaluated the changes in Glu metabolism and microcirculatory perfusion in the HI brain by ^{1}H-MRS combined with IVIM. Glu concentration was increased in the early stage after HI, then transiently recovered and finally increased again, showing a "two-phase" change; perfusion-related parameter f showed a clear decrease, then transiently and slightly recovered, and thereafter continued to decrease. There was a significant negative correlation between the two parameters. Our data highlight the potential of combining changes in Glu concentration and f to explore the close relationship between cerebral dysmetabolism and microcirculatory disturbance after HI.

AUTHOR CONTRIBUTIONS

XW and YD participated in conceiving and designing of the idea. KS contributed to providing the post-processing assistant. YD and KS contributed to analyzing the experiment results. YD also contributed to drafting and editing of the manuscript. XW and YD also participated in critically revising the paper. All authors have read and approved the final manuscript for publication.

FUNDING

The author(s) disclosed receipt of the following financial support for the research, authorship, and/or publication

of this article: This work was supported by the National Natural Science Foundation of China (grant no. 30570541, 30770632, 81271631) and Outstanding Scientific Fund of Shengjing Hospital (item no. 201402).

ACKNOWLEDGMENTS

We would like to thank our colleagues in the Department of Radiology, Shengjing Hospital of China Medical University and MR Engineers whose efforts make this work possible.

REFERENCES

Alexander, G. E., and Crutcher, M. D. (1990). Functional architecture of basal ganglia circuits: neural substrates of parallel processing. *Trends Neurosci.* 13, 266–271. doi: 10.1016/0166-2236(90)90107-L

Bacci, A., Sancini, G., Verderio, C., Armano, S., Pravettoni, E., Fesce, R., et al. (2002). Block of glutamate-glutamine cycle between astrocytes and neurons inhibits epileptiform activity in hippocampus. *J. Neurophysiol.* 88, 2302–2310. doi: 10.1152/jn.00665.2001

Bisdas, S., Braun, C., Skardelly, M., Schittenhelm, J., Teo, T. H., Thng, C. H., et al. (2014). Correlative assessment of tumor microcirculation using contrast-enhanced perfusion MRI and intravoxel incoherent motion diffusion-weighted MRI: is there a link between them? *NMR Biomed.* 27, 1184–1191. doi: 10.1002/nbm.3172

Bisdas, S., Koh, T. S., Roder, C., Braun, C., Schittenhelm, J., Ernemann, U., et al. (2013). Intravoxel incoherent motion diffusion-weighted MR imaging of gliomas: feasibility of the method and initial results. *Neuroradiology* 55, 1189–1196. doi: 10.1007/s00234-013-1229-7

Busija, D. W., Bari, F., Domoki, F., and Louis, T. (2007). Mechanisms involved in the cerebrovascular dilator effects of N-methyl-d-aspartate in cerebral cortex. *Brain Res. Rev.* 56, 89–100. doi: 10.1016/j.brainresrev.2007.05.011

Choi, D. W., and Rothman, S. M. (1990). The role of glutamate neurotoxicity in hypoxic-ischemic neuronal death. *Annu. Rev. Neurosci.* 13, 171–182. doi: 10.1146/annurev.ne.13.030190.001131

Cooper, A. J., and Jeitner, T. M. (2016). Central role of glutamate metabolism in the maintenance of nitrogen homeostasis in normal and hyperammonemic brain. *Biomolecules* 6, pii: E16. doi: 10.3390/biom6020016

Coyle, J. T., and Puttfarcken, P. (1993). Oxidative stress, glutamate, and neurodegenerative disorders. *Science* 262, 689–695. doi: 10.1126/science.7901908

Cui, Y., Zhang, C., Li, X., Liu, H., Yin, B., Xu, T., et al. (2015). Intravoxel incoherent motion diffusion-weighted magnetic resonance imaging for monitoring the early response to ZD6474 from nasopharyngeal carcinoma in nude mouse. *Sci. Rep.* 5:16389. doi: 10.1038/srep16389

Danbolt, N. C., Furness, D. N., and Zhou, Y. (2016). Neuronal vs glial glutamate uptake: resolving the conundrum. *Neurochem. Int.* 98, 29–45. doi: 10.1016/j.neuint.2016.05.009

Dao, D. N., Ahdab-Barmada, M., and Schor, N. F. (1991). Cerebellar glutamine synthetase in children after hypoxia or ischemia. *Stroke* 22, 1312–1316. doi: 10.1161/01.STR.22.10.1312

D'souza, S. W., and Slater, P. (1995). Excitatory amino acids in neonatal brain: contributions to pathology and therapeutic strategies. *Arch. Dis. Child. Fetal Neonatal Ed.* 72, F147–F150. doi: 10.1136/fn.72.3.F147

Federau, C., Hagmann, P., Maeder, P., Muller, M., Meuli, R., Stuber, M., et al. (2013). Dependence of brain intravoxel incoherent motion perfusion parameters on the cardiac cycle. *PLoS ONE* 8:e72856. doi: 10.1371/journal.pone.0072856

Federau, C., Maeder, P., O'Brien, K., Browaeys, P., Meuli, R., and Hagmann, P. (2012). Quantitative measurement of brain perfusion with intravoxel incoherent motion MR imaging. *Radiology* 265, 874–881. doi: 10.1148/radiol.12120584

Federau, C., O'Brien, K., Meuli, R., Hagmann, P., and Maeder, P. (2014a). Measuring brain perfusion with intravoxel incoherent motion (IVIM): initial clinical experience. *J. Magn. Reson. Imaging* 39, 624–632. doi: 10.1002/jmri.24195

Federau, C., Sumer, S., Becce, F., Maeder, P., O'Brien, K., Meuli, R., et al. (2014b). Intravoxel incoherent motion perfusion imaging in acute stroke: initial clinical experience. *Neuroradiology* 56, 629–635. doi: 10.1007/s00234-014-1370-y

Fujima, N., Yoshida, D., Sakashita, T., Homma, A., Tsukahara, A., Tha, K. K., et al. (2014). Intravoxel incoherent motion diffusion-weighted imaging in head and neck squamous cell carcinoma: assessment of perfusion-related parameters compared to dynamic contrast-enhanced MRI. *Magn. Reson. Imaging* 32, 1206–1213. doi: 10.1016/j.mri.2014.08.009

Grant, D. A., Franzini, C., Wild, J., Eede, K. J., and Walker, A. M. (2005). Autoregulation of the cerebral circulation during sleep in newborn lambs. *J. Physiol.* 564, 923–930. doi: 10.1113/jphysiol.2005.083352

Guo, M. F., Yu, J. Z., and Ma, C. G. (2011). Mechanisms related to neuron injury and death in cerebral hypoxic ischaemia. *Folia Neuropathol.* 49, 78–87.

Hagberg, H., Andersson, P., Kjellmer, I., Thiringer, K., and Thordstein, M. (1987). Extracellular overflow of glutamate, aspartate, GABA and taurine in the cortex and basal ganglia of fetal lambs during hypoxia-ischemia. *Neurosci. Lett.* 78, 311–317. doi: 10.1016/0304-3940(87)90379-X

Hauser, T., Essig, M., Jensen, A., Laun, F. B., Munter, M., Maier-Hein, K. H., et al. (2014). Prediction of treatment response in head and neck carcinomas using IVIM-DWI: Evaluation of lymph node metastasis. *Eur. J. Radiol.* 83, 783–787. doi: 10.1016/j.ejrad.2014.02.013

Henry, M. E., Lauriat, T. L., Shanahan, M., Renshaw, P. F., and Jensen, J. E. (2011). Accuracy and stability of measuring GABA, glutamate, and glutamine by proton magnetic resonance spectroscopy: a phantom study at 4 Tesla. *J. Magn. Reson.* 208, 210–218. doi: 10.1016/j.jmr.2010.11.003

Howlett, J. A., Northington, F. J., Gilmore, M. M., Tekes, A., Huisman, T. A., Parkinson, C., et al. (2013). Cerebrovascular autoregulation and neurologic injury in neonatal hypoxic-ischemic encephalopathy. *Pediatr. Res.* 74, 525–535. doi: 10.1038/pr.2013.132

Hu, L. B., Hong, N., and Zhu, W. Z. (2015). Quantitative measurement of cerebral perfusion with intravoxel incoherent motion in acute ischemia stroke: initial clinical experience. *Chin. Med. J.* 128, 2565–2569. doi: 10.4103/0366-6999.166033

Hu, Y. C., Yan, L. F., Wu, L., Du, P., Chen, B. Y., Wang, L., et al. (2014). Intravoxel incoherent motion diffusion-weighted MR imaging of gliomas: efficacy in preoperative grading. *Sci. Rep.* 4:7208. doi: 10.1038/srep07208

Huang, Q. F., Gebrewold, A., Zhang, A., Altura, B. T., and Altura, B. M. (1994). Role of excitatory amino acids in regulation of rat pial microvasculature. *Am. J. Physiol.* 266, R158–R163.

Jackman, K., and Iadecola, C. (2015). Neurovascular regulation in the ischemic brain. *Antioxid. Redox Signal.* 22, 149–160. doi: 10.1089/ars.2013.5669

Jensen, E. C., Bennet, L., Hunter, C. J., Power, G. C., and Gunn, A. J. (2006). Post-hypoxic hypoperfusion is associated with suppression of cerebral metabolism and increased tissue oxygenation in near-term fetal sheep. *J. Physiol.* 572, 131–139. doi: 10.1113/jphysiol.2005.100768

King, M. D., Van Bruggen, N., Busza, A. L., Houseman, J., Williams, S. R., and Gadian, D. G. (1992). Perfusion and diffusion MR imaging. *Magn. Reson. Med.* 24, 288–301. doi: 10.1002/mrm.1910240210

Le Bihan, D., Breton, E., Lallemand, D., Aubin, M. L., Vignaud, J., and Laval-Jeantet, M. (1988). Separation of diffusion and perfusion in intravoxel incoherent motion MR imaging. *Radiology* 168, 497–505. doi: 10.1148/radiology.168.2.3393671

Le Bihan, D., Breton, E., Lallemand, D., Grenier, P., Cabanis, E., and Laval-Jeantet, M. (1986). MR imaging of intravoxel incoherent motions: application to diffusion and perfusion in neurologic disorders. *Radiology* 161, 401–407. doi: 10.1148/radiology.161.2.3763909

Le Bihan, D., and Turner, R. (1992). The capillary network: a link between IVIM and classical perfusion. *Magn. Reson. Med.* 27, 171–178. doi: 10.1002/mrm.1910270116

Le Bihan, D., Turner, R., and Macfall, J. R. (1989). Effects of intravoxel incoherent motions (IVIM) in steady-state free precession (SSFP) imaging:

application to molecular diffusion imaging. *Magn. Reson. Med.* 10, 324–337. doi: 10.1002/mrm.1910100305

Longo, L. D., and Goyal, R. (2013). Cerebral artery signal transduction mechanisms: developmental changes in dynamics and Ca^{2+} sensitivity. *Curr. Vasc. Pharmacol.* 11, 655–711. doi: 10.2174/1570161111311050008

Martin, L. J., Brambrink, A. M., Lehmann, C., Portera-Cailliau, C., Koehler, R., Rothstein, J., et al. (1997). Hypoxia-ischemia causes abnormalities in glutamate transporters and death of astroglia and neurons in newborn striatum. *Ann. Neurol.* 42, 335–348. doi: 10.1002/ana.410420310

Massaro, A. N., Govindan, R. B., Vezina, G., Chang, T., Andescavage, N. N., Wang, Y., et al. (2015). Impaired cerebral autoregulation and brain injury in newborns with hypoxic-ischemic encephalopathy treated with hypothermia. *J. Neurophysiol.* 114, 818–824. doi: 10.1152/jn.00353.2015

Matsumoto, K., Lo, E. H., Pierce, A. R., Halpern, E. F., and Newcomb, R. (1996). Secondary elevation of extracellular neurotransmitter amino acids in the reperfusion phase following focal cerebral ischemia. *J. Cereb. Blood Flow Metab.* 16, 114–124. doi: 10.1097/00004647-199601000-00014

Nougaret, S., Vargas, H. A., Lakhman, Y., Sudre, R., Do, R. K., Bibeau, F., et al. (2016). Intravoxel incoherent motion-derived histogram metrics for assessment of response after combined chemotherapy and radiation therapy in rectal cancer: initial experience and comparison between single-section and volumetric analyses. *Radiology* 280, 446–454. doi: 10.1148/radiol.2016150702

Ohshima, M., Tsuji, M., Taguchi, A., Kasahara, Y., and Ikeda, T. (2012). Cerebral blood flow during reperfusion predicts later brain damage in a mouse and a rat model of neonatal hypoxic-ischemic encephalopathy. *Exp. Neurol.* 233, 481–489. doi: 10.1016/j.expneurol.2011.11.025

Ottersen, O. P., Laake, J. H., Reichelt, W., Haug, F. M., and Torp, R. (1996). Ischemic disruption of glutamate homeostasis in brain: quantitative immunocytochemical analyses. *J. Chem. Neuroanat.* 12, 1–14. doi: 10.1016/S0891-0618(96)00178-0

Ouyang, Y. B., Xu, L., Liu, S., and Giffard, R. G. (2014). Role of astrocytes in delayed neuronal death: GLT-1 and its novel regulation by microRNAs. *Adv. Neurobiol.* 11, 171–188. doi: 10.1007/978-3-319-08894-5_9

Pfeuffer, J., Provencher, S. W., and Gruetter, R. (1999). Water diffusion in rat brain *in vivo* as detected at very large b values is multicompartmental. *MAGMA* 8, 98–108. doi: 10.1016/s1352-8661(99)00013-7

Phillis, J. W., Smith-Barbour, M., Perkins, L. M., and O'regan, M. H. (1994). Characterization of glutamate, aspartate, and GABA release from ischemic rat cerebral cortex. *Brain Res. Bull.* 34, 457–466. doi: 10.1016/0361-9230(94)90019-1

Provencher, S. W. (2001). Automatic quantitation of localized *in vivo* 1H spectra with LCModel. *NMR Biomed.* 14, 260–264. doi: 10.1002/nbm.698

Pryds, O., Greisen, G., Lou, H., and Friis-Hansen, B. (1990). Vasoparalysis associated with brain damage in asphyxiated term infants. *J. Pediatr.* 117, 119–125. doi: 10.1016/S0022-3476(05)72459-8

Pulsinelli, W. A., Levy, D. E., and Duffy, T. E. (1982). Regional cerebral blood flow and glucose metabolism following transient forebrain ischemia. *Ann. Neurol.* 11, 499–502. doi: 10.1002/ana.410110510

Qiao, M., Latta, P., Foniok, T., Buist, R., Meng, S., Tomanek, B., et al. (2004). Cerebral blood flow response to a hypoxic-ischemic insult differs in neonatal and juvenile rats. *MAGMA* 17, 117–124. doi: 10.1007/s10334-004-0058-4

Rego, A. C., Santos, M. S., and Oliveira, C. R. (1996). Oxidative stress, hypoxia, and ischemia-like conditions increase the release of endogenous amino acids by distinct mechanisms in cultured retinal cells. *J. Neurochem.* 66, 2506–2516. doi: 10.1046/j.1471-4159.1996.66062506.x

Rocha-Ferreira, E., and Hristova, M. (2016). Plasticity in the neonatal brain following hypoxic-ischaemic injury. *Neural. Plast.* 2016, 16. doi: 10.1155/2016/4901014

Sofroniew, M. V., and Vinters, H. V. (2010). Astrocytes: biology and pathology. *Acta Neuropathol.* 119, 7–35. doi: 10.1007/s00401-009-0619-8

Suh, C. H., Kim, H. S., Lee, S. S., Kim, N., Yoon, H. M., Choi, C. G., et al. (2014). Atypical imaging features of primary central nervous system lymphoma that mimics glioblastoma: utility of intravoxel incoherent motion MR imaging. *Radiology* 272, 504–513. doi: 10.1148/radiol.14131895

Torp, R., Arvin, B., Le Peillet, E., Chapman, A. G., Ottersen, O. P., and Meldrum, B. S. (1993). Effect of ischaemia and reperfusion on the extra- and intracellular distribution of glutamate, glutamine, aspartate and GABA in the rat hippocampus, with a note on the effect of the sodium channel blocker BW1003C87. *Exp. Brain Res.* 96, 365–376. doi: 10.1007/BF00234106

Tuor, U. I., Morgunov, M., Sule, M., Qiao, M., Clark, D., Rushforth, D., et al. (2014). Cellular correlates of longitudinal diffusion tensor imaging of axonal degeneration following hypoxic-ischemic cerebral infarction in neonatal rats. *Neuroimage Clin.* 6, 32–42. doi: 10.1016/j.nicl.2014.08.003

Wang, H., Wang, X., and Guo, Q. (2012). The correlation between DTI parameters and levels of AQP-4 in the early phases of cerebral edema after hypoxic-ischemic/reperfusion injury in piglets. *Pediatr. Radiol.* 42, 992–999. doi: 10.1007/s00247-012-2373-7

Wang, X. Y., Wang, H. W., Fu, X. H., Zhang, W. Q., Wu, X. Y., Guo, Q. Y., et al. (2012). Expression of N-methyl-d-aspartate receptor 1 and its phosphorylated state in basal ganglia of a neonatal piglet hypoxic-ischemic brain injury model: a controlled study of (1)H MRS. *Eur. J. Paediatr. Neurol.* 16, 492–500. doi: 10.1016/j.ejpn.2012.01.005

Wisnowski, J. L., Bluml, S., Paquette, L., Zelinski, E., Nelson, M. D. Jr., Painter, M. J., et al. (2013). Altered glutamatergic metabolism associated with punctate white matter lesions in preterm infants. *PLoS ONE* 8:e56880. doi: 10.1371/journal.pone.0056880

Wu, W. C., Chen, Y. F., Tseng, H. M., Yang, S. C., and My, P. C. (2015). Caveat of measuring perfusion indexes using intravoxel incoherent motion magnetic resonance imaging in the human brain. *Eur. Radiol.* 25, 2485–2492. doi: 10.1007/s00330-015-3655-x

Xiao, Y., Pan, J., Chen, Y., Chen, Y., He, Z., and Zheng, X. (2015). Intravoxel incoherent motion-magnetic resonance imaging as an early predictor of treatment response to neoadjuvant chemotherapy in locoregionally advanced nasopharyngeal carcinoma. *Medicine (Baltimore)* 94:e973. doi: 10.1097/MD.0000000000000973

Xu, X. Q., Choi, Y. J., Sung, Y. S., Yoon, R. G., Jang, S. W., Park, J. E., et al. (2016). Intravoxel incoherent motion mr imaging in the head and neck: correlation with dynamic contrast-enhanced MR imaging and diffusion-weighted imaging. *Korean J. Radiol.* 17, 641–649. doi: 10.3348/kjr.2016.17.5.641

Yamaguchi, T. (1977). Regional cerebral blood flow in experimental cerebral infarction, with special reference to hyperemia in the ischemic cerebral hemisphere. *Int. J. Neurol.* 11, 162–178.

Yang, S. H., Lin, J., Lu, F., Han, Z. H., Fu, C. X., Lv, P., et al. (2016). Evaluation of antiangiogenic and antiproliferative effects of sorafenib by sequential histology and intravoxel incoherent motion diffusion-weighted imaging in an orthotopic hepatocellular carcinoma xenograft model. *J. Magn. Reson. Imaging* 45, 270–280. doi: 10.1002/jmri.25344.

Zhang, Y. F., Wang, X. Y., Guo, F., Burns, K., Guo, Q. Y., and Wang, X. M. (2012). Simultaneously changes in striatum dopaminergic and glutamatergic parameters following hypoxic-ischemic neuronal injury in newborn piglets. *Eur. J. Paediatr. Neurol.* 16, 271–278. doi: 10.1016/j.ejpn.2011.05.010

Conflict of Interest Statement: The authors declare that the research was conducted in the absence of any commercial or financial relationships that could be construed as a potential conflict of interest.

frontiers in Neurology

ORIGINAL RESEARCH
published: 17 August 2018
doi: 10.3389/fneur.2018.00634

Protectiveness of Artesunate Given Prior Ischemic Cerebral Infarction Is Mediated by Increased Autophagy

*Ming Shao[1], Yue Shen[2], Hongjing Sun[2], Delong Meng[2], Wei Huo[2] and Xu Qi[2]**

[1] Department of Orthopedics, The First Affiliated Hospital of Harbin Medical University, Harbin, China, [2] Department of Neurology, The First Affiliated Hospital of Harbin Medical University, Harbin, China

Background: Ischemic cerebral infarction is a severe clinical condition that can cause serious mortality. Artesunate, an anti-malarial drug that is widely used in cancer treatment, is known to facilitate accelerated cell apoptosis. The aim of this study is to explore the possible neuroprotective effects of artesunate on hypoxic-ischemic cells in rats.

Methods: Middle cerebral artery occlusion (MCAO) rats were treated with artesunate in different doses to observe their survival rate. Primary hippocampal neurons were deprived of oxygen-glucose to induce ischemia symptoms. Western blot was performed to determine the protein expressions of p-mTOR, Beclin-1, and Mcl-1. A five-point scale was used to detect neurological deficit. Cell apoptosis was measured using a TUNEL assay.

Results: Artesunate supplementation protected MCAO rats from death and ameliorated brain injury among them. Artesunate administration decreased the expression of p-mTOR, increased the expressions of Beclin-1 and Mcl-1, and decreased the activity of caspase-3 in both the rats' ischemia cerebral cortices and their primary ischemia hippocampal neurons when compared with artesunate-absent ischemic brains and cells. The neuroprotective effects of artesunate were abolished by either leucine (LEU) or 3-MA, while the effects of rapamycin were reversed by 3-MA. *In vivo* experiments verified the protective effects of artesunate on brain-infarct rats.

Conclusion: The results indicate the protectiveness of artesunate against ischemic cerebral infarction, whereas the protectiveness might increase autophagy through regulating the activity of mTOR.

Keywords: mTOR, autophagy, artesunate, infarction, Ischemic cerebral infarction

OPEN ACCESS

Edited by:
Tijana Bojić,
Vinča Nuclear Institute, University of Belgrade, Serbia

Reviewed by:
Russ Chess-Williams,
Bond University, Australia
Fang Chen,
Nanjing Medical University, China
Aurel Popa-Wagner,
Department of Neurology, University Hospital Essen, Germany

****Correspondence:***
Xu Qi
qixu16125@163.com

Specialty section:
This article was submitted to Autonomic Neuroscience, a section of the journal Frontiers in Neurology

Received: *15 June 2017*
Accepted: *13 July 2018*
Published: *17 August 2018*

Citation:
Shao M, Shen Y, Sun H, Meng D, Huo W and Qi X (2018) Protectiveness of Artesunate Given Prior Ischemic Cerebral Infarction Is Mediated by Increased Autophagy. Front. Neurol. 9:634. doi: 10.3389/fneur.2018.00634

INTRODUCTION

Cerebral infarction, also known as stroke, is the second leading cause of disability and death worldwide (1). Every year, ∼15 million people are diagnosed with a cerebral infarction, while about 5 million people die from the disease globally. Even though progress has been made on fundamental research and clinical treatment, the patients who suffer from cerebral infarction are still unsatisfied. Traditionally, cerebral infarction is thought to be caused by insufficient cerebral blood flow, while oxidative stress and inflammation also play an important role (2–4). Ischemic brain infarcts are a type of cerebral infarction that not only affect the middle cerebral artery, but also induce early mortality (5). Nevertheless, the indistinct mechanism or the clinical method limit the therapy for patients with cerebral infarction.

Artesunate is a traditional anti-malarial Chinese drug that has been proven to play an important role in cancer treatment due to its role in inducing cell apoptosis (5, 6). Studies have suggested that oxidization and inflammation have a vital role in cell death induced by artesunate; for example, artesunate enhances cell apoptosis by stimulating anticancer toxicity (7, 8). Moreover, artesunate induces severer mitochondrial injury that is mediated by ROS (9). A previous study has proven that artesunate has an effect on the therapy of cerebral malaria during its acute phase (10), but whether artesunate affects cerebral infarction is still unclear.

Autophagy is a catabolic process that can damage organelles and specific proteins. The activation of the mammalian target of rapamycin (mTOR) seems to affect protein translation, cellular response and autophagy. Generally, autophagy is known to eliminate toxins, pathogens, and several modified cytoplasmic, and further protects cells against injury. A previous study reported that activated mTOR in amino acid-rich conditions could inhibit the occurrence of autophagy, while when amino acids are limited extracellularly, autophagy recycles intracellular seem to provide an alternative resource for amino acids (11). Other studies have provided key insights into mTOR as an important factor in autophagy. For example, Nazio et al. found that mTOR inhibits autophagy through regulating ULK1 ubiquitylation (12), while Liang et al. supported mTOR as a therapeutic target by regulating YAP in the tuberous sclerosis complex (13). Zhang et al. suggest that mTOR promotes autophagy and protects rats from osteoarthritis by deleting specific cartilage (14). The mechanism of cerebral infarction has also been studied by many researchers, as well as its autophagy. For example, ebselen was recognized to reduce autophagic activation in ipsilateral thalami with cerebral infarction (15). Other studies have indicated that AKT/mTOR signaling is related to ischemic cerebral infarction. Beclin-1 is an autophagy gene that relates to cell death, Mcl-1 is a member of the anti-apoptotic Bcl-2 family, and caspase-3 plays an important role in cell apoptosis through the activation of death-related proteases. All those genes are favorable to detect cell death.

3-MA is an autophagic inhibitor that can be used to block the formation of autophagosome and autophagic vacuoles (16). Leucine (LEU) is a p-mTOR agonist and has been identified to mediate p-mTOR phosphorylation (17). Rapamycin is an inhibitor of mTOR, and has been widely used in regulating the activity of mTOR-signaling pathways (18).

In this study, 3-MA, LEU, and rapamycin were used to analyze the role of artesunate, and it was found that mTOR was mediated in the autophagy of cerebral infarctions. The aims were to explore the mechanism of mTOR on autophagy and determine whether artesunate affects cerebral infarction by regulating the expression of mTOR and autophagy.

MATERIALS AND METHODS

Animals

In this study, a total of 80 Sprague-Dawley (SD) male rats aged 4–6 weeks and weighing 220–250 g each were used. Food and water were provided *ad libitum* in a controlled environment. The study was permitted by the Animal Ethics Committee.

The rats were randomly divided into four groups ($n = 10$ in each group), including Sham (Group 1), middle cerebral artery occlusion (MCAO, Group 2), MCAO+artesunate (30 mg/kg, Group 3) and MCAO+artesunate (60 mg/kg, Group 4). Artesunate was dissolved in the PBS and intraperitoneally injected into the rats 2 h before MCAO. MCAO was performed according to the reference (19). The rats were all under 4% chloral hydrate anesthesia by intraperitoneal injection before the MCAO surgery.

The work was approved by the ethics committee of the First Affiliated Hospital of Harbin Medical University.

Detection of Neurological Deficit, Cerebral Infarct Volume, and Brain Edema

Neurological deficit was detected via motivation ability and visual ability. The five-point scale described previously (20) was used to assess neurological grading; to summarize, "0" presented no apparent deficits; "1" presented left forelimb flexion; "2" presented a decreased grip of the left forelimb while the tail was pulled; "3" presented spontaneous movement in all directions; and "4" presented spontaneous left circling. The experiments were performed by three technicians and the averages of their individual values represented the final results.

Brain edemas were quantified by detecting water content in the rats' brains. After the rats were sacrificed, their brain tissues were taken out and weighed (W1). Then, the tissues were dried and again their weights (W2) were measured. Finally, the water content of the brains was calculated using the formula (W1–W2)/W1 × 100%.

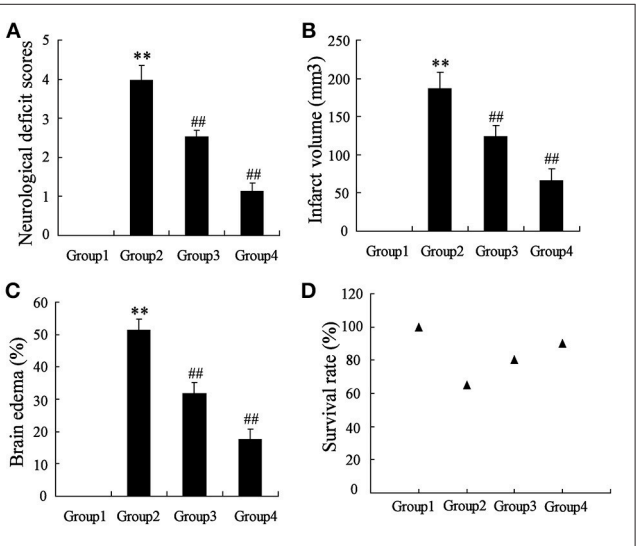

FIGURE 1 | Effects of artesunate on brain injuries. The neurological deficit score **(A)**, infarct volume **(B),** brain edema **(C)**, and the survival rate **(D)** were significantly increased in MCAO rats, while artesunate reversed the results in a dose-dependent manner. $^{**}P < 0.01$ vs. Group 1, $^{\#\#}P < 0.01$ vs. Group 2.

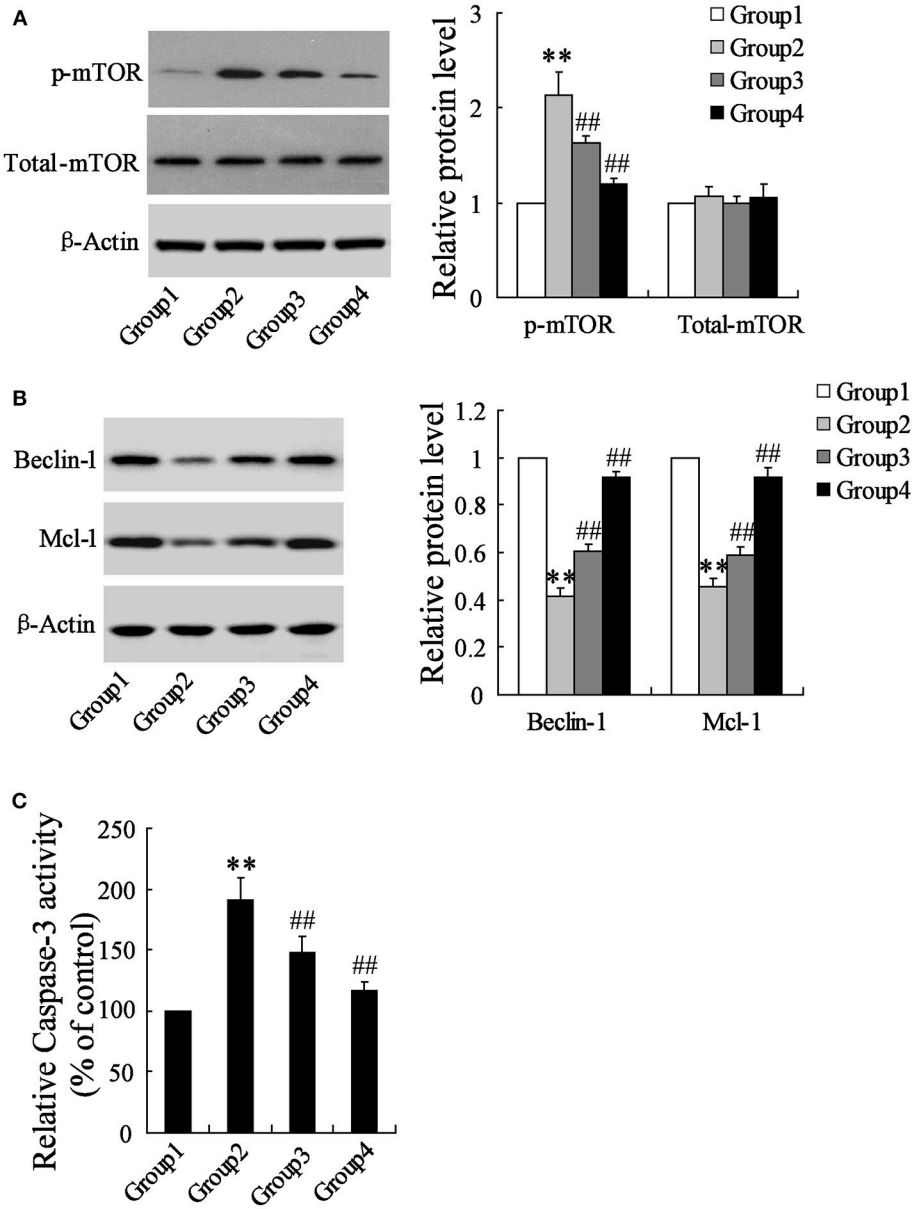

FIGURE 2 | Effects of artesunate on p-mTOR, Beclin-1 and Mcl-1. Ischemia cerebral cortex reflected a significant increase in p-mTOR **(A)**, a significant decrease in Beclin-1 and Mcl-1 **(B)**, and a significant increase of caspase-3 **(C)**, while artesunate supplementation reverses its effects in a dose-dependent manner. $^{**}P < 0.01$ vs. Group 1, $^{\#\#}P < 0.01$ vs. Group 2.

Western Blot

Ischemic cerebrum cells and tissues were lysed using a RIPA Lysis Buffer. Total protein was extracted using a Total Protein Extraction Kit (Takara) according to the manufacturer's instructions, and the quality was detected using the Bradford method. Sodium dodecyl sulfate-polyacrylamide gel electrophoresis (SDS-PAGE) was used to separate the protein extracts. An equal amount of protein was transferred onto a polyvinylidene fluoride membrane, and incubated with primary antibodies (anti-p-mTOR, anti-Beclin-1, anti-Mcl, 1:500, [Sigma, USA]) or β-actin (1:500, [R&D, China]) at 4°C for 24 h. The membranes were then incubated with the secondary antibody (1:1000) for another 2 h at room temperature. The ECL method and Image J software were used to visualize the bands. The antibodies were purchased from Abcam (UK). β-actin acted as an internal control.

Cell Culture and Treatment

Primary rat hippocampal neuron that isolated from SD rats. The cells were cultured in a 24 well-plate with 1×10^4/well and

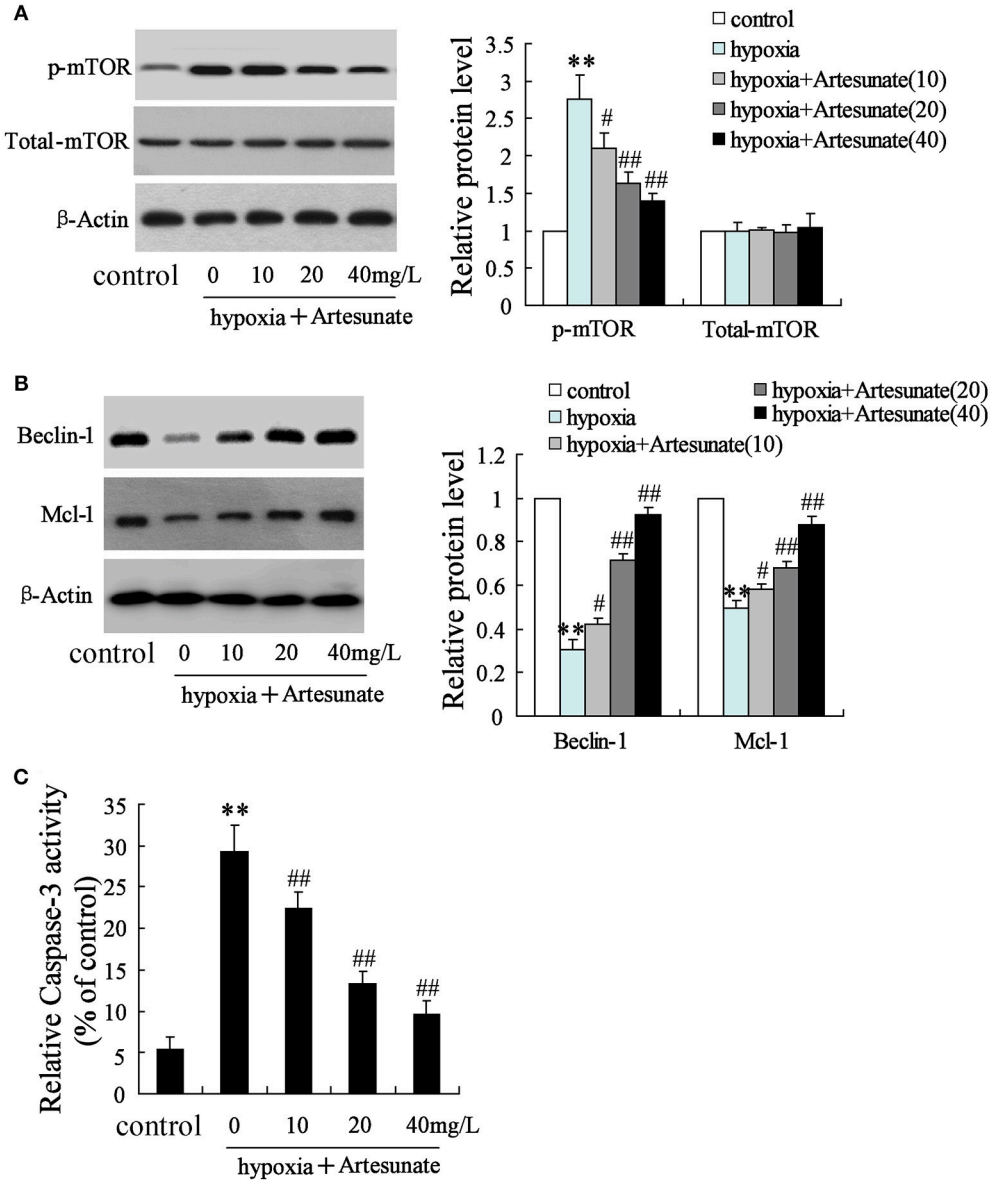

FIGURE 3 | Effects of artesunate with the presence/absence of LEU or 3-MA on ischemic neuron cells. Hypoxia treatment increased the expression of p-mTOR **(A)**, decreased the expression of Beclin-1 and Mcl-1 **(B)**, and promoted cell apoptosis **(C)**, while artesunate supplementation reversed the effects in a dose-dependent manner. $^{**}P < 0.01$ vs. control, $^{\#\#}P < 0.01$ vs. hypoxia.

cultured with DMEM supplemented with 10% fetal bovine serum at 37°C with 5% CO_2 in a humidified atmosphere. After 4 h, the medium was replaced by chemically defined medium, and the half of the volume of the medium was replace every 3 days by an equal volume of chemically defined medium.

Oxygen-glucose deprivation treatment was performed as previously described (21). The cells were exposed to a glucose-free solution of RPBM 1640 medium and cultured at 37°C in an incubator with 5% CO_2 and 95% N_2 for 2 h.

Tunel-Positive Assay

After the cells were treated with artesunate, 3-MA or rapamycin for 2 h and subsequently exposed to gas with oxygen-glucose deprivation for 24 h, TUNEL staining was carried out using a TUNEL Apoptosis Assay Kit (Roche, USA), according to the manufacturer's instructions. The numbers of positive cells were the average value of the ten individual regions of vision.

Activity of Caspase-3

To determine the activity of caspase-3 in rats with different treatments (Sham, MCAO, MCAO+30 mg/kg artesunate and MCAO+60 mg/kg artesunate), the Colorimetric Assay Kit (Genscript, Piscataway, NJ, USA) was used, and the instructions were followed.

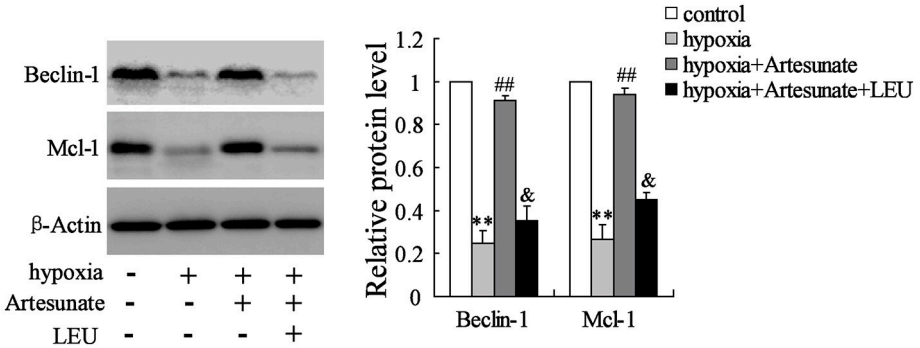

FIGURE 4 | Hypoxia treatment significantly decreased the expression of Beclin-1 and Mcl-1, and the effects were reversed by artesunate supplementation; however, LEU administration abolished the effects induced by artesunate. $^{**}P < 0.01$ vs. control, $^{\#\#}P < 0.01$ vs. hypoxia, $^{\&}P < 0.05$ vs. hypoxia+artesunate.

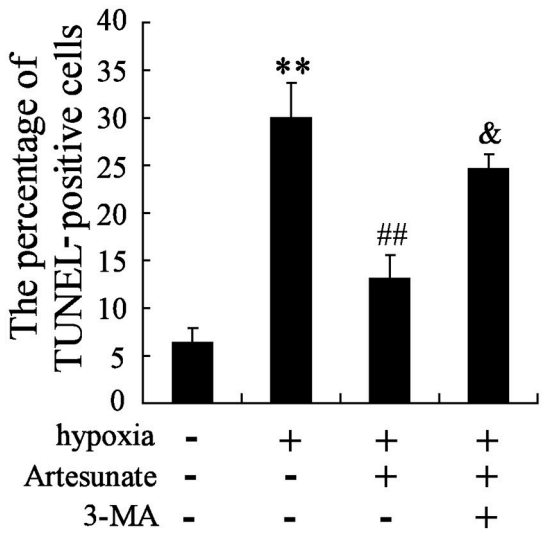

FIGURE 5 | Hypoxia treatment significantly promoted cell apoptosis, and artesunate supplementation reversed the results, whereas 3-MA abolished the effects induced by artesunate (E). $^{**}P < 0.01$ vs. control, $^{\#\#}P < 0.01$ vs. hypoxia, $^{\&}P < 0.01$ vs. hypoxia+artesunate (40 mg/L).

In vivo Experiments

MCAO rats were randomly divided into four groups, including Group 1: MCAO+PBS, Group 2: MCAO+atesunate (60 mg/kg), Group 3: MCAO+atesunate (60 mg/kg) +3-MA (30 mg/kg), and Group 4: MCAO+3-MA (30 mg/kg). After 24 h, the neurological deficit, cerebral infarct volume and brain edema of the rats in the four groups were measured.

Statistical Analysis

All data were expressed as means±SD. The analysis was performed using SPSS18.0. Statistical differences were processed using one-way analysis of variance (ANOVA) combined with the least significant difference *t*-test independent-sample *t*-test. The post-hoc test was carried out to compare the differences in the individual groups. $P < 0.05$ was recognized as a statistically significant difference.

RESULTS

Artesunate Protected the Cerebrum Against Infarction

To determine the effects of artesunate on cerebral infarction, the rats were divided into four groups as previously described, including Sham (Group 1), middle cerebral artery occlusion (MCAO, Group 2), MCAO+30 mg/kg artesunate (Group 3) and MCAO+60 mg/kg artesunate (Group 4). After 24 h, the mortality rates of Groups 1, 2, 3, and 4 were 0, 35, 20, and 10%, respectively (the data were not shown in the article). Cerebral infarction degrees were detected in the living rats. Compared with Group 1, neurological deficit (**Figure 1A**), cerebral infarct volume (**Figure 1B**), and brain edemas (**Figure 1C**) were significantly higher, while the effects were reversed by artesunate (Groups 3 and 4) based on the dose. In addition, when compared with Group 1, the survival rate was lower in Groups 2, 3, and 4, while the artesunate recovered the survival rate based on dose (**Figure 1D**). The results revealed that artesunate significantly ameliorates infractions in neurological deficit, cerebral infarct volume and brain edemas based on dose.

To detect the effects of artesunate on the cerebral cortex in the ischemic region, a western blot and a caspase-3 activity assay were performed. According to **Figure 2A**, the protein expression of p-mTOR was prominently higher in Group 2 compared to Group 1, while it was reversed in Group 3 and Group 4 with the dose-dependent artesunate, while the protein expression of total mTOR showed no significant difference. The protein expressions of Beclin-1 and Mcl-1 was lower in Group 2 than in Group 1; however, it was abolished in Groups 3 and 4 with the dose-dependent artesunate (**Figure 2B**). Furthermore, the activity assay revealed that the activity level of caspase-3 in Group 2 was dramatically higher than Group 1, while its effects were also reversed by artesunate (Groups 3 and 4) in a dose-dependent manner (**Figure 2C**).

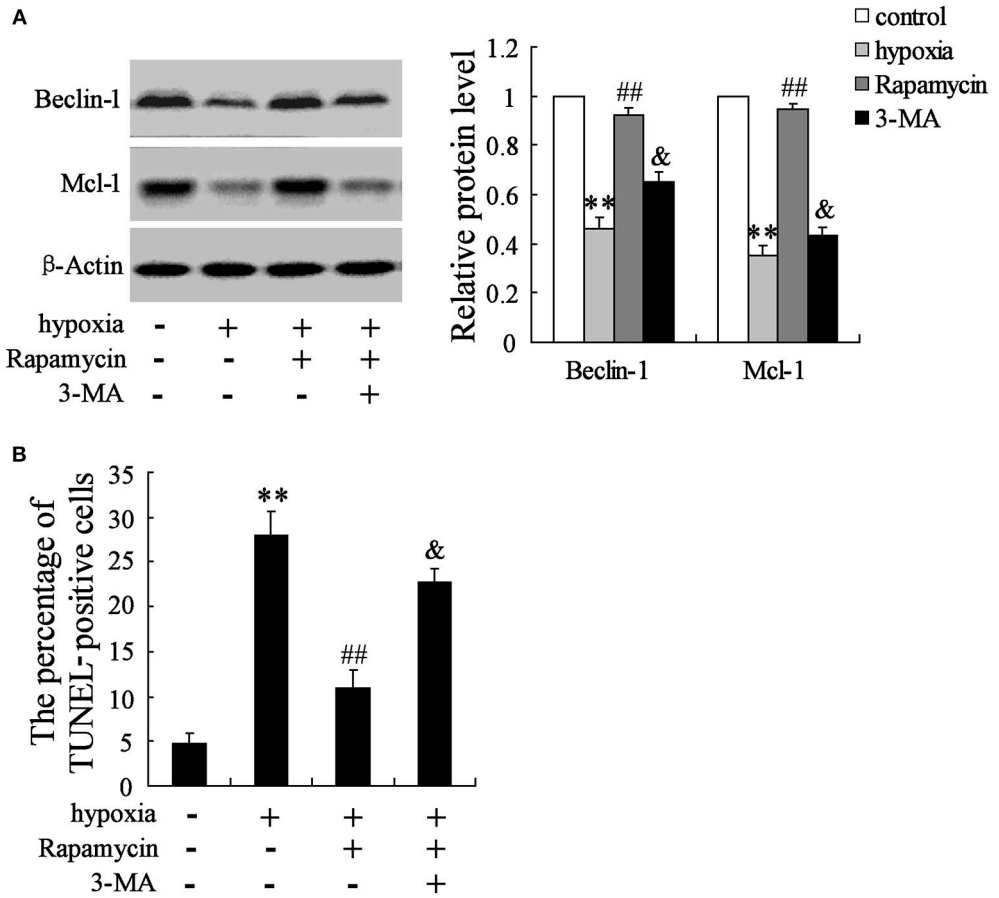

FIGURE 6 | Interaction effects of rapamycin and 3-MA on neuron cells. Hypoxia treatment significantly decreased the expression of Beclin-1 and Mcl-1 **(A)**, but promoted cell death **(B)**. Rapamycin supplementation reversed the effects of hypoxia, while 3-MA administration abolished the effects induced by rapamycin. $^{**}P <$ 0.01 vs. control, $^{\#\#}P < 0.01$ vs. hypoxia, $^{\&}P < 0.01$ vs. hypoxia+artesunate (40 mg/L).

Effects of Artesunate With or Without Leu or 3-MA on Hypoxia-Induced Primary Hippocampal Neurons in Rats

The rats' primary hippocampal neurons were divided into 4 groups and individually pretreated with 0, 10, 20, and 40 mg/L artesunate for 2 h. Afterward, the cells were treated with oxygen-glucose deprivation for 24 h. It was found that hypoxia prominently increased the expression of p-mTOR but not total-mTOR (**Figure 3A**). While hypoxia decreased the expressions of Beclin-1 and Mcl-1 (**Figure 3B**) and increased cell apoptosis (**Figure 3C**), all these effects were abolished by artesunate in a dose-dependent manner.

The primary hippocampal neurons of the rats were pretreated with the presence or absence of artesunate (40 mg/L) and LEU (5 mmol/L) for 2 h, then treated with oxygen-glucose deprivation for 24 h. **Figure 4** demonstrates that hypoxia supplementation significantly decreases the expressions of Beclin-1 and Mcl-1 and artesunate administration seems to reverse its effects, while LEU abolishes its effects.

The hippocampal neurons were pretreated with the presence or absence of artesunate (40 mg/L) and 3-MA (50 mmol/L) for 2 h, then treated with oxygen-glucose deprivation for 24 h. The results revealed that hypoxia stimulation significantly increases cell apoptosis, while this effect is reversed by rapamycin; however, 3-MA supplementation abolishes the effects induced by artesunate (**Figure 5**).

Effects of Rapamycin and 3-MA on Hypoxia-Induced Primary Hippocampal Neurons in Rats

The hippocampal neurons were pretreated with the presence or absence of the p-mTOR inhibitor rapamycin (100 mmol/L) or the autophagy inhibitor 3-MA (50 mmol/L) for 2 h, then treated with oxygen-glucose deprivation for 24 h. As is presented in **Figure 3**, hypoxia stimulation significantly decreases the expressions of Beclin-1 and Mcl-1, but increases cell apoptosis. Rapamycin seems to reverse its effects, while 3-MA abolishes the effects induced by rapamycin (**Figures 6A,B**).

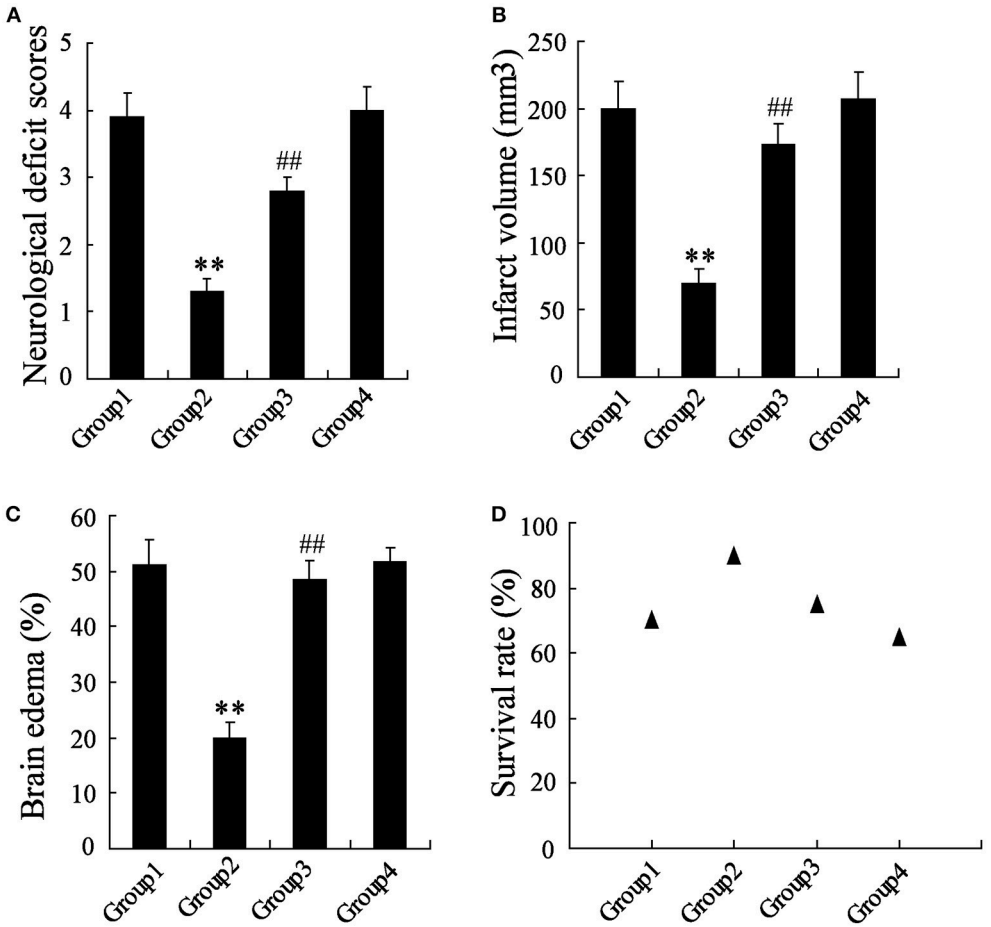

FIGURE 7 | *In vivo* to verify the effects of artesunate and 3-MA on brain injury. The neurological deficit score **(A)**, infarct volume **(B)**, brain edema **(C)**, and survival rate **(D)** were significantly lower in MCAO rats that were supplied with artesunate, while 3-MA supplementation reversed the results in a dose-dependent manner. $^{**}P <$ 0.01 vs. Group 1, $^{\#\#}P < 0.01$ vs. Group 2.

In vivo Examination of the Effects of MCAO, Artesunate and 3-MA

The MCAO rats were randomly divided into 4 groups, including Group 1: MCAO+PBS, Group 2: MCAO+artesunate (60 mg/kg), Group 3: MCAO+artesunate (60 mg/kg) +3-MA (30 mg/kg), and Group 4: MCAO+3-MA (30 mg/kg). After 24 h, the mortality rates of Groups 1, 2, 3, and 4 were 30, 10, 25, and 35% respectively (the data are not shown in the article). The indices of the live rats were detected, and the results revealed that artesunate supplementation decreases neurological deficit score (**Figure 7A**), infarct volume (**Figure 7B**), brain edema (**Figure 7C**), and survival rate (**Figure 7D**) in a dose-dependent manner, while the effects are abolished by 3-MA supplementation.

DISCUSSION

This study exhibited the effects of artesunate as a protective agent in ischemic cerebral infarction in rats. It was found that artesunate protects the brain from MCAO-induced cerebral infarction, based on the dose. Upon the analysis of artesunate *in vivo* experiments, the results revealed that artesunate protects the brain against ischemic infarction.

Mounting studies have reported the current efforts to improve neurorehabilitation. For example, Human induced pluripotent stem cells has been proven to improve the recovery of stroke (22). Another study revealed that Stem cell protected stroke of preclinical models is associated with aging (23). However, the therapy of hypoxia-ischemia induces brain injury was still need further exploration. Hypoxia-ischemia induces brain injury by impairing oxygen supplements, which leads to a variety of biochemical reactions in the body and disturbed normal physiological processes (24). Hypoxia-ischemia can have enormously severe symptoms; for example, it affects oxidative stress and nitrification stress in newborn rats' brains (25), and gestational and perinatal inflammation is associated with hypoxia-ischemia (26). Moreover, many studies have proven that cell death and autophagy induced by hypoxia-ischemia in the brain are an important neuron injury in patients (27–29). In this study, hypoxia-ischemia was performed to obtain brain

infarction cells, which were essential to the study. Previous studies have also declared that hypoxia-ischemia can successfully induce brain infarction cells. For example, Qu et al. found that hypoxia-ischemia induces severe neuronal apoptosis *in vitro* experiments (30), and Savard et al. proved that IL-1β and MMP-9 are mediated in neuronal self-injury in hypoxia-ischemia induced neuron cells (31). All of these observations suggest that hypoxia-ischemia is crucial in brain infarction.

The mammalian target of rapamycin (mTOR) is part of the mTOR Complex 1, with the capacity to regulate cell growth and autophagy. The activation of mTOR is related to many diseases such as cancer, cardiovascular diseases, neurodegenerative diseases as well as brain diseases (32, 33); at the same time, inhibition of mTOR induces autophagy. The expression of phosphorylated mTOR (p-mTOR) is always used to measure the activation of mTOR. From this study, it was found that hypoxia-ischemia stimulation promoted the expression of p-mTOR, while artesunate supplementation impaired the expression. However, other studies provided key inhibitors of mTOR; for example, rapamycin was recognized as an inhibitor of mTOR and affects cell cycle arrest, ribosome biogenesis and autophagy (34).

In this study, Beclin-1, Mcl-1, and caspase-3 were used to assess cell apoptosis. As was presented, the expressions of Beclin-1 and Mcl-1 were significantly decreased in hypoxia-ischemia induced cells, while the expressions of p-mTOR and caspase-3 was significantly increased, which suggested that hypoxia-ischemia stimulation significantly increases cell death and reduces autophagy. Additionally, artesunate supplementation reverses the effects, indicating the protective role of artesunate on neuron cells.

To explore the effects of mTOR on autophagy, p-mTOR agonist leucine (LEU), autophagy inhibitor 3-MA, and p-mTOR inhibitor rapamycin were used individually to observe their effects on cell apoptosis and autophagy. It was found that the protective effect of artesunate on ischemic brain infarction is reversed by both LEU and 3-MA. Moreover, rapamycin also exhibits a protectiveness of neuron cells against ischemia-induced brain infarction, while its effects are abolished by 3-MA. To verify whether the results obtained *in vitro* experiments were acceptable, a *vivo* experiment with MCAO rats was then performed, and the results revealed that ameliorated injury of brain infarction, while its effects were reversed by 3-MA.

CONCLUSION

This study suggests that hypoxia-induced brain infarctions significantly increase the expression of p-mTOR, Artesunate administration seems to protect the brain against infarction by decreasing the expression of mTOR, while the protectiveness is reversed by LEU and 3-MA. Additionally, rapamycin seems to reverse the effects of hypoxia, while 3-MA abolishes the effects of rapamycin. This study suggests that p-mTOR acts as a potential biomarker of brain infarctions, and artesunate provides a potential role for the therapy of ischemic brain infarctions.

CONSENT FOR PUBLICATION

The study was undertaken with the consent of the First Affiliated Hospital of Harbin Medical University.

AUTHOR CONTRIBUTIONS

MS conceived and designed the study and drafted the manuscript. YS collected the data. HS and DM analyzed the data. WH interpreted the data. XQ participated in the study and helped to draft the manuscript. All authors read and approved the final manuscript.

REFERENCES

1. Feigin VL, Forouzanfar MH, Krishnamurthi R, Mensah GA, Connor M, Bennett DA, et al. Global and regional burden of stroke during 1990-2010: findings from the Global Burden of Disease Study (2010) *Lancet* (2014) 383:245–54. doi: 10.1016/S0140-6736(13)61953-4
2. Campbell BC, Christensen S, Tress BM, Churilov L, Desmond PM, Parsons MW, et al. Failure of collateral blood flow is associated with infarct growth in ischemic stroke. *J Cereb Blood Flow Metab*. (2013) 33:1168–72. doi: 10.1038/jcbfm.2013.77
3. Siffroi-Fernandez S, Dulong S, Li XM, Filipski E, Grechez-Cassiau A, Peteri-Brunback B, et al. Functional genomics identify Birc5/survivin as a candidate gene involved in the chronotoxicity of cyclin-dependent kinase inhibitors. *Cell Cycle* (2014) 13:984–91. doi: 10.4161/cc.27868
4. Russek NS, Jensen MB, Histological quantification of brain tissue inflammatory cell infiltration after focal cerebral infarction: a systematic review. *Int J Neurosci*. (2014) 124:160–5. doi: 10.3109/00207454.2013.833509
5. Juttler E, Unterberg A, Woitzik J, Bosel J, Amiri H, Sakowitz OW, et al., Hemicraniectomy in older patients with extensive middle-cerebral-artery stroke. *N Eng J Med*. (2014) 370:1091–100. doi: 10.1056/NEJMoa1311367
6. Liu L, Zuo LF, Zuo J, and Wang J. Artesunate induces apoptosis and inhibits growth of Eca109 and Ec9706 human esophageal cancer cell lines *in vitro* and *in vivo*. *Mol Med Rep*. (2015) 12:1465–72. doi: 10.3892/mmr.2015.3517
7. Alzoubi K, Calabro S, Bissinger R, Abed M, Faggio C, Lang F. Stimulation of suicidal erythrocyte death by artesunate. *Cell Physiol Biochem*. (2014) 34:2232–44. doi: 10.1159/000369666
8. Karpel-Massler G, Westhoff MA, Kast RE, Dwucet A, Nonnenmacher L, Wirtz CR, et al. Artesunate enhances the antiproliferative effect of temozolomide on U87MG and A172 glioblastoma cell lines. *Anti-cancer Agents Med Chem*. (2014) 14:313–8. doi: 10.2174/18715206113136660340
9. Papanikolaou X, Johnson S, Garg T, Tian E, Tytarenko R, Zhang Q, et al. Artesunate overcomes drug resistance in multiple myeloma by inducing mitochondrial stress and non-caspase apoptosis. *Oncotarget* (2014) 5:4118–28. doi: 10.18632/oncotarget.1847
10. Vieira JL, Borges LM, Ferreira MV, Rivera JG, Gomes Mdo S. Patient age does not affect mefloquine concentrations in erythrocytes and plasma during the acute phase of falciparum malaria. *Brazilian J Infect Dis*. (2016) 20:482–6. doi: 10.1016/j.bjid.2016.07.005
11. Katsuragi Y, Ichimura Y, and Komatsu M. p62/SQSTM1 functions as a signaling hub and an autophagy adaptor. *FEBS J*. (2015) 282:4672–8. doi: 10.1111/febs.13540
12. Nazio F, Strappazzon F, Antonioli M, Bielli P, Cianfanelli V, Bordi M, et al. mTOR inhibits autophagy by controlling ULK1 ubiquitylation, self-association and function through AMBRA1 and TRAF6. *Nature Cell Biol*. (2013) 15:406–16. doi: 10.1038/ncb2708

13. Liang N, Zhang C, Dill P, Panasyuk G, Pion D, Koka V, et al. Regulation of YAP by mTOR and autophagy reveals a therapeutic target of tuberous sclerosis complex. *J Exp Med.* (2014) 211:2249–63. doi: 10.1084/jem.20140341
14. Zhang Y, Vasheghani F, Li YH, Blati M, Simeone K, Fahmi H, et al. Cartilage-specific deletion of mTOR upregulates autophagy and protects mice from osteoarthritis. *Ann Rheum Dis.* (2015) 74:1432–40. doi: 10.1136/annrheumdis-2013-204599
15. Li Y, Zhang J, Chen L, Xing S, Li J, Zhang Y, et al. Ebselen reduces autophagic activation and cell death in the ipsilateral thalamus following focal cerebral infarction. *Neurosci Lett.* (2015) 600:206–12. doi: 10.1016/j.neulet.2015.06.024
16. Li J, Hou N, Faried A, Tsutsumi S, Takeuchi T, Kuwano H. Inhibition of autophagy by 3-MA enhances the effect of 5-FU-induced apoptosis in colon cancer cells. *Ann Surg Oncol.* (2009) 16:761–71. doi: 10.1245/s10434-008-0260-0
17. Smith GI, Yoshino J, Stromsdorfer KL, Klein SJ, Magkos F, Reeds DN, et al. Protein ingestion induces muscle insulin resistance independent of leucine-mediated mTOR activation. *Diabetes* (2015) 64:1555–63. doi: 10.2337/db14-1279
18. Li J, Kim, S.G. and Blenis J. Rapamycin: one drug, many effects. *Cell Metab.* (2014) 19:373–9. doi: 10.1016/j.cmet.2014.01.001
19. Liu Y, Tang G, Li Y, Wang Y, Chen X, Gu X, et al. Metformin attenuates blood-brain barrier disruption in mice following middle cerebral artery occlusion. *J Neuroinflammation* (2014) 11:177. doi: 10.1186/s12974-014-0177-4
20. Menzies SA, Hoff, J.T. and Betz AL, Middle cerebral artery occlusion in rats: a neurological and pathological evaluation of a reproducible model. *Neurosurgery* (1992) 31:100–6, discussion:106–7. doi: 10.1227/00006123-199207000-00014
21. Yu AC, Lau LT. Expression of interleukin-1 alpha, tumor necrosis factor alpha and interleukin-6 genes in astrocytes under ischemic injury. *Neurochem Int.* (2000) 36:369–77. doi: 10.1016/S0197-0186(99)00145-X
22. Tatarishvili J, Oki K, Monni E, Koch P, Memanishvili T, Buga AM, et al. Human induced pluripotent stem cells improve recovery in stroke-injured aged rats. *Restorat Neurol Neurosci.* (2014) 32:547–58. doi: 10.3233/RNN-140404
23. Popa-Wagner A, Buga AM, Doeppner TR, Hermann DM. Stem cell therapies in preclinical models of stroke associated with aging. *Front Cell Neurosci.* (2014) 8:347. doi: 10.3389/fncel.2014.00347
24. Alonso-Alconada D, Alvarez A, Arteaga O, Martinez-Ibarguen A, Hilario E. Neuroprotective effect of melatonin: a novel therapy against perinatal hypoxia-ischemia. *Int J Mol Sci.* (2013) 14:9379–95. doi: 10.3390/ijms14059379
25. Hattori I, Takagi Y, Nozaki K, Kondo N, Bai J, Nakamura H, et al., Hypoxia-ischemia induces thioredoxin expression and nitrotyrosine formation in new-born rat brain. *Redox Rep.* (2002) 7:256–9. doi: 10.1179/135100002125000749
26. Xu FL, Cheng HQ, Wang CH, Zhang YH, Guo JJ. [Effects of caffeine citrate on myelin basic protein in neonatal rats with hypoxic-ischemic brain damage]. *Zhongguo Dang Dai Er Ke Za Zhi* (2015) 17:984–8.
27. Liu Y, Shoji-Kawata S, Sumpter, R.M. Jr., Wei Y, Ginet V, Zhang L, et al. Autosis is a Na+,K+-ATPase-regulated form of cell death triggered by autophagy-inducing peptides, starvation, and hypoxia-ischemia. *Proc Natl Acad Sci USA.* (2013) 110:20364–71. doi: 10.1073/pnas.1319661110
28. Kichev A, Rousset CI, Baburamani AA, Levison SW, Wood TL, Gressens P, et al. Tumor necrosis factor-related apoptosis-inducing ligand (TRAIL) signaling and cell death in the immature central nervous system after hypoxia-ischemia and inflammation. *J Biol Chem.* (2014) 289:9430–9. doi: 10.1074/jbc.M113.512350
29. Han W, Sun Y, Wang X, Zhu C, Blomgren K. Delayed, long-term administration of the caspase inhibitor Q-VD-OPh reduced brain injury induced by neonatal hypoxia-ischemia. *Dev Neurosci.* (2014) 36:64–72. doi: 10.1159/000357939
30. Qu Y, Wu J, Chen D, Zhao F, Liu J, Yang C, et al., MiR-139-5p inhibits HGTD-P and regulates neuronal apoptosis induced by hypoxia-ischemia in neonatal rats. Neurobiology of disease. (2014) 63:184-93. doi: 10.1016/j.nbd.2013.11.023
31. Savard A, Brochu ME, Chevin M, Guiraut C, Grbic D, Sebire G, Neuronal self-injury mediated by IL-1beta and MMP-9 in a cerebral palsy model of severe neonatal encephalopathy induced by immune activation plus hypoxia-ischemia. J Neuroinflammation. (2015) 12:111. doi: 10.1186/s12974-015-0330-8
32. Chang L, Graham PH, Ni J, Hao J, Bucci J, Cozzi PJ, et al., Targeting PI3K/Akt/mTOR signaling pathway in the treatment of prostate cancer radioresistance. Critical reviews in oncology/hematology. (2015) 96:507-17. doi: 10.1016/j.critrevonc.2015.07.005
33. Takei N, and Nawa H, mTOR signaling and its roles in normal and abnormal brain development. Frontiers in molecular neuroscience. (2014) 7:28. doi: 10.3389/fnmol.2014.00028
34. Barquilla A, Crespo, J.L. and Navarro M. Rapamycin inhibits trypanosome cell growth by preventing TOR complex 2 formation. *Proc Natl Acad Sci USA.* (2008) 105:14579–84. doi: 10.1073/pnas.0802668105

Conflict of Interest Statement: The authors declare that the research was conducted in the absence of any commercial or financial relationships that could be construed as a potential conflict of interest.

Advantages of publishing in Frontiers

OPEN ACCESS
Articles are free to read for greatest visibility and readership

FAST PUBLICATION
Around 90 days from submission to decision

HIGH QUALITY PEER-REVIEW
Rigorous, collaborative, and constructive peer-review

TRANSPARENT PEER-REVIEW
Editors and reviewers acknowledged by name on published articles

Frontiers
Avenue du Tribunal-Fédéral 34
1005 Lausanne | Switzerland

Visit us: www.frontiersin.org
Contact us: info@frontiersin.org | +41 21 510 17 00

REPRODUCIBILITY OF RESEARCH
Support open data and methods to enhance research reproducibility

DIGITAL PUBLISHING
Articles designed for optimal readership across devices

FOLLOW US
@frontiersin

IMPACT METRICS
Advanced article metrics track visibility across digital media

EXTENSIVE PROMOTION
Marketing and promotion of impactful research

LOOP RESEARCH NETWORK
Our network increases your article's readership